Second Edition

Hydrogeology Field Manual

Willis D. Weight

Hydrogeology Field Manual

Willis D. Weight, Ph.D., P.E.
Montana Tech of The University of Montana
Butte, Montana

Second Edition

New York Chicago San Francisco Lisbon London Madrid
Mexico City Milan New Delhi San Juan Seoul
Singapore Sydney Toronto

The McGraw-Hill Companies

Copyright © 2008, 2001 by The McGraw-Hill Companies, Inc. All rights reserved. Manufactured in the United States of America. Except as permitted under the United States Copyright Act of 1976, no part of this publication may be reproduced or distributed in any form or by any means, or stored in a database or retrieval system, without the prior written permission of the publisher.

0-07-160120-1

The material in this eBook also appears in the print version of this title: 0-07-147749-7.

All trademarks are trademarks of their respective owners. Rather than put a trademark symbol after every occurrence of a trademarked name, we use names in an editorial fashion only, and to the benefit of the trademark owner, with no intention of infringement of the trademark. Where such designations appear in this book, they have been printed with initial caps.

McGraw-Hill eBooks are available at special quantity discounts to use as premiums and sales promotions, or for use in corporate training programs. For more information, please contact George Hoare, Special Sales, at george_hoare@mcgraw-hill.com or (212) 904-4069.

TERMS OF USE

This is a copyrighted work and The McGraw-Hill Companies, Inc. ("McGraw-Hill") and its licensors reserve all rights in and to the work. Use of this work is subject to these terms. Except as permitted under the Copyright Act of 1976 and the right to store and retrieve one copy of the work, you may not decompile, disassemble, reverse engineer, reproduce, modify, create derivative works based upon, transmit, distribute, disseminate, sell, publish or sublicense the work or any part of it without McGraw-Hill's prior consent. You may use the work for your own noncommercial and personal use; any other use of the work is strictly prohibited. Your right to use the work may be terminated if you fail to comply with these terms.

THE WORK IS PROVIDED "AS IS." McGRAW-HILL AND ITS LICENSORS MAKE NO GUARANTEES OR WARRANTIES AS TO THE ACCURACY, ADEQUACY OR COMPLETENESS OF OR RESULTS TO BE OBTAINED FROM USING THE WORK, INCLUDING ANY INFORMATION THAT CAN BE ACCESSED THROUGH THE WORK VIA HYPERLINK OR OTHERWISE, AND EXPRESSLY DISCLAIM ANY WARRANTY, EXPRESS OR IMPLIED, INCLUDING BUT NOT LIMITED TO IMPLIED WARRANTIES OF MERCHANTABILITY OR FITNESS FOR A PARTICULAR PURPOSE. McGraw-Hill and its licensors do not warrant or guarantee that the functions contained in the work will meet your requirements or that its operation will be uninterrupted or error free. Neither McGraw-Hill nor its licensors shall be liable to you or anyone else for any inaccuracy, error or omission, regardless of cause, in the work or for any damages resulting therefrom. McGraw-Hill has no responsibility for the content of any information accessed through the work. Under no circumstances shall McGraw-Hill and/or its licensors be liable for any indirect, incidental, special, punitive, consequential or similar damages that result from the use of or inability to use the work, even if any of them has been advised of the possibility of such damages. This limitation of liability shall apply to any claim or cause whatsoever whether such claim or cause arises in contract, tort or otherwise.

DOI: 10.1036/0071477497

Professional

Want to learn more?

We hope you enjoy this McGraw-Hill eBook! If you'd like more information about this book, its author, or related books and websites, please click here.

To my wife Stephanie, our seven children, our grandchildren, my parents Robert and Charlotte, my mentors and teachers, and students, without whose influence this work could not have been possible.

ABOUT THE AUTHOR

Willis D. Weight, Ph.D., P.E., is Head of the Hydrogeology Program within the Department of Geological Engineering at Montana Tech of The University of Montana in Butte. He is widely recognized for his hydrogeology research and related engineering work.

Copyright © 2008, 2001 by The McGraw-Hill Companies, Inc. Click here for terms of use.

For more information about this title, click here

Contents

Preface xiii

Chapter 1. Field Hydrogeology 1

1.1 Hydrologic Cycle 2
1.2 Water-Budget Analysis 4
1.3 Water-Budget Myth 10
Sustainability 11
Water as a commodity 12
Changes in flow systems 13
1.4 Sources of Information on Hydrogeology 14
1.5 Site Location for Hydrogeologic Investigations 16
1.6 Taking Field Notes 18
Daily information 19
Lithologic logs 19
Well drilling 22
Well completion 24
Pumping tests 25
Water-quality measurements 27
1.7 Groundwater Use 29
1.8 Groundwater Planning 30
Source-water protection studies 31
1.9 Summary 35

Chapter 2. The Geology of Hydrogeology 37

2.1 Geologic Properties of Igneous Rocks 38
Extrusive rocks 38
Andesite 42
Basalt 46
Intrusive rocks 49
2.2 Geologic Properties of Metamorphic Rocks 55
Plate tectonic settings of metamorphic rocks 57
2.3 Geologic Properties of Sedimentary Rocks 59
Weathering 61
Transport of sediment and depositional environments 64
Stratigraphy 67

2.4 Structural Geology 68
Strike and dip 69
Fold geometry 73
Faulting 74
Other observations in structures 78
Structural effects in karst areas 79
2.5 Geologic Time 84
2.6 Using Geologic Information 87

Chapter 3. Aquifer Properties 91

3.1 From the Surface to the Water Table 91
3.2 Porosity and Aquifer Storage 94
Porosity 94
Storativity 101
3.3 Movement of Fluids through Earth Materials 104
Transmissivity 110
3.4 Aquifer Concepts 111
Unconfined aquifers 113
Confined and artesian aquifer 114
Confining layers 116
Hydrostratigraphy 116
3.5 Boundary Concepts 117
Homogeneity and isotropy 119
3.6 Springs 120
3.7 Summary 122

Chapter 4. Basic Geophysics of the Shallow Subsurface 125

4.1 Common Targets for Shallow Geophysical Investigation 126
4.2 Approaches to Shallow Subsurface Investigations 126
4.3 Overview of Geophysical Techniques 127
Methods 127
Limitations 127
4.4 Matching Geophysical Methods to Applications 129
4.5 Geophysical Survey Planning 130
4.6 Seismics 131
Basic principles 131
Refraction surveying 140
Reflection surveying 143
4.7 Surface Wave Methods 148
4.8 Electrical 151
Basic principles and units 151
Resistivity 152
Induced polarization (IP) 162
Spontaneous potential (SP) 163
Telluric and magnetotelluric methods 164
Electromagnetic (EM) techniques 165

Chapter 5. Groundwater Flow 173

5.1 Groundwater Movement 173
Darcy's law 173

Hydraulic head 176
Hydraulic head and Darcy's law 179
5.2 Flow Nets 183
Vertical groundwater flow 188
Gaining and losing systems 189
Refraction of groundwater flow 191
5.3 Level Measurements in Groundwater Monitoring Wells 192
Defining level measurements 194
Access to wells 197
Measuring points 200
Water-level devices 201
Practical design of level-measurement devices 211
Other practical applications 215
Summary of level-measurement methods 220
5.4 Misinterpretation of Water-Level Data 222
Shallow and deep wells 223
Short versus long screen lengths 227
Combining different aquifers 228
5.5 Summary 229

Chapter 6. Groundwater/Surface-Water Interaction 231

6.1 Fluvial Plain 232
Channel orientation and groundwater/surface-water exchange 234
6.2 Hyporheic Zone 236
Channel geomorphology and stream connectivity 237
6.3 Stream Health 240
6.4 Field Methods to Determine Groundwater/Surface-Water Exchange 242
Stream gauging 243
Parshall flumes 249
Crest-stage gauge 251
Minipiezometers 253
Seepage meters 260
Temperature studies 265
Thermal properties 266
Field equipment 272
Tracer studies 273
Chemical mass balance 280
6.5 Summary 282

Chapter 7. Water Chemistry Sampling 287

7.1 Have a Plan 287
Quality assurance 289
What are you sampling for? 290
Make a checklist 291
7.2 Collecting Groundwater Samples 292
Sample retrieval 292
Passive sampling 293
Filtration, preservation, and labeling 294
Chain of custody 297
Cleaning and decontamination 297
7.3 Field Measurements 298
pH and temperature 298

Specific conductance 300
Dissolved oxygen and redox state 303
Alkalinity 304
Turbidity and total suspended solids 307
7.4 Laboratory Analyses 307
Dissolved metals 307
Anions 308
Organic compounds 308
Total dissolved solids 309
Other types of analyses 310
7.5 Interpreting Lab Results 312
Data validation 312
Charge balance 314
Speciation of dissolved inorganic carbon 315
Hardness and sodium adsorption ratio 316
7.6 Tips on Reporting Data 317
7.7 Summary 319

Chapter 8. Drilling and Well Completion 321

8.1 Getting Along with Drillers 321
8.2 Rig Safety 324
Summary of safety points 328
Other considerations 329
8.3 Drilling Methods 330
Cable-tool method 331
Forward (direct) rotary method 335
Reverse circulation drilling 341
Casing advancement drilling methods 344
Auger drilling 346
Direct-push methods 347
Sonic or rotasonic drilling 351
Mini-sonic 351
Cone penetrometer testing (CPT) 351
Horizontal drilling 353
8.4 How to Log a Drill Hole 354
Describing the cuttings 358
Lag time 358
How much water is being made and where did it come from? 359
8.5 Monitoring-Well Construction 360
Objectives of a groundwater monitoring program 361
Installing a groundwater monitoring well 363
Well completion materials 369
Well development 371
Completion of multilevel monitoring wells 373
8.6 Production-Well Completion 374
Sieve analysis 375
Well screen criteria 378
Screen entrance velocity 382
Well completion and development 385
8.7 Water Witching 390
8.8 Summary 391

Chapter 9. Pumping Tests 395

9.1 Why Pumping Tests? 395
9.2 Pumping-Test Design 396
Geologic conditions 397
Distance-depth requirements of observation wells 400
9.3 Step-Drawdown Tests 404
Well efficiency 405
Laminar versus turbulent flow 406
9.4 Setting Up and Running a Pumping Test 411
Power supply and pumps 412
Data loggers, transducers, and well sentinels 418
E-tapes 424
Discharge system 425
Duct tape 427
Setup procedure 427
Frequency of manual readings 431
Safety issues 432
9.5 Things that Affect Pumping Test Results 433
Weather and barometric changes 433
Other apparent sources and sinks 433
9.6 Summary 435

Chapter 10. Aquifer Hydraulics 437

10.1 Wells 438
Cone of depression 438
Comparison of confined and unconfined aquifers 441
10.2 Traditional Pumping-Test Analytical Methods 443
Cooper-Jacob straight-line plot 448
Single-well tests 455
Casing storage 456
Leaky-confined and semiconfined aquifers 458
Specific yield and vertical hydraulic conductivity from unconfined aquifer tests 463
Distance-drawdown relationships 470
Predictions of distance-drawdown from time-drawdown 472
Recovery plots 474
10.3 Specific Capacity 477
10.4 Well Interference and Boundary Conditions 479
Aquifer boundary conditions 481
Image well theory 483
10.5 Partial Penetration of Wells and Estimates of Saturated Thickness 484
Estimates of the saturated thickness in unconfined aquifers 486
10.6 Fracture-Flow Analysis 492
Pumping tests in flowing wells 495
10.7 Summary 498

Chapter 11. Slug Testing 501

11.1 Field Methodology 502
How to make a slug 504

Performing a slug test 505
Slug tests using well sentinels 508
11.2 Common Errors Associated with Performing Slug Tests 509
Monitoring well completion issues 509
Equipment problems 511
11.3 Analyzing Slug Tests—The Damped Case 512
Hvorslev method 513
Bouwer and Rice slug test 516
Common errors made in analyzing slug test data 523
How to analyze slug tests for both damped methods from a single plot 524
11.4 Analyzing Slug Tests—Underdamped Case 525
Nature of underdamped behavior 526
Effective stress and elastic behavior 529
van der Kamp method 533
Kipp method 535
Methodology 537
Comparison of two methods and discussion of storativity 542
11.5 Other Observations 543

Chapter 12. Vadose Zone Hydrogeology: Basic Principles, Characterization, and Monitoring 547

12.1 Energy Status of Pore Water 548
12.2 Water Content 551
12.3 Soil-Water Retention Curves 551
12.4 Darcy's Equation and Unsaturated Flow Parameters 554
Hydraulic gradient 554
Unsaturated hydraulic conductivity 555
12.5 Soil-Water Budget 559
Infiltration 559
Evaporation and transpiration 562
12.6 Water Storage and Deep Percolation 565
12.7 Physical Methods 565
Soil lysimeters 565
Water balance 566
Darcy flux in the vadose zone 566
Numerical models of soil-water flow 566
Chemical methods in the vadose zone 567
12.8 Characterizing Hydraulic Properties 569
Soil-water characteristic curve 569
Saturated hydraulic conductivity 571
Unsaturated hydraulic conductivity 577
Estimating unsaturated hydraulic conductivity 579
12.9 Vadose Zone Monitoring 583
Pressure head soil-water potential 583
Indirect methods 586
Moisture content 589
Soil gas sampling and monitoring 592
Pore liquid sampling 593
12.10 Summary 597

Chapter 13. Karst Hydrogeology 603

13.1 Introduction 603
13.2 Karst Types 606
Covered and exposed karst 606
Cone and tower karst 607
Cockpit karst 608
Pavement karst 608
Fluviokarst 608
Sinkhole karst 609
Karst in the literature 609
13.3 Carbonate Rocks 610
Limestone 611
Folk classification 612
Dunham classification scheme 613
Dolomite 614
13.4 Recharge Areas 615
13.5 Surface Karst Features 616
Sinkholes 616
Sinking streams 620
Karst valleys 620
Karren 622
Epikarst 623
Karst springs 625
13.6 Caves 627
Twentieth century theories on cave formation 629
Controlling factors in cave formation 629
Cave passageways 630
Speleothems 631
13.7 The Karst Aquifer 633
13.8 Land Use Problems in Kart 636
Human impact on karst groundwater resources 636
13.9 Investigative Methods in Karst 638
Groundwater dye tracing 638
Hydrographs and chemographs 639
Geophysical techniques 641
Electrical survey 641
Frequency domain electromagnetic survey 641
Ground penetrating radar 641
Gravity survey 641
Seismic survey 642
13.10 Summary 643

Chapter 14. Tracer Tests—General 651

14.1 Tracer Test Objectives 652
14.2 Tracer Material 652
14.3 Design and Completion of Tracer Test 656
Conceptual design 657
Selection of the initial mass of the tracer or its concentration 658
Point-source infrastructure 662
Observation wells 668

Sampling schedule 668
Monitoring 670
Equipment 671
14.4 Common Errors 673

Chapter 15. Tracer Tests—Dye 675

15.1 Utility of Groundwater Tracing 675
15.2 Characteristics of Ideal Tracing Agents 679
15.3 Common Misconceptions about Tracer Dyes 679
15.4 Dye Nomenclature and Properties 681
15.5 Designing a Dye Tracing Study 686
15.6 Sampling and Analysis for Dyes 689
15.7 Detection Limits for Tracer Dyes 695
15.8 Determining Dye Quantities 696
15.9 Summary 698

Appendix A. Unit Conversions Tables 699

Appendix B. Relationship of Water Density and Viscosity to Temperature 707

Appendix C. Periodic Table 709

Appendix D. Values of $W(u)$ and u for the Theis Nonequilibrium Equation 711

Appendix E. Sources of Cave and Karst Information 713

Appendix F. Water Quality Parameters and Their Significance 719

Glossary 723
Index 741

Preface

The first edition of this book, *Manual of Applied Field Hydrogeology,* resulted from an enquiry by Bob Esposito of the McGraw-Hill Professional Book Group about Montana Tech of the University of Montana's long running hydrogeology field camp, which was began in 1985 by Dr. Marek Zaluski (Chapter 14). This course was continued under the direction of John Sonderegger and myself from 1989 to 1996, when John Sonderegger retired. In 1997 Chris Gammons (Chapter 7) came on board, and he has assisted in directing this course until the time of this printing. Bob asked whether we would consider taking the course notes and field tasks and putting it into book form. A detailed outline and proposal was submitted, which was professionally reviewed. A very distinguished reviewer was exceedingly enthusiastic about a book of this scope being produced. During his review he expressed the opinion that "every hydrogeologist with less than 10 years of experience should own this book." It was also his opinion that there was a burning need to have a reference that inexperienced field hydrogeologists could refer to that would explain things in real world terms. This has been the perspective in putting together the chapters. Ultimately, McGraw-Hill's Senior Editor Larry Hager led the team in completing the first edition.

Feedback from readers and reviewers led to the printing format of the second edition *Hydrogeology Field Manual*. Larry Hager again spearheaded the effort to improve the first edition. Since John Sonderegger had retired, other experts were solicited as contributors to rewrite and expand the first edition. The original chapters were revised and expanded significantly to appeal to a wider audience and expand the scope to appeal to an international audience. The introductory chapters were written to be included as an undergraduate introductory course in hydrogeology, while the other chapters are appropriate to be included for a course or two at the lower graduate level, with a strong field emphasis. The book is specifically useful for a hydrogeology field camp, with enough material to be used for other courses. Chris Gammons, also of Montana Tech's Department of Geological Engineering rewrote

Copyright © 2008, 2001 by The McGraw-Hill Companies, Inc. Click here for terms of use.

Chapter 7 (Water Chemistry Sampling) and Dan Stephens (Daniel B. Stephens & Associates, Inc) from New Mexico rewrote the Vadose Zone chapter (Chapter 12). New material was written to include hydrogeologic studies in karst settings, resulting in the addition of two chapters. The significance of karst hydrogeology was written by David Bednar from Arkansas (Chapter 13), followed by a chapter devoted to dye tracing (Chapter 15) written by Tom Aley of Ozark Underground Laboratories in Missouri. The previous Chapter 13 (Tracer Tests) written by Marek Zaluski was moved to Chapter 14 with a new title (Tracer Tests—General) followed by the new chapter by Tom Aley (Tracer Tests—Dye) to provide two perspectives on this important topic. The result is a book intended for use by students and professionals alike as a reference that can be pulled off the shelf again and again and brought into the field as a useful reference.

Readers are encouraged to study the examples throughout the book. They stand out in a different font and represent helpful hints and examples from many years of the author's experience. They also contain little anecdotes and solutions to problems that can help save hours of mistakes or provide an experienced perspective. Calculations in the examples are intended to illustrate proper applications of the principles being discussed. To help illustrate field examples, the author has taken many photos and created line drawings in a hope to make the reading more understandable and interesting. Examples come from previous field camps, consulting, and work experience.

It is helpful for the practicing hydrogeologist to be able to "read up" on a topic in field hydrogeology without having to wade through hundreds of pages. Students and other entry-level professionals can use this reference to help them overcome the "panic" of the first few times of performing a new task such as logging a drill hole, supervising the installation of a monitoring well, or analyzing slug-test data. It is felt that if this book helps someone save time in the field or reduces the panic of performing a field task then this effort will have been worth it.

It is the consensus of the authors that the only way to understand how to apply hydrogeologic principles correctly is to have a field perspective. Persons that use hydrogeologic data are responsible for their content, including inherent errors and mistakes that may have occurred in the field. Without knowing what difficulties there are in collecting field data and what may go wrong, an "office person" may ignorantly use poor data in a design problem. It is also our experience that there are many people performing "bad science" because the fundamentals are not well understood. When one confuses the basic principles and concepts associated with hydrogeology, all sorts of strange interpretations result. This generally leads to trouble. Like one seasoned hydrogeologist put it, "I have seen hydrogeologists over the years do all sorts of unimaginable things."

When people go fishing, they may try all sorts of bait, tackle, and fishing techniques; however, without some basic instruction on proper methodologies, the lines get tangled, the fish steal the bait or spit out the fly, or the person fishing becomes frustrated. Even people who are considered to be fishing experts have bad days; however, they always seem to catch fish most of the time. *Hydrogeology Field Manual* takes a "teaching how to fish" approach.

It is always a dilemma to decide what to include and what to leave out in writing a book like this. It is the author's hope that the content is useful. The ideas and feedback from you, the readers, have been invaluable and led to the improvements made. Please continue to send ideas that can be considered for the future. A significant effort was made to acknowledge all photographs and figures contributed by others. If any errors are found, they are the responsibility of the authors. We would appreciate readers' comments, corrections, and suggestions for future editions.

Acknowledgments

I would like to thank the many individuals who helped review the chapters and provided some of the photos used in this book. Peter Norbeck and John Metesh of the Montana Bureau of Mines and Geology in Butte, Montana, have provided several helpful comments on some of the chapters. Bill Uthman of the Montana Department of Resources and Conservation (DNRC) provided some helpful suggestions for the expansion of Chapter 1. Mark Sholes, Diane Wolfgram, and Hugh Dresser (emeritus) from the Department of Geological Engineering at Montana Tech of the University of Montana have provided helpful suggestions on Chapter 2. Hugh Dresser provided all of the stereo pairs found in the book. Peter Huntoon provided some of the photos for Chapter 2 and provided helpful encouragement and examples. He was also a mentor to me during my graduate school years. John Sonderegger was gracious enough to "have others that are currently involved" replace his chapters from the first edition (Chapters 7 and 12). John was an invaluable mentor during my early years at Montana Tech. He was always good at asking the right questions. Marvin Speece was instrumental in reviewing Chapter 4.

William "Bill" Woessner of the University of Montana in Missoula was instrumental in providing significant help for Chapter 6 and in providing some of the photos. (Bill Woessner, in the past, taught a week of our hydrogeology field camp.) Stephen Custer of Montana State University provided helpful comments and photos for the new materials in Chapter 6. David Nimick of the USGS in Helena Montana provided excellent feedback about water sampling and the geochemistry

discussed in Chapter 7. Dan O'Keefe of O'Keefe Drilling in Butte, Montana, was very helpful in reviewing the drilling techniques section and in providing photos for Chapter 8. Mark DuBois of Newmont Mining Corporation provided some invaluable editorial comments and was a major contributor of the first edition's errata sheet. Other cooperating specialists, especially Herb and Dave Potts (Potts Drilling in Bozeman, Montana), and Fred Schmidt, Tom Patten, and John LaFave of the Montana Bureau of Mines and Geology in Butte, Montana, have given significant input. Kevin Mellot was very helpful in providing information and scanning several of the slides used in the figures. Readers have provided other valuable comments and suggestions.

I would especially like to thank the contributors for their chapters who have enriched this book and allowed its depth and breadth to become significantly more useful. Curtis Link contributed all of the content for Chapter 4, including all of the line drawings. Chris Gammons has been a colleague and friend now for over 10 years—he contributed all of Chapter 7, and also made valuable suggestions on the introductory chapters. Dan Stephens contributed his expertise in rewriting the Vadose Zone chapter (Chapter 12). Marek Zaluski contributed Chapter 14 and some of the photos. David Bednar and Tom Aley made the karst hydrogeology chapters (Chapters 13 and 15) possible. The combined efforts of the authors represent nearly 200 years of experience.

I wish to thank the many students over the years for being the subjects of photos and providing good questions and discussion. Kay Eccleston was instrumental in transforming all of the chapters into desktop publishing form, and providing the format for all the text, and constructing the whole first edition of the book.

Finally, I wish to acknowledge the support of my wife Stephanie, our seven children (some who were used in the photos), our growing number of grandchildren, and my parents who make life so grand.

WILLIS D. WEIGHT
Boulder, Montana

Chapter

1

Field Hydrogeology

Water is a natural resource unique to the planet Earth. Water is life to us and all living things. After discounting the volumes represented by oceans and polar ice, groundwater is the next most significant source. It is approximately 50 to 70 times more plentiful than surface water (Fetter 1994). Understanding the character, occurrence, and movement of groundwater in the subsurface and its interaction with surface water is the study of hydrogeology. Field hydrogeology encompasses the methods performed in the field to understand groundwater systems and their connection to surface water sources and sinks.

A hydrogeologist must have a background in all aspects of the hydrologic cycle. They are concerned with precipitation, evaporation, surface water, and groundwater. Those who call themselves hydrogeologists may also have some area of specialization, such as the vadose zone, computer mapping, well hydraulics, karst hydrogeology, aquifer storage and recovery (ASR), public water supply, underground storage tanks, source-water protection areas, and surface-water groundwater interaction, actually each of the chapters named in this book and beyond.

The fun and challenge of hydrogeology is that each geologic setting, each hole in the ground, each project is different. Hydrogeologic principles are applied to solve problems that always have a degree of uncertainty. The reason is that no one can know exactly what is occurring in the subsurface. Hence, the challenge and fun of it. Those who are fainthearted, do not want to get their hands dirty, or cannot live with some amount of uncertainty are not cut out to be field hydrogeologists. The "buck" stops with the hydrogeologist or geologist. It always seems to be their fault if the design does not go right. Properly designed field work using correct principles is one key to being a successful field hydrogeologist. Another important aspect is being able to make simple common-sense adjustments in the field to allow the collection of usable data. The more level-headed and adaptable one is, the more smoothly and cost-effectively field operations can be run.

Copyright © 2008, 2001 by The McGraw-Hill Companies, Inc. Click here for terms of use.

Hydrogeology is a fairly broad topic. Entry-level professionals and even well-seasoned, practicing hydrogeologists may not have attempted one or more of the topics described in this manual. New field tasks can be stressful and having to read a large reference book on one subject can be cumbersome. The objective of this book is to provide a brief presentation on the general topics associated with field hydrogeology. Field methods, tasks, pitfalls, and examples using ideal and nonideal behavior will be presented, in hopes of reducing stress and panic the first few times performing a new task.

1.1 Hydrologic Cycle

The hydrologic cycle is an open system powered by solar radiation. Water from the oceans evaporates into the atmosphere, is carried to land as precipitation, and eventually returns back to the oceans. Solar radiation is more intense nearer the equator, where rising air condenses and falls back onto the world's rain forests. The movement of moisture into the atmosphere and back onto the land surface is an endless cycle. Approximately five-sixths of the water that evaporates upward comes from our oceans; however, only three-fourths of the water that falls from the sky, in the form of precipitation, falls back into the oceans (Tarbuck and Lutgens 1993). This means one-fourth of all water that falls to Earth falls on land. Some of this water is stored in ice caps and glaciers, some runs off from the earth's surface and collects in lakes and various drainage networks, some replenishes the soil moisture, and some seeps into the ground. This is important in supplying the land masses with freshwater. Once the water reaches the land, it takes a variety of pathways back to the oceans, thus completing the hydrologic cycle (Figure 1.1). Other than ocean water (97.2%) and frozen water (2.1%), groundwater (0.6%) accounts for a significant volume of the Earth's water (Fetter 1994).

Having a general understanding of the hydrologic cycle is important for perspective, for keeping the big picture in mind. The occurrence and behavior of groundwater in the field can be tied back to this big picture. For example, global climatic conditions may contribute to why there are more or less wet years or help explain why dry years occur, which later affects water availability in storage. Are decreasing trends in hydrographs in wells tied to water use or drought conditions that may have depleted storage?

Example 1.1 The sea temperatures in the equatorial region are being measured in real time on a continual basis (Hayes et al. 1991). There is a significant relationship between the atmosphere and the ocean temperatures that affect the weather around the globe. In normal years, the sea surface temperature is about 8°C warmer in the west, with cool temperatures off the South America coast from cold water upwelling from the deep (NOAA 2000).

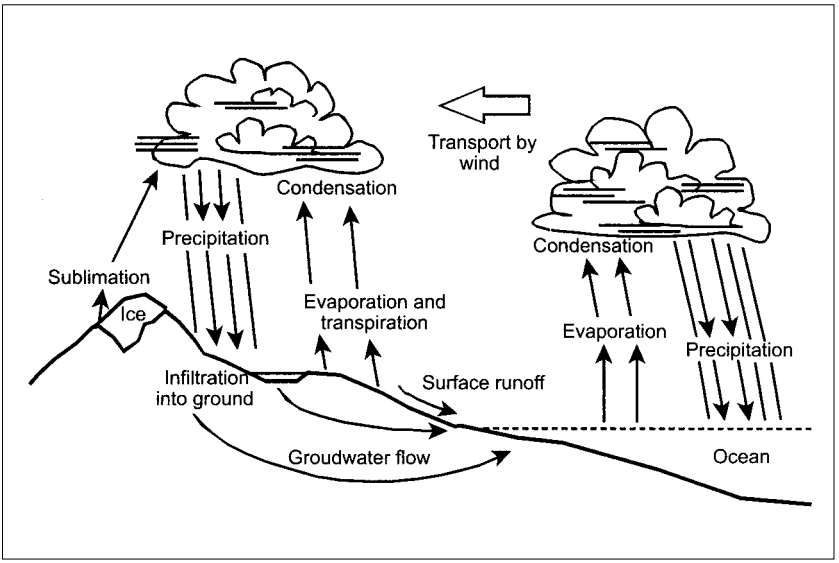

Figure 1.1 The hydrologic cycle.

The upwelling brings nutrient-rich waters important for fisheries and other marine ecosystems. Cool waters are normally within 50 m of the surface. The trade winds blow toward the west across the tropical Pacific, resulting in the surface sea elevation being 0.5 m higher in Indonesia than in Ecuador (Philander 1990). During the year of an El Niño, the warm water off the coast of South America deepens to approximately 150 m, effectively cutting off the flow of nutrients to near-surface fisheries. The trade winds relax and the rainfall follows the warm water eastward, resulting in flooding in Peru and the Southern United States and drought in Indonesia and Australia (NOAA 2000). A strong El Niño year occurred during 1997 to 1998.

Many hydrogeologists may be aware that global conditions are changing, but fail to apply this to the local drainage at hand. It is easy to become focused on only local phenomenon, such as within a given watershed. Sometimes one can get too close to a subject to be able to have the proper perspective to understand it.

There is the story of the four blind men who came in contact with an elephant. Each described what they thought an elephant looks like. One felt the trunk and exclaimed that the elephant must be like a vacuum at a local car wash. Another felt the tail and said that an elephant was like a rope. Yet, another felt the leg and said an elephant must be like a tree. Finally, one felt the ears, so big and broad, and thought the elephant must look like an umbrella. In their own way each was right, but presented only a part of the picture. Understanding the big picture can be helpful in explaining local phenomena.

1.2 Water-Budget Analysis

Most groundwater studies that a typical consulting firm may be involved with take place within a given watershed area (Figure 1.2). The hydrologic cycle is conceptually helpful, but a more quantitative approach is to perform a **water-budget analysis**, which will account for all of the inputs and outputs to the system. It is a conservation of mass approach. This can be expressed simply as:

$$\text{INPUT} - \text{OUTPUT} = \pm\Delta\text{STORAGE} \tag{1.1}$$

The term ΔSTORAGE (change in storage) refers to any difference between inflow and outflow, resulting in a net increase or decrease in the system. An analogy with financial accounting can be used to illustrate. In a bank checking account, there are inputs (deposits) and outputs (writing checks or debits). Each month, if there are more inputs placed into the account than outputs, there is a net increase in savings. If more checks are written than there is money, one runs the risk of getting arrested. In a water-budget scenario, if more water is leaving the system than is entering, mining or dewatering of groundwater will take place. Dewatering may possibly cause permanent changes to an aquifer, such as a decrease in porosity, or compaction resulting in surface subsidence (USGS 1999). Areas where this has been significant include the San Fernando Valley, California; Phoenix, Arizona; and Houston, Texas. Several of the major components of inflow and outflow are listed in Table 1.1

Figure 1.2 Aerial view of a dendritic patterned watershed.

TABLE 1.1 Major Inflow and Outflow Components

Inflow	Outflow
Precipitation	Evapotranspiration
Surface water	Surface water
Groundwater flux	Groundwater flux
Imported water	Exported water
Injection wells*	Consumptive use
Infiltration from irrigation	Extraction wells

*Important for imported water.

It is often difficult to separate transpiration from plants and evaporation from a water surface, therefore, they are combined together into a term called **evapotranspiration** or **ET**. In any area with a significant amount of vegetation close to the water table, there may be diurnal effects in water levels. Plants and trees act like little pumps, which are active during daylight hours. During the day, ET is intense and nearby water levels drop and then later recover during the night. Diurnal changes from plants and diel cycling can also cause changes in water quality in streams (Chapters 6 and 7). Accounting for all the components within water-budget analyses are difficult to put closure on, although they should be attempted. Simplifying assumptions can sometimes be helpful in getting a general idea of water storage and availability. For example, it can be assumed that over a long period of time (e.g., more than one year) that changes in storage are negligible. This approach was taken by Toth (1962) to form a conceptual model for groundwater flow, by assuming the gradient of the water table was uniform over a one-year period, although the surface may fluctuate up and down. This model is also useful when performing back-of-the-envelope calculations for water availability.

Example 1.2 The Sand Creek drainage basin is located 7 mi (11.4 km) west of Butte, Montana (Figure 1.3). The basin covers approximately 30 mi^2 (7,770 ha). In 1992, the land was zoned as heavy industrial. In 1995, there were two existing factories with significant consumptive use. The author's phone rang one afternoon, and the local city manager calling from a meeting on a speaker phone wanted to know how much additional water was available for development. The question was posed as to whether anyone was willing to pay for drilling a test hole so that a pumping test could be performed. After the laughter from the group subsided, they were informed that information to provide a quantitative answer was limited but that a number would be provided as a rough guess until better information could be obtained and that an answer would be forthcoming in a few minutes. Fortunately, there were some water-level data from which a potentiometric surface could be constructed (Chapters 3 and 5). From the potentiometric surface and a topographic map, a hydraulic gradient and an aquifer width were estimated. A probable range of values was estimated for the hydraulic conductivity (Chapter 3), and a guess was given

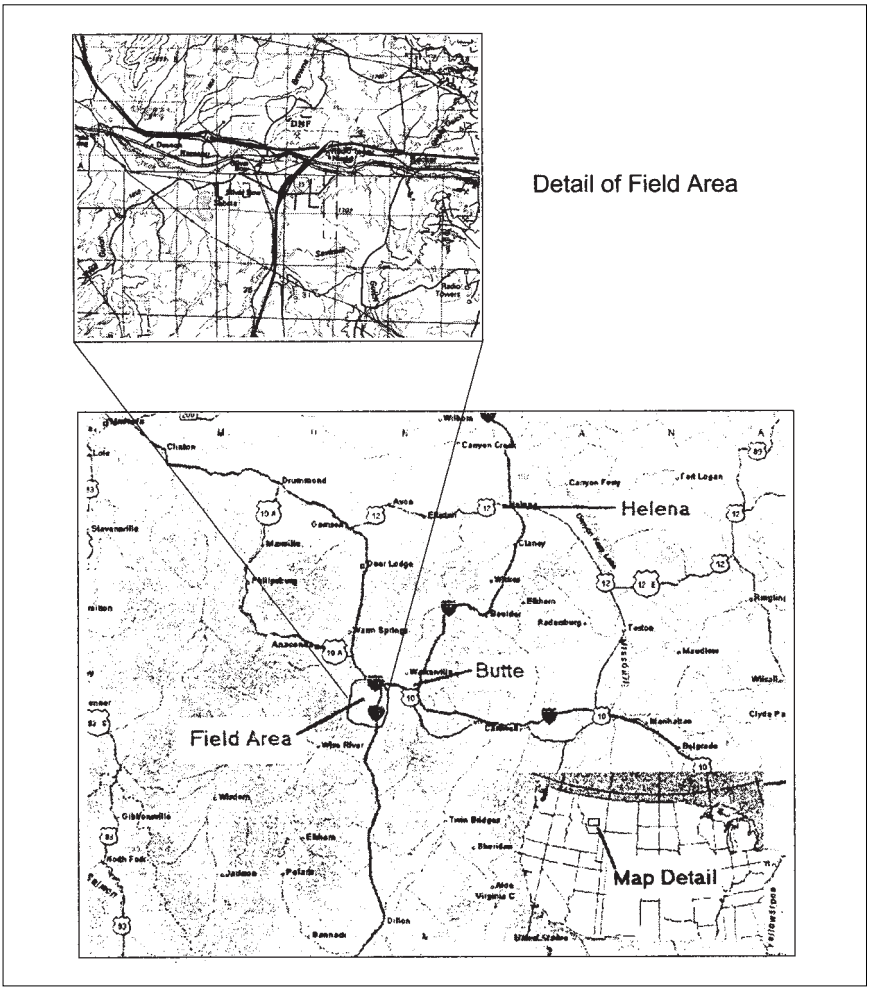

Figure 1.3 Sand Creek drainage basin southwestern Montana and field area detail. [*Adapted from Borduin (1999).*]

for aquifer depth. Darcy's law was used to estimate the volume of water moving through a cross-sectional area within the watershed per unit of time (Chapter 5). This quantity was compared with the water already being used by the existing industrial sources. It was reasoned that if the existing consumptive use was a significant portion of the Darcian flow volume (greater than 20%), it wouldn't look like much additional development could be tolerated, particularly if the estimated contribution from precipitation did not look all that great. The local city manager was called back and provided with a preliminary rough guess of volume ranges. The caveat was that the answer provided was an extremely rough estimate, but did have some scientific basis. It was also mentioned that the estimate could be greatly strengthened by drilling test wells and performing additional studies.

Performing water-budget analyses is more difficult if there is significant consumptive use or if water is being exported. Sometimes there is a change in storage from groundwater occupying saturated media that ends up in a surface-water body. For example, in the Butte, Montana, area, short-term changes in storage can generally be attributed to groundwater flowing into a large open pit known as the Berkeley Pit (Burgher 1992). Water that was occupying a porosity from less than 2% in granitic materials and greater than 25% in alluvial materials was being converted into 100% porosity in a pit lake.

Example 1.3 Many investigations have been conducted in the Butte, Montana, area as a result of mining, smelting, and associated cleanup activities. It was desirable that a water-budget analysis be conducted in the Upper Silver Bow Creek Drainage to better manage the water resources available in the area. Field stations were established at two elevations, 5,410 ft and 6,760 ft (1,650 m and 2,060 m) to evaluate whether precipitation and evaporation rates varied according to elevation. Within the 123 mi^2 (31,857 ha) area, there were no historical pan evaporation data (Burgher 1992) (Figure 1.4). The period of study was from August 1990 to August 1991.

Part of the water balance required accounting for two sources of imported water from outside the area. One source was water from the Big Hole River, imported over the Continental Divide to the Butte public water supply system. Another

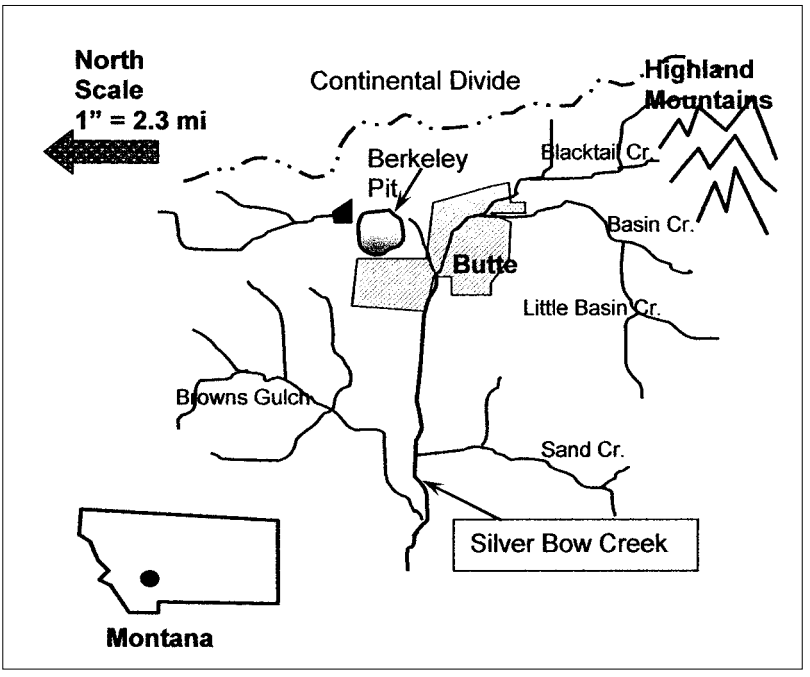

Figure 1.4 Silver Bow Creek drainage. [*Adapted from Burgher (1992).*]

source was water from Silver Lake, a mountain lake west of Anaconda, Montana, connected via a 30-mile (49-km) pipeline to mining operations northeast of Butte.

The water-budget equation used was:

$$P + Q_{\text{imp}} - E_T - Q_{so} - Q_{uo} - Q_{\text{exp}} - \Delta S \pm n = 0 \tag{1.2}$$

where P = precipitation from rain or snow
Q_{imp} = imported water from the Big Hole River and Fish Creek (in parenthesis below)
E_T = evapotranspiration
Q_{so} = surface outflow at the western edge of the valley
Q_{uo} = estimated groundwater outflow
Q_{exp} = exported water through mining activities
S = change in storage in the system groundwater to surface water (Berkeley Pit)
n = error term, net loss or gain

Precipitation was higher at the upper site (13.35 in, 339 mm) compared to the lower site (10.5 in, 267 mm), while evaporation values were similar (23.79 in, 604 mm and 23.46 in, 596 mm). All values in Equation 1.2 were calculated in units of millions of gallons per day, where the error term is used to balance the equation. The results are shown below:

$$112.73 + (9.18 + 5.20) - 113.34 - 12.25 - 0.15 - 1.40 - 5.32 + 5.35 = 0$$

One question that could be asked is, "Is more water within the region being used than is coming in?" Some areas have such an abundance of water that much development can still take place with little effect, while other areas are already consuming more water than their system can stand. An inventory of water use and demand needs to be taken into account if proper groundwater management is to take place.

Example 1.4 The Edwards aquifer of central Texas is an extensive karstified system (Chapters 2 and 13) in Cretaceous carbonate rocks (Sharp and Banner 1997). Historical water-balance analysis shows that this aquifer receives approximately 80% of its recharge via losing streams (Chapter 6) that flow over the unconfined portions of the aquifer (Chapter 3). The amount of recharge has varied significantly over time and seems to be connected to amount of stream flow (Figure 1.5). The average recharge between 1938 and 1992 was 682,800 acre · ft/year (26.6 m^3/s), reaching a maximum of 2,486,000 acre · ft/year (97 m^3/s) in 1992 and a minimum of 43,700 acre · ft/year (1.7 m^3/s) during 1956 (Sharp and Banner 1997). Other sources of recharge include leakage from water mains and sewage lines in urban areas and cross-formational flow where the aquifer thins, especially to the north (Figure 1.5).

Figure 1.5 also reflects discharge by springs and wells (the lower dashed and solid line respectively). Spring discharge follows a subdued pattern of recharge, while pumping discharge indicates an increasing trend over time. Peaks in the trend in pumping rate are inversely proportional to minima in recharge

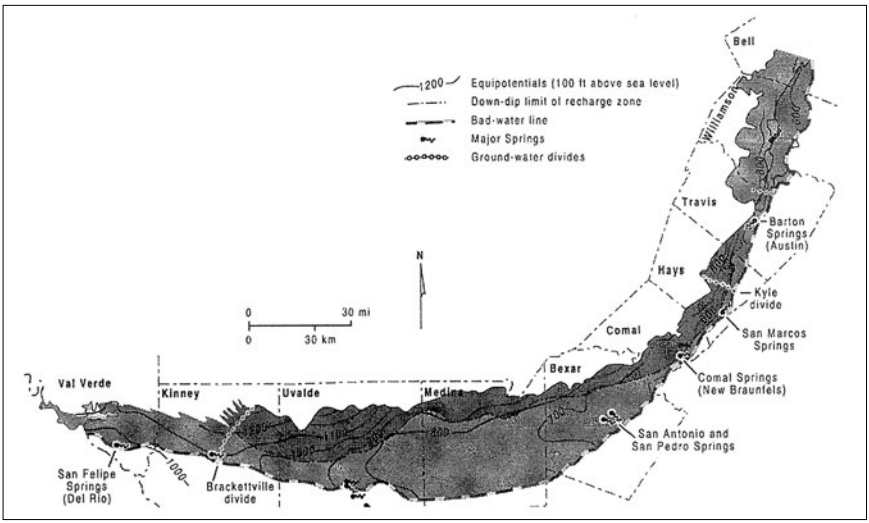

Figure 1.5 Edwards aquifer showing hydraulic boundaries, major springs, and equipotential lines. [*From Sharp and Banner (1997). Reprinted with permission from GSA Today, 1997.*]

(Sharp and Banner 1997). Individual well yields are incredible. A single well drilled in San Antonio is reported to have a natural flow rate of 16,800 gpm (1.06 m^3/s) (Livingston 1942) and another well drilled in 1991 is likely the highest yielding flowing well in the world at 25,000 gpm (1.58 m^3/s) (Swanson 1991).

Figure 1.5 also indicates that other than a few years during the mid-1950s there has always been enough water to meet demands. With the current growth rates in the corridor between San Antonio and Austin Texas, there is a concern about water demands being able to keep up. For example, in 1996 the underdeveloped land north of Austin was being subdivided at a rate of 1 acre every 3 h (Sharp and Banner 1997)!

Complicating matters are the additional roles the Edwards Aquifer plays in supplying water for recreation areas, fresh water critical for nurseries in estuaries for shrimp, redfish, and other marine animals, and spring water for threatened and endangered species that dwell in them (Sharp and Banner 1997). The Edwards Aquifer is a good example of how water-balance studies can assist in addressing the significant decisions that are continually badgered by special and political interests.

The previous discussion and examples point out that water-balance studies are complicated and difficult to understand (see next section). For this reason, many water-balance studies are being evaluated numerically (Anderson and Woessner 1992). A numerical groundwater-flow model organizes all available field information into a single system. If the model is calibrated and matched with historical field data (Bredehoeft and Konikow 1993), one can evaluate a variety of "what if" scenarios for management purposes. For example, what would happen

if recharge rates decreased to a particular level when streamflow also decreased? The areal effects of different management scenarios can be observed in the output (Erickson 1995). A simplified approach can be taken by evaluating flow nets (Chapter 5).

1.3 Water-Budget Myth

In articles by John Bredehoeft (1982, 2002) a presentation is made about *the water-budget myth*. You might be thinking what does this mean and what is going on? The water-budget myth holds that natural aquifer recharge is the measure of the potential yield of the aquifer to wells. It is a myth because it disregards the fact that, over time, the natural recharge to the aquifer determines the natural discharge from the aquifer. The natural recharge rate, however, is a fixed function of environmental conditions and is independent of pumping. (Natural recharge is not affected by pumping). Pumping therefore can only reduce the rate of natural discharge from an aquifer by an amount equal to the groundwater development. Although this was argued to be a false idea many years ago by Theis (1940), where he stated that groundwater development is based on the principle that pumping causes a loss of water somewhere in the hydrologic system. Bredehoeft (2002) and Devlin (2005) point out its persistence in the hydrogeology community.

Groundwater development requires a disruption of the balance or equilibrium between natural recharge and discharge. Groundwater development becomes sustainable only when hydrologic equilibrium is reestablished as groundwater withdrawal is eventually balanced by the capture of an equal amount of discharge from the aquifer. This may require long periods of time (tens to hundreds of years) before a new equilibrium can be reached depending on the distance of pumping from the discharge area and the aquifer properties (Kendy and Bredehoeft 2006). Many streams are partially penetrating (they are only in contact with the upper portion of an unconfined aquifer, Chapters 3, 6, and 10) and therefore the stresses of pumping may be capturing groundwater discharge from the other side of the stream, a phenomenon known as **cross-river flow** (Gamache et al. 2003).

Hydrologic principles state that if wells completely intercept the natural recharge to an aquifer, the natural discharge from an aquifer to surface water will eventually end. If groundwater pumping exceeds natural recharge, both surface water and aquifer storage will be depleted over time. The degree of acceptable groundwater development depends on the amount of stream depletion that can be tolerated (Sophocleous 1997). The capture of natural discharge raises the controversy of stream depletion where pumping impacts stream flow that is already appropriated by downstream users and infringes on prior water rights. When the

quantity of pumping is balanced by a reduction of stream flow (even though this may take a long time), a water right to withdraw groundwater from the well essentially becomes a water right to divert surface water from the stream at that same rate. In groundwater basins where surface-water allocations equal or exceed all of the groundwater discharge, groundwater development ultimately becomes a problem of stream over-appropriation and must be managed by retiring existing water rights to augment or mitigate the effects of the requirements of new water rights. (A holistic approach examining the entire watershed is recommended for groundwater management.)

In groundwater basins where surface-water right allocations are less than the requirements for minimum stream flows or other defined purposes, there may be an opportunity for groundwater development. The quantity of how much additional groundwater discharge can be captured by a pumping well is known as **sustainable yield** (Bredehoeft 2002; Sophocleous 2005).

Sustainability

Sustainable development, as defined by Bredehoeft (2006), is the quantity of water available to meet present-day needs without compromising the needs of future generations. Here, we can learn from Native Americans because they evaluate most problems looking at least seven generations into the future (Medicine Head 2004 and Brandon 2005). Current scientific thought is that sustainable yield should be evaluated using the tool of numerical groundwater modeling on a total basin scale over hundreds of years (Alley and Leake 2004 and Bredehoeft [2002, 2006]). If recharge rates are sufficiently high, some degree of stream depletion can be justified (Devlin and Sophocleous 2005). Watersheds where the concepts of recharge, discharge, and water consumption are poorly understood may result in disastrous outcomes.

Kendy (2003) describes an excellent example from the Hebei Province in the North China Plain of how management practices affect changes in the actual water being consumed in a watershed. Historical precipitation data showed a decrease over time from 54 cm/year pre-1980 to 46 cm/year from 1980 to 2000 while evapotranspiration (ET) showed an increase over time from 46 cm/year to 66 cm/year (Kendy 2003). How could this be? There was a change in farming practices from dry-land farming of a single "rain-fed" crop to an irrigated two-crop system, resulting in a disparity of 20 cm/year net loss. Irrigation waters, originating from surface-water diversions, were supplemented by pumpage to make up the deficit. Although some irrigation water may return through infiltration, the rate of ET is proportional to the type and quantity of crops being farmed. Pumpage rates have recently been reduced but the water-table declines continue because of the large acreages of

land being irrigated. The overall impact has been a steady decline in the water table (1 m/year), diminished surface stream flows, and saltwater intrusion—truly a groundwater management nightmare.

Kendy (2003) emphasizes the point that hydrogeologists need not only consider what happens to groundwater once it is pumped, but should also be concerned about what happens to that water once it reaches the surface, the water actually consumed. Therefore, trying to stabilize an unconfined aquifer through sound management practices means balancing the budget of the entire hydrologic system (a holistic approach), and not just the aquifer. This is the broader thought process that must be included by those involved in groundwater management.

Water as a commodity

As the demand for freshwater increases, so does its need for management. The supply and demand for water pushes it into the realm of a commodity (Southwest Hydrology, 2004). The available water, both surface and groundwaters, are allocated through the water-right process, where the quantity of water is defined along with a specific beneficial use. Once the water right is defined with a title of ownership that can be transferable, it emerges as a commodity (Southwest Hydrology, 2004). Rural agricultural lands are being converted into expanding urbanized areas that have a demand for water. Every product we consume requires water to produce it. As a result, many water laws in the western United States have changed significantly during the past decade and will undergo more changes in the future. The days of unmetered, low-cost irrigation water will likely be replaced with monitored water-use permits, where water can be developed in some areas and transported to water-poor areas for a significant fee.

There is a relatively recent realization by regulators (since the late 1990s) that groundwater development negatively affects surface flow because they are hydraulically connected (Chapter 6). There is a tremendous need to inventory and rethink how management entities allocate water. The general trend is toward conservation and efficiency. The old drainage ditch that conveys water over great distances (many miles or kilometers) may lose up to 75% of their flow from what flowed through the headgate (a diversion structure from a surface stream). Losses are not limited to downward seepage, but are also attributed to evaporation and poor maintenance practices (Figure 1.6). Figure 1.6 shows an unmaintained irrigation ditch where over 0.75 cfs (21.2 L/s) is leaking through the makeshift dam constructed of carpet, approximately 7 ft (2.1 m) wide. This and other breaches in this ditch result in a loss of over 50% of the original flow over a distance of approximately 330 ft (100 m). The quantity of flow lost through this ditch could supply several large-capacity irrigation wells.

Figure 1.6 Breached irrigation ditch approximately 7 ft (2.1 m) wide using carpet as a dam material.

Complaints from "old-time" surface-water users to fix and maintain their ditches will rend the air, but the reality is that water management has been lax and stronger accountability must be part of the governing process.

Changes in flow systems

As water laws and management practices change, it is likely that changes in groundwater-flow systems will also result. For example, water seepage along an older irrigation ditch may be a significant source of groundwater recharge for relatively newer domestic wells. Should the irrigation ditch be retired from service? Annual recharge from ditch losses would result in a declining water table. This commonly occurs as rural farmland is converted into subdivisions and city expansion. Pre-irrigation groundwater flow systems, which were altered because of the addition of irrigation canals and ditches, will again readjust to the new post-irrigation ditch system and the water table will again decline to pre-irrigation levels. Changes in stresses result in groundwater flow systems striving to reach a new equilibrium. Understanding the whole hydrologic system will be needed to manage a system of change. Basin-wide perspectives must be the guiding principle or potential problems as experienced in the North China Plain (Kendy 2003) may result.

1.4 Sources of Information on Hydrogeology

Information on hydrogeology can be gathered from direct and indirect sources. Direct sources would include specific reports where field data have been collected to evaluate the hydrogeology of an area (Todd 1983). Information may include water level (Chapter 5), geologic (Chapter 2), pumping test (Chapters 9 and 10), and groundwater flow direction (Chapter 5). Indirect information are data sources that may be used to project into areas with no information. For example, a few well logs placed on a geologic map and correlated with specific geologic units can be used to project target depths for drilling scenarios.

Since the first edition of this book, there has been an explosion of information accessibility through the Internet. If you need to find specific information about a given topic it is worthwhile to go to your local university. Universities buy the rights to access information databases. Sure you can try a Google search but it is likely you will get tens of thousands of hits that would require days of sorting. On the other hand, at a university you could sit at a computer terminal and click on Databases A–Z and a list of library-purchased databases will appear. A few of the most common ones are GeoRef, Engineering Village 2 (formerly Compendex), or Science Direct. During a topical search, specific references are listed with hotlinks to the full text articles if the library has purchased the database.

Knowing which database to use can be confusing as different vendors buy the rights to use a given database and then change the name for their own marketing purposes. Hence the Compendex database may appear as Engineering Village 2 or Engineering Village II or some other name. An exception to this is GeoRef, which seems to be consistent from library to library.

If you really have to have a thorough search done for very specific information and are willing to pay the required fees (by the minute) you can get a librarian or other search professional to use Dialog or STN databases that will do a simultaneous multi-database search. For example, these programs search a dozen databases simultaneously for very specific information. They are not recommended for general topics.

The following list may give some ideas on where to start. It is by no means an exhaustive list and no specific order is intended:

- Oil field logs or geophysical logs.
- Peer review journals Ground Water, Water Resources Research, Hydrogeology Journal, and a host of other journals with "Water" in their titles (use the Database A–Z search at a local university library).
- Ground Water Online found at www.ngwa.org/gwonline/

- State published or unpublished (incomplete) geologic maps.
- US Geological Survey (on the WEB at www.usgs.gov): This is a source of topographical maps and other published information plus a large section on water supply information, including real-time surface water stations and flows.
- US Evironmental Protection Agency (US EPA) (on the WEB at www.epa.gov)
- The National Oceanographic and Atmospheric Association (NOAA) has a wealth of information about precipitation data (on the WEB at www.noaa.gov).
- Topographic maps are helpful in locating wells (near building) and evaluating topography (for recharge or discharge areas) and making geologic inferences (by evaluating shapes of drainage patterns).
- Structure-contour maps that project the top or bottom of a formation and their respective elevations.
- State surveys and agencies are a great source for published information within a given State; additionally they have well-log and water-quality databases and other production information. These are often organized by county or Section ,Township, and Range.
- Libraries have a wealth of current and older published information. Sometimes the older publications are very insightful. Additionally, many libraries have search engines for geologic and engineering references, such as GeoRef and Compendex (described above).
- Long-time landowners can give valuable historical perspectives and current observations.
- Master's and PhD theses have a variety of qualities, so glean what you can with a grain of salt. Some are very well done while others should not have been published.
- Summary reports prepared by state agencies on geology, groundwater, surface water, or water use and demand.
- Consulting firms and other experienced hydrogeologists.
- US Geological Survey Water Supply Papers and Open File Reports.
- County or city planning governments may have information in Geographical Information System (GIS) formats and have listing of wells, well ownership, or other useful information.
- Some authors or editors attempt to evaluate all references associated with groundwater and then group the references according to topics such as (van der Leeden, 1991). This was a practice done in the pre-1990s and may be very helpful in identifying classic works.

In most states, a well log is required to be filed each time a well is drilled. Included is the depth, lithologic description, perforation or screened interval, the static water level (SWL), and brief pumping or bailing-test information. This can be used to evaluate depth to water, lithologies, and get a general idea of well yield. Sometimes this information is not reported, as some drillers are hesitant to report unsuccessful wells. If no water is found sometimes the well logs do not get filed, when in reality "no water" reported in a well log is good information. Experienced hydrogeologists learn how to combine a variety of geologic and well-log database sources into a conceptual model, from which field decisions can be made.

1.5 Site Location for Hydrogeologic Investigations

As simple as it sounds, the first task is to know where the site is. As a hydrogeologist, you may be investigating a "spill," evaluating a property for a client who is considering buying the property, locating a production well, or participating in a construction dewatering project. It is imperative that you know where the site is, so you can assess what existing information there might be. If this is a preexisting site, there will be some information available; however, if you are helping to "site in" a well for a homeowner or a client for commercial purposes on an undeveloped property, you must know where the property is (see "well drilling" in Section 1.6). Part of knowing where a site is includes both its geography and its geology.

Many water-well drillers are successful at finding water for their clients without the help of a hydrogeologist. Either the geologic setting is simple and groundwater is generally available at a particular depth, or they have experience drilling in a particular area. If they don't feel comfortable with the drilling location, they will always ask the client where they want the hole drilled so that they can't be held liable for problems when things go wrong. The problem is that most homeowners don't have much of an idea about the geology of their site and choose a location based on convenience to their project rather than using field or geologic information. The phone call to you, the hydrogeologist generally comes after a "dry" hole or one with a disappointingly low yield has been drilled. The phone call may also come from the driller or the client. Before carefully looking into the situation, that is, answering questions about what happened and what the drilling was like, you must know where the location of the site is. Unfortunately, sometimes you are given the wrong site-location information and you end up doing an initial geologic investigation in the wrong place. A personal example will help illustrate this concept.

Example 1.5 A phone call came after drilling a 340-ft duster (dry hole). The drill site was chosen near an old, existing homestead cabin. The client (landowner) figured that since the homestead had water, and it was an ideal location for his ranching operation, it would probably make a good site. The driller asked for the location and the drilling commenced. After going 340 ft, with no water in sight, the driller decided to call and get some recommendations. The property consisted of more than 600 acres near a small town in western Montana. The section, township, and range were provided. After an initial investigation in the library, geologic and topographic maps were located. The geologic information was superimposed onto the topographic map, and a couple of cross sections were constructed. The target zone would be a coarser-grained member of a lower Cretaceous sandstone. A meeting time and place were arranged. Within minutes of driving down the road from the meeting site, it became evident that the driller was heading to a location different from what was described. Instead of slightly undulating Cretaceous sedimentary rocks, the outcrops were basalt, rhyolite, and Paleozoic carbonates that had been tilted at a high angle. The dry hole had been drilled into a basalt unit, down geologic dip (Chapter 2). It becomes difficult to recommend anything when the structure and geologic setting are uncertain.

The purpose for well drilling was for stock watering. An initial design was recommended that would not require electrical power. A local drainage area could be excavated with a backhoe and cased with 24-in galvanized culvert material. A 3-in PVC pipe could be plumbed into the "culvert well" at depth and run to a stock tank (Figure 1.7). It was a gravity-feed design and would help keep cows at the far end of his property in the summer.

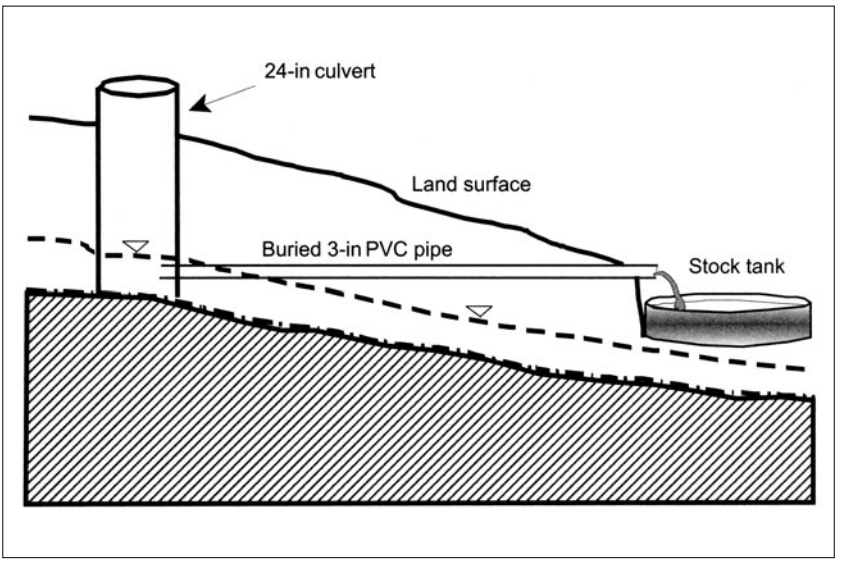

Figure 1.7 Gravity-feed stock tank design from Example 1.5 (not drawn to scale).

After this initial meeting, the rancher informed the author that they tried the backhoe method and found that the area had good aquifer materials, but no water. Once the proper location was known, we went back in the office and evaluated the geology. We determined that this drainage was situated on a large fault and that any infiltrating water collected would be lost quickly into the Paleozoic limestone formations, and would be found only by drilling well below the surface.

In Example 1.5, an understanding of the geology was essential to locating a target for water development. Even if the geologic setting is known, modifications due to structural features may need to be made. Discussion of the geology of hydrogeology is further discussed in Chapter 2.

1.6 Taking Field Notes

A field notebook is your memory of events, locations, people, and figures. Without decent field notes, it will be difficult to reconstruct what happened in the field, let alone remember the important details that are necessary for billing out time and completing reports back at the office. Notebooks should be accessible, sturdy, and weatherproof, or at least you should write with a waterproof pen. Some people prefer to use a pencil (with something hard like a 6H lead), while others prefer pens. What is the problem with using a pencil? Pencils can smear as the pages chafe back and forth in a field bag. After a few times in the field, the information becomes hard to read. A pen can usually be clearly visible for years. After all, one should never erase in a field book. If your field notebook is needed in court, erase marks will be questioned and the book later thrown out as being tampered with. Don't use whiteout or some other coverup to make your field book look prettier for the same reason. After all, it is a field book. Mistakes will be made, and when they occur, neatly draw a line through the mistake and continue on. Your notebook should not be a disorganized mess, because it will be needed to help you remember what happened later on. Some people have a "working" field book and a second field book that the day's work is translated into for neatness. It is a good idea to record or add information each evening or during slack time, or details will be missed. You take notes so you don't have to remember everything.

Inside the cover, put your name, address, and phone number, so you can be reached in the event you lose your field book. Some prefer to staple a business card inside the front cover. The back of the field book should have some blank pages, reserved to write the names, addresses, and phone numbers of contacts or distributors of equipment, supplies, or parts frequently needed. Again, business cards can be stapled directly inside these back pages, for ready access. For some people, it is also helpful to put conversion tables in the field book so that they are accessible for calculations. Your field book is your memory.

Although there are a host of topics that can be recorded in a field book, some examples of the more commonly encountered tasks are presented below.

Daily information

There is some basic information that should appear in a field book each time one ventures out. The location, purpose, and objective of the day's work should be noted. For example, soil sampling along Skunk Creek for ACME remediation study. The day's date and time of departure can be very important. It is a good idea to record the times people arrive and leave a site as a daily itinerary. This could be significant in a law suit if claims are made about who was where, when. It is a good idea to record the people in the party who are present and their phone numbers and names (including the last names). Saying that Jim or Susan was there may not be very helpful a few years down the road. The basic who?, when?, where?, why?, and how? approach to field notes is a good way to remember what should be recorded.

Comments on the weather and how it changes during the day can also be significant in field interpretation. For example, a rainstorm moving in will change the air pressure. In confined aquifers, this may help explain why the water levels increased or slowed down during a pumping test (discussed in Chapter 9). Rainstorms may be the source of why the stage in a stream changed. If the weather is very cold, this may contribute to errors committed in the field from stiff fingers, trying to get the job done quickly, or trying to work with gloves on. Conversely, hot weather can also affect the quality of field data collected as perspiration drops often land right where you need to record information. Equipment is also temperature-sensitive, particularly water-quality equipment. This may contribute to data values drifting out of calibration. Of course, this can occur as one bounces down a bumpy road!

It is a good idea to record detailed observations and descriptions during slack time while your mind is still fresh. Field sketches and diagrams are useful. Many field books have grid lines so that well logs can be drawn vertically to scale. If your drawing or sketch is not to scale, say so in the field book. You may have a field book dedicated to a particular project or get a new one each year. It is advisable to organize or record information in a systematic way. For example, some people like to number the pages sequentially so that a table of contents can be made at the front of the field book. This is helpful if there are a variety of jobs over a broad area. Some of us just prefer to mark the beginning and end of a particular day's effort by noting page 1 of 4, 2 of 4, etc, for example. Whatever system you use, strive to be consistent, complete, and neat.

Lithologic logs

Most companies or agencies have their own forms for filling out lithologic information during drilling (Figure 1.8). This is desirable, but if for some reason you forgot your forms or none are provided, you may have to record lithologic log information in your field book. If you forgot your

Well No. MC-8 1/2

Project Hillcrest School Location 3000 Continental Dr

Engineer W. WEIGHT Installed By D. CROWLEY for the Date 14 SEP 96

Method of Installation H.S.A. Bio-MDX

LOG OF BORING AND WELL

BORING

Depth In ft.	Description	H. Nu Reading
0	Asphalt Surface Gravel	
5	Silty sand dirk gray	
5	Silt, dark carbonaceous micaceous	
	GRAVEL BRN 3/4" Minus Wood chips	
10	Silt, brn clayey, silty	
	Clayey Gravel	
15	Med Sand with fine gravel 3/8" minus	
	Gravel 1/2"-3/4"	
	Sand med coarse @ fine gravel 3/8" minus	
	Water @ 19'	
20		
25	med Sand - Silty matrix	

OBSERVATION WELL INFORMATION

Type of WELL dewatering

Ground Elev. Top of Riser Elev.

Vented Cap

S.W.L.

L.D. of Riser Pipe

Type of Pipe

Type of Backfill Around Riser

Top of Seal Elev.

Type of Seal Material

Top of Filter Elev.

Type of Filter Material 6-9 mesh

Size of Openings 40 Slot

Diameter of Screened Tip

Bottom of Well Elev.

Bottom of Boring Elev.

Diameter of Boring 10 3/4"

L_1 = 20.3'
L_2 = 1.1
L_3 = 16.4
L_4 = 4.10
L_5 = 17.8
L_6 = 10
L_7 = 0.7
L_8 = 10
L_9 = 40

Remarks

L-1 Flush MT/Well Protector
L-2 Surface to Bentonite Seal
L-3 Bentonite Seal
L-4 Filter Pack
L-5 Surface to Top of Screen
L-6 Screen
L-7 Sump
L-8 Pot Hole
L-9 Total Depth

Prepared by W. Weight

Figure 1.8 Form for well logs and well completion diagrams.

field book too, then, shame on you, you forgot your memory. It may be, for example, that you are making field descriptions of surface geology during a site characterization (Nielsen and others, 2006) or recording lithologic information from monitoring wells. (How to log a drillhole is discussed in Chapter 8 and a more detailed discussion of geologic information is presented in Chapter 2.)

Lithologic logs are generally recorded during the drilling process. The type of drilling affects the time that you have to record information (Chapter 8). If you are logging and bagging core, collecting chips, or doing a variety of other tasks, then it can get tricky getting everything done while still recording a meaningful lithologic log.

Example 1.6 I can recall my first attempt at recording lithologic logs for drill holes in overburden on a coal property near Hanna, Wyoming. It was a forward rotary drilling rig, and drillers could drill with air for the first 200 ft or so in relatively soft layered sediments. The mast was almost free-falling at a rate of approximately 20 ft/min. The drillers laughed as I frantically tried to record information. It was bewildering as the various lithologies changed in texture and color before my eyes.

Besides learning to work with your driller, it is helpful to have a shorthand set of descriptions for lithologies and textures (this is discussed further in Chapter 8). Many companies may have their own system, and these can later be incorporated into a software package for visualization. Rock or soil descriptions should be indicated by the primary lithology first, followed by a series of descriptors. Information recorded could include the following:

- Lithology name.
- Grain size and degree of sorting (is this the actual crushed bedrock or soil particles?).
- Color (can be affected by drilling fluids, such as mud).
- Mineralogy (HCl fizz test, or mineral grains observed in the cuttings).
- Probable formation name, etc. For example, an entry might say, sandstone: very-fine to fine-grained, tan, with dark cherty rock fragments, the basal Member of the Eagle sandstone.

You may notice things, such as whether there were coarsening-upward or coarsening-downward sequences in sedimentary deposits, unconformities, or abrupt coloration changes, as would occur if the rocks changed from a terrestrial aerobic origin (red, yellow, tan) to those of an anaerobic origin (grey, dark, or greenish) (Figure 1.9). The relative ability for rocks to react with dilute HCl can be useful in helping distinguish one formation from another or which member you may be in. Record dates and

Figure 1.9 Cross-sectional view of changing lithologies, showing a small-scale (several meters wide) thrust fault.

how samples were taken. For example, were the cuttings washed? (The fines would wash through a sieve, while the chips or coarse fraction would remain behind.) Were they grab samples, split-spoon, or core samples?

Another useful thing to note along with the lithologic log is the drilling rate. There may be a variety of similar rock types, but some may be well cemented and drill slower or faster than others. This may affect the ability for vertical groundwater communication between units, or it may be helpful for a blasting engineer, who needs to know about a very hard sandstone or igneous unit that will require extra blasting agents. Drilling rates can be roughly compared to cone-penetrometer tests. Some drilling may be smooth or "chatterier." For example, a hard sandstone may cause the drill string to chatter because the bit bounces somewhat as it chews up the formation, but the drilling will proceed slowly. Contrasted to this, a coal bed will "chatter" when it is soft and is chewed up quickly. Notice how long it takes between the first "chatter" sound and the appearance of black inky water from the coal bed at the land surface. Use your senses (odors, for example) to notice changes. Additional comments about logging during drilling are made in Chapter 8.

Well drilling

While performing well drilling, you not only need to record the lithologic information, but also the well-completion information. Depending on the

complexity and depth of the well, there may be other key people involved: other geologists, tool pushers, mud loggers, or engineers. Once again, write down the names, addresses, and phone numbers of the driller and these key people, or better yet get their cards and staple them into your book. Hopefully, you have performed some background geologic work and have an idea about what formation you are drilling in and the targeted depth. What is the purpose of the well (monitoring, production, stock well, etc.)? Were there other wells drilled in the area? How deep did they drill for water or product contamination? What were the production zones? What will the conditions likely be (hard, slow drilling, heaving sands, etc.)?

Record a detailed location of the well, using coordinates if possible, township descriptions, or other identifiers, such as latitude and longitude from a global positioning system (GPS). It should be noted that GPS systems vary dramatically in accuracy. Hand held units will get you in the ball park, but to accurately locate (within inches or centimeters) a well, it is necessary to have a base station and a rover unit with expensive software to correct for the global changes that occur during the day (Figure 1.10) (Chapter 5). Will the elevations be surveyed or estimated from a topographic map?

Write down the make and model of the rig and any drilling fluids that were used and when. Did you start with air or begin drilling with mud? It is a good idea to write down a summary of the work completed

Figure 1.10 A global positioning system used in the field. The rover unit is tied to a base station located within 6 km.

by your driller before you arrive. Quantities of materials billed by a driller should corroborate with your field notes to document errors. Big projects may need to be drilled continuously in shift work format until the job is done.

Example 1.7 In western Wyoming in the early 1980s, some deep (1,200 ft, 370 m) monitoring wells were being placed down structural dip of a mining property. Each well took several days, so drilling and well completion took place in 12-h shifts by the geologists and drillers on a continuous basis until the wells were completed. A new drill crew and geologist would arrive every 12 h. It was critical that communication took place between the ones leaving and the ones arriving for continuity.

It is also important for billing purposes to write down incidents of slack time (standby), equipment breakdowns, or "runs" for water. The work submitted should match the field notes taken or inquiries might be made, Each morning or during slack time, measure and record the static-water levels. This is particularly important first thing in the morning after the rig sat all night. The size and type of bit is also important for knowing the hole diameter. Any unusual or problematic situations or conditions should be recorded and discussed with your driller.

Well completion

Once the hole is drilled, the well is completed from the bottom up. Your field book needs to contain sufficient information to construct well completion diagrams back at the office or in the motel room at night. It is helpful to review the information on forms required by the local government, so that all details are covered. For example, was surface casing used? If so, what was the diameter? What about screen type or slot size? What are the diameters of the borehole and pump liner? The mechanics of well completion is discussed in Chapter 8; however, the following items should probably be included in your field book:

- Total depth drilled (TDD) and hole diameter (important for well hydraulics calculations) (Chapters 10 and 11).
- Indication of type and length of bottom cap (or was it left open hole?).
- Is there a sump or tailpipe (a blank section of casing above the bottom cap)?
- Interval of screened or perforated section, slot size and type or size of perforations, outer diameter (OD) and inner diameter (ID) of screen, and material type (schedule 80 PVC)? Is the screen telescoped with a packer, threaded, or welded on?
- Number of sections of casing above the screen, length of each interval, and height of stick up. Twenty-foot (6.1-m) pipe can vary in length.

Fractions of a foot can add up when going several hundred feet into the ground.

- Was the well naturally developed or was packing material used? If packed, what volume was used, height above the screen (number of 100-lb (45.4-kg) or 50-lb (22.7-kg) bags)? Interval of packing material? This is helpful for planning future wells to be drilled.
- Was grouting material used? If so, over what interval?
- What kind of surface seal was used (concrete, neat cement, cuttings)?
- What kind of security system is there for the well cap?
- Was the well completed at multiple depths, and if so, what are the individual screened intervals and respective grouting intervals?
- Was the well developed? What was the static water level before development?
- What method was used (pumping, bailing, lifting with air, etc.) and how long? How many purge volumes or for what duration did development take place?

Pumping tests

There are many details that need to be remembered during a pumping test, let alone many pieces of equipment to gather together. In addition to your field book, for example, it is imperative that you have well logs for all wells that will be included in the pumping test, with well-completion details. Your field book will play a critical role in remembering the details. One of the first items of business is to measure the static-water levels of all wells to be used during the test. Any changes will be important for interpretation. The weather conditions may also affect the water-level responses. Is there a storm moving in? This can result in a low-pressure setting where water levels may rise. In confined systems, the author has observed changes measuring 0.5 to 1 ft (0.15 to 0.3 m) depending on the atmospheric pressure drop and confining conditions. Is there a river or stream nearby? Did the stage remain constant or raise or drop? During Montana Tech's field camps, there have been observed stage drops of 2 ft during a 24-h pumping test. How does this affect the results?

In October 1998, while attending a MODFLOW 98 conference in Boulder, Colorado, several groundwater modelers from around the world were informally interviewed and asked questions about what they thought should be included in a field book. One resounding remark stood out. "Please tell your readers that they should always make backup 'hand' measurements in their field books on changing water levels in wells, during a pumping test! Don't just rely on the fancy equipment."

Another comment was, plot the data in the field so that one knows whether the test has gone on long enough (see Chapter 9). The data would be obtained from measurements recorded in field books or downloaded from software. Along this line, there should be a notation of the pumping rate during the test. Were there changes in discharge rate that took place during the test? Remember that theoretically the pumping rate is supposed to be constant.

Troubles in the field need to be recorded. Sometimes individuals don't want to remember something goofy or embarrassing that happened in the field, but it may be the key to making a proper interpretation. Why didn't anyone get the first 5 min of the recovery phase of the pumping test? The reasons may range from being asleep and didn't notice the silence of the generator as the fuel ran out, or perhaps off taking care of a personal matter, or couldn't get the "darn data logger" to step the test properly. Perhaps a friendly Rottweiler powered through the equipment area and managed to knock out one of the connecting cables (Figure 1.11). I'm sure a documentary on the things that can go wrong during a pumping test would make interesting reading. The following bulleted items will serve as a reminder of the most important general items to record but is by no means an exhaustive list. Additional discussion can be found in Chapter 9.

Figure 1.11 Rottweiler harassing the author during a pumping test.

- Personnel on hand at the site, either assisting or present for observation.
- Static-water levels of all of the wells, prior to emplacement of any equipment.
- Sketch map showing the orientation and distances of observation wells to the pumping well, also include possible boundary effect features, such as steams, bedrock outcrops, other pumping wells, etc., that may affect the results.
- Weather conditions at the beginning, during, and end of the test.
- List of all equipment used. Type of pump, riser pipe, discharge line, flow meters, or devices used to measure flow (e.g., bucket and stop watch or flow meter) Again a sketch or photograph in the field is helpful.
- Exact time the pump was turned on and off for the recovery phase. (It is helpful to synchronize watches for this purpose.)
- Manual water-level measurements of observation wells. Include the well ID, point of reference (top of casing), method of measurement (e-tape or steel tape), and a careful systematic recording of times and water levels in a column format.
- Record of the pumping rate. How was this measured and how often during the test? (times should be written 30 minutes or less).
- Recovery phase of the test. Again, manual measurements, conditions, and times.
- Any other problems or observations that may prove helpful in the interpretation of the results.

Water-quality measurements

Any type of field measurement can have errors. Errors can be made by the equipment being out of calibration or bumped around in the field, or the operator may just get tired during the day. Maybe the weather conditions rendered the collecting of data fairly intolerable. Apparent errors may result from significant diel cycling of water-quality parameters over a 24-h period (Chapter 7). Honest observations in a field book can help someone remember the conditions under which the data were collected and help someone else reviewing the data or their interpretation. The field book can explain why the numbers look strange. For example, many parameters are temperature-sensitive. Along with a pH measurement, there should be a knowledge of what the temperature is to set the calibration knob correctly (Figure 1.12). Many specific conductance meters have a temperature corrections to 25°C internal

Figure 1.12 Surface-water quality analysis in the upper Big Hole River valley, Montana.

within the device. Failing to take into account the temperature can significantly affect the results recorded. Chain of command and other details of the inherent problems that can occur in the field will be discussed in greater detail in Chapter 7. The following items should be considered for field notes:

- What is the sample type (e.g., surface water, domestic well, monitoring well)?
- What were the weather conditions throughout the day?
- What were the date and exact time when the sample was taken? (Many samples are required to reach a lab within 24 h.)
- Who were the personnel present (was the operator alone or was there someone else helping)? Who was present at the respective sampling locations? Did the well owner come out? It may be important to be able to tell who was there.
- What were the methods of calibration and correction for drift?
- What were the units? Were the data temperature-corrected? Remember, many parameters are temperature-dependent and temperature-sensitive!
- If it is a water well sample, what volume of water was evacuated before the samples were collected? What were the purge times and respective volumes? How was the sample taken? Was it via a bailer,

a discharge hose from a pump, or a tap? Which parameters were monitored during the purging (pH, conductivity, temperature)? Where was the discharge water diverted to?

- How long did it take to reach a stable reading? Was the reading taken prematurely before stabilization took place? This can vary significantly between pieces of equipment. Was a stir rod going during the reading or was the container just swished around every once in a while?
- What were the methods of end-point detection? Was a pH meter or color reagents used.
- Were the samples filtered or acidified? How?
- Was the laboratory protocol followed? Were the chain of command papers filled out?
- Units! Units! Units!

1.7 Groundwater Use

It is instructive to evaluate the requirements of water for different purposes. How much water is needed for domestic purposes? In the author's home, we had a water softener that had a built-in digital readout flow meter. When the shower was on, one could read the rate flowing in the pipe (4 to 6 gpm). It also provides an average total use per day. In our case, in the first quarter of 2000 the daily amount was 398 gal. This was for 7 people and includes consumption in the form of showers, hand washing, toilet flushing, drinks of water, and water used for cooking and laundry. Or approximately 57 gallons per day (gpd) per person. This does not account for water used in the yard from the hose. This seems to fit in well with other estimates of water in the range of 50 to 100 gpd (189 to 379 L) per person per day (Fetter 1994 and Driscoll 1986).

In developing countries the daily use requirements for water is approximately 10 gal per day (40 L/day), when the source for water is close at hand (US Corps 2000). The quantity for daily use drops off considerably as the water source becomes more distant. The volume of water for daily use drops to 15 L/day when sources exceed 200 m and drop further to 7 L/day when water supplies exceed distances of 1 km (US Corps 2000).

In Montana, domestic (exempt) well users can have a well drilled on their private property that yields up to 35 gpm (132 L/min) and does not exceed a volume of 10 acre · ft/year (12,300 m^3/year) without a special permit. Yields and volumes in other states will vary, but specific values are established through the legislative process. Wells used for irrigation or public water supply exceeding 100 gpm (378 L/min) or a volume

greater than 10 acre · ft (12,300 m^3/year) require a water-use permit. As part of the technical evaluation the well location (point of diversion), purpose, impacts to other existing users, demonstration of the water being there, and the well design (Chapter 8) are described by a hydrogeologist for evaluation by a state agency. As part of the process a technical review is made of the application and a notice is placed in the local newspaper to advise other users of this taking place. Any complaints must be filed and addressed. Once the water-use permit is granted it is viewed as a water right for groundwater. In the western United States, all water rights are determined 'a-priori doctrine' using the following philosophy "first in time, first in right." A maximum rate and a maximum volume are applied for, conditioned on the water use. The rate is given in gallons per minute (gpm) and the volume is given in acre-feet over a specified time.

Irrigation waters and water rights in the eastern United States are distributed following a Riparian doctrine. In this case, all water users in a given drainage basin share the allocatable water. If flow rates decrease by 10%, the users proportionally decrease water use by 10%. This works in areas where the precipitation is higher and streams are sustained by a fairly continuous source of base flow from groundwater discharge.

The use of groundwater for public water supply along with coordinating where to locate potential contaminating sources (sanitary landfills and industrial parks) falls under the area of groundwater resource management.

1.8 Groundwater Planning

As the demand for groundwater supply increases, there will be a need for improved management practices. This is being addressed in part by evaluating groundwater resources from the bigger picture. Basins and watersheds are being delineated and the information stored as layers within databases in a geographic information system (GIS) format. Each information layer may contain point information, such as wells and points of diversion, or linear features such as roads, fence lines, or property boundaries. Polygon shapes that delineate geology or other features can also be stored. Tables of information that may include depth to water, production rates, or lithologic information can be stored and retrieved. Sources of information for these databases may come from drillers, landowners, or state agencies as groundwater characterization studies or aquifer vulnerability studies are performed.

A significant source of information within each state is being generated from source-water protection (SWP) area studies defined in the 1996 Federal Safe Drinking Water Act Amendments. By the year 2000,

most states had to have a source-water protection plan for all public water-supply wells. This was designed to be a practical and cost-effective approach to protecting public water supplies from contamination. Each source-water plan provides a wealth of information to each state's database and will allow a more comprehensive management plan.

Source-water protection studies

Recharge areas to aquifers or areas that contribute water to surface waters used for public drinking water are delineated on a map. Geologic and hydrologic conditions are evaluated in the delineation study to provide physical meaning to the SWP areas. Assessments are made for contaminant sources within the area. Included may be businesses, surface or subsurface activities, or land uses within SWP areas where chemicals or other regulated contaminants are generated, used, transported, or stored that may impact the public water supply.

Each state develops its own delineation and assessment process, so that information is reported consistently and a minimum of technical requirements have been met. As a hydrogeologist, you may be hired to perform the technical assessment of the geologic and hydrologic information within an SWP area report. An example of the type of information needed is presented in the Montana Department of Environmental Quality Circulars PWS 5 and PWS 6 (Montana DEQ 1999). The following discussion is included for comparison with other State programs and to see what hydrogeologic topics are involved.

PWS 5 is a circular that helps an evaluator determine whether a public water supply has the potential to be directly influenced by surface water. In the circular, surface water is defined as any water that is open to the atmosphere and subject to surface runoff. Included as surface water are perennial streams, ponds, lakes, ditches, some wetlands, intermittent streams, and natural or artificial impoundments that receive water from runoff. Influence to groundwater supply can occur through infiltration of water through the stream bed or the bottom of an impoundment (Chapter 6).

A scoring system of points is used during the preliminary assessment to determine whether the water supply can be classified as groundwater or whether there may be some influence from surface water. For preexisting wells, surface water impacts are scored points by historical pathogenic or microbial organisms that have been detected in a well. Additionally, turbidity, distances from a surface-water source, depths of perforations below surface, and depth to the static water level also contribute to points accumulated. In this case, like the game of golf, the fewer the points, the less likely a surface-water source impacts a given water-supply well.

If the number of points exceeds a limit, then further analysis is required. Springs or infiltration galleries immediately fall under the requirement of performing additional water-quality monitoring. A well may also be required to undergo intensive monitoring for 2 months following the completion of construction to determine its suitability as a public water-supply source. This would include weekly sampling for bacterial content and field parameters of temperature, turbidity, specific conductivity, and pH. The field parameters are also performed on the nearby surface-water source. A hydrograph of water-quality parameters versus time is plotted to compare similarities between surface water and groundwater. It is reasoned that groundwater parameters will not change much, while there may be significant variations in the chemistry of the surface water. Surface-water sources may be used for public water supply if the source water passes the biological and microbial tests.

If a microbial particulate analysis is required for a well, the client is required to conduct two to four analyses over a 12- to 18-month period, according to method EPA 910/9-92-029. The possibility of connection with surface water is indicated by the presence of "insects, algae, or other large diameter pathogens." A risk factor is also specified by the following bio-indicators: giardia, coccidia, diatoms, algae, insect larvae, rotifera, and plant debris. The sampling method is performed using the following steps:

- Connect the sampling device as close to the source as possible.
- Assemble the sampling apparatus and other equipment *without* a filter in the housing to check whether the correct direction of flow is occurring.
- Flush the equipment using water from the source to be filtered, for a minimum of 3 min. Check all connections for leaks. An in-line flow restrictor is desirable to reduce flow to 1 gpm (3.8 L/min).
- Filtering should occur at a flow rate of 1 gpm (3.8 L/min). During the flushing stage, the flow can be checked using a calibrated bucket and stop watch.
- Shut off flow to the sampler. Put on gloves or wash hands and install the filter in the housing. Make sure a rubber washer or o-ring is in place between the filter housing and the base.
- Turn on the water slowly with the unit in the upright position. Invert the unit to make sure all air within the housing has been expelled. When the housing is full of water, return the unit to the upright position and turn on flow to the desired rate.
- Filtering should be conducted at a pressure of 10 psi. Adjustment of the pressure regulator may be necessary.

- Allow the sampler to run until 1,000 to 1,500 gal (3.78 to 5.67 m^3) have been filtered. Mark the time when water was turned on and off.
- Disconnect the filter housing and pour the water from the housing into a ziplock plastic bag. Carefully remove the housing filter and place it in the bag with the water. Seal the bag, trying to evacuate all the air and place it in a second bag and make sure neither bag leaks.
- Pack this into a cooler, making sure the filter does not freeze, as frozen filter fibers cannot be analyzed. Send the filter and data sheet to an acceptable laboratory within 48 h.

If a public water supply source meets the criteria as an appropriate source, a SWP area must be delineated, as defined in the 1996 Federal Safe Drinking Water Act Amendments. In this process, recharge sources that contribute water to aquifers or surface water used for drinking water are delineated on a base map. Included is a narrative that describes the land uses within the delineated area along with a description of the characteristics of the community and nature of the water supply. Methods and sources of information used to delineate the SWP and potential contaminant sources should also be described. An example of the type of information is presented from PWS 6 (1999).

- **Introduction**—describes the purpose and benefit of the SWP plan.
- **Background**—includes a discussion of the community, the geographic setting, description of the water source, the number of residents to be served, well completion details, pumping cycles, the water quality, and natural conditions that may influence water quality at the public water system.
- **Delineation of water sources**—presents the hydrogeologic conditions (aquifer properties and boundaries), source-water sensitivity to contamination (high, moderate, or low), conceptual model based upon the hydrogeologic conditions, method of delineation, and model input parameters (Table 1.2).
- **Inventory of potential contaminant sources**—requires an inventory sheet for the control zone for each well. All land uses need to be listed. These may be classified as residential or commercial (sewered, unsewered, mixed), industrial, railroad or highway right-of-way, and agricultural (dry-land, irrigated, pasture) or forest. A list of contamination sources are listed in Table 1.3.

Once the SWP area has been defined, the affected property owners are advised. If property owners do not like the outcome of the investigation, they may sue under a Takings proviso. Takings issues are not something just for attorneys, but something that should also be familiar to a

TABLE 1.2 Model Input Parameters for a Source-Water Protection Area

Input parameter	Value(s) used	Units	How derived	Remarks
Elevation at well				
Static water level				
Transmissivity				
Thickness				
Hydraulic conductivity				
Hydraulic gradient				
Flow direction				
Effective porosity				
Pumping rate				
100-day total				
1-Year total				
3-Year total				

TABLE 1.3 Common Sources of Groundwater Contamination (U.S. EPA 1990)

Agricultural	Commercial
Animal burial areas	Airports
Animal feedlots	Auto repair shops
Chemical applications (pesticides, fungicides, fertilizers, etc.)	Beauty parlors
	Boat yards
Chemical storage facilities	Car washes
Irrigation systems	Cemeteries
Manure spreading and pits	Construction areas
Industrial	Dry cleaning establishments
Asphalt plants	Educational institutions (labs, storage)
Chemical manufacturing, warehouses, and distribution	Gasoline stations
	Golf courses (chemical applications)
Electrical and electronic products and manufacturing	Jewelry and metal plating
	Laundromats
Electroplates and metal fabrication	Medical institutions
Foundries	Mortuaries
Machine and metalworking shops	Paint shops
Manufacturing and distribution of cleaning supplies	Photography establishments, printers
	Railroad tracks and railyards
Mining and mine drainage	Research laboratories
Paper mills	Road de-icing activities (road salt)
Petroleum products and distribution	Scrap and junkyards
Pipelines (oil, gas, other)	Storage tanks (above and below ground)
Septic lagoons and sludge	**Residential**
Storage tanks	Fuel storage systems
Timber facilities	Furniture, wood strippers, refinishers
Toxic and hazardous spills	Household hazardous products
Transformers and power systems	Lawns, chemical applications
Wells (operating and abandoned)	Septic systems, cesspools
Wood preserving facilities	Water softeners
Naturally Occurring	Sewer lines
Groundwater surface-water interaction	Swimming pools (chlorine)
Iron and magnesium	**Waste Management**
Natural leaching (uranium, radon gas)	Fire training facilities
Saltwater intrusion	Hazardous waste management units
Brackish water circulation	Municipal waste incinerators
	Landfills and transfer stations
	Wastewater and sewer lines
	Recycling reduction facilities

hydrogeologist. Your greatest security in a courtroom situation is to be able to demonstrate that best possible practices have been used in the evaluation. Part of these practices include field studies and field data from which interpretations are made. As a field hydrogeologist, keep in mind the big picture and realize that your work may be revisited in court.

1.9 Summary

Field hydrogeology is an interesting subject. Each time you go into the field, each time you drill a new well or go into a new area, the geology and hydrogeologic conditions change. This is the fun and challenge of it. Keep in mind the big picture of the hydrologic cycle while also paying attention to the detailed items, such as diel water-quality changes in surface streams or storm fronts coming in during a pumping test, and write these observations in your field book. By synthesizing the data, a conceptual model of a given area will emerge. The conceptual model will take shape as additional field data are collected.

Prior to heading for the field, check your sources of hydrogeologic information and make sure you have your field book or you won't be able to remember the details of your daily experiences. Work hard, keep your wits about you, and be safe, and soon your personal experience database will transform you into a valuable team member.

References

Anderson, M.P. , and Woessner, W.W., 1992. *Applied Groundwater Modeling—Simulation of Flow and Transport*. Academic Press, San Diego, CA, 381 pp.

Alley, W.M., and Leake, S.A., 2004. The Journey from Safe Yield to Sustainability. *Ground Water*, Vol. 42, No. 1, pp. 12–16.

Borduin, M.W., 1999. *Geology and Hydrogeology of the Sand Creek Drainage Basin, Southwest of Butte, Montana*. Master's Thesis, Montana Tech of the University of Montana, Butte, MT, 103 pp.

Brandon, Brenda, Personal Communication, November 2005 Spokane Washington Indian reservation.

Bredehoeft, J., and Konikow, L., 1993. Ground-Water Models: Validate or Invalidate. *Ground Water*, Vol. 31, No. 2, pp. 178–179.

Bredehoeft, J.D., Papadopulos, S.S., and Cooper, H.H., 1982. Groundwater: The Water Budget Myth. In *Scientific Basis of Water-Resource Management*, Studies In Geophysics, pp. 51–57. National Academy Press, Washington, D.C.

Bredehoeft, J.D., 2002. The Water Budget Myth Revisited: Why Hydrogeologists Model. *Ground Water,* Vol. 40, No. 4, pp. 340–345.

Bredehoeft, J.D., 2006. On Modeling Philosophies. *Ground Water,* Vol. 44, No. 4, pp. 496–499.

Burgher, K., 1992. *Water Budget Analysis of the Upper Silver Bow Creek Drainage, Butte, Montana*, Master's Thesis, Montana Tech of the University of Montana, Butte, MT, 133 pp.

Devlin, J.F., and Sophocleous, M., 2005. The Persistence of the Water-Budget Myth and Its Relationship to Sustainability. *Hydrogeology Journal*, Vol. 13, No. 4, pp. 549–554.

Driscoll, F.G., 1986. *Groundwater and Wells*. Johnson Screens, St Paul, Minnesota, 1108 pp.

Erickson, E.J., 1995. *Water-Resource Evaluation and Groundwater-Flow Model from Sypes Canyon, Gallatin County, Montana.* Master's Thesis, Montana Tech of the University of Montana, Butte, MT, 69 pp.

Fetter, C.W., 1994. *Applied Hydrogeology, 3rd Edition*. Macmillan College Publishing Company, New York, 691 pp.

Gamache, M., Screiber, R.P., and Weight, W.D. 2003. Estimating Induced Infiltration and Cross-River Flow from Numerical Modeling. *Proceedings in MODFLOW and MORE 2003 Understanding through Modeling,* Vol. 1, International Ground Water Modeling Center, Colorado School of Mines, Golden Colorado, pp.159–163.

Hayes, S.P., Mangum, L.J., Picaut, J., Sumi, A. and Takeuchi, K., 1991. TOGA-TAO: A Moored Array for Real-Time Measurements in the Tropical Pacific Ocean. *Bulletin of the American Meteorological Society*, Vol. 72, pp. 339–347.

Hiscock, K.M., Rivett, M.O., and Davison, R.M. (eds), 2002. *Sustainable Groundwater Development*. GSL Special Publications 193. 344 pp. www.geolsoc.org.uk

Kendy, E., 2003. The False Promise of Sustainable Pumping Rates. *Ground Water*, Vol. 41. No.1, pp. 2–4.

Kendy, E., and Bredehoeft, J.D., 2006. Transient Effects of Groundwater Pumping and Surface-Water-Irrigation Returns on Streamflow. *Water Resources Research*, Vol. 42, No. 8.

van der Leeden, F., 1991. *Geraghty & Miller's Groundwater Bibliography, 5th Edition*. Water Information Center, Plainview, NY.

Livingston, P., 1942. A Few Interesting Facts Regarding Natural Flow from Artesian Well 4, Owned by the San Antonio Public Service Company, San Antonio, Texas, *U.S, Geological Survey Open-File Report*, 7 pp.

Medicine Head, Willis. *Crow Tribal Elder Personal Communication, January, 2004*, Crow Agency, Montana.

Montana DEQ, 1999. *Groundwater Under the Direct Influence of Surface Water*. Montana Department of Environmental Quality Circular PWS 5, 1999 Edition, 30 pp.

Montana DEQ, 1999. *Source Water Protection Delineation,* Montana Department of Environmental Quality Circular PWS 6, 1999 Edition, 21 pp.

Nielsen D.M., Nielsen G., and Preslo, L.M. 2006. *Practical Handbook of Environmental Site Characterization and Ground Water Monitoring, 2nd Edition*, David M, Nielsen ed. RC Press, Taylor Francis Group, Boca Raton, FL, pp. 35–205.

NOAA, 2000. The *El Nino Story.* http://www.pmel.noaa.gov, 4 pp.

Philander, S.G.H., 1990. *El Nino, La Nina and the Southern Oscillation*. Academic Press, San Diego, CA, 289 pp.

Sharp, J.M., Jr., and Banner, J.L., 1997. The Edwards Aquifer: A Resource in Conflict. *GSA Today*, Vol. 7, No. 8, Geological Society of America, pp. 2–9.

Sophocleous, M., 1997. Managing Water Resources Systems: Why "Safe Yield" Is Not Sustainable. *Ground Water*, Vol. 35, No. 4, 541 pp.

Sophocleous, M., 2005. Groundwater Recharge and Sustainability in the High Plains Aquifer in Kansas, USA. *Hydrogeology Journal*, Vol. 13, No. 2, pp. 351–365.

Southwest Hydrology, 2004. Water as a Commodity. *Seven Articles*, Vol. 3, No. 2, pp. 12–31.

Swanson, G.L., 1991. Super well is Deep in the Heart of Texas. *Water Well Journal*, Vol. 45, No. 7, pp. 56–58.

Tarbuck, E.J., and Lutgens F.K., 1993. *The Earth, An Introduction to Physical Geology*. Macmillan Publishing Company, New York, NY, 654 pp.

Theis, C.V., 1940. The Source of Water Derived from Wells: Essential Factors Controlling the Response of an Aquifer to Development. *Civil Engineer*, Vol. 10, pp. 277–280.

Todd, D.K., 1983. *Groundwater Resources of the United States*. Premier Press, Berkeley, CA, 749 pp.

Toth, J.A., 1962. A Theory of Ground-Water Motion in Small Drainage Basins in Central Alberta, Canada. *Journal of Geophysical Research*, Vol. 67, pp. 4375–4381.

US Army Corps of Engineers, 2000. *Evaluation of Water Resources of Guatemala*. Mobile Office. http://www.sam.usace.army.mil/en/wra/Guatemala/Guatemala%20WRA%20English.pdf

U.S. EPA, 1990. *Guide to Groundwater Supply Contingency Planning for Local and State Governments*. EPA-440/6-90-003. U.S. EPA Office of Groundwater Protection, Washington, DC, 83 pp.

USGS 1999. *Land Subsidence in the United States*. Galloway, D., Jones, D.R., and Ingebritsen, S.E., (eds.), U.S. Geological Survey, Circular 1182, 177 pp.

Chapter

2

The Geology of Hydrogeology

Before going into the field or performing fieldwork, the hydrogeologist needs to have a general understanding and a knowledge of subsurface information. Engineers who work with geologic information may have forgotten geologic terms or can't remember what they mean. This chapter is a reference on geologic topics and how they are specifically applied to hydrogeology.

Why is it important to understand the geologic setting? Perhaps the following questions will help. Is the area structurally complex? Are the rocks metamorphic, igneous, or sedimentary? What geologic mapping has been published or conducted in the area? Is there faulting or structural lineaments in the area? Are the formations flat lying or tilted? What surface-water sources in the area pass over formational outcrops? What are the topographic conditions like? Is the area flat lying, rolling hills, or mountainous? What is the climate like? Is it arid or humid? (This will make a big difference on recharge to the system.) What is the location and accessibility to the property? A few hours spent gathering this information will help in developing a conceptual model and in preventing mistakes one would make during field interpretations. Not understanding the general geology or field conditions before going into the field can be disastrous.

If possible, the hydrogeologist should put together a geologic model or conceptual geologic model. The geologic model forms the basis for a conceptual groundwater-flow model, and includes which units may dominate flow and which units or features may inhibit groundwater flow. The geologic stratigraphic units are broken into hydrostratigraphic units, or in other words, aquifers and confining units (discussed in Chapter 3). Metamorphic and igneous rocks may have zones within them that are productive or have significant localized fracture zones. Locations of water production are also areas of concern for potential groundwater contamination. What is the vulnerability of the water supply to contamination? Conceptual geologic models aid in predicting the direction of groundwater flow, its occurrence, and its interaction with surface water.

Copyright © 2008, 2001 by The McGraw-Hill Companies, Inc. Click here for terms of use.

2.1 Geologic Properties of Igneous Rocks

Igneous rocks are an important source of water in some regions. For the most part, **extrusive** igneous rocks (those that have erupted and formed on the land surface) have a greater capacity for water transmission and storage than do **intrusive** igneous rocks (those that formed and cooled beneath the earth's surface). Extrusive and intrusive igneous rocks can generally be distinguished by their texture and mineral composition. Extrusive igneous rocks will generally be finer grained and have fewer distinguishable minerals than intrusive igneous rocks. Both will vary in appearance according to mineral content, with quartz- and feldspar-rich rocks being lighter in color than rocks with a more **mafic** mineral content. Mafic minerals are richer in iron and magnesium. For example, rhyolites and granites will tend to be light in overall appearance and have visible quartz and potassium feldspar, although rhyolite will be fine-grained from rapid cooling, and the granite will be coarse grained. A classification scheme for the various igneous rocks is summarized in Figure 2.1 (See additional discussion of the minerals in igneous rocks in section 2.4 under weathering). Because extrusive igneous rocks generally have more important water-bearing zones, these will be discussed first.

Extrusive rocks

Extrusive rocks are also known as volcanic rocks. They have erupted to the surface either through volcanoes or fissures. The major volcanic mountain ranges around the world form near the margins of plate boundaries. The Cascade Range in Washington and Oregon and the Andes Mountains of South America are forming where crustal plates are colliding. The mineralogically more mafic and denser oceanic crust is subducting (passing) under the lighter continental crust. At depths of 60 mi (100 km), temperatures and pressures are high enough to cause partial melting and mixing of crustal materials, forming molten rock under the surface known as **magma**. Magma is more buoyant than the surrounding solid rock and seeks a pathway to the surface where it emerges as **lava**. As magma rises, volatile gases within the fluid become less constricted and rapidly expand, resulting in an explosive eruption at the surface (Figures 2.2 and 2.3). Sometimes the volatile gases fracture the overlying rocks pneumatically into a **breccia pipe**. Fractures in the breccia pipes may later become mineralized, an important concept for mineral exploration and mining development. Gas bubbles that expand in lava are preserved as the lava freezes to form **vesicular** lavas (Figure 2.4). Gas bubbles increase the porosity but tend to be poorly connected, and therefore do not increase permeability. Some magmas literally expel fluids so quickly that they turn fluids into a foamy froth that cools.

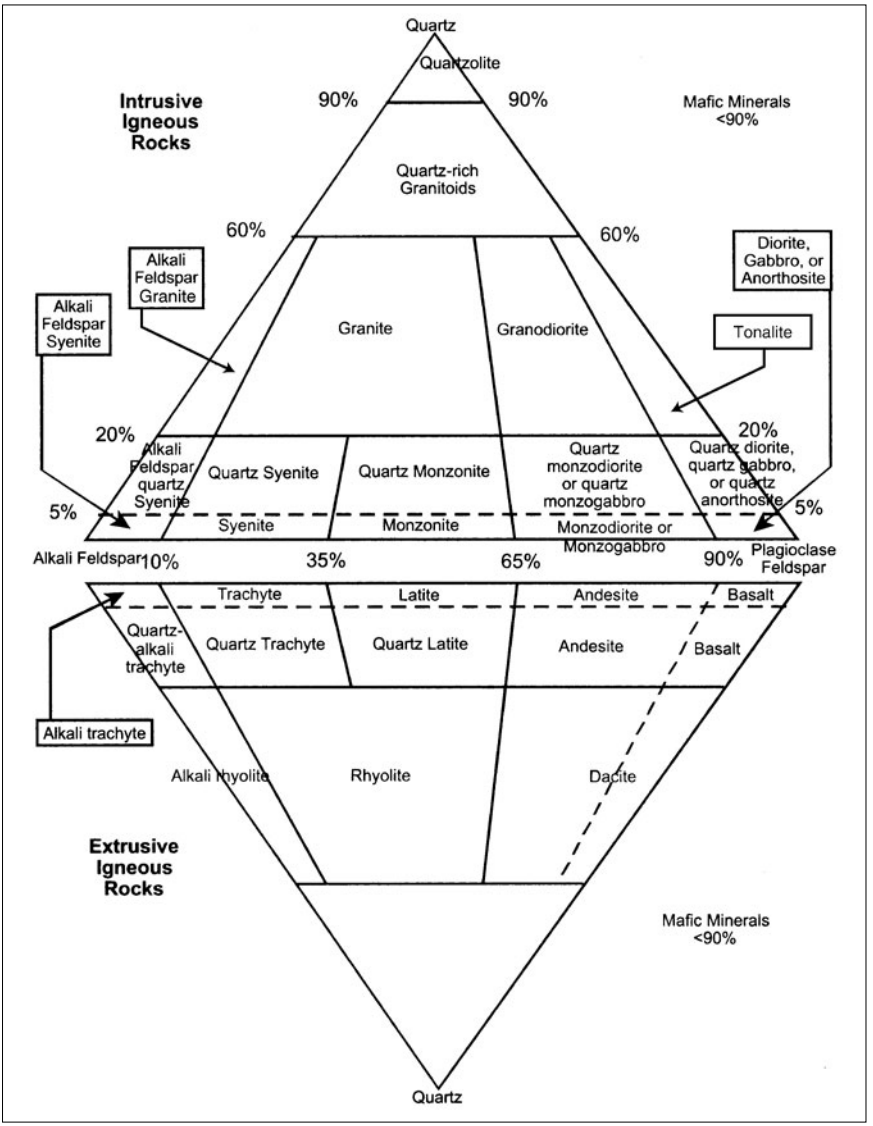

Figure 2.1 Summary classification scheme for the various igneous rocks. [*Modified from Streckeisen* (*1976*).]

This is **pumice**, which may have a porosity of 80% and floats because of the poor interstitial connections.

Other locations where igneous rocks commonly form are places where the crust is extending or pulling apart, known as **rifting**. Igneous activity has occurred, for example, in the Basin and Range province of the United States and in eastern Africa as a result of these forces. Extensional

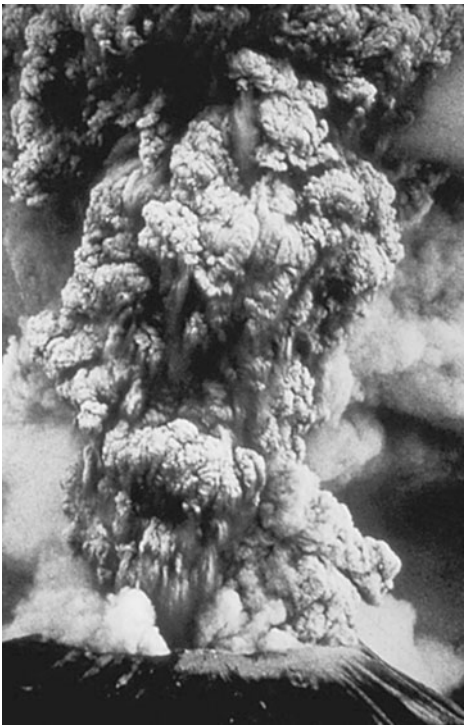

Figure 2.2 Mount St. Helens eruption, May 18, 1990. (*David Frank, USGS.*)

Figure 2.3 Pyroclastic rocks along the coast near La Paz Mexico (note the angular fragments).

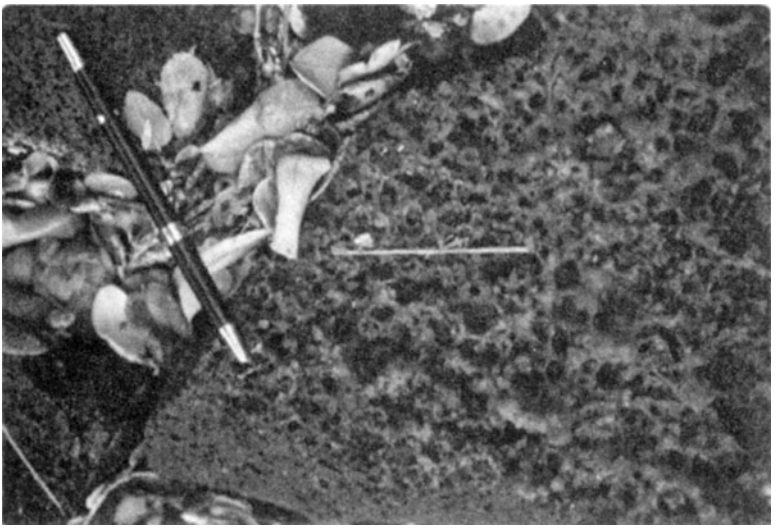

Figure 2.4 Vesicular lava from southeast Hawaii. (*Photo courtesy of Hugh Dresser.*)

areas allow easier routes for deep-sourced magmas to rise to the surface. Most of these magmas are of basaltic composition. Sometimes rifting is initiated in a region and then suddenly ceases from changes in plate-movement direction or heat-flow patterns in the asthenosphere.

The most common extrusive igneous rocks are basalt, andesite, and rhyolite, listed in order of increasing silica (SiO_2) content (Figure 2.1). Silica increases the viscosity of the igneous melt, much as corn starch or flour thickens gravy. The greater the silica content, the more viscous the magma. Thicker magmas that are gas-rich explode more violently. Compositionally, rhyolite is similar to granite, the most common intrusive igneous rock. Generally, granites are more common because magmas of this composition (>70% silica) seldom reach the surface. Rhyolites generally form in areas of high heat flow, for example, in Yellowstone National Park (a continental hot spot) or in New Zealand. Rhyolite eruptions are characteristically violent explosions followed by viscous lava flows that don't move far from the vent (Figure 2.5). Interstitial openings within rhyolitic tuffs and from multiple layers may result in production wells in the tens of gallons per minute range (50 to several hundred m^3/day).

Areas of high heat flow in geothermal settings may also cause the dissolution of minerals. As these waters rise to the surface, they cool and encounter cold-water recharge resulting in near-surface precipitation. This precipitation zone may create a confining layer that seals deeper aquifers from shallow aquifers or from interaction with surface water.

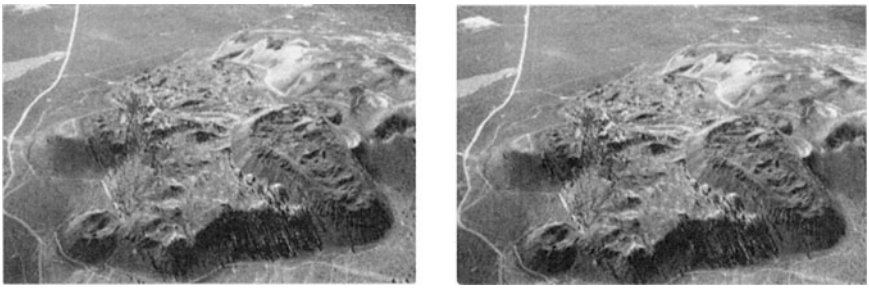

Figure 2.5 Stereo pair of rhyolite flow, north end of Mono Craters, California. (*Photos courtesy of Hugh Dresser.*)

Example 2.1 Near Gardiner, Montana, at the north end of Yellowstone National Park, the Yellowstone River flows northwestward into the Corwin Springs known geothermal area (Figure 2.6). In 1986, a production well on the west side of the Yellowstone River was drilled to a depth of 460 ft (140 m) and aquifer-tested in September of the same year (Sorey 1991). After pumping at a production rate of 400 gpm (25 L/s) for 13 h, La Duke Hot Springs on the east side of the Yellowstone River began to decrease in flow. This prompted a temporary moratorium on the drilling of production wells near Yellowstone Park (Custer et al. 1994). It is interesting that surface sealing from mineral precipitation resulted in a separation of the shallow alluvial system of the Yellowstone River from the deeper rhyolitic rocks. A similar surface-sealing phenomenon occurs in the Rotorua area of New Zealand (Allis and Lumb 1992).

Andesite

Andesitic rocks are intermediate in silica composition between rhyolite and basalt and are associated with the largest, most beautiful volcanoes in the world. Mount Fujiyama of Japan and Mount Rainier are examples (Figure 2.7). Andesitic rock typically forms where partial melting of oceanic and continental crust occur together. The Andes Mountains represent a type locality for this kind of rock. Andesites usually have a violent eruption, from explosively escaping volatile gases, followed by lava flows. During the explosive part, ash and other ejecta spews out onto the flanks of the volcano and surrounding area. The ensuing lava flows cover parts of the ejecta, providing a protective blanket. Subsequent eruptions result in a layering of ejecta and lava that builds up into large steep-sided volcanoes. Given the layered nature of andesitic terranes, there is a potential for water production among the layers.

Example 2.2 Robert Schutt, a professional participant in our year 2000 hydrogeology field camp described drilling conditions near Guatemala City where

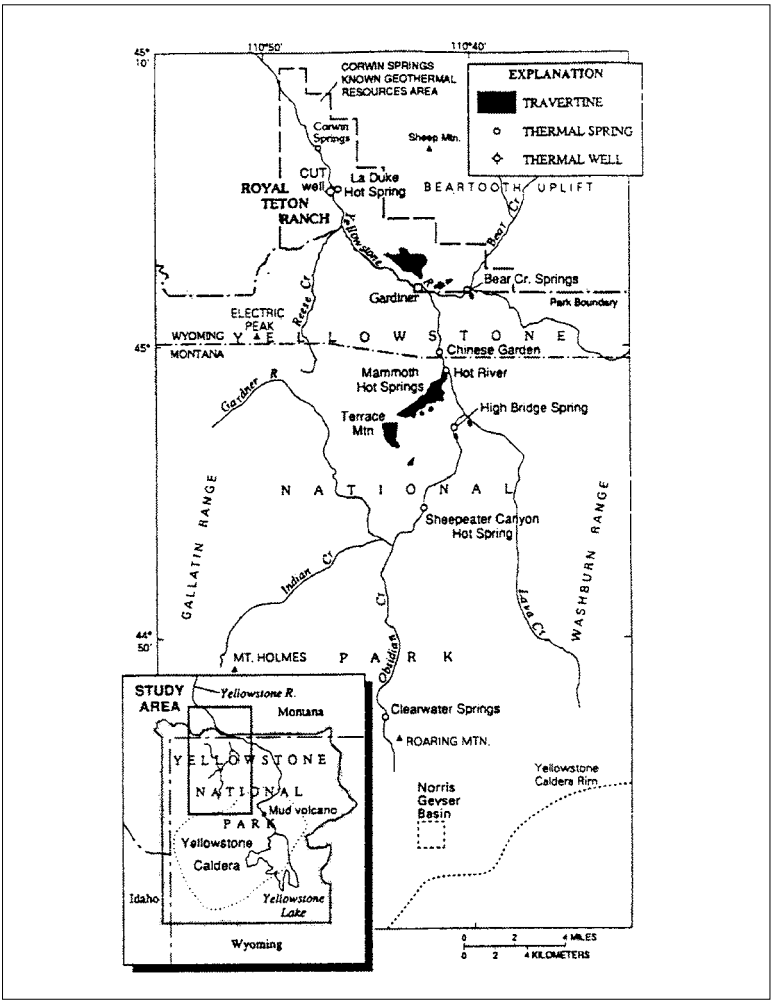

Figure 2.6 Corwin Springs known geothermal resource area near Yellowstone National Park from Example 2.1 (*Sorey 1991*).

his company Daho Pozos drills water wells. A typical production well on the side of a volcano extends to a depth of approximately 800 to 900 ft (244 to 274 m) (Figure 2.8). A typical drilling sequence is as follows: from surface to approximately 400 ft (122 m) is a dry unconsolidated zone of pyroclastics, ash, and pumice followed by approximately 150 ft (45.7 m) of hard andesite lava that serves to confine the next pyroclastic layer below. Once the hard andesite lava layer is penetrated, circulation is lost (Chapter 8), even when drilling with mud. Drilling continues for an additional 250 ft (76.2 m) or so to provide sufficient water with yields up to 300 gpm (1136 L/min).

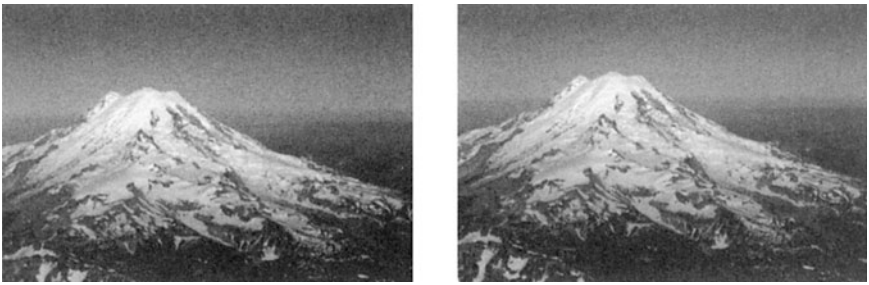

Figure 2.7 Stereo pair of Mount Rainier, Washington. (*Photos courtesy of Hugh Dresser.*)

Below is a well log and geophysical log for a typical production water well provided by Danny Lopez, a hydrogeologist with Daho Pozos (Figure 2.9). The well log indicates the total well depth is 940 ft (286.5 m), the pump was set at 772 ft (235.3 m), and the static water level was at a depth of 621 ft (189.3 m). The achieved production after 24 hours of pumping was 215 gpm (814 L/min). A cement-grouting plug was placed between 380 and 400 ft (115.8 to 121.9 m) to seal off the lower production zone. A gravel pack was placed from 400 ft (121.9 m) to 940 ft (286.5 m). Below the well log is a photo of Danny Lopez standing near

Figure 2.8 Ingersoll-Rand TH-75 drill rig drilling near the Hacienda Carmosa volcano near Guatemala City. (*Photo courtesy of Daho Pozos of Guatemala City, Guatemala.*)

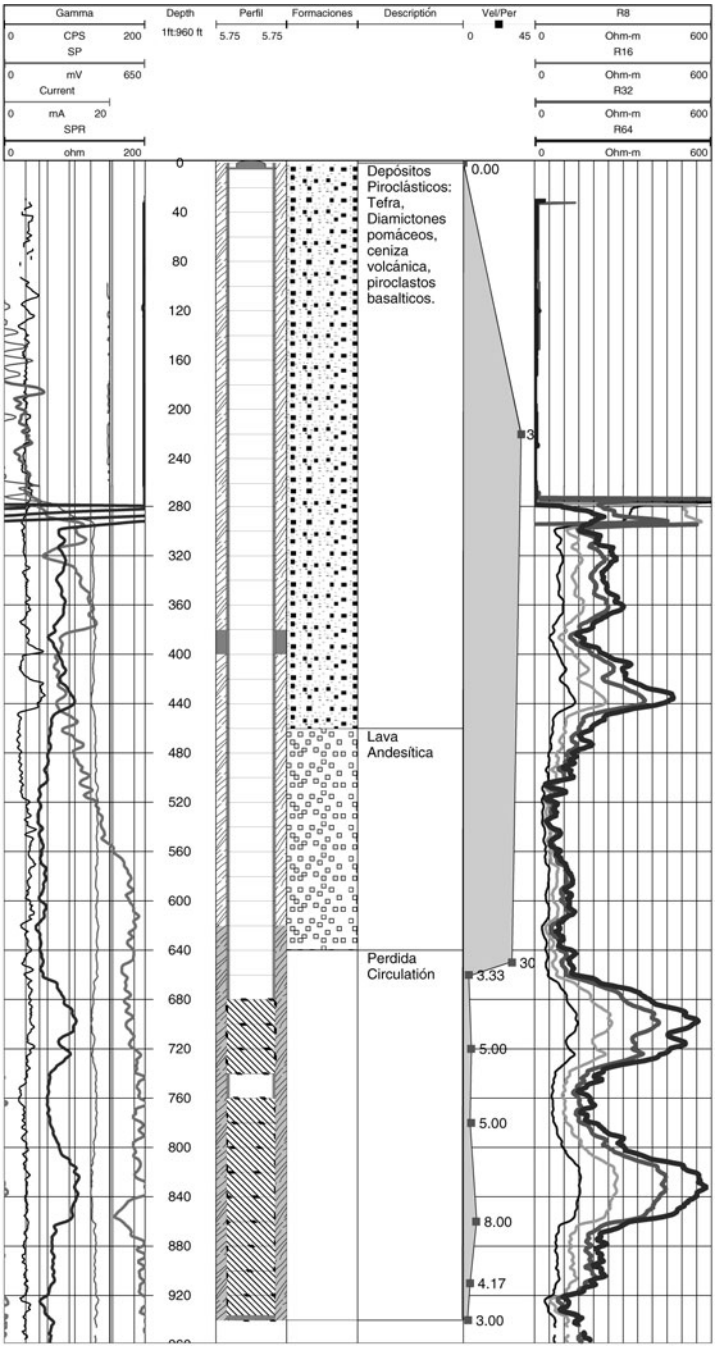

Figure 2.9 Well log and geophysical log showing the sequence of geologic materials (0 to 460 ft pyroclastics and tefra, 460 to 640 ft andesite lava, and 640 to 940 ft pyroclastic conglomerate—lost circulation). The pump depth was 772 ft and the static water level was at 621 ft. (*Courtesy of Daho Pozos, Inc. of Guatemala City, Guatemala.*)

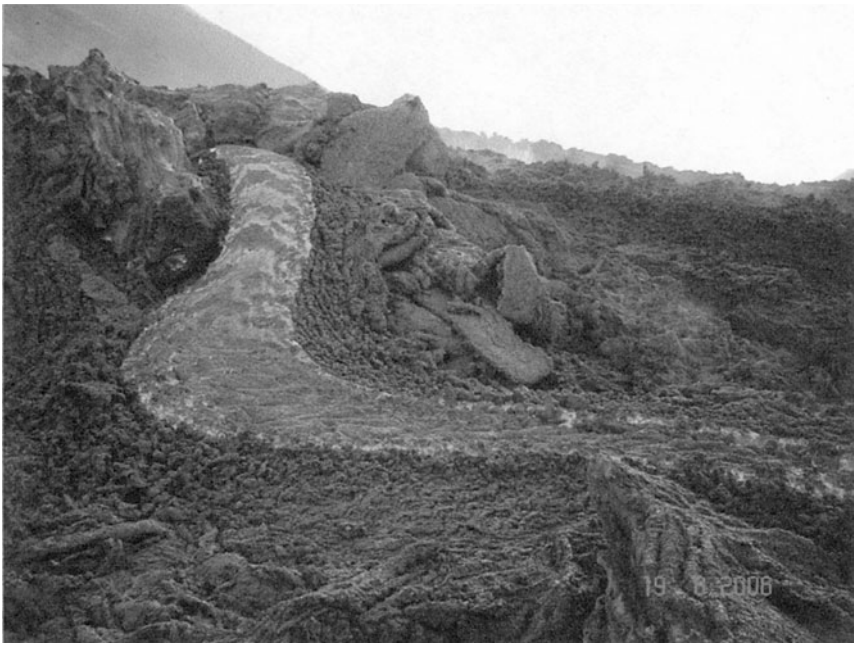

Figure 2.10 Lava flow from an eruption from the Pacaya Volcano near Guatemala City on August 2006. (*Courtesy of Daho Pozos, Inc. of Guatemala City, Guatemala.*)

a lava flow occurring on the Pacaya volcano near Guatemala City that erupted on August 19, 2006 (Figure 2.10).

Another source of water production can be associated with fractures from cooling. Liquid rock, as it cools, tends to form polygonal-shaped columns, known as **columnar jointing** (Figure 2.11). These may provide significant permeability for groundwater flow. Columnar jointing is also commonly observed in basaltic lava flows.

Basalt

The most common extrusive igneous rock is basalt. It is the rock that constitutes oceanic crust and is common within the Pacific Rim in a series of island arcs known as the ring of fire (Figure 2.12). Basalts are common because they form by partial melting of the mantle and constitute the oceanic crust. In areas such as the mid-oceanic ridges and areas where the continental crust is extended, basaltic magmas rise quickly up their vents and flow onto the surface as a dark gray to black lava. These magmas are very fluid because of their low silica content (near 50%). Many basaltic lava flows, where they occur repetitively, are fairly thin, on the order of 15 to 40 ft (4.5 to 12.2 m) thick. At the top

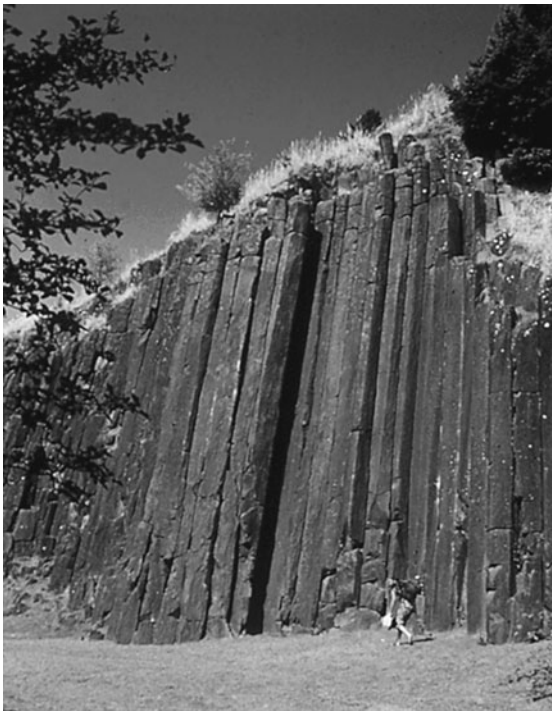

Figure 2.11 Columnar jointing in a basalt flow.

and bottom of these flows are scoria zones of high porosity from burning vegetation and cooling processes. The middle part of basalt flows can be quite dense (Figure 2.13). Some regions can have thicknesses of multiple flows that are in excess of thousands of feet (several hundreds of meters). Many of these are in areas where fissure eruptions have

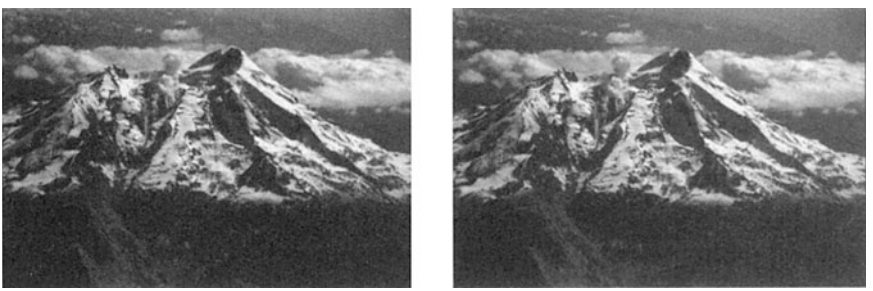

Figure 2.12 Stereo pair of steaming Redoubt Volcano, Chismit Mountains, Alaska. (*Photos courtesy of Hugh Dresser.*)

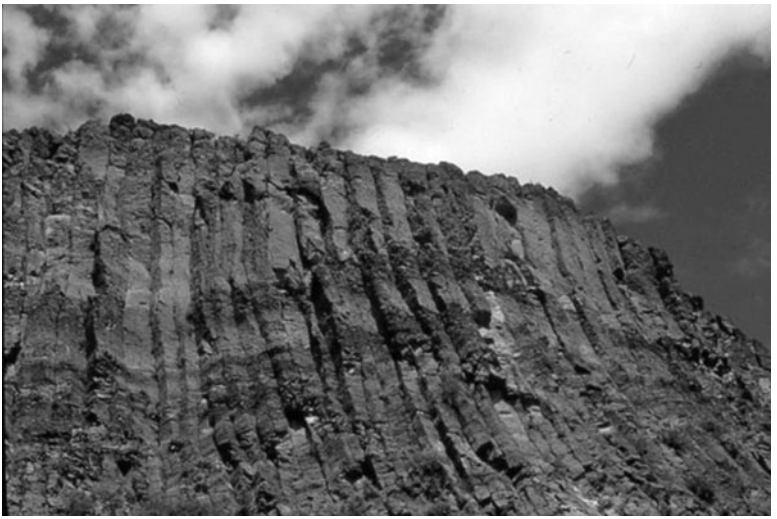

Figure 2.13 Basalt with multiple flows and columnar joining.

occurred. Fissure eruptions like those of the Deccan Plateau in India and the Oregon–Washington area may have resulted from meteorite impact (Alt and Hyndman 1995). Saturated, thinly layered basalt lava flows may result in some of the most prolific aquifers.

Example 2.3 In the eastern Snake River Plain, Idaho, is a very prolific aquifer known as the Eastern Snake River Plain Aquifer. As an undergraduate student, the author worked for Jack Barraclough of the U.S. Geological Survey, Water Resources Division, at the Idaho National Engineering Laboratory (INEL), while participating in several field geologic and hydrologic studies. (It is now known as the Idaho National Engineering and Environmental Laboratory (INEEL)). One project involved logging cores from deep drill holes (greater than 1,000 ft, or 300 m). Basaltic lava flows ranged from 15 to 35 ft (4.5 to 10.7 m) thick. Most were clearly marked by a basal vitrophere or obsidian zone with some **scoria** (a high vesicular or bubbly zone) on the order of 1 to 2 ft (0.3 to 0.6 m) thick, above which was a dense basalt with occasional gas bubbles frozen into position as they tried to rise to the surface (bubble trains). Each dense zone could be distinguished by its olivine content (a mineral characteristic of rock from the mantle), that ranged from approximately 2 to 12%. The top was distinguished by another scoria zone. These layers extended from the surface down to the bottoms of the core holes, separated only by a few thin sedimentary layers, representing erosional hiatuses. It was obvious that there were abundant sources of connected permeability to allow free flow of groundwater.

During the summer of 1979, a deep geothermal production well was attempted, known as INEL#1. Geologists thought they could identify the location of a caldera ring, from surface mapping. A **caldera** is a collapsed

magma camber characterized by ring faults and a crater rim more than 1 mi (1.6 km) across. The concept was that at sufficient depth, fracturing and heat would allow the production of a significant geothermal production well. The proposed purpose of the well was for power generation and heating. The drilling required a large oil rig with a 17-ft platform and 90-ft (27.4-m) drill pipe. Surface casing was set with a 36-in (91-cm) diameter and eventually "telescoped" down to an open hole 12 ¼ in (31.1 cm) in diameter at the total depth of 10,380 ft (3,164 m). The layered basalt flows are over 1,700 ft (518 m) thick at this location. These are underlain by dacitic and rhyodacitic rocks (Figure 2.1). Although the temperatures at depth were up to 325°F (149°C), there was poor permeability and production.

Wells less than 150 m deep at the INEEL can produce in excess of 4,000 gpm (21,800 m^3/day). Some high-capacity production wells start out with a pumping level approximately 1 ft (0.3 m) below static conditions that then recover back to static conditions (Jack Barraclough, personal communication, INEEL, July 1978)! Not all basaltic rocks can be thought of as potentially prolific aquifers. They can vary greatly in their ability to yield water. For example, Driscoll (1986) points out that incomplete rifting about one billion years ago in the central United States produced a massive belt of basalt extending from Kansas to the Lake Superior region. This massive belt contains relatively few fractures or vesicular zones, resulting in poor water production (only a few gpm, 10 to 20 m^3/day). A wide range of hydrologic properties for basalts in Washington State has been reported by Freeze and Cherry (1979) in Table 2.1.

Intrusive rocks

Intrusive igneous rocks are also known as plutonic rocks because they form large bloblike shapes underground that may result from partial melting of colliding plates, rifting, and melting above hot spots. They cool under the Earth's surface. Characteristically, these rocks form a tight network of interlocking grains that compete for space during the cooling process (Figure 2.14). Minerals that are at least 10 times larger than surrounding grains are known as **phenocrysts**. (Phenocrysts are also present in extrusive igneous rocks, but have a matrix around them that is very fine-grained.) Because cooling is slow and volatile gases such as water vapor are present, mineral growth is enhanced. The three most

TABLE 2.1 Range of Hydrologic Properties of Basalts in Washington State

	Hydraulic conductivity (cm/sec)	Porosity (%)
Dense basalt	10^{-9}–10^{-7}	0.1–1
Vesicular basalt	10^{-7}–10^{-5}	5
Fractured basalt	10^{-7}–10^{-3}	10
Interlayered zones	10^{-6}–10^{-3}	20

Figure 2.14 Interlocking crystals in weathering granite, Hammer for scale.

common intrusive igneous rocks whose extrusive counterparts have already been discussed are granites, diorites, and gabbros. Gabbro is compositionally equivalent to basalt. Magma chambers that are larger than 60 mi^2 (100 km^2) are known as **batholiths**. Smaller blob-like bodies are known as stocks. Intrusive features that are discordant and fill vertical to angled fractures are known as **dikes** (Figure 2.15), and

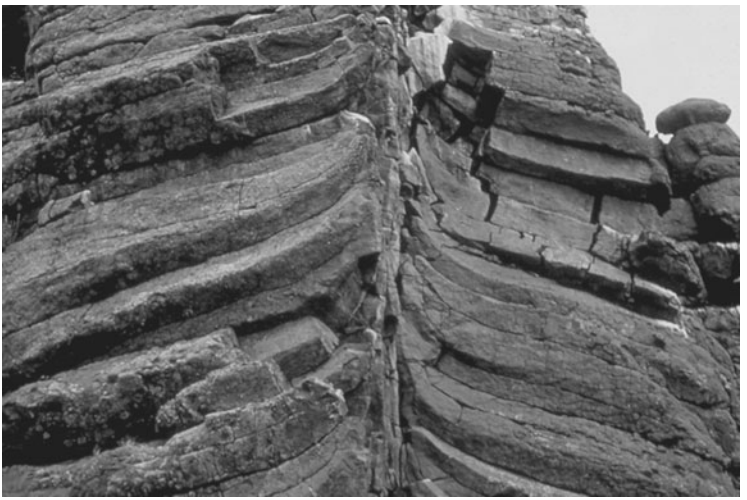

Figure 2.15 Columnar joining in a basalt dike with trapped volatile gas vent, Grose Ventre Range, Wyoming.

concordant intrusive bodies that are injected in between layers are known as **sills**. Each of these may influence groundwater flow directions by obstructing flow paths.

The primary porosity of such rocks tends to be low, less than 1%, although granites with porosities greater than 1% are known (Fetter 1994). The ability of intrusive igneous rocks to produce water generally comes from secondary porosity, generated by fracturing and faulting. Large igneous bodies are subject to the stresses involved in mountain building. These forces may produce fracture patterns oriented obliquely to the principle directions of stress. Fracturing tends to occur in a characteristic crossing pattern that can be observed in the field (Figure 2.16). Sometimes fractures in intrusive igneous rocks are enhanced by **exfoliation,** a process of expansion from unloading as the weathering process strips off overlying materials in relatively thin sheets of rock (shown in Figure 2.28). A list of porosity types and additional discussion of porosity is found in Chapter 3.

Minor drainages often develop in weaker fracture zones promoting recharge to granitic aquifers. Minor fractures can produce some water, however, larger sustained yields require more extensive fracture networks, such as fault zones. Large faults or fractures extend for distances of a mile (1.6 km) or more and are visible on aerial photographs. These longer fracture features are known as **lineaments** (Figure 2.17). Minor drainages that are controlled by these features tend to be abnormally straight, and thus can be recognized as potential target drilling

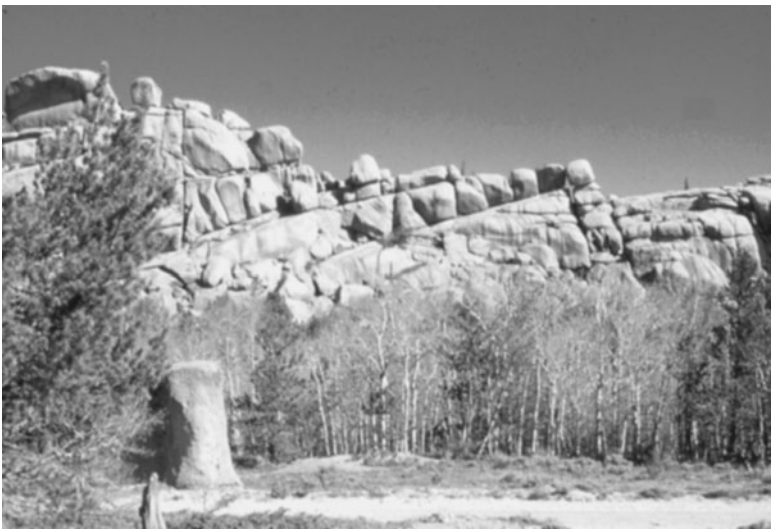

Figure 2.16 Jointed Fracture patterns and weathering in granite, Laramie Range, Wyoming.

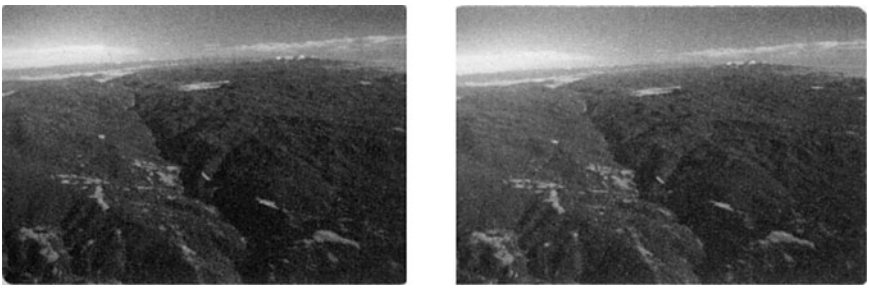

Figure 2.17 Stereo pair Nez Perce lineament in southwestern Montana. (*Photos courtesy of Hugh Dresser.*)

areas. Another perspective of fracture zones being productive, is that they are also the most vulnerable to surface contamination. This is important for well-head or source-water protection issues (Chapter 1).

Example 2.4 In southwestern Montana a large granitic body known as the Boulder Batholith was once a magma chamber for a large volcanic system that has been stripped away by weathering, erosion, and uplift. Its associated mineralization is responsible for a significant amount of the colorful mining history of the old west and current mining activity for precious metals. It extends from Butte to Helena, Montana, and is nicely exposed along Interstate 90 near Homestake Pass (Figure 2.18). This igneous body is disrupted by numerous faults.

Figure 2.18 Fracturing in granitic rocks near Homestake Pass, southwestern Montana. (*See also Figure 2.19.*)

A homeowner from Pipestone, Montana, on the east side of Homestake Pass called seeking the opinion of a hydrogeologist on where to drill a domestic well. The local State agency that keeps records of wells drilled in Montana was contacted to obtain information regarding any existing wells, their drilling depths, and production rates. After plotting this information on a topographic map, it was observed that the most productive wells are aligned with the significant canyons that have exceedingly straight drainage patterns. The projection lineaments of these drainages extend westward into the Homestake Pass area. Production rates varied from 8 to 20 gpm. (43.6 to 109 m^3/day). Domestic wells that were located between drainages and away from major lineament patterns indicated production rates in the 2 to 3 gpm (10.9 to 16.4 m^3/day) range or less. Static water levels in wells were approximately 30 to 70 ft (9.1 to 21.3 m) below ground surface.

This homeowner's property is located between the major lineaments, so prospects for a higher productive well were not very good. The assumption was that away from major fracture zones the smaller patterns were somewhat random. The hope was to drill a deeper well (400 to 500 ft, 122 to 152 m) and intersect sufficient minor fractures to yield a couple of gpm (10 m^3/day). This approach yielded a well 450 ft (137 m) deep, producing 2 gpm (11 m^3/day). The static water was only 40 ft, so there was sufficient water from casing storage to yield significant quantities for a family.

Away from mountain fronts in southwestern Montana are intermontane valleys whose valley fill deposits are asymmetrical. Typically, eastern margins have greater depths to basement rocks than do western margins. In the Pipestone, Montana, area, granitic rocks are covered by a thin layer of sedimentary rocks, so the land surface features appears to be flat lying. The question comes up "how come they can find water and we can't find much?" The answer comes from understanding the subsurface geology and where the major productive fracture zones are.

Previously it was mentioned that intrusive igneous features such as dikes and sills can affect the flow patterns. Many magma chambers experience intermittent periods of activity, with multiple periods of intrusion. Older granitic bodies can be intruded by younger magmas of similar or differing composition. Some fractures may be filled by younger intrusives, inhibiting groundwater flow.

Example 2.5 Located at the south end of Butte, Montana, on the west side of Homestake Pass is a subdivision known as Terra Verde (Figure 2.19). Homeowners prefer to build at as high an elevation as possible for the best possible view of the nearby Highland mountains (Figure 2.20). This results in having to drill deeper wells with a greater uncertainty of success, particularly if the locations they wish to place their homes are not near any lineament features.

In walking around the property of a prospective home builder, the author noticed that there were a series of large pine trees that grew in a straight pattern for at least ¼ mi (400 m). It occurred to the author that this might represent a significant lineament even though it was not readily observable on an

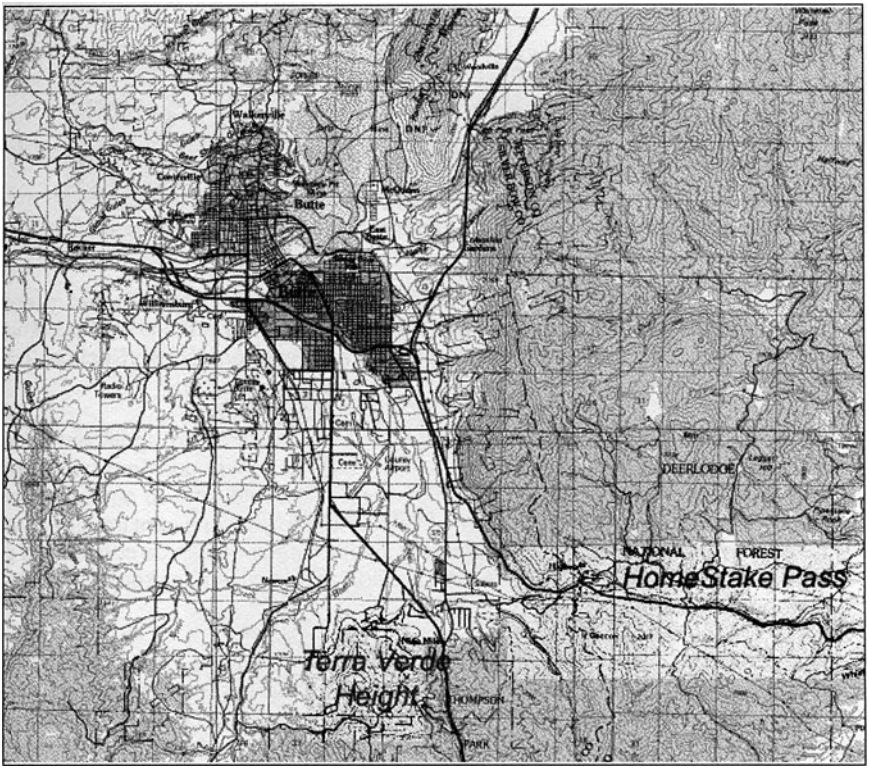

Figure 2.19 Location map of Terra Verde Height subdivision and Homestake Pass, south of Butte, Montana.

Figure 2.20 Highland Mountains looking south, near Butte, Montana.

air photo. The author noticed (imagined?) a second such pattern that crossed the first on the prospective homeowner's property. The second observed or imagined lineament formed a subdued depression at the surface. Down slope there are several **aplite** (very fine-grained, light-colored) dikes. The thinking was that perhaps these dikes resulted in inhibiting groundwater flow allowing greater storage capacity in the "up-gradient" direction. The recommendation was to drill in the lineament crossing pattern area a few hundred feet (several tens of meters) uphill from the dike's outcrop. This formed the reasoning for a best educated guess, presuming that the orientations of the intersecting fractures were nearly vertical. This illustrates the importance of understanding the fracture orientations (Section 2.5) and intersections.

Another recommendation made to the homeowner was that if no significant water was found after drilling 200 ft (60 m), then the probability of finding additional water-bearing fractures was even less likely (lithostatic pressures would tend to squeeze fractures closed). The well was drilled to a depth of 198 ft. At 185 ft, a significant fracture zone was encountered yielding 15 gpm. Encountering the fracture zone can be considered as serendipity, but perhaps the aplite dikes did provide a mechanism for keeping water in the "uphill" area.

This success story prompted another neighbor to call for advice. Unfortunately, the second property owner had already started the expensive process of blasting and constructing a basement for his home, located approximately 1/4 mi (400 m) downslope and to the east of his neighbor. This significantly limited the range of area available to recommend drilling locations, because in Montana it is necessary to dig a trench from the well head to the basement to keep water lines from freezing. After performing a field investigation, surface lineaments were not observed and the aplite dikes located on the first property were also not observed. There was not much to go on. A recommendation was provided with a low but unknown probability for success. The hole was drilled 270 ft, and although the formation was getting softer, the homeowner told the driller to stop. Instead, a water witch was hired to locate the next location, where a 5-gpm (27-m^3/day) well was drilled at a depth of 106 ft (32.2 m). This of course propagates wild ideas about the location and availability of water. More about water witching is found in Chapter 8, Section 8.7.

2.2 Geologic Properties of Metamorphic Rocks

Metamorphic rocks are those that have "changed form" through changes in temperatures and pressures. Rocks that are sedimentary or igneous if subjected to sufficient temperatures and pressures will change form or recrystalize to form a new metamorphic rock. It is important to realize that this process occurs without melting, although fluids may be present to aid in the recrystallization process known as **metasomatism**. The classification of metamorphic rocks is based upon specific composition and texture. Particular mineral assemblages correlate with specific temperature and pressure conditions. Metamorphic rocks are named by describing their mineral content and observing whether they are foliated or not.

The geologic setting where temperatures and pressures are applied may be reflected in the texture of the rocks. Rocks that are involved in colliding plates tend to have a foliated texture (Figure 2.21), whereas rocks forming near hot magma chambers tend to be nonfoliated. Foliation occurs where platy minerals crystalize perpendicular to the stresses being applied. Rocks that are deeply buried will metamorphose even though there may not be any relative tectonic movement. On the other hand, rocks relatively near to the earth's surface (2 mi, or 3 km) may indicate temperature and pressure conditions comparable to deep crustal rocks because they were involved in plate tectonic collisions. Foliation is an important property in controlling the direction of groundwater flow and in identifying potential production zones. Having an understanding of the regional geology is critical to understanding the potential for water development in a local area. Measuring the orientation of foliation structures is discussed in Section 2.5.

There are two general groups of metamorphic rocks, **regional** and **contact** metamorphic rocks. The most common are regional metamorphic

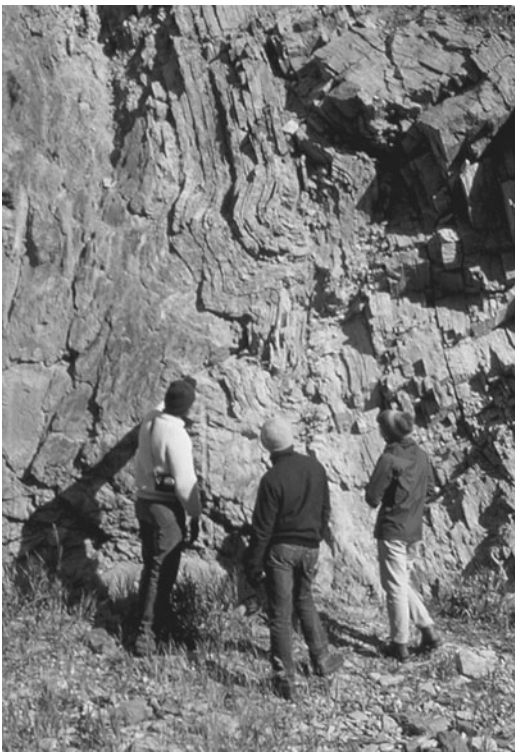

Figure 2.21 Foliated rocks in Hoback Canyon, Wyoming.

rocks. These formed from plate-tectonic movement and tend to occupy large areas.

Plate tectonic settings of metamorphic rocks

The lithosphere is broken into approximately 12 large plates. These all move relative to each other in a variety of ways. Some are divergent (moving apart), some are convergent (moving together), and some move past each other as transform boundaries. Relative plate movement causes a variety of stress conditions in crustal rocks. In convergent areas, such as where the Gorda plate is colliding with the North American plate, subduction of the Gorda plate under the North American plate results in partial melting at depth and the generation of a volcanic arc known as the Cascade Range (Figure 2.22). The volcanoes of the Cascade range erupt above areas of partial melting where active magma chambers are developed. The country rock next to these magma chambers is subject to high temperatures and hot fluids, forming zones of contact metamorphic rocks. The temperature and pressure conditions and available fluids determine the minerals that form, including ore minerals and explains why the country rock in some mining districts have such an "altered and baked" look. Magma being less dense than the solid country rock buoyantly seeks to rise to the surface. Fracturing of the overlying rocks may result in the injection of mineral bearing fluids that harden into dikes and sills. Modern mining districts are often connected to some igneous source that was active in the geologic past.

Rocks away from magma chambers that are involved in plate convergence are subject to tremendous stresses. The pressure conditions are usually measured in the thousands of atmospheres range, with units of

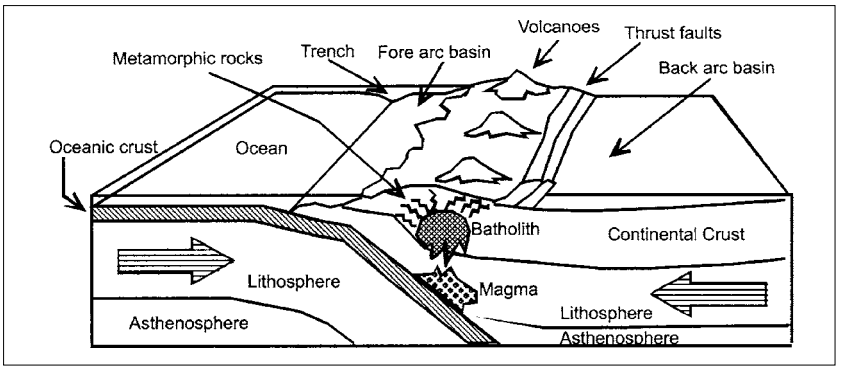

Figure 2.22 Schematic of a converging plate margin with oceanic and continental crust.

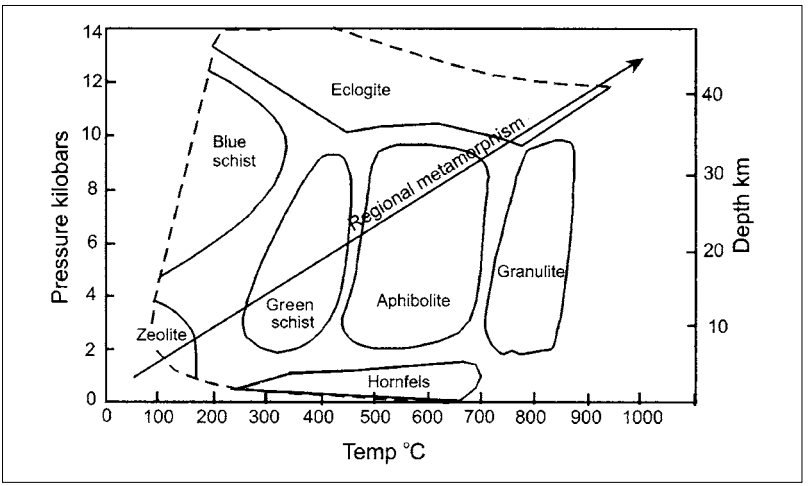

Figure 2.23 Classification of foliated metamorphic facies, showing path of regional metamorphism. Vertical axis is in kilobars of water pressure and depth in kilometers, and horizontal axis is in temperature °C. [*Modified from Turner (1968).*]

kilobars. Temperatures are greater than 200°C. A general classification scheme for metamorphic rocks is shown in Figure 2.23. Rocks are distinguished by minerals present, which form in a characteristic temperature and pressure environment and given a **facies** name. For example, lower temperature and pressure conditions are characteristic of the green schist facies. The name comes from the alteration of basalts to chlorite, with its typical greenish color.

Regional metamorphic rocks usually have a foliated texture unless they are in close proximity to a magma chamber. The degree of metamorphism may affect a metamorphic rock's ability to transmit water. To illustrate the physical changes that occur in rock type with increases in temperature and pressure during metamorphism, an example using a sedimentary rock is provided.

Example 2.6 Suppose that a shale, the most common sedimentary rock, is subject to tectonic stresses. As the conditions of temperature and pressure increase, the clay minerals will recrystalize perpendicular to the applied stresses forming a slate (Figure 2.24). Slates are fine-grained and have poor primary water-yielding capacities. However, if fractured, slates can yield sufficient water for most domestic purposes (Chapter 1).

If the process of increasing temperatures and pressures continues, the slate will first transform into a phyllite and then a schist. Essentially, the clay minerals of the original shale will grow into sheet silicates of the mica group, resulting in a fabric known as **foliation**. Foliated fabric results in an anisotropy for fluid flow (Chapter 3). Flow parallel to foliation may be orders

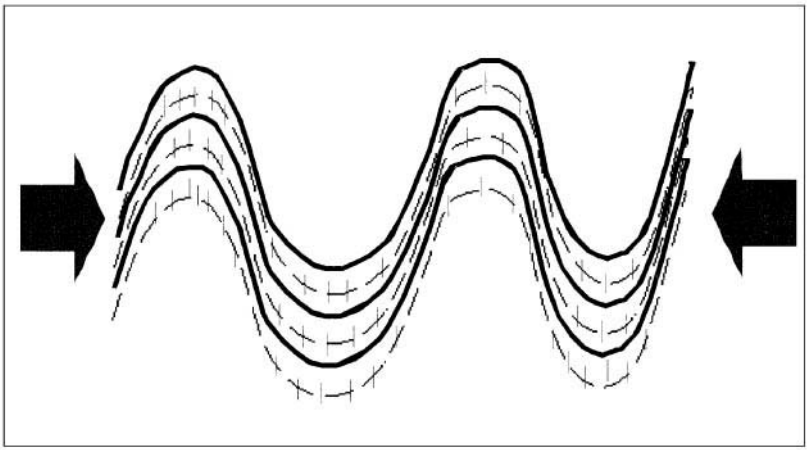

Figure 2.24 Schematic illustrating the reorientation of clay-mineral growth when a shale is subjected to horizontal stresses. (*Heavy and dashed folded lines represent original bedding and clay orientation prior to applied stresses. Vertical markings represent foliation orientation of recrystalized minerals.*)

of magnitude greater than flow perpendicular to foliation. Continued increases in temperatures and pressures result in mineral separation into light and dark bands, forming a gneiss.

In the conditions described in Example 2.6, there is a tremendous competition for space during mineral growth, and the primary yielding capacity for metamorphic rocks tends to be very low. For example, Freeze and Cherry (1979) report intrinsic permeabilities in the range of 10^{-9} to 10^{-11} cm/s for metasediments of the Marquette Mining district in Michigan. A characteristic feature of metamorphic rocks and intrusive igneous rocks is that the hydrologic properties of porosity, permeability, and well yield decrease with depth (Davis and Turk 1964) (Figure 2.25). This is true of most rocks. Generally, igneous and metamorphic rocks are not known as big water producers without secondary porosity and permeability being created by faulting and fracturing.

2.3 Geologic Properties of Sedimentary Rocks

The most common water-bearing materials that produce potable water are sedimentary rocks. These can be consolidated or unconsolidated. Sedimentary rocks, by nature, tend to have high primary porosity and, depending on the depositional environment and particle size, they may have very high hydraulic conductivities. Sedimentary rocks are classified according to grain size and texture. Grain sizes are divided into

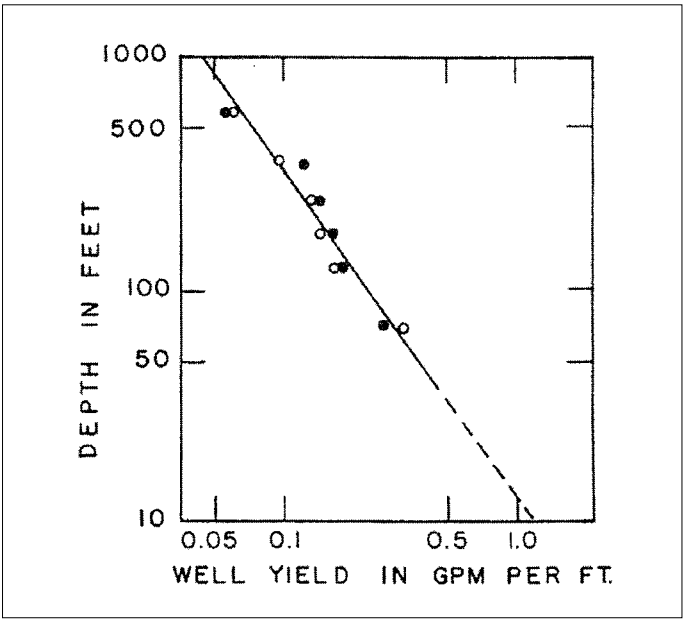

Figure 2.25 Yields of wells in crystalline rock of the eastern United States. Open circles represent mean yields of granitic rock based on a total record of 814 wells; black dots represent mean yields of schist based on a total record of 1,522 wells. [*From Davis and Turk (1964). Reprinted with permission of Groundwater, 1964.*]

gravel, sand, and mud according to a Wentworth-like classification scheme shown in Table 2.2 (Folk 1966). Mud includes all silt and clay-sized particles. The mud fraction is usually analyzed by a pipette or hydrometer method.

TABLE 2.2 Sediment Classification Based Upon Grain Size

Class	Other names	Particle size (mm)	U.S. sieve size
Extremely coarse gravel	Boulders	>256	Wire mesh
Very coarse gravel	Cobbles	64–256	Wire mesh
Coarse gravel	Pebbles	16–64	Wire mesh
Medium gravel	Pebbles	8–16	Wire mesh
Fine gravel	Pea gravel	4–8	Wire mesh
Very fine gravel	Granules	2–4	10–5
Very coarse sand		1–2	18–10
Coarse sand		0.5–1.0	35–18
Medium sand		0.25–0.5	60–35
Fine sand		0.125–0.25	60–120
Very fine sand		0.0625–0.125	230–120
Coarse to very fine silt		0.0039–0.0625	<230
Clay		<0.0039	

Weathering

Sediment particles result from the weathering of igneous, metamorphic, and sedimentary rocks. The ease of weathering depends primarily on climatic conditions and rock type. Climates that are warm and moist produce the highest weathering rates. The composition of minerals in rocks is also a big factor. Rocks that crystalize at high temperatures and pressures tend to weather more quickly than minerals that form at lower temperatures and pressures. An example of this is known as Golddich's (1938) weathering series and is illustrated in Figure 2.26.

Figure 2.26 is essentially the inverse of Bowen's reaction series (1928). Bowen performed a series of laboratory experiments to learn which silicate minerals form first from a molten state. The arrows between the calcium and sodium plagioclase feldspars indicate a continuous series because the ionic radii of these two are similar. Thus they can readily substitute for one another in the crystal lattice. Calcium plagioclase forms at a higher temperature and gives way to increasing sodium content with decreasing temperature. Potassium (K) feldspar is distinguished from plagioclase because potassium's ionic radius is much larger than sodium or calcium. This makes these two minerals immiscible in the molten state. The other side of the diagram represents a discontinuous series of minerals that form as temperatures change. At high temperatures near 1,400 to 1,500°C, olivine forms. As temperatures drop, the olivine is resorbed and pyroxene forms. The type of rocks that cool from a melt depend greatly on the original composition. Rocks that originate

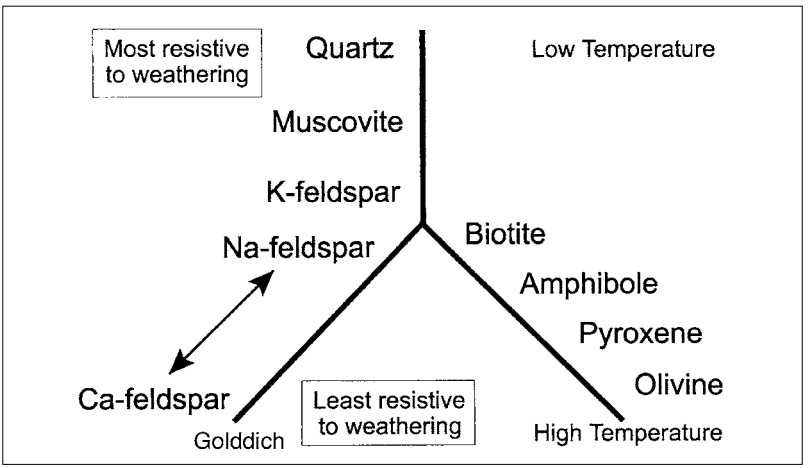

Figure 2.26 Golddich (1938) weathering sequence. (*Illustrates which minerals are more or less resistant to weathering. Quartz is the most resistant and olivine and calcium plagioclase are most easily weathered.*) *The inverse of this diagram is known as Bowen's (1928) reaction series.*

from the mantle form basaltic magmas, those that partially melt from a mixture of oceanic and continental crust are andesitic, and granitic rocks form from molten continental crust (near 600°C). Many metamorphic and sedimentary rocks are composed of the above mineral groups.

The most abundant minerals, the feldspars weather to clay minerals, and this is why shale is the most common sedimentary rock. The other most common mineral in sedimentary rocks is quartz, a principal component in sandstone. Quartz, muscovite, and feldspars are non-ferromagnesian silicate minerals. The higher-temperature minerals of the discontinuous series (Figure 2.26) are ferromagnesian minerals because of their iron and magnesium content. They weather relatively quickly and oxidize soils reddish, yellow, or brown.

Weathering has two general categories, mechanical and chemical. Mechanical weathering includes those processes that act to break down the larger rocks into smaller rocks without changing their physical properties. Another name could be disintegration. For example, a chunk of granite can be broken into smaller pieces by frost wedging, where water enters a crack and freezes. Because water in a solid state occupies 9% more space than in the liquid state, it will wedge or push the rock apart. Then, gravity pulls the fragments downslope. This is why talus slopes form at the bottom of cliffs (Figure 2.27). When granitic rocks, formed at depth, are exposed to lower pressures at the surface they tend to spall off in onion-skin-like layers (exfoliation) (Figure 2.28).

Figure 2.27 Talus slope at the base of a cliff near the east entrance to Yellowstone Park, Wyoming.

Figure 2.28 Onion-skin-like layers of exfoliation in granite, Half Dome, Yosemite Park, California.

Chemical weathering includes processes that change the chemical lattice structure and composition of minerals to reach equilibrium with surface conditions. Another name could be decomposition. Hydrolysis and oxidation are examples. Chemical weathering through water and carbon dioxide act to convert feldspars into clays. Some of the mechanisms of weathering are listed in Table 2.3. Weathering breaks rocks into sediments, which then become available for transport. Angular rocks are especially prone to weathering processes because of increased surface area. The result is the rounding of edges into a more spherical shape known as **spheroidal weathering** (Figure 2.16 and Figure 2.29). In Figure 2.29, both mechanical and chemical weathering processes are breaking down exposed granite in a 100-year-old railroad cut. Mechanical weathering processes are important for enhancing the permeability of geologic materials and providing additional pathways of recharge into aquifer systems. Additionally, dissolution is important in adding dissolved minerals to groundwater and contributing to karstic conditions in carbonate rocks (Chapter 14).

TABLE 2.3 Examples of Mechanical and Chemical Weathering

Mechanical weathering	Chemical weathering
Frost wedging	Hydrolysis
Exfoliation	Oxidation
Heating and cooling	Dissolution
Plants and animals	

Figure 2.29 Exposed granite in a 100-year-old railroad cut, exhibiting spheroidal weathering. The outcrop is approximately 2 to 3 m across.

Transport of sediment and depositional environments

Once sediments have been broken down and decomposed by the weathering process, they can be transported by wind, water, ice, or gravity into a depositional environment. Later, through **diagenesis**, unconsolidated sediments are compacted and cemented into sedimentary rock. Sedimentary rocks contain sedimentary structures that reveal the processes and mechanisms of transport. For example, ripples and trough cross-bedding indicate **fluvial** or stream processes and large cross-bedding up to 15 to 30 ft (4.6 to 9.1 m) high between bedding planes indicate **eolian** or desert wind conditions (Figure 2.30). Glacial deposits tend to be a mixture of large and small particles dumped together in no particular order (Figure 2.31). Having an understanding of depositional environments is necessary to produce a three-dimensional picture of the sediment distribution. This can be a great aid when installing monitoring wells, drawing cross sections, or dividing up units into a hydrostratigraphy (Chapter 3). For example, is this sand channel likely to be continuous or will it quickly pinch out? This is also helpful in interpreting pumping test data and understanding groundwater flow.

Sediments that have been transported by water and wind tend to be sorted and stratified. **Sorting** is a measure of the distribution of grain sizes. Sediments with a narrow range of grain size (all similar sized) are said to be well sorted. An example of a depositional environment where

Figure 2.30 Large cross-bedding typical of an eolian environment.

this occurs is a beach sand. Here, the wave action winnows out the smaller grain sizes, leaving coarser sediments of similar size. In contrast to a well-sorted sedimentary unit is a glacial till where grain sizes from boulders to clay-sized particles are mixed together. In this case, sediments are poorly sorted. Tills, although they may have high porosity, tend to produce units that are poor conductors of water.

Engineering literature uses the term **grading** instead of sorting. A well-graded unit is one with a wide range of grain sizes, like the glacial till example above. The beach sand example would be considered poorly

Figure 2.31 Glacial till showing poor sorting near Leadville, Colorado.

graded. The terms are nearly opposite, so one must be careful in the descriptions. A geologist may be more comfortable using sorting terms, and an engineer may be more comfortable using graded sedimentary terms. Drill logs used for constructing cross sections may have been described by either or both professionals, so it is important to pay attention.

It is recommended that a dictionary of geologic terms, such as that of the American Geologic Institute (Bates and Jackson 1984), be kept in the office library. Table 2.4 presents some of the most common ones, along with generalized characteristics.

TABLE 2.4 Listing of Geologic Terms, Depositional Environments, and General Characteristics

Geologic term	Environment	Comments
Alluvium	Stream, flood plains, or alluvial fans	Coarser-grained channel sediments surrounded by finer-grained sediments away from the channels, including silts and clays. Changes in lithology are commonly abrupt and laterally discontinuous.
Colluvium	Topographic slopes	Loose, incoherent coarse to fine-grained deposits collecting on slopes by gravity.
Drift	Glacial	Geologic materials deposited by ice or melt water. Layered or stratified drift occurs from melt water streams.
Eolian	Desert or pertaining to wind	Well-sorted fine to medium sands, with large cross-bedding.
Fluvial	Streams, rivers, or stream action	Channels fine upward with fair to good sorting, a variety of cross-bedding is visible.
Karst	Limestone dissolution	A topography formed by the dissolution of limestone, dolomite, or gypsum creating caves, sinkholes, and underground drainage.
Lacustrine	Lake	Shales in thinly laminated beds.
	Beach	Well-sorted deposit that is longitudinally extensive along the ocean front but laterally limited in the landward direction. If prograding, these can form sheet sand units.
Paludal	Marsh or swamp	Both are organically rich. Marsh sediments produce fibrous peat, and swamps produce woody peat, which can eventually become coal.
Pelagic	Ocean	Sediments originating in ocean water.
Playa	Ephemeral lake	The lowest part of an undrained basin receives intermittent water. Characterized by clay, silt, sand, and soluble salts.
Turbidite	Continental shelf, slope, or in a lake	Sediments well graded and laminated from moving downslope in a body of water.

Stratigraphy

The hierarchy of names given to rocks is based upon the stratigraphic code. The breakdown of names can range from **group**, to **formation**, to **member**, to **bed**. Groups represent a collection of formations. For example, the Colorado Group represents several marine shales that have been grouped together.

Formations are names given to mappable rock units that have formed in a similar depositional environment at a similar point in time. Generally, they consist of a certain lithologic type or combination of types (Bates and Jackson 1984). They are laterally extensive enough to be mapped and identified in the field. Formations are usually named from where they are best exposed and have been described in detail. For example, the Lahood Formation is a Precambrian marine fan deposit with turbidite sequences. This formation is best exposed near Lahood, Montana, where there are coarse boulders mixed with sandy turbidite beds. To the north, this formation grades into finer-grained, sandy turbidite beds.

Formations are divided into members if there are distinctive characteristics that can be mapped or identified over significantly large lateral distances. For example, the Madison Limestone is divided into the Mission Canyon and Lodgepole members. Each member is distinguished by fossils and paleokarstic features. They are best exposed in the Little Rocky Mountains in northeastern Montana (Figure 2.32).

Formation names often change at state boundaries, which can be confusing for regional studies. For example, the Madison Limestone is

Figure 2.32 Mission Canyon member of Madison limestone exposed in the Little Rocky Mountains on the Fort Belnap Indian Reservation near Hayes, Montana.

Figure 2.33 Monarch coal bed from the Tongue River member of the Fort Union formation near Sheridan, Wyoming.

known as the Redwall Limestone in Arizona, where it weathers into a distinctive reddish wall exposed in the Grand Canyon.

Further subdividing of formations from members to beds is done if they are particularly distinctive. For example, within the Fort Union Formation in eastern Montana and Wyoming is the Upper Tongue River, Lebo Shale, and Lower Tullock members. Within the Tongue River member are laterally extensive coal beds known as the Anderson, Dietz, and Monarch beds. These are important because they form regional aquifers (Figure 2.33). Having an understanding of the local stratigraphy and rock formations is helpful in setting up the geologic framework for a groundwater-flow system.

Formation names are also given to distinct mappable units of igneous or metamorphic rocks. From the perspective of a hydrogeologist, formational units are grouped together based upon the hydraulic properties. Those with a similar enough hydraulic conductivity are combined together into one hydrostratigraphic unit (Chapter 3).

2.4 Structural Geology

Geologic formations may be folded, faulted, or tilted. These represent the response of geological materials to stresses. We live on a dynamic earth. Plate tectonic movements result in applied stresses that can cause geologic formations to be pulled apart, folded, or rumpled like carpet (Figure 2.34). These expressions of deformation are

Figure 2.34 Folded Cretaceous Kootenai formation in southwestern Montana.

known as **strain**. During these processes, the physical properties of formations can change, affecting porosity and fluid conductivity. The science of deciphering the physical orientation of rock relationships within an area is known as structural geology. The deformation and relative timing of tectonic stresses in large regional areas is the purview of **tectonics**.

Disruptive changes in rock formations require well-developed observational skills. The surface expressions of geologic units are identified in the field and located and recorded on a map. Included are rock-type descriptions, observation of fossils that can be correlated with other locations, and the orientation relative to a flat plane. This is done by taking strikes and dips of the bedding planes in sedimentary rocks, foliation orientations in metamorphic rocks, or flow banding in igneous rocks. The locations and orientations of faults are also recorded. The structurally disturbed geological materials can control the direction of groundwater movement and provide areas of higher or lower well yield. Not understanding the orientation of geological formations may result in drilling in the wrong location or missing a desired target.

Strike and dip

A fundamental step in interpreting the orientation of formations in space is taking a strike and dip. The **strike** is the azimuth orientation of the intersection of a horizontal plane with any inclined plane or surface (Figure 2.35). This is usually taken with a Brunton compass. A bull's eye

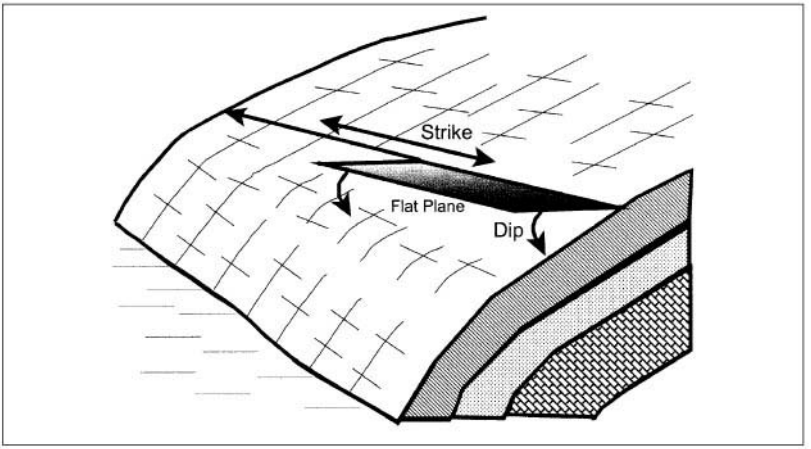

Figure 2.35 Diagram of strike and dip of inclined strata relative to a flat intersecting plane.

bubble indicates when the compass is being held level. The azimuth orientation is read from the compass (Figure 2.36). The strike is indicated with a line drawn on the map in the azimuth orientation. In order for the orientation of the compass to match the orientation of a topographic map in the field, one must first correct for the declination of the Earth's magnetic field. The declination is the horizontal angle between true north and magnetic north at a given location. This is always indicated at the lower left corner of a U.S. Geological Survey quadrangle topographic map.

Figure 2.36 Strike reading taken with a Brunton compass.

The **dip** is the angle from horizontal down to the inclined surface (Figure 2.37). The dip is read by holding the edge of the Brunton perpendicular to the strike line and moving a clinometer until its bubble is centered. Care must be taken to rotate the position of the Brunton back and forth slightly to obtain a maximum inclination for dip. Anything less than the maximum would be an apparent dip and not a true dip.

A field geologist will take several strike and dip readings around an area. In addition to strikes and dips, markings are also made of contacts between formations and faults that are observed. These are usually plotted on an aerial photo or on a topographic map. The different formations are given a distinctive pattern or color code and assembled into a geologic map. Areas that are covered or where faults are inferred or projected are indicated with dashed lines.

The strike and dip of a formation can be estimated from a geologic map if the contacts are accurately drawn on a topographic map, and not in a straight line. This process is known as a **three-point problem**. Three-point problems can be solved with data that do not outcrop if they are from boreholes, mine shafts, or other subsurface information when the dip is uniform (Bennison 1990). The strike is determined by locating where the outcrop of a particular bed intersects the ground surface at the same elevation at two locations. A straight edge is used to draw a line connecting these two points. A perpendicular line is drawn to a third point where the outcrop elevation

Figure 2.37 Dip angle read from a clinometer on a Brunton compass.

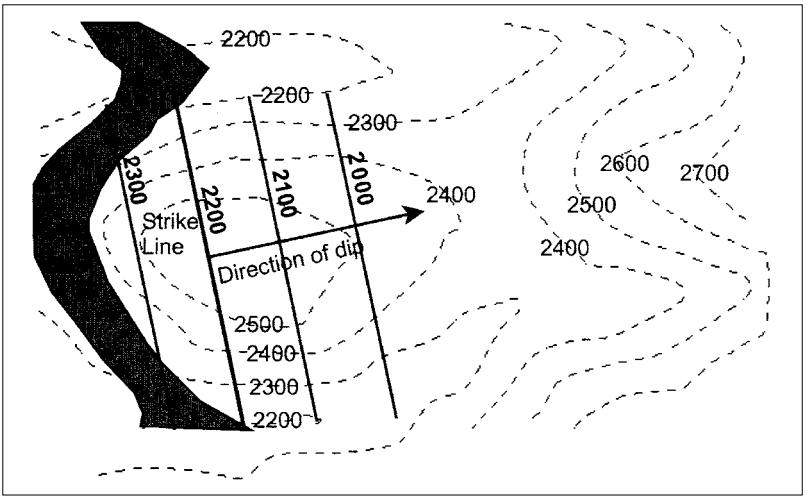

Figure 2.38 Illustration of a three-point problem used to determine the strike and dip from an outcrop and topographic map.

is known and the dip can be calculated or determined graphically. In Figure 2.38, the 2,200-ft contour is used to locate the strike line, and structure contours parallel to the 2,200-ft contour project the planar surface of the bed. Spacing is determined from the 2,300-ft line (another outcrop of known elevation). Doing a three-point problem enables you to know how deep a target is when drilling, projecting inclined planes, or constructing cross sections.

Example 2.7 In 1997, summer students of the Montana Tech hydrogeology field camp were involved in logging a drill hole for the Meadow Village subdivision near the Big Sky Ski Resort south of Bozeman, Montana. The target zone was the basal Cretaceous Kootenai Formation at approximately 1,000 ft (300 m) below the land surface. It was hoped that sufficient permeabilities could produce a well in excess of 100 gpm (500 m^3/day). Since the geologic layers dip approximately coincident with the topographic slope, it was decided to see if the formations being drilled through would be exposed in the canyon walls near Ousel falls in the south fork of the Gallatin River (Figure 2.39). The canyon cuts down a stratigraphic section. At the level of the river, the Thermopolis Shale, the unit just above the Kootenai Formation was exposed. It helped to compare the sedimentary layers exposed at the surface with the drill cuttings. A three-point problem determined the strike and dip of the Thermopolis Shale from the elevation of two exposures in the canyon and the intersection of this same unit in the drillhole. Unfortunately, tight cementation at depth limited the productivity of this well.

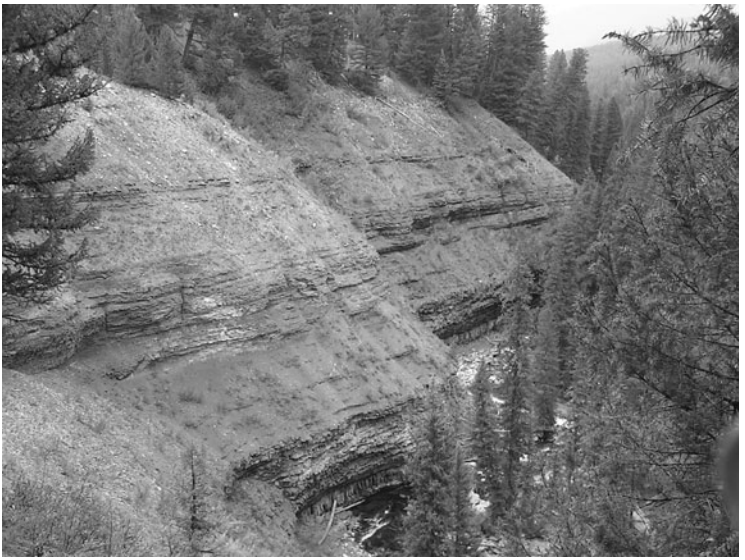

Figure 2.39 Blackleaf formation overlying Thermopolis Shale exposed in canyon wall near Big Sky ski resort in southwestern Montana.

Fold geometry

One form of strain is manifested when rocks subjected to stresses respond by folding. When strata become folded there are some basic parts of the fold that define their geometry. A plane that bisects the structure is known as the axial plane. On either side of the axial plane are the limbs. If the fold axis is oriented vertically, then the fold is symmetrical. If the fold axis is rotated, the fold is asymmetrical. Another feature associated with folds is the orientation of the fold trace (Figure 2.40). The fold trace is aligned at the top of the fold. If the fold trace is inclined from horizontal, then it is said to be plunging. Strike measurements of the axial plane provide the overall orientation of the structure.

In Figure 2.40, two basic types of folds are illustrated. In diagram A, the fold is a syncline, and in B and C anticlines are shown. In synclines the rocks in the middle are youngest, and the reverse is true of anticlines. Photographs of each are shown in Figures 2.41 and 2.42, respectively. The way to keep this straight is to try the exercise in Example 2.8.

Example 2.8 Take a paperback book or manual. If we use the convention of saying page one is the oldest and larger numbers represent younger beds, page one will be on the bottom. If the book is pushed together and the fold is anticlinal, then page one will be to the inside and the larger numbers will be on the outside. This becomes more obvious if the book is cut along the crest of the fold (not recommended if you like this book). In folding the book into a syncline, page one will now be to the outside. Again, refer to Figure 2.40.

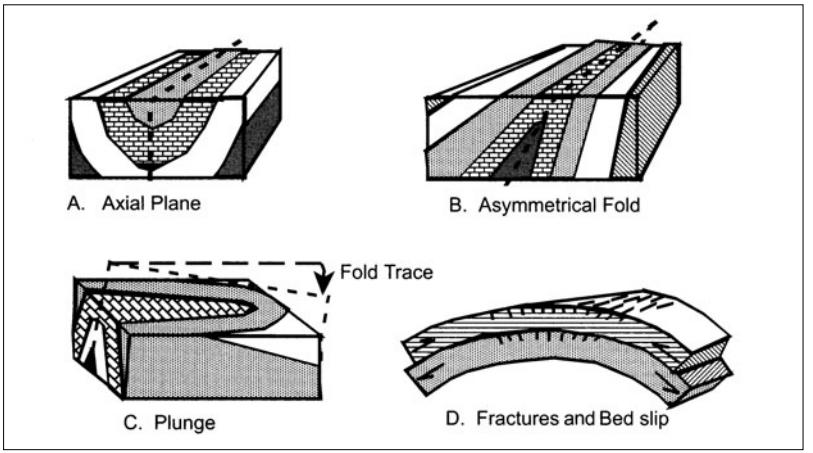

Figure 2.40 Fold geometry: A. axial plane, B. asymmetrical fold, C. plunging fold, and D. rotational fractures around axial plane and slip bed.

Faulting

Another form of strain is a brittle response where rocks rupture from the applied stresses. Rocks that merely break into a pattern of fractures with no displacement are known as **joints**. When rock masses move relative to each other, faulting occurs. If a rock mass breaks into two blocks, then the plane separating the blocks is the fault plane. Typically, this

Figure 2.41 Student standing in the axis of a synclinal fold.

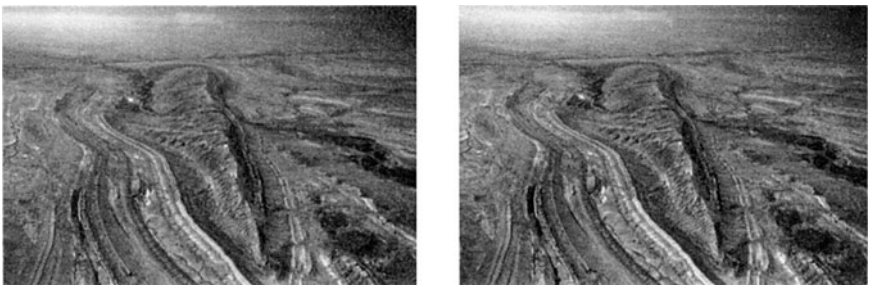

Figure 2.42 Stereo pair Big Sheep Mountain anticline, Bighorn Basin, Wyoming. (*Photos courtesy of Hugh Dresser*.)

plane is inclined. The block on the upside of the inclined fault plane is known as the **hanging wall**, and the lower block is known as the **footwall**. The term hanging wall originated from mining in mineralized areas where reverse faulting was common. The miner would stand on the footwall and hang his lantern on the hanging wall.

Imagine a stack of sedimentary layers from A to D, with layer A being the oldest. A fault divides the layers into two rock masses. If the hanging wall moves down relative to the footwall, the fault is said to be **normal** (Figure 2.43). In this scenario, younger rocks still overlie older rocks (a normal relationship). If the hanging wall has moved up relative to the footwall, the fault is a **reverse** fault. Here, older rocks are overlying younger rocks (an abby-normal or reverse situation). Normal and reverse faults tend to be at a relatively high angle (>45°) (Figure 2.44).

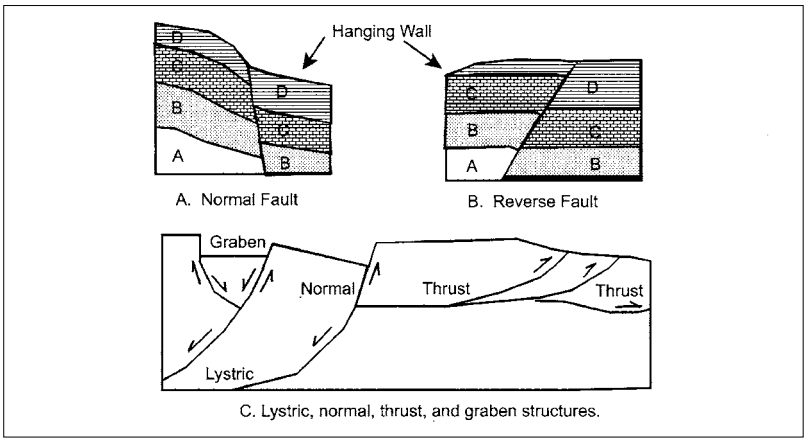

Figure 2.43 Fault structures: A. normal fault, layer A oldest, D youngest; B. reverse fault, layer A oldest; C. variety of structures in cross section, lystric (low-angle normal fault), normal fault, thrust fault (low-angle reverse fault), and a graben valley.

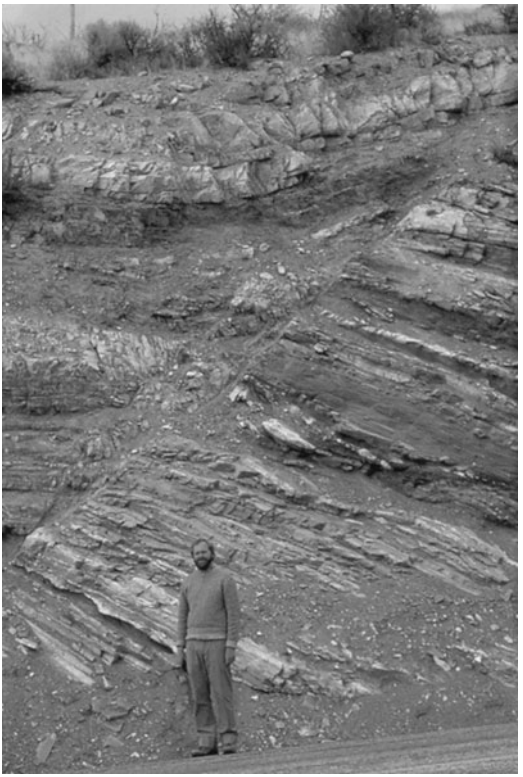

Figure 2.44 High-angle normal fault near the Ruby Mountains, Nevada.

In extensional areas, normal faulting is common with initial high-angle normal faults becoming more horizontal with depth. Where this occurs the fault is said to be **lystric** (Figure 2.43). Also, in extensional areas, a series of blocks may move relative to each other to accommodate the additional space. When this occurs, a whole block may move downward bounded by two normal faults to form a **graben** valley (Figure 2.45). The adjoining uplifted blocks are known as **horsts**. A good example of where this has occurred is in the basin and range province in Idaho, Nevada, Utah, and Arizona (Figure 2.46).

In compressional regimes, the rock masses tend to move into a more compact form. This is where reverse faulting is common. Low-angle reverse faults (commonly less than 15°) are known as **thrust** faults. Rock masses that move as thrust packages tend have high-fluid pressures involved to reduce the friction between rock masses (Hubbert and Rubey 1959). A reverse fault within the Koontenai formation is shown in Figure 2.47.

Faulting can occur within a thin zone or across a wide zone. This has important implications in forming boundary conditions for fluid flow

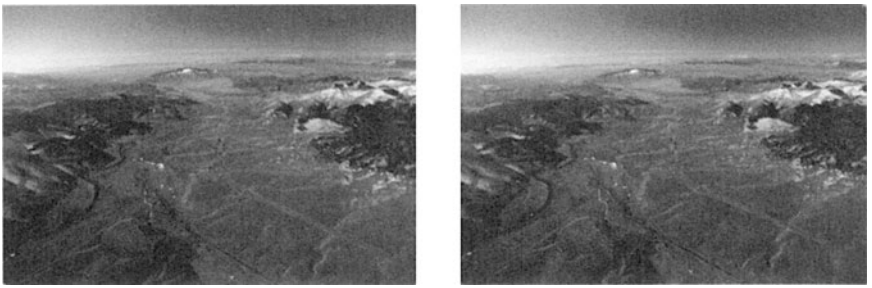

Figure 2.45 Stereo pair graben valley structure near Divide, Montana. (*Photos courtesy of Hugh Dresser*.)

Figure 2.46 Horst mountains and graben valleys of the basin and range near Salt Lake City, Utah.

Figure 2.47 Reverse faulting in the Koontenai formation in southwestern Montana. (*See also Figure* 2.34.)

Figure 2.48 Fault zone approximately 100 ft (30 m) wide at Double Springs, Idaho as a result of the Borah Peak earthquake, October 1984.

(Figure 2.48). A wide shear zone may serve as a conduit to allow confined aquifer waters to move upward. If an aquifer unit is cut by a fault that brings a confining unit next to a permeable unit, the fault may represent a barrier plane to flow.

Other observations in structures

As a geologist maps a structure, such as an anticline, there are other smaller-scale features that can be observed that contribute to understanding the larger structure. For example, one can observe smaller-scale folds within the larger structure known as parasitic folds (Figure 2.49). The strike of these will be similar to the larger structure; however, there is a systematic rotational component depending on which limb of the axis the minor structures are observed (Figure 2.40D). This same phenomenon is true of fractures. The outer edges of strata around a fold, whether the structure be an anticline or a syncline, are subject to extensional stresses. The strata inside a fold are subject to compressional forces. This can greatly affect the fluid flow properties along strike of a structure.

Example 2.9 Within the Paradox basin near Moab, Utah, along the Cane Creek anticline fracture permeabilites and associated enhanced flow conditions were described by Huntoon (Figure 2.47). A potash mine was developed 3,000 ft below the ground surface in a sylvite ore zone, accessible by a 2,790-ft deep shaft along the flank of the Cane Creek anticline. Mining was conducted by room and pillar method and was plagued by gaseous conditions that are common in the Pennsylvanian Paradox Formation and overlying Honaker Trail Formation (Huntoon 1986).

Figure 2.49 Parasitic fold 1 m across within an anticlinal fold several hundred meters wide.

Geologic studies in the Paradox basin reveal that salts within the basin behave plastically. Burial of the salt beds by younger sediments provided continuous lithostatic loading, which when differentially applied resulted in flow structures forming during the accumulation period (Huntoon 1986). During the formation of the Cane Creek anticline, salt beds slowly migrated and bulged in the crest of anticlinal folds. While bulging occurred, the overlying rocks at the crest of fold experienced extensional fracturing and normal faulting (Figure 2.40D) very closely aligned with the strike of the Cane Creek Anticline (Figures 2.50 and 2.51). Beds closest to the mine area are under compression.

It was decided that a solution mining method would be employed to remove the salt by flooding the 150 mi of mining cavities and pumping this to the surface (Huntoon 1986). The Texasgulf 7 well was drilled in the crest of the anticline. The loss of circulation during drilling in the upper extensional beds and subsequent breakthrough into the mine cavity and rapid draining of the drilling fluid provides an interesting story.

Structural effects in karst areas

Karst is a word that was derived from the word "kras" from vicinity of Trieste, Italy, and adjacent Slovenia, which means bare, stony ground (Huntoon 1995 and Quinlan et al. 1996). It does not have a universally accepted definition, but dissolution is its primary process in developing a distinctive surface topography, a topography characterized by sinkholes, caves, and underground drainage (Bates and Jackson 1984).

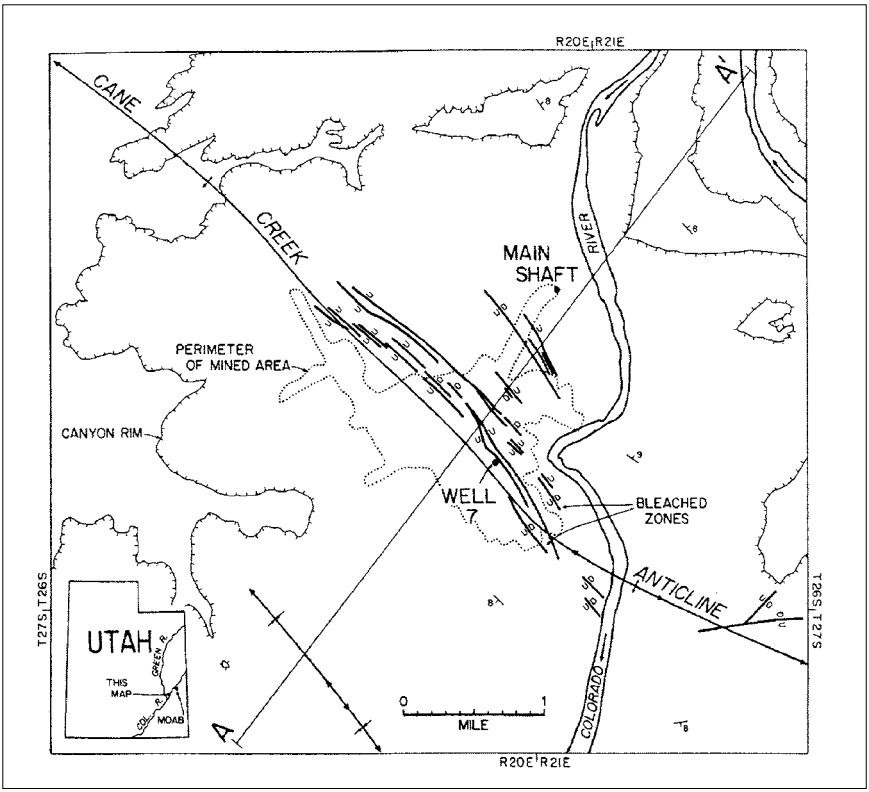

Figure 2.50 Extensional faults along the Cane Creek anticline near Moab, Utah. [*From Huntoon (1986). Reprinted with permission of the National Groundwater Association (1986).*]

Karstic conditions often develop from dissolution of the host rock, along fractures that become enlarged from millimeters to centimeters and even meters, resulting in a triple porosity system (Quinlan et al. 1996) (Figure 2.52). This is significantly different from a porous media system, which tends to have enhanced permeability from secondary porosity features such as jointing and faults.

In Chapter 5, in a discussion of groundwater flow, Darcy's law describes how the volume of groundwater flow is proportional to the hydraulic conductivity and the hydraulic gradient. In porous media systems, the dominant controlling factor is the hydraulic conductivity. Hydraulic gradient is only of incidental concern because production zones in indurated nonsoluble rocks are concentrated within areas of the highest secondary porosity (Huntoon 1995). In Section 2.4, extensional stresses were described in fold structures resulting in enhanced permeability along the strike of such structures. Here, the extensional fracturing was responsible for creating the pathways that dominate fluid flow. In short, the

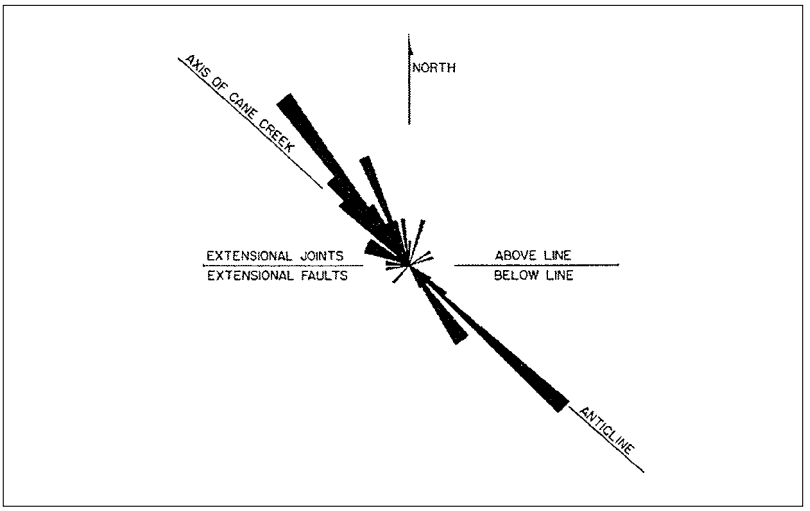

Figure 2.51 Strike relationship of 46 sets of extensional joints and 24 extensional faults near Moab, Utah. [*From Huntoon (1986). Reprinted with permission of the National Groundwater Association* (*1986*).]

largest fractures automatically have the greatest ability for fluid flow, thus resulting in the highest hydraulic conductivities.

It is a mistake to assume karstic flow systems developed in the same way. Many hydrogeologists or geologists may believe that cave systems

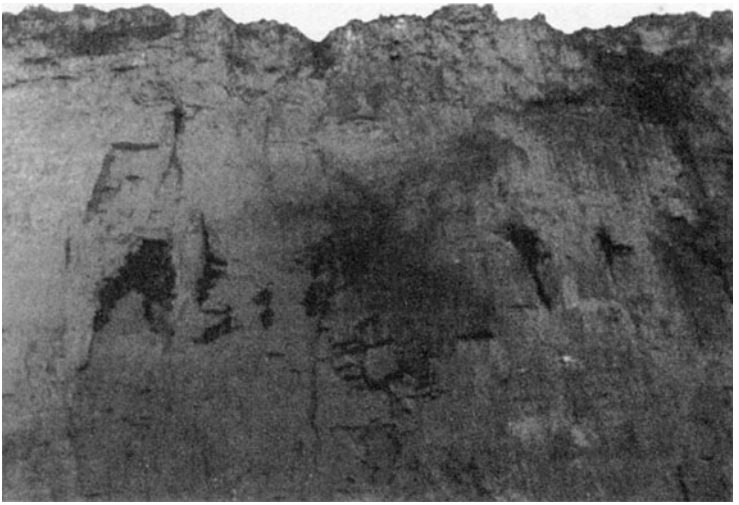

Figure 2.52 Keyhole caves developed in the upper 300 ft of the Mississippian Redwall Limestone, Marble Canyon, Arizona, illustrating triple porosity in one location. (*Photo courtesy of Peter Huntoon.*)

and other karstic features developed where the fractures were largest. However, this is not necessarily true. In soluble host rock karst systems, the greatest fluid flow occurs in the areas of highest hydraulic gradients in concert with available carbon dioxide in the recharge area. Here, fractures and other conduits are enlarged by dissolution of the host rock that develop in conduit systems parallel to fluid flow. There is an organizational hierarchy of dissolution tubes within a complex network that is progressively more organized in the "down gradient" direction (Huntoon 1995). This development can ignore preexisting fracture systems developed by tectonic processes. Furthermore, karst systems change dynamically over time as a result of changes in stage levels and tectonic forces, which result in different flow paths being developed (Quinlan et al. 1996), that may even crosscut older systems (Huntoon 1995).

The network of conduit tubes within a karst aquifer network have multiple interconnections (Huntoon 1995). For this reason, there are numerous opportunities for water to shunt across to other areas in the flow system, particularly in unconfined karst aquifers. The direction of flow and multiple pathways appears to be stage dependent. Tracer studies (Chapters 13, 15) reveal that although they are introduced at a single injection point, they can emerge at diverse exit points (Mills 1989; Huntoon 1995). The scary thing is that at certain stage elevations, springs may be deemed safe because the water-quality data look clean. However, if the stage changes, then a once clean spring may become contaminated just because shunting within the flow system has changed.

Another application of field studies involves basin circulation and regional flow studies. Many carbonate systems outcrop along the upper elevations of mountains in higher precipitation areas. Persons performing fieldwork may erroneously believe that surface streams that enter karst systems account for the water that recharges a basin. In the Rocky Mountain region, cave systems have developed along the flanks of uplifted mountain ranges that reject recharge through a decrease in transmissive properties in the basinward direction (Huntoon 1985).

Example 2.10 Wyoming lies within an area characterized by crustal shortening. This results in elongated mountain uplifts and deep sediment-fllled basins. The mountain uplifts are mountain blocks that have ridden up thrust-fault ramps from Laramide deformation (Huntoon 1985). One should notice that there is a homoclinal margin that parallels uplift and a fault-severed margin (Figure 2.53).

Rocks that outcrop along the homoclinal margins constitute an ideal setting for recharge because these rocks are hydraulically connected to rocks in the basins. In reality, transmissivities within the carbonate rocks decrease basinward, and much of the apparent recharge is rejected through surface springs that discharge at the toe of the mountain front (Huntoon 1985). Huntoon (1985) discusses over 10 cave or sinkhole systems within the Trapper

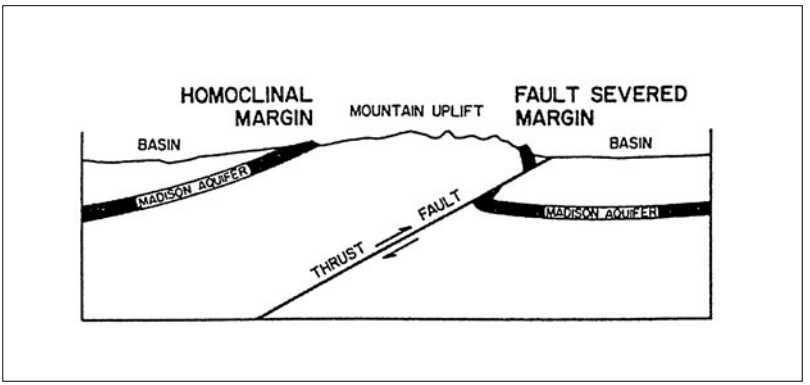

Figure 2.53 Generalized cross section in the Wyoming foreland province. [*From Huntoon (1985). Reprinted with permission from the NGWA (1985).*]

Canyon and Medicine Lodge drainages that lie on the western slope of the Bighorn Mountains (Figure 2.54). Documented stream gauging and other fieldwork indicate that only 25 to 35% of the water observed to enter these cave systems actually may be recharging the basin aquifers (Huntoon 1985).

Apparently, the decreased transmissivities can be explained by the difference in hydraulic gradients found in the recharge areas compared to average gradients within the basins in the same aquifer. In the recharge areas, gradients averaged 400 ft/mi (0.076 ft/ft) compared to an average of 40 ft/mi (0.0076 ft/ft) in the basin (Huntoon 1985). The high gradients were responsibie for developing a karst system with cave-sized conduits (Figure 2.55). The

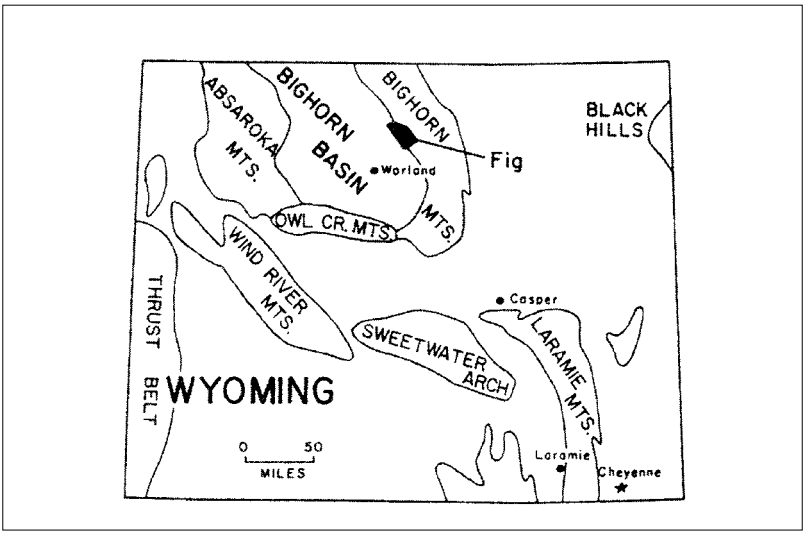

Figure 2.54 Location of recharge areas on east side of Bighorn Basin. [*From Huntoon (1985). Reprinted with permission from the NGWA (1985).*]

Figure 2.55 P-bar cave in the Big Horn dolomite, Big Horn Mountains, Wyoming.

discharge springs at the toe of the drainages are coincident with the decreases in hydraulic gradient and subsequent decreases in transmissivities. A similar phenomenon was observed in the Madison aquifer in the Black Hills (Rahn and Gries 1973).

Hydrogeologic field work in karst systems is markedly different from the traditional approaches used in nonsoluble rock systems such as sedimentary rocks or igneous rock systems with significant secondary porosity. This is why a whole chapter is devoted to karst hydrogeology (Chapter 13), and additional helpful information is found in Chapters 14 and 15, where there is additional discussion on tracer tests.

2.5 Geologic Time

In Section 2.4 is a discussion of stratigraphic hierarchy where geologic units are given formation names, or subdivided further into members or beds. Time units are also assigned with formation names such as the Mississippian Madison Formation or the Permian Quadrant Quartzite. The various geologic time units are divided into Eons, Eras, Periods, and Epochs in units of millions of years (Table 2.5; Geosociety 1999; Gholam et al. 2006).

Geologists have distinguished the different time units in the geologic time scale (Table 2.5) based upon absolute and relative dating methods including the fossil record. The Phanerozoic eon represents the eon of life. Eras (old life, middle life, and recent life) represent times of significant species of life forms. For example, trilobites lived during the

TABLE 2.5 Geologic Time Scale

Eon	Era	Period	Epoch	Millions of years before present
	Cenozoic	Quaternary	Holocene	0.01—present day
			Pleistocene	1.8–0.01
Phanerozoic		Tertiary-Neogene	Pliocene	5.3–1.8
			Miocene	23.9–5.3
		Tertiary-Paleogene	Oligocene	33.7–23.9
			Eocene	54.9–33.7
			Paleocene	65.0–54.9
	Mesozoic	Cretaceous		144–65
		Jurassic		206–144
		Triassic		248–206
	Paleozoic	Permian		290–248
		Carboniferous-Pennsylvanian		323–290
		Carboniferous-Mississippian		354–323
		Devionian		417–354
		Silurian		443–417
		Ordovician		490–443
		Cambrian		543–490
Proterozoic	Late	Precambrian		900–543
	Middle			1600–900
	Early			2500–1600
Archean	Late			3000–2500
	Middle			3400–3000
	Early			3960–3400
Azoic				4560–3960

SOURCES: www.geosociety.org/science/timescale and Kazemi et al. (2006).

Paleozoic era, but became extinct at the end of the Permian Period, while dinosaurs only existed during the Mesozoic era. Periods are further divisions of time representing when significant species of animals appeared, such as the Devonian period (period of fishes) named after its type locale in Devonshire England. Epochs represent additional divisions of time devoted to most recent era (Cenozoic). The Pleistocene epoch is when the earth experienced its most recent ice ages and the Holocene represents time since the last glacial recession.

Absolute time is where exact times and dates can be given, for example, through counting tree rings or other measurable entities. Absolute dating methods typically include radiometric dating methods using unstable isotopes. Recall from basic chemistry that isotopes of a given element have the same number of protons (same atomic number) but differing numbers of neutrons, thus differing in atomic mass. Isotopes that are unstable will spontaneously emit radiation energy through a process known as decay. When one half of the original parent material decays into its daughter product, one half-life is said to have occurred.

The various isotopes have fixed decay rates based upon the temperatures and pressures that exist in the outer layers of the earth. Tritium (^{3}H), for example, has a half life of 12.43 years, therefore it can be used to age date relatively young waters (Kazemi et al. 2006). Potassium (^{40}K)-Argon (^{40}Ar) ratios are used to date age old rocks because of the half-life of 1.25 billion years (USGS 2001). The relationship of time, parent material, daughter products, and decay rate are given in Equation 2.1 (USGS 2001). Radiometric dates in rocks are most commonly obtained from igneous rocks.

$$t = \frac{1}{\gamma} \ln \left(\frac{D}{P} \right) \tag{2.1}$$

where t = age of the rock or water sample
γ = appropriate decay constant
ln = natural log to the base of e
D = number of atoms of the daughter product today
P = number of atoms of the unstable parent material today

Relative dating is where rock relationships and geologic principles are used to determine which rock unit is oldest in sequence without knowing its exact age. The most common geologic principles are listed in Table 2.6 and can be helpful in reconstructing the geologic history. Sometimes faulting or igneous intrusions are responsible for affecting the groundwater-flow paths, so understanding the geology is a must.

Unconformities are generally known by three types: 1) angular (where sedimentary layers meet at an angle to the erosional surface),

TABLE 2.6 Geologic Principles (modified after www.earth.rochester.edu)

Geologic principle	Description
Principle of original horizontality	Geologic materials are basically laid out horizontally (lava flows, river deposits, etc).
Principle of cross-cutting relationships	If a geologic unit cuts across another unit, it is younger than the one it cuts.
Principle of superposition	The oldest rocks will be on the bottom, successive layers are correspondingly younger.
Principle of lateral continuity	Geologic units are laterally continuous in all directions until they thin or pinch out or reach a boundary.
Principle of inclusions	The inclusions or pieces of any rock that become included in another rock are older than the rock they were included in.
Principle of unconformities	Unconformities represent hiatuses in time from erosion, non-deposition, or some other geologic activity.

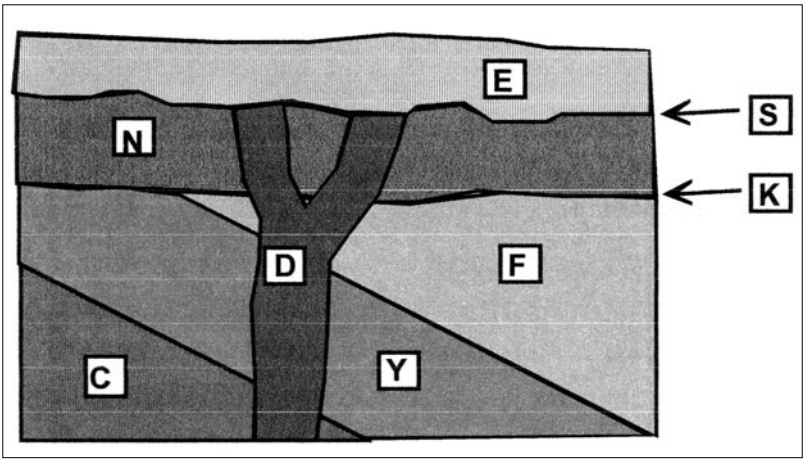

Figure 2.56 Geologic history, where units C, Y, and F are oldest followed by uplift and tilting, then angular unconformity K, layer N, and then dike D. Erosional nonconformity S is followed by layer E, the youngest unit.

2) disconformity (where parallel layers have missing layers between younger and older layers), and 3) nonconformity (where sedimentary rocks come in contact with igneous or metamorphic rocks). A simple geologic history is shown in Figure 2.56.

2.6 Using Geologic Information

The geology of hydrogeology could easily be the topic of many chapters or a book. Geologic concepts and examples are scattered throughout this book, because geology is inseparable from groundwater systems. The geologic features form the framework and boundary conditions for groundwater-flow systems. The more case histories and field examples one studies and experiences, the larger the library of examples one can draw from to solve problems.

If you have avoided studying geology because of the inherent uncertainty in knowing what is occurring at depth, why study hydrogeology? It has the same types of uncertainties. The author's experience is that being able to know exactly what is occurring at depth is an uncomfortable area for many engineers, yet many will think nothing of using field data provided by geoscientists in a computer simulation model or design process. If you use geologic information, you have a responsibility to make sure that the constraints are also known. You are responsible for the information you use in a design or simulation. Take a course or two in geology or read up on it if it is a weakness in your life. It will make you a better professional.

References

Allis, R.G, and Lumb, J.T., 1992. The Rotarua Geothermal Field, New Zealand: Its Physical Setting, Hydrology, and Response to Exploitation. *Geothermics*, Vol. 21, No. 1/2, pp. 7–24.

Alt, D., and Hyndman, D.W. 1995. *Northwest Exposures, A Geologic Story of the Northwest*. Mountain Press, Missoula, MT, 443 pp.

Bates, R.L., and Jackson, J.A, (eds.), 1984. *Dictionary of Geological Terms, 3rd Edition*. American Geological Institute, Anchor Press, Garden City, NY, 571 pp.

Bennison, G.M., 1990. *An Introduction to Geological Structures and Maps. Boutledge*. Chapman and Hall, New York, 69 pp.

Bowen, N.L., 1928. *The Evolution of the Igneous Rocks*. Princeton University Press, Princeton, NJ.

Custer, S.G., Michels, D.E., Sill, W., Sonderegger, J.L., Weight, W.D., and Woessner, W.W., 1994. *Recommended Boundary for a Controlled Groundwater Area in Montana Near Yellowstone Park*. Water Resources Division, National Park Service, Fort Collins, CO, 29 pp.

Davis, S.N., and Turk, L.J., 1964. Optimum Depth of Wells in Crystalline Rock. *Ground Water*, Vol. 2, No. 2, pp. 6–11.

Driscoll, F.G., 1986. *Groundwater and Wells*. Johnson Screens, St. Paul Minnesota, 1108 pp.

Domenico, T.A., and Schwartz, F.W., 1990. *Physical and Chemical Hydrogeology*. John Wiley & Sons, New York, 824 pp.

Fetter, C.W., 1994. *Applied Hydrogeology, 3rd Edition*. Macmillan College Publishing Company, New York, 691 pp.

Folk, R.L., 1966. A Review of Grain-size Parameters. *Sedimentology*, Vol. 6, Elsevier Publishing, Amsterdam, pp. 73–93.

Freeze, A., and Cherry, J., 1979. *Groundwater*. Prentice-Hall, Upper Saddle River, NJ, 604 pp.

Gholam, A.K., Lehr, J. L., Perrochet, P., (2006). *Groundwater Age*. John wiley & sons, Inc., Hoboken, New Jersey, 325 pp.

Golddich, S.S., 1938. A Study in Rock Weathering. *Journal of Geology*, Vol. 46, pp. 17–58.

Hubbert, M.K., and Rubey, W.W., 1959. Role of Fluid Pressure in Mechanics of Overthrust Faulting: I, Mechanics of Fluid-filled Porous Solids and its Application to Overthrust Faulting. *Geological Society American Bulletin*, Vol. 70, pp. 115–166.

Huntoon, W.P. 1985. Rejection of Recharge Water from Madison Aquifer Along Eastern Perimeter of Bighorn Basin, Wyoming. *Ground Water*, Vol. 23, No. 3., pp. 345–353.

Huntoon, W.P., 1986. Incredible Tale of Texasgulf Well 7 and Fracture Permeability, Paradox Basin, Utah. *Ground Water*, Vol. 24, No. 5, pp. 644–653.

Huntoon, W.P., 1992. Hydrogeologic Characteristics and Deforestation of the Stone Forest Karst Aquifers of South China. *Ground Water*, Vol. 30, No. 2, 162 pp.

Huntoon, W.P., 1995. Is it Appropriate to Apply Porous Media Groundwater Circulation Models to Karstic Aquifers? *Groundwater Models for Resources Analysis and Management*, Aly I. El-Kadi (ed.), CRC Press, Boca Raton, FL, pp. 339–358.

Huntoon, W.P., 1997. The Case for Upland Recharge Area Protection in the Rocky Mountain Karsts of the Western United States. In *Karst Waters and Environmental Impacts*, Gunay, G., and Johnson, A.I., (eds.), A.A. Balkema, Rotterdam/Brookfield, 1997.

Mills, J.P., 1989. *Foreland Structure and Karstic Ground Water Circulation in the Eastern Gros Ventre Range, Wyoming*. Master's Thesis, University of Wyoming at Laramie, 101 pp.

Quinlan, J.F., Davies, G.J., Jones, S.W., and Huntoon, P.W., 1996. The Applicability of Numerical Models to Adequately Characterize Ground-Water Flow in Karstic and Other Triple-Porosity Aquifers, *Subsurface Fluid-Flow (Ground-Water and Vadose Zone) Modeling*, ASTM STP 1288, Joseph D. Ritchey and James O. Rumbaugh, (eds.), American Society for Testing and Materials, pp. 115–133.

Rahn, P.H., and Gries, J.P., 1973. Large Springs in the Black Hills, South Dakota and Wyoming, *South Dakota Geology Survey Report of Investigation 107*, 46 pp.

Sorey, M.L. (ed.), 1991. Effects of the Potential Geothermal Development in the Corwin Spring's Known Geothermal Resources Area, Montana, on the Thermal Features of

Yellowstone National Park, *U.S. Geological Survey Water-Resources Investigations Report 91-4052*, pp. A1–H12.
Streckeisen, A.L., 1976. To each Platonic Rock its Proper Name. *Earth Science Review*, Vol. 12, pp. 1–34.
Turner, F.J., 1968. *Metamorphic Petrology*. McGraw-Hill, New York, 366 pp.

Web Resources

www.earth.rockester.edu.2006.
www.geosociety.org/science/timescale.1999.
http://pubs.usgs.gov/gip/geotime/radiometric.htm 2001.

This page intentionally left blank

Chapter

3

Aquifer Properties

It is important to be able to translate the geology (Chapter 2), when it becomes saturated, into hydrogeology. The physical properties of geologic materials control the storativity and ability of fluids to move through them. Rock units that do not allow fluids through them become barriers to fluid flow and in turn change the direction of groundwater movement (Chapter 5). Other features such as fault zones may serve as conduits to fluid flow or act as barriers. In this chapter the physical properties of saturated geologic materials are presented to provide a basic understanding of aquifers, confining layers, and boundary conditions as a basis for understanding groundwater flow presented in Chapter 5. Boundaries are often determined directly through drilling (Chapter 8), pumping tests (Chapters 9 and 10), or geophysical methods (Chapter 4).

3.1 From the Surface to the Water Table

When precipitation hits the land surface, some water enters the soil horizon. This process is known as **infiltration**. Water that accumulates on the surface faster than it can infiltrate becomes **runoff** (Chapter 1, Figure 1.1). The rate at which water infiltrates or runs off is a function of the physical properties of the surficial soils. Some of the important factors appear to be thickness, clay content, moisture content, and intrinsic permeability of the soils' materials (Baldwin 1997). (Additional discussion on intrinsic permeability is given in Section 3.2). Infiltrating water that encounters soils with higher clay content tends to clog the pores, causing precipitation to mound up and run off, unless they are exceedingly dry (Stephens 1996). Sandier soils promote infiltration and exhibit less vegetative growth, while soils with a higher clay content appear to promote plant growth. Glaciated areas provide an example of an environment where many soil types can be found. Glacial sediments deposited via moving water become stratified or layered and tend to be

Copyright © 2008, 2001 by The McGraw-Hill Companies, Inc. Click here for terms of use.

Figure 3.1 Terminal moraine in southwestern Montana, indicating poorly sorted sediments.

well drained; examples include outwash deposits, kames, and eskers. Sediments transported by ice that accumulate along the sides and end of a glacier are poorly sorted and contain a higher content of clay and silt; examples include lateral and end moraines, which are poorly drained (Figure 3.1). In the field well-drained soils can be distinguished by lessor plant growth and a rougher appearance (Figure 3.2). Once

Figure 3.2 Gravel channel exposed in road cut near Sheridan, Wyoming. Coarser sands lack vegetation, while finer-grained upper and lateral floodplain deposits support more vegetative growth.

infiltration occurs, any groundwater that descends below the rooting depth eventually reaches the regional water table as recharge. This has serious implications for dissolved chemicals that accompany the descent waters.

Between the soil horizon and the regional water table is an area referred to as the vadose zone (Figure 3.3). The ability of the vadose zone to hold water depends upon the moisture content and grain size. Wells completed in the vadose zone will have no water in them, even though the geologic materials appear to be wet, while wells completed in saturated fine-grained soils will eventually contain groundwater. Chapter 12 is devoted to the vadose zone and its properties and field methodologies.

Another part of the vadose zone immediately above the regional water table is the capillary fringe. The capillary fringe is essentially saturated, but groundwater is being held against gravity under negative pressure, a phenomenon known as capillarity. In groundwater applications atmospheric pressure is referenced as zero pressure. The water table for example, is at atmospheric pressure, while below the water table, water is under a pressure greater than atmospheric. Water in the capillary fringe and the rest of the vadose zone is under a pressure less than atmospheric. This same phenomenon is observed when one puts a paper towel into a pan of water. The water is attracted to the surfaces of the towel fibers being drawn up through very small pore tubes between the fibers. Similarly, in the capillary fringe groundwater seeks to wet the surfaces of geologic materials with an attraction greater than

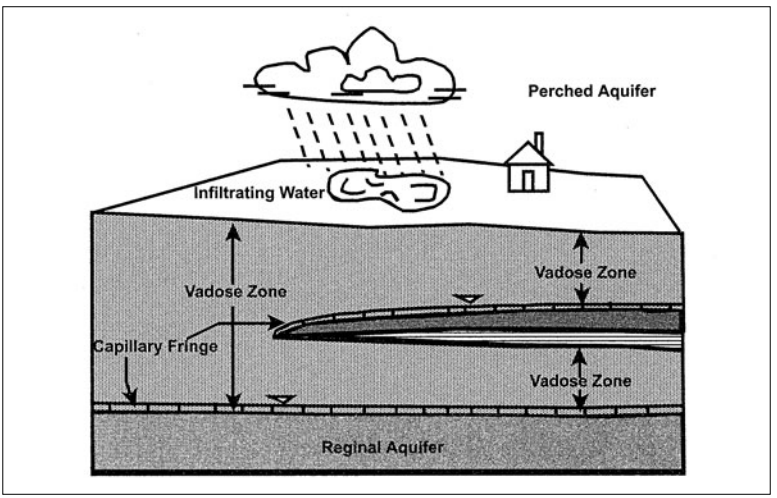

Figure 3.3 Schematic of the vadose zone, infiltrating water, and the capillary zone.

the force of gravity. The thickness of the capillary fringe is grain-size dependent. The finer grained the material, the thicker the capillary fringe because of the smaller pore throats, increased surface area, and surface tension (Chapter 12).

When drilling wells or installing monitoring equipment, one must also be careful that the first water encountered is actually the regional water table and not a **perched aquifer**. Perched aquifers represent infiltrating groundwater that accumulates over confining layers of limited areal extent above the regional water table (Figure 3.3). Perched aquifers may be capable of sustaining enough water for a few residences, but generally not enough for many residences or long-term production. Several water levels in wells in the same area would help one determine whether a perched water table exists or not. Aquifers are defined and discussed in Section 3.4.

Example 3.1 A consulting company was evaluating the drilling depths for production wells for a proposed subdivision. Estimates were being made based upon existing wells in the area. The evaluator did not realize that there were wells completed in a local perched aquifer and regional unconfined aquifer. In the end, he averaged the well depths to estimate drilling costs. This of course resulted in bidding way too low and the consulting company losing money. The crux of the problem was in failing to understand the flow system and that the differences between well depths represented two separate aquifers.

3.2 Porosity and Aquifer Storage

The volume of water that an aquifer can take into or release from storage for a given change in head is often determind by its porosity. The porosity of earth materials is a function of size, shape, and arrangement or packing. The ability of water to move through an aquifer is described by its permeability or hydraulic conductivity (see Section 3.3).

Porosity

The **porosity** is represented as the nonsolid fraction of geologic materials. This is where fluids can be held. In the vadose zone, the porosity or open spaces are filled with air and water (Section 3.3). The total porosity of geologic materials expressed as a percent is represented by:

$$\eta\% = \frac{V_V}{V_T} \times 100\% \tag{3.1}$$

where η = porosity
V_V = volume of the void
V_T = total volume

Figure 3.4 Secondary porosity from faulting. A spring is emanating from the fault zone.

Porosity is often broken down into primary and secondary porosity. Primary porosity is the void space that occurred when the rock or geologic material formed. Secondary porosity refers to openings or void space created after the rock formed (Figure 3.4). Examples of these are given in Table 3.1.

Generally, each aquifer or confining layer is modeled using a single overall porosity unless its lateral changes are known through a distribution of cores. In fractured rock, such as a fractured sandstone or granite, a "dual-porosity" model may be more appropriate. A dual-porosity model assigns a porosity to the fracture zone (secondary porosity) and to the geologic block materials (or rock matrix) (see Chapter 10). Carbonate karstified systems may have a triple porosity where there are microscale and two levels of macroscale pore spaces (larger fractures and caves, see Section 2.6 and Chapter 14). The larger-scale fractures may lead to misleading interpretations of unlimited supply.

TABLE 3.1 Example of Primary and Secondary Porosity

Primary porosity	Secondary porosity
Vesicles	Faults
Intergranular pores	Fractures
Interlayer partings and unconformities	Solution channels
	Stylolites
Spaces between lava flows	Enhanced pathways from plants and animals
Lava tubes	
Intercrystalline pores	

Example 3.2 When John Sonderegger worked for the Alabama Survey, he heard about a pumping test on a Huntsville municipal well (pumped at approximately 2,000 gpm, 7.57 m^3/min) that ran for a week with only a couple of feet of drawdown. The test was continued to 10 days and ran out of water on the 8th or 9th day with a sustainable pumping rate of only a couple of hundred gpm or less (0.76 m^3/min).

Of the total porosity of geologic materials, there is a portion that will drain freely by gravity and an amount retained in the geologic materials. The volume of water that will drain by gravity per unit drop in the water table per unit volume of aquifer is referred to as the **specific yield** (S_y). The water that remains clinging to the surfaces of the solids in the interstices is called the **specific retention** (S_r). Although they are strictly different things, the specific yield is often used as an estimate for the **effective porosity** (η_e), a term used to describe the porosity available for fluid flow. It should be noted that specific yields are estimated from vertical drainage tests, while effective porosities are generally used for horizontal flow calculations, such as to calculate groundwater velocities (Chapter 5). Although one may generally assume that the specific yield and the effective porosity are the same for a coarser-grained aquifer, in some soils there may be a high content of soil aggregates and water may become tied up in dead-end pore spaces. This results in the effective porosity and specific yield being significantly different (Cleary et al. 1992). The specific yield and specific retention make up the total porosity, expressed in the following relationship.

$$\eta = S_Y + S_R \tag{3.2}$$

Example 3.3 Suppose you have a 5-gal bucket full of dry sandy material. You add just enough water until the sand becomes saturated at the 5-gal mark (Figure 3. 5). Assume that it takes exactly 1 gal to fill all of the pores. From Equation 3.1, the percent porosity equals:

$$\eta = \frac{1 \text{ gal}}{5 \text{ gal}} \times 100\% = 20\% \tag{3.3}$$

If a hole was drilled into the bottom of the bucket and the water allowed to drain into a container until it stopped, the specific yield and specific retention could be determined. Assume the amount of water that drained was 0.9 gal. By definition, the specific yield would be:

$$S_Y = \frac{0.9 \text{ gal}}{5 \text{ gal}} = 0.18 \tag{3.4}$$

From Equation 3.4 the effective porosity would be estimated to be 18%. The specific retention would be 0.02 or 2% of the total volume. In most sand and gravel aquifers, the specific retention is quite low (<5%).

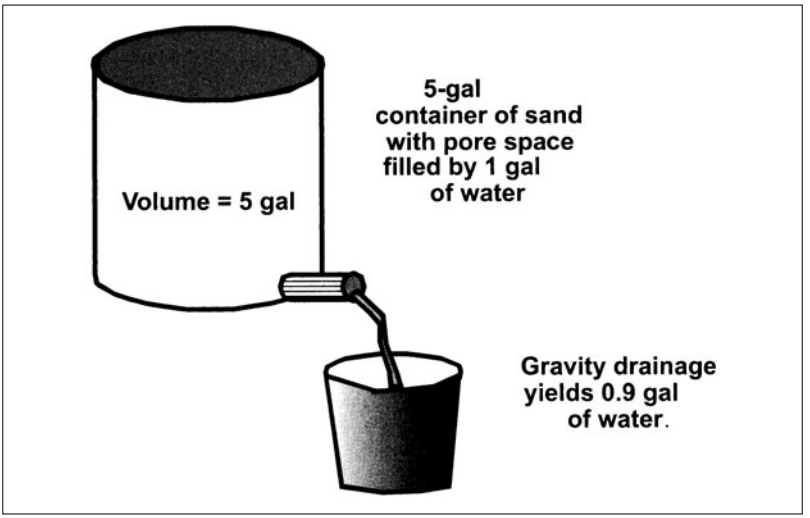

Figure 3.5 Illustration of the concept of specific yield. A 5-gal bucket of sand is filled to the top with 1 gal of water; 0.9 gal drains out by gravity, while 0.1 gal is retained in the pore spaces.

As the grain size decreases, the total porosity increases (Table 3.2, Figure 3.6), but the specific retention increases as well. The smaller the grain size, the greater the surface area for water to cling to.

One notices from Table 3.2 that the porosity of sand and gravel together is less than that of either material separately. This is a function of the packing of grains and sorting. Sorting was described in Chapter 2 and is an expression of ranges of grain sizes. The packing of grains is a function of the size, shape, and arrangement of grains. If one takes spheres of equal size and arranges them, there are two end member packing arrangements that represent the most porous packing (cubic packing) and the least porous (rhombohedral packing) (Figure 3.7). Cubic packing is where grains are stacked vertically on top of one

TABLE 3.2 Ranges of Porosities in Typical Earth Materials [Modified after Driscoll (1986); Freeze and Cherry (1979); Roscoe Moss (1990)]

Unconsolidated materials	η%	Consolidated rock	η%
Clay	40–70	Sandstone	5–35
Silt	35–50	Limestone/dolomite	<1–20
Sand	25–50	Shale	<1–10
Gravel	20–40	Crystalline rock (fractured)	<1–5
Sand and gravel	15–35	Vesicular basalt	5–50

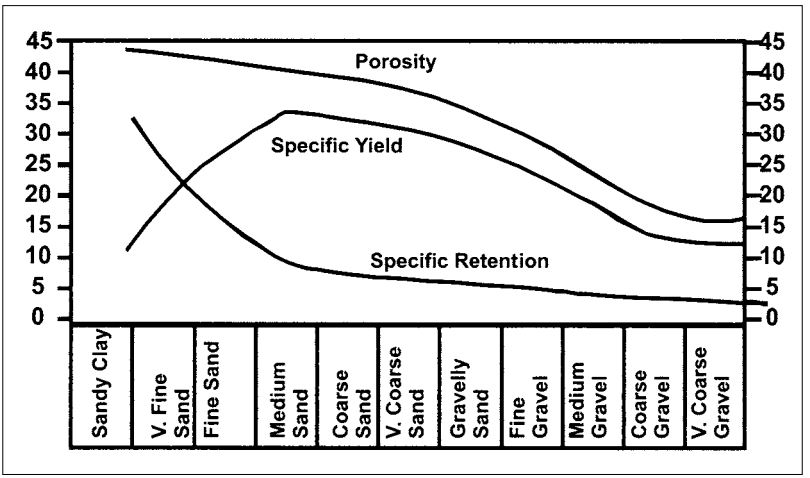

Figure 3.6 Relationship of porosity, specific yield, and specific retention with grain size. [*Modified after Scott and Scalmanini (1978).*]

another with their edges touching. This yields a porosity of 47.6%. In rhombohedral packing the spheres are pushed together in their most compact form, yielding a porosity of 25.9%. Notice in Figure 3.7 how porosity is independent of grain size (r) regardless of packing style. When grains of differing sizes are mixed together, the smaller grains fit between the grains of the larger ones, thus reducing the overall porosity.

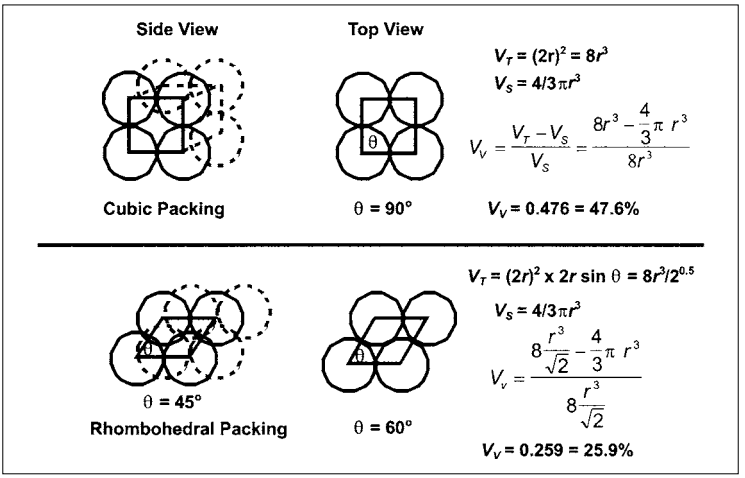

Figure 3.7 Diagram of cubic and rhombohedral packing and determination of porosity. (V_T = Total, V_S = Volume solid, V_V = Void)

In the saturated zone below the water table the porous openings are *completely* filled with water. The total porosity can also be calculated from the following relationship:

$$\eta\% = 100\left[1 - \frac{\rho_b}{\rho_p}\right] \tag{3.5}$$

where η = porosity
ρ_b = dry bulk density (m/L^3)
ρ_p = particle density (m/L^3)

Equation 3.5 is solved using values obtained from cores taken in the field. The volume of saturated material is measured and then weighed (the wet weight). The geologic materials are then placed in a container and cooked at 105°C until dry. The new dry weight compared to the volume represents the dry bulk density (ρ_b). The particle density (ρ_p) is the density of the solid materials. A common value for aquifer materials is that of quartz, 2.65 g/cm^3. The density of groundwater is close to 1.0 g/cm^3 depending on the water temperature (Appendix B). The ratio of the particle density to the density of water is known as the **specific gravity**.

Example 3.4 A core of sandy materials of approximately 80 cm^3 was taken from the field and weighed. The net soil material minus the tare weight was 166 g (wet weight). The soils were saturated and reweighed with a value of 172 g. After placing the sample in the oven at 105°C for several hours the dry sample weighed 148 g (dry weight). The water temperature in the field was 12°C, and the density is 0.99950 g/cm^3 (Appendix B).

The dry bulk density:

$$\rho_b = 148 \text{ g}/80 \text{ cm}^3 = 1.85 \text{ g/cm}^3$$

If the particle density is assumed to be 2.65 g/cm^3, the porosity can be estimated using Equation 3.5 to be:

$$\eta = 100\left[1 - \frac{1.85 \text{ g/cm}^3}{2.65 \text{ g/cm}^3}\right] = 30.2\%$$

Another way the porosity can be estimated is by evaluating the volume occupied by the water in the core at saturation minus the dry weight.

$$\text{Saturation} - \text{dry} = 172 \text{ g} - 148 \text{ g} = 24 \text{ g}$$

This occupies a volume of:

$$V = 24 \text{ g}/(0.99950 \text{ g/cm}^3) = 24.01 \text{ cm}^3$$

Using Equation 3.1:

$$\eta = 100\,\frac{24.02\ \text{cm}^3}{80\ \text{cm}^3} = 30.0\%$$

The discrepancy in values in example 3.4 can be attributed to an assumed particle density in the first case or because of volume errors. The above example was artificially created to illustrate the concept of porosity. In reality, the core must be tapped into a container in the laboratory. During the tapping process differential compaction results in field conditions being lost. It is always harder to place a field core into a container of equal volume. Porosity and specific yield are often determined in a laboratory.

Anderson and Woessner (1992) summarized the results of their findings for specific yield in Table 3.3. It is interesting how the means of unconsolidated materials follow the trend indicated in Figure 3.6. When the reported arithmetic means differ significantly from the midpoint of the range values, this indicates that the distribution is skewed. Notice also that the differences between the unconsolidated sedimentary materials, such as fine and medium sand, compared to their lithified counterparts, fine and medium sandstone, are different because of the volume occupied by cementing agents. Notice also that the specific yield is always less than the total porosity.

In a study conducted at the U.S. Geological Survey laboratory reported by Morris and Johnson (1967), differing earth materials were tested

TABLE 3.3 Ranges of Values of Specific Yield [Adapted from Anderson and Woessner (1992)]

Material class	Material	No. of analyses	Range	Arithmetic mean
Sedimentary	Clay	27	0.01–0.18	0.06
	Silt	299	0.01–0.39	0.20
	Sand (fine)	287	0.01–0.46	0.33
	Sand (Med)	297	0.16–0.46	0.32
	Sand (Coarse)	143	0.18–0.43	0.30
	Gravel (fine)	33	0.13–0.40	0.28
	Gravel (med)	13	0.17–0.44	0.24
	Gravel (coarse)	9	0.13–0.25	0.21
	Siltstone	13	0.01–0.33	0.12
	Sandstone (fine)	47	0.02–0.40	0.21
	Sandstone (med)	10	0.12–0.41	0.27
	Limestone	32	0–0.36	0.14
Wind Deposits	Loess	5	0.14–0.22	0.18
	Eolian Sand	14	0.32–0.47	0.38
Metamorphic	Schist	11	0.022–0.033	0.026
Igneous	Tuff	90	0.02–0.47	0.21

TABLE 3.4A Grain-Size Distribution of Differing Water-Laid Soils [From Morris and Johnson (1967)] Notice how Sums of Numbers Along Rows Add to 100.0

Location	Clay <0.004 mm	Silt 0.004 0.063 mm	V. Fine sand 0.063– 0.125 mm	Fine sand 0.125– 0.25 mm	Med. sand 0.25– 0.5 mm	Coarse sand 0.5– 1.0 mm	V. Coarse sand 1–2 mm	V.F. gravel 2–4 mm	Fine gravel 4–8 mm	Med. gravel 8–16 mm
Brunswick, GA	10.4	19.6	57.2	7.2	3.4	1.6	0.6	—	—	—
McCurtain Co., OK	2.8	8.8	19.2	64.6	4.4	0.2	—	—	—	—
Gallaway Co., KY	4.0	0.2	1.1	19.4	73.4	1.8	0.1	—	—	—
Arapahoe Co., CO	0.3	0.0	0.0	0.2	3.5	24.3	40.5	23.7	6.8	0.7

and evaluated for the physical and hydrologic properties. An example from this study illustrating the grain-size distributions of water-laid sandy materials and their physical and hydrologic properties are shown in Tables 3.4a and 3.4b. It is interesting to note the similarities of specific gravity regardless of the grain-size distribution and the range of grain-size distributions, dry bulk densities, and hydraulic conductivities. It is apparent from the grain-size distributions that there is a correlation between grain-size and hydraulic conductivity (intrinsic permeability, Section 3.3).

Storativity

The amount of water an aquifer can release or take into storage is known as the **storage coefficient**. The numerical value assigned to an aquifer is the **storativity**, a dimensionless value determined from pumping tests (Chapter 10). In a pumping test the storativity represents

TABLE 3.4B Physical and Hydrologic Properties of Water-Laid Soils [From Morris and Johnson (1967)]

Location	Depth (ft)	Specific gravity (g/cm^3)	Dry bulk density (g/cm^3)	Specific retention (%)	Specific yield (%)	Total porosity (%)	Hydraulic conductivity (ft/day)
Brunswick, GA	496–497	2.71	1.58	22.8	18.9	41.7	1.7
McCurtain, Co. OK	—	2.65	1.90	0.7	27.6	28.3	11
Gallaway, Co. KY	—	2.67	1.48	1.0	43.6	44.6	53
Arapahoe, Co. CO	33.5–34	2.61	1.67	2.9	33.1	36.0	802

the storativity from the saturated thickness contributing to the well bore. Storativity is defined according to Equation 3.6.

$$S = S_Y + S_S \times b \tag{3.6}$$

The first term has already been defined as the specific yield (S_y). The second term is the **specific storage** (S_s), dimensioned 1/L, multiplied by the saturated thickness (b). The specific yield is approximately equal to the storativity value for most unconfined aquifers. The usual range of storativity values in unconfined aquifers is 0.03 to 0.3 (Fetter 1994). The value of S_s in unconfined aquifers is practically negligible, unless there are sections within the aquifer where the grain size is very small (interbedded clay lenses). In confined aquifers (Section 3.4), the water released from storage is a function of the compressibility of the aquifer materials and the compressibility of water (Equation 3.7).

$$S_S = \rho \times g(\alpha + \eta\beta) \tag{3.7}$$

where ρ = fluid density, m/L^3
g = gravitational force, L/t^2
α = compressibility of mineral skeleton, (1/(M/Lt^2)
β = compressibility of water, (1/(M/Lt^2)

Specific storage is also known as elastic storage. This is from the flexible nature of mineral skeletons when changes in stress are "felt," such as during a pumping or slug test (Chapter 10). Aquifer dewatering causes the mineral skeleton to be stressed sufficiently that compression of the mineral skeleton takes place, with or without gravity drainage. This phenomenon can also occur during a significant seismic event, such as an earthquake; however, this usually results in permanent structural changes to the mineral skeleton. Permanent structural changes in the mineral skeleton are not restorable. Compressional stresses on the mineral skeleton are also enhanced by overpumping. Earth materials within an aquifer most susceptible to permanent changes are the finer grained materials (Table 3.5). The larger the compressibility value, the easier the material is to compress.

In confined aquifers, storativities range from 10^{-3} to 10^{-6} (0.001 to 0.000001). Because of the compressibility of water, storativity values less than 10^{-6} are not possible in porous media aquifers. When evaluating a report, be aware that the calculated storativities from a software package may be much lower than is possible in real life.

So now the question comes up, what about storativities between 0.001 and 0.03? These fall into the leaky confined or semiconfined range. The

TABLE 3.5 Range of Compressibility Values [Adapted from Freeze and Cherry (1979) and Roscoe Moss (1990)]

Material	Compressibility (m^2/N)	Compressibility (ft^2/lb)
Clay	$10^{-6} - 10^{-8}$	$10^{-5} - 10^{-7}$
Sand	$10^{-7} - 10^{-9}$	$10^{-6} - 10^{-8}$
Gravel	$10^{-8} - 10^{-10}$	$10^{-7} - 10^{-9}$
Fractured rock and sedimentary rocks	$10^{-8} - 10^{-10}$	$1\,0^{-7} - 10^{-9}$
Igneous and metamorphic rock	$10^{-9} - 10^{-11}$	$10^{-8} - 10^{-10}$
Water	4.4×10^{-10}	2×10^{-9}

closer values are to 0.001, the more semiconfining the aquifer is and harder it is for leakage to occur. Contrasted to this, storativities nearer to 0.01 reflect a fairly leaky system (Chapter 10). Figure 3.8 is a schematic of a semiconfined system.

In figure 3.8 the clayey horizon semiconfines the aquifer during the initial stages of pumping. As the cone of influence extends outward, water from above the clay layer eventually contributes to the pumping stress. In a leaky aquifer the clayey horizon would more likely be a silty layer that continues to extend across the diagram. As the hydraulic head becomes reduced from pumping in the lower zone, water from above the silty layer is induced through the silty layer as **leakance**.

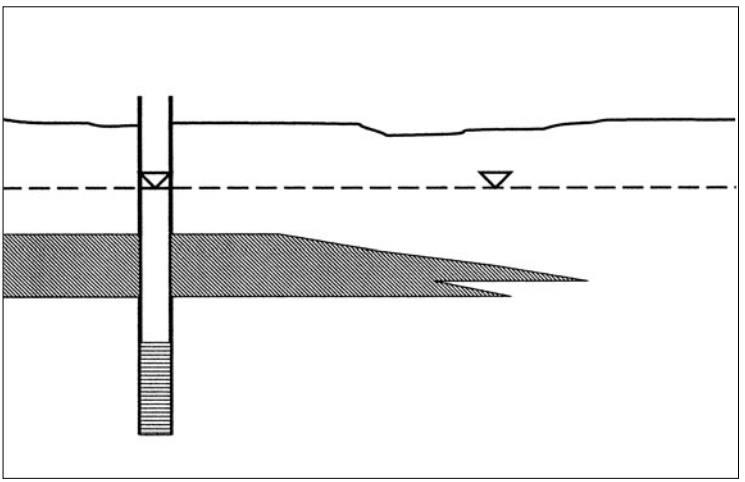

Figure 3.8 Schematic of a semiconfined aquifer where a screened interval occurs below a clay layer that pinches out laterally.

3.3 Movement of Fluids through Earth Materials

Now that we have considered the ability of earth materials to store water, another important term refers to the ability of fluids to move through them. The term most commonly used is **hydraulic conductivity**. It encompasses the ability of a material to conduct fluids under a *unit* hydraulic gradient considering the dynamic viscosity in units of length over time (L/*t*) (Fetter 1994). The **viscosity** is a term that indicates the resistence of fluid to flow. It has units of newton-seconds over meters squared ($N \cdot s/m^2$). Thick fluids like tar or cold molasses have high viscosity, where alcohol is an example of a low viscosity fluid. **Permeability** is another term commonly used to express the ability of fluids to pass through earth materials and often times both hydraulic conductivity and permeability are used interchangeably in groundwater studies, although it should not be done. This needs an explanation.

The conductivity properties of fluids are related to the **specific weight** (γ) and the **dynamic viscosity** (μ) of the fluid (Appendix B). The specific weight represents the gravitational driving force of the fluid. The ability of fluids to move is also inversely proportional to the resistance of fluids to shearing (Fetter 1994). This is expressed in Equation 3.8.

$$K = k_i \frac{\gamma}{\mu} = k_i \frac{\rho g}{\mu} \tag{3.8}$$

where k_i = intrinsic permeability, Darcy (9.87×10^{-9} cm^2)
γ = specific weight = density × gravity
ρ = density (m/L^3)
g = force due to gravity (L/t^2)
μ = dynamic viscosity (m/L*t*)

The **intrinsic permeability** (k_i) represents the physical flow properties of the geologic materials. It is essentially a function of the pore size openings only (no fluids are included). The larger the pore opening, the larger the intrinsic permeability. This relationship can be seen in Tables 3.4a and 3.4b. The specific weight (γ) indicates how a fluid of a given density will be driven by gravity. The dynamic viscosity (μ) indicates that the less resistive the fluid, the more conductive the earth material is. Those that equate hydraulic conductivity to intrinsic permeability consider most fresh groundwater to have insignificant changes in specific weight and dynamic viscosity; therefore, the ability of groundwater to move is mainly proportional to the intrinsic permeability alone. This should not be done because the hydraulic conductivity will change by a factor of 3 just by changing the water temperature between 2 and

30°C. This is also not true when contaminants interact with groundwater with different fluid properties, such as nonaqueous phase liquids (NAPLs) or with saline waters.

Example 3.5 What is the hydraulic conductivity for water at 2, 16, and 30°C if the intrinsic permeability is 0.2 darcy?

Solution We start by seeing what a darcy is (modified from Fetter 1994):

$$1 \text{ darcy} = \frac{1 \text{ cP} \times 1 \text{ cm}^3/\text{s}/1 \text{ cm}^2}{1 \text{ atm}/1 \text{ cm}} = 9.87 \times 10^{-9} \text{ cm}^2 \tag{3.9}$$

where cP = centipoise, a unit of viscosity = 0.01 dyn · s/cm^2, and
atm = atmosphere = 1.10132×10^6 dyn/cm^2

From Appendix B one can obtain the density and viscosity values as a function of temperature. An example calculation for water will be done at 2°C with the results for the other two temperatures following.

At 2°C for water,

$$\rho = 0.99994 \text{ g/cm}^3$$

$$\mu = 0.01673 \text{ g/s} \cdot \text{cm}$$

Acceleration from gravity is given as $-g = 980$ cm/s^2

$$0.2 \text{ darcy} \times 9.87 \times 10^{-9} \text{ cm}^2 = 1.97 \times 10^{-9} \text{ cm}^2$$

From Equation 3.8, the hydraulic conductivity of water at 2°C is:

$$K = K_i \frac{(\rho g)}{\mu} = 1.97^{*}10^{-9} \times \frac{0.99994 \text{ g/cm}^3 \times 980 \text{ cm/s}^2}{0.01673 \text{ g/s} \cdot \text{cm}}$$

$$= 1.16 \times 10^{-4} \text{ cm/s}$$

Similarly, substituting the appropriate values from Appendix B for density and viscosity at temperatures of 16°C and 30°C respectively (0.99894 and 0.99565 g/cm^3 for density and 0.01111 and 0.00801 g/s · cm for viscosity) we obtain hydraulic conductivity values for water:

$$\text{At } 16°\text{C}, K = 1.74 \times 10^{-4} \text{ cm/s, and}$$

$$\text{At } 30°\text{C}, K = 2.4 \times 10^{-4} \text{ cm/s}$$

Hydraulic conductivity values for earth materials range over 12 orders of magnitude (Figure 3.9). The distribution of hydraulic conductivity is log-normally distributed, so averaged values should be geometric means

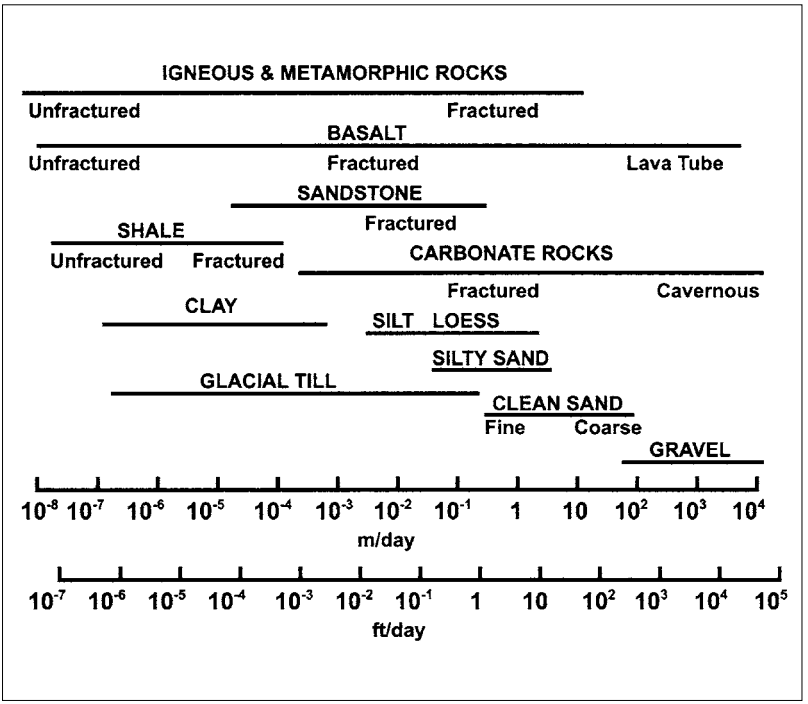

Figure 3.9 Ranges of hydraulic conductivity values for earth materials. [*Adapted from Anderson and Woessner* (*1992*).]

or some other transformation. Obtaining precise or accurate values for hydraulic conductivity is unlikely, so when they are reported as such they should be viewed with a jaundiced eye. This leads to caution for those who report hydraulic conductivity values. Just because your calculator gives a number to many decimal places, your responsibility as a hydrogeologist is to report only that level of precision that you feel is justified. Typically this would be with a maximum of two significant figures (Table 3.6).

Hydraulic conductivity is reported in a variety of different units in the literature and in software packages. A hydrogeologist needs to be able to convert back and forth from one unit system to another through unit conversions and by knowing a few simple conversion factors (Appendix A). It may be that you are out in the field with only your field book and a calculator and you have to make a decision based upon some numbers.

Example 3.6 An estimate of hydraulic conductivity at 2×10^{-4} cm/s was estimated for a fine sandy material. The number needed to be converted into ft/day to perform a calculation for average linear velocity during a tracer

TABLE 3.6 Ranges of Hydraulic Conductivity Values for Various Earth Materials [Adapted from Domenico and Schwartz (1990)]

Material type	Material	Hydraulic conductivity cm/sec
Unconsolidated	Unweathered marine clay	8×10^{-11}–2×10^{-7}
	Clay	1×10^{-11}– 4.7×10^{-7}
	Silt, loess	1×10^{-7} – 2×10^{-3}
	Fine sand	2×10^{-5} – 2×10^{-2}
	Medium sand	9×10^{-5} – 5×10^{-2}
	Coarse sand	9×10^{-5} – 6×10^{-1}
	Gravel	3×10^{-2} – 3
	Till	8×10^{-10} – 2×10^{-4}
Sedimentary rocks	Shale	1×10^{-11} – 2×10^{-7}
	Siltstone	1×10^{-9} – 1.4×10^{-6}
	Sandstone	3×10^{-8}–6×10^{-4}
	Limestone, dolomite	1×10^{-7} – 6×10^{-4}
	Karst and reef limestone	1×10^{-4} – 2
	Anhydrite	4×10^{-11} – 2×10^{-6}
	Salt	1×10^{-10} – 1×10^{-8}
Crystalline rocks	Unfractured basalt	2×10^{-9} – 4.2×10^{-5}
	Fractured basalt	4×10^{-5} – 2
	Weathered granite	3.3×10^{-4} – 5.2×10^{-3}
	Weathered gabbro	5.5×10^{-5} – 3.8×10^{-4}
	Fractured igneous & metamorphic rocks	8×10^{-7} – 3×10^{-2}
	Unfractured igneous & metamorphic rocks	3×10^{-12} – 2×10^{-8}

test (Chapters 13 and 14). The only resources you have are a writing utensil, a field book, and a calculator.

$$K = 2 \times 10^{-4} \frac{\text{cm}}{\text{s}} \times \left(\frac{1 \text{ in}}{2.54 \text{ cm}}\right) \times \left(\frac{1 \text{ ft}}{12 \text{ in}}\right) \times \left(\frac{60 \text{ s}}{1 \text{ min}}\right) \times \left(\frac{1440 \text{ min}}{1 \text{ day}}\right)$$

$$= 0.6 \text{ ft/day}$$

The average linear velocity was estimated to be:

$$V_{\text{ave}} = \frac{K}{\eta_e} \times \frac{\delta h}{\delta l} = \frac{0.57 \text{ ft/day}}{0.26} \times \frac{3 \text{ ft}}{145 \text{ ft}} = 0.045 \text{ ft/day}$$

The hydraulic conductivity can be estimated for sandy materials where the **effective grain size** (d_{10}) is between 0.1 mm and 3.0 mm (Hazen 1911), where d_{10} represents the smallest 10% of the sample. (It is important to pay attention to the limits over which this is applicable). The effective grain size is determined from a grain-size distribution plot from passing a dried field sample through a series of sieves (see Chapter 8 and Example 3.7). In a grain size plot the d_{50} is the median grain size. Grain

size plots are helpful in determining the sorting. The sorting is estimated with the **uniformity coefficient** (C_u) expressed in Equation 3.9.

$$C_u = \frac{d_{60}}{d_{10}} \tag{3.9}$$

Values less than 4 are well sorted, and values greater than 6 are considered to be poorly sorted (Fetter 1994). The Hazen equation (1911) relating hydraulic conductivity to effective grain size and a sorting coefficient is shown in Equation 3.10. The most common error made by users of this equation is to forget to convert the grain-size parameters from millimeters to centimeters.

$$K = C(d_{10})^2 \tag{3.10}$$

where K = hydraulic conductivity in (cm/s)
d_{10} = effective grain size (cm)
C = sorting and grain-size coefficient in (1/cm/s)

The coefficient C is assigned according to sorting *and* grain size (Table 3.7). The grain size is determined by evaluating the median grain size (d_{50}) from a grain-size distribution curve (Example 3.7). Values that are poorly sorted and finer grained receive smaller coefficient numbers. I recommend that the coefficients in Table 3.7 only be estimated to the nearest value of 10.

Shepard (1989) evaluated the data from published studies relating grain size to hydraulic conductivity by plotting hydraulic conductivity (in ft/day) versus median grain size (d_{50}) on log-log paper. Various plots were made based upon sediments from different depositional environments (Chapter 2), each forming a straight-line plot. The slope of the plot was related to an exponent (Equation 3.11). The values of the exponent range between 2.0 for glass spheres of equal size and 1.5 for poorly sorted unconsolidated materials. Example C values and exponents are shown in Table 3.8.

$$K = C_F \times d_{50}^{i} \tag{3.11}$$

TABLE 3.7 Hazen Equation Coefficients in $(cm \cdot s)^{-1}$ Based on Sorting and Grain Size

Description	Coefficient
Poorly sorted to well-sorted very fine sand	40–80
Poorly sorted to moderately sorted fine sand	40–80
Moderately sorted to well-sorted medium sand	80–120
Poorly to moderately sorted coarse sand	80–120
Moderately sorted to well-sorted coarse sand	120–150

TABLE 3.8 Hydraulic Conductivity (K in ft/day) Related to Shape Factors (C), Based on Depositional Environment and Median Grain Size (mm) [Adapted from Shepard (1989)]

Deposit. Environ. (Shape Factor)	0.0l mm K ft/day	0.1 mm K ft/day	1.0 mm K ft/day	10.0 mm K ft/day	Exponent
Glass beads (40,000)	4.0	400	40,000	—	2
Eolian dunes (5,000)	1.0	70	5,000	—	1.85
Beach deposits (1,600)	0.5	28	1,600	—	1.75
Channel deposits (450)	0.23	10	450	20,100	1.65
Sedimentary rock (100)	0.1	3.2	100	3,160	1.5

where K = hydraulic conductivity (ft/day)
C_F = shape factor, (based upon depositional environment) in units which convert mm^2 to ft/day
d_{50} = median grain size in mm
i = exponent (between 2.0 and 1.5) = slope on log-log plot

Example 3.7 A grain-size distribution based upon water-laid deposits from McCurtain County, Oklahoma (triangles), and Arapahoe County (boxes), Colorado (from Morris and Johnson 1967), is plotted in Figure 3.10. The respective hydraulic conductivities are calculated based upon the Hazen (1911) method and the relationship developed by Shepard (1989). These are compared with the hydraulic conductivities determined in the laboratory by Morris and Johnson 1967). The values used in the equations are given in Table 3.9.

Equations 3.9 and 3.10, and Table 3.7 are used to evaluate the hydraulic conductivity using the Hazen (1911) method, and Equation 3.11 and

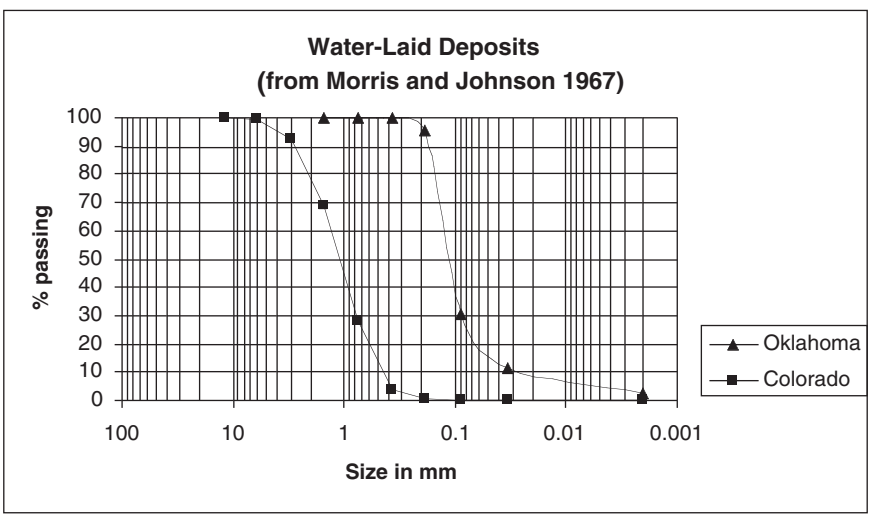

Figure 3.10 Plot of grain size versus percent finer by weight. Triangles represent McCurtain Co., Oklahoma, and boxes represent Arapaho Co., Colorado.

TABLE 3.9 Summary of Calculations to Evaluate Hydraulic Conductivities in ft/day for Two Water-Laid Sand Deposits

Location	d_{10} mm	d_{50} mm	d_{60} mm	C_u	C	K_{hazen} ft/day	C_F	Exp	$K_{shepard}$ ft/day	K_{lab} ft/day
Oklahoma	0.06	0.17	0.18	3.0	90	9	1000	1.7	54	11
Colorado	0.67	1.5	1.8	2.6	150	2080	1200	1.75	3360	802

Table 3.8 are used to evaluate the hydraulic conductivity using the Shepard (1989) relationship. Both are compared to the coefficient of permeability reported by Morris and Johnson (1967). The results are shown in Table 3.9 with an example calculation below.

Although the sand from Oklahoma has an effective grain size less than 0.1 mm, a well-sorted sample may allow the calculations to be useable. The uniformity coefficient indicates a well-sorted sand with a d_{50} in the fine sand range (between 0.125 and 0.25 mm). Converting the median grain size into centimeters and using a Hazen (1911) C factor of 90 yields:

$$K_{\text{Hazen}} = 90(0.006\text{ cm})^2 = 3.2 \times 10^{-3}\,\frac{\text{cm}}{\text{s}}\left(\frac{86400}{1\text{ day}}\right)\left(\frac{1\text{ ft}}{30.48\text{ cm}}\right)$$

$$= 9.2\text{ ft/day}$$

For the Shepard (1989) method it is noticed that the sands are water-laid and well sorted, a shape factor C_F between beach and channel deposits was selected, with an exponent of 1.7 to yield the following hydraulic conductivity:

$$K_{\text{Shepard}} = 1000 \times (0.18\text{ mm})^{17} = 54\text{ ft/day}$$

All values were within one order of magnitude, but the Hazen (1911) method appears to have better agreement with the laboratory calculated value.

Example 3.7 illustrates how estimates for hydraulic conductivity vary based upon grain-size analysis. It is the author's experience that similar discrepancies also occur when performing pumping tests (Chapters 9 and 10) and slug tests. Conversions from one system to another are also illustrated in the example. Table 3.10 gives conversions for the more commonly used hydraulic conductivity values.

Transmissivity

The hydraulic conductivity can be estimated based upon grain-size relationships or directly in the field by performing slug tests (Chapter 11). Hydraulic conductivities are also estimated from pumping tests

TABLE 3.10 Conversion Factors for Commonly Used Hydraulic Conductivity Values

Multiply	By	To obtain
1 gal/day/ft^2	0.1337	ft/day
1 cm/s	2835	ft/day
1 m/day	3.2808	ft/day
1 gal/day/ft^2	4.72×10^{-5}	cm/s
1 ft/day	3.53×10^{-4}	cm/s
1 m/day	1.16×10^{-3}	cm/s
1 gal/day/ft^2	4.07×10^{-2}	m/day
1 cm/s	864	m/day
1 ft/day	0.3048	m/day
1 cm/s	21203	gal/day/ft^2
1 ft/day	7.481	gal/day/ft^2
1 m/day	24.54	gal/day/ft^2

(Chapters 9 and 10), by first obtaining a **transmissivity** (T) value. The transmissivity is directly related to the hydraulic conductivity by the following relationship:

$$T = K \times b \tag{3.12}$$

where K = hydraulic conductivity
b = saturated thickness

During a pumping test the estimated saturated thickness contributing to the screened interval varies depending on the time of pumping, geology, and whether an aquifer is confined or unconfined. More discussion on this topic is found in Section 10.5. The common approach is to assume the **saturated thickness (*b*)** in an unconfined aquifer represents the thickness of saturated materials from bedrock to the water table and in a confined aquifer, b is simply the thickness of the aquifer between confining units. One must realize that this assumes there is no low hydraulic conductivity barrier layers within the aquifer and/or that the entire thickness is screened. This could only be true in thin aquifers.

3.4 Aquifer Concepts

An aquifer is a formation, part of a formation or group of formations that contain *sufficient* saturated permeable material to yield *significant* quantities of water to wells or springs. Water within the zone of saturation is at a pressure greater than atmospheric pressure (Section 3.1). The definition is useful because of its flexible application, depending on water use within an area. For example, in a dry semiarid region, any aquifer that can produce 10 gpm for stock watering purposes would be considered

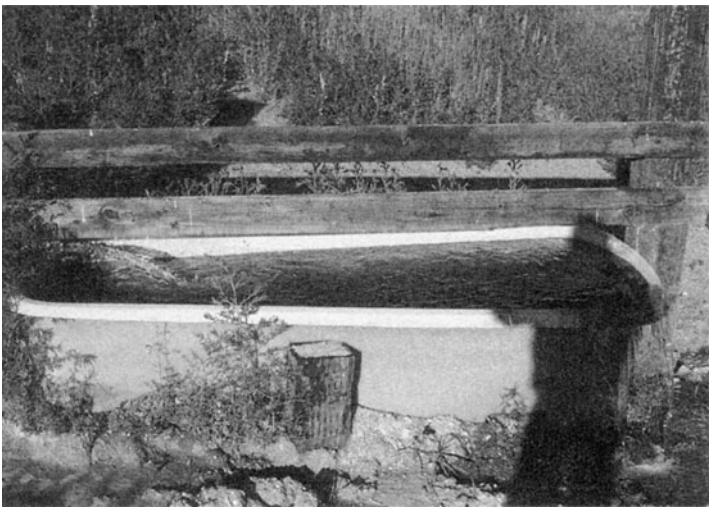

Figure 3.11 Well discharge for stock watering (windmill).

to be sufficient and significant (Figure 3.11). Contrasted to this, a center-pivot irrigation production must produce a minimum of 500 gpm for a 160-acre piece (quarter-section) of land to be considered sufficient and significant (Figure 3.12). In the latter case, a 10-gpm domestic well in the same area as the pivot well may not be considered very significant.

Figure 3.12 Pivot irrigation system in southwestern Montana.

An aquifer can be made up of a single formation, for example, the Permian Quadrant Quartzite in southwestern Montana, which is tightly cemented at outcrop, but is fairly friable and porous at depth. Other aquifers that consist of groups of formations are probably better known as aquifer systems. Well-known examples are the Floridian Aquifer System (Miller 1986) and the High Plains Aquifer System (Gutentag et al. 1984), both of which consist of units of varying lithologies and ages. Some aquifers may only consist of one member within a formation or a single bed. Within the Fort Union Formation, exposed in eastern Montana and Wyoming, is the Tongue River member containing several thick subbituminous coal beds. The Anderson, Dietz, and Monarch coal beds extend regionally and are important sources of water for stock. Aquifer units are separated by confining units of varying physical properties.

Unconfined aquifers

When water infiltrates into the ground, gravity pulls it downward until it encounters a confining layer. Because flow is inhibited, the zone of saturation literally piles up above this confining layer. The saturated thickness represents the height of the pile, and since the porosity of the overlying materials is connected to the land surface, it is called an **unconfined aquifer**. It could also be viewed as an open system. The top of this saturated material is called the **water table** and is located where the pressure is atmospheric (Figure 3.13). It also represents a physical

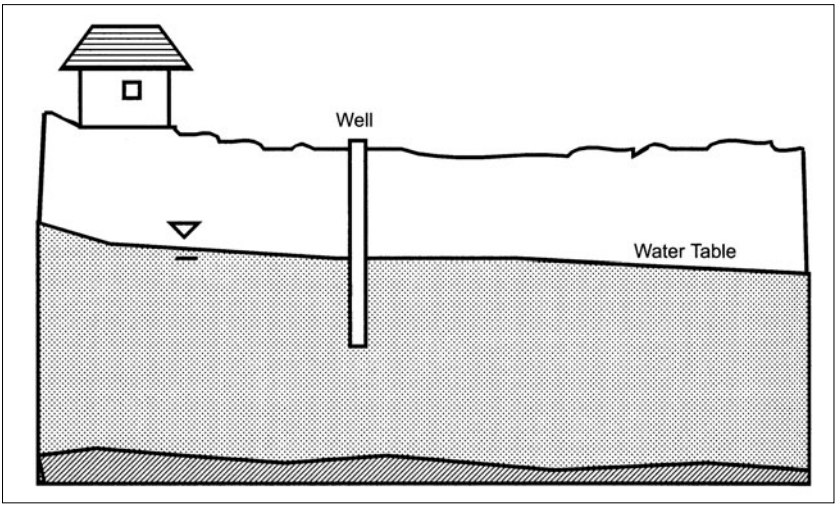

Figure 3.13 Unconfined or water table aquifer with pore spaces connected to the surface.

moving boundary that fluctuates according the amount of recharge or discharge. Groundwater beneath the water table is under a pressure greater than atmospheric, because of the weight of water above a given point of reference. This concept will be explained in more detail in Chapter 5.

Confined and artesian aquifer

Geologic materials that outcrop at the surface at a relatively high elevation (recharge area) receive water by infiltration recharge (Figure 3.14). Materials of sufficient transmissivity that become saturated and are overlain and underlain by confining layers become aquifer units with trapped groundwater. The elevation of the zone of saturation propagates a pressure throughout the system from the weight of the water. When this occurs, there is sufficient pressure head within the system to lift the water within cased wells above the bottom of the upper confining layer or top of the aquifer (Figure 3.15). By definition, this is a **confined** or **artesian** aquifer. Both terms refer to the same condition.

Generally, most confined aquifers receive recharge through vertically leaking geologic materials above or below them (Freeze and Cherry 1979). When water levels in cased wells rise to the land surface and become flowing wells, they are still considered to be from a confined aquifer

Figure 3.14 Mountain recharge in south western Montana.

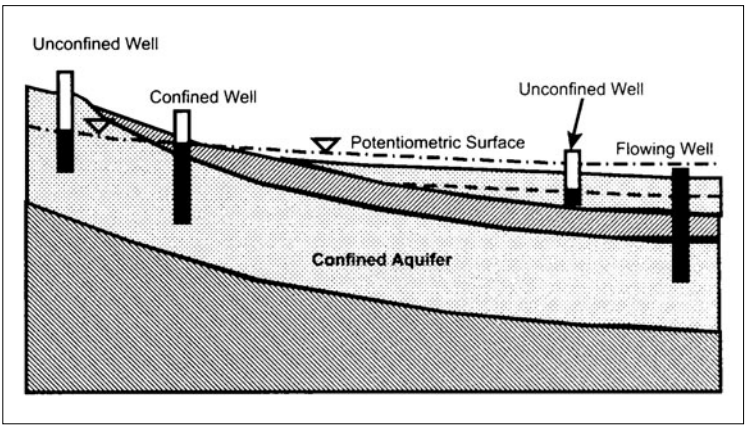

Figure 3.15 Confined aquifer and surficial unconfined aquifer setting. Three wells completed in the lower aquifer, two of which are confined. Overall the head in the upper unconfined aquifer is less than the lower confined aquifer.

(Figure 3.16). The height to which water levels rise forms a surface known as the **potentiometric surface** (Figure 3.15). Notice in Figure 3.15 that the confined aquifer and unconfined aquifer have different potentiometric surfaces. In an unconfined aquifer the potentiometric surface is the water table. The slope of this surface is called the **hydraulic gradient**. The slope of the hydraulic gradient is proportional to the hydraulic conductivity. The lower the hydraulic conductivity, the greater the slope of the hydraulic gradient (Chapter 5). Each aquifer has its own

Figure 3.16 Attempt to measure field parameters from a flowing well in Petroleum County, Montana.

potentiometric surface, from which groundwater flow and other interpretations are made (Chapter 5). It is important to construct separate potentiometric surfaces for each aquifer to evaluate vertical connectivity (Chapter 5).

Confining layers

If aquifers yield significant quantities of water, **confining layers**, although they store water, generally slow or inhibit fluid flow through them. Some prefer to use separate terminology for varying types of confining layers. For example, layers that pass water slowly may be referred to as **aquitards**, while those that are considered to be impermeable are called **aquicludes** (Fetter 1994; Freeze and Cherry 1979). Substances may have *very* low hydraulic conductivity, but nothing is really impermeable, including geotextiles, the most compacted clay, and the tightest bedrock. Hydraulic conductivities that are six orders of magnitude (a million times) less permeable than another substance may *just* appear to be impermeable.

For practical purposes, confining layers can be defined as those geologic materials that are more than two to three orders of magnitude less permeable than the aquifer above or below it. Those less than two orders of magnitude different are hydraulically connected enough to be a single aquifer unit. Using this as a basis, formational stratigraphy is regrouped and reevaluated in terms of hydrostratigraphy.

Hydrostratigraphy

When one considers the definitions of aquifers and confining layers in performing a site characterization or defining the geology of an area, it is also important to define the **hydrostratigraphy**. This involves the combining or separation of units with similar hydraulic conductivities into aquifers or confining layers. It may be, for example, that the Ordovician and Mississippian formations (group of formations) collectively form one large Madison Aquifer, while the Cretaceous Muddy Sandstone (part of a formation) forms another. These may be isolated from aquifers above or below by a part of a formation, a single formation or a group of formations or units. The hydrostratigraphy is used along with structural data to build a **conceptual model** of a flow system (Chapter 5).

Example 3.8 On the Hualapai Plateau, Arizona, it was desired to drill wells for water development rather than depending upon temporary stock tanks behind earthen dams (Huntoon 1977). The earthen dams were only successful if flash floods occurred to trap relatively poor-quality water. The target zone was the lowermost Rampart Cave member of the Muav limestone,

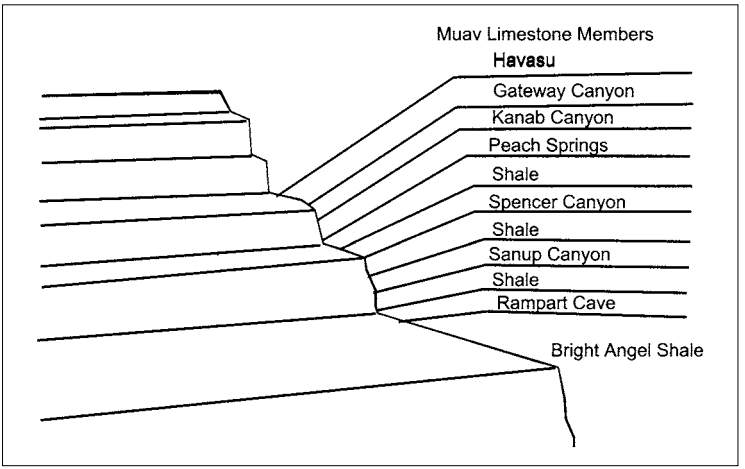

Figure 3.17 Detailed Cambrian section of the lower part of the Muav Limestone on the Hualapai Plateau, Arizona. [*Adapted from Huntoon* (*1977*).]

some 1,500 ft below the canyon rim. The Cambrian section was originally described by Nobel in 1914 and 1922 and then in detail by McKee and Resser in 1945. They honored the nomenclature designated by Nobel (1922) but assigned all shale units as part of the Bright Angel Shale and the limestone units as part of the Muav Limestone. This posed a problem because the depositional environment was that of the transgressive sea where the two formations intertwine and subunits extend for miles. The lowest three members of the Muav Limestone are interbedded with shale units that are unnamed (Figure 3.16). The hydrogeologist hired to define the target zones said that if they drilled past the limestone into upper part of the shale, they would reach maximum production (Huntoon 1977). The problem was that drilling took place through the Peach Springs member of the Muav Limestone and the driller terminated in the uppermost unnamed shale (Figure 3.17). The hydrogeologist failed to inform the driller that there were other limestone and shale units that needed to be penetrated before the target zone would be encountered. In most drill locations, they had stopped short of the target by 150 to 250 ft (Huntoon 1977).

A given conceptual model of the physical behavior of groundwater movement depends somewhat on scale. There are regional groundwater studies and local groundwater studies. The hydrostratigraphy of a small site (e.g., 5 acre, 2.0 ha) would likely be defined by local drill-hole information.

3.5 Boundary Concepts

The hydrostratigraphy, structural changes, and adjacent earth materials all affect groundwater flow and the separation of saturated materials into aquifer units. Each aquifer will have its own potentiometric surface

and a hydraulic gradient corresponding to its hydraulic conductivity. If there are multiple aquifers in a particular area, it is important to identify the potentiometric surface of each aquifer separately. Figure 3.18 shows the potentiometric surface of four aquifers: an unconfined bedrock aquifer, unconfined sand and gravel aquifer (dashed line), and two other confined aquifers (solid lines). Note how the potentiometric surface of the intermediate layer (well B) is lower than the others, but the potentiometric surface of the lowest layer (well C) is higher than that of wells A and D. The slope of the potentiometric surfaces are toward or away from the reader, except the bedrock aquifer, which slopes toward the alluvial system. Because groundwater always moves from areas of higher total head to areas of lower total head, the groundwater from the lowest system (well C) wants to move vertically through a confining layer toward the intermediate aquifer. Additionally, the groundwater from the surficial unconfined aquifer wants to leak downward toward the intermediate (well B). Groundwater will always move as long as there is a slope or head difference from one area to another, thus creating a hydraulic gradient. There may be a horizontal component to groundwater flow (within aquifers) and a vertical component (between aquifers and in recharge or discharge areas) of groundwater flow. Groundwater continues to move until equilibrium is reached.

In considering the boundary conditions of Figure 3.18, the granitic bedrock and the clay layers separate the three sand and gravel aquifers

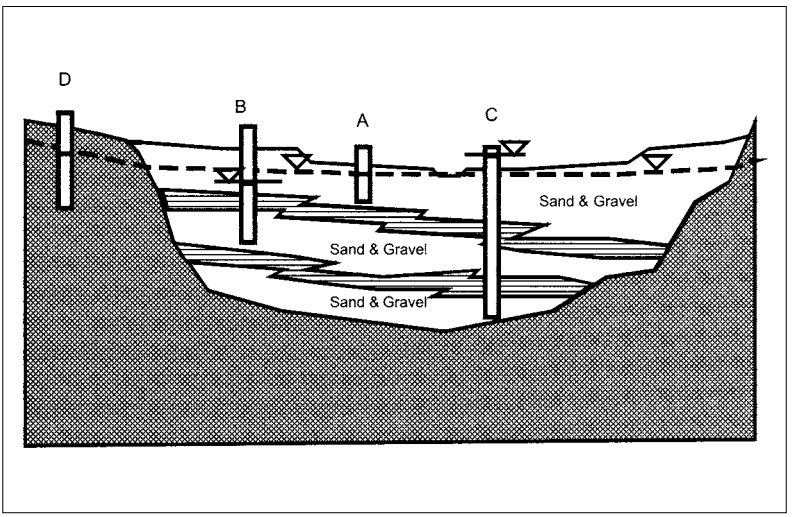

Figure 3.18 Schematic illustrating four aquifer units: well A, an unconfined aquifer connected to the river; well B, an intermediate confined aquifer; well C, completed in a confined aquifer; and well D, completed in bedrock.

from each other, evidenced by the differing water-level elevations. Given the low porosity of the granite, long-term yields from well D would be expected to be minimal compared to well C. It is apparent that the lowest layer is receiving recharge up river from a higher elevation than the other two sand and gravel aquifers. What would the water levels in wells be like if the bedrock were siltstone instead of granite? Think of the physical properties of siltstone compared to granite.

Another example shows how structural effects and changes in aquifer properties create aquifer boundaries (Figure 3.19) In the diagram there are two springs. Boulder Springs is a contact spring where a unit of higher hydraulic conductivity intersects the land surface. Why is Basin Springs there? What effect is the Basin Fault having on the system? Notice that the river is losing water. Are the slopes of the hydraulic gradient within the different units appropriate?

Homogeneity and isotropy

There are two terms that are often confused and/or ignored in hydrogeologic studies that are related to the physical and flow properties of an aquifer, **heterogeneity** and **anisotropy**. Heterogeneity refers to the lateral and vertical changes in the physical properties of an aquifer. For example, the grain-size packing, thickness, porosity, cementation, and hydraulic conductivity at one location (site A) can be compared to the same physical properties at another location (site B) (Figure 3.20).

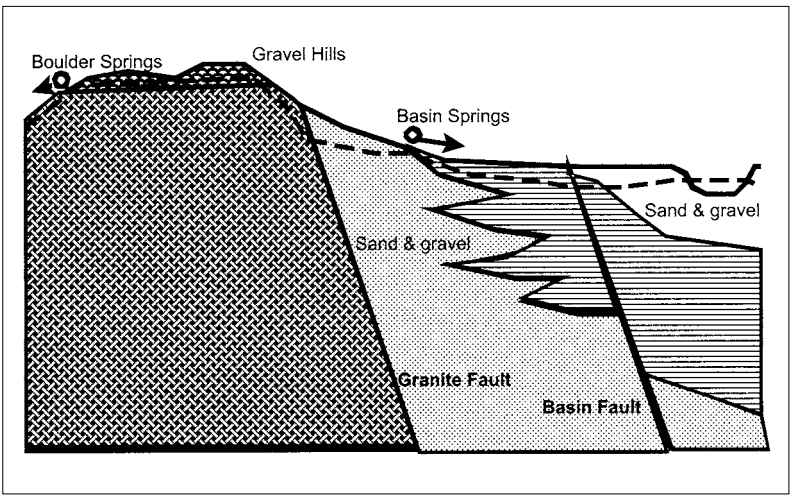

Figure 3.19 Diagram illustrating aquifer boundary conditions. Boundary conditions are caused by varying hydraulic conductivities of rock units and structural offsets. The horizontal pattern signifies shale.

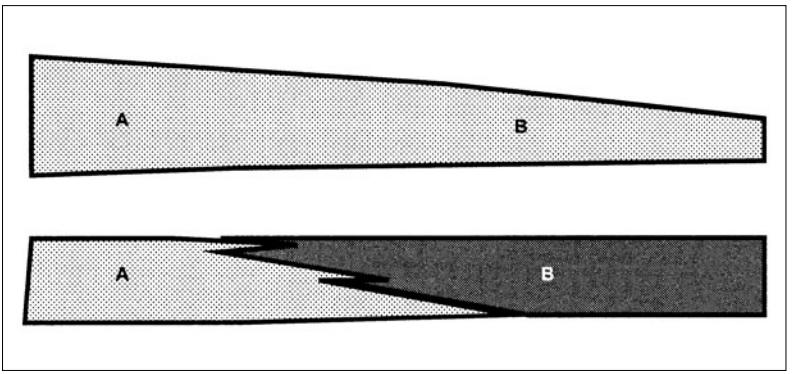

Figure 3.20 Schematic showing heterogeneity. In the upper diagram, the thickness changes from point A to point B. In the lower diagram, the grain-size and packing changes from point A to point B.

If the variability of the physical properties relative to the volume of the system of interest is small, the aquifer is said to be **homogeneous**. A **heterogeneous** aquifer will have a different saturated thickness, porosity, or some other physical property from location to location. For example, if a sandstone becomes finer grained laterally (as in a facies change) or thins or thickens laterally, it is *not* homogeneous.

Anisotropy refers to differences in hydraulic properties depending on the direction of flow. If a porous media were made up of spheres in cubic packing, the permeability of the media would be the same in all directions. In most depositional environments the sediments are laid down in a stratified manner, so that the vertical hydraulic conductivity is *very* different from the horizontal hydraulic conductivity. This difference can be from percentages to an order of magnitude or more. In considering a Cartesian coordinate system, where Z represents the vertical dimension, within the X-Y plane there is a preferential flow in one direction over the other. A summary of these concepts is shown in Figure 3.21. Faults, fractures, bedding planes, and other features are potentially important causes of anisotropy and heterogeneity.

3.6 Springs

Springs are an important source of hydrogeologic information. They occur because the hydraulic head in the aquifer system intersects the land surface (Figure 3.22). By paying attention to their distribution, flow characteristics, and water qualities, much valuable information can be derived without drilling a single well. Springs can sometimes provide more information than wells.

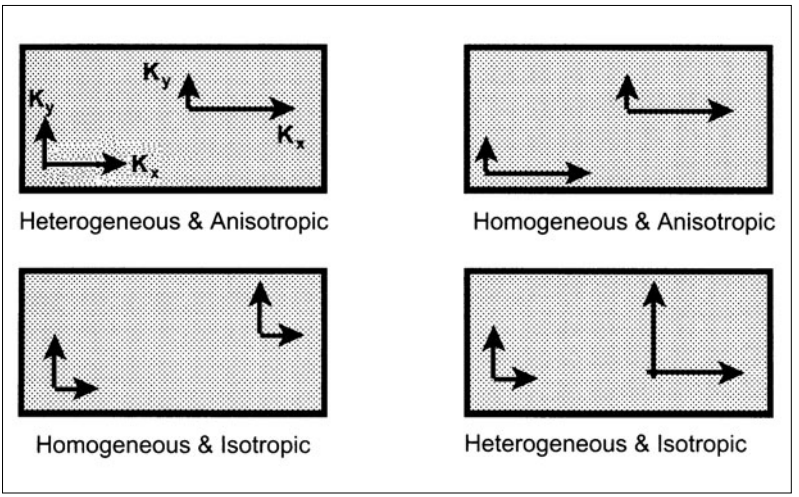

Figure 3.21 Combinations of heterogeneity and isotropy. [*Adapted from Freeze and Cherry* (*1979*).]

Perhaps the most common springs are contact springs. In an area of layered sedimentary rock, springs will develop if recharge enters a higher hydraulic conductivity unit overlain by a lower hydraulic conductivity unit. In the field, these are observed as places where trees and other vegetation flourishes in an otherwise dry area. Look for game trails that lead into the vegetation, the animals know where water is.

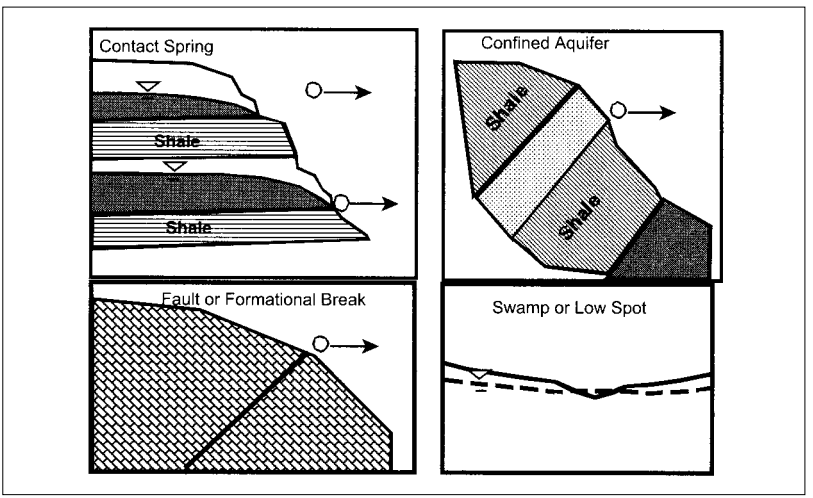

Figure 3.22 Cross-sectional views of a variety of springs: contact spring, confined aquifer is charge, fault, or depositional plane, and swamp or low spot.

TABLE 3.11 Physical Characteristics of Springs

Characteristic	Comments
Provides elevation of minimum head	As single points or a string of points on a topographic map
Hydrostratigraphy defined	Vegetation at discharge points separated by areas lacking in vegetation
A point of maximum hydraulic conductivity	Either coarser-grained or more fractured
Discharge type, fractures, porous discharge	Type of aquifer permeability observed
Discharge rate	Volume and frequency may be steady or vary
Discharge time	Steady flow indicates a larger system than one that stops flowing after a short time
Type of aquifer	Confined or unconfined
Groundwater quality	General chemistry of aquifer
Place to age date	Provides a place of maximum residence time in the aquifer
Thermal data	Circulation depths or thermal influences
Periodicity	Is there a regular discharge interval?
Can be used to understand structural relationships	Discharge areas can be correlated with geologic structures

Springs from confined aquifers occur either in structurally complex areas where the recharge area is high, relative to the location of the rock outcrops lower in the system. They occur either from folded beds, depositional contacts, or fault planes. They represent places of discharge where minimum hydraulic head occurs locally within an aquifer system. A summary of the physical characteristics of springs is listed in Table 3.11.

3.7 Summary

The subsurface geology when saturated is divided into hydrostratigraphic units consisting of aquifers and confining units. The physical properties of aquifers include their ability to store and transmit water while confining layers tend to inhibit flow and serve as barriers to flow. Porosity represents the volume of pore space that can be occupied by groundwater. Porosity can be estimated from cores taken in the field and then tested for their water content. The effective porosity is that part of porosity available for fluid flow. It is often estimated to be the value for specific yield.

Hydraulic conductivity is a measure of the transmissive qualities of saturated earth materials. It can be estimated based upon grain size or by stressing the aquifer through pumping tests. The rate at which water can move through an aquifer is reflected by the slope or hydraulic gradient of the potentiometric surface; high hydraulic conductivity materials

have a flatter hydraulic gradient than low hydraulic conductivity units. The hydrostratigraphy is placed within the geologic framework to create a conceptual model of groundwater flow. Fault zones and bedrock may serve as barriers and control the distribution of hydraulic head. In deciphering the structure of an area and determining aquifer characteristics, springs in the area provide direct quantitative information about the aquifer and its chemistry.

References

Anderson, M.P., and Woessner, W.W., 1992. *Applied Groundwater Modeling: Simulation of Flow and Advective Transport*. Academic Press, San Diego, CA, 381 pp.

Baldwin, D.O., 1997. *Aquifer Vulnerability Assessment of the Big Sky Area, Montana*. Master's thesis, Montana Tech of the University of Montana, Butte, MT, 110 pp.

Cleary, R.W., Pinder, G.F., and Ungs, M.J., 1992. *IBM PC Applications in Ground Water Pollution & Hydrology*, Short course notes. National Ground Water Association, San Francisco, CA.

Domenico, P.A., and Schwartz, W.W., 1990. *Physical and Chemical Hydrogeology*, John Wiley & Sons, New York, 824 pp.

Driscoll, F., 1986. *Groundwater and Wells*. Johnson Filtration Systems, St. Paul, MN, 1108 pp.

Fetter, C.W., 1994. *Applied Hydrogeology, 3rd Edition*. Macmillan, New York, 691 pp.

Freeze, A., and Cherry, J., 1979. *Groundwater*. Prentice-Hall, Upper Saddle River, NJ, 604 pp.

Gutentag, E.D., Heimes, F.J., Krothe, N.C., Luckey, R.R, and Weeks, J.B., 1984. *Geohydrology of the High Plains Aquifer in Parts of Colorado, Kansas, Nebraska, New Mexico, Oklahoma, South Dakota, Texas, and Wyoming*. U.S. Geological Survey Professional Paper 1400-B.

Hazen, A., 1911. Discussion: Dams on Sand Foundations. *Transactions, American Society of Civil Engineers*, Vol. 73, 199 pp.

Huntoon, P.W., 1977. Cambrian Stratigraphic Nomenclature and Ground-water Prospecting Failures on the Hualapai Plateau, Arizona. *Ground Water*, Vol. 15, No. 6, pp. 426–433.

McKee, E.D., and Resser, C.E., 1945. *Cambrian History of the Grand Canyon Region*. Carnegie Institute, Washington Publication 563, 168 pp.

Miller, J.A., 1986. *Hydrogeological Framework of the Floridian Aquifer System in Florida and Parts of Georgia, Alabama, and South Carolina*. U.S. Geological Survey Professional Paper 1043-B.

Morris, D.A., and Johnson, A.I., 1967. *Summary of Hydrologic and Physical Properties of Rock and Soil Materials, as Analyzed by the Hydrologic Laboratory of the US Geological Survey 1948–1960*. U.S. Geological Water-Supply Paper 1839-D.

Nobel, L.F., 1914. *The Shinumo Quadrangle, Grand Canyon District, Arizona*. U.S. Geological Survey, Bulletin 549, 100 pp.

Nobel, L.F., 1922. A *Section of the Paleozoic Formations of the Grand Canyon at the Bass Trail* . U.S. Geological Survey Professional Paper 131, pp. 23–73.

Roscoe Moss Company, 1990. *Handbook of Ground Water Development*. John Wiley & Sons, New York, 493 pp.

Shepard, R.G. 1989. Correlations of Permeability and Grain Size. *Ground Water*, Vol. 27, No. 5, pp. 633–638.

Stephens, D.B., 1996. *Vadose Zone Hydrology*. Lewis Publishers, CRC Press, Boca Raton, FL, 347 pp.

This page intentionally left blank

Chapter

4

Basic Geophysics of the Shallow Subsurface

Curtis A. Link

Montana Tech of The University of Montana,
Butte, Montana

This chapter provides a basic introduction to the principles and applications of geophysical techniques as they might be applied to problems related to hydrogeology. The goal of geophysics is to determine properties and parameters of subsurface materials (usually rock or sometimes soils) from measurements made at the surface of the earth. Even though the scale of the problem may change, the physics of the basic techniques remains the same.

Many of the techniques and methods presented can be applied at various scales such as those encountered in oil exploration, in understanding shallow lithological parameters, or in determining properties at the mantle or core level.

Since this chapter covers a variety of techniques, it is impossible to explore each method in detail. Our goal is to provide readers with a basic understanding of the various geophysical techniques that are most commonly used such that they can determine which techniques are most applicable to particular problems.

The format of the chapter will be to introduce each technique; discuss data acquisition, processing, and interpretation principles; and provide one or more application examples from the literature.

Copyright © 2008, 2001 by The McGraw-Hill Companies, Inc. Click here for terms of use.

4.1 Common Targets for Shallow Geophysical Investigation

This chapter is meant to provide basic information on the most common geophysical techniques. However, for those unfamiliar with the methods and techniques of geophysics, it might be useful at this point to list some of the applications suitable for shallow geophysical investigations (list from Greenhouse et al. 1998). Please note that specific methods are site-dependent and the quality of results is dependent on the target, geologic environment, surface features, and other factors that affect the contrast of the target to the surrounding medium.

- Archeology
- Bedrock topography
- Forensics
- Mine waste
- Stratigraphy
- Buried drums, tanks, etc.
- Unexploded ordnance
- Faults, fractures, voids
- Water table
- Landfills and pits
- Contaminants—organic, inorganic

4.2 Approaches to Shallow Subsurface Investigations

Of course, the best way to determine properties of the subsurface is to observe or measure the materials directly. This is generally very difficult and usually impossible. The next best approach is to sample the subsurface materials at selected locations and extrapolate or interpolate the properties between sample locations. This is a typical and effective process whose success is limited mostly by the number of sample locations and the spacing between them. Large sample location spacings lead to increasingly unreliable predictions. Another common problem is that the materials of interest are often hazardous and it is usually desirable and often critical to avoid contamination of a surrounding zone by the hazardous material. An obvious example is the location of a corroded steel drum containing toxic substances. Physically probing for the drum poses the risk of puncturing it and exacerbating the problem. Using geophysical magnetic surveying techniques, the drum can

be located allowing a careful excavation of the drum and its remains (Reynolds 1997).

Geophysical techniques provide an alternative to the sample/interpolate approach. Geophysical methods allow calculation of subsurface properties without subsurface sampling. An effective approach to characterizing a site is to combine geophysical methods with observations from several sample locations to do a *guided* interpolation between the sample points; guided in the sense that the image of the properties between the sample points produced by the geophysical method does not have the level of detail obtained at the sample points themselves, but that the lower resolution geophysical image is derived from the actual intervening earth materials. This is in contrast to interpolating properties between sample points without any direct information from the intervening materials.

A further advantage of geophysical methods is that large areas can be surveyed quickly at a relatively low cost. Instead of being viewed as an additional cost, a geophysical survey should be considered as adding value by making the entire site investigation more cost-effective (Reynolds 1997).

4.3 Overview of Geophysical Techniques

A geophysical investigation often forms part of a larger study. As such, the geophysicist is responsible not only for the **acquisition** and **processing** of the geophysical data but also the **interpretation** of the final results for presentation to the client. Careful consideration and a close working relationship with the client is required if the geophysicist is to present results in a form consistent with the expected results. For example, in the case of a seismic refraction survey, the client probably is not interested in seismic velocity variations, but in the types of materials present and their properties (Reynolds 1997). The final form of the results should certainly be agreed upon before the investigation begins.

Methods

Geophysical techniques can be broadly classified into two groups. **Passive** methods, which detect variations in the natural earth fields such as gravitational or magnetic, and **active** methods, in which artificial signals are transmitted into the earth and subsequently recorded after passing through and being modified by earth materials (Reynolds 1997).

Limitations

Although geophysical methods are extremely useful in providing information about the subsurface, it is important to be aware of their limitations.

A common limitation is the lack of sufficient contrast in earth properties (Burger 1992). This problem manifests itself in not being able to detect or distinguish zones or properties of interest in the subsurface. Sometimes it is possible to use a different method or combine methods to alleviate the problem.

Another difficulty arises due to the nature of the problems and the methodologies employed. Few, if any, of the problems encountered in geophysical investigations have unique solutions. This arises from the fact that most of the geophysical solutions developed result from a process called inverse modeling. **Inverse modeling** is the process of observing the effects (i.e., geophysical measurements) and then solving for the cause (e.g., seismic layer velocities). This is in contrast to **forward modeling**, which would be equivalent, for example, to knowing the seismic layer velocities and then calculating the travel times that would be measured (Burger 1992). This relationship is shown schematically in Figure 4.1. This inherent nonuniqueness makes it necessary to use all available information in the interpretation and sometimes the processing stage. For example, when performing a seismic refraction survey, it is desirable to have shallow well logs and some sense of the shallow geology to control and limit obviously incorrect solutions in the processing and interpretation steps.

Still another limitation is **resolution**. Resolution, as defined by Sheriff (1991), is the ability to separate two features that are very close together or, alternatively, as the smallest change in input that will produce a detectable change in output. The desired resolution of relevant parameters may not be possible for specific geophysical methods or it may be cost prohibitive.

Finally, another limitation is **noise**. Noise can take a variety of forms. Sheriff (1991) defines noise as any unwanted signal or, as a disturbance

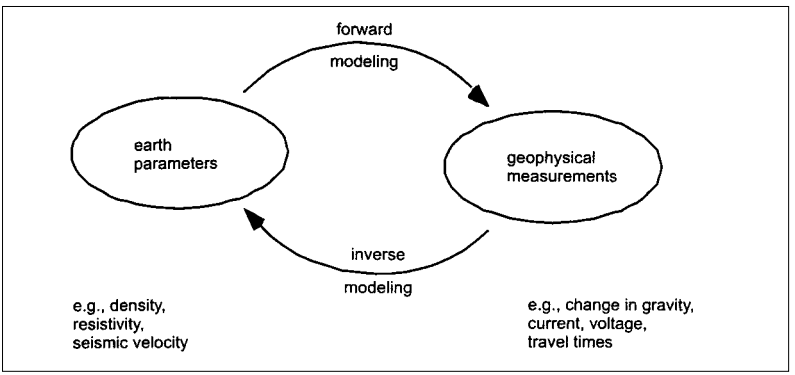

Figure 4.1 Schematic showing the complementary nature of forward and inverse modeling.

that does not represent part of a signal from a specific source. Noise can arise in the instruments used, result from uncontrollable conditions, or be related to operator error. Noise can mask the expected contrasts of earth parameters or manifest itself as error or uncertainty in the inversion process.

4.4 Matching Geophysical Methods to Applications

Because of the different properties measured by the different geophysical methods, it is necessary to match the correct method for the desired application. Reynolds (1997) provides a useful listing of the various geophysical methods and their main applications (Table 4.1). Further detail for each of the methods, including examples and case studies, will be shown in their respective sections.

TABLE 4.1 Geophysical Methods and Main Applications [From Reynolds (1997)]

Geophysical method	Dependent physical property	Applications (see key below)									
		1	2	3	4	5	6	7	8	9	10
Gravity	Density	P	P	s	s	s	s	!	!	s	!
Magnetic	Susceptibility	P	P	P	s	!	m	!	P	P	!
Seismic refraction	Elastic moduli; density	P	P	m	P	s	s	!	!	!	!
Seismic reflection	Elastic moduli; density	P	P	m	s	s	m	!	!	!	!
Resistivity (ER)	Resistivity	m	m	P	P	P	P	P	s	P	m
Spontaneous potential (SP)	Potential differences	!	!	P	m	P	m	m	m	!	!
Induced polarization (IP)	Resistivity; capacitance	m	m	P	m	s	m	m	m	m	m
Electromagnetic (EM)	Conductance; inductance	s	P	P	P	P	P	P	P	P	m
EM-VLF	Conductance; inductance	m	m	P	m	s	s	s	m	m	!
Ground penetrating radar (GPR)	Permitivity; conductivity	!	!	m	P	P	P	s	P	P	P
Magneto-telluric (MT)	Resistivity	s	P	P	m	m	!	!	!	!	!

P = primary method
s = secondary method
m = usable, but not necessarily the best approach, or undeveloped for this application
(!) = unsuitable
Applications:
1. Hydrocarbon exploration (coal, gas, oil)
2. Regional geological studies (100s of km^2)
3. Exploration/development of mineral deposits
4. Engineering site investigations
5. Hydrogeological investigations
6. Detection of subsurface cavities
7. Mapping leachate and contaminant plumes
8. Location definition of buried metallic objects
9. Archaeogeophysics
10. Forensic geophysics

4.5 Geophysical Survey Planning

It cannot be overemphasized that the prime objective of the geophysical survey should be clear from the beginning, especially before planning of the survey begins. Constraints and methodologies of surveys vary as the objectives do, and it is impossible to establish guidelines that will work, for example, for all electrical resistivity surveys. It should also be emphasized that there may not be an ideal method to apply. Sometimes, even with the use of two or more methods, the best results that can be obtained may be only to eliminate possibilities, for example, determining the absence of the water table at a particular depth. In addition, clearly defining the objective before a project begins can simplify the final stages of the project, which often involve interpretation, by ensuring that the deliverables are agreeable to both parties.

There have been only a few published guidelines on geophysical survey planning and execution: British Standards Institute BS 5930 (1981), Hawkins (1986), the Geological Society Engineering Group Working Party Report on Engineering Geophysics (1988), and Reynolds (1997). Also, little attention has been paid to survey design, at least for smaller scale investigations. This is in contrast to seismic exploration by the hydrocarban industry, which devotes considerable resources to survey planning and design and uses sophisticated survey design software packages to optimize recording parameters and strategies.

It is instructive to include Reynolds's (1997) quote from Darracott and McCann (1986):

> Dissatisfied clients have frequently voiced their disappointment with geophysics as a site investigation method. However, close scrutiny of almost all such cases will show that the geophysical survey produced poor results for one or a combination of the following reasons: inadequate and/or bad planning of the survey, incorrect choice or specification of technique, and insufficiently experienced personnel conducting the investigation.

It is the goal of this chapter to help increase the "satisfaction level" of individuals or organizations who have chosen to use geophysical methods as a sole or companion approach to a site investigation.

Cost is another factor associated with survey planning and design. Costs span the range from those for a simple one-method survey conducted by a geophysicist with local college student assistants requiring minimum travel to a multiple-method survey done in a remote area requiring a full field crew and various forms of logistic support, which might even include helicopters. Costs also vary with the amount of postacquisition processing or interpretation expected. Again, this can vary from a single product from a simple survey (e.g., a single refraction line interpretation) to multiple versions of numerous products that might require significant amounts of time spent on testing.

It is worthwhile to remember that the geophysical component of a site investigation is usually a relatively small fraction of the total cost and should be viewed with that perspective. Indeed, the judicious use of geophysics can save large amounts of money by allocating resources more effectively (Reynolds 1997). For example, a reconnaissance survey might be able to identify zones for more detailed work without the expense of performing a detailed investigation over the entire study area.

4.6 Seismics

This section on seismics will cover the basic principles and applications of **seismic refraction** and **reflection**.

Basic principles

The physical basis of seismology can be summarized simply. A disturbance (e.g., a vibration such as a sledge hammer blow) is created in a localized area, which then propagates as a vibration through the surrounding materials. The form of this propagating **wave** is spherical in a homogeneous medium. If the medium consists of different materials with different **elastic** properties, the shape of the wave front changes based on the nature of the materials. The propagating wave vibration is then recorded by an instrument called a **seismograph**, which is connected to sensing devices called **geophones**. The recording is typically done at the earth's surface where the original **seismic source** disturbance is created.

A geophone consists of a coil and magnet device attached or coupled to the ground, usually by means of a metal spike. As the ground surface vibrates in response to a propagated wave disturbance, the case of the geophone, which usually contains the magnet, moves relative to the coil, which is suspended by top and bottom springs. This relative motion induces a voltage which is proportional to the relative velocity of the coil with respect to the magnet (Sheriff 1991; Evans 1997). The voltage is recorded and analyzed for (1) the voltage signal shape characteristics and (2) the times at which the characteristic parts of the signal occur. The timing information is used with the geometry (locations of the seismic sources and receivers) to determine the earth propagation velocities and structure. This velocity and structure information is then interpreted to represent a geological cross section.

A simple example illustrating the wave propagation process occurs when a pebble is thrown into a still pond. Everyone is familiar with the circular wave patterns spreading out from the point where the pebble entered the water. With a stop watch and measuring tape, one can in fact determine the **speed of propagation** of the surface water waves. Also, with careful observation, one can determine some of the common wave characteristics such as **wavelength**, **period**, and **frequency**.

An illustration of a simple waveform and its characteristics is shown in Figure 4.2.

For "real-world" propagating waves, amplitude and wavelength (related to frequency) vary depending on the propagation conditions and media. The relationship among wave propagation velocity, frequency, and wavelength is given by:

$$\upsilon = f\lambda \tag{4.1}$$

where υ = wave propagation velocity
f = frequency in cycles/second or Hz
λ = wavelength

Figure 4.3 shows a plot of 24 waveforms as recorded in a refraction survey. Each waveform is called a **trace**. The traces are numbered sequentially, horizontally across the top of the plot. The vertical dimension of each trace shows the voltage variation with time as recorded from individual geophones. The dark portion of the trace is called the **peak** and indicates positive voltage; the open **trough** is negative. Time increases downward in units of milliseconds (ms). Note the changing waveform for each trace and how the pattern changes from trace to trace. The trace variations are characteristic of the propagation medium. The change from zero voltage to a positive or negative voltage is called the **first break** (e.g., trace 1, where the line intersects the trace) and indicates the **first arrival** of the propagated wave energy. The arrow points to the trace where there is a change in slope of the first arrival alignments. This indicates the occurrence of **refraction**. Analysis of the first arrival slopes (sloping lines) gives the velocities and thickness of the earth layers (see section on refraction).

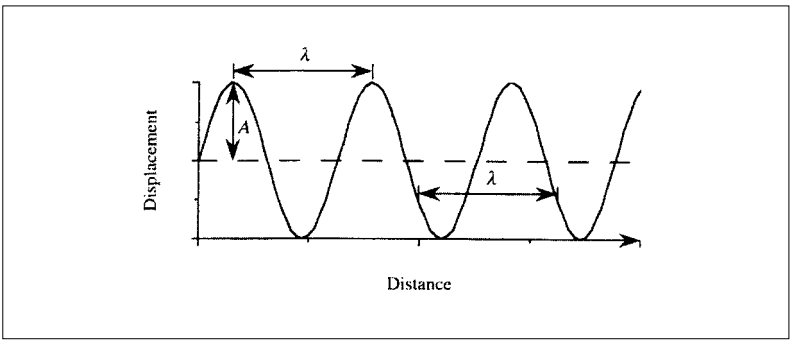

Figure 4.2 Schematic illustrating some of the characteristics of a wave and common terminology: wavelength (λ), amplitude, crest or peak, and trough. [*After Burger* (*1992*).]

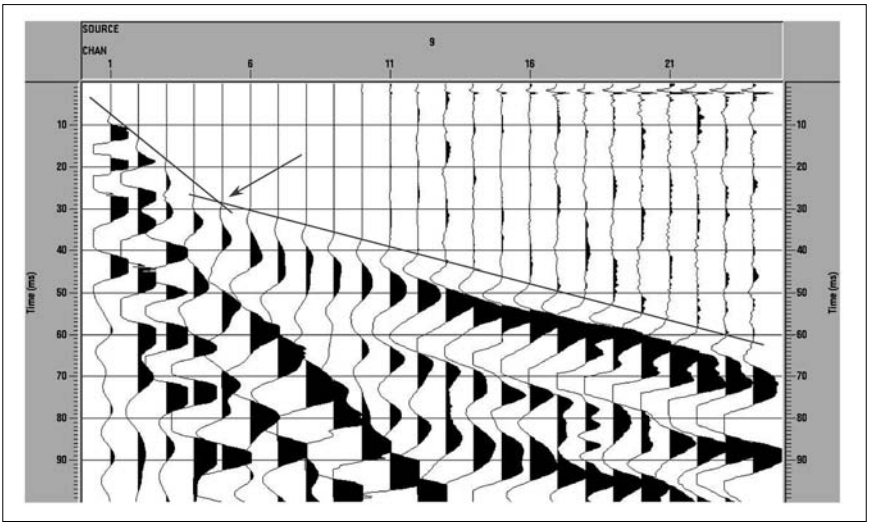

Figure 4.3 Plot of seismic data traces as recorded in a refraction survey. Traces are numbered 1 to 24, from left to right, and show signal variation with time from top to bottom (time in ms). Note the changing waveforms on each trace and the change in slope of first arrival times.

Figure 4.4 depicts seismic wave propagation in a simple medium. Notice that what is labeled as the **ray** is perpendicular to the **wavefronts**. Many of the diagrams used to depict seismic waves show only rays to simplify the drawings. This is especially convenient when illustrating the concepts of reflection and refraction. However, it is important to keep in mind that even though the concept of a ray is useful, seismic waves propagate as spherical wavefronts (homogeneous medium),

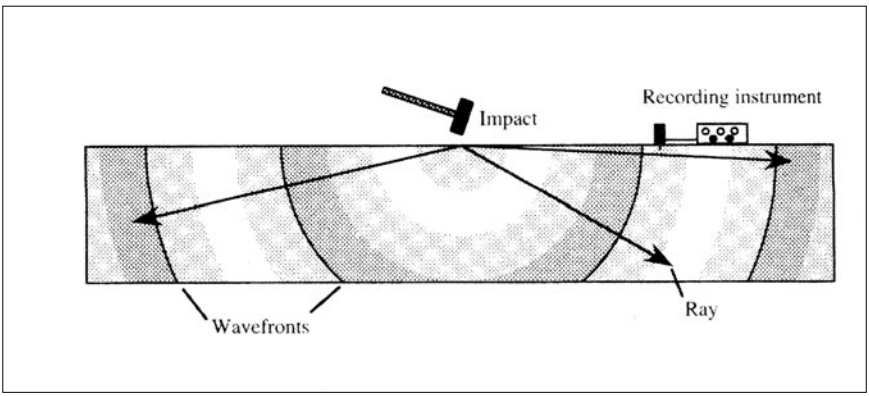

Figure 4.4 Illustration of wavefronts and a single ray in a simple medium. [*After Burger* (*1992*).]

and the ray only approximates the wavefronts when the amount of curvature of the wavefronts is very large (i.e., tightly focused wavefronts). This is called the **high-frequency approximation**.

Seismic waves can be categorized into two groups: body waves and surface waves. For many purposes, surface waves are considered noise. However, recent work has made use of the dispersion characteristics of Rayleigh mode surface waves to determine additional subsurface properties including shear velocity.

Seismic body waves can propagate in two main modes: **compressional** (P or P-wave) and shear (S or S-wave) waves. The modes are distinguished by the direction of particle movement associated with the particular mode. Figure 4.5 is an illustration of the particle motion associated with P-wave propagation. For P-waves, particle motion is in the direction of wave propagation; for S-waves, particle motion is perpendicular to the direction of propagation.

The most common types of geophones are sensitive to ground displacement in the vertical direction (see ground motion components in Figure 4.5). Depending on the angle of emergence of the seismic wave, the vertical component may only represent a small fraction of the energy associated with the propagating wave.

Useful information about earth properties is often contained in S-wave recordings. Shear waves are often more sensitive to conditions such as anisotropy due to layering and fluid content in formations. To record S-waves, geophones that are sensitive to particle motion in the horizontal direction must be used. The horizontal direction is usually specified as **in-line** (in the direction of the line of geophones deployed) or

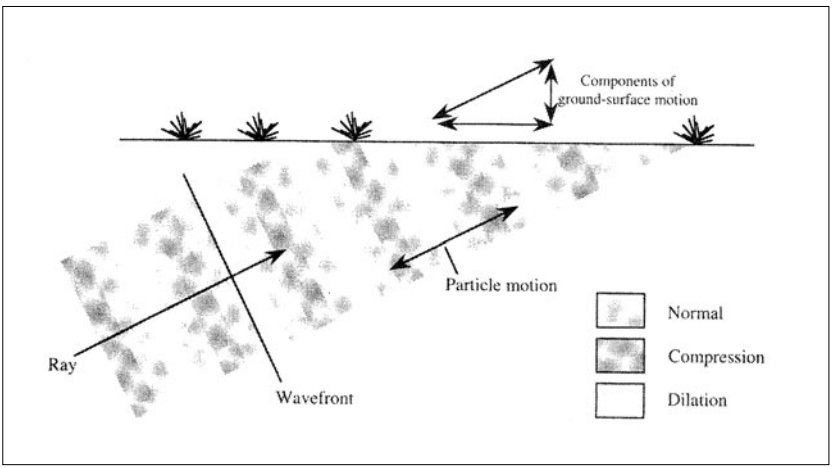

Figure 4.5 Schematic showing particle motion for compressional or P-wave. [*After Burger* (*1992*).]

cross-line (perpendicular to the line of deployed geophones). For recordings of S-waves, geophones are usually used that can record three components: the vertical as well as the two horizontal components. These are called **3-C** recordings.

Seismic surveys can generally be accomplished in three ways: **refraction** surveys, **reflection** surveys, and **tomography** surveys. Reflection and refraction surveys are described in the following sections.

Reflection principles. Even though refraction methods comprise the highest proportion of shallow seismic surveys, it is useful to look at the process of reflection first. The basic principle controlling reflection is shown in the Figure 4.6 and can be stated as, "the angle of incidence equals the angle of reflection." Figure 4.6 shows an incident seismic ray (recall that a ray is a geometric construct that is perpendicular to spherical wavefronts) on a plane interface separating two geologic media with different properties.

In this example, the properties that affect the seismic wave propagation are seismic velocity and bulk density. Because density doesn't vary as much as velocity in a normal sedimentary sequence, usually only seismic velocity is specified as the variable. Table 4.2 shows values for density (ρ) and compressional (υ_p), and shear (υ_s) seismic velocities for various rock types.

The convention for referring to the angles associated with propagation is to measure the angles from the normal to the interface. Thus, the **Law of Reflection** can be stated as:

$$\theta_{\text{incidence}} = \theta_{\text{reflection}} \tag{4.2}$$

It should also be noted that the amplitudes of reflected waves are lower than the amplitudes of the incident wave. This follows from the

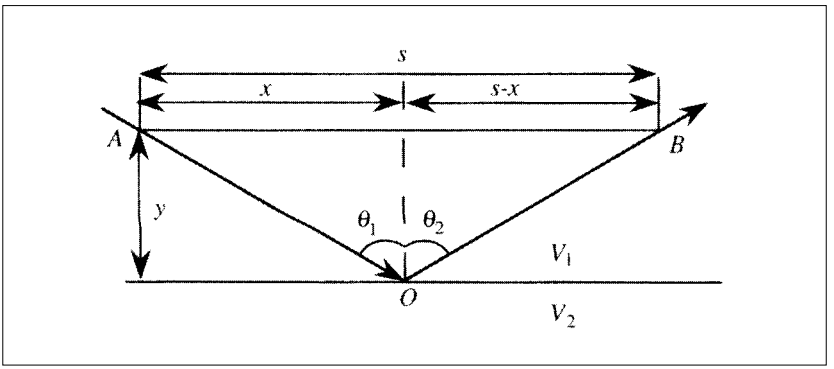

Figure 4.6 Illustration of the principle of reflection.

TABLE 4.2 Seismic Velocities and Densities for Common Rock Types [After Burger (1992)]

Rock type	Density ρ (g/cm^3)	υ_p m/s	υ_s m/s
Shale (AZ)	2.67	2124	1470
Siltstone (CO)	2.50	2319	1524
Limestone (PA)	2.71	3633	2319
Limestone (AZ)	2.44	2750	1718
Quartzite (MT)	2.66	4965	3274
Sandstone (WY)	2.28	2488	1702
Slate (MA)	2.67	4336	2860
Schist (MA)	2.70	4680	2921
Schist (CO)	2.70	5290	3239
Gneiss (MA)	2.64	3189	2053
Marble (MD)	2.87	5587	3136
Marble (VT)	2.71	3643	2355
Granite (MA)	2.66	3967	2722
Granite (MA)	2.65	3693	2469
Gabbro (PA)	3.05	5043	3203
Diabase (ME)	2.96	6569	3682
Basalt (OR)	2.74	5124	3070
Andesite (ID)	2.57	4776	2984
Tuff (OR)	1.45	996	659

Values selected from Press (1966).

conservation of energy and looking at the redistribution of the incident wave energy. In fact, the amplitude of a seismic wave decays due to not only loss of energy at reflections but also spherical spreading and attenuation. **Spherical spreading** is the decay of amplitude associated with an expanding wavefront. If one unit of energy is present initially at the time of the wave initiation, that unit of energy is subsequently spread over an increasingly larger area (proportional to r^2) of the expanding wavefront resulting in decreasing energy density which is proportional to the square of the wave amplitude. Thus spherical spreading can be compensated for by using a correction factor of 1/r (r is distance from point of wave initiation). **Attenuation** is the exponential decay in amplitude associated with vibrational energy loss (heat) of the propagating wave. Rock materials can be characterized by an attenuation coefficient with units of decibels (dB) lost per cycle (wavelength). Multiple seismic reflections (**multiples**) can occur in a layered earth with subsequent energy loss at each reflection. This occurs in addition to spherical spreading and attenuation. A familiar example of multiples is the case of being inside an elevator with mirrored walls and observing your reflection. Each reflection entails an additional loss of energy proportional to the properties of the incident and reflecting media.

Refraction principles. The law of refraction, or **Snell's law**, describes what happens to waves as they are transmitted through an interface. Snell's law can be stated as:

$$\frac{\sin(\theta_{\text{incident}})}{v_1} = \frac{\sin(\theta_{\text{refracted}})}{v_1} \tag{4.3}$$

This is illustrated in Figure 4.7, which shows Snell's law for a single interface. It is important to note that the phenomenon occurs at every interface, plane or curved, where there is a difference in elastic properties (seismic velocities and densities). Thus, for a multilayered case, refraction occurs at each interface and the ray can bend away from the interface normals ($\upsilon_1 < \upsilon_2$) or toward them ($\upsilon_1 > \upsilon_2$).

Figure 4.8 shows a case of three layers with seismic velocities $v_1 < v_2 > v_3$ (assuming constant density). Note the direction of bending of the seismic ray with respect to the normal: for $v_1 < v_2$, the ray bends away from the normal; for $v_2 > v_3$, the ray bends toward the normal.

A phenomenon that occurs in the process of refraction is called **critical refraction**. Critical refraction occurs when the refraction angle in Snell's law is equal to 90°. A refraction angle of 90° means that the refracted wave travels along (parallel to) the medium interface. This phenomenon results in what are called **head waves**. Head waves result from the energy traveling along the interface at velocity v_2 "leaking" energy into the upper medium which can only travel at velocity v_1. The head wave energy leaves the interface at an angle equal to the incident angle (critical angle) as shown in Figure 4.9. Example 4.1 shows the critical angle calculation.

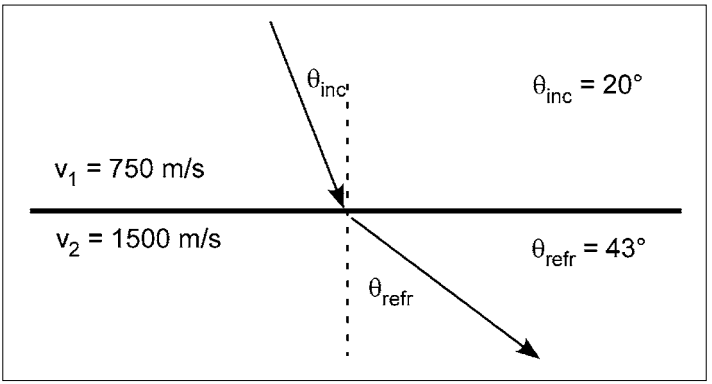

Figure 4.7 Example of Snell's law (refraction) for a single interface ($v_1 < v_2$).

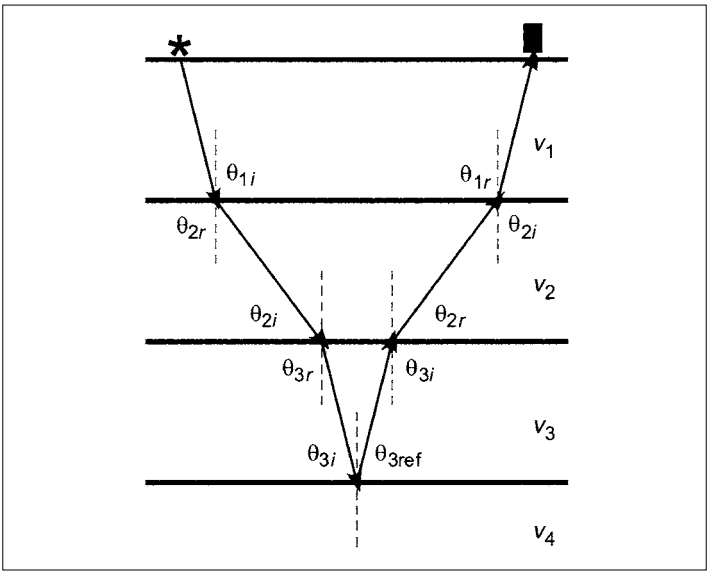

Figure 4.8 Example of Snell's law showing refraction from medium 1 to medium 2, refraction from medium 2 to medium 3, reflection at the interface between medium 3 and medium 4, and then refraction back to the geophone at the surface.

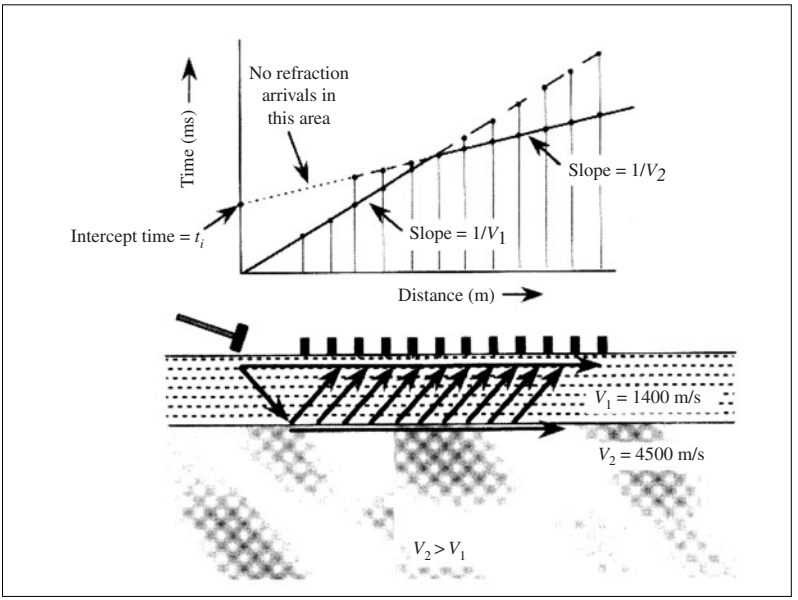

Figure 4.9 Example showing critical refraction and head wave propagation in a simple geological model. [*From Burger* (*1992*).]

Example 4.1 Critical angle calculation

For a two-layered medium with $v_1 = 1{,}000$ m/s and $v_2 = 1{,}500$ m/s, what is the angle of incidence for a critically refracted ray?

Solution:

$$\frac{\sin\theta_1}{v_1} = \frac{\sin\theta_2}{v_2}$$

$$\sin\theta_1 = \frac{v_1}{v_2}\sin\theta_2$$

$$\sin\theta_1 = \frac{v_1}{v_2}\sin 90^\circ = \frac{v_1}{v_2}$$

$$\theta_1 = \sin^{-1}(v_1/v_2) = \sin^{-1}\left(1{,}000\,\frac{m}{s}\,/1{,}500\,\frac{m}{s}\right)$$

$$\theta_1 = 41.58^\circ$$

Figure 4.9 shows critical refraction and the resulting head waves. Note how the critically refracted wave traveling along the interface between medium 1 and medium 2 gives rise to head waves in medium 1. Analysis of the recorded arrival times is based on calculations for three segments: time for energy to propagate from the seismic source to the interface at the seismic velocity v_1, time for the energy to propagate from the point of contact with the interface to the point of exit from the interface at v_2, and time for the energy to propagate to the surface at the speed v_1.

The simple geological model shown in Figure 4.9 would produce a refraction record similar to the actual one shown in Figure 4.3. The time/distance plot at the top of Figure 4.9 shows the first break times picked from the refraction record plotted against geophone offset (distance). This **t-x** plot is then used for analysis. The slopes of the lines drawn on the first breaks along with the **intercept time** solve the simple refraction problem:

- Velocity of layer 1
- Velocity of layer 2
- Thickness of layer 1

The solution for this simple refraction problem is given by:

$$h_i = \frac{t_i}{2}\,\frac{v_2 v_1}{(v_2^2 - v_1^2)^{1/2}} \tag{4.4}$$

where t_i = intercept time picked from the t-x plot (Figure 4.9)
v_1 = inverse of the slope of line 1 (Figure 4.9)
v_2 = inverse of the slope of line 2

Refraction analysis increases in complexity as geological models become more realistic, starting from the single, horizontal subsurface

just described to multiple horizontal interfaces, single dipping interfaces, and multiple dipping interfaces. In addition, heterogeneities in the subsurface make it difficult to fit straight lines to first break picks. For example, a "pod" of slower material will delay propagating energy such that the time increases for a particular geophone or geophones. So, those first breaks will not lie on a straight line.

Thus it can be seen that the process of picking the first breaks is actually an interpretation in itself. At this point, it is worth noting that the subsurface *does not* really look like the simple layers described. In fact, the subsurface is better described by properties that change continuously rather than discretely.

Refraction surveying

Targets. The seismic refraction method is useful when the target is shallow and low-dipping and consists of materials with different elastic properties. Refraction surveying is often used to detect the water table or a shallow bedrock interface. It can and should, if possible, be used with other techniques such as electrical resistivity. This combination works especially well if the target is the water table. Mapping of the water table using this approach can be done relatively cheaply and quickly in areas with limited water well information.

Limitations. A significant limitation of the refraction method is that it requires that material velocities increase with depth. If a medium contains a layer with a lower velocity than the layer above it, the layer with the lower velocity is called a **hidden layer** and will not be detected by the refraction method. The reason this occurs can be easily seen by looking at the example for the critical angle calculation. The angle of incidence is undefined for $v_1 > v_2$ using the critical angle condition of $\theta_2 = 90°$. Thus, for a typical shallow geological scenario of interbedded sands, clays, and gravels, a low velocity layer would remain undetected using the refraction method.

Equipment. Refraction surveying can be accomplished with equipment as minimal as a sledgehammer, geophones and cabling, and a seismograph. It helps to have additional field hands to improve efficiency. In addition, it is necessary to have some means of analyzing the data. This could be done by hand, but it is convenient and more efficient to use software designed for that purpose.

Common seismographs available for purchase or rent typically have 24 channels, which means that 24 individual geophones or groups can be used. Unless you are doing refraction (or reflection) surveys on a

regular basis, it is better to rent the equipment or to contract someone who can do the survey for you.

Seismic sources can be as simple as a sledgehammer and striking plate (Figure 4.10). For deeper targets or greater penetration, modified guns can be used, for example, the Betsy Seisgun, which uses 8 gauge shells, or modified rifles (e.g., modified .30-06). Another popular source is the accelerated weight drop. This consists of a metal ram of substantial mass (50 kg) accelerated to a striking plate on the ground with a thick elastic band. The mechanism is then rearmed using hydraulics (Figure 4.11).

Local universities and colleges are often good sources for rental equipment. A number of companies rent geophysical equipment. An internet search will provide contacts for equipment rental services as well as full-service geophysical contracting services.

Site selection and planning. For geophysical investigations, it is always important to determine as much as possible about the local geology, both

Figure 4.10 Example of sledgehammer/striking plate as a seismic source.

Figure 4.11 Photograph of accelerated weight drop source with 100 lb ram mounted on an all-terrain vehicle. The striking plate is directly under the ram. A battery-operated motor operates the hydraulic pump to rearm the ram.

surface and subsurface, before undertaking fieldwork (Burger 1992). More effective surveys result from this a priori knowledge, and the information can be critical in processing and interpretation of the data. Geophysical solutions are implicitly nonunique and a priori information is often crucial in eliminating physically unrealizable solutions from the many possible solutions.

Example 4.2 Figure 4.12 is an example of the results obtained from a refraction survey conducted by Lankston (1990) for a potential waste disposal site. With careful data acquisition and analysis, a geologic section can be formed showing excellent vertical as well as horizontal resolution.

Example 4.3 This example describes a refraction survey in a mining reclamation area in Montana. The location is a creek drainage that has been running dry after historical placer mining activity. The Bureau of Land Management is investigating the feasibility of installing underground "dams" on the bedrock in an attempt to pool groundwater. The goal of the investigation was to determine bedrock depth.

A refraction survey was performed using three landstreamers consisting of 24 gimbaled geophones per streamer with 1 m geophone separation. A sledgehammer source was used stacking the individual shots 16 times. Figure 4.13 shows results obtained from processing the data using a refraction processing package called SIPQC (Rimrock Geophysics Inc.). Bedrock depth is approximately 7 m, a reasonable depth for attempting the restoration project.

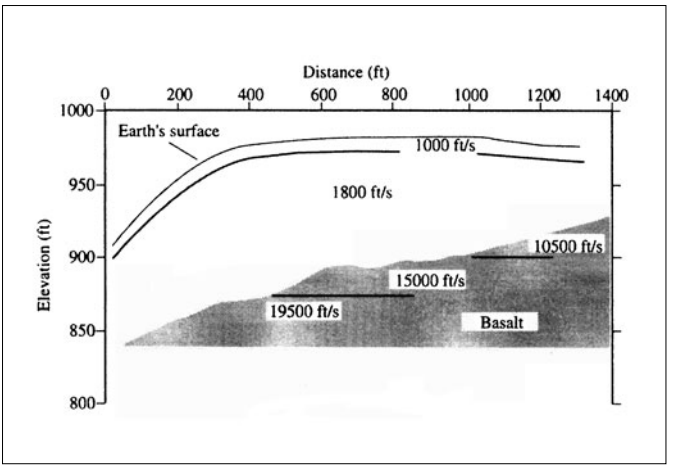

Figure 4.12 Example of a geologic section derived from a refraction study. The particular method used for refraction data analysis is able to determine lateral velocity changes as well as vertical. [*From Burger* (*1992*), *after Lankston* (*1990*).]

Reflection surveying

Although refraction surveying is the predominant technique in shallow seismic investigations, the increasing capabilities of inexpensive computers and availability of processing software has made reflection surveying an attractive alternative in many cases.

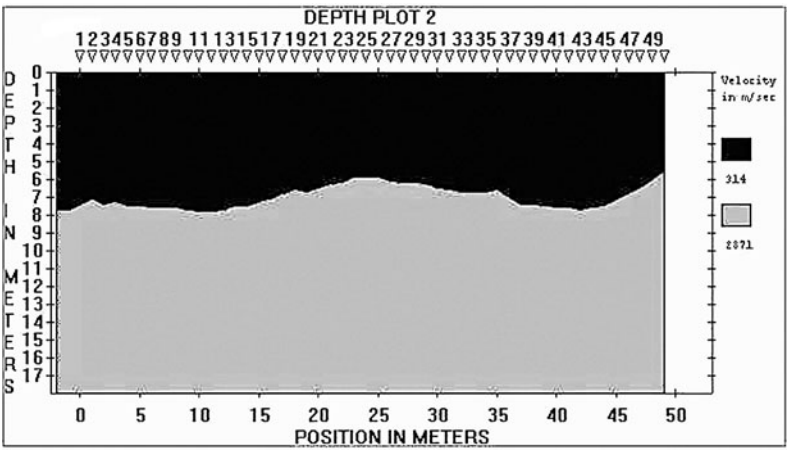

Figure 4.13 Refraction result for mining reclamation project in Montana. Bedrock depths show undulation of bedrock interface. Velocity of overburden is low at approximately 300 m/s while velocity of Mississippian age limestone bedrock is high at approximately 3000 m/s.

Reflection surveying is fundamentally different from refraction surveying because it uses reflections from a geologic interface rather than recording the refracted head wave traveling along the interface. One of the major difficulties to deal with in reflection surveying is the lower amplitude of the recorded reflection compared to a refraction. This has led to innovations in processing reflection recordings, which include **stacking** as the most important noise-reducing technique. Stacking is the process of assembling source/receiver combinations from different shot records that reflect from the same subsurface point. These combinations arise from different source/receiver locations; thus they have different travel path lengths (Figure 4.14). The reflection arrives at a different time for each pair. A correction is calculated to remove this time difference and the traces are then summed at each time increment. The effect is to enhance coherent events on the trace and suppress random and unwanted noise. This **zero-offset** trace is then plotted with other zero-offset traces at the x-location corresponding to the reflection point. This set of common depth point (CDP) traces is then plotted and called a **seismic section**. On the seismic section, adjacent reflection events line up, allowing an interpreter to analyze the section for geologic interfaces corresponding to the reflections (Figure 4.15).

Targets. The seismic reflection method is useful for mapping variable subsurface structure and stratigraphy (Greenhouse et al. 1998). The main benefit of the reflection method is that it is able to provide more detail and resolution in the interpreted results than the refraction method. However, this increased resolution comes at a price—the presence of favorable conditions that permit recording good reflection shot records. (A shot record is the set of traces resulting from a single source

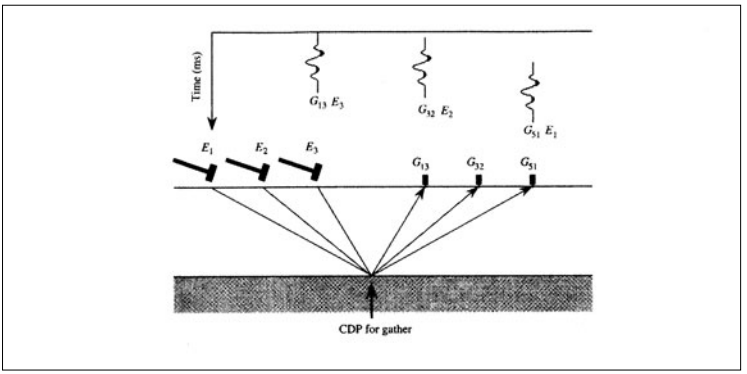

Figure 4.14 Schematic showing three source/receiver pairs that each record a reflection from a common point (CDP). The individual traces exhibit different arrival times which are corrected in subsequent processing. [*From Burger* (*1992*).]

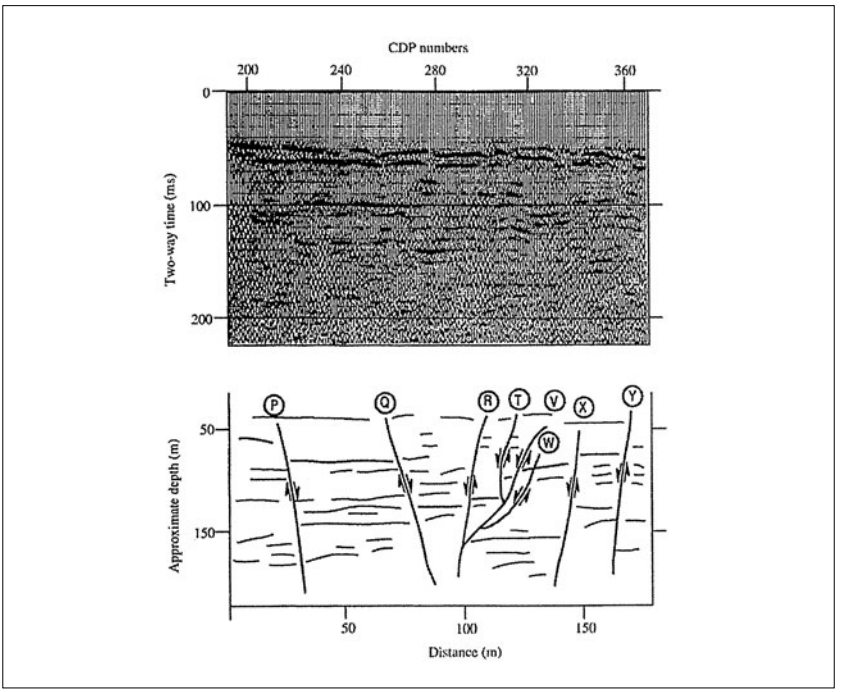

Figure 4.15 Example of a stacked seismic section and geologic interpretation for a shallow seismic reflection survey from southwestern Oklahoma. Stacked reflection traces in top panel; geologic interpretation in bottom panel. [*From Burger* (*1992*) and *Miller et al*. (*1999*).]

location and multiple geophone locations (see Figure 4.3). It is usually necessary (or at least recommended) to perform tests to determine if reflections can be recorded in an area of interest. If no evidence of reflections occurs on a shot record, a refraction survey or other approach would be advisable.

Optimum conditions for the reflection method in shallow environmental and geotechnical studies occur when the overburden is fine-grained and saturated, conditions not conducive to ground-penetrating radar (Greenhouse et al. 1998). The reflection method can be particularly valuable in hazard assessment. Detailed information can be obtained from the shallow subsurface in zones of active faults or in areas of potential collapse due to sinkholes or mining activity (Burger 1992).

Limitations. Reflection surveying is mainly limited by lithologic conditions, in other words, whether reflections can be recorded or not. In addition, more resources are required to analyze the data records. Reflection surveying typically records more data than the refraction method. This requires increased computer storage capability.

Processing reflection data using the common reflection point (CRP) method generally requires software to perform the proper trace sorting and corrections. A simpler approach, the **optimum offset** method (Hunter et al. 1984), can be applied without additional software and is simple to implement and quite efficient (Figure 4.16).

Equipment. Equipment for shallow reflection surveys is similar to that required for refraction surveys. A sledgehammer might be an effective source in some areas but often reflection surveying requires more seismic source energy. A shotgun or rifle type source can be used effectively in those cases. Other types of sources include weight dropping, elastic wave generators (using a large elastic band to input seismic energy to the ground), and small-scale vibratory sources.

Most of the processing concerns choosing appropriate parameters. Very sophisticated and complex packages are used by the oil industry. More modest packages useful for geotechnical applications include WINSEIS (Kansas Geological Survey), EAVESDROPPER, PROSEIS, and SPW. Seismic UNIX, or SU, is a free processing software package available from the Colorado School of Mines Center for Wave Phenomena.

Following are two examples showing the application of the seismic reflection method.

Example 4.4 Figure 4.17 shows a seismic section resulting from a survey done by the shallow seismic group at the University of Kansas/Kansas

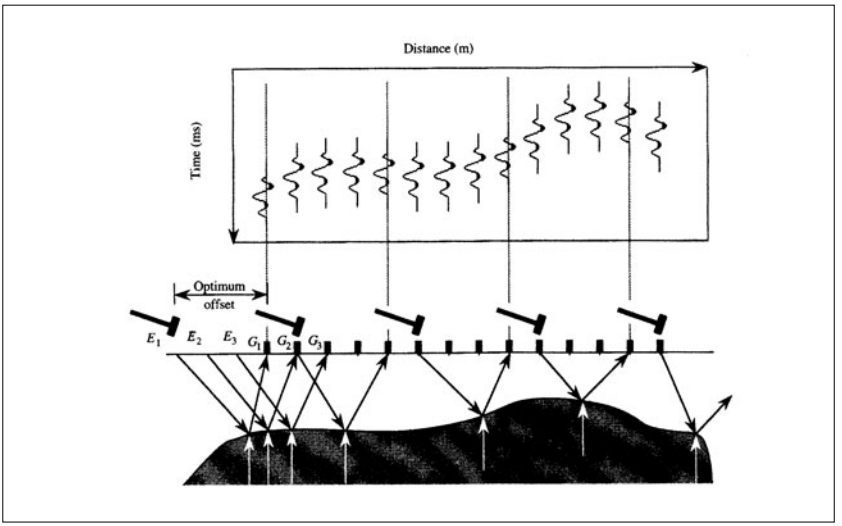

Figure 4.16 An example of common-offset profiling. Position of light-colored arrows indicates reflection points relative to the position of the recording geophone. [*From Burger* (*1992*).]

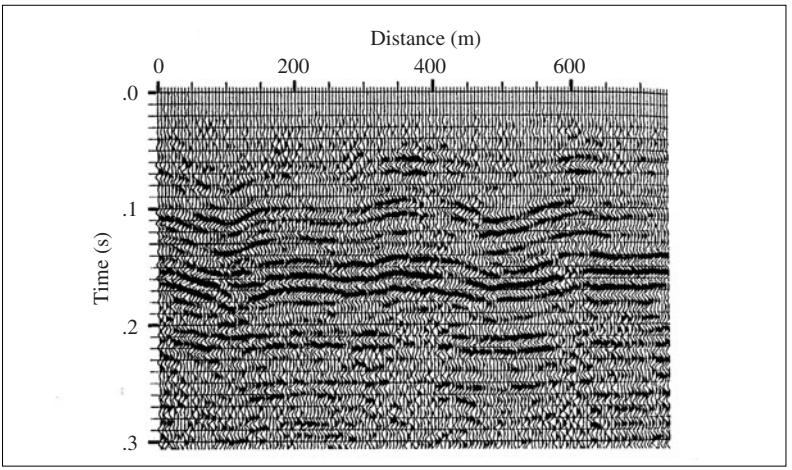

Figure 4.17 An example of a processed CDP seismic reflection record showing stratigraphic changes caused by sinkholes formed by salt dissolution. [*From Burger* (*1992*). *Figure courtesy of R.D. Miller and D.W. Steeples, Kansas Geological Survey*.]

Geological Survey. This group is well known for their innovations and work in the area of shallow seismics. The section shows evidence of dissolution structures in the discontinuity of stratigraphic boundaries.

Example 4.5 Figure 4.18 illustrates the detection of faults cutting coal seams using the seismic reflection method. The subvertical lines on the section are interpreted fault locations and do not result from the seismic data processing. Other useful examples and guidelines can be found in Ward Volumes I–III (1990).

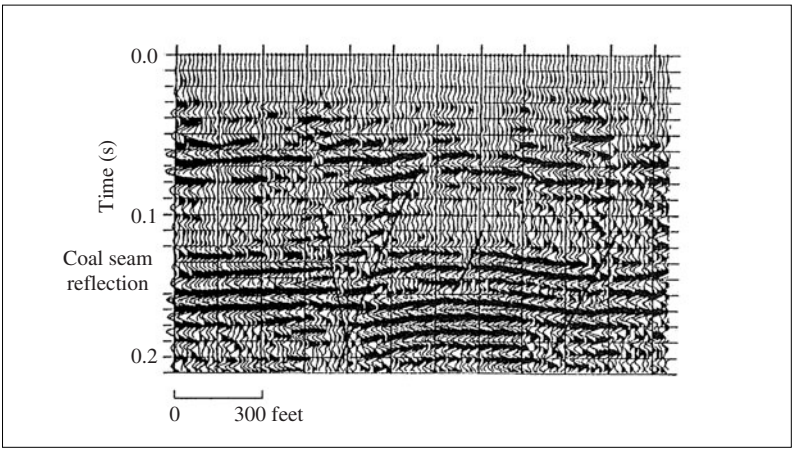

Figure 4.18 Another example of a CDP seismic section illustrating locations of faults cutting coal seams. [*From Burger* (*1992*), *after Gochioco and Cotton* (*1989*).]

4.7 Surface Wave Methods

A relatively new methodology applied to shallow seismic investigations is **surface wave analysis**. Recalling that seismic waves can be characterized as body waves (P-wave, S-wave) and surface waves, it is useful to note that body waves make up less than 30% of the energy in a seismic wave while surface wave modes can contain over 70%. Surface wave energy is usually considered noise as it interferes with body wave seismic arrivals. However, surface waves have a useful characteristic that make them noteworthy. That property is **dispersion**. Dispersion is the variation of velocity with frequency. The dispersion of body waves is small under most circumstances but surface waves may show appreciable dispersion in the presence of near-surface velocity layering (Sheriff 1991). Most importantly, dispersion is most influenced by S-wave velocity and a shallow S-wave velocity profile with depth can be calculated from the dispersion characteristics of the vertical or Rayleigh mode of surface waves.

What makes this approach so attractive is that the surface wave energy used to calculate an S-wave profile is recorded with conventional P-wave, vertical geophones. In principle, both P-wave and S-wave velocity profiles can be produced from the same data set. This represents a great increase of information for little or no extra field effort. In addition, P-wave and S-wave velocity can be used to calculate a third parameter of interest: Poisson's ratio. Note however that recommendations for recording surface waves are to use geophones of lower natural frequency (e.g., 4.5 Hz). Typically shallow seismic investigations record data using geophones of higher natural frequency, for example, 30 Hz or higher. Thus, recording surface wave modes and body wave modes with the same instrumentation may compromise one of the modes depending on the frequency of the geophones used. Also, optimum recording of surface waves may require a longer shot offset (distance from shot to nearest geophone) than for recording body waves, again, recording of one or the other modes may be compromised.

The technique described above is called Multichannel Analysis of Surface Waves or MASW. The Kansas Geological Survey has been in the forefront in developing the MASW method and produces software for surface wave analysis. A recent upgrade has the capability to perform passive source (e.g., road traffic as seismic source) as well as active source (e.g., sledgehammer) surveys. Two useful references describing MASW methodology and case histories are Miller et al. (1999) and Xia et al. (2002).

Recent projects at Montana Tech have been performed using one type of geophone to record data for body wave analysis and surface analysis. Our geophones are 30 Hz natural frequency, gimbaled, in a **landstreamer** arrangement. We have recorded and analyzed data from a test

site with a buried concrete structure, over an earthen dam that has developed leaks, over a buried mine shaft under a street intersection, at a site contaminated by treatment of timbers for underground mines, and at a local swimming pool.

Figures 4.19 to 4.21 show results from the swimming pool project. The local swimming pool has been in a constant state of repair due to leakage presumably caused by shifting from changing soil conditions. An electrical and seismic survey were performed to investigate subsurface conditions that might have been responsible for the ground movement. Figure 4.19 shows a portion of two P-wave velocity profiles near the pool. The profiles were produced using refraction tomography software (Rayfract) that produces a continuous velocity profile with depth. The data were recorded with a 24-channel landstreamer using 1 m geophone spacing and a 5 m sledgehammer shot offset with a shot moveup of 3 m.

Figure 4.20 shows the S-wave velocity profiles created using the Kansas Geological Survey software SurfSeis. The shear wave velocities range from approximately 200 m/s at the surface to approximately 400 m/s at depth. The profiles are produced by interpolating between the 1D shear velocity profiles calculated at the center of each geophone spread layout.

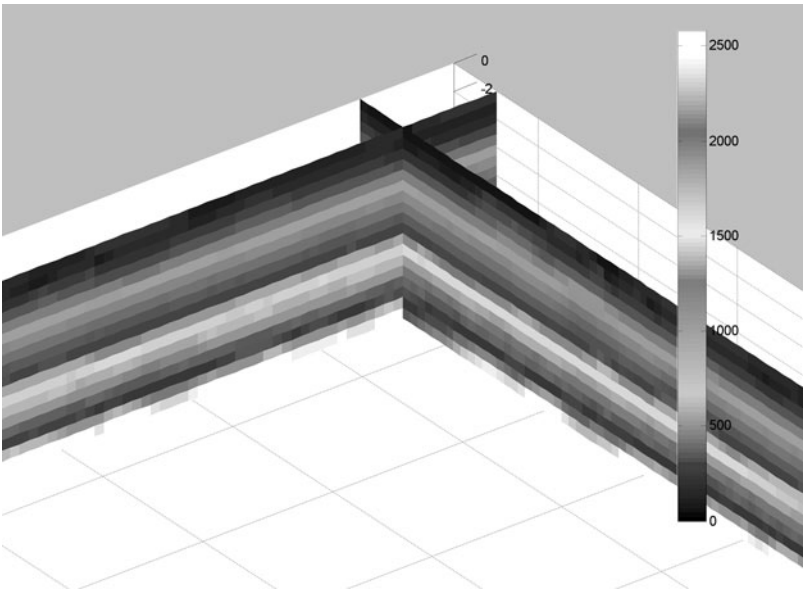

Figure 4.19 Intersecting P-wave velocity profiles showing good agreement of velocity at intersection. Profiles were created using refraction tomography software. Velocity increases from approximately 500 m/s at the surface to 2500 m/s at depth.

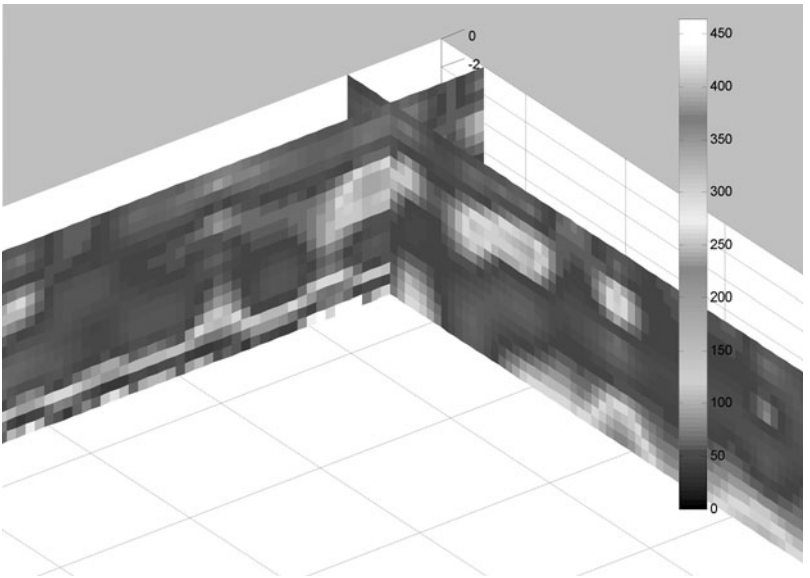

Figure 4.20 Intersecting S-wave velocity profiles for the swimming pool project. S-wave velocities indicate several pods of higher values along both profiles. S-wave velocities range from approximately 200 m/s at the surface to approximately 400 m/s at depth.

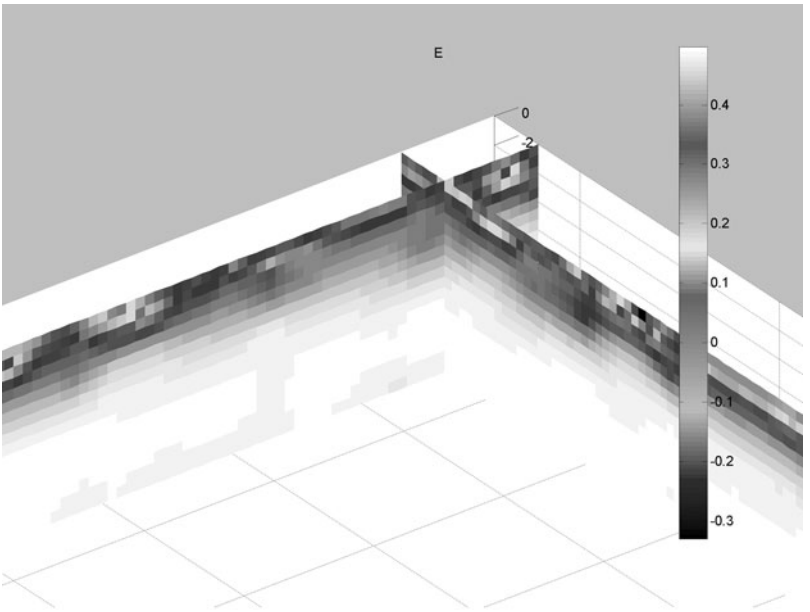

Figure 4.21 Intersecting Poisson's ratio profiles created from P-wave and S-wave velocity profiles. High Poisson's ratios at depth indicate unconsolidated material.

Next we calculated Poisson's ratio from the P-wave and S-wave velocity profiles. Both profiles need to have the same extents and pixel dimensions. Poisson's ratio is calculated from

$$\sigma = \frac{V_p^2 - 2V_s^2}{2(V_p^2 - V_s^2)}$$

where V_p is P-wave velocity and V_s is S-wave velocity. If the profiles are displayed in the program Surfer by Golden Software, the calculations can be easily done using grid math and then displayed. Figure 4.21 shows the Poisson's ratio results for the swimming pool project. Poisson's ratio ranges from approximately 0.05 in isolated zones near the surface to 0.45 at depth.

4.8 Electrical

Basic principles and units

The methods introduced in this section are based on measurements and interpretations resulting from earth materials with different electric properties. The quantities measured are either **conductivity** (ability of a material to conduct current under an applied electric force, i.e., voltage) or **resistivity** (property of a material that is a measure of resistance to current flow).

Resistivity is the reciprocal of conductivity (as resistance is the reciprocal of conductance) and its units are ohm · m (Ω · m). The units of **conductivity** are mhos/m or the more commonly used SI unit msiemens/m (mS/m). A commonly used unit for groundwater conductivity is the microsiemen/cm (μS/cm). A conductivity of 1 mS/m is equivalent to 10 μS/cm. Resistivity (ρ) in Ω · m and conductivity (σ) in mS/m are easily converted using the following relationship

$$\rho = \frac{1000}{\sigma}$$

The commonly used term **resistance** depends not only on the material but also its dimensions and is measured in the familiar unit ohm. The fundamental property of the material is its resistivity, usually denoted by the variable ρ. **Conductance** is the inverse of resistance, and its unit is the siemens (S), which is the reciprocal of the ohm.

The most fundamental issue in undertaking a geophysical survey is the detectability of the target. As discussed earlier, detection requires sufficient contrast in physical properties and suitable factors of scale, shape, and depth of the target (Greenhouse et al. 1998). The other factor that goes hand-in-hand with detectability is resolution. Detecting a target and resolving it are two different but complementary issues.

This section covers the broad category of electrical techniques. The presentation of topics generally follows the trend from methods with higher levels of resolution to methods of lower resolution.

In going from a discussion of seismic techniques to the broad category of electrical methods, two differences become evident. First, the diversity of electrical methods that exists, and second, the relative complexity in deriving quantitative interpretations from field data compared to seismic methods (Burger 1992).

Electrical methods generally fall into two categories: (1) those in which current is applied to the earth and (2) those using natural energy sources.

Applied current methods. In **electrical resistivity** (ER) methods, direct or low-frequency alternating current is applied at the ground surface and potential difference (voltage) is measured between two points. **Induced polarization** (IP) is a technique that uses the time-dependent decay of the potential difference to obtain information about the polarization properties of the earth materials. A third method, **electromagnetic surveying** (EM), uses a primary electromagnetic field produced by alternating current to induce a secondary field in subsurface conductive bodies. The difference between the primary and secondary fields provides information on subsurface characteristics (Burger 1992).

Natural current methods. Natural current methods take advantage of naturally occurring currents in the earth. **Tellurics** is the method of measuring the potential differences at the earth's surface resulting from variations in the flow of natural (telluric) currents through earth materials. **Magnetotellurics** is similar but measures the magnetic field as well as the electric field. **Spontaneous potential** (SP) is another method that detects potential differences arising from electrochemical effects in subsurface bodies, for example, ore bodies that lie partly above the water table.

Resistivity

Electrical resistivity methods (ER) can provide moderately detailed information about the subsurface in areas with reasonable resistivity contrasts. Burger (1992) provides a list based on his personal experiences for commonly encountered conditions (Table 4.3).

Another useful list is found in Ward (1990), who presents resistivity ranges for common geologic materials (Figure 4.22). Note the variation in resistivity over six orders of magnitudes for these common materials.

The main advantages of ER methods are their low cost and simple equipment requirements. When current is injected into the ground in

TABLE 4.3 Resistivities of Common Shallow Subsurface Conditions [After Burger (1992)]

Material	Resistivity ($\Omega \cdot$ m)
Wet to moist clayey soil and wet clay	1s to 10s
Wet to moist silty soil and silty clay	Low 10s
Wet to moist silty and sandy soils	10s to 100s
Sand and gravel with layers of silt	Low 1000s
Coarse dry sand and gravel deposits	High 1000s
Well-fractured to slightly fractured rock with moist-soil-filled cracks	100s
Slightly fractured rock with dry, soil-filled cracks	Low 1000s
Massively bedded rock	High 1000s

an ER procedure using a pair of electrodes, the patterns of subsurface current flow reflect the resistivities of the subsurface. These patterns can be inferred by measuring the variations in voltage at the surface using another pair of electrodes (Greenhouse et al. 1998).

Figure 4.23 shows distributions of current lines in a simple model. Using the principle that the measured voltage or potential is proportional to the current density, all else being equal, variations in **current density** (proportional to the spacing of current lines) near the surface will result in variations in **apparent resistivity**. Apparent resistivity is a function of the measured potential difference, current injected into the surface, and the spacings of the electrodes.

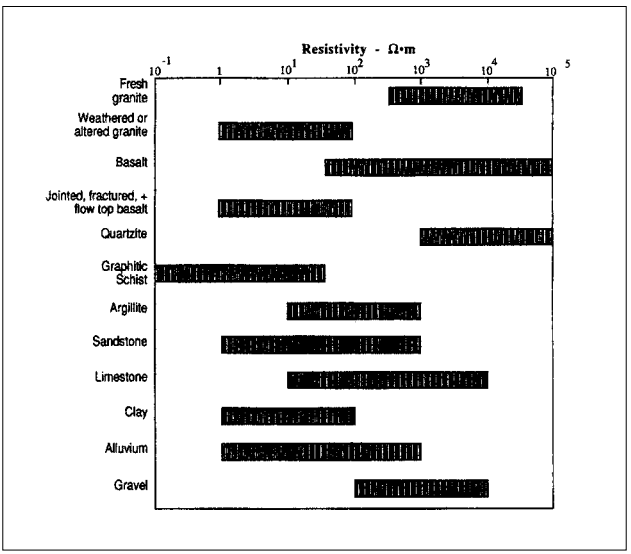

Figure 4.22 Range of resistivities of common rocks and soils. [*From Ward* (*1990*).]

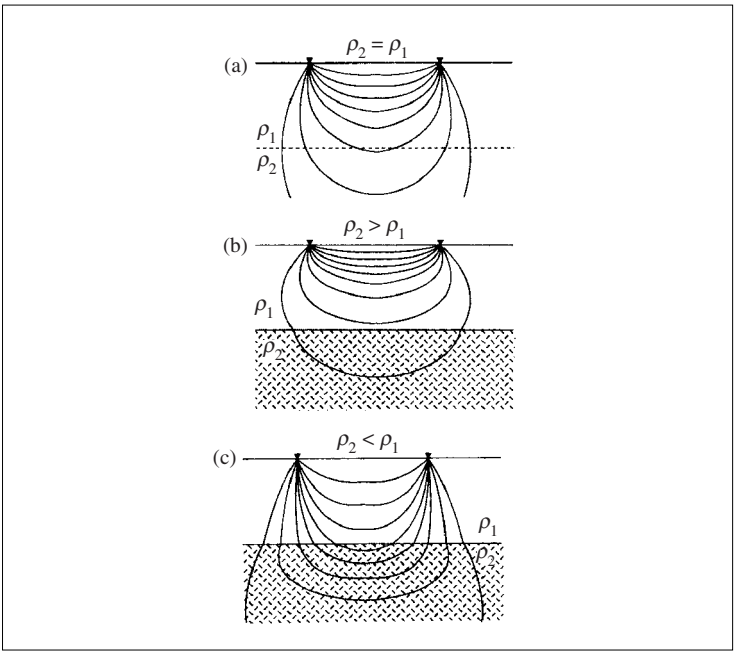

Figure 4.23 Distribution of current lines for a horizontal interface separating two media: (a) homogeneous subsurface; (b) material with greater resistivity beneath the interface —current line spacing increases in the top medium; (c) material with lower resistivity is beneath the interface—current line spacing decreases in the top medium. [*From Burger* (*1992*).]

The spacing of current lines depends on the resistivities of the geologic media. (Burger 1992). Greenhouse et al. (1998) draw a useful analogy between the flow of fluid through a permeable medium and the flow of electricity through a conductive medium. They state that the fluid potential and specific discharge are analogous to voltage and current density, respectively.

Targets and resolution. It is useful to look at an example for a two-layer case and a simple electrode arrangement (Figure 4.24). The plot shows modeled apparent resistivity plotted against electrode spacing. Note that electrode spacing is logarithmic. As electrode spacing is increased, more current penetrates to a greater depth; however, the shallow material is also included in the measurement. Therefore, in order for the measured apparent resistivity to approach the resistivity of the second layer, a large volume of the subsurface must be sampled, which is why logarithmic electrode spacing is necessary (Burger 1992).

It should be emphasized that apparent resistivity is a combination of the true resistivities and, as such, requires interpretation to determine the true resistivities of the media.

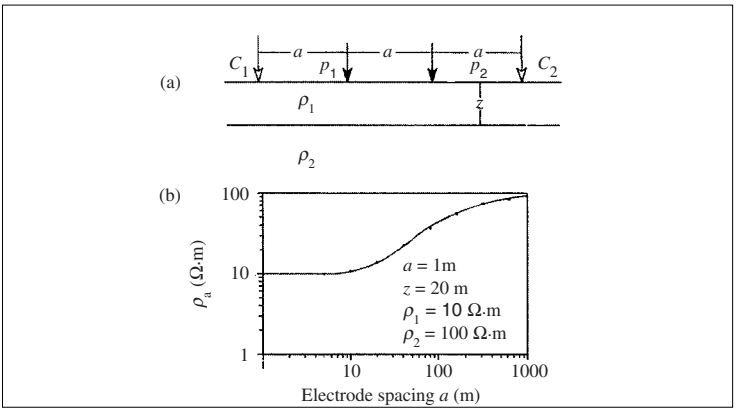

Figure 4.24 Example of modeled apparent resistivity versus electrode spacing for a simple geologic model. Layer 1 resistivity 10 Ω · m, layer 2 resistivity 100 Ω · m, layer 1 thickness 20 m, layer 2 thickness ∞. [*From Burger* (*1992*).]

Field methods

Survey types. ER surveys are usually accomplished in two ways: **profiling** or **sounding**. Many surveys do both simultaneously. In profiling, the lateral distribution of resistivity is studied by maintaining a relatively constant depth of investigation where the depth of investigation is controlled by the electrode spacing. Profiling is used in situations where layer properties vary more horizontally than vertically. Sounding, on the other hand, is used when the zone of investigation varies vertically more than horizontally. In many cases, data are acquired in both profiling and sounding mode (Greenhouse et al. 1998).

Electrode configurations. The electrode patterns used in resistivity surveying are called **arrays**. The commonly used arrays are the Wenner, Schlumberger, and dipole-dipole. Other arrangements are used that are variations of these basic types but these have withstood the test of time. Figure 4.25 is a schematic showing the array arrangements.

Equipment. In its simplest form ER surveying requires relatively inexpensive equipment compared to methods such as seismic. The basic equipment consists of a current source (generator or battery pack), transmitter/receiver (which may be in a single module), wire, and current/potential electrodes (Greenhouse et al. 1998).

In practice, low-frequency alternating current is injected into the ground rather than DC. Manufacturers of equipment include ABEM, Androtex, Iris, Bison, Campus OYO, Soiltest, and Scintrex (Greenhouse et al. 1998). The new generation ER equipment records data digitally and can take advantage of programmable electrodes.

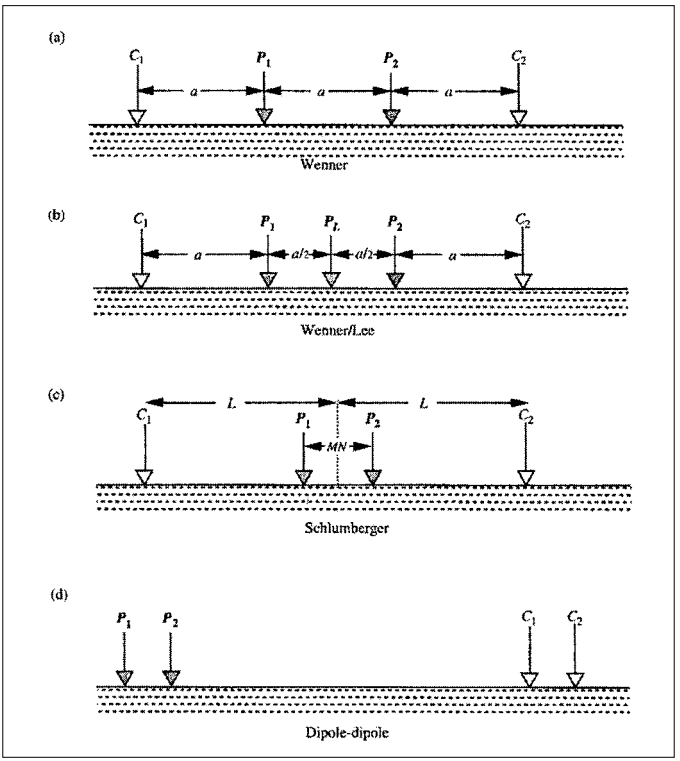

Figure 4.25 Schematic of most common electrode arrays for ER surveying. Electrode spacing is a, current electrodes are C_i, and potential electrodes are P_i. [*From Burger* (*1992*).]

Penetration. In principle, there is no limit to the penetration of the ER method as depth of penetration is controlled by the electrode spacing. Targets can be possibly hundreds of meters below the surface. In practice, penetration is controlled by the types of materials and the strength of the recorded signal compared to background variations or noise. As a rule of thumb, it is difficult to resolve a layer that is thinner than the depth to its upper surface (Greenhouse et al. 1998).

Surveying strategies. As is the case for all geophysical surveys, resistivity survey goals should be specifically defined before fieldwork begins. The appropriate equipment must be selected and geologic control should be available if at all possible. Geologic control becomes critical in the interpretation phase when multiple geologic models can be found to fit the data.

The next step is to decide the type of survey: constant-spread (profiling), expanding-spread (sounding), or a combination. If the goal of the survey is to determine apparent resistivity (ρ_a) information with depth, then

sounding using an expanding-spread traverse is the clear choice. An example of this would be to determine the depth to bedrock with an overburden of saturated, silty sands. Another traverse should be run perpendicular to the first to determine lateral variations in both directions (Burger 1992).

If the survey goal is to map lateral variations in resistivity, then a constant-spread survey or profiling is the correct choice. If multiple traverses are recorded and several electrode spacings can be used at each location, then a contour map of ρ_a can be produced for each electrode spacing. This approach would be useful for detection of a gravel bar, for example (Burger 1992).

Concerning electrode spacing, an often used guideline is that depth of penetration is equal to electrode spacing. This is not completely correct as the amount of current penetrating the subsurface depends not only on electrode spacing but also on the resistivities of the media. If surveying is being conducted in an area for the first time, it is usually advisable to plot ρ_a readings as surveying progresses to determine if the electrode spacings are sufficient to "see" the resistivity of the deepest zone of interest.

Interpretation of results

Curve matching. Curve matching is a relatively straightforward approach to estimating the true resistivities of subsurface materials. This approach works best for the simple case of a single horizontal interface and expanding-spread traverse. The technique is a way to match field measurements of ρ_a and scaled electrode spacing to theoretical curves that have been calculated for various layer thicknesses and resistivities. Figure 4.26 is a plot showing an example of curve matching for a two-layer model with an upper layer resistivity of 100 $\Omega \cdot$ m and a lower layer resistivity of 43 $\Omega \cdot$ m and a top layer thickness of 10 m.

Analytical methods. With the proliferation of fast, cheap personal computers, analytical methods have largely replaced curve-matching methods. This is typically an inversion approach that requires an initial guess for a starting model and then refines that model by iteratively reducing the error between forward calculations from the current state of the model and the field data. The iterative process is stopped when the error meets a specified criterion.

This is a fast, effective approach that produces a solution in a short time. However, as with any inversion process, the resulting final model is one of many possible models. The result must be compared to existing geologic information to determine its feasibility.

Pseudosections. Sounding data are usually plotted as apparent resistivity (ρ_a) versus electrode spacing, while profiling ER data are plotted as apparent resistivity versus profile distance. It is also possible to plot

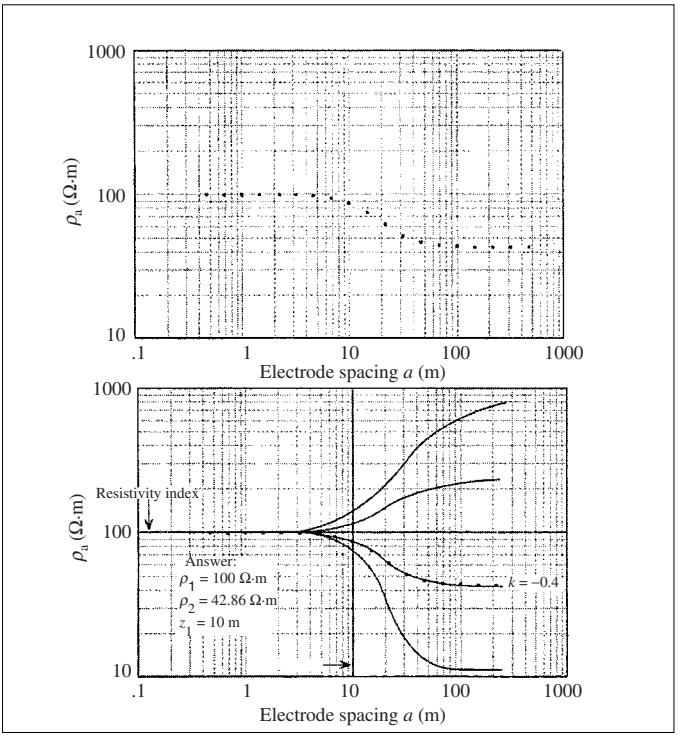

Figure 4.26 Curve-matching example. Top plot shows field measurements. Bottom plot shows field measurements overlaid on a set of theoretical curves. The closest matching curve indicates the best-fit model parameters. [*From Burger* (*1992*).]

data in a format called **pseudosection**. This format plots ρ_a recorded with a variety of electrode spacings with the spacing as a measure of the depth to the apparent resistivity. The result resembles a geologic cross section, but it must be kept in mind that the depth is an estimate only.

Figure 4.27 is an example of (a) an observed pseudosection, (b) a computed pseudosection from a finite-element algorithm, and (c) the model of the subsurface used to produce the computed results in (b).

Example 4.6 Figures 4.28, 4.29, and 4.30 are examples taken from Burger (1992) illustrating the use of the ER method for two contamination problems and a karst investigation.

Figure 4.28 shows an apparent resistivity contour map (a) generated from constant-spread traverses. The goal of the survey was to map a buried stream channel. The section in (b) shows the interpreted geology from the resistivity survey and borehole information.

Figure 4.29 is a schematic example of how ER can be use to study the extent of leachate plumes leaking from landfills. It is based on patterns

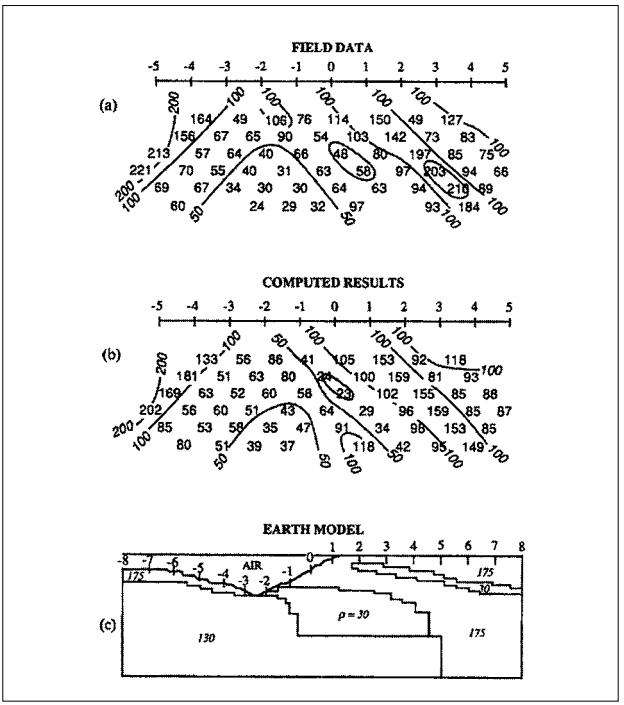

Figure 4.27 Example of (a) observed pseudosection, (b) computed pseudosection from a finite-element algorithm, and (c) model of the subsurface used to produce the computed results in (b). [*From Ward* (*1990*), *after Hohmann* (*1982*).]

observed in studies of several landfills located at various sites throughout the United States. The resistivity contours are determined from variations in apparent resistivities compared to normal values associated with the landfill site (Burger 1992).

Figure 4.30 shows apparent resistivity plotted against offset from an ER survey performed in a karst region in Illinois. The spread used a Wenner array with an electrode spacing of 30.48 m. The bottom plot shows the geologic interpretation. Apparent resistivity highs correspond to limestone and voids; apparent resistivity lows correlate with clays.

Example 4.7 The following example shows the results of an ER survey conducted in the same creek drainage that is described in Example 4.3 in the seismic section. The survey was performed using a dipole-dipole array with a dipole spacing of 10 m (a = dipole electrode spacing). For each setup of current electrodes, potential readings were taken at spacings of 1a, 2a, 3a, 4a, 5a, and 6a. After data were recorded for the six electrode spacings, the current electrodes were moved up a distance 1a. This approach combines both the sounding method (increasing electrode spacing) and the profiling method (lateral movement of electrodes).

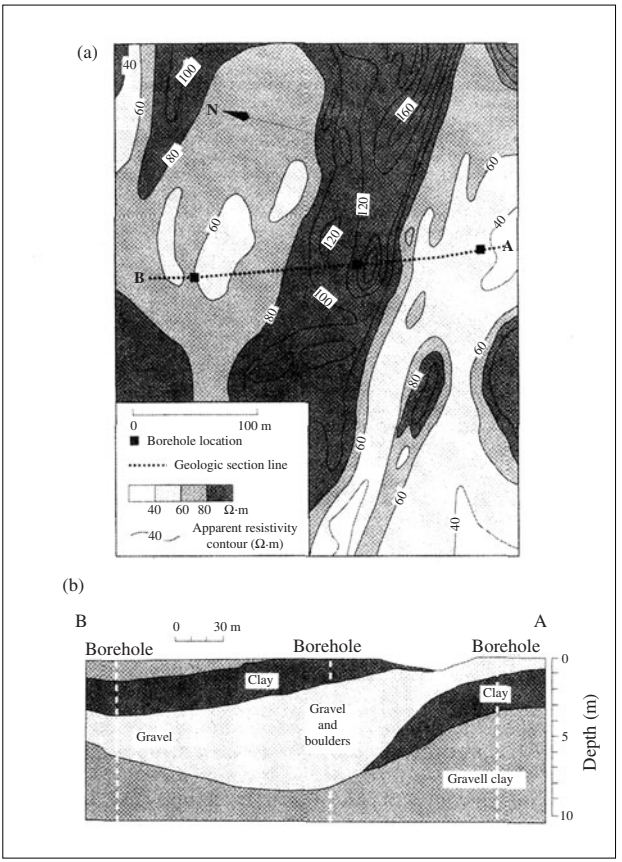

Figure 4.28 Contour map of apparent resistivity values from constant-spread traverses and locations of boreholes (a). Interpreted geologic cross section through the boreholes(b). [*From Burger* (*1992*), *after Zohdy et al.* (*1974*).]

Figure 4.31 shows the results of the 2D resistivity inversion for data collected from 15 different current electrode setups and associated n = 1 to 6 potential electrode setups. The upper plot shows the apparent resistivities calculated from the recorded voltages and currents. These are plotted using the conventional **pseudosection** technique in which the data are plotted beneath the midpoint between the dipoles at a depth of half the distance between the dipole centers. These results are then contoured.

The bottom plot shows the results of the resistivity inversion. The plot shows a somewhat homogeneous upper layer of high resistivity (300 $\Omega \cdot$ m) grading fairly quickly into a lower layer of low resistivity (30 $\Omega \cdot$ m). The transition between layers occurs at about a depth of 9 m, the interpreted depth to bedrock from seismic refraction. The upper layer material consists of large cobbles and boulders of limestone and other competent sedimentary rocks in a poorly sorted sand matrix. This layer is dry. The lower layer is interpreted

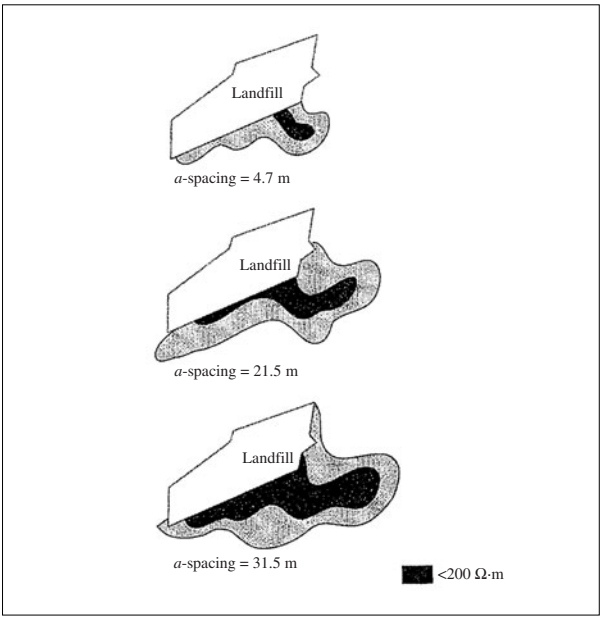

Figure 4.29 Schematic showing a spreading leachate plume as determined from ER surveys. Each plot is generated at a greater depth. [*From Burger* (*1992*).]

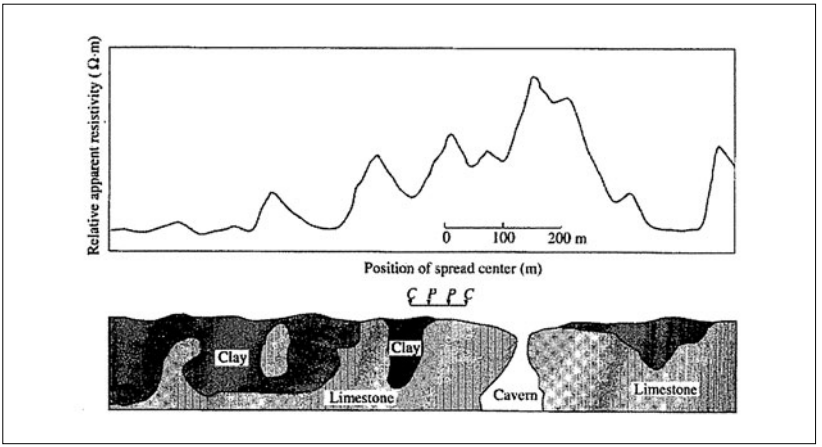

Figure 4.30 Results from an ER survey in a karst region in Illinois. Apparent resistivity is plotted against offset for constant-spread survey (top) with electrode spacing of 30.48 m (electrode arrangement denoted as CPPC). Geologic interpretation of apparent resistivity where high ρ_a corresponds to limestone and voids and low ρ_a to clays. [*From Burger* (*1992*), *after Hubbert* (*1944*).]

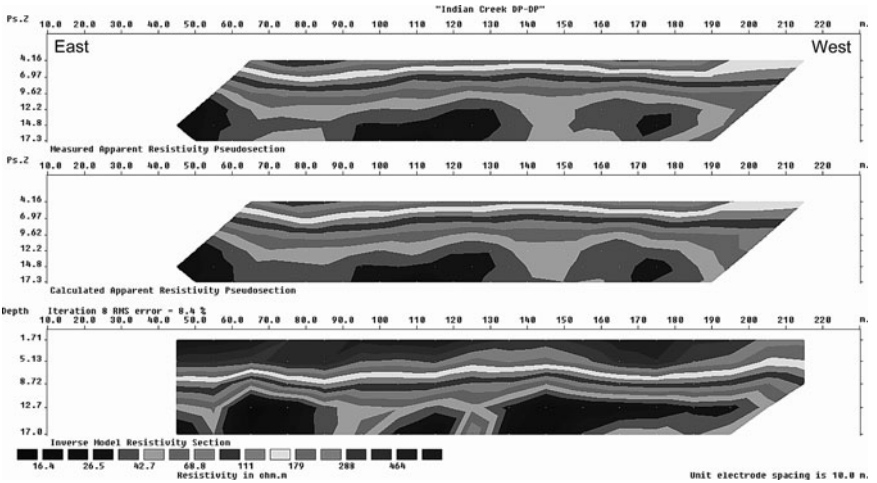

Figure 4.31 2D resistivity inversion results. Top plot shows contoured values of apparent resistivities calculated from voltages and currents. Bottom plot shows result of 2D inversion for resistivity. Depth of zone of rapidly changing resistivity in center of bottom plot agrees well with calculated depth to bedrock of 9 m from seismic refraction. Center plot shows forward modeled apparent resistivities calculated from the inverted resistivity model (bottom plot). Note good agreement with the measured apparent resistivities (top plot).

to be the weathered top of a Mississippian age limestone with possible features controlling the groundwater flow. The low resistivity value may result from saturated conditions.

The middle plot is the forward calculated apparent resistivity using the resistivity results in the bottom plot as an earth model. This plot should, and does, agree well with the measured apparent resistivity values in the top plot.

Induced polarization (IP)

The description of the next four methods will be necessarily brief following the format of Burger (1992). The descriptions will mainly provide a sense of applications, limitations, and advantages and how these methods are similar to or differ from electric resistivity methods. Detailed descriptions of these methods can be found in many books. A particularly useful reference is Ward (1990). A useful tutorial and more information can also be found in the CD-ROM by Greenhouse et al. (1998).

The induced polarization or IP method takes advantage of the fact that when the current applied to a medium is turned off, the potential difference does not immediately return to zero. This voltage decay indicates that the material has become polarized, analogous to a rechargeable battery. This decay of voltage with time is referred to as an *induced potential in the time domain* (Burger 1992). There is also an approach that uses different frequencies of alternating current. This is called IP in the frequency domain.

A useful measure of the effect of IP in the time domain is chargeability. Chargeability is defined as the ratio of the area under the voltage curve to the potential difference measured before the current was turned off. A theoretical relationship between ρ_a and chargeability allows calculation of relationships between subsurface geometries and apparent chargeabilities (Burger 1992).

Electrode arrays are typically the Schlumberger or dipole-dipole. Apparent chargeability is plotted against electrode spacing, similar to apparent resistivity plotted against electrode spacing. Curve matching with calculated theoretical curves is then used to determine the subsurface model (Burger 1992).

IP applications. IP has probably found more use in the search for base metals rather than the usual ER applications such as groundwater studies. IP tends not to be as cost-effective as ER methods because of the more complex interpretation methods. So it is generally used where the potential payoff is higher.

The equipment for IP is similar to ER with two exceptions: A timing circuit is required, and a recording unit is necessary to record the decay of potential with time. Thus, standard equipment used for ER cannot be used for IP, but IP can be used for measuring apparent resistivities (Burger 1992).

IP could be useful in a situation where ER methods cannot distinguish several layers because of similar resistivities but which might have different chargeabilities (see Ward 1990, Vol. 1).

Spontaneous potential (SP)

Natural potential differences measurable at the surface may arise from electrochemical reactions at depth that cause currents to flow. For example, in an ore body that lies partly above the water table, oxidation takes place above the water table and reduction below it. These processes are the cause of different charge concentrations that cause a flow of current. Sulfide bodies are probably the most common example of this condition. For this reason, most SP surveys are used for locating ore bodies, especially sulfide ores (Burger 1992).

SP applications. Equipment for SP surveys is minimal. Two electrodes, wire, and a millivoltmeter constitute the basics. Nonmetal electrodes must be used as metal electrodes produce their own self-potential. Porous-pot electrodes are used, consisting of a ceramic container with holes filled with a solution of copper sulfate and a copper tube.

SP surveys are quick and efficient, and the required equipment is minimal. However, quantitative interpretation is difficult and depths of sources are difficult to model (Burger 1992). In addition, SP effects can

be masked by other sources such as telluric currents. SP exploration, therefore, is not a common shallow exploration method except in the obvious case of a shallow sulfide body. Corwin (1990) gives a detailed discussion of SP methods (Burger 1992).

Telluric and magnetotelluric methods

At any moment, naturally occurring electric currents are flowing in the earth. These currents are induced by the flow of charged particles in the ionosphere. These subsurface telluric currents tend to flow in uniform patterns over large areas. However, variations in resistivity and geometry cause fluctuations in the currents. Thus, measuring the potential differences associated with telluric current flow should give information about the subsurface variations in resistivity (Burger 1992).

Telluric currents vary with time. Thus, the field procedure is to set up a base station at which two pairs of electrodes are placed at right angles. Voltage is then continuously monitored at the base station. Two additional pairs of electrodes are then moved along a grid. Comparison between readings taken at the base station and readings taken at the grid locations yields a potential difference that is caused by the subsurface variation effect on current density (Burger 1992).

Telluric methods can also include measurement of magnetic field intensity variations with voltage. This process is called magnetotellurics. Both sets of data are then used to compute apparent resistivity functions, which are then compared with theoretical curves to determine thicknesses and true resistivities. Magnetotellurics requires a magnetometer capable of measuring weak magnetic field variations that fluctuate frequently (Burger 1992).

The main disadvantage of the natural source magnetotelluric methods is the erratic signal strength. A relatively recent development introduced the principle of an artificial signal source that was dependable and strong enough to speed up data acquisition and improve the reliability of results. The controlled-source magnetotelluric method typically operates in the frequency band 0.1 Hz to 10 kHz, while the natural source magnetotelluric (MT) method uses the range 10^{-3} to 10 Hz. Audio-frequency magnetotellurics (AMT) operates in a still higher range from 10 to 10^4 Hz (Reynolds 1997).

Telluric and magnetotelluric applications. The telluric and magnetotelluric method has been more popular in Europe and the Soviet Union. The natural-source methods are not capable of providing a great level of detail and are thus used in more regional type surveys to determine, for example, basin geometries and other features of that scale (Burger 1992).

Audio-frequency magnetotellurics have been used in groundwater/geothermal resource investigations and in the exploration for major base metal deposits over the depth range from 50 to 100 m to several kilometers. The main application of the MT method, however, has been in hydrocarbon exploration, especially in terrains where the seismic method is difficult to use or ineffective (Reynolds 1997).

Since the 1970s, controlled-source AMT (CSAMT) has been used in an increasing range of applications and, since the 1980s, especially within the geotechnical and environmental community. Reynolds (1997) considers CSAMT to be an underutilized method with many potential applications.

Figure 4.32 shows some plots generated from CSAMT data. It is worth noting that processing CSAMT data is a relatively complicated process accomplished in two phases: preprocessing and interpretative processing (Reynolds 1997).

Electromagnetic (EM) techniques

Background. Among all the geophysical methods, the EM techniques have the broadest range of different instrumental systems in use corresponding to the broad range of applications of these methods. Recent developments in portability and ease of use have resulted in the increasing popularity of EM methods. Modern EM systems provide a powerful suite of sophisticated instruments. Coupled with major advances in computer interpretation techniques, EM techniques have become increasingly available to engineering and environmental applications (Reynolds 1997).

In its simplest form, EM surveying involves passing alternating current through a wire loop producing a local magnetic field called the primary field. This in turn produces current flow in the earth, which produces a secondary magnetic field that varies in amplitude and phase from the primary. This secondary field is measured by a receiver coil in which current flow is induced by the secondary field. Knowing the primary field, it is possible to isolate the secondary field, which contains information about the subsurface in which it was generated (Burger 1992).

Although the secondary field contains information about the distribution of conducting (resistive) material in the subsurface, quantitative interpretation is fairly complex. However, signatures of good conductors are sufficiently clear that the method is well suited to reconnaissance surveys (Burger 1992).

No electrodes are involved, so fieldwork can be fairly rapid and airborne data collection is common. The EM method is relatively inexpensive, but depth penetration is poor and good conductors are necessary (Burger 1992).

Instruments. Commonly used EM instruments are the EM31 and EM34 manufactured by Geonics Limited. Both instruments operate on the

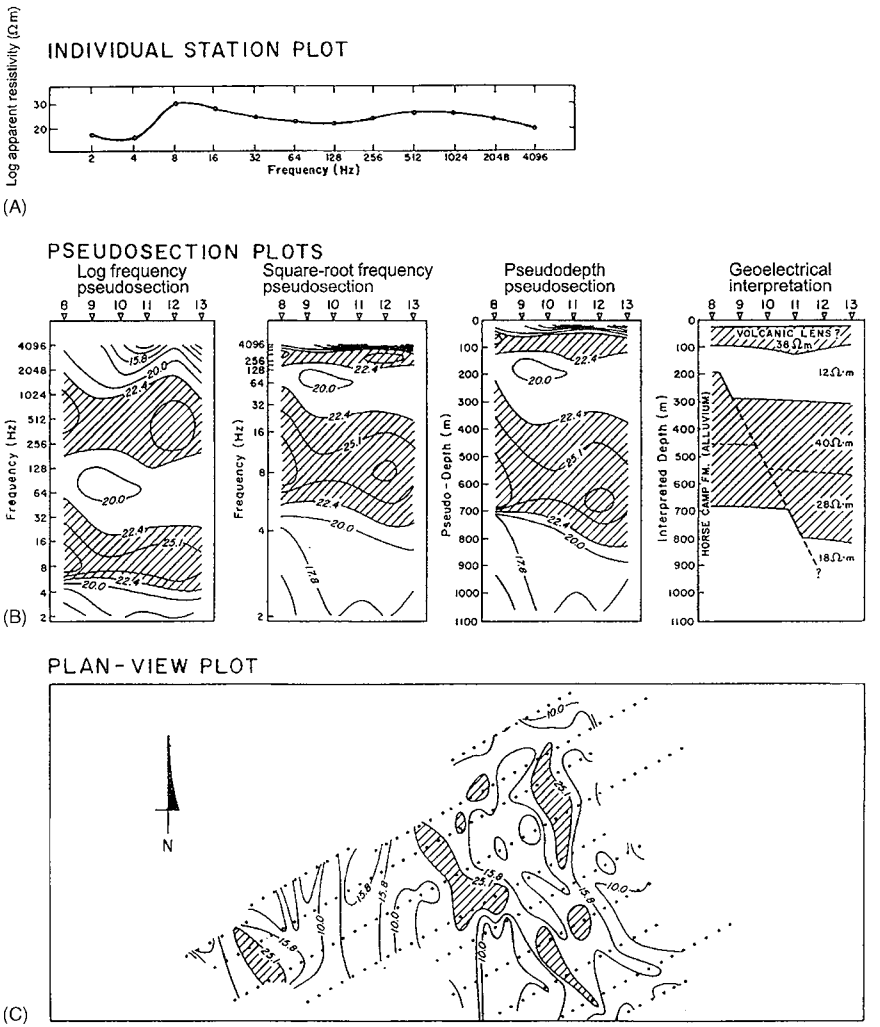

Figure 4.32 Display types for CSAMT data. (A) Individual station plot of apparent resistivity (log) versus frequency. (B) Various pseudosection displays with the corresponding geoelectric/geologic interpretation. (C) Plan-view plot of parameter of interest. [*From Reynolds* (*1997*), *after Zonge and Hughes* (*1991*).]

same principle; however, the EM31 has a fixed spacing of 3.7 m between transmitter and receiver coils (Figure 4.33). The instrument can be used in a vertical dipole mode with penetration depth of approximately 6 m and a horizontal dipole mode with penetration depth of approximately 3 m. The operating characteristics of the two operating modes allows interpretation of subsurface conductivities with depth.

The EM34 uses different length cables to obtain transmitter/receiver separations of 10, 20, and 40 m (Figure 4.34). These transmitter spacings

Figure 4.33 EM31 being used in the field. Simple rotation of the instrument 90° about the long axis gives vertical or horizontal dipole orientation. (*Geonics, Ltd.*)

give approximate penetration depths as shown in Table 4.4. The different dipole orientations are achieved by holding the antenna loops in a vertical plane (e.g., between legs) for a horizontal dipole or in a horizontal plane (e.g., on the ground) for a vertical dipole orientation.

The EM31 provides a rapid method of measuring the ground conductivity, but only to a depth of about 6 m. The EM34 provides a much greater depth of investigation, but requires two people to operate and

Figure 4.34 EM34 being used in horizontal dipole mode. (*Geonics, Ltd.*)

TABLE 4.4 Approximate Penetration Depths for EM34 Spacings and Dipole Orientations

Spacing (m)	Horizontal dipole penetration (m)	Vertical dipole penetration (m)
10	7.5	15
20	15	30
40	30	60

only takes discrete measurements. However, in spite of these limitations, these simple methods still provide one of the most cost-effective approaches for measuring the ground conductivity (which can be converted to resistivity). Neither method provides direct information regarding the depth of investigation; however, curve fitting methods can be used for the six data combinations of the EM34 to solve a simple layered earth problem. Also, if EM31 measurements are made in both dipole orientations at varying heights above the ground surface, curve fitting can also be used to solve the shallow two-layered earth problem (i.e., σ_1, σ_2, z).

A particularly useful website discussing EM as well as other geophysical methods and specific applications is http://www.cflhd.gov/agm/geoMethods/ by the U.S. Department of Transportation Federal Lands Highway Program.

EM applications. The range of applications is large (Reynolds 1997), although Burger (1992) suggests that most of the applications of EM surveying have been for ore exploration. However, Burger (1992) suggests McNeill (1990) for a good, modern review of groundwater applications of EM.

The applications of EM methods depend on the type of equipment being used but can be broadly categorized as in Table 4.5 (Reynolds 1997). Not all EM methods are equally appropriate to the applications

TABLE 4.5 Range of Applications for EM Surveying—Independent of Instrument Type [After Reynolds (1997)]

Mineral exploration
Mineral resource evaluation
Groundwater surveys
Mapping contaminant plumes
Geothermal resource investigations
Contaminated land mapping
Landfill surveys
Detection of natural and artificial cavities
Location of geological faults, etc.
Geological mapping
Permafrost mapping, etc.

listed. For example, ground-penetrating radar (GPR) (see next paragraph) has limited use in the direct investigation of landfills because of the high conductivity levels that are usually present, which attenuate the propagating radio waves rapidly with depth.

One of the main advantages of EM methods is that the process of induction does not require direct contact with the ground as do the methods that use electrodes. This allows increased efficiency in field operations and permits the method to be used in aircraft and vessels with obvious advantages (Reynolds 1997).

GPR can be considered an EM method but is usually considered separately. Reynolds (1997) suggests Nabighian (1987, 1991) for a comprehensive and detailed discussion of the various EM methods with the exception of GPR (see Ward 1990, Vols. I, II, and III).

Goldstein et al. (1990) present a case study where ground conductivity measurements were used to delineate contaminated water emanating from a series of water storage lagoons in California. The final interpretation of their data is shown in Figure 4.35.

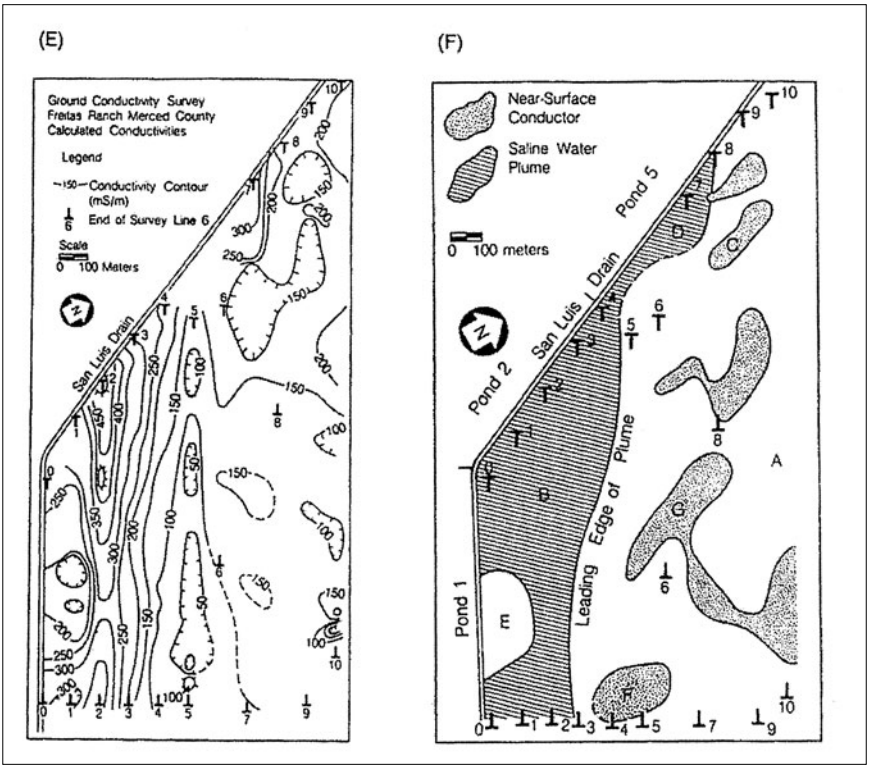

Figure 4.35 Final processed data is conductivity map (E) and final interpretation map from study site at Kesterton, California. [*From Reynolds* (*1997*), *after Goldstein et al.* (*1990*).]

References

British Standards Institute, 1981. *Code of Practice for Site Investigations, BS* 5930. London, BSI.

Burger, H.R., 1992. *Exploration Geophysics of the Shallow Subsurface*. Prentice-Hall, Upper Saddle River, NJ.

Corwin, R.F., 1990. The Self-Potential Method for Environmental and Engineering Applications, in Ward, S. H., (ed.), *Geotechnical and Environmental Geophysics, Vol. I, Review and Tutorial*. Society of Exploration Geophysicists, Tulsa, OK, pp. 127–145.

Darracott, B.W., and McCann, D.M., 1986. Planning Engineering Geophysical Surveys, in Hawkins, A.B., (ed.), *Site Investigation Practice: Assessing BS 5930*. Geological Society Engineering Geology Special Publication, No. 2, pp. 85–90.

Evans, B.J., 1997. *A Handbook for Seismic Data Acquisition in Exploration*. Geophysical Monograph Series No. 7, Society of Exploration Geophysicists.

Geological Society Engineering Group Working Party, 1988. Engineering Geoophysics. *Quarterly Journal of Engineering Geology*, Vol. 21, No. 3, pp. 207–271.

Gochioco, L.M., and Cotten, S.A., 1989. Locating Faults in Underground Coal Mines Using High-Resolution Seismic Reflection Techniques, Geophysics, 54, 1521–1527.

Goldstein, N.E., Benson, S.M., and Alumbough, D., 1990. Saline Groundwater Plume Mapping with Electromagnetics, in Ward, S. H., (ed.), *Geotechnical and Environmental Geophysics, Vol. II, Environmental and Groundwater*. Society of Exploration Geophysicists, Tulsa, Oklahoma, pp. 17–25.

Greenhouse, J.P., Slaine, D.D., and Gudjurgis, P., 1998. *Applications of Geophysics in Environmental Investigations*. CD-ROM.

Hawkins, A.B. (ed.), 1986. *Site Investigation Practice: Assessing BS 5930*. Geological Society Engineering Geology Special Publication No. 2.

Hearst, J.R., and Nelson, P.H., 1985. *Well Logging for Physical Properties*. McGraw-Hill, 571 pp.

Hohmann, G.W., 1982. *Numerical Modeling for Electrical Geophysical Methods*. Proceedings of International Symposium of Applied Geophysics Tropical Region, University do Para, Belem, Brazil, pp. 309–384.

Hubbert, M.K., 1944. An Exploratory Study of Faults in the Cave in Rock and Rosiclare Districts by the Earth Resistivity Method in Geological and Geophysical Survey of Fluorspar Areas in Hardin County, Illinois, U. S. *Geological Survey Bulletin 942*, Part 2, pp. 73–147.

Hunter, J.A., Pullan, S.E., Burns, R.A., Gagne, R.M., and Good, R.L., 1984. Shallow Seismic Reflection Mapping of the Overburden-Bedrock Interface with the Engineering Seismograph—Some Simple Techniques, *Geophysics,* 49, pp. 1381–1385.

Lankston, R.W., 1990. High-Resolution Refraction Seismic Data Acquisition and Interpretation, in Ward, S. H., (ed.), *Geotechnical and Environmental Geophysics, Vol. I: Review and Tutorial,* Society of Exploration Geophysicists, Tulsa, OK.

McNeill, J.D., 1990. Use of Electromagnetic Methods for Groundwater Studies, in Ward, S.H., (ed.), *Geotechnical and Environmental Geophysics, Vol. I: Review and Tutorial*. Society of Exploration Geophysicists, Tulsa, OK. pp. 191–218.

Miller, R.D., Xia, J., Park, C.B., and Ivanov, J., 1999. Using MASW to Map Bedrock in Olathe, Kansas: 69th Annual International Meeting, *SEG, Expanded Abstracts*, pp. 433–436.

Nabighian, M.N., 1987. *Electromagnetic Methods in Applied Geophysics, Vol. 1*. Society of Exploration Geophysicists, Tulsa, OK.

Nabighian, M.N., and Macnae, J.C., 1991. Time Domain Electromagnetic Prospecting Methods, in Nabighian, M. N., (ed.), *Electromagnetic Methods in Applied Geophysics, Vol. 2a*. Society of Exploration Geo physicists, Tulsa, OK. pp. 427–520.

Press, F., 1966. Seismic Velocities, in Clark, S.P., Jr., (ed.), *Handbook of Physical Constants,* revised edition. Geological Society of America Memoir 97, pp. 97–173.

Reynolds, J.M., 1997. *An Introduction to Applied and Environmental Geophysics*. John Wiley & Sons.

Robinson, E.S. and Coruh, C., 1988. *Basic Exploration Geophysics*. John Wiley & Sons.

Sheriff, R.E., 1991. *Encyclopedic Dictionary of Exploration Geophysics*. Society of Exploration Geophysicists, Tulsa, OK.

Ward, S.H. Ed., 1990. *Geotechnical and Environmental Geophysics*, *Vol. I, Review and Tutorial*. Society of Exploration Geophysicists, Tulsa, OK.

Ward, S.H. Ed., 1990. *Geotechnical and Environmental Geophysics*, *Vol. II, Environmental and Groundwater,* Society of Exploration Geophysicists, Tulsa, OK.

Ward, S.H. Ed., 1990. *Geotechnical and Environmental Geophysics*, *Vol. III, Geotechnical*. Society of Exploration Geophysicists, Tulsa, OK.

Xia, J., Miller, R.D., Park, C.B., Hunter, J.A., Harris, J.B., and Ivanov, J., 2002. Comparing Shear-Wave Velocity Profiles Inverted from Multichannel Surface Waves with Borehole Measurements: *Journal of Soil Dynamics and Earthquake Engineering*, *Vol. 22,* 181–190.

Zohdy, A. A.R., Eaton, G.P., and Mabey, D.R., 1974. *Application of Surface Geophysics to Ground Water Investigations*. Techniques of Water-Resources Investigations of the United States Geological Survey, Book 2, pp. 49–50.

Zonge, K.L., and Hughes, L.H., 1991. Controlled-Source Audio-Frequency Magnetotellurics, in Nabighian, M.C. (ed.), *Electromagnetic Methods in Applied Geophysics*, *Vol. 2, Applications, Part B*. Society of Exploration Geophysicists, Tulsa, OK, pp. 713–809.

This page intentionally left blank

Chapter

5

Groundwater Flow

5.1 Groundwater Movement

Groundwater is generally always moving. Movement occurs from higher hydraulic head in **recharge** areas (natural or artificial), where precipitation is generally higher, to **discharge** areas of lower hydraulic head (wells, springs, rivers, lakes, and wetlands). The reason groundwater moves is because there always seems to be a "change in head" somewhere in a groundwater system. This "change in head" results in a slope (hydraulic gradient) in the potentiometric surface (Chapter 3). Gravity is the driving force that moves water. Infiltrating groundwater moves downward until it reaches a horizon with low enough hydraulic conductivity to begin mounding. Groundwater moves so slowly (feet/year to feet/day) that mounds of water in recharge areas may build up before their effects in the system can be equilibrated. If you picked up one corner of a bathtub full of water, gravity would cause the water to move toward the low corner. If the bathtub were filled with saturated sand and you picked up a corner (you would be very strong!), water would still move, to the lower corner but much more slowly. The quantity of groundwater movement through porous media is defined through **Darcy's law** (Figure 5.1).

Darcy's law

In the mid-nineteenth century, Henry Darcy (1856) systematically studied the movement of water through sand columns. He was able to show that the volumetric rate (Q) of groundwater was proportional to the intrinsic permeability (see Chapter 3) of the porous media (k) and the change in head (hydraulic gradient)) over the length of the sand column

Copyright © 2008, 2001 by The McGraw-Hill Companies, Inc. Click here for terms of use.

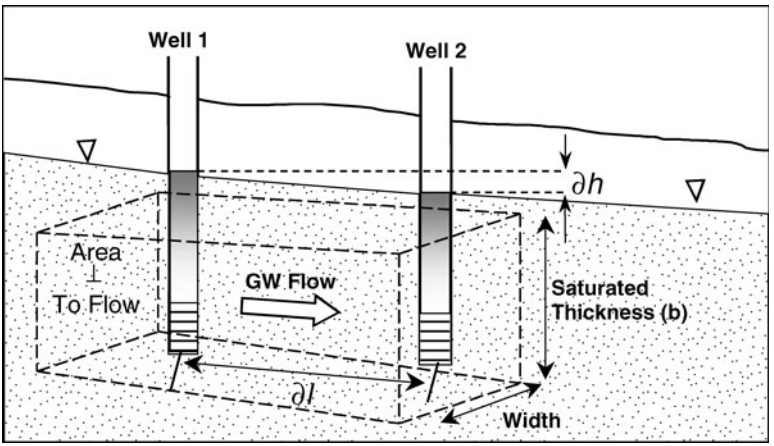

Figure 5.1 Schematic of Darcy's law showing change in head (δh) over the flow path length (δl) and the area perpendicular to flow (aquifer width times thickness (b) for horizontal flow).

(Figure 5.1). This can be expressed as Darcy's law:

$$Q = K\frac{\partial h}{\partial l}A = KiA \tag{5.1}$$

where Q = volumetric discharge rate (L^3/t)
$\partial h/\partial l = i$ = hydraulic gradient (L/L) or slope of the potentiometric surface.
$A = b \times w$, the cross-sectional area perpendicular to flow (L^2), (in horizontal flow, the saturated thickness (b) multiplied by the width of the aquifer (w) or a part of the width of an aquifer)
K = hydraulic conductivity (L/t)

There is a significant difference between the hydraulic conductivity (K) and the intrinsic permeability (k), although they tend be to used interchangeably in practice because the fluid properties of most uncontaminated groundwaters are similar at similar temperatures (Chapter 3, Example 3.5). Waters with total dissolved solids (TDS) less than 5,000 mg/L have similar enough viscosities and specific weights (Fetter 1994).

Darcy's law can also be viewed as:

$$Q = q \times A \tag{5.2}$$

where:

$$q = K\frac{\partial h}{\partial l} = Ki \tag{5.3}$$

q = the Darcian velocity, also known as the specific discharge

Even though the Darcian velocity or **specific discharge** (q) has units of velocity (L/t), it does not represent a true groundwater velocity. This is because the porous media occupies some of the area perpendicular to flow. To account for this, one must include the effective porosity (n_e) of the porous media. The n_e represents the porosity available for fluid flow. The true velocity is really an average linear velocity (V_{ave}) as the water moves around the grains from one point (high head) to another (low head). This value is also known as the **seepage velocity** (V_s), expressed as:

$$V_s = \frac{K}{n_e}\frac{\partial h}{\partial l} = \frac{q}{n_e} \tag{5.4}$$

where all terms have been defined previously.

Example 5.1 The seepage velocity (Vs) or average linear velocity can be used to estimate the time of travel of groundwater for a nonreactive dissolved contaminant as it is being carried along by groundwater moving down hydraulic gradient. The general relationship is:

$$\text{Time of travel} = \frac{\text{distance traveled}}{V_s}$$

Weird application: Franco Horowitz escaped from a low security work farm and dumped a highly soluble deadly contaminant "methyl death" down his ex-wife's domestic well. He was sent to prison after being convicted for assault from chasing her lover, the town mayor, with a tire iron. The town mayor has a domestic well 200 ft down-gradient and Franco was seeking revenge. We are going to assume it takes one day for "methyl death" to begin a direct flow path toward the mayor's well. If the hydraulic gradient is 45 ft/mi (1 mi = 5280 ft), the effective porosity is estimated to be 0.22, and the hydraulic conductivity is approximately 20 ft/day how long will it take "methyl death" to reach the mayor's well?

We apply the above relationship after using equation 5.4 to solve for V_s, the groundwater velocity of "methyl death."

$$V_s = \frac{K \times \partial h}{n_e \times \partial l} = \frac{20\ \text{ft/day} \times 45\ \text{ft}}{0.22 \times 5280\ \text{ft}} = 0.775\ \text{ft/day}$$

$$\text{time of travel} = \frac{200\ \text{ft}}{0.775\ \text{ft/day}} = 260\ \text{days}$$

Discussion: This relationship is used to make a back-of-the-envelope "first approximation" estimate for time of travel. Since V_s represents the average linear velocity, the leading edge of the plume for "methyl death" may arrive much sooner than 260 days. As the mayor uses his well the cone of depression from pumping will intermittently steepen the slope of the hydraulic gradient. Therefore, to report a number more precise than 260 days is silly because most of the parameters used in the estimate for time of travel were also estimated.

Darcy's Law is valid in the saturated zone, in multiphase flow, and in the vadose zone, although adjustments to Equation 3.1 have to be made. For example, the hydraulic conductivity (K) in the vadose zone becomes a function of the moisture content (Fetter 1993) (Chapter 12).

Hydraulic head

In Chapter 3 potential, hydraulic head, and total head are mentioned. Here these concepts will be developed.

Whenever water moves from one place to another, it takes work (W) to accomplish this. The work performed in moving a unit mass of fluid is a mechanical process and is known as the fluid potential (Φ)(Freeze and Cherry 1979). The forces moving the fluid have to overcome the resistant frictional forces of the porous media. The work calculation represents three types of mechanical energy (Freeze and Cherry 1979). The total fluid potential (Φ_T) (the mechanical energy per unit mass) is expressed as the sum of the three components of the Bernoulli equation, which are velocity potential, elevation potential, and pressure potential (The dimensions of work and energy are the same: ML/t^2.):

$$\Phi_T = \frac{v^2}{2} + gz + \frac{P}{\rho} \tag{5.5}$$

where v = fluid velocity (L/t)
g = acceleration due to gravity (L/t^2)
z = elevation above a datum (L)
P = pressure = Force/A, $(ML/t^2)/L^2 = ML/t^2$
ρ = fluid density, (M/L^3)

M. King Hubbert (1940) showed that the fluid potential at any point is simply the total hydraulic head multiplied by the acceleration due to gravity (g).

$$\Phi_T = gh_t \tag{5.6}$$

Since g is very nearly constant near the Earth's surface, fluid potential and hydraulic head are nearly perfectly correlated (Freeze and

Cherry 1979). If the components of the Bernoulli equation (Equation 5.5) (expressed as energy per unit mass) are divided by gravity, we obtain the three components of total hydraulic head expressed as fluid potential on a unit weight basis.

$$h_t = \frac{v^2}{2g} + Z + \frac{P}{\rho g} \tag{5.7}$$

Dimensionally, these are all measured in terms of length (feet or meters). The first term is known as the *velocity head* (h_v), the second term is called the *elevation head* (h_z), and the last term is called the *pressure head* (h_p). Since groundwater moves so slowly (feet/year to feet/day), the velocity head (h_v) is considered to be negligible (see Example 5.2). Therefore, the total head (h_t) at any point in a groundwater system (confined or unconfined) can be expressed in terms of the elevation head (h_z) and the pressure head (h_p). Equation 5.7 can be simplified to:

$$h_t = h_z + h_p \tag{5.8}$$

Example 5.2 The typical hydraulic conductivity of a fine to silty sand is approximately 0.3 ft/day (1×10^{-4} cm/s). Is the velocity head negligible?

Solution: The hydraulic conductivity must be converted to a velocity using Equation 5.4 by making some assumptions. If the effective porosity can be assumed to be 25% and a gradient of 0.008 ft/ft is used, then the velocity can be calculated.

By using the first "head" term in Equation 5.7 one can calculate the relative velocity head.

$$v = \frac{[(0.3 \text{ ft/day})(0.008 \text{ ft/ft})]}{0.25} = 9.6 \times 10^{-3} \text{ ft/day}$$

$$\frac{v^2}{2g} = \frac{[(0.0096 \text{ ft/day})(1 \text{ day}/86{,}400 \text{ s})]^2}{2(32.2 \text{ ft/s}^2)} = 1.92 \times 10^{-16} \text{ ft}$$

This appears to be a negligible value.

The total head in an unconfined aquifer is reflected by the elevation of the water table. At the water table the pressure is at atmospheric pressure. Hydrogeologists reference atmospheric pressure as zero pressure (zero feet of head). Thus, water below the water table is at a pressure greater than atmosheric (positive head), while water in the vadose zone, including the capillary fringe is at a negative pressure head. When these elevations are contoured, a surface is generated that is also known as the potentiometric surface. The **potentiometric surface** of an

unconfined system is the water table. The potentiometric surface, therefore, is a surface reflecting the total head, which includes elevation head (h_z) and pressure head (h_p).

In a confined aquifer the total head is also represented by water levels in cased wells. For an aquifer to be confined, by definition the water level rises above the physical top of the aquifer (Chapter 3). This occurs because confined aquifers are pressurized. Pressurization results from an aquifer being confined from above and below by units of lower hydraulic conductivity, while recharge waters entering the system (at some position laterally) do so at a significantly higher elevation than the elevation of the aquifer at the position of the cased well (Figure 3.15, Chapter 3). Since water levels in confined aquifers rise proportionally to the pressure within the aquifer system, their elevations represent points of total head in the potentiometric surface. When these points are contoured one can determine the slope of this surface and estimate the direction of groundwater flow. Examples 5.3 and 5.4 and Figure 5.2 illustrate the concept of total head in an unconfined and confined aquifer relative to a common datum. The most commonly used datum is mean sea level (MSL).

Example 5.3 A well completed in a unconfined aquifer and a confined aquifer are compared at two points within the well to show that the water level represents the total head (Figure 5.2). Note now the water level at point C is above the top of the aquifer (point D) indicating this aquifer is confined.

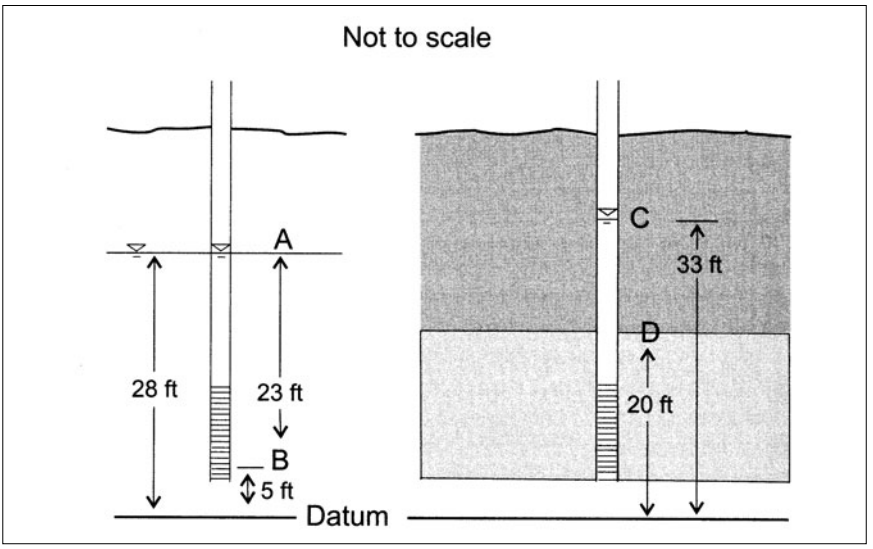

Figure 5.2 Comparison of heads at A, B, C, and D in Example 5.2.

Solution: Equation 5.8 can be used to calculate the heads at A, B, C, D.

$h_A = h_z + h_P = 28\text{ ft} + 0\text{ ft} = 28\text{ ft}$, $h_B = h_z + h_P = 5\text{ ft} + 23\text{ ft} = 28\text{ ft}$

$h_C = h_z + h_P = 33\text{ ft} + 0\text{ ft} = 33\text{ ft}$, $h_D = h_z + h_P = 20\text{ ft} = 13\text{ ft} = 33\text{ ft}$

Hydraulic head and Darcy's law

Between the Bernoulli equation and Darcy's law, most groundwater problems associated with fluid flow can be solved. Groundwater models are designed to solve for head distributions, from which Darcy's law is applied to determine the quantity of flow. Where most people have trouble, however, is in the proper interpretation of the Bernoulli equation and the correct application of Darcy's law.

Remember that the total head is composed of the elevation head and the pressure head. The pressure head is created by the weight of the water above a datum. Pressure is often times measured in pounds per square inch (psi). There is a simple relationship between pressure head and equivalent hydraulic head (Equation 5.9):

$$1\text{ psi} = 2.31\text{ ft of } H_2O \tag{5.9}$$

Let's see where this came from. Recall from the Equation 5.7 that the pressure head can be expressed as:

$$h_p = \frac{P}{\rho g} \tag{5.10}$$

Pressure (P) is equal to force/area, where force (F) is equal to mass times acceleration due to gravity (g). The denominator essentially represents a force over a volume (vol). Therefore, there is an inherent g in both the numerator and the denominator:

$$\frac{P}{\rho g} = \frac{mg/A}{\rho g} = \frac{mg/A}{mg/\text{vol}} \tag{5.11}$$

If it can be assumed that the density of water (ρ) is approximately 62.4 lb/ft^3 and the area (A) is converted from square inches to square feet:

$$1\text{ psi} = \frac{1\text{ lb}/1\text{ in}^2}{62.4\text{ lb/ft}^3} \times \frac{144\text{ in}^2}{1\text{ ft}^2} = 2.31\text{ ft} \tag{5.12}$$

Where, gravity in the numerator and denominator (Equation 5.11) have already been cancelled out. The relationship in Equation 5.9 can also be conceptualized by taking a piece of 1-in inner diameter (ID) PVC pipe and filling it with water. The weight of the water would be one pound.

This means that if flowing wells are capped and equipped with a pressure gauge, the pressure read in psi could be converted into feet of water. If psi readings are small (a few psi), then a stand pipe can be added to get a true reading for total head (Figure 5.3).

Example 5.4 A well completed in Death Valley, California, is capped and has a pressure-gauge reading of 23 psi. The ground surface elevation is −234 ft (using mean sea level as a datum, Section 5.3) and the well casing is capped at 2.5 ft above ground surface. What is the total head at this location that would be used as a point on a potentiometric surface?

Solution: Using Equation 5.9, we obtain the equivalent pressure head, and using Equation 5.8, we determine the total head:

$h_p = 23 \text{ psi} \times 2.31 \text{ ft/1 psi} = 53.1 \text{ ft of pressure head}$

$h_z = -234 + 2.5 = -231.5 \text{ ft of elevation head}$

$h_t = h_p + h_z = 53.1 + (-231.5) = -178.4 \text{ ft, relative to mean sea level}$

Now that you have a basic understanding of hydraulic head and Darcy's law, Examples 5.5, 5.6, and 5.7 illustrate some applications.

Example 5.5 As a graduate student in Laramie, Wyoming, I lived in a small house with a basement apartment. In the springtime, the basement apartment would flood from seeping groundwater. The landlord and his son were down there mopping the water up and wringing it into buckets, which they would throw out onto the lawn. After observing them make a couple of trips to the

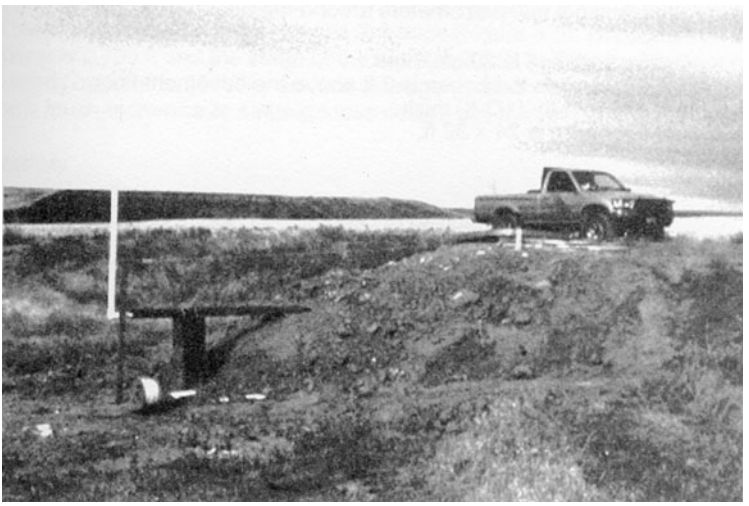

Figure 5.3 Well with stand pipe.

yard, I took pity and suggested they design a sump-pump system to handle groundwater seepage from the high water table. As an example of using Darcy's law for vertical flow, we can assume the walls are impermeable and that all the water is seeping through the concrete slab of the basement. We can use this information to determine the hydraulic conductivity of the concrete slab. Suppose the following information was determined after a brief field excursion, which included placing a few piezometers around the house (Figure 5.4):

Rate of water seepage is 20 gal/ h.
Average head outside the house is 3 ft above the basement floor.
Basement slab is 4-in (1/3-ft) thick.
Basement floor area is 24 × 32 ft.

Solution: If it can be assumed that the physical properties of the concrete slab are homogeneous and isotropic, Equation 5.1 can be manipulated algebraically to obtain the result.

$Q = 20$ gal/h $\times$ 1 ft^3/7.48 gal $\times$ 24 h/1 day $= 64.2$ ft^3/day
$A = 24$ ft $\times$ 32 ft $= 768$ ft^2, the area perpendicular to upward vertical flow
$\partial h = 3.0$ ft
$\partial l = 1/3$ ft, the distance over which the head change occurs
$i = 3.0$ ft/0.33 ft $= 9$

$$K = \frac{Q}{Ai} = \frac{(62.4 \text{ ft}^3/\text{day})}{(768 \text{ ft}^2)9} = 9.0 \times 10^{-3} \text{ ft/day}$$

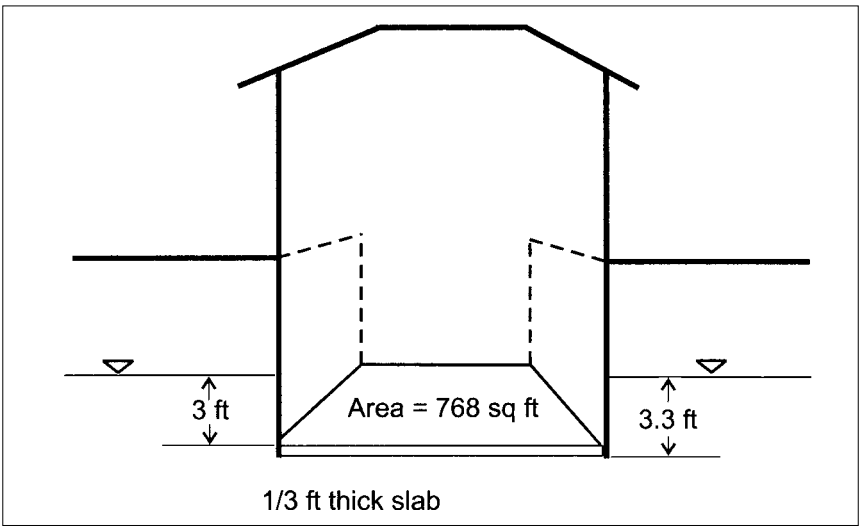

Figure 5.4 Basement flooding problem.

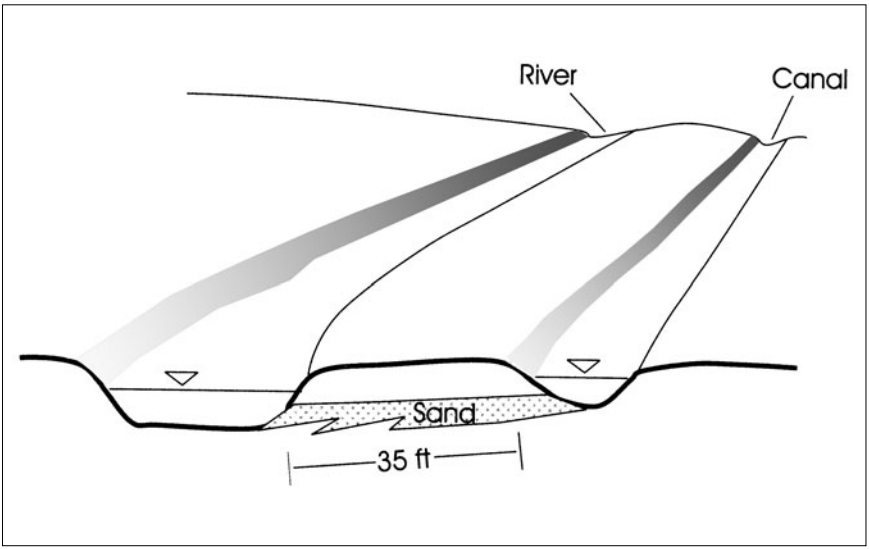

Figure 5.5 Leakage from canal to river.

Example 5.6 (An example from Dr. Bruce Thompson from New Mexico) Suppose that along the Rio Grande River there is a canal that runs parallel to the river. Because of flooding, the surficial materials are fine-grained and clayey. However, there is a connection through a sandy layer between the canal and the river that averages 2-ft thick (Figure 5.5). Suppose that the stage of the river is 2,110 ft and the stage of the canal is 2,113 ft. If the hydraulic conductivity of the sandy material is 10 ft/day and the average distance from the canal to the river is 35 ft, how much **leakance** or seepage loss occurs per mile of canal back to the river?

Solution: Equation 5.1, Darcy's law, can be used to calculate the result.

Change in head is: $\partial h = 2{,}113–2{,}110 = 3$ ft
Flow path length over which the head changes is: 35 ft
Area perpendicular to flow is: 1 mile $\times$ 2 ft = 5,280 ft $\times$ 2 ft. = 10,560 ft^2
Leakance Q = (10 ft/day) (3 ft/35 ft) (10,560 ft^2) = 9,050 ft^3/day per mile of canal.

Example 5.7 One of the best ways to visualize Darcy's law and gain a perspective of the area perpendicular to flow is by imagining that the room you are in is a confined aquifer. Pretend that a series of wells drilled from the roof and completed within the aquifer (the room) reveal a gradient of 0.007 from one side of the room to the other. If you assigned a hydraullc conductivity to the aquifer materials, can you determine the amount of flow through the room?

Solution: Since flow is horizontal from one side of the room to the other, the distance from one wall to the other along the flow path is the flow length (dl) over which the head changes (∂h). The area perpendicular to flow (A) is the height of the room from floor to ceiling multiplied by the width of the wall.

5.2 Flow Nets

One of the ways to graphically represent a 2-D view of groundwater flow, either planar (x,y) or cross-sectional (x,z), is through a **flow net**. The net consists of two sets of lines, flow lines and **equipotential lines**, or contours, of equal hydraulic head. In the case of homogeneity and isotropy flow lines are parallel to groundwater flow and the equipotential or potential lines are perpendicular to flow. The spacing of the equipotential lines reflect the hydraulic gradient (Figure 5.6). The usual spacing of the flow lines and potential lines are selected so that they roughly form a box. This gives the appearance of a net. The quantity of flow (Q) between any two flow lines is the same based on the principle of conservation of mass. If there are sources (recharge contributions) or sinks (discharge areas), the effect would result in the bending (divergence for injection or convergence for discharge) of flow lines. This will be discussed in more detail later on. In a given flow net, the areas of highest transmissivity have the flattest gradients and therefore the largest boxes. Some excellent examples on how to construct flow nets, with wonderful

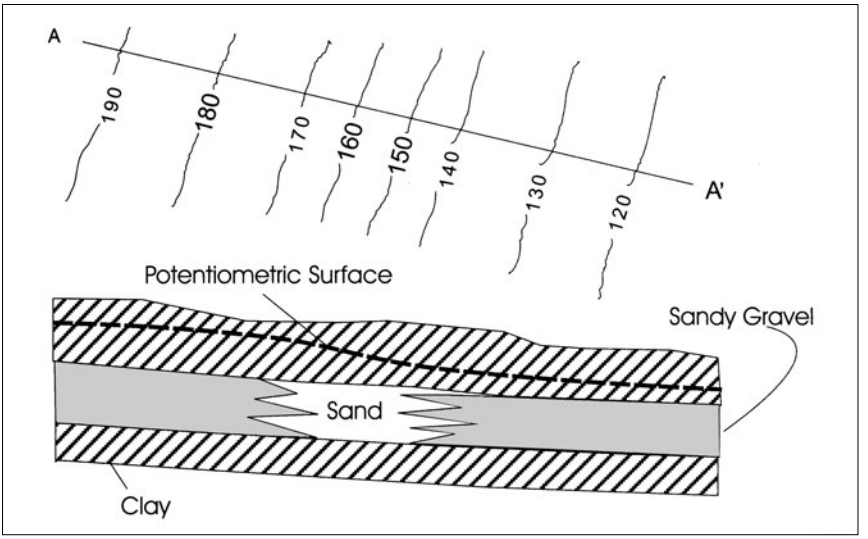

Figure 5.6 Plan view and cross-sectional view of a potentiometric surface map in a confined aquifer. [*Modified after Heath and Trainer (1981).*]

drawings and examples related to flow beneath concrete or earthen structures, are given by Watson and Burnett (1993). It is my experience that flow nets can be easily created using a variety of software (Waterloo Hydrogeologic, Groundwater Modeling Systems, and others).

The steepening of the hydraulic gradient in Figure 5.6 suggests that the transmissivity of the aquifer has changed. This may be attributed to a region of lower hydraulic conductivity (K) or a thinning of the aquifer (b).

Two examples (Examples 5.8 and 5.9) will be given from litigious cases. In example 5.8 a gasoline spill cleanup took place without investigating possible contamination sources up-gradient (a bad idea). In Figure 5.7 of the example is an oblique view of the potentiometric surface of a shallow water table. One can observe the steeper gradient on the right of figure 5.7, where finer-grained (siltier) sediments prevail. On the left side of the figure the hydraulic gradient flattens, corresponding to a coarser-grained sandy aquifer material.

Example 5.9 takes place at a railroad fueling site at a town in north-central Montana near the Canadian border. The site was under investigation as a likely source for diesel and halogenated hydrocarbons contamination of the shallow aquifer in a residential area. The technical personnel representing the railroad assumed that the geology at the railroad property continued northward into the residential area. Additional drilling and correlation analysis of the available drillhole data indicated a marked coarsening of aquifer sediments in the residential

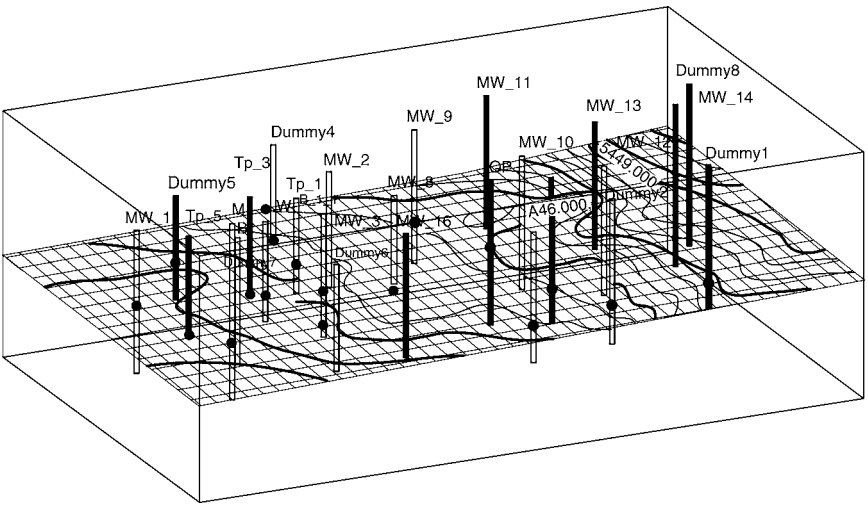

Figure 5.7 Oblique view of a water-table surface from wells completed in a shallow unconfined aquifer in western Montana. MW stands for monitoring well. The scale of the grid spacing is approximately 10 × 10 ft (3 × 3 m).

area, including a paleochannel that aided in distributing the contaminants throughout the neighborhood (Weight, 2004). The change in grain-size to becoming coarser grained is also revealed by a flattening of the hydraulic gradient in Figure 5.8.

Example 5.8 In a city in western Montana was a business that stored and sold gasoline from the 1950s through the 1980s. During the 1980s several leaks and spills were documented, resulting in contamination of the local soils. A brief investigation during the early 1990s revealed a BTEX (Benzene, Toluene, Ethyl Benzene, and Xylene) plume in the shallow aquifer (less than 20 ft or 6.1 m). Although some of the backhoe pits which extended to the water table indicated other possible sources (evidenced by surface sheens and odors) in the up-gradient pits, this was not pursued. In an effort to clean up the site soils were excavated followed by the installation of a soil vapor extraction system. This effort "appeared" to clean up the vadose zone to a zero detection limit, at least temporarily. The insurance company representing the land owner was approached by the state agency that financed the cleanup to recover operating expenses plus interest.

A review of the documents and field data associated with the case indicated a strong possibility that at least one other contamination source existed up-gradient

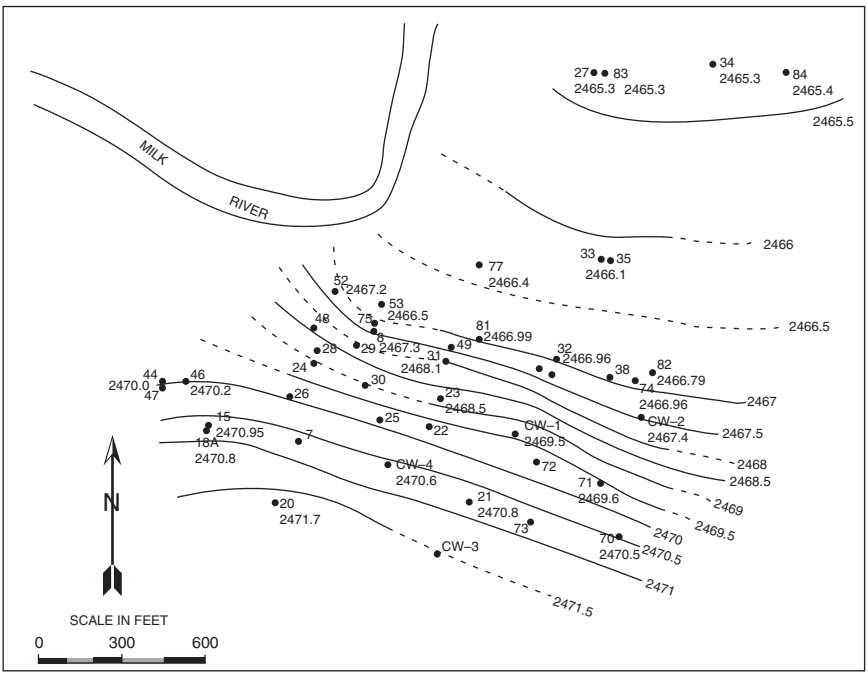

Figure 5.8 Potentiometric surface map of a shallow aquifer near the Milk River in north-central Montana. Contour interval is ½ ft (0.15 m). The steeper hydraulic gradient is where the railroad property is.

of the site. Additional monitoring wells and sampling points were installed to evaluate the extent of off-site sources. The additional data points, after being sampled, revealed at least one additional upgradient source of BTEX chemicals. Water level data from all wells were used to construct a water-table surface map (potentiometric surface, Figure 5.7). Figure 5.7 represents an oblique view of the water table taken from a numerical model. The data were contoured using a 1/2 ft (0.15 m) interval, with every third contour marked in bold (the original contaminated soils were thought to be between MW 1 and MW 4 in the figure and MW 2 was considered to be up gradient during the early 1990s). The drill cuttings from monitoring wells MW 10 through MW 14 (on the right-hand side of Figure 5.7) showed a predominance of siltier materials compared to wells at the original site near MW 1, MW 3, and MW 4 at the left of the diagram showing a predominance of sand. Notice how the slope of the potentiometric surface corresponds well to the geologic materials of the aquifer.

Example 5.9 Along the Montana hi-line (a highway that runs east-west across northern Montana just south of the Canadian border) in north-central Montana is one of several railroad towns. The railroad site had been a fueling facility since the 1880s, and was converted from steam to diesel power in the 1940s. Since that time a sizable pool of free product (approximately one half million gallons, 1.9 million liters) had built up on the water table. The direction of groundwater flow is north to northeast toward a residential area. A class action law suit from the local residents resulted in an investigation of all existing data, followed by new drilling with subsequent water-quality sampling and aquifer analysis.

The claim by technical folks representing the railroad was that geologic conditions at the fueling site continued northward into the residential area. The drillhole data and the potentiometric surface maps contradicted this interpretation (Weight 2004). Figure 5.8 represents a mutually agreed upon interpretation of water level contours of the local shallow aquifer. The contour interval is 1/2 ft (0.15 m). Using lithologic log descriptions from drillhole data and considering the depositional environment of the area, it became clear that a paleochannel extends, from where the Milk River bends northward, eastward across the residential area. Notice how the hydraulic gradient is very flat east of the Milk River (representing the paleochannel and associated floodplain deposits), while the tighter contours represent the clayey silt materials prevailing at the railroad property.

When one uses flow nets to estimate flow, it is important to make calculations through flow lines where the hydraulic gradient is similar, rather than averaging the gradient over a larger region. Calculations using Darcy's law are only valid where the hydraulic conductivity or transmissivity is constant. Where this is true, the flow net will show a uniform gradient corresponding to the hydraulic properties.

Getting back to Figure 5.6 the hydraulic gradient between contours 190 and 170 is uniform; therefore the hydraulic properties between these contours are similar. Between contours 170 and 140 the hydraulic gradient is also similar but its slope has changed (it is steeper, contours are closer together) indicating a change in aquifer properties (finer-grained or thinner). The widening of the hydraulic gradient between

contours 140 and 120 indicates the aquifer has changed once again (become coarser-grained or thicker). Hence, when performing calculations using Darcy's law one must be sure the hydraulic gradient (I = dh/dl) is matched with the corresponding aquifer hydraulic properties of K or T.

If the location at hand is not in a recharge or discharge area, the flow is generally considered to be mostly horizontal (horizontal flow). This can occur if the material is relatively permeable in flat terrain. Here the potential lines are assumed to be more or less vertical. As a practical matter, this means that wells completed at different depths within the same aquifer at the same location will have the same water level elevation.

Rarely, within a given aquifer unit, is the distribution of horizontal hydraulic conductivity the same. This phenomenon is a function of the depositional environment of the sediments. There are usually lenses of varying hydraulic conductivity or fining upward or downward sequences within an aquifer. The coarser units tend to have faster relative velocities than the finer-grained units. This contributes to varying contaminant arrival times than would be predicted using the average linear velocity from Equation 5.4 (Figure 5.9). In plan view flow nets and in 2-dimensional groundwater modeling, however, the vertical distribution of horizontal conductivities (and other characteristics) are averaged over the entire saturated thickness.

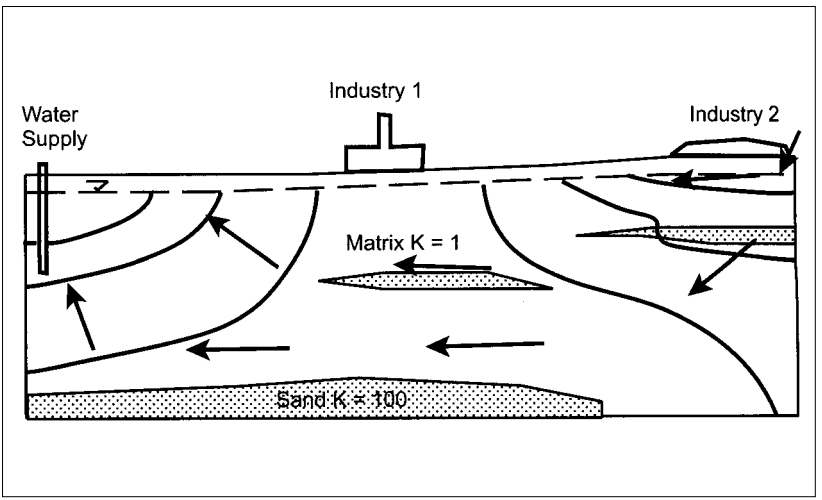

Figure 5.9 Potential lines and flow arrows for a recharge-discharge area with two potential sources affecting a public water supply.

Vertical groundwater flow

In discharge areas, recharge areas, or undulating topography, there is always a significant vertical component to groundwater flow (Figure 5.10). This means that water levels in wells completed at different depths within the same aquifer unit will be different. The best way to determine this is to complete two or more wells at varying depths within the same drillhole as a nested set. There should be a trend of downward or upward changes in water levels with depth, depending on whether the location is a recharge or discharge area. Wells completed in the central region of Figure 5.10 will have similar water levels, whereas wells completed deeper in the discharge area will show higher relative heads than wells completed nearer to the surface. The reverse will be true in a recharge area.

The water level observed in any well is reflective of the head at the midpoint of the screened interval. Piezometers (Chapter 6) with screen lengths less than 1/2 ft (0.15 m) provide strategic point estimates of hydraulic head. Monitoring wells with screen lengths longer than 10 ft (3 m) may not provide a sufficiently accurate distribution of hydraulic head to understand the vertical nuances of groundwater flow. Depending on the goal of the project it just may be a matter of scale.

At a given contamination site, it is important to know if there is a significant component to vertical flow and which way that component is. For example, wells with long screened intervals may have components of groundwater flow entering the well and components leaving the well (McIlvride and Rector 1988). For example, in a discharge area, the higher potential lines are intercepted at the lower part of the well. This

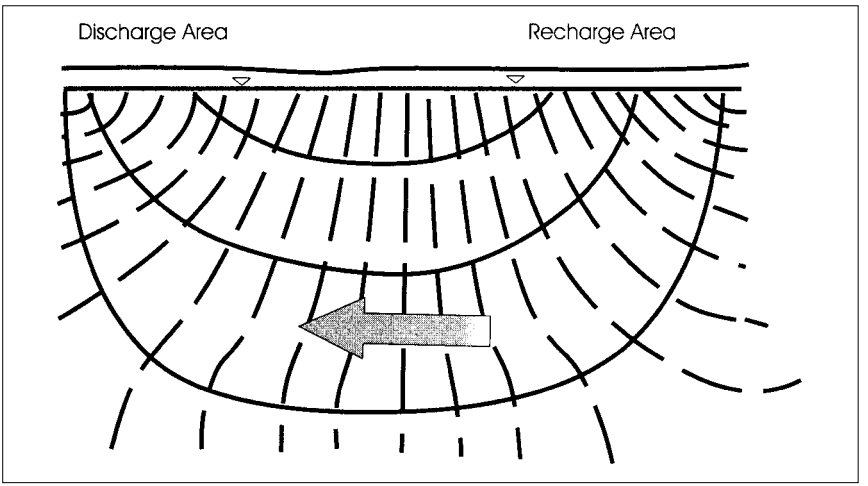

Figure 5.10 Flow net showing recharge and discharge areas with no vertical exaggeration. [*Modified from Toth (1962).*]

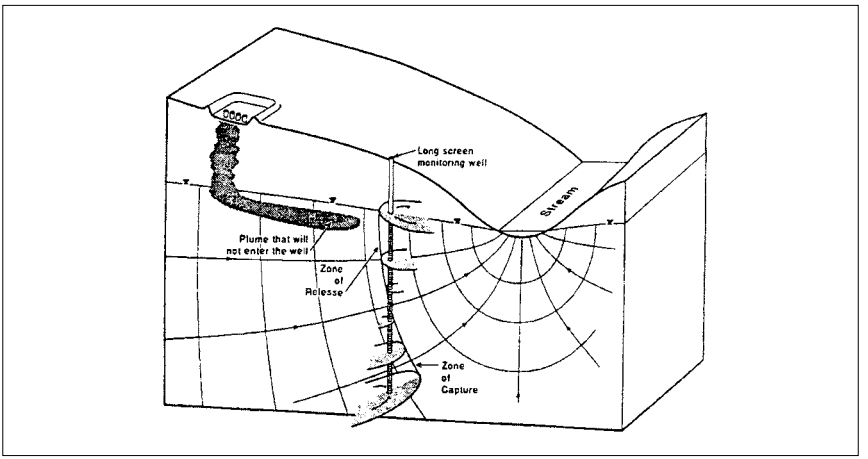

Figure 5.11 Water circulation within fully screened monitoring wells in discharge areas. [*From Mcllvride and Rector (1988).*]

results in water flowing into the well in the lower portion of the well screen (Figure 5.11). In the upper portion of the well screen, the water level in the well is higher than the surrounding potential lines within the aquifer. This results in water in the upper portion of the well moving from the well out to the formation. Any contamination that would potentially intercept the upper portion of the well would go around the well and may not be detected.

Gaining and losing systems

Many perennial streams receive groundwater discharge (gaining streams) along their courses that sustain their flow even during the driest months, even if no tributaries enter. In this case, the river represents the lowest point of hydraulic head in a groundwater surface-water system. The equipotential lines in a flow net bend such that the flow lines converge on the stream ("V" upstream) (Figure 5.12 Location "D"). Here the water table slopes toward the stream. Although in a 2-D plan view of a flow net, all potential lines appear to be vertical, in a discharge area (e.g., a gaining stream) the potential lines actually dip in the direction of stream flow. This means that flow lines are actually curvilinear (Wampler 1998) (Figure 5.13).

In the arid west of the United States, many streams maintain sustained flow in the mountains, but lose their water into alluvial fans or the sediments of larger valleys. As streams enter areas with lower precipitation, it may be that the water table slopes away from the river or is several feet below the river stage. Here, Darcy's law would indicate that water

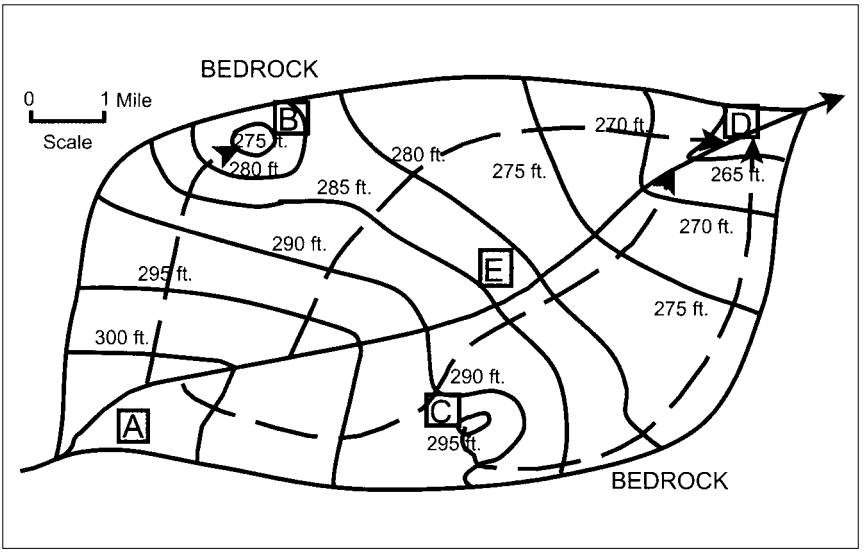

Figure 5.12 Schematic of groundwater/surface water flow in a valley surrounded by bedrock: losing stream (A), discharge area (B), recharge area (C), gaining stream (D), and neither gaining nor losing conditions (E). [*Adapted from Davis and Dewiest* (*1966*).]

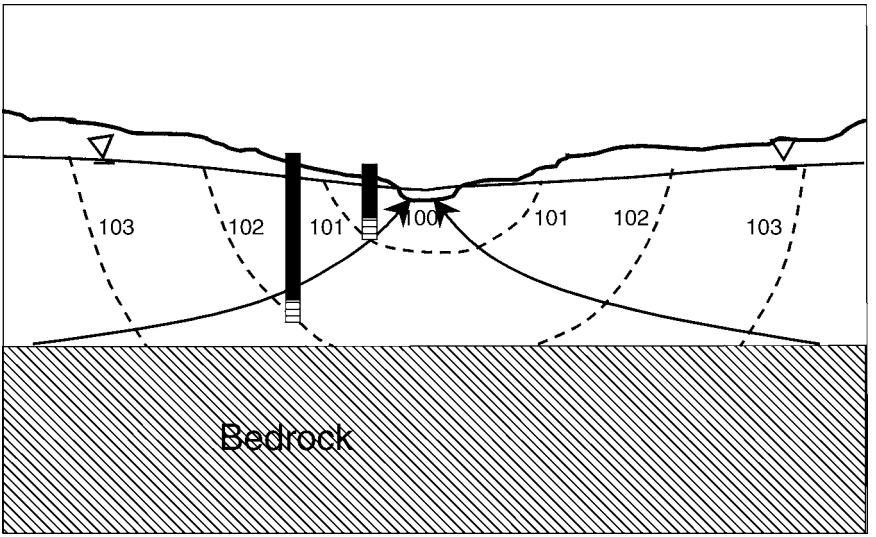

Figure 5.13a Schematic of a flow net of a gaining stream or groundwater discharge area. Notice how the deeper well has higher head than the shallow well indicating upward flow. Not to scale.

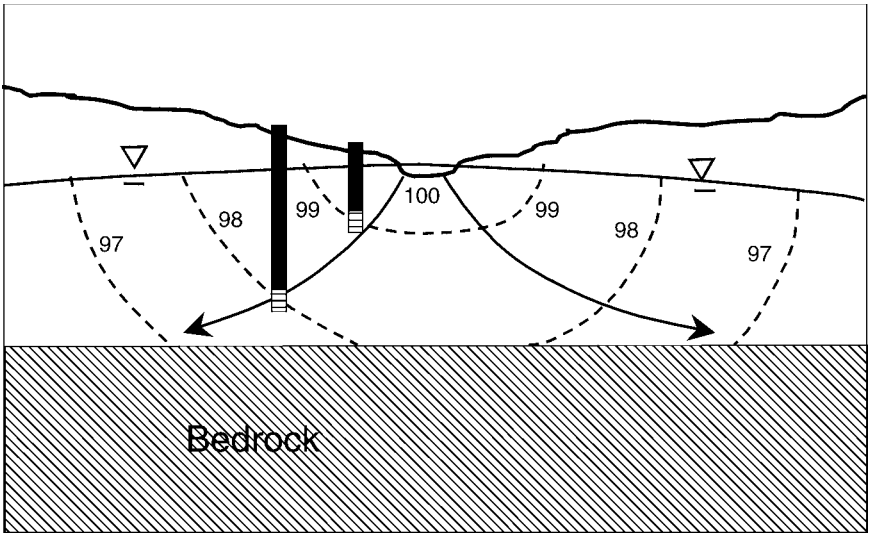

Figure 5.13b Schematic of a flow net of a losing stream or groundwater recharge area. Notice how the deeper well has a lower head than the shallow well indicating downward flow. Not to scale.

will move from the river out to the aquifer. This is a losing stream. In this case, the potential lines bend so that they "V" downstream (Figure 5.12 Location "A"), and also dip away from the direction of stream flow.

A given stream valley can have both components of losing stretches and gaining stretches as shown in Figure 5.12. In the recharge and discharge areas, there are vertical components (3-D components) of flow; whereas, in the areas where groundwater flow parallels the stream, flow is essentially horizontal (2-D, the mid-section of Figure 5.10). This becomes significant later on in the interpretation of water-level data (Section 5.4).

Refraction of groundwater flow

As water passes from porous materials of a certain hydraulic conductivity into a differing hydraulic conductivity, the flow lines will bend or refract according to the principles described by Snell's law. This phenomenon is observed in a clear glass of water with a straw sticking out of it. The straw seems to bend at the air/water interface. This is due to the refraction of light as light rays pass from the less dense medium of air into the denser medium of water. Snell's law applied to groundwater flow is described by:

$$\frac{K_1}{K_2} = \frac{\tan(\sigma_1)}{\tan(\sigma_2)} \tag{5.13}$$

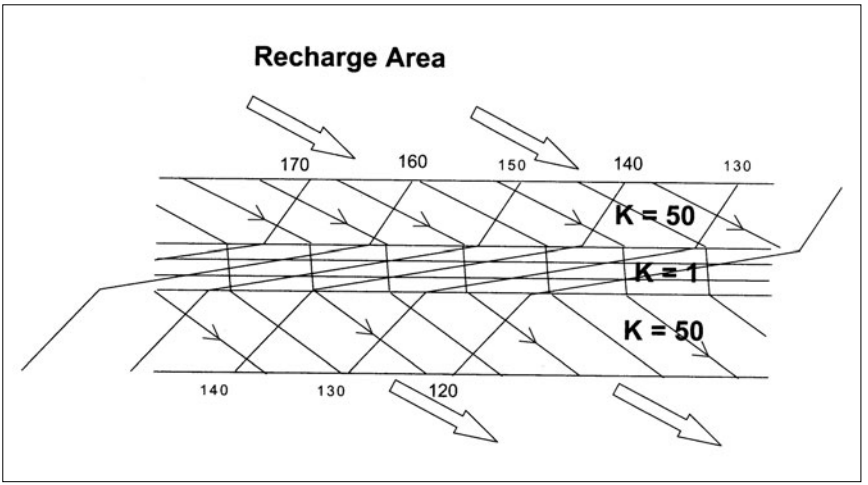

Figure 5.14 Flow lines refract between or at the boundary of dissimilar materials of differing hydraulic conductivity.

This phenomenon is illustrated in Figure 5.14 . What you see is that flow lines or stream lines move vertically through low conductivity layers (at wider spacing) and somewhat horizontally through higher conductivity layers.

In terms of pipe flow, if:

$$Q_1 = Q_2 = v_1 A_1 = v_2 A_2 \tag{5.14}$$

then the closer together (tightly spaced) stream lines represent areas with horizontally faster velocities (moving through flatter gradients), and the wider spaced streamlines represent areas with slower vertical velocities (moving through steep hydraulic gradients).

Since streamlines will refract when they encounter geologic materials with differing hydraulic conductivities, it is extremely difficult to predict where these streamlines will go. Many depositional environments will create lenses of materials with differing hydraulic conductivities. This becomes significant when one considers locating a landfill or attempts to predict where a source of contamination came from. Depending on the geology and the flow system, a contamination source that appears to be obviously close may not be the source in question at all, but may have come from some more distant source (Figure 5.9).

5.3 Level Measurements in Groundwater Monitoring Wells

The basis for determining the direction of groundwater flow is based upon static water-level data. Level measurements in groundwater monitoring

wells are one of the most fundamental tasks performed at any site. It is one of the first things done when arriving to a site and performed on a routine basis. Water levels can be collected manually with a portable field device or rigged to collect continuous data with a data-logger sentinel. It is possible to telemetrically send these data back to the office, powered by a solar panel providing the ability to have real-time access to critical monitoring points (Figures 5.15 and 5.16). Water-level data are of little value without knowing the well-completion information and what the relative elevations are. Grave errors can result if one assumes that all water-level data for a given area are collected from the same aquifer unit, ignores recharge and discharge areas, and fails to survey the measuring points!

The purpose of this section is to present the practical aspects of obtaining level-measurement data and to describe the most commonly used devises to obtain them. It is instructive to present the most common sources of error from field mistakes and idiosyncracies of the equipment to give the reader a better understanding of the pitfalls one can fall into. The pitfalls one can make in interpreting water level data are discussed in Section 5.4.

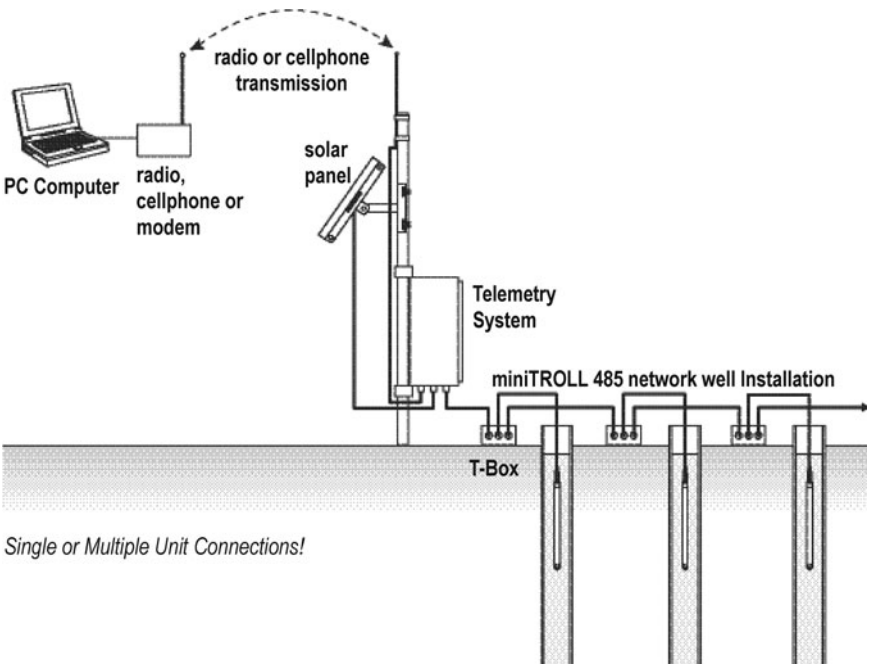

Figure 5.15 Schematic of an enhanced telemetry system designed by In-Situ, Inc. of Fort Collins, Colorado.

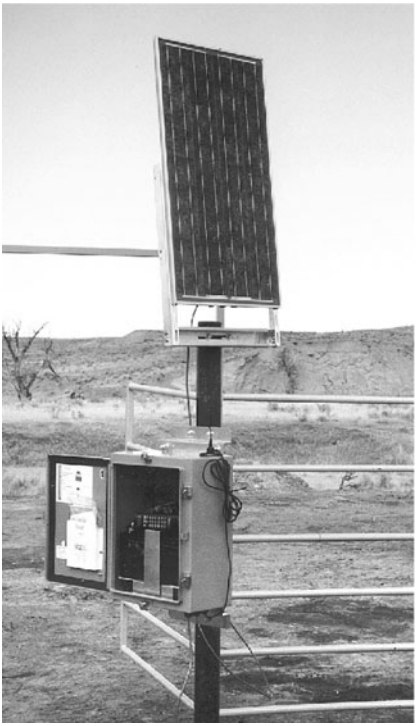

Figure 5.16 Solar-powered telemetry system.

Defining level measurements

For a given project area or data set, it is imperative that there be some consistency among those who collect the data. One of the first considerations is where the common datum is. Many use mean sea level (MSL) as a datum. This would mean that all data would be reduced to elevations above MSL. For some projects, an arbitrary relative datum may become the base datum. For example, you are out in the field and there is no convenient way to tie into a benchmark of known elevation. You still need to evaluate the relative elevations or may have security reasons for keeping your database as arbitrary elevations. Keeping exact elevations from being known by others may be important if a public presentation is being conducted in a politically sensitive area. Whatever ends up being used as the base station needs to be a relatively permanent feature that is not likely to be disturbed. It would be disastrous to select a large rock or drive a stake that is later excavated and removed during construction or by curious children.

Surveying the well locations and measuring points is critical to proper interpretation of the data. Surveying can be done by estimating on a topographic map, by tape and measure, by simple level surveys, total

station systems that give northing, easting, and elevation, or by the global positioning systems (GPS). For example, level surveys provide a relative vertical positioning, but are not capable of providing northing and easting positions. GPS systems are very useful for widely spaced monitoring locations, distributed farther than is practical with traditional surveying equipment.

The handheld GPS units are widely used by drillers and geologists with accuracies within 10 ft (3 m) if the receivers have Wide Area Augmentation System (WAAS) capabilities. The WAAS provides greater accuracy and precision by incorporating ground stations in the United States to correct for ionospheric disturbances and timing of the 24 Department of Defense satellites and corresponding satellite orbit errors (Garmin 2006). Without the WAAS, GPS units are typically accurate to within 50 ft (15 m). The GPS satellites circle the earth twice a day, each in a precise orbit. Continuously a signal is being transmitted that GPS receivers "lock" unto. With three satellites a latitude and longitude (2D) location can be calculated, with more satellites vertical estimates can also be made. Again handheld units are not very accurate (approximately 50 ft or 15 m or so) in the vertical. This is hardly accurate enough to use for constructing potentiometric surface maps www.garmin .com (2006).

To obtain survey-grade vertical GPS accuracy a more expensive system that includes a base station (positioned at a known surface elevation) configured with a rover unit must be used. This type of system can bring vertical accuracies within less than a centimeter. To accomplish this, a tripod is positioned over a point of known vertical elevation, with the base station unit and rover unit coupled together at the exact same elevation (Figure 5.17). Software in the base unit is given instructions via a handheld keypad and told the rover unit has been correlated with the base station. Once this initial setup has taken place the rover unit must be held continuously out the window of a vehicle between stations, so as not to lose the connective signal. A bull's-eye bubble is held against the rover unit to maintain as near vertical position as possible and the portable keypad is activated to mark each way point (Figure 5.18). The farther away from the base station (some units are limited to a distance of 14 mi or approximately 20 km, depending on the unit cost), the greater the drift in vertical accuracy. Also, the battery life of some units may only be for 8 to 10 h, so closure of the survey should be accomplished before the batteries lose power, although this isn't absolutely necessary. Closure is ideally completed by bringing the rover unit back to the base station and coupling the unit once again for a final reading. A software package that accompanies the GPS unit is used to reduce the hand held keypad data and perform any corrections.

Figure 5.17 GPS base station and rover unit during initial setup.

Figure 5.18 GPS rover unit being held vertical at a way point.

Most software systems accompanying the expensive GPS units also have a mission planning subroutine with an almanac file that can project the conditions of satellite receiving capabilities for up to 60 days in advance. One keys in the latitude and longitude of the location of the survey site along with the date and a projection printout is generated that shows what times during the day the signal may be weak or strong.

Access to wells

Taking level measurements in wells is straightforward, provided access to wells is known in advance. In a site where level measurements are being taken from wells constructed by a variety of contractors, there may be an assortment of security devices and locks. Each may require its own key or some special way to remove the cap. For example, monitoring wells that are constructed in playgrounds or in paved roadways may have a flush-mount security plate (Figure 5.19). In this case, a socket or wrench is required to remove the surface metal plate before a subsequent lock can be reached. A bucket with whisk brooms and an array of screwdrivers can be invaluable in removing sediment trapped in the spacing between the cap and its housing and in the mount bolts. This flat completion method allows vehicles to run over the well locations or individuals to run around without tripping.

Figure 5.19 Flush-mount well cap.

Removing a well cap. To save on costs for more regional studies, monitoring networks are sometimes expanded to include domestic, stock-water, or other existing wells. Nothing is more frustrating in fieldwork than not to have access to a well. This may be something as simple as forgetting the keys to the well caps or the gate to get in. Many stock wells or domestic wells will typically have a well cap attached by three bolts (Figure 5.20). These are usually more than finger tight to prohibit animals from knocking off the well caps, and to discourage the casual passerby from intruding. An indispensable device is the handy multitool purchased at most sporting goods or department stores. These should be equipped with pliers that can be used to loosen the bolts and free the cap. This is a good excuse to tell your spouse that you need one, it makes a great safety award.

Well caps that become wedged over a long season from grit, changes in air temperature, or moisture can usually be loosened by taking a flat stick or your multitool and tapping upward on the sides of the well cap until it loosens up. This process will eventually allow access to the well. Tight fitting polyvinyl chloride (PVC) well caps can be modified with slits on the sides of the well cap, to allow more flexibility. Another important point to remember is to place the well cap back on and resecure any locking device the way you found it. Well owners can get really mad about such neglect and may not allow a second opportunity for access.

Figure 5.20 Typical well cap.

In areas where gas migration takes place, (coal mines, or landfill areas) gas pressures may build up under well caps if they are not perforated with a breathe hole. One field hydrogeologist was measuring water levels in a coal-mining region and had a thought to kick the well cap. When the cap blew 150 ft into the air he contemplated what would have happened to his head. This resulted in a company policy of drilling breathe holes in well caps or in the casing to bleed off methane gas pressures. Pressure changes in any monitoring well from changing weather conditions may affect the static water level, therefore, drilling a small hole below the well cap in PVC casing can alleviate pressure effects.

Opening tight-strung gates and negotiating fences. Another obstacle in gaining access to wells in the western United States is barbed-wire fences. After one obtains permission to obtain level measurements in rural areas, it is important to leave all fences and gates the way they were found. Some gates are tough to open and are tougher to close. There is actually a technique to opening and closing a tightly strung gate. The gate is usually held at the bottom and the top by a looped wire attached to the fence post. The trick is to place the gate post into the bottom loop and pull toward the top loop (sort of like a head lock in the sport of wrestling), with the fence post braced against your shoulder for more leverage (Figure 5.21). It is embarrassing to have a coworker or support vehicle wait long periods of time for you to close a gate. Merely pushing the gate post toward the fence results in safety problems and frustration. The headlock method works much better. In some cases, in extremely tight fences a "cheater bar" will be

Figure 5.21 Accessing a well through a barbed-wire gate.

hanging there along the fence post. In this case, you again place the gate post into the lower loop and then use the "cheater bar" to pull the fence close enough to attach the upper loop. Both apply the same principle.

Some fences may have an electrically hot top wire to keep livestock in. In this case if you touch the wire, you will get shocked. The wire looks distinctively different from the other wires and is located near the top of the fence. Test the wire by gently tossing something metal at the suspected wire. Having rubber boots on can be helpful. Hot fence wires can be especially problematic for fences keeping buffalo in. Network mogul Ted Turner has a fence in Montana that puts out 5,000 V (although the amperage is low) to the unwary animal. It is shocking enough to keep a buffalo away but also strong enough to knock a person down and stop their heart from beating for a couple of minutes.

Measuring points

Once a datum has been established, data collected in a fieldbook are brought back to the office. All persons collecting data should clearly indicate whether data were collected from top of casing (TOC) or ground surface (GS), and so forth. Are the data recorded as depth from TOC or depth from GS or from some other point of reference? For example, a well casing cut off below the floor of a shed may be recorded from the shed floor surface. The distance that the casing extends above the ground surface is referred to as the "stick up." All these become important later on as a level survey is conducted and relative elevations need to be established.

Identifying measuring points (MPs) may not be as straightforward as would seem. Sometimes when several monitoring wells are constructed in a short period of time, simple annoyances, such as not cutting the casing off horizontally, can occur. It may be that a piece of steel casing was cut off with a torch, or a section of PVC casing was cut diagonally. This is not only a problem with placement of a well cap, but creates a myriad of problems when different individuals are going out into the field to take measurements. Where do you take the measurement? At the lowest part of the cut, the top of the cut, or somewhere in between? Probably you were not responsible for the well completion, but still need to collect meaningful data.

It is suggested that markings be clearly made on the casing indicating where to take a measurement. On steel casing, it is helpful to take a hacksaw or file and make three nick marks close together. A dark permanent marker can also be used to make an, upward arrow pointing to the three marks. A similar arrangement can be used on PVC casing; however, the dark permanent marker works well enough that hacksaw or file markings are usually not necessary (Figure 5.22). This works best

Figure 5.22 Marking point on a PVC casing.

if all markings are made inside the casing. Markings on the outside, even with bright spray paint, tend to fade quickly in the weather. If a name plate is not with the well, it is also helpful to indicate well name and completion information, such as total depth drilled (TDD) and screen interval, on the inside of the well cap.

Water-level devices

There are a host of water-level devices used to collect level-measurement data. Don't be fooled into thinking one is best; for the different devices each have their own unique applications. Manual devices such as steel tapes and electric tapes, or E-tapes, are discussed first, followed by those with continuous recording capabilities, such as chart recorders, transducer-data-logger combinations, and self-contained mini loggers.

How to take a level measurement. The basic procedure of taking a level measurement involves gaining access to the well, removing the well cap, and lowering a device down the well to obtain a reading. Normally, this procedure takes only a matter of a few minutes depending on the well depth, device used, and whether the well is a dedicated monitoring well or a domestic well being used as a monitoring well. As simple as this procedure sounds, if one is not aware of the weaknesses and idiosyncracies of the equipment, serious errors in readings can result that affect the

quality and interpretation of the data. These are discussed in this section and in "The transducers and data loggers section."

Most level measurements are taken under static conditions. Dynamic conditions occur during a pumping test. If the intention is to take a static water-level measurement and the well is in use or was recently used, it is important to allow recovery to equilibrium conditions before taking the measurement. For example, a stock well may be on all the time or the pump activated by a timer. The pump can be shut off for a while (until there are no changes between readings). Then take a reading and turn the pump back on or reset the timer. Once again, if timers are not reset or pumps turned back on, then you may not be given a second chance.

Steel tapes. Most data collected before the late 1970s were likely collected with a steel tape. Steel tapes represent the "tried-and-true" method that still has many important applications today. Water levels from the 1940s on were all measured this way until electric tapes (E-tapes) became the norm. The proper way to use a steel tape is to apply a carpenter's chalk to approximately 5 to 10 ft (1.5 to 3 m) of tape before lowering it into the well. The tape is lowered to some exact number next to the measuring point, for example, 50 ft (15 m). The tape is retrieved to the surface, where the "wet" mark on the tape, accentuated by the carpenter's chalk, is recorded (Figure 5.23). A reading like 50 ft minus 4.32 ft would yield a reading of 45.68 ft depth to water below the MP.

Figure 5.23 "Wet" mark on steel tape.

There is usually a historical knowledge of the approximate depth to water to guide this process. Otherwise it is done by trial and error. Usually a good reading can be made even on a hot day, with the wet chalk mark, otherwise the tape dries quickly. Getting a clean marking may require more than one trip with the tape, hence its loss in popularity.

Sometimes the only way to get a water level *is* with a steel tape. In many pumping wells, with riser pipe and electrical lines, or wells with only a small access port the only way to get a water level is with a thin steel tape. Steel tapes are rigid and tend to not get hung up on equipment down the hole. A 300-ft (100-m) steel tape is an important part of any basic field equipment. It can also be used to measure distances between wells or other useful tasks.

Electrical tapes (E-tapes). By the early 1980s, E-tapes began to dominate the market and are currently considerd as basic equipment. The first devices were usually marked off in some color-coded fashion every 5 ft (1.5 m), with 10-ft markings and 50- or 100-ft markings in some different color. E-tapes now are usually marked every 1/100th of a foot (3 mm) (Figure 5.24). All E-tapes function with the same basic principle. A probe is lowered into the water, which completes an electrical circuit, indicated by a buzzer sound or an activated light or both. The signal from the water level is transmitted up the electronic cable of the E-tape to the reel where the signal occurs. Each has its own appropriate function. During a pumping test with a generator running, it may be hard to hear a buzzer sound, or you may have a hearing impairment from hanging around drill rigs too long without wearing ear protection. In this case a light is helpful. In very bright sunlight, your light indicator may be hard to detect and the buzzer is more helpful. It should be noted that if oils or other floating organics are present in the well, they will not be detected and may provide a false water-level reading.

Most E-tapes have a sensitivity knob from the conductivity sensor in the probe. The sensitivity knob is usually a turn dial that ranges from

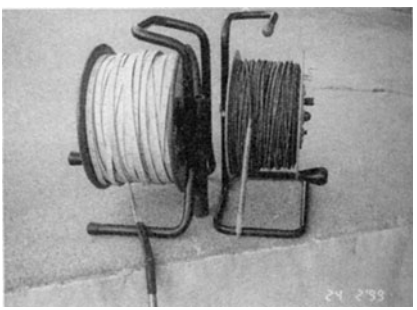

Figure 5.24 E-tapes with probes marked every one-hundredth of a foot.

1 to 10. Probe sensitivity is needed for a variety of water qualities. Low sensitivity (1 to 3) will give a clear signal in high total dissolved solids (TDS) waters, such as those found in Cretaceous marine shales. The higher the TDS in the water, the lower the sensitivity needed to detect a water level. Relatively pristine or low TDS waters require that the turn dial be adjusted to a higher sensitivity setting (8 to 10) to get a clear signal. A good general rule is to put the dial in midrange (4 to 6) and lower the probe until a buzz/light signal is indicated. If little attention is paid to the sensitivity setting, the hydrogeologist may obtain false readings. This may be one of the first questions asked to a field technician when trying to explain why a water-level reading does not make sense.

To take a water-level reading using an E-tape, turn the device on by moving the sensitivity knob dial to midrange. Lower the probe until the light goes on or the buzzer sounds. This gets you close to where the reading will be. At this point, lift the E-tape line above the depth that activates the buzzer and gradually lower the probe until the buzz sound is repeated. Hold this spot on the E-tape line with your thumbnail or with a pointer, like a pencil (Figures 5.25a, 5.25b). The E-tape line should be held away from the measuring point toward the center of the well and shaken lightly to remove excess water and the process repeated. If the light signal is clear and the buzz is crisp, the reading is probably accurate.

False readings are fairly common if one does not pay attention to the sensitivity knob setting. In some wells, condensation inside the casing can trigger a false reading. The sound of the buzzer may not be clear or the light may flicker instead of providing a clear, bright reading. In this case, the sensitivity should be turned down to the lowest setting that yields a good signal. This will be variable, depending on the water quality involved. Cascading water from perforated sections above the actual water level can also be problematic. This can occur during a pumping test, where one is trying to get manual readings in the pumping well that

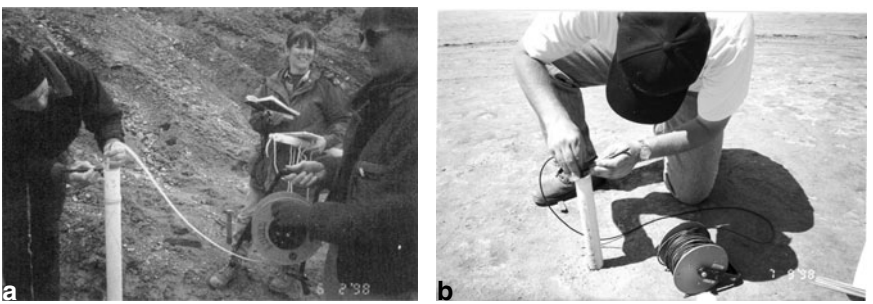

Figure 5.25 (a) Taking water level reading using E-tape. (b) Student with thumb marked on E-tape and location pointed at with pencil for a clear level reading.

has been perforated at various depths. In pristine waters, it may be difficult to get a reading at all. In this case, lower sensitivity knob settings may not be discerning enough to detect when the water table has been reached. Detection may or may not sound off until the probe has been submerged well under the water surface. In this case, turn the dial to the high sensitivity range (8 to 10) and the buzzer or light should give a clearer signal. It is always a good idea to lightly shake the line and repeat the process until a clear reading is obtained.

E-tapes come in a variety of designs. Some have round or flat marked electronic cable lines and probes come in a variety of sizes. Some are easier to use, but most used by hydrogeologists and field technicians today tend to be marked every 1/100th of a foot (3 mm). Many drillers still have devices marked every 1 or 5 ft. Common spool lengths range from 100 ft (30.5 m) to 700 ft (213.2 m) although lengths of 2500 ft (762 m) are routinely used in mining applications. It is usually handy to have a couple of different depth capabilities. There are a number of multi-parameter probes that will measure water quality parameters in addition to static water levels.

Water levels taken in monitoring wells tend to be uninhibited by riser pipe and electrical lines. These pose the fewest concerns as to probe size. Pumping wells, however, may present some challenges. Here, probes may wind around or get hung up in wiring or spacers placed down the well to hold the riser pipe in the central part of the well. Getting hung up can be a real problem, not to mention costly. Here is where steel tapes or the cheaper 5-ft marked E-tapes can be helpful, particularly those with a very narrow probe size. In some cases a service call to a well driller may be cheaper than paying for a new E-tape.

Chart recorders. Many times it is advisable to perform a continuous recording of level measurements. One device that has been used for many years is a chart recorder, such as a Steven's Recorder. A device like this uses a drum system onto which a chart is placed. The position of the water level in the well is tracked by having a weighted float connected to a beaded cable that passes over the drum and is connected to a counterweight (Figure 5.26). As the drum turns forward or rolls backward with the movement of the water level, a stationary ink pen marks the chart. The pen is only allowed to move horizontally to correspond with time set by a timer. Timers can be set for 1 month or up to 3 months. Chart paper is gridded where each column line usually represents 8 h. The row lines mark the vertical water-level changes.

Since the turning of a drum can be significant, control of movement is through setting the ratio of float movement to drum movement of the chart paper. This is known as setting the gear ratio. For example, a 4:1 (four to one) gear ratio means that the float will move four times the

Figure 5.26 Chart recorder in the field.

distance the drum would turn forward or backward. This helps keep the pen on the chart paper.

Once the chart is replaced with new paper, the information from the chart has to be reduced or converted into numbers. A technician often logs numbers from a chart into a file for data analysis or hydrograph plotting. Corrections for drift are made by noting the time and date at the end of the chart and then applying a linear correction from the beginning time. For example, if the final marking on the chart is 12 h short (because the timer setting is off) of the supposed time, a correction factor is applied to "stretch" the data to match up with real time. Reduced data are easily adjusted on a spreadsheet.

Frequently, wells located near surface water streams are fitted with a chart recorder to compare the groundwater and surface-water elevations or in an area where water-level fluctuations are significant. Other reasons may be for placement during winter months or remote areas when access is difficult.

The chart recorder is positioned directly above the well on some kind of constructed platform (Figure 5.26). The platform sits above the well casing, with the float attached to a beaded cable lowered down to the

water surface. A hole cut in the platform allows the beaded cable to pass up over the drum and then through another hole cut in the platform for the counter weight. The top of the well casing and the recorder can be encased in a 55-gal drum that can be locked.

Errors and malfunctions can occur in a variety of ways. For example, the batteries can go dead on the timer or the pen can become clogged. The beaded cable occasionally comes off the drum from lack of maintenance or from rapid water-level changes. Replacement floats can be jury-rigged with a plastic 1- or 2-L soda bottle weighted by sand, if one cannot find a replacement float in a timely way. The chart recorder is being phased out and replaced by enhanced telemetry systems or well sentinels, but was included for those still using them.

Enhanced telemetry systems. When monitoring conditions change rapidly, wells are located in remote sites, or require real-time data, enhanced telemetry systems (ETS) may be a cost-effective way to go. These systems provide wireless signal technology, which provides greater control over the data, and has the benefit of reducing the number of site visits (travel and man-power costs reduced). The basic layout was shown in Figure 5.15.

Telemetry options include very-high and ultra-high frequency (VHF/UHF) radio, cell-phone modem, license free spectrum radio, or telephone-line modem, while power options include either 100–240 VAC line power or solar-charged battery power (In-Situ Inc., 2005). Distance capabilities for wireless technology is expanding rapidly and is now (2007) becoming a viable option. The technology is changing so quickly that a cost analysis to implement such a system to offset rising travel costs is worth looking into.

Transducers and data loggers. Transducers are pressure-sensitive devices that "sense" the amount of water above them. The "sensing" is performed by a strain gauge located near the end of the transducer, which measures the water pressure. The water pressure can be converted into feet of head above the strain gauge by Equation 5.9, repeated here for convenience as Equation 5.15:

$$1 \text{ psi} = 2.31 \text{ ft of } H_2O \tag{5.15}$$

The above relationship is important in knowing the maximum pressure or how deep the transducer can be placed below the static water surface. Typical ranges of pressure transducers are 5, 10, 15, 20, 30, 50, 100, 200, 300, and 400 psi. For example, a 10-psi transducer should not be placed more than 23 ft below the static water surface. If it is, the transducer may become damaged. Another problem may occur when the

data logger will not record any meaningful data. Personal experience indicates that the data logger will give level readings of zero. Transducers of 400 psi have been used in deep mine shafts to gauge recovering water levels.

During a pumping test, one should estimate the range of water-level changes that will take place during a test. The pumping well is usually equipped with the highest range followed by lower water-level ranges for observation wells located at various distances away. If the transducer is to be placed in an observation well, it is a good idea to lower the transducer to an appropriate depth and let it hang and straighten out before defining the initial level measurement. A common error is to forget to establish the base level in each well as a last setting in the data logger before the beginning of the test. If this is done immediately as the transducer is placed into the well, especially with the placement of the pump and riser pipe, the water levels may not have equilibrated. It is also a good idea to select a base level other than zero. Fluctuations of the water level may occur above the initial base reading, resulting in negative numbers for drawdown. This can be problematic when trying to plot the data in a log cycle. Placement of the transducer in the pumping well should be just above the top of the pump. The transducer should be secured with electricians tape, with additional tape being placed approximately every 5 ft (1.5 m) as the pump and riser pipe are being lowered into the well (Figure 5.27).

Data loggers record level-measurement readings from pressure transducers and store these values into memory. The stored data can be retrieved for analysis. Transducers and data loggers are indispensable equipment for taking rapid succession readings from multiple wells during a pumping test or a slug test. Loggers can record data in log-cycle mode, which allows hundreds of readings within the first few seconds of turning the pump on or during the initial recovery phase. Data loggers can also record data on a linear time scale determined by the user. In this way, a data logger is similar to a chart recorder; however, the information stored is already in digital format and does not need to be corrected or reduced (Figure 5.28).

Care must be taken in the field to make sure pressure transducers are connected to the data loggers. Sometimes, even though a proper connection is made, the cable line from the transducer to the data logger may be kinked or damaged, thus prohibiting accurate data collection. Most cables have a hollow tube that allows the strain gauge to sense changes in air pressure. The typical field procedure is to make a loop greater than 1 in (2.5 cm) with duct tape and attach this to the well casing, also with duct tape. The duct-tape loop may slip in hot weather, so a dowel or similar object can be placed to prevent kinking. The cable can be protected in heavy traffic areas by placing boards on the ground,

Figure 5.27 John D lowering a1-hp pump down a 4-in (10.2 cm) production well. The pressure transducer is attached with electrician's tape above the pump on the riser pipe.

with the cable located between the boards. Most field technicians are encouraged to obtain manual backup readings to the data-logger readings using E-tapes in case the automatic system fails.

Well sentinels. Well sentinels can be placed into wells to record data over a long time period similar to chart recorders. For example, In Situ Inc. has one called the Troll or mini-Troll. Solinst Inc. has one called the Levellogger (Figure 5.29) and Schlumburger has one called the Diver. They are stainless-steel, titanium, or ceramic probelike devices with their own built-in pressure transducers and data loggers. These can be programmed directly via communications software loaded on a personal computer. To overcome issues of barometric changes most manufacturers also recommend using a barometric data logger (Barologger) in concert with a well sentinel. This allows for level corrections from barometric

Figure 5.28 Data loggers in use in a field setting.

Figure 5.29 A small-diameter well sentinel that measures level and temperature.

changes. Well sentinels can also be equipped with a variety of water-quality probes in addition to a pressure transducer (level measurement). Measurements of specific conductance, pH, dissolved oxygen, and temperature are popular options. These can be very helpful in monitoring changes in water quality over time. For example, during a pumping test, changes in water quality may indicate helpful information that aids in interpretation. A case example occurred during a pumping test in mining impacted waters near Butte, Montana. A steady-state head condition was being approached during the test. It was clear to see that a recharge source was contributing cleaner water to the pumping well, indicated by a higher pH and lower specific conductance, possibly from a nearby stream or from a gravel channel connected to a nearby stream. The water-quality data nicely augmented the interpretation of the pumping test.

Practical design of level-measurement devices

Based upon the above discussion there are some practical considerations one should be aware of when purchasing level-measurement devices. This section will go into more detail on the designs of probes, cables and battery placement. Most of these have implications for the popular manual E-tapes, although other methods will be addressed.

Probe design. The purpose of the probe is to detect the static water level. Some detection sensors are near the middle, while others are located near the bottom of the probe (Figure 5.30). With an E-tape, when the

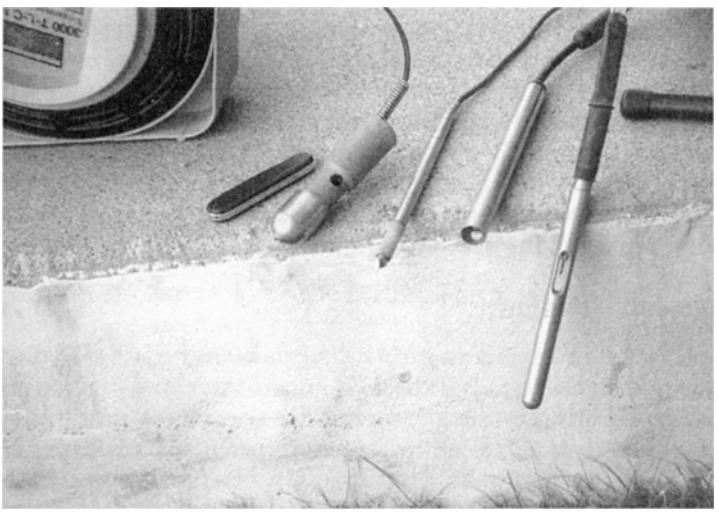

Figure 5.30 Probe sensors.

static water surface is encountered, an electrical circuit is completed, which activates a light or audible buzzer. Both are desirable. The sensor may be made of copper or some other metal; probes are mostly made of stainless steel. The sensor may be accessible on the outside of the probe, or through a hole in the probe with the sensor in the middle, or, the bottom inside of the probe. In the latter case, the bottom part is somewhat hollow, like a bell housing, with a wire sensor extending across the hollow section. In the case of a transducer, the size needed depends on the application. Several are in the 5/8-in (1.6-cm), although 3/8 in (0.95 cm) or 5/16 in (0.79 cm) are made by most manufacturers. These are suitable for use in 1-in piezometers, but if mini piezometers (Chapter 6) of smaller diameter are being measured, significant displacement can occur. This is also one reason for having the sensor at the bottom of the probe.

It was mentioned that sometimes false readings are made when the E-tape probe scrapes off moisture down the side of the casing. Condensation is especially problematic in hot weather or very cold weather. The hole in the middle and bell-like probe housing with the sensor near the bottom is designed to avoid this problem. Whether this is a problem depends on the application. For monitoring wells, probe diameter is not a problem down to a well diameter of about 1 in (2.5 cm); however, for mini-piezometers or well plates with small access ports, probe diameters may be too large. The shape of older probes tends to be more cylindrical and blocky, sometimes with abrupt edges that provide places for them to become hung up on protrusions in the well, like centralizers, or wiring in pumping wells. Newer designs have probes that are more sleek and tapered and have depth capabilities.

Smaller well probes, usually equipped with an outside sensor, tend to be tapered and have smaller diameters. The minimum size is down to 1/4 in (6.4 mm), which easily allows measurement in a 1/2-in (1.3-cm) mini-piezometer or access through a port in the top of a well plate. These can be very effective for shallow wells with depth capacities usually less than 100 ft (30.4 m). Another example of this kind of design is by Slope Indicator, which has a 5/16-in (8-mm) probe with depth capacity up to 700 ft (213 m).

Sometimes you may wish to get a water level in a production well that does not have convenient access. In this instance, instead of having a ridgid probe, a string of brass or stainless-steel beads covers the water-level sensor (This design is carried by drillers more than anyone else). These devices will snake through a difficult access port better than anything else. They are marked every foot (30.5 cm) or every 5 ft (1.5 m), with a brass plate located on the cable for each marking. Once again, these may give false readings from scraping along the casing.

Electronic cable design. Another variation in level-measuring devices is in the cable and reel design. E-tapes have a crank handle that allows the cable to spool onto a reel. Some are freestanding, while others require the person to handle the whole thing to maneuver it. Some manufacturers provide both capabilities, with the freestanding design requiring an extra charge. Having some kind of freestanding capability is desirable for taking repeated measurements and wanting to set the device down in between readings. This helps keep the reel, probe, and cable cleaner. Another useful design is a simple braking stop that keeps the reel from turning when it is helpful to "hold" a position. This is usually a plastic or rubber stop that can be twisted in or out or a lever arm that is moved half of a rotation or so to keep the reel from turning.

Some reels and spooling designs have too small a housing for the cable. When the probe is fully reeled in, some of the wraps may slip off, creating a tangled mess. Whenever too much cable is placed on too small a reel, there will be problems. Another aspect of level-measuring devices is the cable design itself. Electronic cables come in a flat, tapelike design, or round, or variations in between. Most of the tape designs have the electronics fully encapsulated in an unbreakable ultra-violet radiation-resistant plastic, with two reinforcing wires or thin metal cables that pass through the outer edges for added strength and resistence to cable stretch. This is a good idea. Markings occur on both sides in hundredths of a foot and fractions of a meter. A drawback to this cable design is in the spooling on the reel. The tapelike design allows easier slippage on the reel. Newer models allow for replacement lines in the field.

Round electronic cable designs are also marked to 1/100th ft (3 mm) but have no capability for having metric markings without another separate E-tape. The choice is either in feet or meters, not both. The round electronic cable has a reinforced mesh design around the transmitting signal wire for strength. Round cables tend to not slip like the flat tapelike cables do, but one worries more about cable stretch with round-cable measurements, especially in measurements that are deep.

Other errors in level measurements. Another aspect of any measurement is whether the kinks and bends in the electronic cable lead to inaccurate readings. This can also be argued with steel tapes too. Generally, as one uses the same device for each measurement, the results tend to be consistent. If minor changes occur in the data that are significant to a project, one should investigate whether there was a change in field technicians or equipment or both.

Other discrepancies could be the result of improper reading of the measuring device. There are fewer errors associated with taking readings from E-tapes marked every 1/100th ft (3 mm) than with those marked every 1 ft (30.5 cm) or every 5 ft (1.5 m). Typically errors amount

to reading a 6 or a 9 upside down. In tapes where markings are more widely spaced, readings are referenced either from the next mark above or the one below. This is done with a retractable 10 ft (3 m) tape marked every 1/100th ft (3 mm). For example, if the water level is at 18.00 ft (5.48 m), the distance from the thumbnail to the next marking would be either 3 ft (0.91 m) from the 15-ft (4.57 m) mark or 2 ft (0.61 m) subtracted from the 20-ft (6.09-m) mark. The field technician would essentially think "15 plus 3 ft or 20 minus 2 ft." If one is always consistent at reading from the marking below or above, it is easier to detect errors later on. If one arbitrarily changes how to follow protocol in the field, serious interpretation problems may result. For example, in a high-transmissivity aquifer, 1/10th ft (0.03 m) can make a big difference in interpreting the direction or rate of groundwater flow.

Battery location. As obvious as it sounds, the location where batteries are housed can be a big factor on level-measurement device maintenance. Some new models and many earlier models required that all of the cable be unreeled before having access to the battery compartment. Some allow the reel housing to become separated to allow access to the batteries. A good design is where the batteries are quickly accessible through a plate cover on the reel housing (Figure 5.31). This is a simple remove-the-plate and change-the-batteries scenario. When purchasing a level-measuring device, accessibility and easy maintenance can be a

Figure 5.31 Students replacing batteries on the reel housing.

deciding factor if all other features are the same. Most level-measuring devices are powered with a 9-V battery.

Level-measuring devices also have a battery or light tester button. One merely presses a button and the light or buzzer or both go off. Some allow the user to choose whether they want to have the light active or the buzzer active and can test each separately. If the buzzer signal or light is weak, it is a good idea to replace the batteries. Having extra batteries on hand is always a good idea. The multitool is helpful for removing a few screws, should changes of batteries be required.

Other practical applications

Some of the problems associated with level measurements come from well completion rather than device design. For example, pumping wells arranged with spacers and centralizers are more likely to encounter a hang-up of the equipment than a monitoring well dedicated only to water-level measurements. Once a level-measurement device becomes stuck, how can it be retrieved from the well? Should E-tapes be used to sound the depth of wells? Additionally, what should be done about decontamination of equipment before it is lowered into other wells? What do you do if the well is flowing? How do you obtain a measurement on a flowing well?

Retrieving lost equipment. When pumping wells are being used to obtain level-measurement readings, there is always a risk of getting the equipment stuck. This may be during a pumping test, where an operator is trying to follow the pumping level in a well, with an E-tape or simply trying to obtain a level measurement from a domestic well. Extending upward from the top of the pump is the riser pipe and electrical lines to power the motor (Figure 5.32). If the pump is fairly deep, plastic centralizers are placed to keep the riser pipe and wiring near the middle of the casing.

In cold climates, pitless adapters are used to make a connection from a waterline pipe placed in a trench from the house to the well (Figure 5.33). An access port is welded to the casing, approximately 6 to 8 ft below the ground surface to prevent freezing of waterlines. An elbow connector from the riser pipe fits into the **pitless adapter**. This way the riser pipe elbow can be removed from the pitless adapter and the pump can be pulled from the well for servicing.

It is amazing how a level-measuring probe can become stuck down a well. When probes become lodged, it is usually because the probe has wound around the riser pipe and electrical lines. Sometimes the probe will slip through the electrical lines and become wedged as it is being retrieved or hung up on a pitless adapter. Some well owners will have a rope or

Figure 5.32 Pump with riser pipe, being tightened with aluminum wrenches.

cable attached to the pump, that extends up to the surface for pump retrieval. If an E-tape probe threads through a gap between the cable and another obstruction, it will become stuck. There are other cases where the probe actually forms a slipknot during the process of obtaining a level measurement. The electronic cable line loops outward as an obstruction is encountered, and the probe ends up falling back through the loop.

When an E-tape becomes stuck, the first task is to try and free the probe. Depending on how far down the probe is, one can try different methods. Sometimes success occurs from loosening the electronic cable and striving to jiggle the probe free. If this doesn't work and the probe is within 20 ft (6.1 m), a "fishing" device can be made from one or more sections of 1-in PVC electrical conduit pipe, typically 10 ft (3 m) long. In the bottom piece, a slit or long notch about 6 in (15.2 cm) long is cut.

Figure 5.33 Trenching from well to building below frost depth to allow a pitless adaptor to be connected to the riser pipe below the ground surface.

The level-measuring cable is hooked into the notch. By sliding the conduit pipe toward the probe, there is more leverage available to move the probe around. In the event the well probe really becomes stuck, it may be necessary to pull the pump and riser pipe to retrieve the E-tape. This can be a real pain, particularly in a production well that has a lot of heavy piping. If you want to save the E-tape, it is cost-effective to call in a service truck with a cable-and-hoist capability to pull up the piping and pump. The cost of service is a minor percentage of the cost of a new E-tape.

Sometimes if someone pulls really hard on an electronic cable, the line breaks and the cable and probe fall down the well. In this case, after one pulls out the pump and riser pipe it is possible to "fish out" the offending object with a treble hook attached to 30- to 50-lb test monofilament fishing line. Treble hooks may be helpful in hooking onto things that unwittingly fall down a well.

Untangling equipment. When an E-tape cable lines slip off of a reel, a tangled mess can occur. Rather than trying to fight the reel, it is worthwhile

to unspool the reel by having someone walk the probe and cable out until the problem area is resolved. Sometimes untangling becomes akin to untangling kite strings or fishing lines. Time and patience can be well worth the effort.

In some cases the electronic cable line may become damaged. It is possible to reattach the probe to a convenient marking on the cable (such as at 100 ft). In this case the repaired device can be used as a backup E-tape. Most manufacturers also have replacement cables. One must compare the economics of purchasing a new probe over the time and effort to repair or replace a new electronic cable line.

Decontaminating equipment. As an operator performs a level-measurement survey of a series of monitoring wells, it is important to decontaminate, or DECON, the equipment. Merely going from one well to the next with the same device may cause cross-contamination. DECON practices vary from company to company. Something as simple as rinsing with an Alconox-water solution rubbed with a brush to steam cleaning (Figure 5.34) or a submergence bath may be required. A small amount of Woolite into a bucket of water makes a great DECON solution. It depends on the nature of the site. If the monitoring is for trends in water levels, a simpler DECON step would be taken, compared to monitoring wells completed in a plume of toxic organics. For water-quality sampling it may be better to use dedicated bailers tied onto and then left inside each well.

Newer level-measuring devices are designed to have the electronic reel built as a module that can be removed for DECON purposes or the

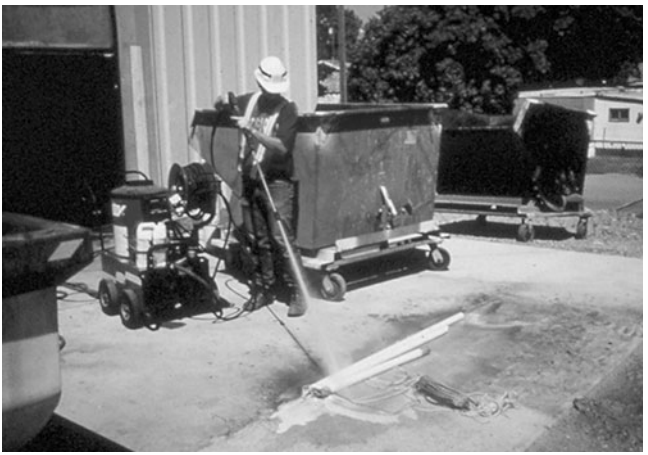

Figure 5.34 Worker decontaminating slug-testing equipment with a steam cleaner.

electronics are encased in an epoxy coating for easier decontamination. It is significant to realize that certain chemicals may adsorb onto probes (Fetter 1993). Most probes are constructed of stainless steel because this tends to be less reactive than other materials, except in mining-impacted waters where pHs are low and dissolved metals are high. It is also helpful to have clean-looking equipment when you go knock on a landowner's door.

Level measurements in flowing wells. When a well is drilled into a confined aquifer whose recharge area is sufficiently high, the pressure head at the well head may be sufficiently high to result in artesian flow. The volume of flow at the surface is a function of hydraulic head and the casing diameter. Predicting the actual rate of flow at the surface is difficult to do, even if the shut-in pressure is known. From field observations two wells with identical total hydraulic heads but different casing diameters will flow differently at the surface as a function of casing diameter. For example, a 4-in ID well with a shut-in pressure of 5 psi (11.6 ft of head) may flow at 5 gpm (1.26 L/s), while a 2-in ID well nearby, also with shut pressure of 5 psi (11.6 ft of head), flows at 5 gpm (0.32 L/s). If enough stand pipe is added to each well the result is that each has the exact same static water level. A reduction of casing diameter at the surface results in a reduction in the rate of flow.

Flowing artesian wells can be capped and equipped with a pressure gauge so the pressure head at the cap can be read directly (Figure 5.35). In this case the elevation of the cap would be surveyed and the pressure gauge reading converted into feet of head and added to the elevation head. If the pressure head is less than 5 psi (11.6 ft of head) then a well can be fitted with a standpipe sufficiently high to keep the well from flowing and direct level-measurements made. During a pumping test if the pressure head is too great, sometimes a pressure transducer can be plumbed directly into the well casing where the head reading is recorded on a data logger. A section on running pumping tests on flowing wells is given in Chapter 10.

Example 5.10 In Petroleum County, Montana, several wells have been drilled into several confined aquifers, such as the Cretaceous Basal Eagle Sandstone, and the 1st, 2nd, and 3rd Cat Creek (Brayton 1998). These wells had been flowing for decades until a rehabilitation program took place to control free-flowing wells. Some of the wells were controlled by installing flow reducers, while others were redrilled and completed with new casing and insulation and located below the frost zone to keep from splitting from freezing (Figure 5.36). This resulted in saving millions of gallons of water and the recovery of water levels on the order of 5 ft in just 1 year (Brayton 1998; Weight et al. 1999).

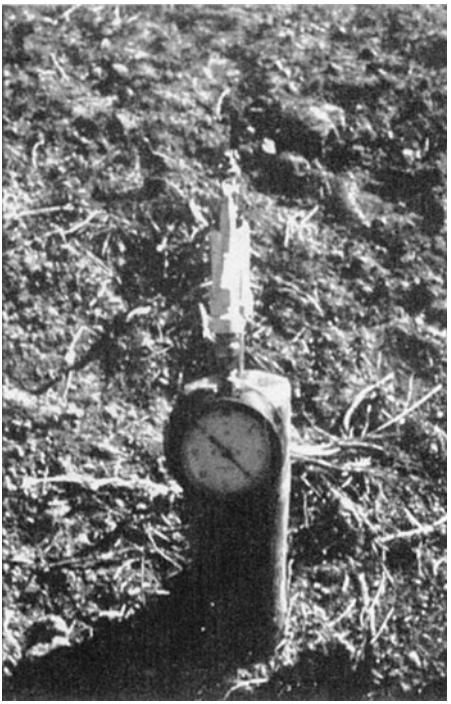

Figure 5.35 Well cap pressure gauge.

Summary of level-measurement methods

Level-measurement devices are necessary to obtain static-water-level data. Each has its own application and design. Generally, it may be helpful to have a variety of designs and depth capabilities.

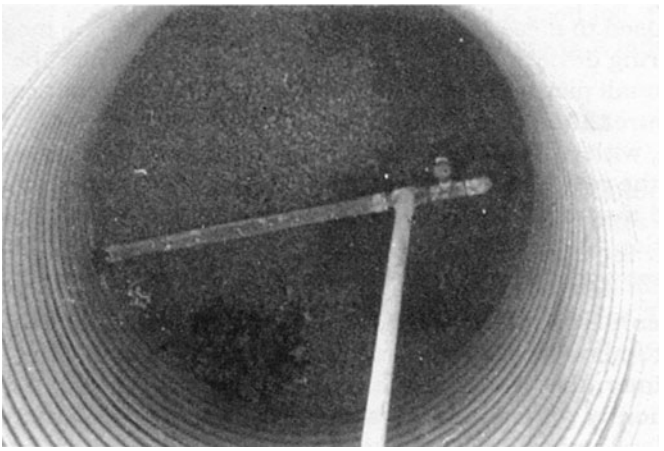

Figure 5.36 Well Installed below frost zone.

Summary of manual methods

1. Establish a common datum. It may be worth defining a particular elevation above MSL so that maps of different scales can be constructed later on.
2. Make sure that the base station is a relatively permanent feature, unlikely to be moved or removed later on.
3. Don't forget your keys, wrenches, and multitool to remove the well cap.
4. Establish a measuring point (MP) physically on the well casing or the location from which all water-level measurements will take place.
5. To prohibit effects from weathering, make all markings on the inside of the well or under the well cap.
6. Use a carpenter's chalk with a steel tape for a clearer reading.
7. E-tapes should have their sensitivity dials adjusted as appropriate to the water quality to get a crisp, clear buzz or light indication.
8. Always move the E-tape cable line to the middle of the well, shake lightly, and repeat, to make sure the reading is the same.
9. Record the depth to water from TOC or GS. The "stick up" should also be measured and recorded. Remember to put the well cap back on after the reading and secure the well.
10. Do not use your E-tape to sound well depths.
11. Make sure your field notes are clear, because getting back to some wells again may be difficult.

If wells are locked or inside locked gates, one must remember the appropriate keys or tools necessary to gain access. Multitools are handy to remove tightened bolts and loosen wedged well caps. Steel tapes are helpful to gain access to small openings in well caps and can be used to measure field distances. E-tapes are the most common level-measuring device and come in a range of designs. Probe size is important for small piezometers and pumping wells, and proper care must be taken to ensure the readings are accurate. Flat electronic cable designs are easy to read, with English and metric markings, and resist stretching, but may slip on the reel. Round cable designs do not slip but have markings on one side and may stretch on deeper readings. Other design features, such as the location of the battery housing and maintenance capabilities, may be important for choosing from among devices.

Chart recorders have been helpful in monitoring continuous hydrograph data in the past. Chart recorders are being replaced by enhanced

telemetry systems (ETS) or a network of well sentinels. Phone jacks have provided the greatest distances for sending information from EHS, but "wireless" technologies are expanding the possibilities for flexibility and speed. EHS are the way to go for obtaining "real-time" data, while well sentinels can be uploaded at the end of a season.

Pressure transducers and data loggers are indispensable for rapid succession readings needed during pumping and slug tests. These are more expensive, but are easier to manipulate during the data reduction and analysis stage. Pressure transducers may be helpful in obtaining levels on flowing wells.

Summary of automated methods

1. Lower each transducer down the well to allow the cable to straighten and then spool each transducer cable to the data logger. Allow a 1-in loop in the cable (to sense air-pressure changes), secured with duct tape and then taped to the well so that it doesn't move. Place a dowel in the loop.
2. Check the psi range of the transducer or well sentinel and make sure it isn't lowered into a water depth that exceeds its capacity.
3. Attach the transducer in the pumping well above the pump with electricians tape and secure the cable to the riser pipe every 5 ft (1.5 m) to the surface.
4. Make sure each transducer is connected to the data logger. (This can be checked from the data logger).
5. Establish the base level as a last item before starting the pumping test and use a value other than zero.
6. Back up the automated system with manual E-tape level measurements.

Getting level-measurement devices stuck down a well is a real possibility in pumping wells. Fishing techniques may be used as a first step, but it may be necessary to call a service rig to free an E-tape probe. This would only be a percentage of the cost of a new probe. Decontamination of level-measuring devices is essential to prevent cross-contamination. Simple rinsing or brushing using an Alconox-water solution or steam cleaning can do a good job. Having clean equipment is important when showing up at the door of a landowner.

5.4 Misinterpretation of Water-Level Data

The misinterpretation of water-level data is a relatively common occurrence among those just getting started in field hydrogeology. It takes time and experience to think through certain questions to put together

a reasonable conceptual flow model. Some of the following reasons for making errors in interpreting water-level data can be grouped as topics. The following list is by no means exhaustive, but will hopefully get the hydrogeologist thinking.

- Vertical component of flow
- Misunderstanding the difference between water levels in wells and the elevation of the water table
- Combining shallow and deep wells completed in the same aquifer
- Combining long and short screen lengths for wells completed in the same aquifer
- Combining level data for wells completed in different aquifers
- Combining level data from different times, seasons, or completion dates.

Shallow and deep wells

The first three topics can be essentially discussed together. Even if the geology of an area is fairly uniform, there is usually a vertical component to flow emanating from recharge to discharge areas (see Figure 5.10). The flow path of water particles is generally rectilinear (Wampler 1998). This means that very few water particles actually move along the top surface of the water table; rather they take a rectilinear path among local, intermediate, or regional flow systems. The development of the different systems is a function of the dimensions of the basin. Deeper basins tend to have a greater variety of systems developed (Fetter 1994). In humid areas where there is a fairly constant source of precipitation recharge, increased topography also affects the local flow regime. For example, more undulations in the surface topography result in greater numbers of local recharge and discharge areas (Fetter 1994). This must be taken into account when deciding on the depth and placement of wells. It also will affect one's interpretation of water-level data. For example, it may mean that wells completed at different depths may be screened within different parts of a local or intermediate system.

When one combines level measurement data from wells completed shallow and deep an improper interpretation of groundwater flow may result (Saines 1981). The question arises, how deep must the well completions be before they represent a different flow system? Can I use level measurement data from 30 ft (9.1 m) wells, 100 ft (30.5 m) wells, and 300 ft (91.4 m) wells and still be in the same groundwater-flow system? The answer is complicated by the proximity of wells to recharge or discharge areas, variable screen lengths, the hydrostratigraphy (Chapter 3), and physical dimensions of the valley. Rather than drilling

more wells sometimes the number of wells needed can be reduced by incorporating water-quality data. It may be that water-quality signatures are typical of certain flow systems. The following three examples will help illustrate the above issues.

Example 5.11 A study was conducted along Blacktail Creek in Butte, Montana, to investigate why local residents were experiencing basement flooding (Figure 5.37). The Geology in the immediate vicinity of Blacktail Creek consists of fine-grained sediment lenses mixed with sandy units. The sandy units appear to be laterally connected, with the fine-grained sediments generally constrained within the flood plain area of the creek. Nested wells completed at depths of 15 and 30 ft, respectively, within 100 ft (30.5 m) of the Creek showed water-level differences of 1 ft (0.3 m) between wells. Deeper wells indicated a water level approximately 1 ft (0.3 m) higher than shallow wells, indicating an upward gradient. Differences between nested pairs indicated that if all data were combined, a confused interpretation would result.

The question exists whether all groundwater within the residential area comes from more than one flow system. Water-quality samples from the area indicate the possibility that waters from mining-impacted areas may be influencing waters discharging into the area. A schematic of this interpretation is presented in Figure 5.38.

Example 5.12 Butte, Montana, is nestled in a valley surrounded by mountains including those of the North American continental divide. Like many intermontane basins of southwestern Montana, the basement rocks of the valley are structurally tilted to the east, resulting in thicker deposits on this side. In this case, the eastern sediments are approximately 900-ft thick and only about 100- to 200-ft thick on the western margin. Sediments are generally coarse grained, with lessor discontinuous clay lenses that locally have a confining

Figure 5.37 Well drilling along Blacktail Creek, Butte, Montana.

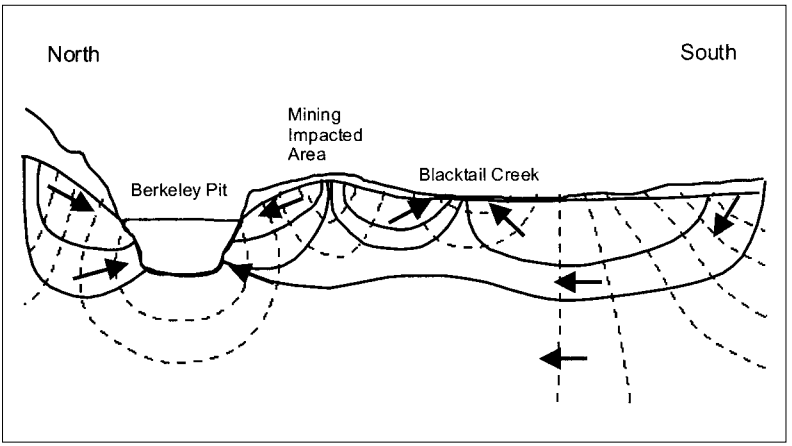

Figure 5.38 Schematic of Example 5.8 interpretation.

affect. The valley slopes to the north in a gradual gradient as does groundwater flow. Shallow wells that penetrate to "first" water indicate a gradient of 15 ft/mi (or 0.003) (Botz 1969).

Two of the local drainages, Little Basin Creek and Blacktail Creek, initiate their headwaters in the Highland mountains to the south and flow northward into the Butte valley. The streams are bedrock controlled as they flow out onto the weathered granitic valley-fill materials, losing most of their water, which results in basin recharge. Deep circulation occurs in the valley, and stream flow picks up again as groundwater begins to discharge to the north. Wells completed near the discharge area to the north at depths of 120 ft (36.5 m) and 35 ft (10.7 m), respectively, show differences of 2 ft (0.61 m) between wells with an upward gradient, while nested wells in other parts of the valley show equal water-level elevations and in the recharge area there is a downward component of flow. This essentially is the scenario depicted in Figure 5.10.

Example 5.13 A watershed committee in Dillon Montana was concerned about the drilling of new production wells during a period of extended drought. They wanted to know what the impacts of new production wells would have on the Beaverhead River (Figure 5.39). The Quaternary fluvial deposits and anastamosing sloughs associated with the floodplain of the Beaverhead River are approximately 3 mi (5 km) wide in the study area. Flanked on both sides of the floodplain to the east and to the west are Tertiary sediments that extend to the surrounding mountains. Additionally on the west side, to the north, are Tertiary volcanics from which irrigation-well production may exceed 1000 gpm (63 L/s). Precipitation recharge is augmented by leakage from a distribution of canals originally sourced from the Beaverhead River many miles upstream. The general groundwater-flow system originates from the mountains and flows toward the floodplain of the Beaverhead River.

Figure 5.39 View of Albers Slough and the Beaverhead River floodplain taken from the Tertiary bench on the west side looking east.

The budget for this project was very low, so new drilling was out of the question. To better understand the groundwater-flow system(s) a network of more than 40 wells, mostly from stock and domestic sources, were permitted to be measured on a bimonthly basis over a period of 2 years (Weight and Snyder 2006). Well depths ranged from approximately 30 ft (10 m) to several hundred feet (>100 m). Hydrographs of the level measurement data were created coupled with a study of stream flow and precipitation data. Survey grade GPS elevations were determined for each of the monitoring well and river measuring points. The following observations were determined from the level measurement data:

- Level measurement data within the floodplain correlated well with stage elevations of the Beaverhead River indicating the floodplain is well connected with the river.
- Level data from wells less than 100 feet (30 m) on the west side appear to be influenced by recharge from surface-water irrigation return flows.
- A 50 to 100 ft (15 to 30 m) thick clay layer on the west side separates the shallower level elevation data (wells completed less than 100 ft, 30 m) from “deep” wells completed greater than several hundred feet (>100 m).

The shallower wells have an average elevation level 50 ft (15 m) higher than the deeper wells.

- The Tertiary volcanics also appear to be a source of recharge to the Tertiary sediments on the west side. They show an average level elevation 80 to 100 ft (24 to 30 m) higher than other west side wells.
- East side Tertiary sediments have a greater thickness, are coarser-grained, and have a higher average transmissivity than sediments on the west side.
- Level measurement data on the east side show a cyclical pattern in all well hydrographs, reflecting the influence of irrigation pumping and the timing of precipitation infiltration recharge from the nearby mountains.

Water-quality data indicated a clear distinction from Beaverhead River surface water sources and groundwater irrigation return-flows. Specific conductivity reading and pH data for surface water was higher than for groundwater, while groundwater temperatures were typically lower than surface water.

Short versus long screen lengths

Another source of interpretation errors may come from wells completed with varying lengths of screen. It may be that wells at a site designed to monitor free product of a light nonaqueous phase liquid (LNAPL), such as gasoline, also have wells completed deeper to monitor cleaner water at depth, all within the same aquifer. Are all of the water levels telling the same story? It may be helpful to evaluate what the water level in a well indicates.

The level measurements in a well represent the average head at the mid-point of the screened interval, including elevation and pressure head. The longer the screen length, the more vertical head changes that may be included in the average. Piezometers are distinguished from wells by having a relatively short length of screen (less than 1 ft or 0.3 m). The purpose of piezometers is to obtain hydraulic head data from a point. They are especially useful in distinguishing the vertical distribution of hydraulic head. Sometimes at a given site there are a combination of well completions, ranging from production wells with tens of feet of screen, to monitoring wells with shorter lengths of screen (5 ft or 1.5 m), to driven well points and piezometers with short screen lengths completed near the top of the aquifer (Chapter 6). The hydrogeologist needs to be careful in considering the geology, the hydrogeologic setting, and the well completion when coming up with a conceptual groundwater-flow model. This is particularly important if one is in a recharge or discharge area (Section 5.2).

A well completed to detect an LNAPL , such as the example described in Figure 5.11, tends to have long screen lengths extending above and below the water table. This is done to be able to monitor levels during seasons of high and low elevations. If the well is completed in a recharge or discharge area, the average head may be below or above the water table. Consider the schematic in Figure 5.40.

Combining different aquifers

A woman from a conservation district in eastern Montana called one day to say she had monthly water-level and water-quality data for 24 months. Could I please make some sense out of it and tell whether there were any water-quality trends? My first question to her was, could I please obtain a base map and well completion information, including lithologic logs? One must know how many aquifers and confining units may be involved before proper interpretation can be performed. Understanding this is crucial to interpreting the direction of groundwater flow and contaminant movement.

Example 5.14 A consulting engineer was estimating drilling costs based upon water-level data within a subdivision area of a couple of square miles (5.2 km^2). Within the area was a perched aquifer and a regional aquifer with wells completed in both (Figure 5.41). The engineer did not understand the geologic setting and averaged the well-completion depths for both aquifers to obtain an estimate for total drilling footage. This resulted in a poor estimate of total drilling costs and surprises in the field when drilling began.

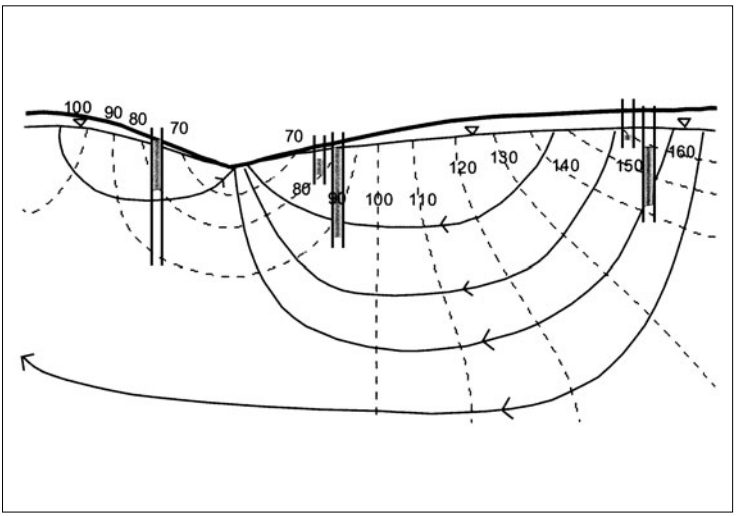

Figure 5.40 Water levels in a recharge area and discharge area, showing an average water level for a longer screen length shaded.

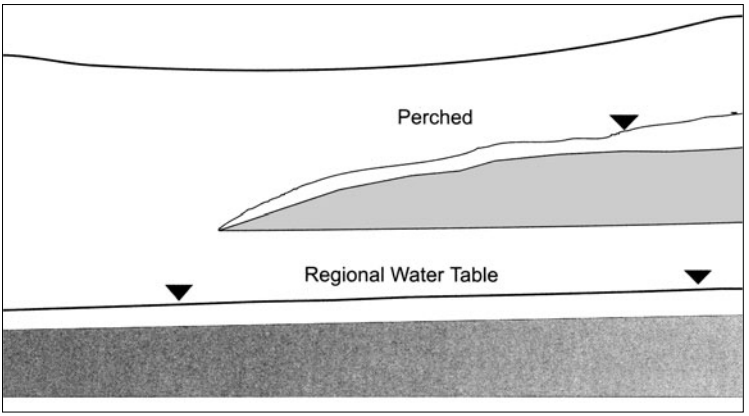

Figure 5.41 Schematic of perched and regional aquifers from Example 5.14.

5.5 Summary

Groundwater is generally always moving from higher to lower hydraulic head. The slope of the "head" surface or potentiometric surface of an aquifer is known as the hydraulic gradient. The total head at each location on the potentiometric surface is determined using components of the Bernoulli equation, where the velocity head term was shown to be negligible from most applications. The quantity of groundwater movement moving through a defined cross-sectional area is solved using applications of Darcy's law. Two-dimensional applications of Darcy's law can be performed by constructing flow nets. Recharge areas are defined where flow lines diverge from a given area and flow lines converge in groundwater discharge areas.

As groundwater encounters hydrogeologic units of differing hydraulic conductivity the flow lines refract or bend, thus changing the flow path. The flow path through finer-grained units tends to be somewhat vertical, while flow through coarse-grained units is more horizontal. Level measurements in wells define the potentiometric surface at a given location. The various principles and problems associated with taking level measurements were discussed along with the merits of each type of equipment. The point was made that each level measuring device has its own application.

There are many reasons groundwater-flow systems are poorly understood. The misinterpretation of level measurements was suggested as a key factor. Ignoring vertical flow, combining shallow and deeply completed wells, and combining wells with short and long well screens contribute to the difficulty of interpreting level-measurement data. Care must be taken to make sure the level-measurement data are from a known aquifer. Mixing level-measurement data from different aquifers leads to misinterpretations of groundwater flow and may cause a host of problems.

References

Botz, M.K., 1969. Hydrogeology of the Upper Silver Bow Creek Drainage Area, Montana. *Montana Bureau of Mines and Geology Bulletin* 75, 32 pp.

Brayton, M.D., 1998. *Recovery Response from Conservation Methods from Wells in the Basal Eagle Sandstone, Petroleum County, Montana*, Master's Thesis, Montana Tech of the University of Montana, 68 pp.

Davis, S.N., and Dewiest, R.J.M., 1966. *Hydrogeology*. John Wiley & Sons, New York, 463 pp.

Fetter, C.W., 1993. *Contaminant Hydrogeology*. Prentice-Hall, Upper Saddle River, NJ, 500 pp.

Fetter, C.W., 1994. *Applied Hydrogeology*, *3rd Edition*. Macmillan, New York, 691 pp.

Freeze, A., and Cherry, J., 1979. *Groundwater*. Prentice-Hall, Upper Saddle River, NJ, 604 pp.

Heath, R.C., and Trainer, F.W., 1981. *Introduction to Groundwater Hydrology* . Water Well Journal Publishing Company, Worthington, OH, 285 pp.

Hubbert, M.K., 1940. The Theory of Ground-water Motion. *Journal of Geology*, Vol. 48, pp.785–944.

McIlvride, W.A., and Rector, B.M., 1988. Comparison of Short- and Long-Screen Monitoring Wells in Alluvial Sediments. *Proceedings of the Second National Outdoor Action Conference on Aquifer Restoration, Ground Water Monitoring and Geophysical Methods*, Vol. 1, Las Vegas, NV, pp. 375–390.

Saines, M., 1981. Errors in Interpretation of Ground-Water Level Data. *Ground Water Monitoring and Remediation*, Spring Issue, pp. 56–61.

Toth, J.A., 1962. A Theory of Groundwater Motion in Small Drainage Basins in Central Alberta. *Journal of Geophysical Research*, Vol. 67, pp. 4375–4381.

Toth, J.A., 1963. A Theoretical Analysis of Groundwater Flow in Small Drainage Basins. *Journal of Geophysical Research*, Vol. 68, pp. 4795–4811.

Watson, Ian, and Burnett, A.D., 1993. *Hydrology: An Environmental Approach*. Buchanan Books, Cambridge, 702 pp.

Wampler, J.M., 1998. Misconceptions about Errors in Geoscience Textbooks, Problematic Descriptions of Ground-Water Movement. *Journal of Geoscience Education*, Vol. 46, pp.282–284.

Weight, W.D., Brayton, M.D., and Reiten, J., 1999. Recovery Response from Conservation Methods in Wells from the Basal Eagle Sandstone, Petroleum County, Montana. *1999 GSA Abstracts with Programs*, Vol. 31, No. 4, A60 pp.

Weight, W.D., 2004. Integrating Site Characterization Data into a Numerical System: a Case Study from Northern Montana. *Abstract in Proceedings of the 2004 North American Environmental Field Conference and Exposition*, Tampa, Fl. Nielson Environmental Field School .

Weight, W.D., and Snyder, D., 2006. Basin Analysis of Groundwater Changes in the Northern Dillon, Montana area. *Abstracts in Proceedings of the AWRA Montana Section Annual Meeting*, Polson, Montana.

Chapter

6

Groundwater/Surface-Water Interaction

Another topic a hydrogeologist must be familiar with is how groundwater and surface water interact within rivers and drainage systems. This was briefly addressed in Chapter 5 under gaining and losing streams and in more detail under the discussion of water-level interpretations (Section 5.4). However, in this chapter, an extended treatment of this topic is presented, including concepts of channel geometry and groundwater exchange, the hyporheic zone, and stream health (Meyer 1997; Winter et al. 1998; Woessner 2000; Hauer and Lamberti 2006).

Traditionally, hydrogeologists considered groundwater/surface-water interaction in terms of water rights and streamflow reduction by evaluating distance-drawdown relationships and pumping wells adjacent to streams (Walton 1970; Sophocleous et al. 1995; Modica 1998; Winter et al. 1998). Flowing streams are complex systems with intricate interactions with living organisms (Hansen 1975; Grimm and Fisher 1984; Dahm et al. 1998, Hauer and Resh (2006)), streamflow dynamics (Bencala and Walters 1983; Huggenberger et al. 1998; Newbury and Bates 2006), and groundwater discharge and recharge (Castro and Hornberger 1991, Gore 2006). Additionally, streams are situated within a fluvial plain that may be meandering or braided and may have stratigraphically complex relationships, including rapid changes in grain size distributions, facies, and vegetation distribution (Anderson 1989; Mial 1996; Gross and Small 1998). There is a need to perform fieldwork to better conceptualize groundwater/surface-water interaction within the fluvial plain and within active and non-active channels (Woessner 2000).

Some of the reasons for having a basic understanding of groundwater/surface-water interactions are to better understand groundwater flow in fluvial plains for water-resource management, watershed or catchment (Stanford 2006) assessment, watershed restoration, impacts to streamflows

Copyright © 2008, 2001 by The McGraw-Hill Companies, Inc. Click here for terms of use.

including water rights and minimum flows for riparian habitat. More work in the future will need to be performed as companies and regulatory agencies work together on preimpact assessments from mining, housing development, logging, construction, and postconstruction design. The purpose of this chapter is to discuss issues regarding groundwater/surface-water interactions and stream health, and present the basic principles the hydrogeologist will need to know to perform meaningful field studies.

6.1 Fluvial Plain

The **fluvial plain** represents the bigger picture of where fieldwork is performed. The fluvial plain is a fairly planar feature consisting of the active stream channel, flood plain, and associated fluvial sediments, which also include older sediments associated with previous stream positions (Woessner 2000). In intermontane basins, the fluvial plain is bounded by highlands or terraces on either side (Figure 6.1). The fluvial plain system as described by Woessner (2000) is also referred to as an alluvial valley or a riverine valley (Dahm et al. 1998; Winter et al. 1998). It is beyond the scope of this chapter to discuss the various shifting inter-habitats within the fluvial plain. For example, parafluvial habitats recently reworked by backfull flooding include the permanently connected channels and parafluvial zone with flood channels, islands, bars and levees, and springbrooks. Conversely fluvial habitats are

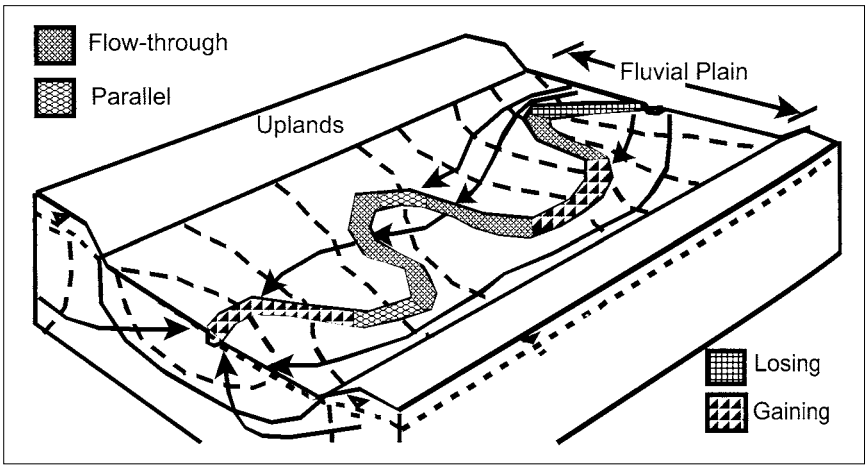

Figure 6.1 Block diagram of the fluvial plain. Isopotentials and water table are represented by dashed lines and groundwater movement by flow arrows; reaches are broken into losing, gaining, flow-through, and parallel stretches. [*Adapted from Woessner (2000). Used with permission of Groundwater (2000).*]

characterized by areas only reworked by big floods or ice jams that are frequently inundated and contain riparian vegetation (Stanford 2006).

Characterizing a fluvial plain is difficult, because of the many dynamic processes occurring. Each stream carries a quantity of sediment and flow volume proportional to the gradient of the stream. During spring runoff, stream velocities and flow volumes are great enough to incise certain meandering stretches and may overflow the banks depositing sediments onto the flood plain. The lateral continuity of sediments change rapidly over distances of tens of feet (meters to tens of meters). Geological models of these systems vary significantly as one evaluates the differences between meandering streams (Figure 6.2) with lower gradients to braided stream systems (Figure 6.3) with high sediment loads (Anderson 1989; Mial 1996; Gross and Small 1998; Huggenberger et al. 1998).

Example 6.1 A research site along Silver Bow Creek approximately 9 mi (14.5 km) west of Butte, Montana, was selected to evaluate the hydrogeology of a mining-impacted streamside tailings setting. A number of wells and piezometers were placed to evaluate groundwater flow, aquifer characteristics, geology, and water-quality distribution. Over the years, the students from the hydrogeology field camp have added more wells, so well density is quite high. Figures 6.4 and 6.5 show a plan view and cross-sectional view of sediments at the site.

One general result of the depositional processes within the fluvial plain is that units of higher hydraulic conductivity tend to follow the main axis of the valley, although they can migrate laterally during the meandering process (Winter et al. 1998; Woessner 1998). The trend of groundwater flow is down-plain with fluid transport mechanisms controlled by the higher hydraulic conductivity units (Woessner 2000).

Figure 6.2 Meandering stream in southwestern Montana.

Figure 6.3 Braided Sream north of Banff Canada.

Channel orientation and groundwater/surface-water exchange

There are at least four general flow scenarios associated with groundwater/surface-water in the fluvial plain: losing, gaining, flow-through, and parallel (Winter et al. 1998; Woessner 1998, 2000) (Figure 6.1 and Figure 6.6). (See also Figure 5.13.)

Streams where the head underneath and adjacent to the stream is greater than the stream stage, the stream gains water from the sediments within the fluvial plain (a groundwater discharge area, an

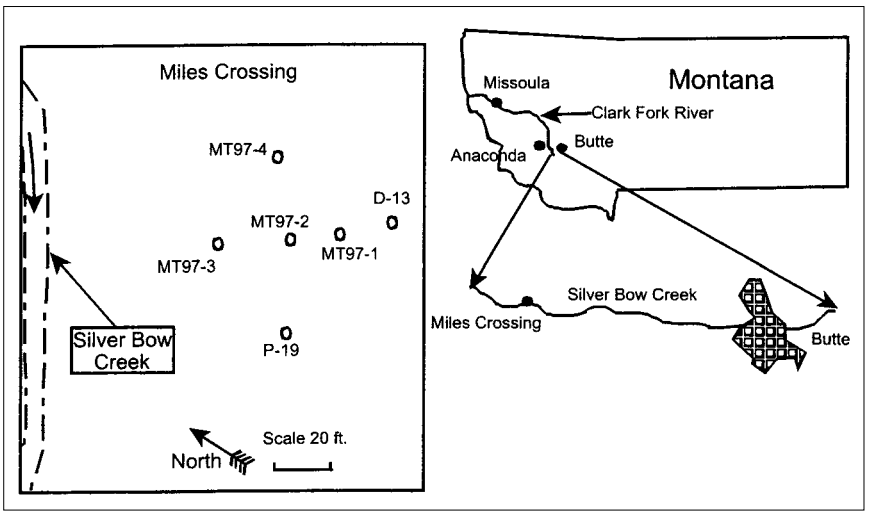

Figure 6.4 Location map for Miles Crossing, Montana, fluvial environment.

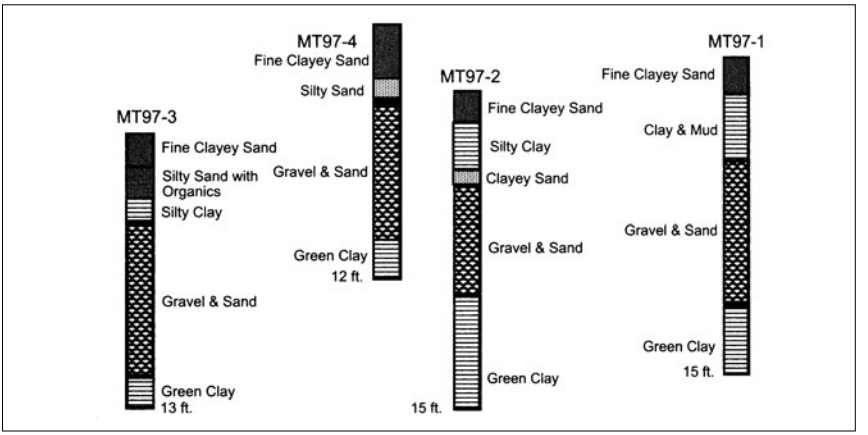

Figure 6.5 Cross-sectional view of lithologic changes in a fluvial environment near Miles Crossing, southwestern Montana.

upwelling zone) (Figure 6.6A). Conversely streams that lose water (provide recharge to the aquifer, a downwelling zone) have stages that are greater than the hydraulic head in the sediments underlying and adjacent the stream channel (Figure 6.6B).

In a flow-through scenario, the head on one side of the stream bank is higher than the head on the other side of the bank (Figure 6.6C). This often occurs when the stream meanders and becomes oriented perpendicular to the fluvial plain and general direction of groundwater flow (Huggenberger et al. 1998; Woessner 1998). When the stream stage and

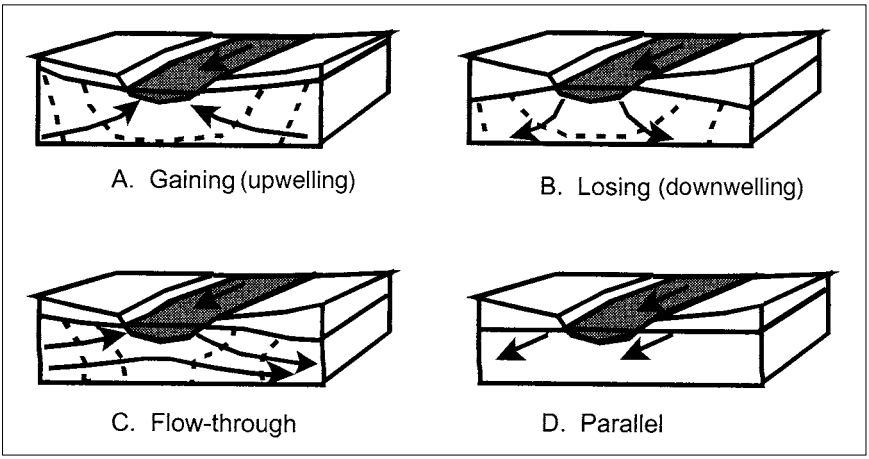

Figure 6.6 General flow scenarios associated with groundwater/surface water in the fluvial plain. [*Adapted from Woessner (2000). Used with permission of Groundwater 2000.*]

hydraulic head in the adjacent sediments are equal, then parallel flow or "zero exchange" occurs (Figure 6.6D)(Woessner 1998). In this last case, the stream flow and groundwater flow are parallel to each other, although some minor exchanges may be occurring at the streambed scale (Woessner 2000).

Channels can take on a variety of shapes, configurations, and time of flow factors. Again, it is beyond the scope of this chapter to discuss streams that are braided versus anastomosing or meandering and their respective hydrogeologic interactions, but by mentioning these and presenting the general concepts of the fluvial plain an increased awareness of the issues will occur. The discussion is also limited to perennial systems where riparian habitat is present with active hyporheic zones. More work needs to be done on intermittent systems that flow part of the year and develop some of the dynamics mentioned. Ephemeral streams represent channels where flow occurs only from snow melt or precipitation runoff. Most of these are losing streams.

6.2 Hyporheic Zone

Surface water and groundwater are considered by hydrogeologists as a single system, since interaction occurs along the total stream length where hydraulic connection with shallow groundwater occurs (Winter et al. 1998; Woessner 2000). This is indicated by the covariation of hydrographs of stream stage and shallow groundwater wells (Stanford and Ward 1993). Although covariation responses can be tracked, this does not necessarily mean that mixing is taking place. Combining the perspectives of stream and riparian ecologists, biologists, geochemists, and hydrogeologists, the **hyporheic zone** can be viewed as the mixing zone of stream water and groundwater (Stanford and Ward 1988; Triska et al. 1989; Winter et al. 1998; Woessner 2000, Dahm et al. 2006).

Groundwater discharge areas and influxes along meanders from parallel flow in the longitudinal direction may serve as higher nutrient exchange sites that enhance algal growth, the base food web used for any stream system (Dahm et al. 1998, Lowe and LaLiberte 2006). This may also affect the distribution of macroinvertebrates within active streams (Wright 1995; Wallace et al. 1996; Hauer and Resh 2006). However, macroinvertebrates may be found throughout the floodplain of large alluvial systems in the western United States over a mile (2 to 3 km) distant from the active channel, when high porosity and permeability paleochannels are connected within the flood plain (Sanford and Ward 1993).

At the fluvial plain scale (Figure 6.1), upland waters flow toward the floodplain of a stream system. Discharge occurs in the **riparian zone**. The riparian zone is commonly referred to as the interface between the terrestrial and aquatic zones (Gregory et al. 1991). It is characterized

by trees (i.e, cottonwoods, alders, and spruces) and other large vegetation and generally does not contain surface water except during episodic floods (Dahm et al. 1998). In smaller stream systems, the riparian zone may be characterized by willows, sedges, or other shrubs (Figure 6.7).

Within the fluvial plain system, on the stream side of riparian zones, groundwater and nutrient exchanges are occurring primarily along parafluvial sections, where water enters the gravel at riffles and exits at pools or moves through gravel bars and meander sections discharging on the other side (Wroblicky et al. 1998).

Channel geomorphology and stream connectivity

The exchange of groundwater and surface water discussed above can be partially explained by understanding the geomorphology within fluvial plain systems. Stream reaches can be categorized as constrained, unconstrained, **aggrading,** or **degrading**. Constrained stream reaches can be defined as fluvial plains less than four times the width of the active channel and unconstrained at greater than four times the active channel (Dahm et al. 1998). Aggrading reaches are those that are depositing sediment, while degrading reaches are where active downcutting and erosion are occurring. Straight channelized sections and canals tend to be areas where groundwater/surface-water interaction becomes disconnected. Additionally, unconstrained degrading streams rarely have losing reaches within them (Dahm et al. 1998). A summary of nutrient

Figure 6.7 Riparian zone characterized by willows and shrubs along the Clark Fork River, southwestern Montana.

retention studies in groundwater discharge, recharge, and parallel flow scenarios along with various channel configurations was hypothesized by Dahm et al. (1998) and is shown in Figure 6.8.

Dahm et al. (1998) hypothesize that the geomorphologic and hydrogeologic conditions represented in Figure 6.8 portray the retentive capacities of solutes and their ability to alter the volume and direction of interactive exchange between the active stream, the riparian zone, and the alluvial aquifer. The highest interactions between groundwater and surface water are hypothesized to occur in tributaries and aggrading reaches, while channelized reaches are believed to be disconnected (Dahm et al. 1998).

Nutrient retention can be viewed as solute sources that have sufficient residence times and interactive exchanges between surface waters and groundwater to promote a complex variety of biochemical processes occurring throughout the fluvial plain (Dahm et al. 1998). These processes may also be complicated by an intermittent vadose zone within gravel bars and in the riparian zone, providing an increased oxygenated environment.

A summary of nutrient exchange processes within the hyporheic zone of streams can be divided into chemoautotrophic and electron-accepting conditions (Dahm et al. 1998). Stumm and Morgan (1996) present an example of the various processes, including energy yields by taking a pH solution of 7 and using CH_2O as a typical organic substance. These are presented in Table 6.1.

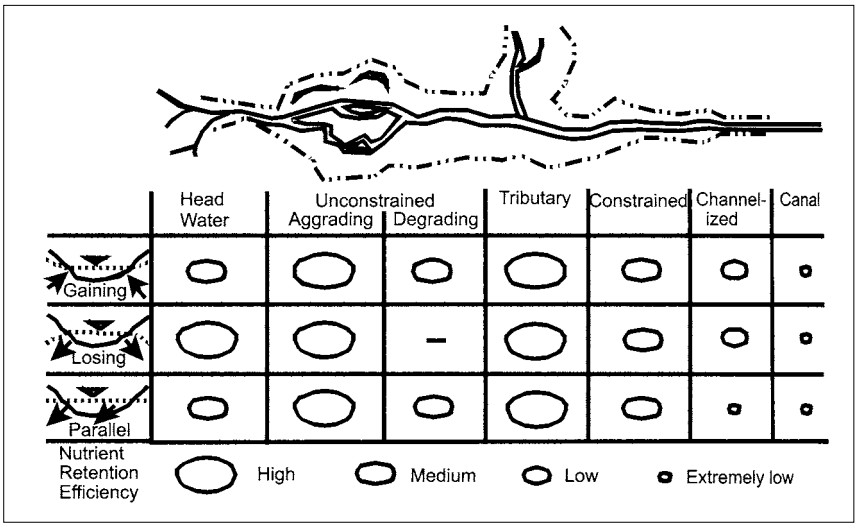

Figure 6.8 Hypothesized nutrient retention efficiencies in various groundwater/surface-water settings and channel configurations. (Losing reaches rarely occur in degrading sections of unconstrained stream.) [*Adapted from Dahm et al. (1988).*]

TABLE 6.1 Chemoautotrophic and Electron Acceptors in the Fluvial Plain [From Stumm and Morgan (1996)]

Chemoautotrophic processes	Kcal/Equiv	Electron accepting processes	Kcal/Equiv
Nitrification $NH_4^+ \rightarrow NO_3^-$	−10.3	Sulfate reduction $SO_4^{-2} \rightarrow S^{-2}$	−5.9
		Methanogenesis $CO_2 \rightarrow CH_4$	−5.6
Iron oxidation $Fe^{+2} \rightarrow Fe^{+3}$	−21.0	Iron reduction $Fe^{+3} \rightarrow Fe^{+2}$	−7.2
Sulfide oxidation $S^{-2} \rightarrow SO_4^{-2}$	−23.8	Denitrification $NO_3^- \rightarrow N_2$	−28.4
Methane oxidation $CH_4 \rightarrow CO_2$	−9.1	Aerobic respiration $CH_2O \rightarrow CO_2$	−29.9

Theoretically, microbial activity follows a definite progression from aerobic to anaerobic conditions as a sequence of electron accepting substrates as they pass through distinctly different redox states (Azadpour-Keeley 2005). A summary of the different substrates represented and their respective redox states is summarized in Figure 6.9. A pneumonic that seems to help one remember the electron-capture sequence from aerobic to anaerobic

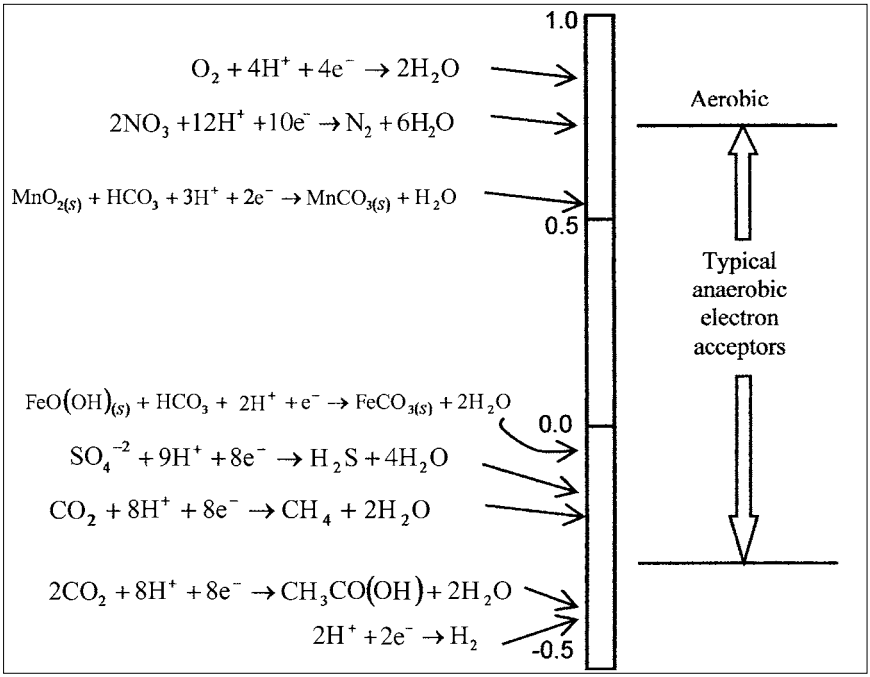

Figure 6.9 Electron-donor and acceptor sequences from aerobic to anaerobic conditions under various redox potentials in volts, assuming a pH of 7 after (Azadpour-Keeley, 2005).

conditions is "Oh No My Friggin Shoes are Melted." The mnemonic stands for Oh = Oxygen, No = Nitrate, My = Manganese, Friggen = Iron (Fe), Shoes = Sulfate, Melted = Methane. Azadpour-Keeley in a very-well referenced book chapter discusses the progression and microbial conditions for contaminated groundwater plumes from a field sampling perspective; however, the general principles discussed there have application to various conditions within a fluvial plane from well-oxidized hyporheic-interaction zones to stagnant swampy areas. By measuring dissolved oxygen, nitrate, manganese, iron, and sulfate along with eH one can gain a perspective of what the conditions are like (see Chapter 7).

The redox potential within the riparian zone is a function of residence time and metabolism rates within mixing zone of upland waters and hyporheic waters and their chemical characteristics (Dahm et al. 1998). Organic carbon decomposition can be carried out through the reduction of terminal electron accepting processes listed in Table 6.1 and Figure 6.9. The rates and distribution of biogeochemical processes are still not well understood. Additionally, there are a number of metabolic pathways that oxidize dissolved or particulate matter and selected nutrients (Dahm et al. 1998; Tank et al. 2006). For example, Hill (1993) has shown that riparian zones are efficient removal sites for nitrate from upland flow areas, with nitrogen removal exceeding 80% from a survey of streams.

At the tens of feet or meters scale, groundwater/surface-water exchange can be partially evaluated through the use of minipiezometers and comparing the head differences between groundwater and surface water (Lee and Cherry 1978; Woessner 2000). A schematic of flow conditions for overall gaining or losing scenarios is presented in Figure 6.10.

Figure 6.10 shows how streambed topography can affect localized water exchanges even though the reach may be losing overall (Figure 6.10A) or gaining (Figure 6.10B). Hydraulic head data can be coupled with basic water-quality surveys (dissolved oxygen, specific conductance, and temperature) to provide a multi-disciplinary approach. Additional perspectives can be gained by studying nutrient patterns and the distribution of macroinvertebrates (Hauer and Resh 2006; Brunke, M., and Gonser 1997).

One of the keys to understand biochemical processes is tied to an understanding of the fluvial plain hydrogeology. Places of relative constant influx or infiltration and the distribution of macro- and microbial fauna all contribute to gauging the health of a given stream.

6.3 Stream Health

A healthy stream as proposed by Meyer (1997) is an ecosystem that is sustainable and resilient in maintaining its ecological structure and function over time. This structure leads to discussions of stream,

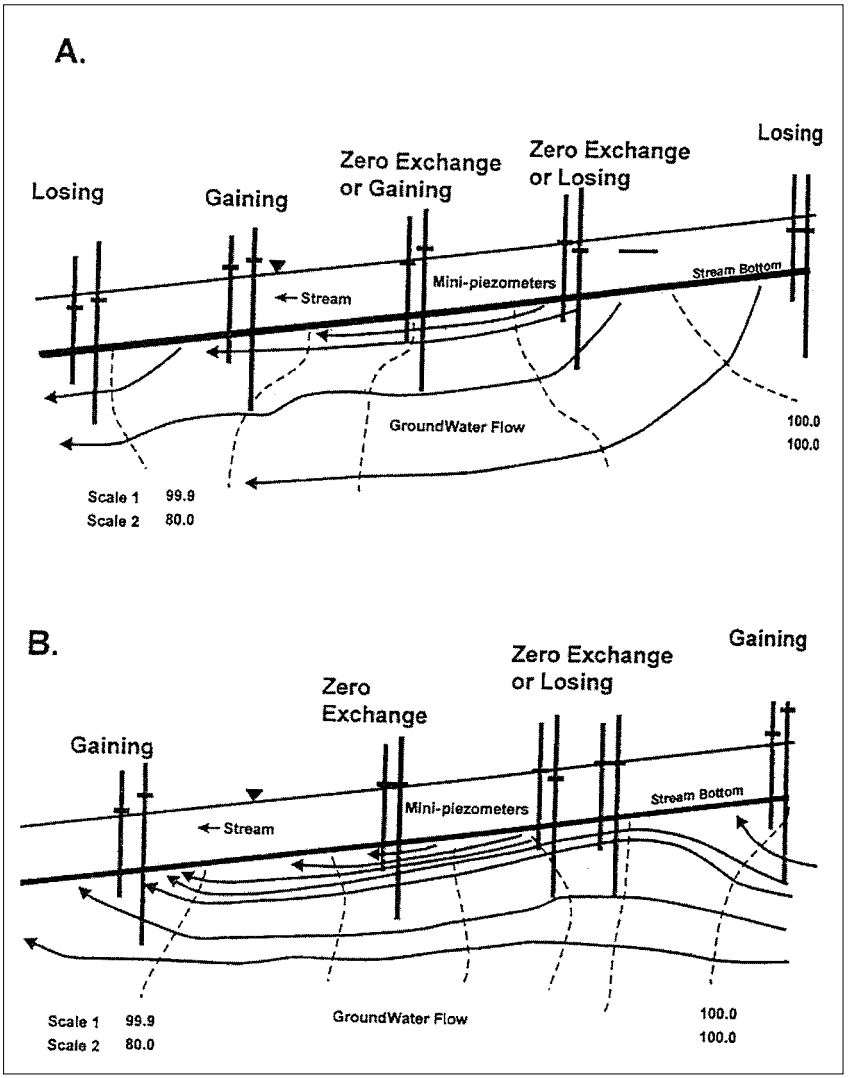

Figure 6.10 Streambed topography and localized water exchanges. [*From Woessner (2000). Reprinted with permission of Groundwater 2000.*]

hyporheic, riparian zone, and fluvial plain functions and their respective critical components (Woessner 2000). Ecologists and scientists may provide measures of stream health, but defining the respective goods and services expected of a stream requires input of societal values (Meyer 1997). Examples of goods and services valued by policy makers are shown in Table 6.2. As societal values change, so do the policies and laws that are implemented for stream maintenance and restoration.

TABLE 6.2 Goods and Services Valued by Healthy Streams [After Meyer (1997)]

Goods	Services
Clean water for drinking, washing, and other uses	Cleansing and detoxifying water
Adequate supply for irrigation and industry	Maintaining water supply
Uncontaminated foods (seafood, crayfish, shellfish)	Reducing sediment inputs in coastal areas
Challenging waterways for kayaking	Providing aesthetic pleasure
Sites for swimming	Produce fish for angling
An environment for meditation and renewal	Decomposing organic matter
Unique species and wildlife to observe	Storing and regenerating essential elements

The concept of stream health is analogous to human health, in that the absence of disease in humans can be compared to the absence of pollution, acids, and toxins (Meyer 1997). This can be measured by macroinvertebrate studies, the presence or absence of fish populations, or other biotic indicators (Wright 1995; Wallace et al. 1996). Excellent additional treatment of this topic can be gleaned from reading Carter et al (2006) and Culp and Baird (2006). Biota are useful stress indicators but do not give a full picture of the fluvial plain. Flowing waters receive multiple, potentially interacting stressor sources (municipalities, industry, and non-point source agricultural) that make it difficult to establish cause and effect relationships (Culp and Baird, 2006). The focus of modern medicine is more on wellness and maintaining health rather than curing diseases (Meyer 1997). Stream health is conceptually similar but requires a multi-disciplinary assessment for a proper evaluation. Both terms are imprecisely defined, but useful.

Another measure of stream health is how quickly it recovers from a disturbance. This is how resilience can be evaluated, although rates of recovery have not been applied to stream health (Meyer 1997). Comparative studies are needed between impacted and natural stream reaches (Woessner 2000). The purpose of presenting this chapter is to heighten the awareness of hydrogeologists in the complex issues and to consider their role in designing fieldwork for stream restoration and evaluating impacts from hazardous waste contamination in the hyporheic zone.

6.4 Field Methods to Determine Groundwater/Surface-Water Exchange

There are several field methods hydrogeologists use to evaluate the interaction of groundwater and surface water in fluvial plains.

A combination of these will usually provide a better understanding of the flow system. Perhaps the most common ones are:

- Stream gauging
- Parshall Flumes
- Crest-stage gauge
- Minipiezometers and wells
- Seepage meters
- Temperature studies
- Tracer studies
- Chemical mass balance

If a hydrogeologist teamed up with an ecologist, additional insights on riparian functionality and general stream health can be included to obtain a more complete picture (Palmer 1993; Woessner 2000). The scope of this chapter is to include only a cursory presentation of the issues important to stream biota and focus more on the physical phenomenon of groundwater/surface-water interaction and the associated field tasks facing the hydrogeologist. Additional sources of ecological assessment and impact are discussed extensively in Hauer and Lamberti (2006).

Stream gauging

Stream gauging is the field method of quantifying flow along a given stretch of stream. In smaller streams this is done by using a handheld velocity meter and stadia rod to obtain point velocities along a stream cross section (Figure 6.11). This can be done as long as the current flow and depth are not great enough to affect the safety of the field person. In larger and deeper streams, gauging is performed at a bridge or from a cage suspended from a cable-pulley system. In deeper, higher-velocity streams, a weighted **Price** meter is used to determine stream velocities per fraction of cross-sectional area (USGS 1980). A Price-type meter has a horizontal wheel approximately 5 in (12.7 cm) in diameter, with small cups attached. The wheel rotates in the current on a cam attached to the spindle. An electrical contact creates a "click" sound with each rotation. The clicks are transmitted to a headset worn by the field person to obtain a clear signal. The clicks are counted for 30 or 60 s or sent to a direct readout meter. The number of clicks is compared with a calibration curve to obtain the velocity.

Streams have a parabolic velocity profile that is affected by the bottom and sides of the stream (Fetter 1994)(Figure 6.12). The average velocity is found at approximately the 0.6 depth from the surface, although an average of the 0.2 and 0.8 depths are also used (Buchanan and

Figure 6.11 Stream gauging with a handheld velocity meter and stadia rod.

Sommers 1969). The fastest part of current occurs in the middle and center of the stream. If no velocity-measuring equipment is available, a quick estimate of flow can be obtained by using the **float method**. In the float method, a distance of 10 to 20 ft (3 to 6 m) is paced along the bank of a straight stretch of stream. A stick is tossed in the middle of the stream above the first marking and timed how long it takes to move from the first to the second marking. This yields an average velocity for the center of the stream. The estimated velocity

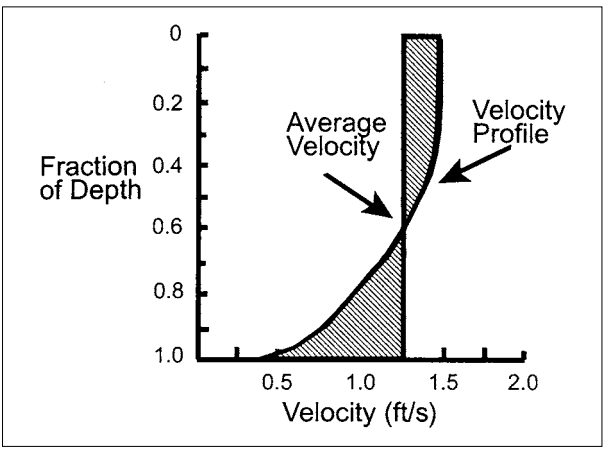

Figure 6.12 Velocity of stream as a function of depth. (The 0.6 depth is near the average velocity.) [*After Fetter (1994).*]

should be multiplied by a correction factor of 0.75 or 0.80 to account for friction along the sides and bottom of the channel. The correction factor is applied according to the uniformity of the profile across the stream. Edges with higher friction factors, such as vegetation, would have the 0.75 correction applied, where streams with a more uniform velocity would have the 0.8 factor applied. The cross-sectional area is estimated by measuring several depths across the stream where the flow "looks" average. The velocity times the area yields a flow in cubic feet per second (ft^3/s), or cubic meters per second (m^3/s) depending on the equipment used.

Larger stream systems may have dedicated gauging stations to evaluate long-term monitoring (Figure 6.13). The distances between stations are typically miles to tens of miles (kilometers to tens of kilometers) apart. In order to establish a gauging station, a detailed cross section of the stream is surveyed during low-flow conditions. Multiple discharge readings are made at different stage elevations to establish a functional relationship between depth and flow, known as a stage-discharge curve (Figure 6.13). It is important to resurvey the cross section every several years to make sure the flows are accurate. Drift of points from the curve indicates changes in the cross section have occurred.

An inlet pipe allows water to enter the stilling well (often constructed of corrugated pipe). The float moves up and down according to the stage, strung by a beaded cable, which passes over a pulley at the recorder with a counterweight hanging on the other side. The shed housing the system is known as the dog house. The stage is recorded via a float-recorder system or using well sentinels (described in Chapter 5).

Some watersheds have gauging stations near the watershed outlet, before there is a confluence with another channel. However, to understand

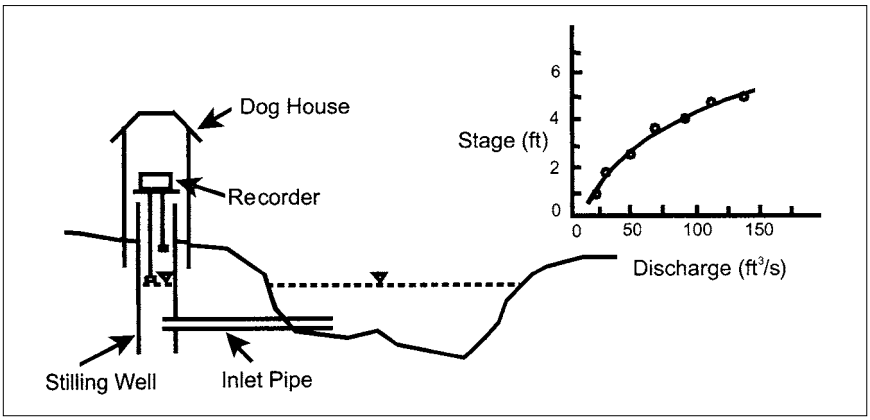

Figure 6.13 Schematic showing a gauging station and associated stage discharge curve.

the dynamic local groundwater/surface-water interactions occurring within a watershed, it is necessary to take multiple discharge readings along the stream. One must account for every contribution be accurate. For example, there may be minor tributaries, springs, irrigation ditches, or pipe discharge occurring along the stream that may not be readily apparent. A detailed evaluation of all gains and losses within a stretch at the same time is known as a **synoptic survey**. For the purposes of discussion, it is assumed that these streams and associated tributaries can be gauged with a current meter attached to a wading rod at least some time during the field season.

For smaller streams, the U.S. Geological Survey used or still uses a **pygmy** meter, similar to the Price meter; however, all the components are at a smaller scale. Cups attached to a wheel spin proportionally to the current. It is critical to perform a "spin test" prior to use and properly maintain this equipment. A spin test is conducted by blowing on the cups to allow them to free spin for a minute or so. If they stop within 30 to 40 s, there is something wrong that needs to be fixed. It may be that a drop of lubricant is needed or a nick in the spindle tip may be the problem. Maintaining these meters so that they will pass the spin test is probably the most common problem with these devices. For this reason, most hydrogeologists have made the switch to using meters equipped with sensors to measure velocity.

Current meters with sensors are able to measure a wider range of velocities. For example, one of these current meters creates a magnetic field as the moving water passes the sensing device (Figure 6.14). Changes in velocity are correlated with changes in voltage amplitude.

Figure 6.14 Flow meter with sensing device to indicate stream velocity.

Velocities are directly read from a meter that hangs around the operator's neck. The great thing about this type of device is that it can be used in streams or irrigation ditches with weeds or other debris that would normally clog up a spinning wheel. In comparing velocity results during field camps using both types of current meters, correlations were found to be within the error ranges found with multiple readings using the same device. The USGS gauges all stream locations three times before making a comparison of readings. Discrepancies when comparing measurements have been given the following ratings: excellent (2%), good (5%), fair (8%), and poor (over 8%) (USGS 1980).

An ideal site would be a stream stretch that is relatively straight and free from obstructions and vegetation (Sanders 1998). The field operator should test the stream for depth, strength of current, and the bottom for safety and stability before wading out with the equipment. A tag line is stretched across the stream with graduated markings and secured, so that velocity measurements can be accurately divided at the appropriate intervals. A 100-ft (30.5 m) cloth tape works well for many applications. The stream width should be divided into approximately 20 sections, so that less than 5 to 10% of the total discharge passes through any given section. This provides more repeatable results. Flow in small gaining streams with stream properties prohibiting the use of gauging equipment can be estimated using tracer methodologies discussed later on in this chapter. The field operator should bring:

- Field book
- Waders
- Graduated tagline or 100-ft (30.5-m) cloth tape
- 10-ft (3-m) retractable measuring tape, for making shorter measurements
- Writing utensils and extra supplies
- Extra batteries for field equipment
- Calculator

The current meter should be attached to the wading rod, and the operator should stand on the downstream side facing upstream. A velocity reading is taken within each section. Hold the rod out with the cups or current sensor facing upstream set at the 0.6 depth, unless the water depth is more than 2.5 ft (0.75 m) (USGS 1980). The wading rod should be kept vertical. When the water depth is greater than 2.5 ft (0.75 m), readings should be taken at the 0.2 depth and 0.8 depth to obtain an average. The total flow is calculated by summing the individual velocities and multiplying the result by the respective cross-sectional areas

(Equation 6.1). A repeat is made of each measurement. An example sample data sheet for stream velocity measurements is also presented.

$$Q = \sum_{i=1}^{n} v_i A_i \tag{6.1}$$

Stream Velocity Measurements Data Sheets										
Date	Stream			Weather						
Location										
Meter type				Meter coefficient(vel/rev)						
Observer				Stage gauge reading						
Comments										
Angle Coef.	Dist. from edge	Width	Depth	Obs. point depth	Revs	Elapsed Time	Velo-city	Angle adj.	Area	Dis-charge

Example 6.2 Approximately 5 mi west of Butte, Montana, is the Sand Creek drainage basin. A hydrogeologic study was conducted to create a "transitional baseline" in the midst of industrial development and water-use changes (Borduin 1999). A significant area of the drainage basin has been zoned heavy industrial. Stream gauging was conducted along Silver Bow Creek and Sand Creek and other tributaries to document fluxes and gaining and losing stream sections. Later, this information was used to compare numerical modeling results of the basin to compare modeled stream fluxes with field gauged data. Agreement of potentiometric surface data and stream fluxes was an indication that calibration objectives were being achieved. Stream reaches less than 5 ft (1.5 m) wide were divided up every 0.5 ft for velocity measurements. Wider stream reaches were divided into enough widths to represent approximately 10% of the total flow. A direct readout current meter was used to obtain point velocities at the 0.6 ft depth. An example is shown in Table 6.3 for a reading along Silver Bow Creek with associated calculations.

Stream gauging is useful when net gains and losses are obvious (flow changes are greater than 10%); however, when performing a synoptic survey within a drainage basin or along a significant length of stream, there are many sources of error (Roberts and Waren 1999). Some of the following can render a stream gauging survey inconclusive:

TABLE 6.3 Example of Stream-Flow Calculations Site 1, Silver Bow Creek. August 27, 1998 [From Borduin (1999)]

Distance (ft)	Depth (ft)	Velocity (ft/sec)	Area (ft^2)	Discharge (ft^3/sec)
Left bank = 1	0.9	0.16	0.9	0.144
3	0.97	0.26	0.97	0.252
4	1.4	0.36	1.4	0.504
5	1.5	0.48	1.5	0.72
6	1.87	0.76	1.87	1.421
7	2.1	1.04	2.1	2.184
8	2.35	1.05	2.35	2.468
9	2.4	1.15	2.4	2.76
10	2.65	1.09	2.65	2.889
11	2.45	1.05	2.45	2.573
12	2.2	0.99	2.2	2.178
13	2.0	0.94	2.0	1.88
14	1.77	0.74	1.77	1.31
15	1.9	0.68	1.9	1.292
16	1.8	0.48	1.8	0.864
17	1.8	0.43	1.8	0.774
18	1.95	0.34	1.95	0.663
19	1.7	0.26	1.7	0.442
20	1.3	0.14	1.3	0.182
21	0.75	0.0	0.75	0.0
			Total	25.5

- Gauging during runoff
- At the time of a precipitation event when stream flow is changing
- Diurnal changes that occur from overnight to early morning to early evening affected by healthy vegetation growth.
- Ignoring or missing small contributions from minor tributaries, springs, irrigation ditches, or pipe discharge can result in significant water-budget errors.
- Gauging during periods of low flow or similar times during the day yields improved confidence in the results.

Parshall flumes

During a synoptic study of stream discharge, it is very important to identify and gauge all surface water inputs or outputs. This includes irrigation diversions and irrigation return flows. In the semiarid Western states, irrigation ditches are extremely common and are often difficult or impossible to locate from a topographic map. Ditches are sometimes easier to spot in the field or from an aerial photo, and can be traced upgradient to their origin at the stream source. However, there is no substitute for simply walking down the entire drainage, catching any

unmapped diversions and returns. In a synoptic study of Big Lake Creek, south of Wisdom, in southwestern Montana, a downstream traverse uncovered 10 to 12 irrigation diversions with significant flow over approximately 10 mi of creek. Only a few of these diversions were obvious from preliminary reconnaissance work.

Near the point of divergence, landowners will often place a headgate with a weir or flume to control and quantify the amount of water withdrawn from the stream (Figure 6.15). In southwestern Montana, Parshall flumes are especially common. The Parshall flume is essentially a tapered box with a rectangular cross section, flaring both upstream and downstream, and with a slight constriction in the middle (the throat). The total discharge in cubic feet per second (cfs) is computed knowing the depth of the water and the width of the flume at the throat (University of Wyoming 1994). Care should be taken in the field to make sure that the flume is in good condition. Problems include obstructions and making sure that the flow is laminar and that there is no evidence of water passing around or underneath the flume box (Fig 6.16). If high precision and accuracy is required, it is a good idea to check the flume measurement with your own estimate of flow based on velocity transects. Although Parshall flumes are made to rigid specifications, problems can occur with faulty installation or wear and tear. Because the relationship of flume width, water depth, and stream discharge is nonlinear, there is no simple equation to calculate stream discharge. Instead, the hydrogeologist must consult a Parshall flume table for the appropriate conversion (University of Wyoming 1994 and WWE).

Figure 6.15 V-notch weir used to estimate discharge from a mine adit.

Figure 6.16 Parshall flume installed in a small stream to measure flow.

Crest-stage gauge

Sometimes it is helpful to know what the peak stage was during a flooding event in a remote area or an ephemeral drainage. If no permanent gauging system is available and the location is important to evaluating peak flows, a **crest-stage gauge** can be installed (Buchanan and Sommers 1968). A crest-stage gauge is essentially a calibrated stick inserted inside a clear tube. The tube is constructed so that water can enter at the bottom and allow air to escape at the top. A material such as ground-up cork is inserted in the tube so that when the stage increases, the cork floats along with the rising stage. When the stream reaches a maximum stage (or crests) and begins to drop, the cork will adhere to the calibrated stick and the inside of the tube. The tube and stick can be placed inside a PVC casing to protect the gauge, which is attached with metal strapping to a fence post on the downstream side of an ephemeral drainage (Figure 6.17).

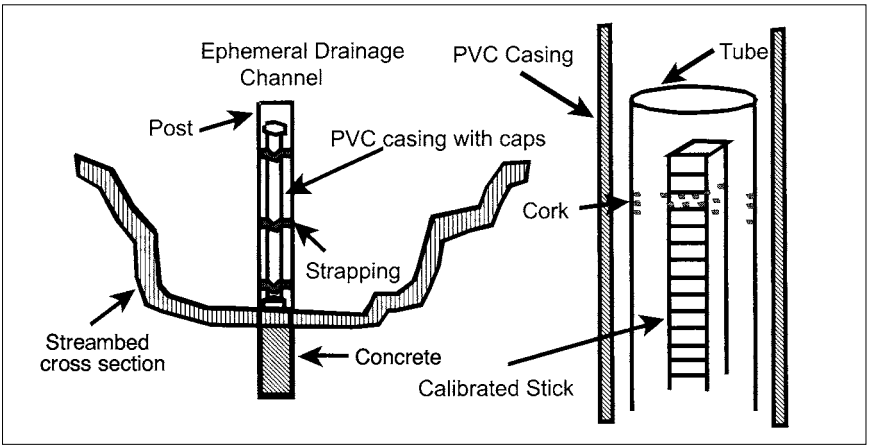

Figure 6.17 Crest-stage gauge attached to a fence post with metal strapping. (Holes drilled around the base of the PVC casing and the tip cap allow air circulation. A detailed diagram on the right shows a clear tube, calibrated stick, and cork material. Cork material floats during high stage and adheres to the tube and stick as the stage decreases.

Example 6.3 While performing baseline studies for a prospective coal mine in southwestern Wyoming, it was necessary to obtain peak discharges for several ephemeral drainages that occurred during spring runoff. None of the drainages contained water except in response to spring snow melt and precipitation events. The crest-stage gauge design presented in Figure 6.17 was used at a couple of locations along each drainage to obtain upstream and downstream values. Each post was set approximately 3 ft (0.9 m) into the stream channel in concrete. Each crest-stage gauge location was surveyed to obtain a cross-sectional area. An estimate of the velocity was made by using the Manning equation. The Manning equation uses four parameters to estimate the velocity (Equation 6.2).

$$V = \frac{1.49R^{2/3}S^{1/2}}{n} \tag{6.2}$$

where V = average estimated velocity, ft/s
R = hydraulic radius, ft^2/ft and R = Area/WP
WP = wetted perimeter (Figure 6.18)
S = estimated slope of the water surface
n = Manning roughness coefficient

The Manning equation, where length is measured in meters and time in seconds is:

$$V = \frac{R^{2/3}S^{1/2}}{n} \tag{6.3}$$

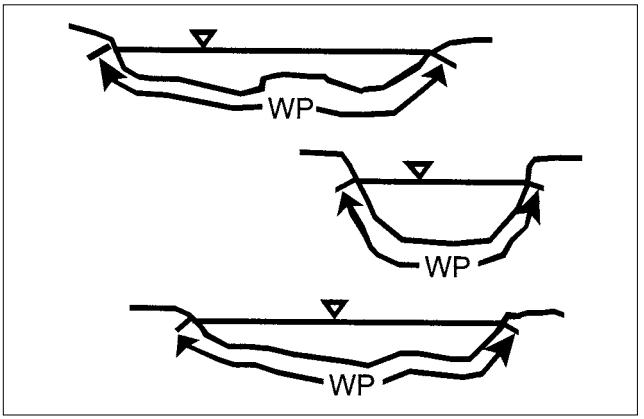

Figure 6.18 Schematic showing the wetter perimeter (WP), the bottom surface from edge to edge used in the Manning equation. (*Note that the WP is wider than the width of the channel.*)

The Manning roughness coefficient ranges from 0.025 for streams that are straight, without brush and weeds or riffles and pools to 0.15 for channels containing dense willows (Chow 1959). Some of the more common values for streams with grasses, rocks, and pools range from 0.035 to 0.045. See Chow (1959) for tables and photographs of all types of roughness coefficients. To make a reading, the PVC cap is removed and the tube with the calibrated stick is pulled out. After a reading is taken, the cork material is washed to the bottom of the tube, to be ready for the next event.

For areas with established gauging stations, a crest-stage gauge would be installed next to the bank at average flow. In this case, the crest-stage gauges would have to be checked more frequently. The ground-up cork material will only record the peak stage height. If there were multiple peak events, only the highest one is recorded. It will be hard to distinguish which peak event was recorded by the crest-stage gauge.

Minipiezometers

Elevations of hydraulic head for local and intermediate groundwater flow systems are usually determined from level measurements from wells (Chapter 5). Wells tend to be more permanent features installed using power equipment or drill rigs contrasted with minipiezometers that are manually placed and retrieved (Lee and Cherry 1978). In evaluating groundwater/surface-water interactions or in determining the head differences at a smaller scale (meters to tens of meters), **minipiezometers** are great tools. Minipiezometers can be constructed with a variety of construction materials including stainless steel, different

types of tubing, or PVC. Minipiezometers are screened over a short length (a few inches or centimeters) and therefore provide "point" estimates of hydraulic head at a particular depth (Figure 6.19). Figure 6.19 shows the adding of slot openings on a 1-in (2.5-cm) pipe, with a duct tape "bottom cap."

The mixing of surface water and groundwater takes place within the near-channel sediments (Woessner 2000). The mixing process can be very complicated (discussed in Section 6.2) and at many different scales because of the dynamics of surface-water movement and heterogeneities within the near channel sediments (Bencala et al. 1983, Huggenberger et al. 1998). Minipiezometers can be installed along the stream bank or in the streambed to partially evaluate the different flow regimes, as depicted in Figure 6.6.

Installation of minipiezometers into stream sediments devoid of cobbles is pretty simple; however, stream beds armored with rocks and cobbles are nearly impossible to install manually. A few installation methods are presented. The examples will assume we are using 1/2-in

Figure 6.19 Piezometer with a duct tape bottom cap and being slotted with a hacksaw.

(1.2-cm) stainless steel electrical conduit as "casing" material. Electrical conduit is typically sold in 10-ft (3-m) lengths at minimal cost. These may be cut to any shorter lengths with a hacksaw. Perforations can also be made with a hack saw, staggering the cuts for increased casing strength. A loosely fitted bolt is "scotch" taped to the bottom of the piezometer, to keep the tube from crimping (Lee and Cherry 1978). At the top end, another bolt is used for support and in keeping the top open during pounding with a mallet or heavy hammer. The author has found reasonable success pounding on a block of wood placed on the top of the minipiezometer (Figure 6.20). Once the piezometer is driven 1 ft (30 cm) or more into the sediments, the minipiezometer tube is twisted and pulled back slightly to free the bolt, which is left in the sediments (Lee and Cherry 1978). This process could be referred to as the **bolt method**.

When a significant fraction of gravel is found in the sediments, the bolt method may not provide sufficient support for the piezometer tube. In this case, a metal support rod similar in length to the piezometer can be used effectively (the **support-rod method**). An ideal material to fit inside the thin piezometer tubing material is a steel grounding rod. The

Figure 6.20 Installing a minipiezometer.

smoother the support-rod material, the better (English 1999). Good results can also be obtained with a heavy gauge copper wire. Steel rebar turns out to be a poor choice because the ribbed edges pull sediments into the piezometer when retracting, and will bend relatively easily when encountering cobbles and rocks. The technique is to insert the support rod inside the piezometer tubing and pound it in with a hammer. The support rod should only protrude an inch (2.5 cm) or so beyond the end of the piezometer and extend a short distance above the top end. The stress of the pounding is all taken up by the support rod. Once retraction of the rod has taken place, some water can be poured into the piezometer to flush the screened zone and evaluate the connection with the stream sediments. The screened zone can be constructed by cutting slots with a hacksaw or drill holes with the perforations wrapped with 0.2-mm nylon mesh or fiberglass cloth (Lee and Cherry 1978). The support-rod method is the most efficient method in gravelly conditions, but may not work if the stream-bedrock density is too great.

When the stream-bedrock density is too great or one must install piezometers into bedrock, one may need to resort to the **plate-jack method**. A piezometer location is first hand-augured to provide a description of geologic materials to as great a depth as possible. Once the auger can no longer penetrate, a heavy gauge 1-in (2.5-cm) pipe is placed into the hole and driven with a fence driver (Figure 6.21a). This is done to penetrate to the desired depth (up to 2 m or more in weathered bedrock). At this point hand retrieving the 1-in (2.5-cm) pipe is nearly impossible or extremely hard on the back. The plate-jack is a 1/4-in (6.4-mm) steel plate with a torch-cut hole cut approximately 6 in (15.2 cm) in diameter to accommodate being placed over the driven 1-in pipe. A handy-man jack is bolted to the plate at the jack base with chains welded to it as a means to lift the 1-in (2.5-cm) pipe back out of the borehole (Figure 6.21b).

The piezometer is "completed" by being placed into the borehole with sand packing being added to a level above the top of the slot openings. Bentonite chips or other sealants are added to the surface to isolate the slotted horizon. Level measurements and water-quality sampling can then be done. The plate-jack method can be used where access to the piezometer locations is difficult but the equipment can be moved from place to place using a wheelbarrow.

It is important to test the hydraulic connection of a "just completed" piezometer. Some folks place piezometers into the ground and then move to the next piezometer without testing whether a connection with the aquifer was made. A simple procedure to test this is to pour water down the piezometer until it reaches the top and then see if the level drops over time. Small bubbles coming up the piezometer are a sign that displacement is occurring and connection has been made.

A

B

Figure 6.21 In 6.21a 1-in (2.5-cm) heavy-gauge pipe is being driven into the ground with a fence driver (note the auger cutting piled to the right). In 6.21b the jack-plate is being used to lift the 1-in (2.5-cm) pipe out of the ground. The chains are wrapped around the pipe. (*Photos courtesy of Andrew Sudbrink.*)

Example 6.4 The Milk River traverses eastward along the hi-line of north-central Montana through the town of Havre, Montana. A dispute over contamination of hydrocarbons migrating to a residential area from a rail yard led to an investigation, including evaluating whether contaminants had reached the Milk River. Several piezometers were placed near the edge of the river to provide level and water-quality information. Hand-auguring was done to describe the sediments to a depth of approximately 2 ft (0.61 m), followed by placement of the piezometers. To test connectivity with the saturated stream sediments, water from the river was poured into each piezometer. In each case the water level crowned and showed no sign of connectivity. A surging tool was made from a willow branch and inserted into the piezometer (Figure 6.22). After pumping the surge tool up and down for 15 to 30 s water was added again to the piezometer. This process was repeated until each piezometer showed connection with the aquifer materials.

The water-level difference between the piezometer and the stream stage indicates the change in head with depth. The respective levels can be found by lowering a small diameter E-tape down the piezometer to get a reading and then dangling the E-tape from the top of the piezometer.

Figure 6.22 Photo along the Milk River in northern Montana, where the author is using a willow as a surge tool to obtain connectivity of the piezometer to saturated stream sediments.

To obtain a clearer understanding of the vertical gradient profile in gaining streams, it may be helpful to have a group of piezometers placed at graduated depths (1, 2, and 3 ft or 30, 60, and 90 cm).

Something should be said about where to place a minipiezometer. A minipiezometer should not be placed in the middle of the stream where current is high and difficult to read levels. Near the edge of a stream or just next to the channel will allow installation and readings without fighting current effects. If multiple minipiezometers are being placed "as a nest," it may be helpful to place adjacent to the channel; however, placing up on the bank away from the stream will require a greater depth of penetration. It is also helpful to have the tops of nested piezometers to be level one with another so that rapid comparisons of water levels can be made, even though they may be driven to different depths. Vertical gradients from minipiezometers are measured by comparing the heads in the respective piezometers with the perforation zones (Figure 6.23).

Another way of measuring differential hydraulic head readings between stream stage and minipiezometers is from a method described by Lee and Cherry (1978). This method is also practical for obtaining water quality samples from stream sediments. The bolt method, described above, is used to drive a piece of nonperforated piezometer tubing (casing) into the stream sediments. Once the desired depth has been reached, a smaller-diameter plastic tube with a perforated tip is inserted into the bottom. The tubing (casing) is carefully pulled out and the sediments collapse against the plastic tube. The bottom bolt is again left in the sediments near the tube tip. A measuring scale can be held against the tube as it is extended vertically to compare differences. If

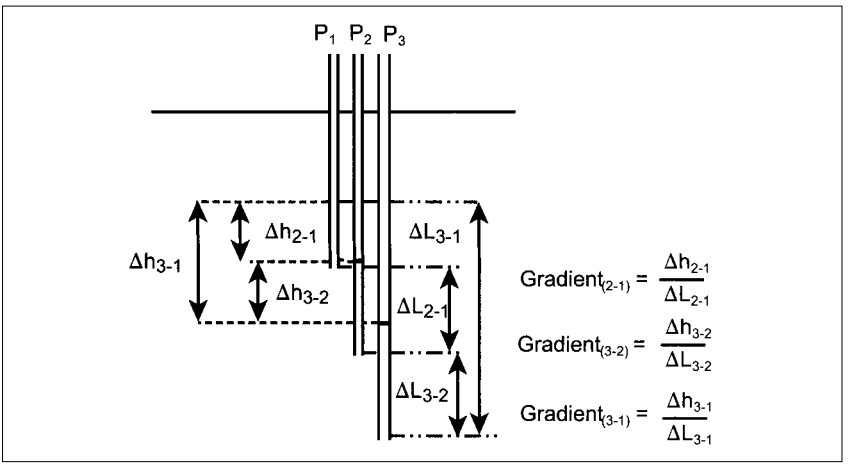

Figure 6.23 Diagram illustrating how to calculate vertical gradients in nested minipiezometers. (In this case, all gradients are negative, indicating downward movement.)

the stream is gaining and the tube is bent close to the stream elevation, water will flow from the tube and water-quality parameters can be measured. If the stream is losing or under parallel flow conditions, a bag can be attached to the tubing and held under the stream surface to obtain a sample (Figure 6.24).

Example 6.5 Near Silver Gate, Montana, a study was conducted to understand the relationship between surface water and groundwater in the Soda Butte Creek drainage before entering Yellowstone National Park (Figure 6.25). As part of the study, groundwater flow-paths were evaluated using domestic wells in the area. Groundwater/surface-water interactions were evaluated by installing nested minipiezometers, stream gauging and comparing groundwater and surface-water quality data (English 1999). Over 20 nested pairs of minipiezometers were installed to evaluate vertical gradients and compare seasonal trends (Table 6.4 and Figure 6.26).

Seepage meters

The seepage flux between groundwater and surface water can be measured directly using a **seepage meter**. A seepage meter is constructed by inserting an open-bottomed container into the stream sediments and then measuring the time it takes for a volume of water to flow into or out of a bag connected to the container (Lee and Cherry 1978). The bag can be protected by a #10 can, (such as a coffee can) held in place with a rock. A hole is drilled into the container and fitted with a plastic barbed fitting. Tygon or plastic tubing is inserted to provide an extension to which the bag can be attached (Figure 6.27). Another tube can be attached to the top of the

Figure 6.24 Seepage meter on Box Elder Creek, Petroleum County, Montana. The bag is downstream of the stick.

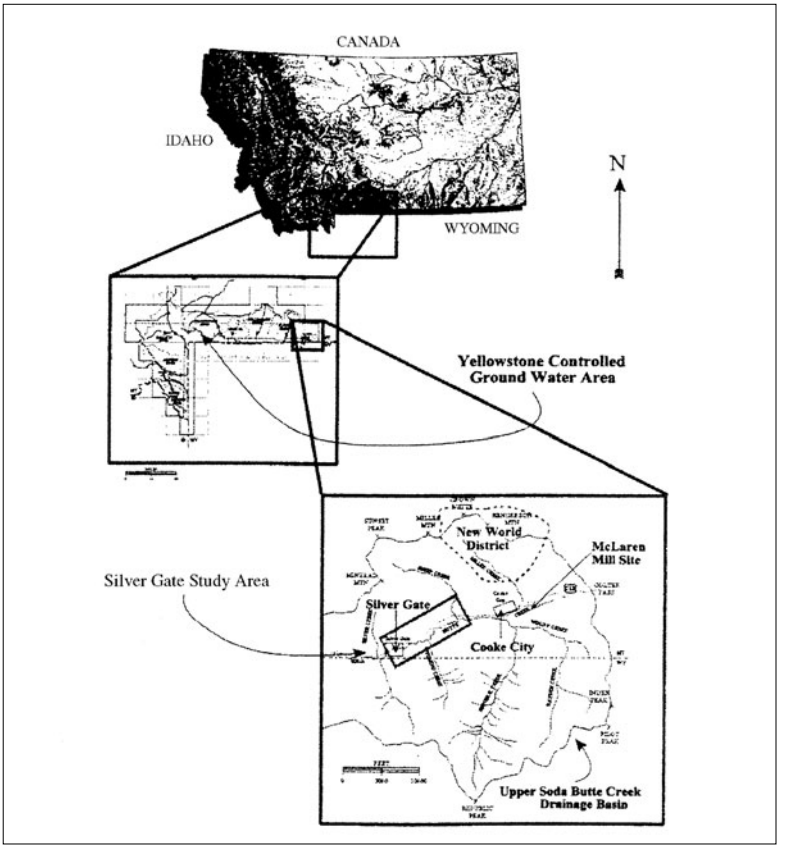

Figure 6.25 Silver Gate study area location map in south-central Montana, within the upper Soda Butte Creek drainage. [*From English* (*1999*).]

container, near one edge, to serve as a vent for any gases released from the sediments. Metal- or stiff-sided containers work best. Good results can be obtained by cutting a 5-gal (18.9-L) bucket in half horizontally or using a 55-gal (0.208-m^3) drum with sides cut to approximately 1 ft (30 cm) in length. The larger the surface area of the container, the more representative

TABLE 6.4 Vertical Hydraulic Gradients for Paired Minipiezometers near Sliver Gate, Montana [From English (1999)] (See Figure 6.26)

Piezometer ID	Vertical W.L difference (ft.)	6 Aug 1998 gradient	6 Oct 1998 gradient	2 Dec 1998 gradient	18 Mar 1999 gradient
19s & 19d	4.7	0.019 up	0.021 up	0.023 up	0.021 up
20s & 20d	4.0	flat	0.008 up	0.005 up	0.005 up
21s & 21d	3.5	flat	0.006 down	0.006 down	0.006 down
22s & 22d	3.5	flat	flat	flat	0.020 down

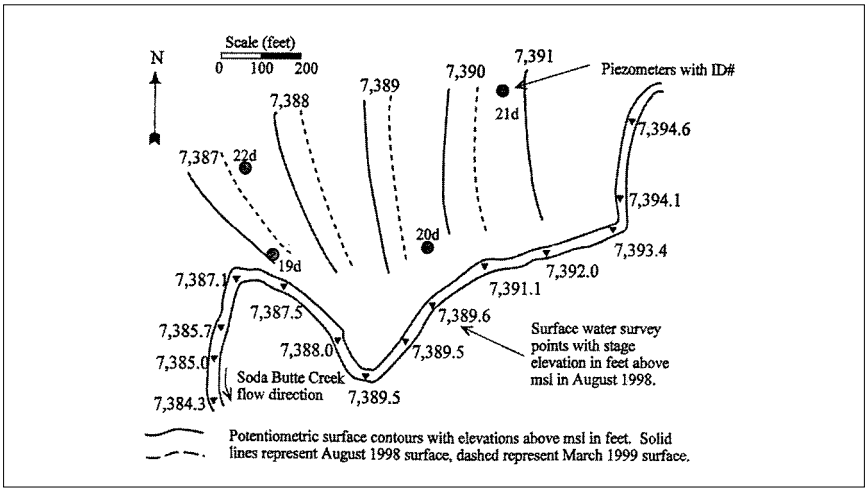

Figure 6.26 Shallow groundwater flow in the marshy area by Silver Gate is toward the west and does not appear to be strongly influenced by Soda Butte Creek until it reaches the western edge of the marshy area. (See Table 6.4) [*From English (1999)*.]

the averaged seepage rate is. Seepage-meter installation has the highest success in lakes or surface streams with low current velocities that do not have significant gravel or rocky armor fraction.

The seepage meter is installed by pushing and twisting the container back and forth slowly into the sediments with the container slightly tilted. Tilting allows the vent tube to work better (Lee and Cherry 1978). It is essential that the container cavity be filled with water with no air

Figure 6.27 Seepage meter in Flathead Lake evaluating discharge. (*Photo courtesy of Bill Woessner*.)

bubbles. The bag is attached to the plastic tubing and clamped until ready for timing. If the flow is upward, the empty bag does not need to be preweighed (Figures 6.27 and 6.28). A Mylar balloon works well because it is strong, lightweight, and has a narrow filling access port that is easily clamped to the tubing. If the stream is losing, the bag needs to be filled or partially filled with water and weighed before attaching and clamped to the tube extending from the container (not the vent tube). When the operator is ready, the tube is unclamped and the time noted. Once the bag empties or fills it is reweighed and the time noted once again. The bag can be protected from the current in the stream by punching a hole through the top of a #10 can (coffee can size) and running the tube from the container into the can before attaching the bag. The can/bag configuration can be held down with a rock (Figure 6.28).

The volume of water represents the flow (Q) of Darcy's law (Chapter 5). The hydraulic gradient (I, change in head per distance) could be determined by installing a minipiezometer to the depth of the seepage meter and reading it directly. The area (A) affected by seepage is the cross-sectional area of the container. From this a hydraulic conductivity (K) can be calculated from Equation 6.4.

$$K = \frac{Q}{IA} \tag{6.4}$$

The hydraulic conductivity (K) is not a seepage velocity. The average linear seepage velocity (v_s) is determined by multiplying K by the hydraulic gradient (I) and dividing by the effective porosity (Equation 6.5) of the unconsolidated sediments (25 to 35%) (Chapter 3).

$$V_s = \frac{K}{n_e} I \tag{6.5}$$

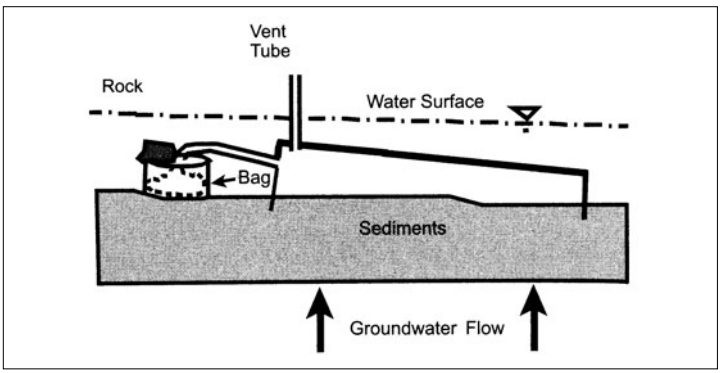

Figure 6.28 Schematic of installed seepage meter (gaining scenario).

TABLE 6.5 Seepage Meter Results at Streams Crossing the Eagle Sandstone Outcrop [From Brayton (1998)]

Location	Volume lost, mL/h
NW 1/4, NE 1/4, SW 1/4 , Section 25, T14N, R27E	60
SE 1/4, SW 1/4, NE 1/4, Section 11, T14N, R27E	30
SW 1/4, SW 1/4, SW 1/4, Section 6, T14N, R28E	72
NE 1/4, NE 1/4, NW 1/4, Seetion 15, T15N, R27E	230

Example 6.6 In east-central Montana, a study was conducted to evaluate the recovery of hydraulic head from rehabilitated flowing wells completed in the Basal Cretaceous Eagle Sandstone (Brayton 1998). Artesian wells had been flowing since before the 1960s and through rehabilitation and conservation efforts, recoveries of hydraulic head in excess of 5 ft (1.5 m) was achieved. As part of the study, seepage meter tests were performed in streams in the outcrop areas of the Eagle Sandstone to evaluate recharge (downward gradient) from surface flow.

A 5-gal (18.9-L) bucket was fitted with a nylon nipple on the bottom (Figure 6.24). A 500-mL bag full of water was attached and allowed to sit for 1 h. At that time, the quantity of water was remeasured to obtain a volume lost per time (Table 6.5).

Care was taken to ensure that the stream sediments were well connected to the Eagle Sandstone aquifer. Minipiezometers were also installed near the seepage meter sites and all indicated a downward gradient.

Another type of seepage meter that uses the same electromagnetic flow principle discussed earlier for stream velocity meters was described by Rosenberry and Morin (2004). They were able to test an expensive commercial electromagnetic flow meter (EFM) in the tubing between the seepage meter and the plastic bag (Figure 6.27), along with a datalogger sensor and pressure transducer to record seepage rates over time correlated to stage level. The beauty of using this type of system is that seepage rates in lakes, estuaries, and tidal areas likely vary over time and this system allows one to capture these changes. They were able to measure seepage rate changes over three orders of magnitude, from 30 mL/min to 30 L/min (Rosenberry and Morin, 2004). An excellent correlation between EMF and plastic bag results was also presented.

Other important observations made by Rosenberry and Morin (2004) include the following:

- Although EMF and bag measurements for seepage rates compared very well, the greatest divergence (bag at 92% of flow of EMF) occurred at the highest flow rate (278 cm/day).
- 10 to 30 min were required for the meter to stabilize. The seepage rate appears to be artificially large immediately following installation and then tapers out.

- Disturbance of the lake bed surface sediments from repeated installations or raking the lake bed surface with a garden rate increases the seepage rate compared to undisturbed areas, indicating a thin crust of lower permeability develops on lake bed sediments,
- Wave action increases the noise in the data, creating wave-induced flow changes, therefore additional research and applications in other settings and conditions are needed to better understand the range of applications.

The EMF tested by Rosenberry and Morin (2004) was a commercially available flow velocity meter designed for measuring vertical flow in boreholes (water wells). Since the technology exists, it seems that a seepage meter devise with a battery-powered data logger system could be designed to be more portable and at reduced cost.

Temperature studies

Another important surface-water/groundwater exchange that has expanded significantly since the first edition is the use of temperature data to evaluate the hydrogeology of many settings. In many studies temperature is used as a surrogate for flow when analyzing the movement of groundwater and its interaction with surface water (Stonestrom and Constantz 2003; Conant Jr. 2004; Burrow et al. 2004; Anderson 2005; and Hatch et al. 2006). A very comprehensive paper that discusses the theory of heat used as a tracer, with applications to identify surface-water infiltration, flow through fractures, and flow patterns in groundwater basins at a variety of scales, with over 150 references from a variety of sources, was presented by Anderson (2005). A few of these are included in this section to present the main ideas and discuss applications important to those trying these for the first time.

Whenever there is a temperature difference between two points along a flow path, heat will be carried advectively with the groundwater (Stonestrom and Constantz 2003). When groundwater is not moving heat will move from higher temperatures to lower temperatures through conduction (analogous to molecular diffusion in a contaminant transport setting, Anderson 2005). Temperature data can reveal much about the interaction of groundwater with surface water. For example, the temperature of surface water typically behaves diurnally between morning and evening, while groundwater temperatures tend to remain more constant (Conant 2004). Therefore if temperatures in stream sediments remain fairly constant over time, one can interpret that groundwater discharge (upwelling) is having a strong influence on streambed temperatures. Conversely, if stream sediment temperatures fluctuate in temperature similar to surface-water temperatures it is likely that

groundwater is being recharged by downwelling stream waters. The hydraulic properties of stream sediments can be estimated numerically by monitoring streambed temperatures.

Thermal properties

It is instructive to explore some of the thermal parameters of geologic materials to better understand the parameters of the numerical models. Much of this discussion was derived from Stonestrom and Constantz (2003). Thermal conductivity, denoted by k, is the ability of a material to conduct heat. The units are given in watts per meter per degree Celsius (W/m°C). Thermal conductivities of materials vary over a much narrower range than do hydraulic properties because of how heat moves through the cross-sectional area of the flow path. Heat moves directly through the matrix material and the pore spaces, while hydraulic conductivity moves in a tortuous path around and through the matrix. Thermal conductivity has a linear function when nearly saturated, but becomes very nonlinear at lower moisture levels. A listing of the thermal conductivities of materials from a variety of sources listed in Stonestrom and Constantz (2003) and Anderson (2005) is given in Table 6.6.

TABLE 6.6 Thermal Conductivity of Selected Materials form Sources Listed by Stonestrom and Constantz (2003) and Anderson (2005)

Materials	Thermal conductivity (W/m°C)
Air	0.024
Liquid water	0.60
Ice	2.2
Dry Snow	0.1–0.7
Quartz	8.4
Average saturated soils	2.9
Saturated soils with organic matter	0.25
Saturated sediments (sand, loam, etc.)	1.4–2.2
Saturated Tottori sand	2.2
Saturated Clarion sandy loam	1.8
Saturated Harps clay loam	1.4
Dry sediments	0.18–0.26
Dry Sandfly Creek sand	0.25
Dry Yolo silt loam	0.26
Dry Clarinda clay	0.18
Shale	1–2
Sandstone	2–4.5
Limestone	2–4
Granite	3–4
Basalt	1.5–2.5

Specific heat capacity is the amount of heat released or absorbed per mass of material per change in temperature (up or down) by 1°C. When one multiplies the specific heat capacity by the material density, one obtains the volumetric heat capacity measured in Joules per cubic meter per degree Celsius (J/m^3°C). Typical values for dry sediments range from 1.1 to 1.3 $\times$ 10^6 J/m^3°C while saturated sediments range from 2.5 to 3.2 $\times$ 10^6 J/m^3°C. Heat capacities ranked by phase from highest to lowest have the following sequence: liquid water > organic solids > mineral solids >> soil gases (Stonestrom and Constantz 2003). (The heat capacity of liquid water at 20°C is 4.2 $\times$ 10^6 J/m^3°C). Another parameter in the models is thermal diffusivity. Thermal diffusivity is the ratio of thermal conductivity to volumetric heat capacity measured in meters per second squared (m/s^2). Typical values are 0.15 to 0.25 $\times$ 10^{-6} m/s^2 for dry sediments, while saturated sediments range from 0.5 to 1.5 $\times$ 10^{-6} m/s^2. The above mentioned thermal properties along with other parameters, such as porosity, dispersivity, and hydraulic conductivity are used in the numerical models.

The USGS program VS2DH (Healy and Ronan 1996) assumes that streambeds are near saturation and therefore use a linear thermal conductivity function. Complications arise as the composition of stream sediments vary laterally, thus changing the physical properties. The software is free and it can be downloaded along with the documentation at http://water.usgs/nrp/gwsoftware/.

A good field example of how to use temperature data to evaluate the distribution of groundwater flux in a sandy streambed environment is given in Example 6.7. Examples of how temperature data were used to evaluate hydraulic conductivities are found in Stonestrom and Constantz 2003; Su et al. 2004; and Burrow et al. 2005). Example 6.7 is followed by specific field methods to install and retrieve temperature data from different sensor equipment.

Example 6.7 Conant Jr. (2004) provides one of the first good examples of presenting detailed spatial and time-varying temperature sensor data to quantify the distribution and flux along a stream reach. This was part of an investigation to quantify the flux of dissolved-phase tetrachloroethene (PCE) to the stream. In the study subsurface temperatures were measured along 1-m transects, spaced across the stream at 2-m intervals over a 60-m reach of the Pine River in Ontario, Canada. The surficial streambed geology consists of fine sand, with areas of gravel and cobbles. The surficial fluvial sediments are underlain by semi-confining silts, clays, and peats, which locally resulted in water levels extending 0.5 to 1.5 m above the stage of the river (Conant Jr. 2004).

The spatial distribution of streambed temperatures were mapped along transects during the summer in late July and during the winter when the difference in temperature between surface water and groundwater was greatest. Groundwater temperatures were measured with a probe equipped with a temperature sensor that was inserted into the sediments at a depth of 0.2 m

for approximately 30 s before taking a reading. This allowed a rapid succession of readings along transects resulting in hundreds of readings being taken during each time period (Conant Jr. 2004).

In addition to the spatial temperature sensor data, vertical profiles of temperature in the streambed were measured to evaluate changes in temperature with depth. Vertical profiles were measured at 0.1 m intervals to a depth of 0.5 to 0.6 m at driven points. The vertical profiling revealed that the ideal depth for groundwater measurements would have been at 0.3 m (1 ft); however, penetrations to this depth at many locations would have resulted in destroying the probe.

Hydraulic properties of the sediments were estimated by performing numerous slug tests (Chapter 11) in 34 distributed piezometers. Water-quality profiles were measured using the Waterloo Profiler and drivable multilevel samplers. During late July surface-water temperatures showed diel cycling patterns (Chapter 7) fluctuating 4°C between morning and evening, while groundwater temperatures remained constant (Conant Jr. 2004). The constancy of the groundwater temperatures were tested in the morning and evening at various locations to verify this relationship.

Vertical fluxes in $L/m^2 \cdot day$ were determined at the piezometer locations where slug testing was performed to estimate horizontal and vertical hydraulic conductivity values. The change in head (dh) was measured from the level measurement in the piezometer and the river stage and the flow path length (dl) was assigned from the center of the piezometer screen to the top of the streambed. Porosity values needed for velocity calculations were estimated using Time Domain Reflectometery (TDF) equipment (Chapter 4), where measurements were taken near the piezometers. A sample calculation of vertical flux converted from m/day flowing through an area of 1 m^2 to $L/m^2 \cdot day$ is given using Equation 6.6 followed by a velocity calculation (using Euation 5.4). All calculations were normalized to 10°C (the ambient groundwater temperature) and placed into a table (Conant Jr. 2004). The velocities were used to estimate the time for contaminated groundwater to move through approximately 2 m of stream sediments.

$$\text{Groundwater flux} = q_v = -K_v \times \frac{\partial h}{\partial l} \tag{6.6}$$

where K_v = vertical hydraulic conductivity

$$q_v = 5.86 \times 10^{-3}\,\text{cm/s} \times 0.047$$

$$= 2.75 \times 10^{-4}\,\text{cm/s}\left(\frac{1\text{ m}}{100\text{ cm}}\right)\left(\frac{86{,}400\text{ s}}{1\text{ day}}\right)(1\text{ m}^2)\left(\frac{1000\text{ L}}{1\text{ m}^3}\right) = 238\left(\frac{\text{L}}{\text{m}^2/\text{day}}\right), \text{ and}$$

Groundwater velocity (vertical) is:

$$V_v = 238\,\frac{\text{L}}{\text{m}^2\text{ day}}\left(\frac{1\text{ m}^3}{1000\text{ L}}\right)\left(\frac{1}{0.45}\right) = 0.53\text{ m/day}$$

Summer and winter groundwater fluxes were plotted against streambed temperatures at each piezometer location. The summer fluxes increase as streambed temperatures decrease (compared to surface-water temperatures), and in winter fluxes increase as streambed temperatures decrease (compared with warmer groundwaters). This is a common pattern noted by other investigators (Stonestrom and Constantz 2003 and associated references). The resulting trends were approximated and are shown in Figure 6.29.

The "best fit of data" shown in Figure 6.29 is a second order polynomial fit with significant R^2 values (0.81 for winter and 0.66 for summer). The winter fit is better (tighter fit) because the surface-water temperature range was less variable than in summer (Figure 6.29). The scatter of data (points not shown) around the second order polynomial fit in Figure 6.29 can largely be attributed to viscosity changes from variable mixing temperatures affecting the hydraulic conductivities (Chapter 5).

The equations corresponding to the "best fit of data" were used to estimate fluxes where only temperature data were available (Figure 6.30).

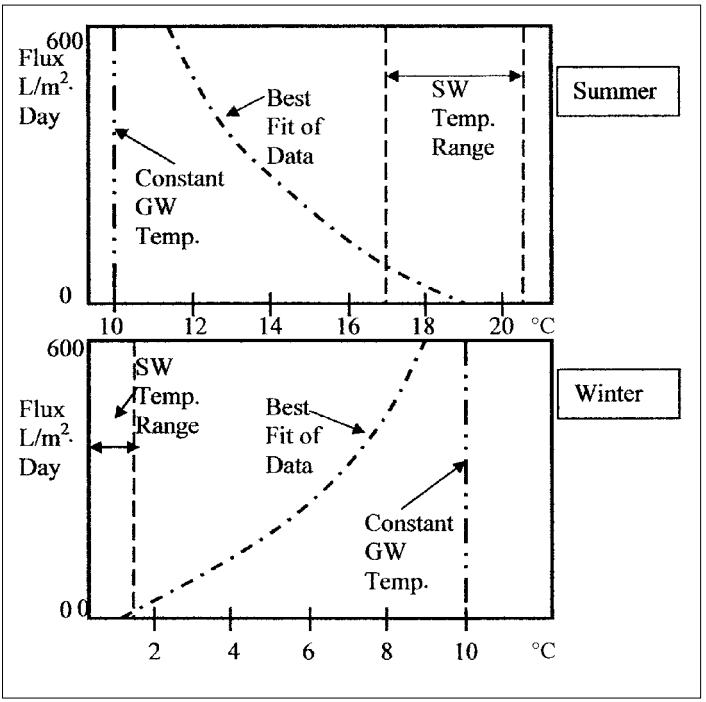

Figure 6.29 Flux discharge in $L/m^2 \cdot$ day versus temperature in °C (X axis) plotted for summer and winter conditions along a 60-m reach of the Pine River Ontario, Canada, modified from Conant Jr. 2004.

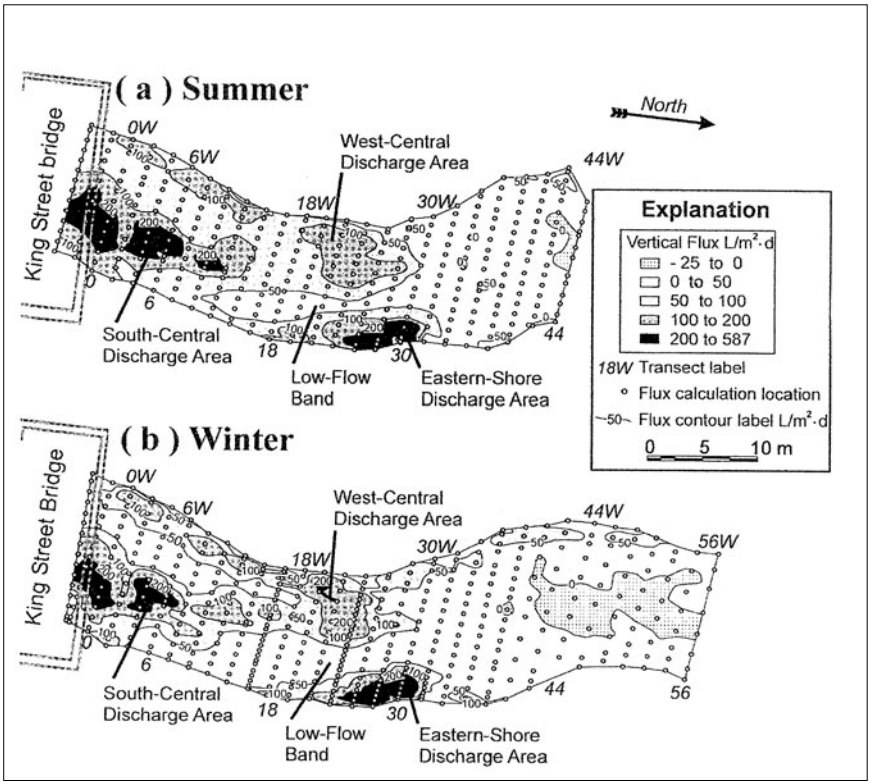

Figure 6.30 Distribution of groundwater fluxes in $L/m^2 \cdot$ day in a 60-m stretch of the Pine River in Ontario, Canada. (*From Conant Jr.* (*2004*), *reprinted from Ground Water with permission of the NGWA, copyright 2004.*)

The contours of groundwater flux data show distinctive patterns of high discharge and band of low flux that corresponds to higher clayey content in the streambed sediments.

It should be noted that the example by Conant Jr. (2004) is site-specific (geologic setting) and time-specific, therefore the graphs in Figure 6.29 should not be used at other sites. They are given as an illustration of how temperature data can be used to estimate trends in physical flow properties in a groundwater/surface-water setting. The limitations for this application are described in the paper but can be summarized as the following:

- Groundwater temperatures underlying the aquifer are essentially constant.
- Surface-water temperatures are spatially uniform.
- The difference between groundwater and surface-water temperatures is large or at a maximum.

- Flow conditions have been constant for a long time before readings were taken (effects from stage changes, bank storage, or induced infiltration from pumping are not present).
- Thermal properties of shallow deposits are essentially uniform.

Based upon discussions with other investigators, larger, more armored streams prove difficult for detailed spatial analysis because of difficulty of penetration through cobbles and excessive stream velocities in the riffles (Stephen Custer, personal communication, Figure 6.31). Some streambed sediments are confining enough in gaining reaches to create heaving sands conditions (Chapter 8). Being able to gain sufficient penetration to measure groundwater temperatures becomes an issue if the exchange from the head of gravel bars to pools is deep reaching. One

Figure 6.31 Steve Custer power drilling a piezometer borehole on the Gallatin River, Montana. Note the heavy cobble armor in the stream. (*Photo courtesy of steve custer.*)

wonders whether groundwater flux is being measured or a mixture of ground and surface waters related to hyporheic flow.

Field equipment

Temperature data at specific locations have been collected using well sentinels equipped with temperature sensing capabilities. Various manufacturers sell combinations of level and temperature sensor dataloggers to measure head (level) and temperature simultaneously (Figure 5.29). The output data appears as another column in the output next to level data. Well sentinels can also include a host of other water quality parameters, however the costs increase correspondingly. There has been a need to expand the capabilities of obtaining spatial and temporal temperature data. For example, evaluate temperature gradients, the movement of heat with groundwater flow, and heat as a tracer described in the references. Manufacturers have designed a variety of sensor equipment at increasingly reduced costs. Some of the more commonly used sensors are pictured and described in Stonestrom and Constantz (2003), however a practical review of the different capabilities of differing temperature dataloggers was more recently presented by Johnson et al (2005). Well sentinels have been described for level measurements in Chapter 5, with additional applications in Chapters 9 and 10; however, a simple inexpensive stand alone temperature logger is given as another illustration of field use.

Johnson et al (2005) performed an evaluation of wireless/stand alone temperature loggers. Many of the devices previously described in the references above were compared with the Thermochron iButton manufactured by Dallas semiconductor or Dallas, Texas at (http://www.ibutton.com/). The iButton temperature logger was originally developed to monitor temperature sensitive cargo during transit (e.g., meat). (It has a temperature range from −40°C to 85°C). An example of how to use these devices is in Example 6.8. Johnson et al (2005) pointed out four principal advantages of the iButton logger over other wired or stand alone temperature loggers.

1. Being wireless, the instrument does not have to be located in a control-recording system.
2. Its small size (just over 17 mm) allows for deployment in small-diameter, hand-driven or direct-push monitoring wells.
3. Multiple loggers are easily suspended within a fully screened monitoring well (Chapter 8) to obtain a high-resolution (within 0.5°C) vertical temperature profile, and
4. The relatively low cost (ratio of 10 units to one) allows for detailed spatial and temporal studies.

Example 6.8 To use iButton temperature loggers one must purchase a starter kit ($125 in 2007) that comes with an iButton, a mounting bracket, an iButton dual receptor/receiver, and a USB to 1wire/iButton adaptor that is inserted into a PC computer. The communication software and drivers are downloaded at http://www.ibutton.com/ibuttons/1921Kit.html/. If f has trouble getting set up one can call the technical support number listed at the Web site. One must push the iButton fairly hard into the dual receptor and it will snap into place (Figure 6.32).

Figure 6.32 shows the dual receptor, an iButton logger in a bracket, and a couple of loose iButtons. Each iButton logger has a unique identification code and can record up to 2048 measurements per deployment. They support a lifetime of one million readings.

As an example of configuring iButtons for a vertical temperature profile, take a wooden dowel or thin PVC tubing to mount the iButton brackets to at a desired spacing. One can place two iButtons (front and back) at each location for additional data control and as a backup, should one unit fail to work properly. Foam packing material can be attached between the iButton intervals to isolate the different chambers. More or less duct tape (Chapter 9) can be added until a good fit is achieved. The dowel or PVC tubing configuration can then be inserted into the monitoring well Figure 6.33.

Tracer studies

Tracer studies have been used for years in determining "time of travel" in streams (Wilson 1968; Kilpatrick 1970). Methods include injecting

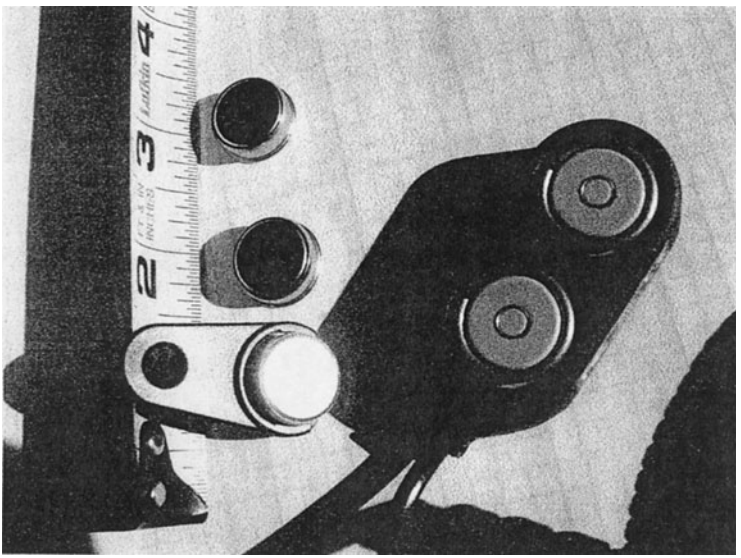

Figure 6.32 Close-up of iButtons, one in a bracket and the dual receptor/receiver.

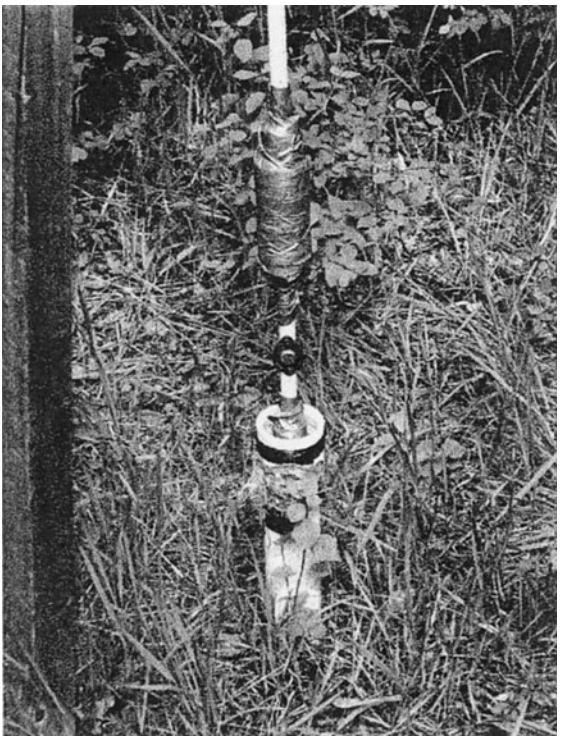

Figure 6.33 Deployment of iButtons mounted on a PVC tube, separated by packing materials attached with duct tape into a 2-in (5.1-cm) fully screened monitoring well near the Middle Fork of the Flathead River. (*Photo courtesy of Bill Woessner.*)

chloride or bromide or a fluorescent dye (Smart and Laidlaw 1977). Tracer studies conducted for aquifer velocities and aquifer properties are presented in Chapters 13, 14 and 15. However, separate discussion of tracer-study applications for groundwater/surface-water interactions is needed because of the trends shown about storage (Bencala and Walters 1983) and dynamic movement within stream sediments (Castro and Hornberger 1991). Additionally, tracer applications to estimate flow discharge for small gaining streams are discussed and presented after Example 6.7.

Time-of-travel studies are useful when stream velocities cannot be measured from ice cover or steep rocky channels, or when one wishes to evaluate dispersal patterns from waste or thermal pollution (Kilpatrick 1970).

A detailed comparison of eight fluorescent dyes was presented by Smart and Laidlaw (1977). Their evaluation yielded a recommendation of three: rhodamine WT (orange), lissamine FF (green) and amino G (blue). Evaluation criteria such as pH of waters, temperature effects,

salinity (for estuarine studies), resistance to adsorption, and toxicity were used in the analysis. Kilpatrick (1970) found that rhodamine WT could be used at a lower concentration (20% solution compared to 40% solution) than rhodamine BA and at a lower cost.

For time-of-travel studies, the Equation 6.7 from Kilpatrick (1970) is helpful.

$$V_d = 3.4 \times 10^{-4} \left(\frac{Q_m L}{V} \right)^{0.93} C_p \tag{6.7}$$

where V_d = Volume of dye in liters
Q_m = Discharge in the reach in ft^3/s
L = Length of reach in miles
V = Mean stream velocity in ft/s
C_p = Peak concentration and micrograms per liter (μg/L) desired at the lower end of the reach

Equation 6.7 represents the case where $C_p = 1$ μg/L at the lower end of the reach and for a stream velocities that range between 0.2 and 5.0 ft/s. To increase the peak concentration at the lower end of the reach (C_p), a proportionately greater volume of dye is needed. The U.S. Geological Survey does not recommend exceeding 10 μg/L as a peak concentration (Kilpatrick 1970; Kilpatrick and Cobb 1985). Equation 6.7 is presented graphically in Figure 6.34 to evaluate dye volumes directly.

Tracers are also helpful in determining the movement of groundwater in near-channel sediments. This may have implications for understanding the hyporheic zone (Section 6.2) and stream ecology (Stanford and Ward 1988, 1993; Meyer 1997; Dahm et al. 1998; Dahm et al. 2006).

A stream reach can be selected that has a riffle zone or shallowing area where the tracer can readily enter the streambed sediments (Figure 6.35). Ideally, there is a place on the downstream end where most of the tracer influenced water can be accounted for (a discharge point). The sampling points should be distributed along the stream reach to be able to obtain a representative distribution of the tracer throughout the stream sediments and within the channel.

Example 6.9 A tracer study was conducted in the North Fork of Dry Run Creek in Shenandoah National Park in Page County, Virginia, by Castro and Hornberger (1991) to evaluate groundwater/surface-water interaction within fluvial sediments in a steep mountain stream (gradient 0.057). A 225-m reach was selected where the spatial variability of the channel characteristics was great. The width of the alluvial materials varied between 22 m and 77 m (Figure 6.36). The surficial flow pattern was dominated by pools and riffles and the study was conducted at low flow.

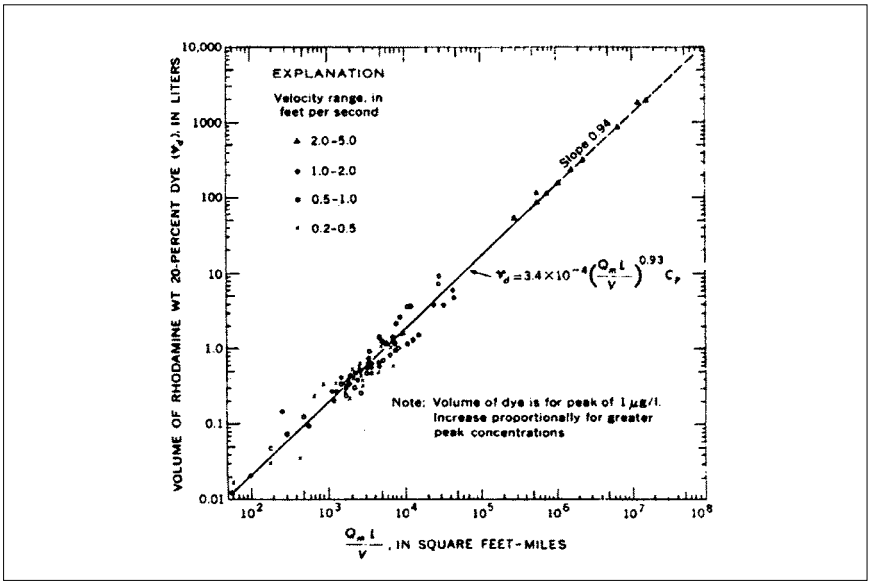

Figure 6.34 Quantity of rhodamine WT 20% dye required for slug injection to produce a peak concentration of 1 µg/L at a distance downstream, L, at a mean velocity, V, and a maximum discharge, Q_m, in the reach [*From Kilpatrick (1970)*].

The (KBr) tracer was mixed with stream water in a 378-L (100-gal) polyethylene tank. On the day before the test, the solution was mixed via a small pump for 8 h. During the test, the tank was stirred manually twice a day during the injection period. The tracer concentration in the tank was 48.6 g/L. The tracer was introduced into the stream at a riffle zone at a rate of 50 mL/min over the 93-h injection period (approximately 0.05 to 0.1% of the

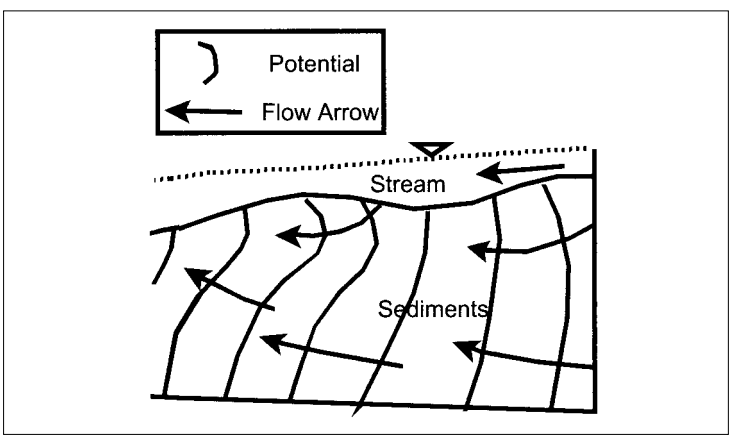

Figure 6.35 Longitudinal profile of a stream indicating where surface water enters stream sediments. [*Adapted from Lee and Cherry (1978).*]

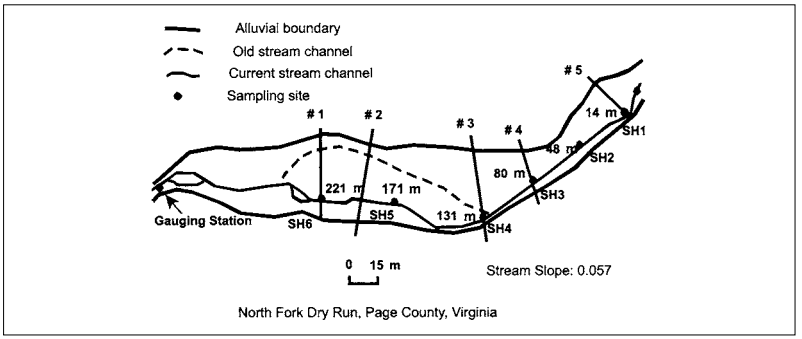

Figure 6.36 Plan view of study area in Shenandoah National Park, Virginia. [*Adapted from Castro and Hornberger (1991). Used with permission of American Geophysical Union (1991.)*]

total discharge). The injection rate was checked using a bucket and stopwatch several times during the injection period.

Six surface water sampling sites (SH1 through SH6) and a series of transects were established to evaluate the distribution of tracer in the sediments (Figure 6.36). Groundwater samples were obtained from hand-dug wells along each transect near the active channel and from an old abandoned channel within the alluvial plain. Each hole was dug deep enough to fill each hole with 0.15 to 0.3 m of standing water. Additionally, a few cased wells were drilled with completion depths ranging from 0.75 to 1.75 m. These were up to 24 m from the active stream to provide sampling stations from deeper sediments (Figure 6.37).

Samples were collected from the stream and gravel bed every 0.5 to 1.0 h until the arrival of the leading edge of the tracer. Subsequently, samples were collected every 4 h while concentrations were relatively constant during injection of the tracer. Following tracer injection, samples were collected at 0.5 to 1.0, 4, 8, and 24 h, and ultimately weekly (Castro and Hornberger 1991).

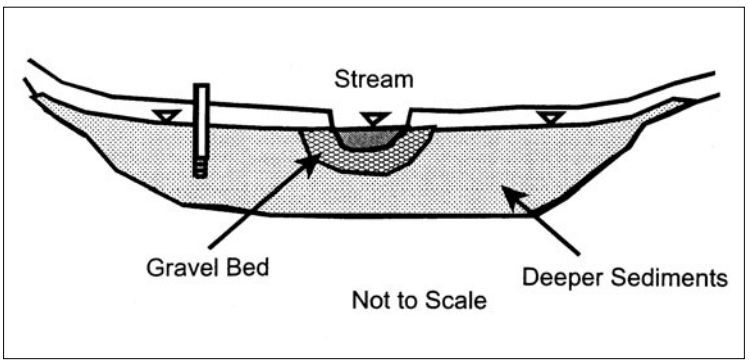

Figure 6.37 Schematic cross section showing mixing zones in the stream, gravel bed, and deeper sediments.

A specific ion electrode (accurate to 0.25 mg/L) was used to measure bromide concentrations (peak concentrations were near 30 mg/L). This was used in conjunction with a pH/conductivity/temperature meter. Because of the low ionic strength of the stream water, all samples and standards, prior to analysis, were mixed with an ionic strength adjuster (ISA), 2 *M* potassium nitrate, to the ratio of 1:10 (ISA:sample) (Castro and Hornberger 1991). Standards were made with upstream water and compared with standards made with deionized water with no differences found.

Significant tracer concentrations were found in wells at distances of 8 m and 16 m from the active stream channel after concentrations within the stream had cleared, supporting the concept of long-term storage. Concentration tails (abrupt concentration arrivals followed by gradual decreasing trends; see Chapter 13) at surface-water sites waned after 4 to 6 days, while similar tails in wells lingered approximately 20 days before clearing to background levels. This study showed how mixing within the hyporheic zone is active at significant distances away from the main channel and that movement away from and back into the channel through the bottom sediments does occur.

Another type of tracer test in surface-water/groundwater interactions is the continuous tracer injection method. This was developed by the USGS (Kirkpatric and Cobb 1985) for low-flow streams that are gaining (groundwater discharge) and have too little discharge to measure using gauging equipment. It is important to stress that this method works well for reaches that are gaining and 1 km or less in length.

The procedure is to continuously inject a known quantity of tracer for 24 h to saturate the sample measuring sites. A tracer reservoir consisting of Rhodamine WT dye, chloride, or bromide at a known concentration is input into the stream from a reservoir at a constant rate (Figure 6.38), using a very accurate delivery pump, such as a one made by Fluid Metering Inc. (www.fmipump.com). A peristaltic pump is not sufficiently accurate to deliver the constant quantity required.

Once a steady-state concentration is measured at the bottom end of the stream, one proceeds quickly to the other sampling sites up stream to the reservoir location. The flow in the stream is calculated using the simple relationship shown in Equation 6.8.

$$\text{Flow(L/min)} = \frac{\text{injection rate (mg tracer/min)}}{\text{tracer concentration in downstream sample (mg/L)}} \tag{6.8}$$

Example 6.10 A study was conducted to determine the source of zinc loading at the reclaimed Comet mine site up High Ore Creek in southwestern Montana (Sudbrink 2007). A series of piezometer transects were installed using the plate-jack method (Figure 6.21), along with surface-water gauging sites to establish the interaction of groundwater with surface water. The stream flow during spring runoff was measurable using gauging equipment (>2 cfs, 56.6 L/s),

Figure 6.38 Continuous injection of Rhodamine WT dye in a continuous injection tracer test. Shown is the reservoir (5-gal jug) and injection pump with tubing.

however by late summer the flow dropped to a fraction of a cfs (<28.3 L/s), which was estimated using the continuous injection tracer method. Two tests were conducted. The first test (July 28, 2005) was injected above a rock-lined channel, resulting in some uncertainty in the results (HOC 1 thru HOC 3), therefore a second test was done (August 25, 2005) beginning below the rock-lined channel with comparable yet more confident results. The data are shown in Table 6.7.

TABLE 6.7 Stream Flow Estimates on High Ore Creek in Southwestern Montana Using the Continuous Injection Tracer Method. (From Sudbrink 2007.)

July 28, 2005			August 25, 2006	
Station	Tracer cfs	Flow meter	Station	Tracer cfs
HOC 1	0.19	0.13		
HOC 2	0.19			
HOC 3	1.9			
HOC 4	0.26		HOC 4	0.246
HOC 5	0.26		HOC 5	0.250
HOC 6	0.27		HOC 6	0.275
HOC 7	0.27		HOC 7	0.278
HOC 8	0.28		HOC 8	0.283
HOC 9	0.29		HOC 9	0.305
HOC 10	0.30		HOC 10	0.325
HOC 11	0.32		HOC 11	0.344
HOC 12	0.33	0.23	HOC 12	0.379
Gain	0.14	0.10	Gain	0.133

Chemical mass balance

The purpose of this section is to give a brief presentation on water-quality indicators at groundwater/surface-water settings and how a mass balance approach can be used to compare general groundwater and surface-water qualities in accounting for gaining streams. A more complete presentation on water chemistry is given in Chapter 7.

If minipiezometers are installed in a gaining stream reach and the tops are close enough to the stream surface, they will flow like miniartesian wells. These can then be tested for water quality parameters such as specific conductance, temperature, and dissolved oxygen to distinguish water-quality differences between groundwater and surface water. In losing stretches, minipiezometers would have to be completed differently. The minipiezometer casing is driven to the desired depth and plastic tubing is inserted to the bottom of the casing. The minipiezometer casing is twisted and carefully pulled out, leaving the tube as the piezometer. A plastic bag is attached to the tubing and held under the water surface to induce flow into the bag (Lee and Cherry 1978). The bagged water can then be tested for water quality parameters. Redox potential and nutrient dynamics can also be studied within the hyporheic zone (Dahm et al. 1998). The usual practice, however, is to insert a small tube and pull a water-quality sample with a peristaltic pump.

Sometimes a mass-balance approach can be used to account for influxing groundwater into a stream. It is necessary to obtain stream water-quality samples from places where stream gauging data have also been collected. The groundwater quality must be characterized from "representative" well samples collected near the active stream. It is a good idea to identify whether significant changes with time are occurring, as this may complicate the analysis. If the two water chemistries are distinctive enough, it is possible to make a comparison between the two and perform an estimate of the influx of groundwater. The approach is to use Equation 6.9:

$$Q_{sw,\text{in}} \times WQP + S_{gw,\text{in}} \times WQP = Q_{sw,\text{ out}} \times WQP \qquad (6.9)$$

where $Q_{sw,\text{in}}$ = stream flow into the area, in L^3/t
WQP = water quality parameter of choice (consistent with flow term)
$S_{gw,\text{in}}$ = groundwater flow into the area, in L^3/t
$Q_{sw,\text{out}}$ = stream flow out of the area, in L^3/t

The objective is to use the streamflow and water-quality data to evaluate the groundwater flow into the area ($Q_{gw,\text{in}}$). It can be tested using several parameters for comparison purposes.

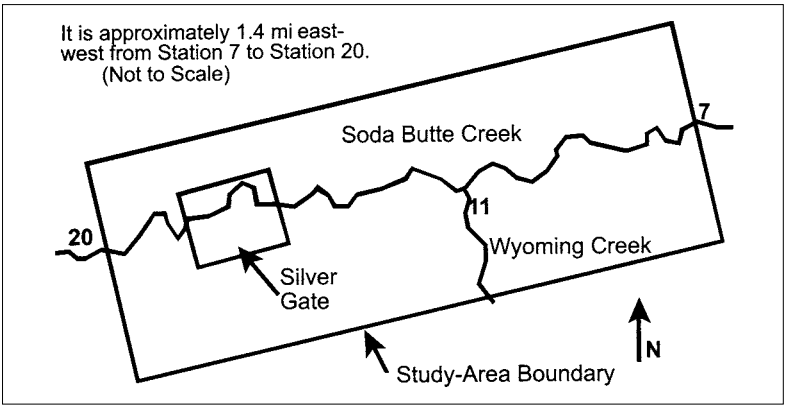

Figure 6.39 Schematic of Soda Butte Creek near Silver Gate, Montana, showing surface water gauging station and water-quality sites used in a mass-balance analysis of groundwater influx into the study area.

Example 6.11 In the study conducted by English (1999) near Silver Gate, Montana, a mass balance approach was taken to estimate the influx of groundwater into Soda Butte Creek as it flows through the study area (Example 6.5). Stream gauging stations 7, 11, and 20 were used in the analysis along with their respective water chemistries, along with local shallow wells (less than 65 ft below ground surface) (Figure 6.39). Station 7 is on Soda Butte Creek just downstream from the confluence of a tributary (Sheep Creek). Station 11 is on Wyoming Creek, a tributary in the middle of the study area, just before it merges with Soda Butte Creek. The water quality and gauging data only reflect this contribution. Station 20 is on Soda Butte Creek at the exit point of the study area. The respective water qualities and gauging data are shown in Table 6.8.

Using the following form of Equation 6.9 and calcium as an example, the groundwater inflow ($Q_{gw,\text{in}}$) was estimated. This same process was

TABLE 6.8 Water Quality and Stream Gauging Data near Silver Gate, Montana [From English (1999)]

Well	Depth (ft bgs*)	SC (μmhos/cm)	Ca (mg/L)	Mg (mg/L)	Na (mg/L)	Cl (mg/L)
5-well ave	35–65	270	32.68	7.35	4.23	0.66
SW Station	Flow (L/s)	SC (μmhos/cm)	Ca (mg/L)	Mg (mg/L)	Na (mg/L)	Cl (mg/L)
7	192.86	189	22.1	5.84	3.93	0.52
11	15.86	81.1	5.37	1.96	8.1	0
20	277.82	218	26.5	6.02	3.87	0.6

*Below ground surface

TABLE 6.9 Summary of Estimated Groundwater Influx in L/sec, Based on Groundwater Quality Data near Silver Gate, Montana [From English (1999)]

Specific cond.	Calcium	Magnesium	Sodium	Chloride	Average
82.1	93.4	70.8	45.3	99.1	78.1

repeated for the other five water-quality parameters to obtain an average estimate for ($Q_{gw,\text{in}}$). The results are tabulated in Table 6.9.

$$192.86 \text{ L/s} \times [22.1 \text{ mg/L}] + 15.86 \text{ L/s} \times [5.37 \text{ mg/L}]$$

$$+ Q_{gw,\text{in}} \times [32.68 \text{ mg/L}] = 277.82 \text{ L/s} \times [26.5 \text{ mg/L}]$$

The average estimate of groundwater influx from stream gauging was 76.5 L/s (2.7 cfs).

6.5 Summary

Groundwater/surface-water interactions within riverine systems are complex. A variety of flow scenarios occur at many scales. Interactions of groundwater/surface-water within the hyporheic and riparian zones, coupled with biotic distributions and chemical gradients suggest the need for hydrogeologists to team up with other professionals to understand these systems. The field methodologies presented will assist the hydrogeologist in collecting meaningful data to better manage the mass balance components occurring within a watershed.

References

Anderson, M.P., 1989. Hydrogeologic Facies Models to Delineate Large-Scale Spatial Trends in Glacial and Glaciofluvial Sediments. *Geological Society of America Bulletin*, 101, pp. 501–511.

Anderson, M.P., 2005. Heat as a Ground Water Tracer. *Ground Water,* Vol. 43, No. 6, pp. 951–968.

Azadpour-Keeley, A., 2005. Microbiological Field Sampling and Instrumentation in Assessment of Soil and Groundwater Pollution. *In Environmental Instrumentation and Analysis Handbook*, Downs, R. and Lehr, J.H. (eds), John Wiley and Sons, Inc. 1068 pp.

Bencala, K.E., and Walters, R.A., 1983. Simulation of Solute Transport in a Mountain Pool-and-Riffle Stream: A Transient Storage Model. *Water Resources Research*, Vol. 19, No. 3, pp. 718–724.

Bencala, K.E., 1993. A Perspective on Steam-Catchment Connections. *Journal of North American Benthological Society*, Vol. 12, No. 1, pp. 44–47.

Borduin, M.B., 1999. *Geology and Hydrogeology of the Sand Creek Drainage Basin, Southwest of Butte, Montana*. Master's Thesis, Montana Tech of the University of Montana 103 pp.

Brayton, M., 1998. *Recovery Response from Conservation Methods in Wells Found in the Basal Eagle Sandstone, Petroleum County*, Montana. Master's Thesis, Montana Tech of the University of Montana, 68 pp.

Brunke, M., and Gonser, T., 1997. The Ecological Significance of Exchange Processes between Rivers and Groundwater. *Freshwater Biology*, Vol. 37, No. 1, pp. 1–31.

Buchanan, T.L., and Sommers, W.T., 1968. *Stage Measurement at Gauging Stations*. Techniques of Water-Resources Investigations of the U.S. Geological Survey, Book 3, Chapter A7. U.S. Geological Survey, Washington, DC.

Buchanan, T.L., and Sommers, W.T., 1969. *Discharge Measurements at Gauging Stations*. Techniques of Water-Resources Investigations of the U.S. Geological Survey, Book 3, Chapter A8. U.S. Geological Survey, Washington, DC.

Burrow, K.R., Constanz, J., and Fujii, R., 2005. Using Heat as a Tracer to Estimate Dissolved Organic Carbon Flux beneath a Restored Wetland. *Ground Water*, Vol. 43, No. 4, pp. 545–556.

Carter, J.L., Resh, V.H., Hannaford, M.J., and Myeres, M.J., 2006. Macroinvertebrates as Biotic Indicators of Environmental Quality; In *Methods in Stream Ecology, 2nd edition*; Hauer, F.R. and Lamberti, G.A. (eds.). Academic Press, Elsevier Inc., Burlington, MA, pp. 805–831.

Castro, N.M., and Hornberger, G.M., 1991. Surface-Subsurface Water Interaction in an Alluviated Mountain Stream Channel. *Water Resources Research*, Vol. 27, No. 7, pp. 1613–1621.

Chow, V.T., 1959. *Open Channel Hydraulics*. McGraw-Hill, New York.

Conant, B. Jr., 2004. Delineating and Quantifying Ground Water Discharge Zones Using Streambed Temperature. *Ground Water*, Vol. 42. No. 2, pp. 243–257.

Culp, J.M., and Baird, D.J., 2006. Establishing Cause-Effect Relationships in Multi-Stressor Environments; In *Methods in Stream Ecology, 2nd edition*; Hauer, F.R., and Lamberti, G.A. (eds.), Academic Press, Elsevier Inc., Burlington, MA, pp. 835–854.

Dahm, C.N., Grimm N.B., Mamonier P., Valett H.M., and Vervier P., 1998. Nutrient Dynamics at the Interface between Surface Waters and Groundwaters. *Freshwater Biology*, Vol. 40, pp. 427–451.

Dahm, C.N., Valett, H.M., Baxter, C.V., and Woessner, W.W., 2006. Hyporheic Zones; In *Methods in Stream Ecology, 2nd edition*; Hauer, F.R., and Lamberti, G.A. (eds.), Academic Press, Elsevier Inc., Burlington, MA, pp. 119–142.

English, A., 1999. *Hydrogeology and Hydrogeochemistry of the Silver Gate Area, Park County, Montana*. Master's Thesis, Montana Tech of the University of Montana, 131 pp.

Fetter, C.W., 1994. *Applied Hydrogeology*, *3rd Edition*. Macmillan College Publishing Company, New York, 691 pp.

Gore, J.A., 2006. Discharge Measurements and Streamflow Analysis; In *Methods in Stream Ecology, 2nd edition*; Hauer, F.R., and Lamberti, G.A. (eds.), Academic Press, Elsevier Inc., Burlington, MA, pp. 51–77.

Gregory, S.V., Swanson, F.J., McKee, W.A., and Cummins, K.W., 1991. An Ecosystem Perspective of Riparian Zones. *Bioscience,* Vol. 41, pp. 540–551.

Grimm, N.B., and Fisher, S.G., 1984. Exchange between Interstitial and Surface Water: Implications for Stream Metabolism and Nutrient Cycling. *Hydrobiologia*, *Vol. III*, pp. 219–228.

Gross, L.J., and Small, M.J., 1998. River and Floodplain Process Simulation for Subsurface Characterization.*Water Resources Research*, Vol. 34, No. 9, pp. 2365–2376.

Hansen, E.A., 1975. Some Effects of Groundwater on Brown Trout Redds. *Transactions of American Fisheries Society*, Vol. 104, No. 1, pp. 100–110.

Hatch, C.E., Fisher, A.T., Revenaugh, J.S., Constantz, J., and Reuhl, C., 2006. Quantifying Surface Water-Groundwater Interactions Using Time-Series Analysis Using Thermal Streambed Records: Methods Development. *Water Resources Research*, Vol. 42, W10410, doi:10.1029/2005WR004787, 2006.

Hauer, F.R., and Lamberti, G.A.(eds.), 2006. *Methods in Stream Ecology, 2nd edition*, Academic Press, Elsevier Inc., Burlington, MA, 877 pp.

Hauer, F.R., and Resh, V.H., 2006. Macroinvertebrates; In *Methods in Stream Ecology, 2nd edition*; Hauer, F.R., and Lamberti, G.A. (eds.), Academic Press, Elsevier Inc., Burlington, MA, pp. 435–463.

Healy, R.W., and Ronan, A.D., 1996. Documentation of the Computer Program VS2DH for Simulation of Energy Transport in Variably Saturated Porous Media-Modification of the U.S. Geological Survey's Computer Program VS2DT. *U.S. Geological Survey Water-Resources Investigation Report 96-4230*, 36 pp.

Hill, A.R., 1993. Nitrogen Dynamics of Storm Runoff in Riparian Zones. *Journal of Environmental Quality*, Vol. 25, pp. 743–755.

Huggenberger, P., Hoehn, E., Beschta, R., and Woessner W., 1998. Abiotic Aspects of Channels and Floodplains in Riparian Ecology. *Freshwater Biology*, Vol. 40, pp. 407–425.

Johnson, A.N., Boer, B.R., Woessner, W.W., Stanford, J.A., Poole, G.C., Thomas, S.A., and O'Daniel, S.J., 2005. Evaluation of an Inexpensive Small-Diameter Temperature Logger for Documenting Ground Water–River Interactions. *Groundwater and Remediation*, November 2005, Vol. 25, Issue 4, pp. 101–105.

Kilpatrick, F.A., 1970. Dosage Requirements for Slug Injections of Rhodamine BA and WT dyes. In *Geological Survey Research*, U.S. Geological Professional Paper 700-B, pp. B250-B253.

Kilpatrick, F.A., and Cobb, E.D., 1985. Measurement of Discharge Using Tracers. Techniques of Water-Resources Investigations of the U.S. Geological Survey, Book 3, Chapter A16.

Lee, D.R., and Cherry, J.A., 1978. A Field Exercise on Groundwater Flow using Seepage meters and Mini-piezometers. *Journal of Geological Education*, Vol. 27, pp. 6–10.

Lowe, R.L., and LaLiberte, G.D., 2006. Benthic Stream Algae: Distribution and Structure; In *Methods in Stream Ecology, 2nd edition*; Hauer, F.R., and Lamberti, G.A., (eds.), Academic Press, Elsevier Inc., Burlington, MA, pp. 327–339.

Meyer, J.L., 1997. Stream Health: Incorporating the Human Dimention to Advance Stream Ecology. *Journal of the North American Benthological Society*, Vol. 16, No. 2, pp. 439–447.

Mial, A.D., 1996. *The Geology of Fluvial Deposits: Sedimentary Facies, Basin Analysis, and Petroleum Geology*. Springer-Verlag, New York, 582 pp.

Modica, E., 1998. Analytical Methods, Numerical Modeling, and Monitoring Strategies for Evaluating the Effects of Ground-water Withdrawals on Unconfined Aquifers in the New Jersey Coastal Plain. *USGS Water Resources Investigation Report*, 98–4003, 66 pp.

Newbury, R.W., and Bates, D.J., 2006. Dynamics of Flow; In *Methods in Stream Ecology, 2nd edition*; Hauer, F.R., and Lamberti, G.A. (eds.), Academic Press, Elsevier Inc., Burlington, MA, pp. 79–101.

Palmer, M.A., 1993. Experimentation in the Hyporheic Zone: Challenges and Prospects. *Journal of the North American Benthological Society*, Vol. 12, No. 1, pp. 84–93.

Roberts, M., and Waren, K., 1999. North *Fork Blackfoot River Hydrologic Analysis*. Montana Department of Natural Resources and Conservation, Helena, MT, 36 pp.

Rosenberry, D.O., and Morin, R.H., 2006. Use of an Electromagnetic Seepage Meter to Investigate Temporal Variability in Lake Seepage. *Ground Water*, Vol 42. No. 1, pp. 68–77.

Sanders, L.L., 1998. *A Manual of Field Hydrogeology*. Prentice-Hall, Upper Saddle River, NJ, 381 pp.

Smart, P.L., and Laidlaw, I.M.S., 1977. An Evaluation of Some Fluorescent Dyes for Water Tracing. Water *Resources Research*, Vol. 13, No. 1, pp. 15–33.

Sophocleous, M., Koussis A., Martin, J.L., and Perkins, S.P., 1995. Evaluation of Simplified Stream-Aquifer Depletion Models for Water-Rights Administration. *Ground Water*, Vol. 33, No. 4, pp. 579–588.

Stanford, J.A., and Ward, J.V., 1988. The Hyporheic Habitat of River Ecosystems. *Nature*, Vol. 335, pp. 64–66.

Stanford, J.A., and Ward, J.V., 1993. An Ecosystem Perspective of Alluvial Rivers: Connectivity and the Hyporheic Corridor. *Journal of the North American Benthological Society*, Vol. 12, No. 1, pp. 48–60.

Stonestrom, D.A., and Constantz, J., 2003. Heat as a Tracer of Water Movement near Streams. In *Heat as a Tool for Studying the Movement of Ground Water Near Streams*, Stonestrom, D.A., and Constanz, J. (eds.), USGS Circular 1260. Reston, Virginia: USGS, pp. 1–6.

Stanford, J.A., 2006. Landscapes and Riverscapes; In *Methods in Stream Ecology, 2nd edition*; Hauer, F.R., and Lamberti, G.A. (eds.), Academic Press, Elsevier Inc., Burlington, MA, pp. 3–21.

Stumm, W., and Morgan, J.J., 1996. *Aquatic Chemistry*, *3rd Edition*, John Wiley & Sons, New York, 1022 pp.

Su, G.W., Jasperse, J., Seymour, D., and Constantz, J., 2004. Estimation of Hydraulic Conductivity in an Alluvial System Using Temperatures. *Ground Water,* Vol. 42, No. 6, pp. 890–901.

Tank, J.L., Bernot, M.J., and Rosi-Marshall, E.J., 2006. Nitrogen Limitation and Uptake; In *Methods in Stream Ecology, 2nd edition*; Hauer, F.R., and Lamberti, G.A. (eds.) Academic Press, Elsevier Inc., Burlington, MA, pp 213–238.

Triska, F.J., Kennedy, V.C., Avanzino, R.J., Zellweger, G.W., and Bencala, K.E., 1989. Retention and Transport of Nutrients in a Third-Order Stream in Northwestern California: Hyporheic Processes. *Ecology,* Vol. 70, No. 6, pp. 1893–1905.

University of Wyoming, College of Agriculture, 1994. *Irrigation Water Measurement, Irrigation Ditches and Pipelines*. Cooperative Extension Service Bulletin 583 R, University of Wyoming Laramie, WY, 70 pp.

U.S. Geological Survey (USGS), 1980. *National Handbook of Recommended Methods for Water-Data Acquisition (Updates).* Office of Water Data Coordination, U.S. Geological Survey. Reston, VA, U.S. Department of Interior.

Wallace, J.B., Grubaugh, J.W., and Whiles, M.R., 1996. Biotic Indices and Stream Ecosystem Process: Results from an Experimental Study. *Ecological Applications*, Vol. 6, pp. 140–151.

Walton, W.C., 1970. *Groundwater Resource Evaluation*. McGraw-Hill, New York, 664 pp.

Wilson, J.F., 1968. An Empirical Formula for Determining the Amount of Dye Needed for Time-of-Travel Measurements in Geological Survey Research. *U.S. Geological Survey Professional Paper 600-D*, pp. D54-D56.

Winter, T.C., Harvey, J.W., Franke, O.L., and Alley, W.M., 1998. Ground Water and Surface Water: A Single Resource. *USGS Circular,* 1139, 79 pp.

Woessner, W.W., 1998. Changing Views of Stream-Groundwater Interaction. In Van Brahana, J., Eckstein Y., Ongley L.W., Schneider R., and Moore, J.E., (eds.), *Proceedings of the Joint Meeting of the XXVIII Congress of the Intemational Association of Hydrogeologists and the Annual Meeting of the American Institute of Hydrology*. American Institute of Hydrology, St. Paul, MN, pp. 1–6.

Woessner, W.W., 2000. Stream and Fluvial Plain Ground-Water Interactions: Re-scaling Hydrogeologic Thought. *Ground Water*, Vol. 38, No. 3, pp. 423–429.

Wright, J.F., 1995. Development and Use of a System for Predicting the Macroinvertebrate Fauna in Flowing Waters. *Australian Journal of Biology*, Vol. 20, pp. 181–197.

Wroblicky, G.J., Campana M.E., Valett, H.M., and Dahm, C.N., 1998. Seasonal Variation in Surface-Subsurface Water Exchange and Lateral Hyporheic Area of Two Stream-Aquifer Systems. *Water Resources Research*, Vol. 34, pp. 317–328.

This page intentionally left blank

Chapter

7

Water Chemistry Sampling

Chris Gammons

Montana Tech of The University of Montana
Butte, Montana

The purpose of this chapter is to give an overview of some practical considerations regarding how to plan, conduct, and interpret the results of a water-quality study. The discussion focuses mainly on groundwater, but can be applied to surface water sampling as well. Because this topic is very broad, it is not possible to cover everything in a single chapter. A good overview of groundwater sampling protocols and procedures is the U.S. Geological Survey (USGS) Open-File Report 95-399 (USGS 1995). Detailed information on practical and theoretical aspects of water chemistry measurements can be found in Hem (1985). A more recent reference focusing on field methods is the National Field Manual for the Collection of Water-Quality Data (USGS 2005). A large number of textbooks cover more theoretical aspects of environmental water chemistry. Good choices for entry-level students or professionals include Drever (1997), Kehew (2001), and Eby (2004). More advanced textbooks include Langmuir (1997) and Stumm and Morgan (1995). Fetter (1999) and Bedient et al. (1999) are two of the many books that deal with contaminant transport, including both inorganic and organic compounds.

7.1 Have a Plan

The most important step in any water quality investigation is to understand what question or problem you are trying to address, and to design a sampling and analysis plan that will best answer this question within budgetary constraints. With modern instrumentation, it is now possible to analyze any water sample for a bewildering number of analytes and field parameters. But how many of these are critical to the project?

Copyright © 2008, 2001 by The McGraw-Hill Companies, Inc. Click here for terms of use.

Can the project goals be met without collecting *any* samples for laboratory analysis? Although most large-scale projects will require water- quality data, some field problems can be solved by use of simple manual equipment, such as a pH meter, a conductivity meter, or a portable spectrophotometer. In most cases, a rapid field survey using these methods will help screen locations for more detailed field sampling and laboratory work at a later date.

A useful question to ask early in the planning stages is the following: Is the question or problem I am trying to address better served by collection of samples from many different locations at one time, or by collection of samples at many different times at a few locations? For example, a study that seeks to characterize the concentrations of nitrate in an alluvial aquifer on a basin-wide scale would most likely start off by sampling as many groundwater wells as possible, distributed more or less evenly across the area of interest. Ideally, the sample set would include several locations that are far-removed from any nearby source of nitrate contamination to establish a reference or background concentration against which groundwater that has been "polluted" by human activity can be compared. On the other hand, if monitoring of drinking water is the main issue of concern, then it may make more sense to place a few monitoring wells upgradient of the supply well and sample these for a large number of analytes at regular intervals (e.g., monthly, quarterly, or annually) over a long period of time. Other examples of how time-series data may be useful include tracking the rate of migration of contaminant plumes, evaluating the long-term success of remediation activities, or looking at the effects of climate or seasonal land-use practices (e.g., irrigation) on groundwater quality.

Once a method of approach has been defined to meet the project goals, it is highly recommended to formalize these ideas into a Sampling and Analysis Plan (SAP) project document. Rather than a collection of hastily jotted down notes, the SAP should be a carefully written, complete summary of the overall project objectives and methods. To begin with, the SAP should detail the location and frequency of all samples to be collected. It should specify to what level of concentration each analyte will be quantified (often referred to as the "critical reporting value"), the laboratory that will perform this work, and what the estimated costs will be. Standard procedures should be summarized in appendices, and should include information on field safety, equipment operation and maintenance, pre-sampling procedures (such as acid-washing of bottles, preparation of standards, equipment checkout), sampling procedures (calibration protocols, well purging, sample collection), and post-sampling procedures (sample storage, holding times, equipment cleaning and storage). The SAP should also detail any specific quality assurance/quality control (QA/QC) procedures and targets that must be

met during the course of the project. The SAP should be reviewed and endorsed by the project supervisor, and ideally will be sent out for independent review prior to collection of any critical data. Once approved, the SAP should travel with field personnel for reference during collection of field data. Any deviations from the SAP should be noted by the field worker and reported to the project leader.

Quality assurance

The term "quality assurance" is widely used in the environmental field, but its meaning may be vague to a newcomer. Table 7.1 lists six principal quality attributes as defined by the U.S. Environmental Protection Agency (EPA) that should be optimized in any environmental study

TABLE 7.1 Data Quality Attributes for Water Sampling

Attribute	Definition	Practical considerations
Precision	The measure of agreement among repeated measurements of the same property under identical or substantially similar conditions	Precision is optimized if the same equipment and SOPs are followed for all measurements. Quantified by field replicates.
Bias	Systematic or persistent distortion of a measurement process that causes error in one direction	Bias is minimized if field instruments are properly calibrated and SOPs are followed. Check lab bias by running spikes and submitting certified standards as unknowns
Represent-ativeness	The measure of the degree to which data suitably represent a characteristic of a population, parameter variations at a sam pling point, a process condition, or an environmental condition	Examples: purge three well volumes before sample collection; avoid sample contamination from external sources; measure pH and alkalinity in the field (before samples degrade).
Comparability	A qualitative expression of the measure of confidence that two or more data sets may contribute to a common analysis	Comparability will be optimized if different field personnel follow the same standard procedures. Use same equipment when possible.
Completeness	A measure of the amount of valid data obtained from a measurement system	Avoid skipping measurements and procedures. Make checklists. Take good notes.
Sensitivity	The capability of a method or instrument to discriminate between measurement responses representing different levels of the variable of interest	Verify that the analytical methods are capable of detecting the analyte of interest to the required reporting value. Take measures to minimize sample contamination.

(EPA 2002). These include: *precision, bias, representativeness, comparability, completeness,* and *sensitivity*. The combined error from *imprecision* and *bias* determines the overall *accuracy* of the data that are collected. Accuracy is optimized by making sure that all field equipment is clean and properly serviced, and by developing and following standard operating procedures (SOPs) for all sampling and analytical procedures. *Representativeness* refers to how well a given sample or measurement truly reflects the environmental condition of interest. For example, how representative of the aquifer conditions is a groundwater sample that is obtained by bailing a single grab sample from static water in the well? Not very. This is why hydrogeologists have adopted the procedure of purging a well volume at least three times before collecting a sample. Following a standardized procedure also assures *comparability* and *completeness*. A common problem in many big projects is that different field personnel wind up collecting data using different pieces of equipment and different procedures. This makes it difficult to compare the data from one field season to another. As well, people should be discouraged from skipping measurements in the interest of saving time, as this can lead to gaps in the final project database. Finally, with respect to *sensitivity*, the SAP should insure that the method of analysis being employed is capable of detecting the analyte of interest at concentrations below the critical reporting value, and that the sampling SOPs minimize any chance of trace contamination (from filtration equipment, etc.).

It is always a good idea to submit your own QA samples to the laboratory, along with each batch of environmental samples. The type and frequency of QA samples to be collected will be spelled out in your project SAP, but typically these samples include field blanks (i.e., laboratory water passed through the same sampling and filtration equipment and preserved in the same manner as the field samples) and field replicates (identical samples collected in different bottles). You may also consider sending a certified multielement standard of known concentration to the lab (being sure not to identify it as such by the sample ID name). A wide variety of certified standards are available from major chemical supply companies. Another good practice is to occasionally send a few replicate samples to different labs.

What are you sampling for?

Each project will have its own specific set of data to collect, and it is difficult to make general recommendations. However, as a rule it is always a good idea to collect a complete set of field parameters, including water temperature, specific conductance, pH, dissolved oxygen, Eh or ORP, and alkalinity. A routine chemical analysis will also usually include

quantification of a full suite of major and minor cations by inductively coupled plasma (ICP-ES or ICP-MS), and a suite of major anions by ion chromatography (IC). Additional data may help to characterize the chemistry of the waters of interest, as shown in Table 7.2. Most of these procedures are discussed in more detail below. It is worth stressing that seemingly random observations about the color or general appearance of the water sample (such as "the sample was effervescing an odorless gas upon pumping to the surface") may become very important later on. So take good notes, and pass on any information of this type to your project leader.

In projects that involve regulatory compliance, it is usually important to specify between data collection that is "critical" versus "noncritical." Critical data include any measurements or results that have a major bearing on the overall objectives and outcomes of the project. Such data will typically undergo rigorous QA scrutiny to ensure they are of the highest possible quality. Noncritical data include any supporting measurements that help to characterize the environmental system, but do not have a direct bearing on the project outcomes. Although noncritical data may not require QA testing and validation, good field procedures should nevertheless always be followed.

Make a checklist

Once your SAP is complete and you are ready to go in the field, make a checklist of supplies and equipment that you will need. There is nothing worse than spending half a day loading and driving to a field site and then realizing you forgot the key to unlock the well back in the office.

TABLE 7.2 List of Possible Types of Data to Collect for Groundwater Studies

Basic/essential information	Class	Optional information	Class
Water temperature	*i*	Stable isotopes ($\delta^{18}O$, $\delta^{2}H$) of water	*a*
Conductivity (SC, C25)	*i*	Nutrients (nitrate, phosphate, ammonia)	*ts*
pH	*i*	H_2S (very important if present)	*i*
Dissolved oxygen	*i*	Dissolved Fe(II)/Fe(III)	*ts*
ORP or Eh	*i*	Organic compounds	
Alkalinity	*ts*	Dissolved organic carbon	*ts*
Dissolved metals	*a*	Organic contaminants	*ts*
Major anions	*ts*	Pathogens	*ts*
Turbidity	*ts*	Total dissolved solids	
Color/appearance of water	*i*	Age dating	*ts*

i = immediate (collect data *in-situ* or immediately after bringing to surface); *ts* = time-sensitive (analyze as soon as practical); *a* = can be archived (shelf life ≥ 6 months)

TABLE 7.3 Example Checklist

SAP and SOPs	Rope and reel	Alkalinity kit
Field notebook	Cooler & ice	Turbidity meter
Pencils, pens, sharpies	Water-level indicator	Portable spectrophotometer
Sample bottles (assorted)	Datasonde (calibrated)	Reagents for Fe(II)/Fe(III)
GPS	Laptop, calculator	Reagents for H_2S
Keys	Communication cables	Spare batteries
Chain of Custody forms	Manual pH-SC-DO-Eh meters	Multi-tool knife, wrench set
Filtration supplies	Calibration standards	Duct tape, packing tape
Peristaltic pump and tubing	Nitric and hydrochloric acid	Kimwipes
Battery (charged)	Automatic pipet and pipet tips	Garbage bags
2-L point sampler	Powder-free gloves	Ziplock bags
Messenger	Safety glasses	10 L de-ionized (DI) water
Flow cell	5-gal calibrated bucket	DI squirt bottles

Example 7.1 Table 7.3 is an example checklist from a recent project involving collection of groundwater samples in a flooded mine shaft near Butte. In this project, water samples were collected using a point sampler, a nylon rope, and a hand reel. Downhole water quality parameters were collected with a datasonde, and a second set of parameters were collected at the surface using handheld probes. Additional measurements at the surface included alkalinity, turbidity, Fe(II)/Fe(III) speciation, and H_2S concentration. Filtration was accomplished using a peristaltic pump and large diameter filters.

7.2 Collecting Groundwater Samples

Sample retrieval

For collection of groundwater samples, the most common methods are to use a portable submersible pump, a peristaltic pump, a bailer, or a point sampler. The simplest system for relatively shallow (less than about 20 ft deep), small-diameter monitoring wells is to use a peristaltic pump, flexible plastic tubing, and a portable battery. This method is limited to relatively low-flow rates (less than 1 or 2 gal/min), and therefore will not be practical if it is necessary to purge a well that is more than 2 in in diameter. One advantage of a peristaltic pump is that no moving parts contact the water being sampled, making it possible to pump water that is highly corrosive or turbid. For deeper or larger-diameter wells, a submersible pump powered by a generator or DC battery will be needed. A relatively small 1-hp pump similar to what one uses in a hot tub can be carried around by hand and will deliver up to 30 gal/min. Attention should be paid to make sure the discharge from the pump is directed as far as possible from the well and does not enter any nearby surface water body.

A bailer is a hollow cylinder, usually plastic with a check valve at the bottom, that is lowered down a monitoring well to retrieve a water sample. The bailer is lowered until it is completely submerged, and then raised and dropped a few times to fill the cylinder. The bailer is then retrieved and the water is discarded to a 5-gal bucket to monitor the purge volume. This process is repeated until the well is sufficiently flushed, usually after three well volumes, or when all field parameters have stabilized. Although this sounds like hard work, bailing shallow 2-in monitoring wells is often faster than using a peristaltic pump. One problem is that the turbulence caused by raising and lowering the bailer can make the water muddy. To minimize this problem, avoid lowering the bailer all the way to the screen or bottom of the well. Provided the well is properly purged, a representative sample will be obtained simply by bailing from a few feet below the static water level. For some projects with multiple wells it may be more convenient to prevent cross-contamination to have a dedicated bailer permanently assigned to each well. Each bailer can be stored inside its designated well above the water line with a piece of string.

Our group in Butte does a lot of flooded mine shaft sampling, and in this case it is impossible to "purge the well." Instead, we use point samplers, which are hollow cylinders with two articulated caps that are spring-locked in the open position. After the point sampler is lowered to the desired depth, a small weight or "messenger" is sent down the cable which trips the spring and causes the caps to clamp shut, trapping the water sample inside. The sampler is then lifted out of the hole as quickly as possible. Using this method we have been able to get samples of mine shaft water from depths up to 1000 ft below the static water level. Point samplers are also widely used when sampling lakes (Figure 7.1).

Passive sampling

Wells work great in sand and gravel, but how does one collect a representative groundwater sample from sediment with a high percentage of silt and mud? Driving a monitoring well into the muck at the bottom of a shallow lake or wetland is a dirty job, and it is virtually impossible to pump such a well to obtain a decent water sample. In this case, a better option may be to use a *passive* sampling method, such as a "peeper" or "diffusion sampler." Most peepers are some variation of a vertical column containing several hollow compartments at different depths that are separated from the water-saturated sediment by a semipermeable synthetic membrane. The sample compartments are typically filled with deoxygenated, distilled water before deployment. The peeper is then pushed into the subsurface to the desired depth, and left for several weeks. During this time solutes diffuse across the membrane until the

Figure 7.1 Using a 2-L point sampler (white device in upper right) to collect water samples from an acidic lake in Patagonia, Argentina.

water chemistry inside each sample compartment is the same as that in the immediately adjacent sediment. The peeper is then removed and each of the compartments is sampled as quickly as possible, sometimes in a N_2- or Ar-glovebox to avoid oxidation of redox-sensitive species. The use of peepers to collect pore water chemistry profiles in sediment with low hydraulic conductivity soils is still not widely practiced, but has much potential. Another application of diffusion samplers that is gaining popularity is in the sampling of volatile organic carbon compounds (VOCs). Some recent studies suggest that pumping a monitoring well can change the concentration of VOCs that partition into the gas phase, and therefore a more representative sample is collected by a variant of the diffusion method described above. More information can be found in the excellent review article of ITRC (2006).

Filtration, preservation, and labeling

Most SOPs will call for collection of filtered groundwater samples, whereas surface waters may be either filtered or nonfiltered. The term "dissolved metal" is operationally defined as any substance that passes through the filter that is used in the field. For groundwater sampling

0.45-μm filters are most commonly used, although filters with smaller diameter are also comm-ercially available, down to about 0.1 μm. The advantage of using 0.45-μm filters is that they will capture almost all of the algae and bacteria and most of the suspended solid in the water, while still being of sufficient pore size to allow rapid filtration of relatively large (>1 L) sample volumes. Speaking of volume, be sure to collect enough sample for all your laboratory needs. When in doubt, collect a larger sample size. It is very frustrating to run out of sample before all of the analytical work is completed.

There is a bewildering array of filter styles and materials on the market, and the choice of what product to use is nontrivial. Many workers use a disposable in-line filter with a plastic housing that attaches to any flexible tubing (Figure 7.2 F, G). These are one-use only filters that can process a large volume of water (depending on the turbidity) but are also somewhat expensive. A slightly different approach is to use a screw-tight plastic filter holder with individual filter sheets (Figure 7.2 B, C, D). The filter housing is awkward to carry around and rinsing between samples consumes large amounts of distilled water, but this method turns out to be much less expensive per sample. Finally,

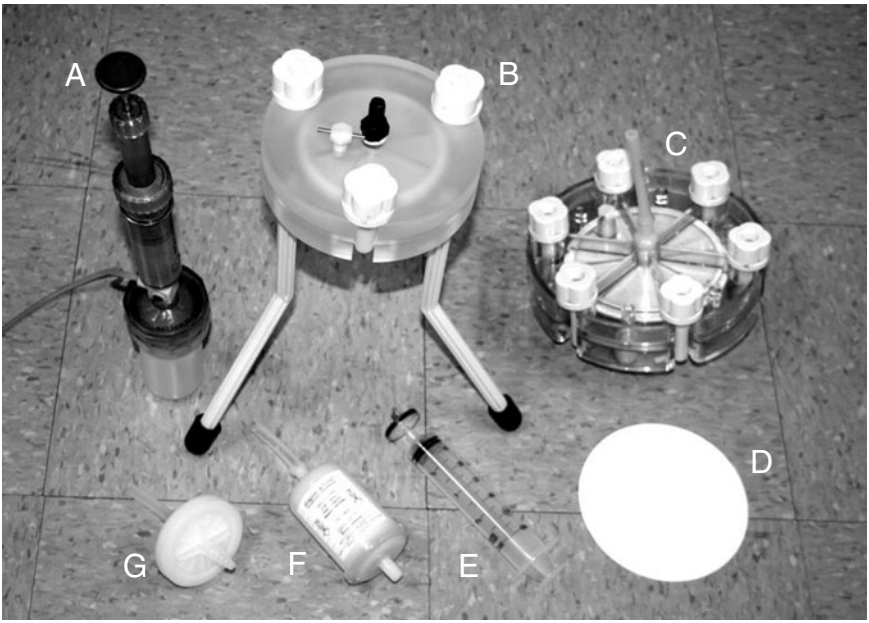

Figure 7.2 Some example filter styles for water sampling. A: hand-pump portable filter; B and C: plate filters with disposable filter membranes (D); E: syringe with small disposable filter (~ $1 each); F: high capacity in-line disposable filter (> $10 each); G: medium capacity in-line disposable filter (> $5 each).

in cases where it is impossible to carry a battery and pump, it may be more convenient to use a small hand-operated filter (Figure 7.2 A) or plastic syringes (e.g., 60 mL) and syringe filters (Figure 7.2 E). These small filters will clog quickly if the water is turbid, and they are also notorious for trace metal contamination, especially zinc. Preliminary QA tests with blank water are always recommended to determine the concentrations of trace metals that are leached out of a given filtration setup. Once a filter size and type is selected, the same filters should be used throughout the life of the project.

Nitric acid (HNO_3) is the most common reagent used for preservation of samples for trace metal analysis (ICP-ES or ICP-MS). Sulfuric acid (H_2SO_4) is used for nitrate and phosphate, and hydrochloric acid (HCl) is usually used to preserve redox-sensitive species, such as Fe^{2+}/Fe^{3+}. Different levels of acid purity may be required, depending on your project. "Trace metal grade" acid is the most common type used for routine sample collection. A small bottle of concentrated acid can be transported into the field (e.g., in the sample cooler), and a pipet can be used to dispense a precise amount of acid into each bottle after the samples are collected. The exact amount of acid to add will be specified in your SAP; we typically acidify groundwater samples to 1% v/v (by volume). Samples collected for dissolved metal analysis must be filtered first prior to addition of the acid. Some workers prefer to use pre-weighed capsules of acid in individual plastic ampoules. Whereas this method avoids having to transport a bottle of concentrated acid into the field, it is somewhat awkward to open the capsules and this can lead to minor spills as well as non-identical amounts of acid going into different sample bottles. Some labs may provide sample bottles with a small amount of acid already in them. Although this may be okay for your application, be aware that concentrated acid can leach metals out of plastic bottles, even pre-acid washed bottles. All appropriate safety precautions should be made when handling nitric acid, including wearing safety goggles and gloves.

It is worth saying a few things about labeling. Chances are good that the sampler will be using a sharpie or similar waterproof pen to label plastic sample bottles in the field. Essential information that should go on the bottle includes—at a minimum—the date of collection and the sample ID, as well as some indication as to whether or not the sample was filtered and preserved. Our group uses the prefixes "F" or "R" for filtered or raw, and "U" or "A" for un-acidified or acidified. Thus, a sample that has been filtered and preserved with HNO_3 would be labeled "FA-HNO_3." Be aware that sharpies are notorious for smudging or wearing off completely. To avoid this, wrap a sheet of transparent packing tape over the label. This will save a lot of headaches, especially if the samples will be transported a long distance. Most SOPs for analysis of water samples call for refrigeration during transport and storage, so bring a

cooler with plenty of ice. Be sure to double-bag all samples and pack them so that they will not be "swimming" in water when the ice melts.

Chain of custody

Regulatory work requires chain-of-custody (COC) forms to be filled out by the field sampler and shipped along with the environmental samples to the laboratory. COC forms can be custom-made for each project, or can be supplied by the lab. Essential information includes a list of the sample IDs, the dates of collection, the sample volumes, whether the samples were filtered and preserved, the project name, who collected the sample, and a description of what types of laboratory analyses are required for each sample. Always double-check the sample IDs marked on the bottles with the list on the COC form. Anyone who handles the samples on route to the lab must sign and date when they received and relinquished them. The laboratory will also sign and date the COC form when the samples arrive, and will check the condition of the samples, noting any spillage or whether the cooler had warmed above an unacceptable temperature during shipping. The laboratory then checks the sampling dates to determine how quickly the various analyses need to be performed (e.g., anion analysis usually needs to be completed within 2 weeks of sampling). The COC forms are eventually mailed back to the project leader, and become part of the permanent record of the project.

Cleaning and decontamination

Following clean field procedures is as much a valuable skill as taking good field notes or having the stamina to put in a long field day. This is particularly important when analysis of trace metals or organic compounds is going to be performed. The U.S. Geological Survey Water-Quality Field Manual (USGS 2005) has an entire chapter devoted to cleaning field equipment between samples. Although some of these procedures may be overly rigorous for your specific application, there are several reasons why clean sampling methods are important. These include minimizing sample contamination between sites, extending the lifetime of your sampling equipment, and avoiding exposure of yourself or your employees to potentially toxic chemicals. Here are a few pointers:

- The sampler should wear disposable, powder-free gloves and change the gloves frequently, that is, between samples or whenever the gloves are potentially contaminated by contact with uncleaned surfaces or objects.
- Always rinse any sampling or filtration equipment with copious amounts of distilled water before use, and again after use while the materials are still wet. Do not allow any equipment to be stored for an extended period of time without proper cleaning.

- Transport equipment and supplies (including sample bottles) in a sealed storage container or in plastic bags. Avoid contact with dust. This is especially critical when driving on dirt roads.
- Avoid airborne particles getting into the water samples. This is really important on windy days near sites where soil is highly contaminated.
- Use alcohol, alconox, or a dilute bleach solution to rinse equipment when sampling for organic compounds (exception: don't use for dissolved or total organic carbon analyses). In this case, the sampler should wear sturdy plastic gloves that can tolerate organic solvents. Alcohol is flammable, so dispose of waste rinse in a suitable container.
- Avoid generator or vehicle exhaust fumes when sampling for volatile organics.
- Be sure all electrodes are properly stored in appropriate storage solutions (usually supplied when the electrode is purchased).
- Make sure any electronic device is turned off and remove batteries from any piece of equipment that will not be used within the next month or two.

7.3 Field Measurements

Prior to collecting a water sample, a number of field observations and measurements are typically recorded. These include the well ID#, depth to static water level, date and time, method of sample collection (e.g., whether a well was bailed or pumped), whether or not the well was purged prior to sampling, and the volume of purge water. Several important water quality measurements should be taken at the same time as the sample is retrieved, including water temperature, pH, specific conductance, dissolved oxygen, and redox state. Ideally, these parameters will be measured in-situ, with a submersible datasonde (Figure 7.3). If this is not possible, then make measurements as soon as possible after the sample is pumped or bailed to the surface. If the well is being pumped, then a good practice is to divert all or a portion of the water through a "flow cell," which has ports for inserting electrodes and thus making measurements without allowing the water to contact air. Stabilization of field parameters after one or more well volumes is an indication of successful purging of a well. The following are additional notes and suggestions for each of the field parameter measurements.

pH and temperature

Most pH meters have a built-in temperature probe, and routine measurements should be capable of a precision of ±0.1 pH units and ±0.1°C. For best results, pH meters should be freshly (within 6 h) calibrated with at least

Figure 7.3 Using a Hydrolab Minisonde to record water quality measurements.

2 pH buffers that span the range of pH of the waters being sampled. Bring your buffers with you for calibration checks in the field. Also, bring an ample supply of distilled or deionized water for rinsing the electrode between measurements, but don't use deionized water to store the electrode. Instead, the electrode tip should be stored in a pH 4 or pH 7 buffer solution, in a KCl buffer solution, or in whatever water with moderately high salinity is available. Do not allow the tip of the pH electrode to dry out.

There are many types of pH electrodes on the market. Glass electrodes are the most sensitive and are well-suited to lab work, but are breakable and have a port for adding electrolyte solution that often leaks. Many field workers prefer gel electrodes which are unbreakable (or nearly so) and are permanently sealed. However, gel electrodes can be very slow to equilibrate, especially at cold temperatures or for water whose pH is poorly buffered. In such cases, a gel electrode may take as much as 15 min or longer to reach a stable pH value.

The pH of a deep groundwater sample can change after the sample is pumped or bailed to the surface. Examples 7.2 and 7.3 underscore the need to take pH measurements in the field, and to do this in-situ (with a submersible probe) if possible.

Example 7.2 Vertical gradients in pH were recently measured in a flooded mine shaft near Butte, Montana. A detailed pH profile was obtained by lowering a submersible datasonde down the shaft. The pH of samples bailed to the

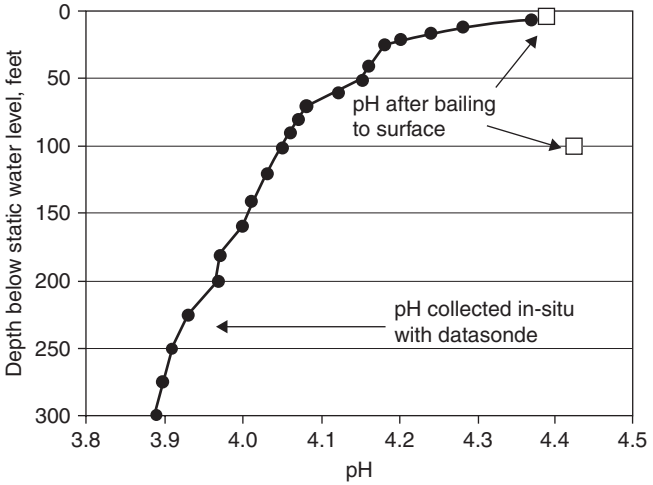

Figure 7.4 Comparison of in-situ pH (determined with a submersible datasonde) with the pH of samples bailed to the surface for mine shaft water in Butte, Montana. (*C. Gammons, unpublished data*)

surface was also measured using a manual pH meter. As shown in Figure 7.4, the surface pH value for the 100 ft deep sample was significantly higher as compared to the in situ datasonde pH value. The deeper water effervesced CO_2 gas while bailing to the surface, which is the probable reason for the change in pH.

Example 7.3 The same water samples mentioned in the previous example were observed to turn reddish-brown upon storage (even in tightly sealed bottles with no head space), due to oxidation of dissolved ferrous iron to insoluble ferric hydroxide:

$$Fe^{2+} + 1/4O_2 + 5/2H_2O = Fe(OH)_3(s) + 2H^+ \quad (7.1)$$

Because reaction (7.1) produces protons, the pH of these mine waters measured in the laboratory were very often much lower than the field pH (Figure 7.5).

Specific conductance

Specific conductance (SC or C25) is the ability of a water sample to conduct electricity at a reference temperature of 25°C. Salty water conducts electrons much easier than freshwater, and the conductivity of water of a given salt content increases with increase in temperature. Most modern SC meters have a built-in temperature sensor so that the absolute conductivity of the sample at the field temperature is automatically converted to specific conductivity at 25°C. Many older conductivity

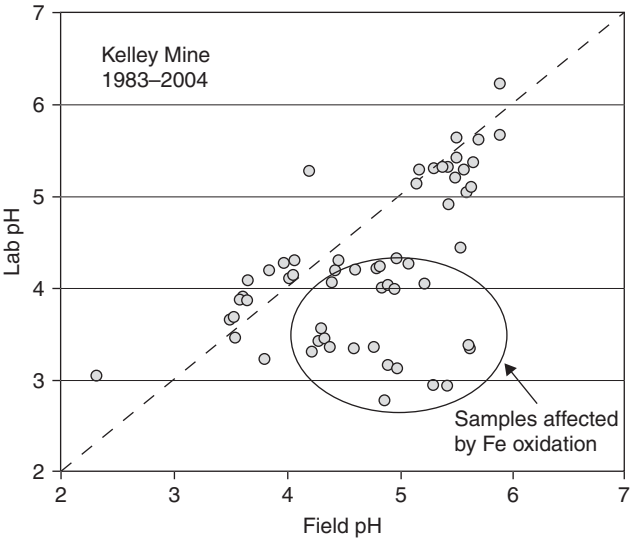

Figure 7.5 Comparison of field pH and lab pH for Fe-rich water in a flooded mine shaft. (*C. Gammons, unpublished data*)

meters do not have this option, and the measured conductance will need to be adjusted manually to 25°C. SC is most commonly expressed in units of μS/cm (micro-siemens per cm) or mS/cm. A siemen is the same as a mho, and the latter is easy to remember since it is the backwards spelling of "ohm," the unit of electrical resistance. As usual, be careful with units. Some SC meters will automatically shift from μS/cm to mS/cm when the electrode is placed in water with high salinity.

An SC meter is a very useful tool for rapid water quality assessment, as it can be used as a proxy for total dissolved solids. This can help, for example, to predict how large a dilution factor should be applied prior to laboratory analysis. As well, our group has found SC to be particularly useful in investigations of groundwater/surface-water interaction. For example, if a given reach of a stream is gaining flow from discharge of shallow groundwater, then it will usually show a change in SC since the influent groundwater almost always has a different (usually higher) SC value than that of the stream. In contrast, if the SC of a stream is invariant with distance over a given reach, it is likely that the river is not receiving influent groundwater or is losing water to the subsurface. Before collecting any stream sample, it is strongly advised to measure SC at a number of locations across the profile to see if the surface water is well-mixed. If the water along the near bank has a much different chemistry than the main flow of the stream, a grab sample at this location will not be representative of the entire stream flow.

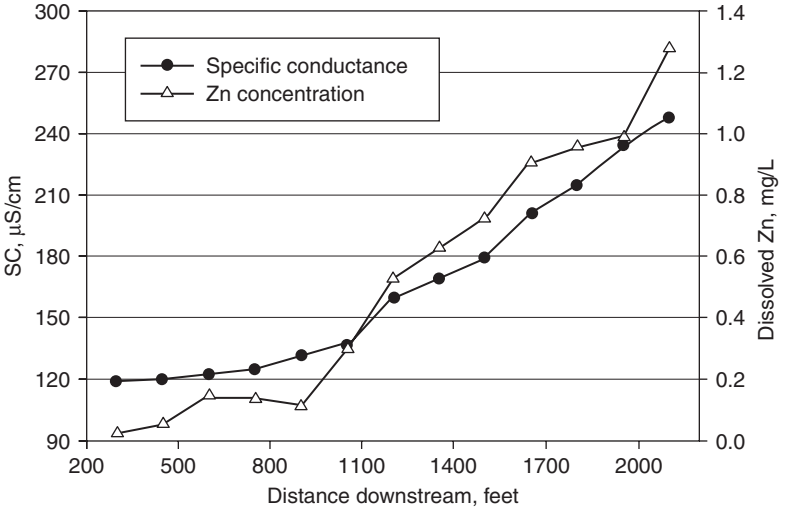

Figure 7.6 Changes in specific conductance (SC) and Zn concentration along upper High Ore Creek, Montana, near the abandoned Comet Mine. [*From Gammons et al. (2007)*]

Example 7.4 Figure 7.6 shows changes in SC and dissolved Zn concentration in a section of High Ore Creek, Montana (Gammons et al. 2007). The steady increase in both SC and Zn was due to discharging shallow groundwater that had been contaminated by interaction with buried mine waste. Because the increase in streamflow through this reach was small (less than 0.1 cfs), the influent groundwater must have had very high SC and Zn concentration.

Example 7.5 In some cases, field SC measurements can also be used to rapidly estimate stream flow. For example, the following data were obtained at a section of High Ore Creek where a small tributary stream entered: $SC_1 = 595$, $SC_2 = 82$, $SC_3 = 526$ µS/cm, where the subscripts 1, 2, and 3 referred to High Ore Creek above the tributary, the tributary, and High Ore Creek below the tributary, respectively. The flow of High Ore Creek upstream (Q_1) was measured from a Parshall flume and found to be 1.1 cfs (ft^3/s). An SC mass balance equation was then used to estimate the flow of the tributary and High Ore Creek downstream:

$$SC_1 \cdot Q_1 + SC_2 \cdot Q_2 = SC_3 \cdot Q_3 \tag{7.2}$$

Since $Q_1 + Q_2 = Q_3$, we can set $Q_2 = x$, and $Q_3 = (1.1 + x)$. Rearrangement of Equation 7.2 gives:

$$x = \frac{Q_1 \cdot (SC_1 - SC_3)}{(SC_3 - SC_2)} = \frac{1.1 \cdot (595 - 526)}{(526 - 82)} = 0.17 \tag{7.3}$$

from which $Q_2 = 0.17$ cfs and $Q_3 = 1.27$ cfs were obtained.

Dissolved oxygen and redox state

The redox state of water is typically characterized by a combination of dissolved oxygen (DO) and oxidation-reduction potential (ORP or Eh) measurements. In very broad terms, groundwater can be classified into three categories with respect to its redox state: (1) *oxic* (containing DO well above the practical quantification limit of around 1 mg/L), (2) *suboxic* or *transitional* (DO near or below detection, but no H_2S), and (3) *anoxic* or *sulfidic* (H_2S present at detectable levels). The fate and transport of trace metals and other contaminants can change dramatically depending on the redox state of the water. Depletion of DO in groundwater may be an indication of O_2-consuming reactions such as decay of organic matter or oxidation of sulfide minerals.

Dissolved oxygen is usually measured by Winkler titration or using a DO meter with a galvanic or luminescent DO electrode. Winkler titrations are somewhat time consuming and cumbersome to do in the field, but are a good way to check the accuracy of your DO electrode. Galvanic DO electrodes are the most common type used on multiparameter instruments, although luminescent DO (LDO) probes are becoming increasingly popular for the more expensive units. Because a galvanic DO electrode will consume O_2 during its operation, the solution must be stirred or flowing to get an accurate measurement. LDO electrodes do not have this problem, and are also reputedly more accurate and less prone to instrument drift. Using any of the above methods, it is straightforward to quantify DO in the range of 1.0 to >10 mg/L. Below about 1 mg/L, DO measurements are problematic, and caution should be used to interpret data near the detection limit. In many cases, the trace amounts of DO that are recorded by the equipment will be a false artifact of atmospheric contamination, chemical interferences, or pressure effects.

For suboxic or anoxic water, an Eh or ORP electrode should be used to quantify redox state. The ORP electrode has a platinum wire tip that should be kept clean and protected from damage. To take an ORP reading, simply attach the ORP electrode to your pH meter, and switch the "mode" button from pH units to mV. Although Eh and ORP both have units of volts or mV, they are different things, and the user needs to be careful. Whereas Eh is defined as the electrical potential of a sample relative to the standard hydrogen electrode (SHE), ORP is the potential of the water sample relative to the particular reference electrode that is used in the field. Most ORP electrodes use a Ag-AgCl reference cell, although there are also some calomel ($Hg\text{-}HgCl_2$) electrodes around. The conversion from Ag-AgCl to SHE is typically on the order of 200 to 220 mV (see column B of Table 7.4), which makes a big difference in the final reported Eh values. This voltage correction is temperature dependent, and also varies slightly with the concentration of KCl in the electrode filling solution. To check the

calibration of an ORP electrode, measure the mV reading in a bottle of fresh ZoBell's solution at a known temperature. The result should be close to what is shown in column C of Table 7.4. To convert from ORP to true Eh, the following equation can be used:

$$Eh_{sample,\,T} = ORP_{sample,T} + Eh_{ZoBell's,T} - ORP_{ZoBell's,T} \qquad (7.4)$$

where $ORP_{sample,T}$ and $ORP_{ZoBell's,T}$ are the measured ORP values of the water sample and ZoBell's solution at the field temperature, and $Eh_{ZoBell's,T}$ is the theoretical Eh of ZoBell's at the field temperature (given in column A of Table 7.4).

Example 7.6 Our group recently sampled a river in southwestern Spain that was highly acidic due to acid mine drainage. The field ORP of the river water was +420 mV and the temperature was 20.2°C. The ORP of a ZoBell's solution standard placed in the river at the same temperature was 219 mV. The true Eh of the water sample was then calculated using Equation 7.4 and was determined to be 420 + 443 – 219 = 644 mV.

Alkalinity

Alkalinity is defined as the sum of the concentrations of titratable bases in a water sample. For practical purposes alkalinity can be expressed as:

$$\text{Alkalinity (moles/liter)} = mHCO_3^- + 2mCO_3^{2-} + mOH^- (+mHS^-) \qquad (7.5)$$

Although natural waters may contain other basic compounds (such as borate, phosphate, or $Mg(OH)^+$), these are usually very minor contributors to the total alkalinity. Alkalinity is an important measurement because it is the most convenient way to determine the concentrations

TABLE 7.4 The Temperature Dependence of the Electrical Potential (mV) of Zobell's Solution and the Ag-AgCl Reference Electrode

	Column A	Column B	Column C
Temp.°C	Eh (SHE) of ZoBell's solution	Eh (SHE) of Ag/AgCl (3.5M KCl)	ORP of ZoBell's relative to Ag-AgCl (3.5M KCl)
0	490	221	269
5	478	218	260
10	467	215	252
15	455	212	243
20	443	208	235
25	431	205	226
30	418	201	217

of dissolved bicarbonate (HCO_3^-) and carbonate (CO_3^{2-}) in an environmental water sample. Although many laboratories will measure alkalinity (for a price), it is always a good idea to perform a quick alkalinity titration in the field soon after the samples are brought to the surface. Even samples that are filtered and stored on ice can "go bad" between the time you collect them and when the lab gets around to doing the measurement (see Example 7.7 below).

Alkalinity is measured by potentiometric titration. A known volume (usually 100 mL) of filtered, unacidified groundwater is titrated with dilute acid (usually H_2SO_4) to a pH endpoint of ~ 4.5. The volume of acid that is needed to lower the pH of the sample to 4.5 is then used to calculate the alkalinity of the sample. For field titrations, the most convenient approach is to use a digital titrator (Figure 7.7) and an appropriate cartridge (usually 0.16 N H_2SO_4 for dilute samples, 1.6 N H_2SO_4 for concentrated samples)[1]. You will also need a 250 mL Erlenmeyer flask, a portable magnetic stirrer and stir bar, and a way to measure out 100 mL of sample, such as a pipet, a volumetric flask, or a portable balance. The accuracy of your alkalinity titration will be poor if you simply "eye-ball" the 100 mL mark on the Erlenmeyer flask. For rapid measurement without the need for a pH meter, a small packet

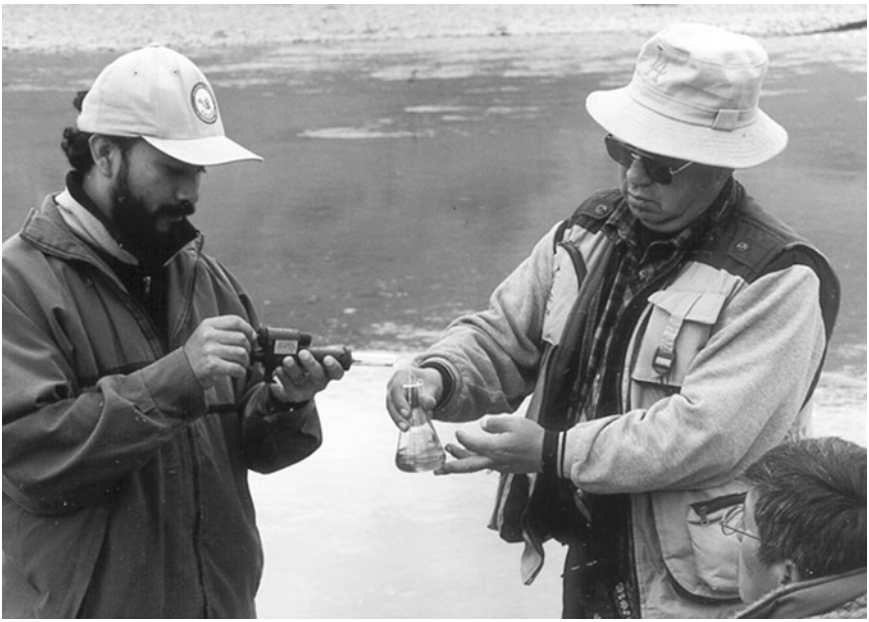

Figure 7.7 Using a digital titrator to determine alkalinity of a river in Peru.

[1] 0.16N H_2SO_4 = 0.08M H_2SO_4, where N = "normal," and M = "molar."

of bromcresol green-methyl red indicator dye can be added to your water sample. As long as pH is above 5, the color will be blue-green. As the pH drops below 5 with continued addition of H_2SO_4, the color will shift to lavender, and then pink at the pH endpoint of 4.5. Although alkalinity often increases with increase in pH, this is not always the case. However, any water sample with an initial pH less than 4.5 has zero alkalinity (by definition).

Units of alkalinity are particularly troublesome. Common units include mg/L (as $CaCO_3$), mg/L (as HCO_3^-), and meq/L (milli-equivalents per liter of total alkalinity). If you are using a HACH digital titrator, the units corresponding to the digital readout are specified on the side of the cartridge. For example, if a 0.16N H_2SO_4 cartridge is used, the alkalinity (for a 100-mL sample) in units of mg/L as $CaCO_3$ is equal to the digital readout divided by 10. To convert from mg/L as $CaCO_3$ to meq/L, the alkalinity value is divided by 50 (this is the gram formula weight of calcite divided by two, realizing that each mole of $CaCO_3$ has two equivalents of base). To convert from meq/L to mg/L as HCO_3^-, the alkalinity value is multiplied by 61 (the gram formula weight of bicarbonate). Be careful with units!

Example 7.7 Field alkalinity measurements and filtered water samples were taken each hour from a river in western Montana that had very high pH (pH > 9) due to abundant photosynthesis by algae and aquatic macrophytes. The alkalinity of each sample was analyzed in the laboratory several days later. Figure 7.8 summarizes the results. Whereas the field alkalinity data showed a smooth trend over 24 h, the lab data were very scattered, and most

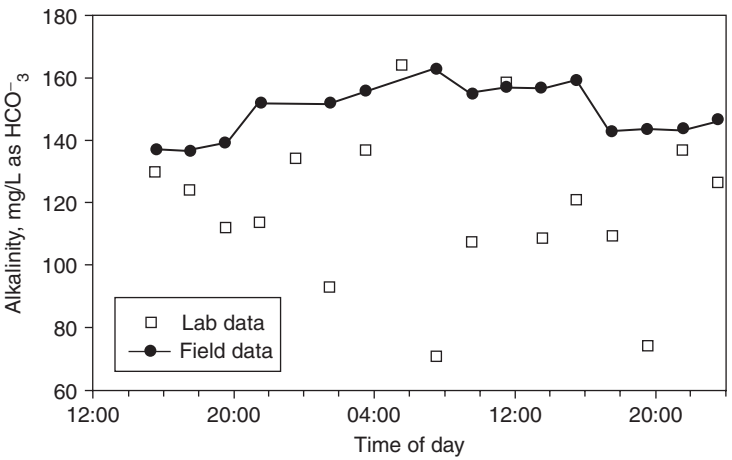

Figure 7.8 A comparison of field and laboratory alkalinity data collected from the Mill-Willow Bypass, a tributary to the upper Clark Fork River, over a 24-h period in August, 2005. (*C. Gammons, unpublished data*)

of the values were lower than the field measurements. This problem was attributed to precipitation of calcite in the nonacidified bottles after they were sealed. As shown by Equation 7.6, precipitation of calcite would have lowered the bicarbonate alkalinity of the samples:

$$Ca^{2+} + 2HCO_3^- = CaCO_3(s) + CO_2(g) + H_2O \quad (7.6)$$

Thermodynamic modeling later showed that the river samples were strongly supersaturated with calcite owing to the high pH of the water, supporting the hypothesis that calcite precipitation was the cause of the poor lab alkalinity data.

Turbidity and total suspended solids

Turbidity is an important measurement to collect if suspended solids are a concern, and is a useful measure of how well a given monitoring well has been developed prior to sampling. If the water being pumped is turbid and brown, then chances are the well was never properly developed or was completed in fine-grained sediment with no filter packing. Turbidity is quantified using a turbidity meter which measures the amount of light that is scattered at 90° to the incident beam, and is usually reported in units of NTU (nephelometric turbidity units).

The concentration of total suspended solids (TSS) is determined by filtering a known volume of raw water (usually 1 L) and weighing the residual dried solid. Because groundwater samples are usually filtered prior to laboratory analysis, TSS measurements are often omitted in the SAP. However, with some relatively simple equipment, filtration of a 1-L sample can be done quickly in the field, with the pre-weighed filters stored for later drying and weighing. The stored filter papers can also be used for mineralogical, chemical, or microbiological characterization of the suspended particles. The particles will transform as they dry up and oxidize, so forethought should be given as to how any such data will be used.

7.4 Laboratory Analyses

Dissolved metals

Groundwater samples collected for metals analysis will typically be filtered and then acidified in the field (Section 7.2), and stored on ice or in the refrigerator prior to analysis. Concentrations of dissolved (filtered) metals in environmental water samples are usually quantified by Inductively Coupled Plasma Emission Spectroscopy (ICP-ES, also known as ICP-OES or ICP-AES). In cases where a lower detection limit is needed, samples may be analyzed by Inductively Coupled Plasma Mass Spectroscopy (ICP-MS) or graphite furnace atomic absorption spectroscopy (GFAAS). The advantage of ICP-ES and ICP-MS over

GFAAS is that a full suite of 15 to 30 elements can be analyzed at the same time with the former methods, whereas with GFAAS each metal must be analyzed separately. Because of its higher sensitivity, ICP-MS is more expensive than ICP-ES. Beginners should not confuse these two techniques, as they employ quite different instrumentation. Also, one should not refer to their analytical method as simply "ICP," as this does not discriminate between mass versus emission spectroscopy. Most EPA methods for metal analysis specify a maximum 6-month holding time. Many commercial laboratories will supply coolers, sample bottles, acid reagents, and chain-of-custody forms at little or no additional cost. If this interests you, call the lab ahead of time and arrange for the supplies to be mailed in plenty of time before your fieldwork.

Anions

Samples for anion analysis are normally filtered and unacidified, and stored on ice or in the fridge until analysis. Most analytical methods for anions specify a maximum 2-week holding time, so be sure to send your samples to the lab quickly. Ion chromatography (IC) is the method of choice for the geologically common anions including bromide (Br^-), chloride (Cl^-), nitrate (NO_3^-), and sulfate (SO_4^{2-}). Nitrite (NO_2^-) and phosphate (PO_4^{3-}) may be added to the list if concentrations are expected to be above the analytical detection limits. IC cannot quantify bicarbonate or carbonate ions: these solutes are determined by alkalinity titration (Section 7.3). Colorimetric methods have also been developed for most anions, and these are sometimes used when concentrations of species such as nitrate, nitrite, or phosphate are below the detection limit of the IC. HACH Company has developed a large number of tests that can be done on site relatively cheaply with a portable spectrophotometer. These tests should be backed up with plenty of QA checks (including standards, spikes, and duplicate samples) if the data are critical.

Organic compounds

There are many types of organic substances that can be quantified in a given groundwater sample. These include naturally occurring soluble organic compounds (usually referred to as dissolved organic carbon, or DOC), man-made contaminants, and pathogens (protozoa, bacteria, viruses). Although DOC is often skipped in a sampling plan, most groundwater will contain at least a few mg/L of organic carbon from natural sources, such as humic and fulvic acids, carboxylic acids, etc. (Drever 1997). Some forms of DOC can be complex trace metals, and DOC is an essential nutrient for many forms of bacteria. Water samples for DOC measurement are gently filtered (to avoid rupture of suspended

bacteria or algal cell walls) and collected in opaque glass bottles prior to analysis using a total carbon analyzer. There is typically a 2-week holding time for DOC measurement, so get your samples to the lab quickly.

The list of man-made compounds that have been detected in groundwater is exceedingly long. Many of these chemicals are toxic, and the US EPA has created a list of 126 priority pollutant organic compounds, as well as a list of standard methods for their analysis (e.g., see Fetter 1999). Most of the target compounds are analyzed by gas chromatography (GC), or a combination of gas chromatography and mass spectroscopy (GC/MS). Many of the priority pollutants are volatile, and some are sparingly soluble in water leading to the accumulation of "free product," or nonaqueous phase liquid (NAPL). For their own safety, fieldworkers should take great care handling environmental samples from highly contaminated sites, and also need to be diligent about decontaminating equipment between samples. If you are involved with a project that deals with organic contaminants, chances are good that detailed SOPs regarding safety, sampling methods, and quality control already exist. Follow these procedures.

There has been increased attention to the presence of *pesticides* and *pharmaceutical* compounds in groundwater (Barbash and Resek 1996; Heberer 2002; EPA 2006). Pesticide contamination of groundwater is a problem that has long been recognized in agricultural areas. Pharmaceutically Active Compounds (PhACs), also referred to as Pharmaceuticals and Personal Care Products (PPCPs), are of current interest because many of these commercial products are very slow to biodegrade, are mobile in shallow groundwater or surface water, and pose an unknown threat to human health. Although a complete chemical analysis for the full range of pesticides or PPCPs that may be present in a given sample is very expensive, the methods of sample collection and preservation are not. As well, preliminary screening may identify one or more target compounds that can serve as a proxy for the full suite of contaminants likely to be present.

Total dissolved solids

Before ~ 30 years ago, a total dissolved solids (TDS) analysis was performed by evaporating a known volume of filtered water to dryness and weighing the mass of residual solids. This mass divided by the original mass of water gives the TDS, usually expressed in mg/L. However, in recent decades it has become a common practice to calculate TDS as the sum of the concentrations of all major and minor dissolved species in the water as determined by ICP-ES, alkalinity, and IC. Interestingly, the values obtained by these two methods are usually different. The reason is that

a sample with moderate or high Ca-bicarbonate content will precipitate a fair amount of calcite on evaporation (reaction 7.6), and in the process will liberate $H_2O(g)$ and $CO_2(g)$ that was originally bound in dissolved bicarbonate ion. So, TDS measurements based on evaporation are usually lower than TDS based on chemical analyses. This distinction may be very important if TDS is a parameter that is closely monitored or regulated, as is the case for some high-salinity waters used for irrigation or produced as a by-product of oil and gas extraction (see Van Voast 2003, for a good example). Although TDS is generally proportional to SC, the relationship is semi-quantitative. Therefore, SC should not be substituted for TDS if the latter is a critical measurement.

Other types of analyses

Depending on the project, there are a number of additional types of chemical and isotopic analyses that can be performed on a given groundwater sample. For example, our group has found Fe(II)/Fe(III) speciation to be particularly helpful in the study of waters impacted by mining (Pellicori et al. 2005). Taking advantage of the fact that dissolved iron compounds are often brightly colored, several different colorimetric tests have been developed to discriminate one Fe oxidation state from the other. Our group uses the FerroZine procedure (Stookey 1970), which is both sensitive and low cost. Regardless of which method you choose, Fe speciation should be performed as quickly as possible after sample collection. If this is not possible, samples may be preserved by filtration (to remove Fe-rich suspended solids, and also to remove Fe-oxidizing bacteria), acidification with HCl (not HNO_3) to pH < 2, minimizing contact with air by filling the sample bottle with no head space, refrigeration, and storage in an opaque container or in the dark, to avoid photoreduction of Fe(III) to Fe(II).

Some strongly reducing groundwaters will contain dissolved sulfide, and if so they will have a strong smell of rotten eggs. HACH offers a simple and highly sensitive field colorimetric method for quantifying sulfide (sum of H_2S and HS^-) in such waters, based on the methylene blue reagent (Figure 7.9). Because dissolved sulfide concentrations drop quickly after sample collection (due to the combined effects of oxidation plus loss of gaseous H_2S), any sulfide measurement should be performed on site immediately after sample collection. The presence of even trace (< 0.01 mg/L) levels of H_2S in a groundwater will make it undrinkable, and will drastically reduce the concentrations of heavy metals such as Fe, Cu, and Zn that form insoluble metal sulfides.

If your project involves identifying groundwater sources or recharge rates, you may consider collecting samples for stable isotope analysis or age dating. The stable isotope ratios ($^{18}O/^{16}O$ and $^{2}H/^{1}H$) of water can be

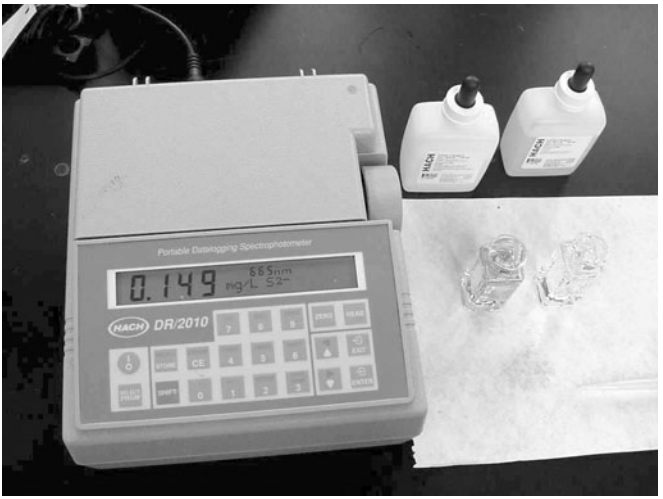

Figure 7.9 Using a portable spectrophotometer to determine the concentration of dissolved sulfide in a flooded underground mine in Butte, Montana.

very useful to track sources of recharge water, to provide evidence of groundwater mixing, and also to quantify the extent of evaporation (Gammons et al. 2006). More explanation is beyond the scope of this chapter, and the reader is referred to Clark and Fritz (1997) for an excellent summary. Many hydrogeologists are surprised when they discover how inexpensive stable isotopes can be (often less than $80 for a combined O and H isotopic analysis), and how easy it is to collect the samples: simply fill a small bottle to the top (no head space) with filtered water, seal tightly, and send to the lab. No refrigeration is needed. Even if your project has no plans for isotopic work this year, it may be worth archiving a set of filtered samples in case you decide to employ isotopes at a later date. Water samples can be stored indefinitely prior to stable isotope analysis, so long as they are tightly sealed. Also, because 10 mL is plenty of sample for O and H isotopic analysis, shelf space should not be a problem.

A detailed treatment of different methods to date groundwater would fill a textbook in its own right (e.g., see Kazemi et al. 2006). Cook and Solomon (1997) provided an early overview of different methods that have been developed, including tritium (^{3}H) analysis, ^{3}He-^{3}H analysis, and use of chlorofluorocarbons (CFCs). ^{3}He-^{3}H (helium-tritium) is the most precise method for dating relatively young (< 50 years) groundwater, but sample collection requires specialized equipment and the cost may be prohibitive for routine monitoring studies. Analysis of tritium by itself is much simpler and cheaper than ^{3}He-^{3}H, but can only be used to discriminate between water that is older than ~ 1952 from

water that is younger, 1952 being the date when nuclear testing produced a "slug" of tritium in the atmosphere. CFC analyses are also relatively inexpensive and can be used (with caution) to date relatively young groundwater to a precision of a few years, but again require specialized sampling equipment and are prone to contamination from CFC sources other than the atmosphere.

7.5 Interpreting Lab Results

Data validation

All commercial laboratories will follow an approved EPA analytical method that is appropriate for their equipment and the type of analysis being performed. The analytical method will include a large number of internal quality control checks, such as lab blanks, lab duplicates, lab spikes, and continuing standards (often referred to as instrument performance checks (IPC) or continuing calibration verification (CCV)). Most laboratories will report the results of the QA checks along with the table of analytical results, although sometimes QA reporting is only supplied upon request at an additional cost. If the lab sends a QA report, do not lose this information. Each user (or his/her supervisor) should verify that all QA checks for elements of critical importance were passed during the analytical session.

Normally a full set of lab QA checks is run every batch of 10 unknown samples, including a lab duplicate, a lab spike, an IPC, and a lab blank. The *lab duplicate* is a re-analysis of the first unknown sample in the preceding set. Typically, lab duplicates should agree within 10%, unless concentrations are very close to the IDL (instrument detection limit). In a *lab spike*, a known amount of spike solution containing a mixture of all of the elements of interest is added to the first unknown sample. Knowing the mass of spike added and its concentration, the nominal increase in concentration for the sample is calculated, and the % spike recovery in the QA sample is given as follows:

$$\%\ \text{spike recovery} = [(C_1 - C_0)/C_s] \times 100 \tag{7.7}$$

where C_1 is the concentration of the spiked sample, C_0 is the concentration of the same sample before the spike, and C_s is the expected increase in concentration from the spike. Lab spikes are an excellent way to test for matrix interferences in a given batch of samples, and should have recoveries within ±20% of 100%. Poor spike recovery is common when the sample concentration is high relative to the spike contribution, and in such cases does not necessarily indicate a problem with the analysis. An instrument performance check (IPC, or CCV) is a multielement standard of known composition which is run every 10 unknowns to

check that the instrument calibration is still acceptable. IPCs should agree within 10% of their nominal values. Finally, the laboratory blank is a sample of distilled and deionized water with the same acid matrix as the unknowns. The lab blanks should give concentrations below the IDL for all elements of concern. If not, there may be a problem with acid reagent contamination, or with carry-over of metal between samples (e.g., from insufficient flushing).

If an EPA standard method is being followed, then it is up to the analyst to examine the results of the QA check to be sure they pass all validation criteria. If not, then the data are flagged for the element of concern, or the samples are reanalyzed. In addition to the laboratory QA checks discussed above, field blanks and field duplicate samples should be collected during each period of sample collection. The results of these QA checks should also be scrutinized for signs of possible contamination (e.g., from sample bottles or filtering equipment), and summarized as an important part of the final report.

Example 7.8 Table 7.5 shows an example ICP-AES laboratory report collected for some river samples. In this analytical session, the % spike recovery and RPD of the IPC sample were both outside of the acceptable ranges

TABLE 7.5 Example ICP-AES Laboratory Report (All Data are in mg/L)

Sample Name	Ca	Cu	Fe	K	Mg	Mn	Na	Zn
IDL	0.02	0.003	0.001	0.5	0.1	0.0005	0.5	0.0005
IPC-nominal	10	0.5	0.5	0.5	10	0.5	10	0.5
Spike contribution	19.5	0.489	0.5	4.9	4.89	0.5	9.77	0.489
Sample unknown								
CG-1	12.7	0.122	0.046	0.76	3.42	0.146	1.82	0.040
CG-2	13.2	0.111	0.054	0.67	3.56	0.144	1.95	0.039
CG-3	13.3	0.096	0.031	0.71	3.55	0.141	1.90	0.039
CG-4	13.2	0.101	0.038	0.71	3.48	0.132	2.24	0.038
CG-5	13.1	0.115	0.035	0.73	3.45	0.133	2.08	0.040
QA checks								
CG-1 Lab dup	13.1	0.125	0.047	0.77	3.49	0.148	1.87	0.040
RPD of dup	2.4%	2.5%	1.9%	1.1%	2.0%	2.0%	2.8%	1.0%
CG-1 Lab spike	29.8	0.586	0.501	5.29	7.97	0.612	13.7	0.493
% Spike recovery	87.6%	94.9%	90.9%	92.3%	93.0%	93.3%	**122%**	92.6%
IPC	9.96	0.499	0.493	5.20	10.2	0.510	13.5	0.499
RPD of IPC	−0.4%	−0.3%	−1.4%	3.9%	2.1%	2.1%	**35.4%**	−0.3%
Lab blank	<.02	<.003	<.001	<.50	<.10	<.0005	<.50	<.0005

IDL = instrument detection limit; IPC = instrument performance check; Lab Dup = laboratory duplicate sample; RPD = reproducibility (RPD = difference/mean)

for Na. Consequently, the Na data are shaded to show that the QA checks did not pass. Because Na was not a critical analyte for this project, the samples did not need to be reanalyzed.

Charge balance

All water samples are electrically neutral, meaning that the sum of the positively charged cations must be exactly equal to the sum of the negatively charged anions. Therefore, a very useful test of the completeness and accuracy of your field and laboratory data is to perform a charge balance calculation. Charge balance is usually calculated by the following equation:

$$\text{Charge balance (\%)} = \frac{\Sigma\text{meq cation} - \Sigma\text{meq anions}}{(\Sigma\text{meq cations} + \Sigma\text{meq anions}) \div 2} \times 100 \tag{7.8}$$

where "meq" means "milli-equivalents per liter," and is the concentration of each solute in mg/L divided by its gram formula weight, and multiplied by its charge. (A periodic table to determine gram formula weights is found in Appendix C.) For example, 29.2 mg/L Mg^{2+} will contribute $29.2/24.31 \times 2 = 2.4$ meq of (+) charge. Example 7.9 shows a charge-balance calculation for a mine water in Butte. As a general rule, the charge balance error should be within ±5% of zero using Equation 7.8, although in most cases the error will be less than 1 or 2% if good field and lab procedures are followed. If the charge balance is outside 5%, it could mean one of several things: (1) problems with field measurements (e.g., alkalinity), (2) problems with the lab analysis (e.g., poor standardization or failure to correct the results for laboratory dilutions), (3) incorrect assignment of the charge for one or more of the major solutes or, (4) the list of compounds that were analyzed was incomplete. The third type of error is a problem for acidic, Fe-rich waters such as the Berkeley pit lake where it is often uncertain whether the dissolved iron is ferrous (Fe^{2+}) or ferric (Fe^{3+}). (For groundwater with pH > 4, you can assume that all Fe will be Fe^{2+}, since the solubility of ferric iron is very low at near-neutral pH.) As an example of the fourth source of error, our group was once puzzled by consistently poor charge balances for surface water samples from the Big Hole River in southwest Montana. The problem was eventually attributed to high concentrations of dissolved organic carbon (>10 mg/L as C). Because many forms of DOC carry a negative charge (e.g., the COO^- groups on humic and fulvic acids), failure to include DOC in the charge balance calculation resulted in an apparent excess of cations.

Example 7.9 The following data (Table 7.6) were collected from a flooded mine shaft sample in Butte, Montana (GWIC ID#142793, collected 4/8/2003). The sum of the meq/L of cations and anions agreed within 0.5%, indicating a

TABLE 7.6 Charge-Balance Calculation for the Ophir Flooded Mine Shaft

cations	mg/L	gfw	meq/L	anions	mg/L	gfw	meq/L
Ca^{2+}	110	40.08	5.49	HCO_3^-	218	61.03	3.57
Mg^{2+}	29.2	24.31	2.40	CO_3^{2-}	0.0	60.03	0.00
Na^+	24.5	22.99	1.07	SO_4^{2-}	240	96.06	5.00
K^+	4.6	39.10	0.12	Cl^-	38.7	35.45	1.09
Mn^{2+}	11.2	54.94	0.41	F^-	0.4	19.00	0.02
Zn^{2+}	1.8	65.37	0.06	Br^-	0.2	79.91	0.00
Fe^{2+}	0.3	55.85	0.02				
		total	9.55			total	9.69

Charge balance = $(9.55-9.69)/(9.55+9.69)/2 \times 100 = -0.36\%$

very good charge balance. Note that in this calculation, it was necessary to estimate the concentrations of HCO_3^- and CO_3^{2-}. Because the pH of this water was < 7, the concentration of CO_3^{2-} was vanishingly small, and HCO_3^- could be approximated from alkalinity. These assumptions may be invalid for high pH water samples, as discussed later in the next section.

Speciation of dissolved inorganic carbon

A complete chemical analysis of a given groundwater sample will require information on the concentrations of bicarbonate (HCO_3^-) and carbonate (CO_3^{2-}) ions. For most waters with pH <8, the concentration of bicarbonate can be computed from the measured alkalinity because at these pH values HCO_3^- is the dominant titratable base in the water. However, as pH rises above about 8.0, there is an increasing contribution to the total alkalinity from CO_3^{2-} and OH^- ions (Table 7.7). In this case, the speciation of alkalinity and inorganic carbon is best done using a geochemical modeling program, such as Visual MINTEQ (a recent, user-friendly

TABLE 7.7 The Distribution of Total Alkalinity between HCO_3^-, CO_3^{2-}, and OH^- at Different pH Values

pH	% as HCO_3^-	% as CO_3^{2-}	% as OH^-
7	99.9	0.1	0.0
7.5	99.7	0.3	0.0
8	99.1	0.8	0.0
8.5	97.3	2.6	0.1
9	91.9	7.7	0.3
9.5	78.1	20.8	1.1
10	52.5	44.0	3.4
10.5	24.3	64.8	10.8

The calculations assume T = 20°C, ionic strength = 0.001 m, and $PCO_2 = 10^{-3.5}$ bars (close to atmospheric saturation).

variant of the original EPA program described by Allison et al. 1991) or PHREEQC (developed and distributed by the USGS). Both of these programs are widely used and are freely available from the internet, but it will take a while for a beginner to get familiar with them. The user first creates an input file that specifies the field temperature, pH, alkalinity, and concentrations of solutes as determined by the laboratory. The input file is then run through a speciation program, and an output file is created that lists the concentrations and chemical activities of each solute. Both Visual MINTEQ and PHREEQC can do redox calculations and gas-water reactions, and will compute the partial pressure of dissolved $CO_2(g)$ for your water sample. These programs will also perform a "speciated" charge balance calculation, which is an excellent QA check on the reliability of your field and lab data. More advanced functions such as calculation of mineral saturation indices and adsorption modeling are also built into the software, but are beyond the scope of this chapter.

Hardness and sodium adsorption ratio

Hardness is related to the concentration of dissolved Ca^{2+} and Mg^{2+} in a water sample. It is easily calculated by the following formula (from Drever 1997):

$$\text{Hardness (in mg/L of } CaCO_{3,eq}) = (\text{mg/L Ca}) \times 2.5 + (\text{mg/L Mg}) \times 4.1 \quad (7.9)$$

Historically, the term "hard water" had to do with the tendency of a water sample to precipitate calcium carbonate scale upon evaporation, hence the convention of reporting hardness in units of $CaCO_3$ equivalents. However, it is possible for a water to have high Ca and Mg content (and therefore high hardness) but low dissolved carbonate content. Acid mine waters and Ca-Cl-rich brines are two examples.

Sodium adsorption ratio (SAR) is frequently used to quantify the potential for "sodium toxicity" from irrigation water. SAR is calculated as follows:

$$\text{SAR} = \frac{[\text{Na}]}{\sqrt{\{[\text{Ca}] + [\text{Mg}]\}}} \quad (7.10)$$

where the brackets [] denote concentrations in millimoles per liter. (A millimole per liter is simply the concentration in mg/L divided by the gram formula weight.) Continuous irrigation with water containing SAR > 10 may be detrimental to crops that are sensitive to sodium (U.S. Salinity Lab 1954). This is another serious issue with respect to discharge waters from coal-bed methane wells (Van Voast 2003).

7.6 Tips on Reporting Data

Sooner or later you will be required to summarize your field and laboratory data for a final project report, thesis, or journal publication. The following are a few tips and suggestions.

First, pay close attention to *units*. This is the most common source of confusion and error in data reporting. Each column in the data table should have units explicitly stated, either at the top of the column or in a footnote. For compounds such as SO_4, SiO_2, HCO_3, PO_4, or NO_3, be clear about whether the value in the table denotes mg/L as the element, or as the compound. For example, 20 mg/L NO_3 as NO_3 is equivalent to 4.5 mg/L NO_3 as N. Big difference! It matters little which convention you choose in your own table as long as you are clear which unit convention you have adopted.

Second, pay attention to *significant figures*. Most commercial laboratories will round off their analytical results to an appropriate number of significant figures, which is usually 1, 2, or 3 depending on the method of analysis and the concentration of the sample. However, if you receive lab data in "raw" form, or do manipulations in a separate spreadsheet, the data will likely have an undetermined number of significant figures. All such data should be rounded off to a number of digits that is appropriate to the precision of the analysis. For example, 342.45 mg/L SO_4 is more realistically reported as 340 mg/L SO_4, given the ±5% precision of a typical IC analysis.

Third, be consistent about how you report data that are below the instrument detection limit (IDL). Many authors will simply list the IDLs in a separate row at the top or bottom of the table, and then specify the low analyte concentrations as "b.d." (below detection). However, if the sample was diluted prior to analysis (which is often the case for ICP-ES or ICP-MS analyses of polluted waters), then the practical quantification limit (PQL) for that sample is actually the IDL multiplied by the dilution factor. To avoid confusion, the best approach is to specify the PQL for all analytes that are below detection within the main body of the table. For example, if a sample diluted 10 times had a Cd concentration below an IDL of 2 μg/L, the result would be reported in the data table as "< 20 μg/L." For *statistical analysis*, a common convention is to assign below-detect data a value of 1/2 the PQL. Whereas this may be allowable for the spreadsheet that serves as the statistics database, it is not a good idea to do this in tables that are published in your final report, as you are essentially making up numbers that may or may not be valid.

In some cases, parameters such as pH, SC, ORP, and alkalinity will be determined both in the field and the laboratory. The question then becomes, which set of data should be given in the final report? There is no universal recommendation that can be made here. In general, laboratory measurements will have higher precision, accuracy, and comparability than data collected in the field by different workers using different field equipment that may or may not be properly calibrated. However, if field SOPs are followed with diligence, then these data may in fact be more valuable than the lab

results because the chemistry of a given sample can change after collection (see Examples 7.2, 7.3, and 7.7). A good compromise would be to report *both* the field and lab measurements in the final table of results.

Finally, it is stressed that the *date* of sample collection should be included in all data tables. This is especially true for surface water samples, but groundwater samples can also show seasonal or long-term variations in water chemistry. For surface water samples, it is also recommended to include the *time of day* alongside the date. Our research has shown that the chemistry of rivers and streams can change dramatically on a diurnal (24-h) basis.

Example 7.10 Figure 7.10 shows an example data set collected from the Big Hole River, Montana, during mid-summer, low-flow conditions. The pH and DO of the water both increased during the day, owing to photosynthesis by algae and aquatic plants. As shown by the following reaction, photosynthesis not only produces DO, but also consumes dissolved CO_2:

$$CO_2(aq) + H_2O = CH_2O \text{ (organic carbon)} + O_2(aq) \qquad (7.11)$$

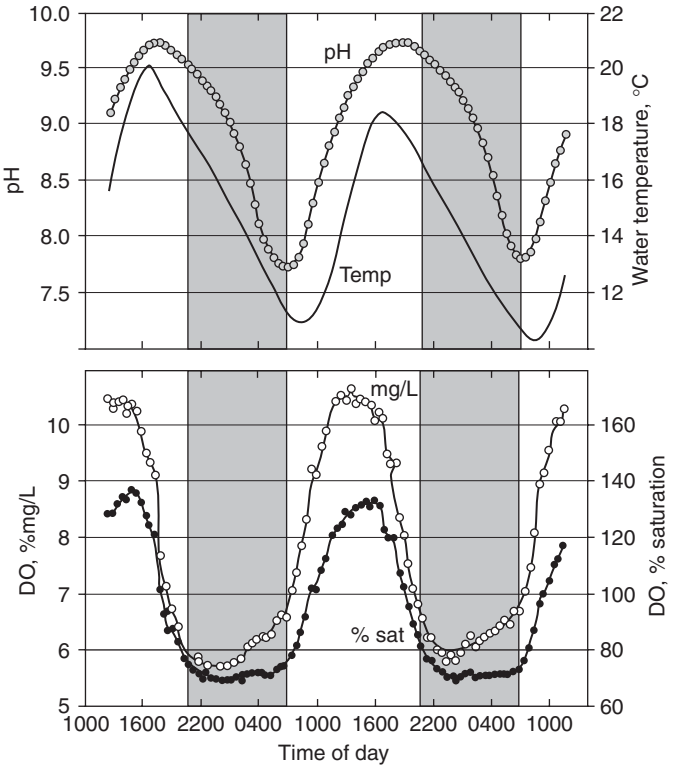

Figure 7.10 Diurnal variations in pH, temperature, and dissolved oxygen (DO) in the upper Big Hole River, August, 2000. [*C. Gammons, unpublished data*]

Because CO_2 is a weak acid, a decrease in its concentration typically results in an increase in pH. Although this example focuses on pH and DO, almost any parameter that you can measure, including the concentrations of major solutes, trace metals, and nutrients, will – in some cases – show diurnal fluctuations in a surface water body (Brick and Moore 1996; Nimick et al. 2003), making the time of sample collection a critical variable that should be reported in the final table of results.

7.7 Summary

The most important step in any water-quality study is to carefully formulate the question that you are trying to address, and then to write a Sampling and Analytical Plan (SAP) for how you will carry out the work. Careful thought needs to be given as to where, when, and how often you will sample, what equipment and supplies you will need, which measurements will be taken in the field, what types of samples will need to be collected for laboratory work, which laboratory will do the work, and the estimated total project costs. Depending on the nature of your work, you may also need to specify what quality assurance (QA) steps will be taken, and how the final data will be validated. Regardless of whether rigorous QA documentation is mandatory for your project, always take steps to insure that the environmental samples and field data that you collect are of the highest quality possible, given the amount of time and money you have available.

This chapter has given an overview of most of the common technical procedures that groundwater specialists are likely to encounter when collecting or analyzing samples for chemical parameters. However, it is always a good idea to seek additional information before heading into the field, especially if you are not confident in a given procedure. A lot of material is available on the internet, but it is sometimes of questionable reliability. The resources mentioned at the beginning of this chapter have all been carefully peer-reviewed, and much of this information is available on-line. Also, do not hesitate to talk to another human being! This author has spent many hours speaking on the phone with technical service representatives for supply companies, for example, and sometimes that is the fastest way to solve a question about how to do something.

References

Allison, J.D., Brown, D.S., and Novo-Gradac, K.J., 1991. MINTEQA2/PRODEFA2, A Geochemical Assessment Model for Environmental Systems: Version 3.0 Users Manual. *Environ. Res. Lab*., U.S. Environmental Protection Agency.

Barbash, J.E., and Resek, E.A., 1996. *Pesticides in Ground Water: Distribution, Trends, and Governing Factors*. Ann Arbor Press.

Bedient, P.B., Rifai, H.S., and Newell, C.J., 1999. *Ground Water Contamination*, 2nd ed. Prentice-Hall, Upper Saddle River, NJ.

Brick, C.M., and Moore, J.N., 1996. Diel Variation of Trace Metals in the Upper Clark Fork River, Montana. *Environmental Science and Technology*, Vol. 30, pp. 1953–1960.

Clark, I., and Fritz, P., 1997. *Environmental Isotopes in Hydrogeology*. Lewis Publishers, New York.

Cook, P.G., and Solomon, D.K., 1997. Recent Advances in Dating Young Groundwater: Chlorofluorocarbons, $^{3}H/^{3}He$ and ^{85}Kr. *Journal of Hydrology*, Vol. 191, pp. 245–265.

Drever, J. I., 1997. *The Geochemistry of Natural Waters*, 3rd ed. Prentice-Hall, Upper Saddle River, NJ.

Eby, G.N., 2004. *Principles of Environmental Geochemistry*. Brooks/Cole, Pacific Grove, CA.

EPA, 2002. *Guidance for Quality Assurance Project Plans*. U.S. Environmental Protection Agency, EPA QA/G-5, 111 pp, http://www.epa.gov/QUALITY/qs-docs/g5-final.pdf

EPA, 2006. Pharmaceuticals and Personal Care Products (PPCPs) as Environmental Pollutants. http://www.epa.gov/esd/chemistry/pharma/index.htm

Fetter, C.W., 1999. *Contaminant Hydrogeology*, 2nd ed. Prentice-Hall, Upper Saddle River, NJ.

Gammons, C.H., Poulson, S.R., Pellicori, D.A., Roesler, A., Reed, P.J., and Petrescu, E.M., 2006. The Hydrogen and Oxygen Isotopic Composition of Precipitation, Evaporated Mine Water, and River Water in Montana, USA. *Journal of Hydrology*, Vol. 328, pp. 319–330.

Gammons, C.H., Milodragovich, L., and Belanger-Woods, J., 2007. Influence of Diurnal Cycles on Monitoring of Metal Concentrations and Loads in Streams Draining Abandoned Mine Lands: An Example from High Ore Creek, Montana. *Environmental Geology*, in press, [doi 10.1007/s00254-007-0676-z].

Heberer, T., 2002. Occurrence, Fate, and Removal of Pharmaceutical Residues in the Aquatic Environment: A Review of Recent Research Data. *Toxicology Letters*, Vol. 131, pp. 5–17.

Hem, J.D., 1985. *Study and Interpretation of the Chemical Characteristics of Natural Water*, 3rd ed. U. S. Geol. Surv. Water-Supply Paper 2254, 263pp, http://pubs.usgs.gov/wsp/wsp2254/pdf/wsp2254a.pdf

ITRC, 2006. *Technology Review of Passive Sampler Technologies*. Interstate Technology and Regulatory Council, 115 pp, http://www.itrcweb.org/documents/DSP_4.pdf

Kazemi, A.A., Lehr, J.L., and Perrochet, P., 2006. *Groundwater Age*. Wiley-Interscience, Hoboken, N.J., 325 pp.

Kehew, A.E., 2001. *Applied Chemical Hydrogeology*. Prentice-Hall, Upper Saddle River, NJ.

Langmuir, D., 1997. *Aqueous Environmental Geochemistry*. Prentice-Hall, Upper Saddle River, NJ.

Nimick, D.A., Gammons, C.H., Cleasby, T.E., Madison, J.P., Skaar, D., and Brick, C.M., 2003. Diel Cycles in Dissolved Metal Concentrations in Streams — Occurrence and Possible Causes. *Water Resources Research*, Vol. 39, Paper 1247, doi:10.1029/WR001571.

Pellicori, D.A., Gammons, C.H., and Poulson, S.R., 2005. Geochemistry and Stable Isotope Composition of the Berkeley Pit Lake and Surrounding Mine Waters, Butte, Montana. *Applied Geochemistry*, Vol. 20, pp. 2116–2137.

Stookey, L.L., 1970. Ferrozine – A New Spectrophotometric Reagent for Iron. *Analytical Chemistry*, Vol. 42, pp. 779–781.

Stumm, W. and Morgan, J.J., 1995. *Aquatic Chemistry*, 3rd ed. Wiley, NY.

USGS, 1995. Groud-Water Data-Collection Protocols and Procedures for the National Water-Quality Assessment Program: Collection and Documentation of Water-Quality Samples and Related Data. *U.S. Geological Survey, Open-File Report 95-399*. Available online at: http://water.usgs.gov/nawqa/OFR95-399.html

USGS, 2005. National Field Manual for the Collection of Water-Quality Data. *U.S. Geological Survey Techniques of Water-Resources Investigations, Book 9*. Available online at: http://water.usgs.gov/owq/FieldManual/

U.S. Salinity Lab, 1954. Diagnosis and Improvement of Saline and Alkali Soils. *U.S. Dept. of Agriculture Handbook 60*, 160 pp.

Van Voast, W.A., 2003. Geochemical Signature of Formation Waters Associated with Coalbed Methane. *AAPG Bulletin*, Vol. 87, pp. 667–676.

Chapter

8

Drilling and Well Completion

Perhaps one of the more common tasks a hydrogeologist will be involved with is obtaining subsurface information, which can be found through a variety of methods, including geophysical (Chapter 4), hand tools, and drilling methods. This chapter presents the common drilling methods and explains how monitoring and production wells are installed. A hydrogeologist does not need to know how to run a drill rig but should be familiar with drilling methods, terms, and well-completion strategies so that meaningful subsurface information can be obtained. Also, the hydrogeologist, with some guidance, will be better informed to make decisions in the field.

Hydrogeologists need to be able to work safely with the drill crews in obtaining subsurface information. It is helpful to know the basics of drilling methodologies, how to describe drill cuttings, and what is involved in well completion. The approach taken here is to familiarize entry-level hydrogeologists or professionals unfamiliar with drilling operations with what they should know to safely proceed.

Understanding the geology of an area (Chapter 2) is helpful in knowing which drilling methodologies would be most productive and result in obtaining the best subsurface information. Examples of drilling in different geologic settings are presented throughout to show applications of the appropriate drilling method in a given geologic environment.

8.1 Getting Along with Drillers

Drillers are an interesting breed and can make your life highly productive and successful or exceedingly miserable. The biggest factor, generally, is you and your attitude. A friendly, helpful, congenial, useful attitude (Boothman, 2000) on your part can go a long way to getting the best information possible. During any given day, things can and will go wrong, but it is up to you to decide how you will let your circumstances govern your actions.

Copyright © 2008, 2001 by The McGraw-Hill Companies, Inc. Click here for terms of use.

Example 8.1 If you have little experience working with drillers the following experience, related by Tom Aley (Chapter 15), is a good illustration on the proper attitude to have. This is what I recall Tom had to say:

"At my first experience working with drillers on a drilling project, I figured I didn't know what I was doing and needed their help, so I bought a dozen donuts and a pot of coffee and brought these to the site. Then I said, "Guys I don't know much about drilling, maybe you can help me get the job done. We got along great and I had a good experience."

This illustration shows how having a useful attitude can go a long way to a win-win situation.

Drillers are generally very professional and knowledgeable about what they do. They know when "first" water has been found or what the conditions are like at depth (Figure 8.1). Nothing is more irritating to them than to have a young inexperienced person tell them how to do their job. If you get on their bad side, watch out. It has been the author's experience from

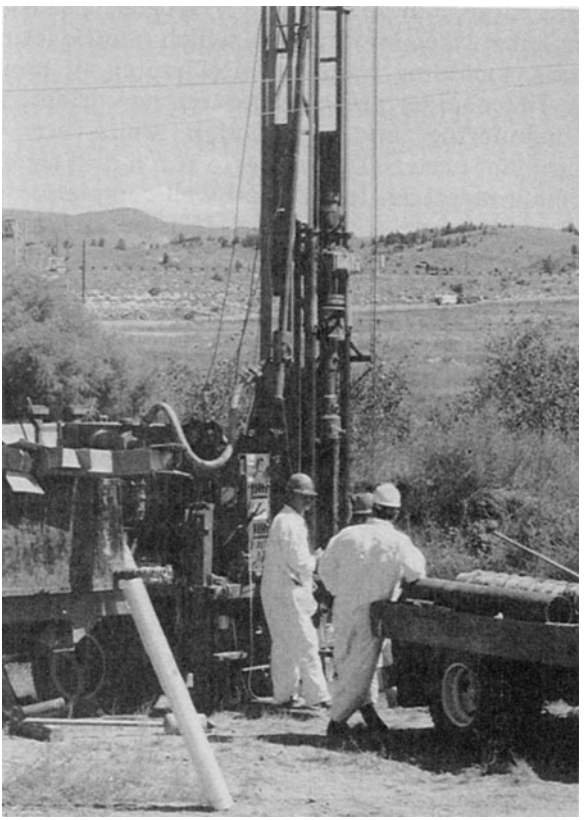

Figure 8.1 Discussing drilling conditions during monitoring well installation. (*Photo courtesy of O'Keefe Drilling.*)

being involved with a variety of drilling conditions in various parts of the world that disgruntled drillers do unpleasant things to smart aleck geologists or hydrogeologists. For example, while you are away, your briefcase may be rearranged, your vehicle sabotaged, or your person may be adorned with lubrication grease. It is better to be polite, act interested, and ask questions: for example, Did we just go through a gravel layer? Are we making a bit more water? Was that last drill rod 120 ft or 140 ft?

There is a fine line between the drillers making footage and your obtaining complete information. It is your responsibility to obtain good subsurface information. If the drillers are going too fast, you need to politely ask them to slow down. How the job is bid is an important factor. Is payment by the job, by the foot, or by the hour? Being cognizant that a job needs to be done and that drillers need to make a living, too, leads to a cooperative relationship. The bottom line, however, is that you, the hydrogeologist, are responsible for the subsurface information.

Other factors that help or hinder a working relationship are the little things. Do you collect your cuttings and then sit in the vehicle until the next drill rod is ready to go in? Or do you always sit in your vehicle while the drill rods are being coupled together and going into the hole (**"tripping in"**) or being pulled out of the ground (**"tripping out"**)? Simple gestures like helping shovel cuttings out of the way, helping guide a **sand line**, or retrieving a tool helps the process run smoother and contributes to a positive working relationship (Figure 8.2). While the driller helper has

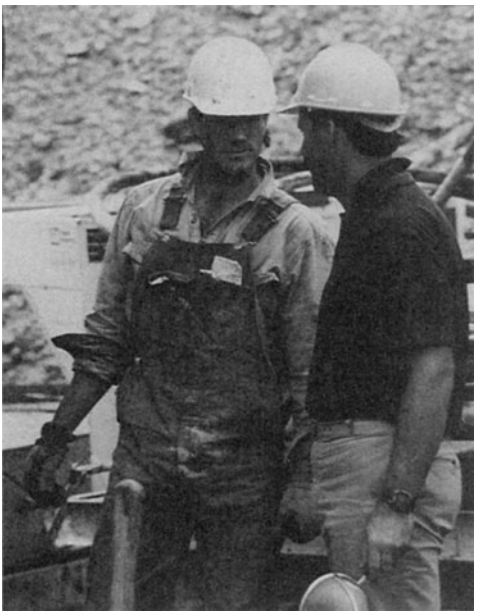

Figure 8.2 Driller and geologist in conference. (*Photo courtesy of O'Keefe Drilling.*)

gone for water do you assist or stand around? This is something each professional has to decide for him- or herself, but can make a big difference in how a job gets done. Company policies may address these issues, but being helpful is a good way to be.

Sometimes breakdowns occur, the equipment needs attention, or something may be inadvertently dropped down the hole and a "fishing" expedition is under way (see Example 8.12, Section 8.6). In some cases, there is nothing you can do but stay out of the way. Being patient and understanding that "things happen" is more helpful than yelling at your help.

8.2 Rig Safety

In the above discussion, no information is required at your peril. Always think safety. There are few pieces of equipment with more moving parts than a drill rig. If you are within the mast length of the drill rig, then you need to be checking and looking around. You need to look up as often as you check your rearview mirror while driving a vehicle (every few seconds) because a hardhat cannot save you from a falling drill pipe. Equipment can break loose, cables can break, and conditions can change in a heartbeat. Always have a sense of caution and safety in mind.

The minimum appropriate attire at the drill site is steel-toed shoes, a hardhat, gloves, and safety glasses (Figure 8.3). If you are working at a hazardous waste site, other protective clothing will be required. Loose clothing is susceptible to becoming snagged by a rotating machine, pulling you in or getting torn up.

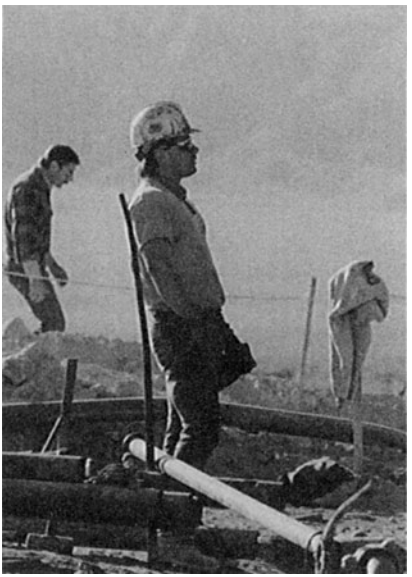

Figure 8.3 Minimum safety equipment: hardhat, steel-toed boots, safety glasses, and gloves. (*Photo courtesy of O'Keefe Drilling.*)

The safest place to stand near a drill rig is on the driller side (Figure 8.4). The driller is in charge of the controls and is the most knowledgeable person about what is going on. He or she is the person you need to have an ongoing dialog with and will be most helpful in answering your questions. The "helper" side is generally the direction where more things fall and more moving items are located. The helper's job is to help make connections, place pipe into position, or place "slips," wrenches, or other equipment in place.

If you want to help, observe what the helper does and then ask at the appropriate time. Never put your hands, fingers, or other where you can be pinched, trapped, or will compromise safety. No drill hole is worth an injury. If you don't feel comfortable helping, then stand back and get out of the way. Another obvious, but important point is, there is a fair amount of welding and grinding at times. Do not stare at the bright lights, it can damage your eyes (Figure 8.5). Grinding wheels can throw hot, sharp metals pieces, so please stand back.

If you need to write something down that will take longer than the few seconds needed to keep looking up, move well away to the driller's side or walk over to your vehicle. If you have to write something down that will take time, tell the drillers and have them wait. You may miss something important. Work methodically, conscientiously, and safely. Remember, your vehicle should have been parked farther away than the length of the drill mast. The best thing to do is ask the driller where to park, because he or she may have some maneuvering plans for the water truck or other equipment.

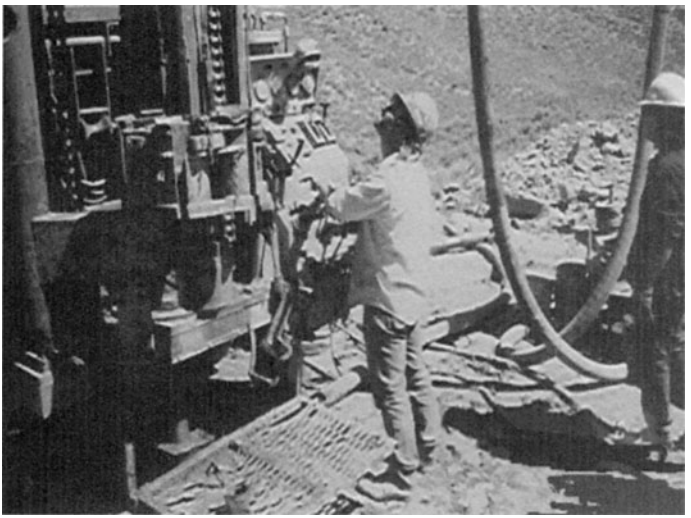

Figure 8.4 The driller's side of the rig is the safest place to stand. (*Photo courtesy of O'Keefe Drilling.*)

Figure 8.5 Welding on another section of casing.

Before you drill, it is a good idea to call a toll-free number to have the utility lines located. This has to be arranged 48 h in advance, so plan ahead. A person will be dispatched to locate water (marked blue), power (marked red), gas (marked yellow), phone or TV cable (marked green or black) in spray paint in the ground surface (Figure 8.6). Contacting the local courthouse or city government can be helpful in locating sewer or other utility lines. Installing monitoring wells and making a spark from encountering a gas line while drilling can be interesting.

Figure 8.6 Drill site with utility lines marked on the surface.

Example 8.2 An elementary school in Butte, Montana, was having basement flooding problems year after year, each spring. School district maintenance officials were interested in knowing why they had a problem and not just how to solve the problem. The biggest problem appeared to be that a 72-in (1.8-m) culvert was directing runoff water from a drainage originating at the Continental Divide under an interstate highway toward the school.

Another significant problem was that the school was located on fill materials in a floodplain (Figure 8.7). Surface water and groundwater would move toward the school and back up against the fill materials and basement wall as the water table rose each spring. By summer time, the groundwater levels dropped more than 10 ft (3 m) below the basement slab. A dewatering system was designed to alleviate the problem until the various parties of county and state could work out disputes on how to correct the surface drainage.

As part of the investigation, a series of monitoring wells were installed. Before drilling, the toll-free telephone number was called and the utility lines were located. While drilling one hole near the front of the school, a light-colored powder came up with the cuttings at a depth of 7 ft (2.1 m). Smelling the power revealed that we were drilling into concrete. A decision was made to abandon the hole, as it was thought it might be an unmarked sewer line. Later on, it was discovered from an oldtimer that it was more likely that we were drilling into a concrete block that was part of the fill material. This illustrates the need to use all your senses, be cautious, and make good use of the available resources in finding out information about a site.

Drill rigs make good lightning rods. If stormy conditions are possible, keep a wary eye open. Often, you can watch clouds approaching from a particular direction. The sound of thunder is a sure sign that lightning

Figure 8.7 Elementary school site (bottom center) built on fill placed in the middle of a drainage. (*Photo courtesy of Hugh Dresser*.)

is not far away. A simple conversation with the driller will result in a mutual waiting period for the storm to pass over. Drill rig masts can also extend up into power lines. In conversations with other drillers, it is the author's understanding that a rig should be more than 15 to 30 ft (4.6 to 9.1 m) away from power lines or arcing may occur. A phone call to a power utility may result in it placing insulated covers over the power lines so that drilling can proceed safely. Ask your driller what he or she would suggest.

Drilling operations attract people. Drilling in remote areas often draws curious onlookers (Figure 8.8). Flag off your safety area so that onlookers are kept back. People getting too close can slow down working operations and increase the potential for hazards. A smile and firm demeanor usually gets the message across. One of the biggest problems drillers encounter is clients that do not follow the safety rules. As a hydrogeologist on site, make sure the clients are wearing the minimum safety equipment or politely tell them to back over to a safer place.

Summary of safety points

- Have a useful attitude.
- Always look up, as you would check a rearview mirror.
- Park your vehicle a full drill mast length away from the rig or ask the driller where to park, as he or she may have a particular method of maneuvering equipment.
- Stand on the driller's side of the rig.

Figure 8.8 Curious children from the Peoples Republic of China.

- If you have to write a long time (more than approximately 3 s), move away from the rig to the driller's side.
- Don't watch people weld.
- Never drill without locating utility lines or identifying other hazards, such as power lines.
- Thunder usually means lightning, so stop what you are doing until this danger has passed over.
- Use caution when drilling near power lines.
- Rope off your area to keep curious onlookers back.
- Prior to donning personal protective equipment or respirators, work out a communication protocol, so that signals are clear.
- Never, never, never compromise safety, it can be fatal.

Other considerations

Common sense is an important part of your tool box. Most of the time it is the hydrogeologist's responsibility to tell the driller where to drill. The direction of the wind is a significant factor. If you have a serious wind blowing from the front of the rig toward the back, you are going to eat the dust and cuttings swirling around you. This is especially unpleasant when drilling with air and a forward rotary rig in a coal bed.

Have plenty of layers of clothing to put on or take off. Nothing is more miserable than being cold or hot while you are trying to collect data. Your hands do not write well when the fingers are stiff and your lips are blue. At the same time, dripping perspiration on your log book can damage what you have written down. Layers allow flexibility in staying comfortable. A person too cold or too hot is more inclined to make mistakes. This affects safety and the quality of information collected.

Drilling near hazardous waste sites and other conditions require an extra dose of common sense. Dressing out in level "A" personal protective equipment (PPE) can affect your performance (Figure 8.9). Heat stroke is often as dangerous as the hazards you are being protected from. Communication and frequent breaks will often be necessary. A particular communication protocol needs to be worked out in advance with all parties involved, along with step-by-step procedures before drilling begins. Sometimes methane or other gases may be present in certain situations. In this case, keeping a detection device operating to identify these gases will be necessary. Safety should never be inappropriately compromised.

Example 8.3 In eastern Montana, a number of coal mines are operating in the Fort Union Formation. Drilling is part of the ongoing exploration and production process. During a very cold day −10°F (−23°C), a propane torch was

Figure 8.9 Performing field tasks dressed out in level "A" personal protective equipment (PPE).

being used to thaw out some of the fluid lines on the rig. The TIP gas detector was inadvertently shut off because of the use of propane. This was a coal well, and methane gas was emitting from the well. The torch ignited the methane and the drill rig burned for 3 days before it could be pulled off the drill site!

It is not the intention of this section to provide a treatise on safety; however, pointing out several of the more common hazards found near drill rigs may prove helpful. To obtain more information and discussion about the principles of safety, the reader may consult Spellman and Whiting (1999).

8.3 Drilling Methods

A variety of drilling methods have been developed over time to account for the many geologic conditions. Some formations are very hard, such as granite, while others are soft or unconsolidated such as sand and gravel found in an alluvial setting. Drilling and subsequent well completion should be considered together when deciding which drilling method is most appropriate. Some methods may be faster than others but may result in disturbing the aquifer to the point of reducing yield. For example, if the production zone is completed in unconsolidated sediments, high-pressure drilling fluids may actually cause damage to the aquifer (disturb existing natural packing by suspending and mixing grains). In this case, production wells need to be drilled using a slower,

less-disruptive method so that production-zone disturbance is minimized. This chapter will explore the most common truck-mounted drilling methods. For a more complete discussion of drilling applications in the water-well industry, the reader is referred to Driscoll (1986).

Monitoring wells provide a point of access to the aquifer. They need to be constructed so that the hydraulic head and water-quality information collected is representative of the aquifer under investigation. Again, the drilling method will depend on the geologic conditions. The well-completion materials need to be appropriate for the water quality of the site, which may include such factors as pH, presence of organics, water temperature, or depth.

Cable-tool method

Perhaps one of the oldest drilling methods used is a percussion approach known as the cable-tool method. These technologies were developed by the Chinese some 4,000 years ago (Driscoll 1986). In this drilling method, a heavy drill bit is repeatedly lifted and dropped by a walking beam or spudding beam attached to a spooled cable via a pitman arm (Figure 8.10). The motion of the bit is up and down in a strokelike fashion, so that the bit strikes the bottom of the hole each time it is dropped. The spudding

Figure 8.10 Cable-tool drill rig.

beam is also the reason they are known as "spudder" rigs, although the author also knows of the spudding beam being referred to as a walking beam or rocker arm (from the up-and-down rocking motion).

The lifting and dropping of the drill tool results in the breaking up and crushing of geologic materials. Drilling continues until the drill tool advances a few feet (1 m) beyond the end of the casing. It is the author's experience that the casing exhibits a "bouncing" action while geologic materials are still inside the casings. Once the bit reaches the end of the casing, the bouncing stops and the drilling sound becomes more like a thud. The drilling action is usually followed by driving casing down the hole as the drilling proceeds.

The casing is driven by means of a "pounding plate" bolted to the drill tool (Figure 8.11). The stroking action of the rocker arm lifts and drops the drill tool causing the "pounding plate" to strike the casing with a loud clang! The clanging continues until the casing has been driven a few feet (1 m) below where drilling ceased. During this part of the operation, it is advised to have hearing protection. It is an effective drilling method in unconsolidated and softer materials, but most effective in brittle formations such as shales and limestone. It can be used in hard formations but may be very slow. The well casing associated with this method usually ranges from 4 in (10.1 cm) to 24 in (0.61 m), with depth capacities up to 2,000 ft (609 m) (NGWA 1998).

After the materials are broken up or crushed, they are bailed to the surface via a separate cable and spool. If the hole is dry, the bailing operation

Figure 8.11 A drive or "pounding" plate which is bolted to the drill tool to drive the casing.

is done by first pouring a couple of 5-gal (18.9 L) buckets of water down the hole or running a hose attached to a water truck to facilitate mixing with the cuttings. A heavy bailer equipped with a closing valve is lowered to the bottom of the hole through an auxiliary cable. One common name for an auxiliary cable is the sand line. The bailer is a long tube with an opening/closing valve (Figure 8.12), a **dart valve** bailer is an example. When the bailer is lowered to the bottom of the hole, the dart valve is compressed and the water/cuttings mixture gushes into the bailer. When the bailer is lifted the valve closes, thus trapping the mixture. The sand line retrieves the bailer where it is brought to the land surface. This can be lowered into a discharge chamber. When this is done, the dart valve once again compresses, and the water/cuttings mixture is released out through the discharge chamber (Figure 8.13). The cuttings can be directed away from the working area by digging a shallow trench.

Once the hole has been drilled a few feet (a meter or so), casing is pounded or driven to the bottom of the hole to keep the hole from sloughing (as previously described). Depending on the casing and tool-handling capabilities of the rig, the length of casing driven or added varies. The spudding wheel turns proportionally to the drilling rate. One can observe whether the formations are hard or soft by how much the spudding wheel rotates. It has been the author's experience for smaller diameter wells (6 to 8 in, 0.15 to 0.2 m) that 10 ft (3 m) is welded on each time. This results in an overall drilling rate of approximately 10 ft (3 m) per hour. Rates may vary significantly, but this rate is given for comparison with other methods.

Figure 8.12 Dart valve bailer on a cable-tool drill rig.

Figure 8.13 Discharge chamber to direct cuttings away from the drilling.

The cable-tool method is ideal when time is not of the essence, the geologic materials are relatively soft or brittle, and the formation disturbance needs to be minimized. Attempting the drill in hard materials may result in drilling rates too slow to be cost effective, unless the rig is capable of handing a much larger heavier bit. Cable-tool rigs are also useful in drilling shallow, larger-diameter holes, 18 to 24 in (0.46 to 0.61 m), used for construction supports, such as caissons.

The author has found this drilling method especially useful in drilling unconsolidated materials that may contain **heaving sands**. Heaving sands are loosely consolidated sand zones with relatively high confining pressures. When the drill hole breaches one of these zones, the sand gushes into the casing. The remedy is to drill out the intruding sand and attempt to proceed with the hole. This is very disruptive to the formation and is exacerbated using the forward rotary method.

Example 8.4 An irrigation well capable of 250 gpm was desired for irrigating a cemetery in Butte, Montana. The sediments consisted of unconsolidated weathered granitic materials, alternating beds of fine gravel, sand, and clay (Figure 8.14). The clay beds confined or semiconfined some of the sandy zones. Recharge to the sandy zones were from elevations sufficiently high to produce heaving sands or sands subject to high confining pressures. These are usually found immediately under a clay horizon. The cable-tool method was used to drill an 8-in (0.2-m) cased well. Heaving sand events occurred on several occasions while drilling the 170-ft (52-m) well. The sands would intrude approximately 15 to 20 ft (4.6 to 6.1 m) into the casing. The fine gravel zones were stable enough to complete a production zone in the well.

Figure 8.14 Split-spoon core sediments from Example 8.4.

Forward (direct) rotary method

The forward rotary or direct rotary method is perhaps the most versatile drilling method for smaller-diameter drilling (less than 12-in diameter wells). Greater drilling depths can be achieved than for other methods, and it is well suited for drilling in harder geologic materials. Part of the versatility comes from the variety of drilling additives that enhance the drilling environment.

In the forward rotary method, a bit and drill pipe string are rotated by means of a power drive system. The power drive can be at the top of the drill string (a top-head drive) (Figure 8.15) or near the working level of the drillers, a table-drive system.

In a table-drive system, the top of the drill string is a **kelly** bar, which is turned inside the table. The kelly slides through drive bushings in the rotary table. When these are in their proper place, the table turns the kelly and the drill-string bit configuration and feeds it down hole (Driscoll 1986). The shape of the kelly bar is often square or hexagonal and approximately 3 ft (1 m) longer than the drill pipe (Driscoll 1986). Connected to the bottom of the kelly is a short (less than 1 m) removable section used to connect the first drill pipe to the kelly. This removable section or "sub" is there to save on wear and tear of the threads at the end of the kelly. A similar "sub" is used to connect the bit to the lower most drill pipe. The drill string is lifted up the mast via a heavy cable with the top section laterally connected to a heavy chain collectively known as the **drawworks**. The driller can raise and lower the drill string by the drawworks while the kelly slides past the kelly bushings in the table. The chain moves in a circular fashion within the mast. The hydrogeologist usually

Figure 8.15 Forward rotary rig with top-head drive.

observes the rate of drilling by observing chalk markings made on the chain by the driller or numbered increments made down the mast.

The diameter of the drill pipe is smaller than the diameter of the borehole cut by the bit. The drill pipe is thick but hollow enough to allow the flow of drilling fluids. Drilling fluids are injected via a hose connected to the top of the drill string from a pumping system. The fluids exit through ports in the bit that help lubricate it and keep it cool. The cuttings are forced up the annulus between the borehole wall and the drill pipe to the land surface (Figure 8.16).

During mud drilling, a pit is excavated (or a portable pit with baffles is used when cuttings must be removed from the site). The pump intake hose is placed on one side of the baffles where drilling additives can be easily mixed. The returning fluid and cuttings are discharged back into the opposite side of the pit. The baffles filter or separate the cuttings from the intake side. When there is a continuous movement of fluids through the drill pipe to the bit and a return of fluids and cuttings up the annulus of the borehole to the land surface, this is known as circulation. The drilling fluids added during forward rotary drilling are designed to "maintain" circulation.

This is a hierarchy of drilling fluids in order to increase hole stability:

- Air
- Water

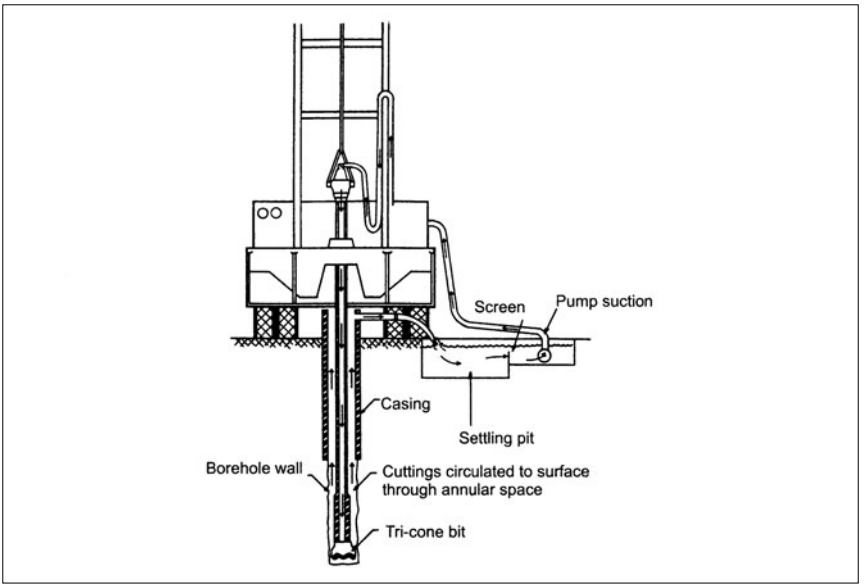

Figure 8.16 Direct rotary circulation system. [*From NWWAA (1984).*]

- Foam (a detergent)
- Stiff foam (foam with polymer added)
- Mud

Once a certain drilling fluid is used, there is no returning to a previously used fluid. For example, once a stiff foam is required to maintain borehole stability, the driller can't go back to using just water.

An air compressor on the rig is designed to produce sufficient airflow to lift the cuttings to the surface. The driller stands near the control station and monitors the flow volume of air or fluid. The drawworks and other controls are also handy from this position.

The author has observed holes drilled with air in softer layered sediments achieve drilling rates of 100 ft/h (30 m/h.) In unconsolidated sediments and in clays drilling with air is not viable. Unconsolidated sediments will collapse against the drill pipe and clays "ball up" and do not reach the surface. By adding water or mist, the circulation may once again be restored. Drilling with air is viable in very hard formations until "first water" is encountered.

When drilling with water or other fluids, some of the cuttings coat the borehole wall, thus providing stability. If the borehole caves or washes out, the cuttings may not return to the surface, even with a thick additive like stiff foam. At this point, the driller may have to drill with mud to provide

a wall cake needed for a stable hole. Once the driller uses mud, then there is no turning back, since water or other fluids would cut through the wall cake and the hole may lose circulation once again. Drilling with mud should also be avoided to keep from sealing off production zones.

When hole diameters exceed 12 in (0.3 m), most air compressors are not able to supply sufficient air volume to lift the cuttings to the surface.

This can be overcome by using an auxiliary compressor. Sometimes two drill rigs are "plumped" side by side to use the combined strength of both compressors. This is often necessary to complete 10- or 12-in (0.25- or 0.3-m) wells. Wells with even larger diameters become impractical using this drilling method unless the drill rigs are very large; even then maximums are reached at diameters of approximately 22 in (0.56 m) (Driscoll 1986).

Another versatile thing about forward rotary drilling is the variety of bit types available for use. Two of the most common bits are the tri-cone and the drag bit. A tri-cone bit has bearings that turn as the bit is rotated. Each cone has patterned cutting teeth or is studded with bumps or buttons that are designed for the hardness of the geologic materials (Figures 8.17a, 8.17b). Generally the shorter the teeth or buttons, the harder the materials. Short buttons may be studded with tungsten carbide while larger teeth may be constructed of hard-surfaced alloy steel or other materials resistant to abrasion. Drag bits are fashioned with nonrotating metal cutters that are used for rapid penetration, such as through soft shales. Ask your driller about bits and their function.

Figure 8.17a A series of drag bits used in soft formations.

Figure 8.17b In front are a variety of tri-cone bits, the larger the teeth the softer the formation.

Forward rotary drilling is ideal for harder geologic materials and faster drilling scenarios. Although forward rotary drilling methods can drill through most geologic materials, there are at least four general conditions when this method is not recommended:

1. Rock materials that do not allow circulation, such as highly fractured basalts or karstic limestone (Chapters 2 and 13).
2. Soft unconsolidated materials with high confining pressures.
3. Zones that change from soft to hard and back to soft once again.
4. Large diameter wells (greater than 22 in or 0.56 m).

In highly fractured rocks or limestones with large void spaces, drilling fluids do not remain in the borehole because they are lost out into the formation. If there are heaving sands or other unstable conditions, forcing drilling fluids up the borehole may actually result in decreasing the hydraulic conductivity of the formation. Another problem occurs when the geologic zones alternate between hard and soft horizons. This is illustrated by Example 8.5.

Example 8.5 A family in southwestern Montana was interested in building a home in a topographic saddle between two hills. They called a drilling company to get their well drilled. The drillers were hopeful they could complete the well before the Labor Day weekend. A forward rotary drilling method was employed. The drillers went through some fairly hard zones and then soft

zones. Worried that they might get the bit stuck in the hole, the drillers advised the property owners that if they continued drilling they would have to pay for the bit. Were they prepared to pay if it became stuck (approximately $5,000 U.S. at the time)? The owners said no. The drillers pulled off the well and left with no explanation.

Shortly thereafter the author received a call from the property owners seeking advice on what to do next. After receiving an explanation of the problem and being advised of the location of the property, the geology of the site was researched and plotted on a topographic map (Figure 8.18). The well site, chosen by the property owners, was near one of the hills to protect their home from the prevailing north winds. As it turned out, the geology of the hill near the well site consists of Cambrian sedimentary rocks and the saddle area consists of basalt (Chapter 2). The author reasoned that the well was drilled in a "chill" zone near the contact between the sedimentary and igneous rocks. The chill zone resulted in layers of basalt alternating between soft weathered zones and hard unweathered zones. This was confirmed in the field by looking at the cuttings and other field evidence. Figure 8.19 illustrates the layering that occurs in rock formations in igneous rocks. Under the ledges, the softer materials can accumulate and bunch up around the drill pipe, closing off the diameter of the hole. When the drill string is pulled upward, the bit may become stuck at the ledges.

The author suggested that if they could drill away from the "chill" zone, perhaps the rock would be brittle or hard all the way down and the hole diameter would remain uniform. Since an E-tape was not available (Chapter 5), the depth of the water table was estimated by dropping a small rock and timing when it hit water. This was repeated three times with consistent values. The depth was estimated to be approximately 100 ft (30 m). With this information, we drove to the top of the hill to examine the property area. It was noticed that a linear drainage extended from the top of the saddle area and seemed

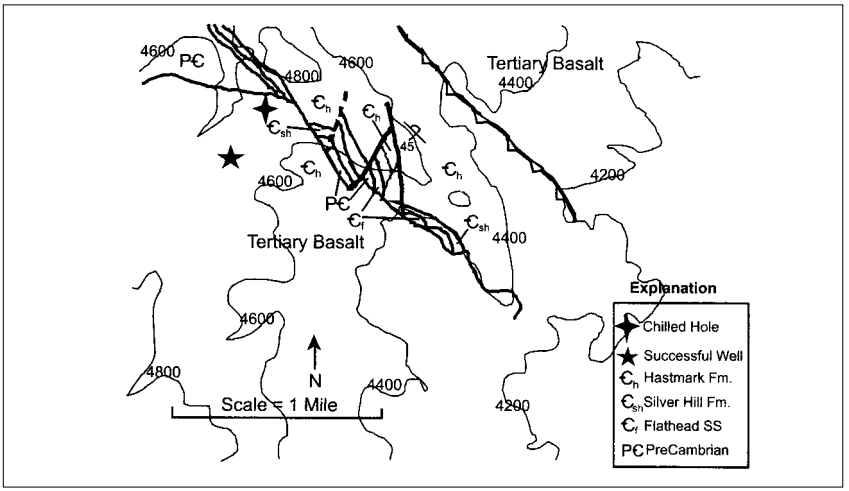

Figure 8.18 Surface geology and elevation contours from Example 8.4.

Figure 8.19 Layering in granite from exfoliation.

to correspond with a fault in the geologic map. By drilling near the fault, it was hoped that increased fracture permeability would be encountered. A site was recommended, and the author later sought more information on the thickness of the basalt. Fortunately an oil well had been drilled within the property indicating that the basalt was approximately 400-ft thick and underlain by lacustrine shales (Chapter 2). The author reasoned that recharge waters from precipitation would "pile up" on the shales and that a drill hole with a depth of 250 ft (76 m) or so would do the job.

The property owners called another driller to perform the task. This driller wouldn't drill at that high an elevation unless he consulted with a water witch (Section 8.7). Interestingly enough, the "witcher" picked the same place that was recommended by the author (the site was flagged) and a successful well was drilled with a depth of 200 ft (61 m).

Reverse circulation drilling

Unlike forward rotary methods, where continuous circulation is required before drilling can continue, reverse circulation drilling avoids the problems of losing cuttings and drilling fluids into the formation by taking up all cuttings and drilling fluids up through the drill pipe. This is a reverse drilling process from forward rotary methods. Drilling fluids are introduced between the borehole wall and the drill pipe and then drawn up at the bit. The discharge hose is located at the top of the kelly where water and cuttings may be diverted out through a cyclone and dropped to the ground or are directed back into a mud pit (Figure 8.20).

Figure 8.20 Author collecting cuttings from the bottom of a cyclone.

Perhaps the most common application of reverse circulation methods is for drilling larger diameter wells from 24 to 72 in (0.61 to 1.8 m) (NGWA 1998). The cost for drilling larger diameter wells is not much greater than for smaller diameter ones in unconsolidated materials and the well-completion applications are very straightforward. A summary of useful applications for reverse circulation drilling of larger diameter wells in unconsolidated or soft formations is given by Driscoll (1986):

- This method causes very little disturbance of the natural porosity and permeability of formation materials, an important consideration for production zones when other methods may disrupt the aquifer characteristics.
- Large diameter wells can be drilled quickly and economically.
- No casing is required during the drilling operation.
- Well screens are easily installed as part of the well completion process.
- Borehole wall erosion is less likely because down-hole fluid velocities are low.

There are also some conditions that must be met in order for this method to be effective (Driscoll 1986):

- Formations should be soft sedimentary rocks with no large boulders. Drawing boulders up through the center of the drill pipe is a problem.
- The static water level should be more than 10 ft (3 m) below the land surface to be able to maintain a sufficiently high hydrostatic pressure

along the outside of the borehole. Problems also arise if the static water level is high and adequate water for drilling is lacking.

- Drilling using this method requires a high volume of available water with requirements ranging up to hundreds of gallons per minute (tens of liters per second). If this cannot be obtained, this method will not work well.
- Drill rigs, equipment, and components are very large and expensive and require more room to work.

Another reverse circulation drilling method that has very successful applications is known as the dual-wall reverse circulation method. Instead of fluids moving along the outside of the drilling pipe, there are two fluid passageways through the drill pipe (Figure 8.21). The drilling fluids pass down the outer passageway, and the cuttings and fluids are drawn up through the center passageway. The inner sleeve is sealed by an "O" ring. During this method, the only place the drilling fluids contact the formation is near the bit. This allows a continuous sampling of the formation with minimal disturbance and reduces the chances of cross contamination.

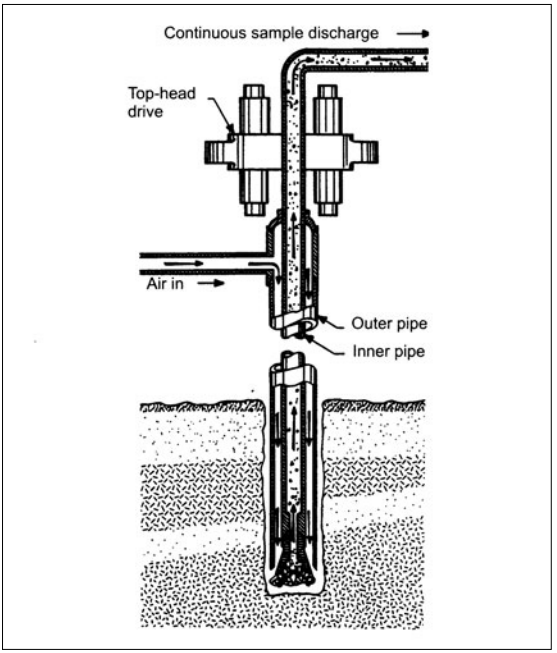

Figure 8.21 Dual-wall reverse circulation diagram. [*From Driscoll* (*1986*).]

The author first became aware of dual-wall reverse circulation drilling in placer gold exploration applications. Any cuttings within 3 in (7.6 cm) of the bit are drawn up through the pipe. Drilling recovery rates using this drilling method are in excess of 95%. Heavy minerals, like gold, would not likely make it to the surface using another drilling method. This is the method of choice for exploration test drilling at properties with heavy metals, although sonic drilling (discussed later on) is gaining in popularity. Representative samples can be obtained using this method. Although drill pipe outer diameters (OD) range from 3 1/2 to 9 5/8 in (8.9 to 24.4 cm), the most common drill pipe size is 4 1/2 OD with a 2 1/5 ID (11.4 cm OD and 6.4 cm ID) (Driscoll 1986).

Casing advancement drilling methods

In cable-tool drilling, casing advancement is an integral part of the drilling process. Two other casing advancement methods will be discussed in this section: top-head forward rotary and wire-line drilling. Casing advancement methods are helpful when the borehole conditions are unstable or there may be a danger of contamination of materials from up-hole to down-hole. In top-head forward rotary methods, the casing driver is usually at the top of the mast. The drillpipe and casing are suspended together below. At the bottom of the first piece of casing is a thick forged drive shoe that is welded to the bottom to keep the casing from crimping as it is driven. The drill bit and casing advance simultaneously or the drill bit may advance a few feet (a meter or so) ahead of the casing before it is driven.

The casing driver is a piston percussion-driven system activated by air pressure. The bit grinds up the cuttings, as in forward rotary drilling, and the cuttings are blown up through the annular space between the casing and the drill pipe to a discharge tube near the bottom of the casing driver (Figure 8.22). When the bit advances ahead of the casing, the bit can be retracted inside the casing before driving the casing. There are many advantages to this method over traditional forward rotary methods in spite of the additional cost of the casing hammer and the noise of operation. Most drillers who use this method wear hearing protection attached to their hardhats (Figure 8.23). It is also advisable for the hydrogeologist logging the hole to wear hearing protection.

Several advantages of this method have been summarized by Driscoll (1986):

- Unstable formations that would result in too much disturbance using forward rotary methods can now be attempted with a good rate of success.
- The borehole is stable through the entire drilling operation.
- Penetration rates are rapid in most drilling environments.

Figure 8.22 Collecting cuttings from the discharge tube. The drilling fluid is foam.

- Loss of circulation is no longer a problem since cuttings are blown up through the casing.
- Specific zones can be tested for water production and sampling without up-hole contamination.
- This method can be used in all weather conditions.

In wire-line drilling, the casing serves as the drill string (NGWA 1998). The bit is attached to the bottom of the first piece of casing and

Figure 8.23 Hearing protection on hardhats; driller measuring flow rate.

advances along with drilling. As the hole advances, new casing is added to the drill string. All tools can be withdrawn upon completion of the hole. Wire-line drilling is ideal for continuous coring applications at depths where tripping-in or tripping-out can be cumbersome. The core barrel can be retrieved via a sand line by slinging a brass messenger down the sand line to the top of the core catcher. The sand line can then be pulled up with the core to the surface. A new core barrel can be sent back to the bottom of the hole and reattached to the bit already in place. In this way continuous coring can occur.

Example 8.6 The author spent a couple of months in the Peoples Republic of China performing wire-line coring on a coal property a couple of hundred kilometers west of Beijing. The drilling was unstable with soft overlying formations and coal thicknesses in excess of 50 ft (15 m). The surface consisted of 80 to 100 ft of silty loess (Figure 8.24). This was underlain by a few tens of feet of unconsolidated fine gravel before we encountered stable layered sediments of Pennsylvanian age. A surface casing was set to isolate the soft overlying materials and continuous coring of the Pennsylvanian rocks occurred to depths in excess of 300 ft (100 m). The wire-line coring was very convenient to obtain continuous core at relatively deep depths below very unstable drilling conditions.

Auger drilling

Two methods of auger drilling are presented, solid-stem and hollow-stem auger drilling. The applications are more common for monitoring well completion rather than production wells, although shallow (approximately

Figure 8.24 Wire-line drilling in China; canyons reveal silty loess.

100-ft or 30-m) production wells can be completed in soft formations (NGWA 1998) using this method. The chief advantage of auger drilling is that it requires no drilling fluids when drilling the hole. This is especially significant for contamination sites that require monitoring wells. Drilling depths can reach 200 ft or more depending on the geologic formation and capabilities of the drill rig.

Solid-stem auger drilling is often used when the well can be completed "open hole." This means that all of the auger flights can be retrieved from the hole before placing the casing. Solid-stem auger drilling can usually achieve greater drilling depths than hollow-stem augers (HSA) because the shafts on auger flights are narrower; however, the hole diameters are usually smaller. The auger flights are rotated via a rotary head drive with a hydraulic-feed mechanism that allows either downward pushing or upward pulling (Driscoll 1986). The kelly bar is hexagonal and is attached to the first flight with two rod bolts that are often turned "finger tight." As additional flights are added, they are usually tightened with a wrench or air-powered drill. As one driller put it "anything below ground gets wrenched."

As the augers turn, the geologic materials spiral upward to the surface. It is confusing at first to tell which depth the cuttings came from, so it is a good idea to communicate with your driller. Cuttings depths can be correlated between the sound and "feel" of the drilling and the associated materials observed. An experienced driller will be able to tell you what you are in. For example, "We hit that gravel about a foot ago," even though the gravel may not be observed at the surface for another 10 ft (3 m) of drilling. Sometimes cuttings do not make it to the surface and cannot be sampled until the auger flights are pulled.

Many auger flights are 5 ft (1.5 m) long except for the first flight that has a cutter head attached, extending the length an additional foot or so (Figure 8.25). This, of course, depends on the diameter of hole being drilled and size of the drill rig, etc. The author's experience is primarily with smaller-diameter wells (less than 4 in or 0.1 m). Additional discussion on larger-diameter wells can be found in Driscoll (1986). Completing monitoring wells is discussed in Section 8.5.

Direct-push methods

Another method of obtaining subsurface information with or without completing a well is through direct-push methods. The technology and expansion of direct-push subsurface tools has expanded rapidly since the first edition of this book. There are a wider variety of drill-rig sizes, coring length capabilities, well-installation diameters, and aquifer testing and sampling tools. Direct-push drill rigs are truck or van mounted or manufactured as tracking units with widths as narrow as 12 in (0.3 m), which allows easy maneuverability in smaller areas.

Figure 8.25 First flight with cutter head.

All units are equipped with a hydraulic system to push a 4-ft (1.2-m), 5-ft (1.5-m), or 6-ft (1.8-m) core barrel into the ground (Figure 8.26). A stainless-steel core tube captures the core [typically 1 7/8 in (4.8 cm)], inside a plastic tube. The tube can be laid on a core tray or back of a truck, where it can be sliced in half with a knife for inspection (Figure 8.27), or may be sealed for laboratory soil-gas work. Coring systems can be readily altered to an augering system in the field within minutes. This allows the flexibility of continuous coring followed by installing a 3/4-in, 1-in, 2-in, or 3-in (1.9-cm, 2.5-cm, 5.1-cm, or 7.6-cm) or larger diameter monitoring well (Figure 8.28).

The strength of these devices is in the ability to perform soil-gas surveys or delineating plumes with volatile organic carbon sources or to define bedrock in relatively shallow aquifer systems. There is a capability to extract soil gases directly into a gas chromatograph on the rig or pull a groundwater sample via a peristaltic pump, suction pump, or through the casing with a retractable tip (Figure 8.29). The upper tool in Figure 8.29 shows the tip refracted to expose the stainless-steel

Figure 8.26 Track-mounted direct-push drill rig.

screen for water sampling. A check ball enhances the ability of lifting fluids from deeper depths. It is a relatively quick way to obtain several point samples in a short period of time with minimal surface impact, since no well completions are needed. This is ideal for investigative and site evaluation work.

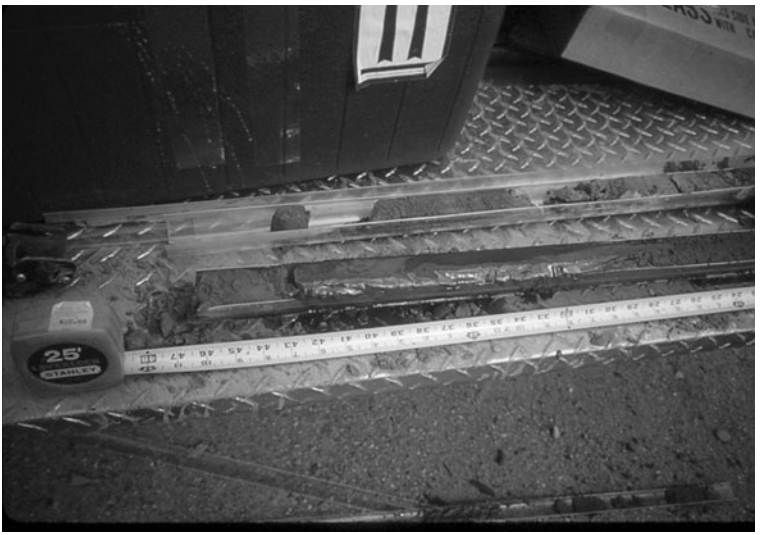

Figure 8.27 Plastic tubes from direct-push cores, cut in half for inspection. Note the sheen of diesel in the core.

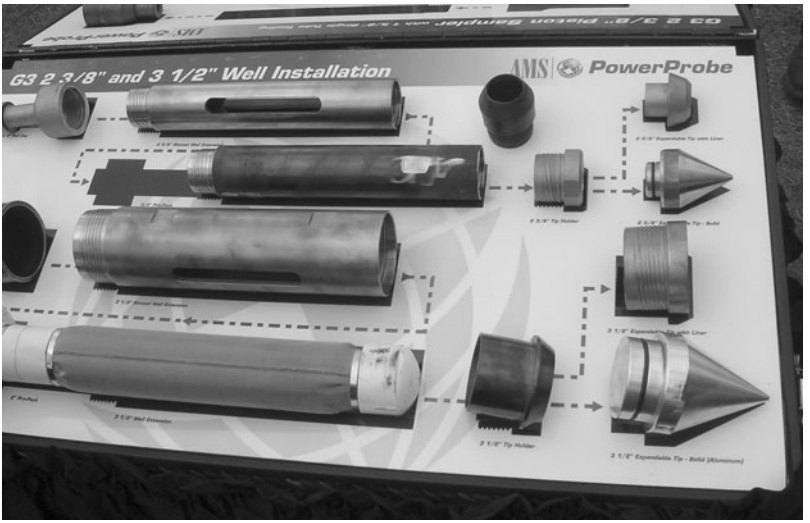

Figure 8.28 Array of well-completion and sampling tools for 2 3/8-in (6-cm) to 3 1/2-in (8.9-cm) monitoring wells.

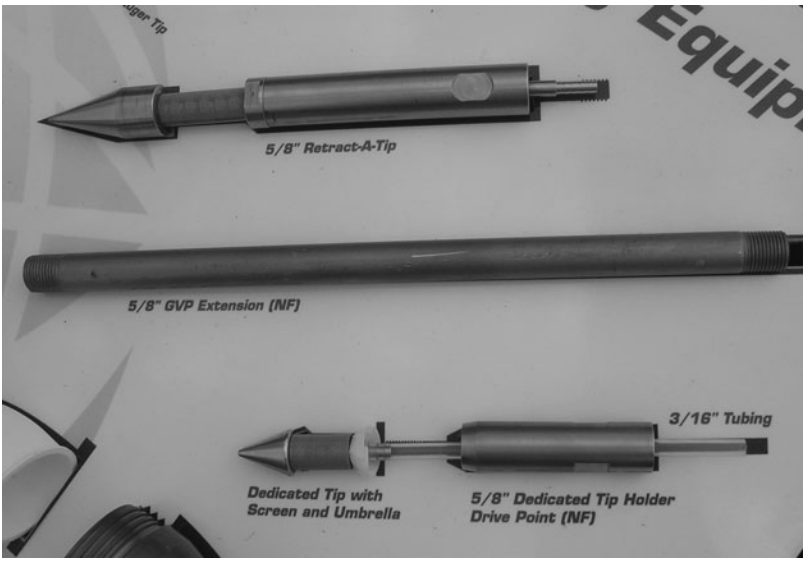

Figure 8.29 A series of direct-push down-hole tools. The upper tool is a retractable tip that exposes steel screen for water sampling. In the middle is an extension piece and the lower tool is a dedicated screened zone near the driving tip.

Direct-push methods are only effective in unconsolidated materials or softer sediments. Depth capacities are usually in the 20- to 50-ft (6.1- to 15.2-m) range, although drillers exceeding depths of 100 ft (30 m) are documented by Geoprobe Systems' 100 club (Geoprobe 1999).

Sonic or rotasonic drilling

Sonic drilling is a relatively newer drilling method that is expanding its applications in the obtaining of subsurface information. Sonic drilling is especially known for being able to take continuous cores in unconsolidated sediments, including till and alluvial deposits, and frozen and solid materials, because of its unique process of coring without drilling fluids.

The heart of the sonic system is the rotation of two imbalanced counter rotating weights or rollers, which are driven by high-speed motors. During rotation, a high-frequency vibration resonance takes place that is delivered directly to the drilling rods. The synchronization of the rollers ensures that the entire length of the drill pipe becomes a penetrating tool with little friction between the drill rod and borehole interface (Precision sampling 2006; and Midwest Drilling 2004). While resonant vibration is occurring, the drill rods are also being rotated to improve the cutting effect. Thus explains why the name Rotasonic is also applied to this drill rig. Coring depths in excess of 400 ft (122 m) are achieved with these rigs.

Mini-sonic

A mini-sonic drill rig is approximately a 1/3-size version of the larger rigs (Figure 8.30). The rig in Figure 8.30 has 18-in (0.46-m) wide tracks and also comes in 24-in (0.61-m) wide track models. Drilling can be vertical or angular and achieve depths of approximately 150 ft (46 m). The imbalanced counter weights are rotated at approximately 5000 revolutions per minute (rpm), while the drill string can be rotated up to 100 rpm.

Drill rods are laid in a receiving unit and coupled mechanically (a safety measure), which keeps the helper away from the drill string (Figure 8.31). In monitoring-well installation applications a smaller diameter drillhole can be followed with a larger diameter casing to seal off an upper zone. Drilling inside the casing in a "telescoped" fashion can occur without the danger of carrying near-surface contamination downward.

Cone penetrometer testing (CPT)

Another newer application of obtaining subsurface information using an older technology is cone penetrometers testing or CPT. The CPT system is a truck-mounted system using a sensitive cone-shaped probe head that

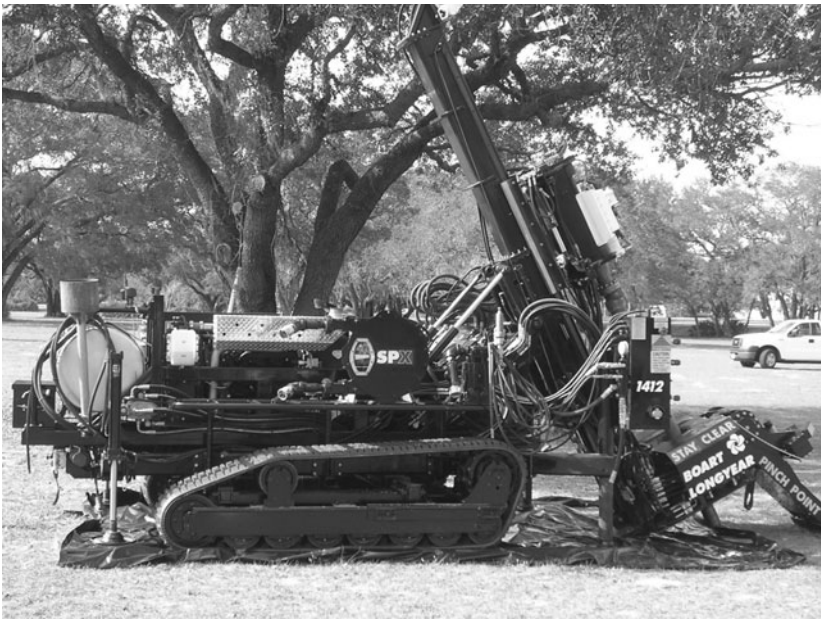

Figure 8.30 Track-mounted mini-sonic drill rig.

Figure 8.31 Coupling of additional drill rod on the mini-sonic drill rig. Coupling is done mechanically to increase safety during drilling.

is hydraulically pushed into unconsolidated sediments. The equipment includes the CPT probe, down-hole tools and a computer-data logger for data collection. The probe head is equipped with a low-pressure transducer, an inclinometer, a friction sleeve (containing strain-gauge load cells), and a pore pressure transducer (Precision sampling 2006). The standard cone has a surface area of 10 cm^2 and a surface angle of 60°. The CPT system can use electrical and acoustical energy to transmit signals to a receiving unit at the surface. The resistance to penetration is continuously measured with depth and correlated to grain size to characterize soil types and identify zones of increased permeability for water sampling or production. An example of a CPT log is shown in Figure 8.32.

Horizontal drilling

An older technology that has expanded rapidly during the 1990s is horizontal drilling. Horizontal drilling has been used in placing utility lines for years but has found new uses in the environmental field. Horizontal drilling has found many applications in drilling and completing wells under permanent structures such as landing strips, airport fueling areas, roadways, tank farms, and other areas that would be problematic for remediation if there were a host of vertical wells.

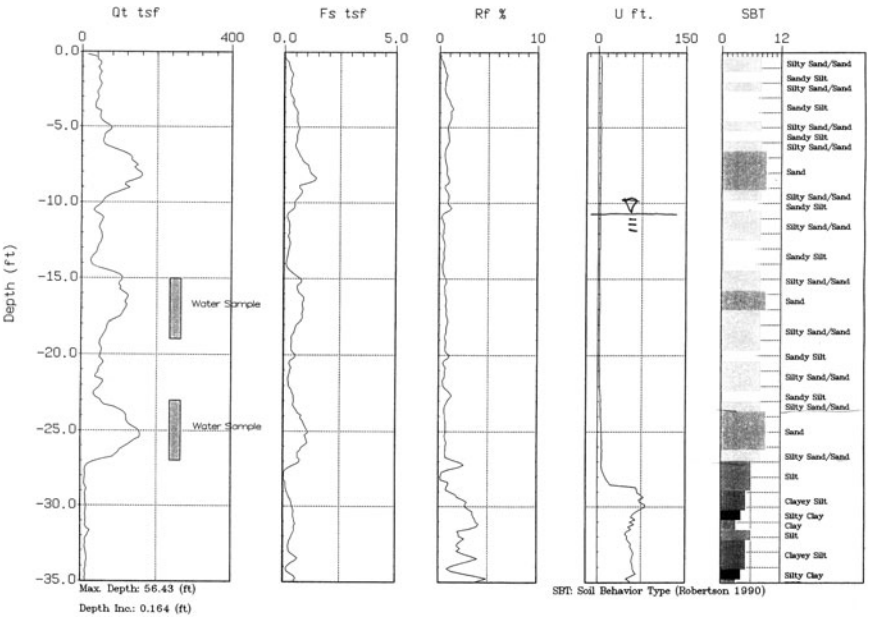

Figure 8.32 Information derived from a CTP log.

Figure 8.33 Horizontal drilling rig performing utility line work.

Drilling is accomplished by a rotating disklike bit that is directed at a low angle to the surface. Control is maintained by rotating the disk in a continuous motion. Changes in the direction are made via the orientation of the bit. Often times a "foot" person with a surface-detecting device works with the driller to identify exact positioning of the bit, particularly if one is drilling along existing utility lines (Figure 8.33). There are an increasing number of drilling companies that perform horizontal drilling services and would be happy to provide additional information; most have a web site. One printed source of information is the annual rigs issue of *Water Well Journal* (July issue).

8.4 How to Log a Drill Hole

Before newcomers begin logging subsurface information, it is helpful to be familiar with the different drilling methodologies described above and the section on rig safety before attempting to log your first hole. You need to know how the cuttings arrive at the surface and the objectives of the drilling project. In addition to logging a hole, you are also responsible to see that the drilling project is completed. There needs to be a balance between making good footage for the driller and also obtaining the needed subsurface information. The hydrogeologist is responsible for the data that are collected.

It is typically your responsibility to locate where to drill. How will you decide? Will the locations be premarked? Were they located by someone

else, which means that you have to be able to read a map and locate yourself? Do you know where the site is and where to begin? Is it necessary to call a utility line locator? Remember that you need 48 h advanced notice (Section 8.2). Are there any issues regarding personal protective clothing? These may sound like obvious questions, but for someone new they are a significant source of stress and point out the need for a predrilling meeting with the driller and other involved parties.

In addition to knowing the drill-site locations (or enough sites to get started), there are a number of tasks that one can prepare before going into the field. Does your company have a standard form they use for drill logs? Maybe you are using a field book from which you will be transferring information to a standard form. Consult Chapter 1, Section 1.6, on field note taking. Will you be taking samples that will be stored? Will you collect them every 5 ft (1.5 m) or at a major lithology change? Will these be chip samples, core samples, or something else (Figure 8.34)? Do you have whatever containers, bags, or boxes prepared so the drillers don't have to wait for you?

Make a list and be sure you are prepared to go into the field. Some common items needed are:

- Site location map
- A topographic map, if it is not included on the site map
- Geologic map, if possible, or at least have well logs from other wells in the vicinity
- Field book, well log forms
- Hand lens, grain-size chart, acid bottle, or hardness tester

Figure 8.34 Chip samples in compartmentalized container.

- Containers for samples, or materials needed for samples, core boxes, etc.
- Chain-of-custody information if needed for samples
- Writing utensils, with extra backup writing capability
- If using a laptop, extra batteries or a power source
- Appropriate clothing, rain gear, etc.
- Drinking water and food
- Reading material for breakdowns or delays
- Cell phone or other communication device for emergencies

This is not an exhaustive list, but serves to jog one's memory. It will be essential to have a cursory idea of site geology, even if you have never been to the site before. Which drilling method is most appropriate for the conditions? Is forward rotary better or auger drilling?

You will need to know how to tell how deep you are in the ground. When the driller sets up at the hole and raises the mast, he or she will level the rig. When the bit rests at the ground surface, this is surface or zero drilling depth on your log. If there are preexisting numbers painted down the mast, you need to note where the zero marking coincides. Another way to keep track of footage is to mark the drawworks chain, every 5 ft (1.5 m) or so with a bright colored grease marker (the driller will do this for you). Another way is mark directly on the drill casing with chalk (Figure 8.35). It is best to ask the driller the most appropriate way to keep track of drilling footage.

Example 8.7 illustrates logging a drill hole while using the forward rotary drilling method. Initially drilling is with air and then switched to water and then to foam.

Example 8.7 The driller asks you if you are ready and the deafening sound from the air compressor is directed down through the kelly into the drill pipe. Air begins gushing out the ports at the end of the bit and dust begins to blow. The driller engages the power drive system and the rotary table begins to turn. The cuttings begin to blow around at the base of the drill rig and pile up. The driller helper begins to shovel the cuttings to channel the fluids and cuttings away from the back of the rig.

You have prefilled out most of the header of your logging form and stand near the driller with your sieve ready to catch cuttings. You do so frequently and look up frequently to make sure you are aware of what is going on. In your log book you write down descriptions for every 5 ft (1.5 m) or at major lithology changes. Generally, lithology changes more frequent than 3 ft (1 m) will require too much writing to keep up with drilling. You start piling representative cuttings sequentially on the ground to be able to refer back to them, or place them in premarked bags. After 50 ft or so you notice the samples are getting moist and you ask, did we hit water yet (Figure 8.36)?

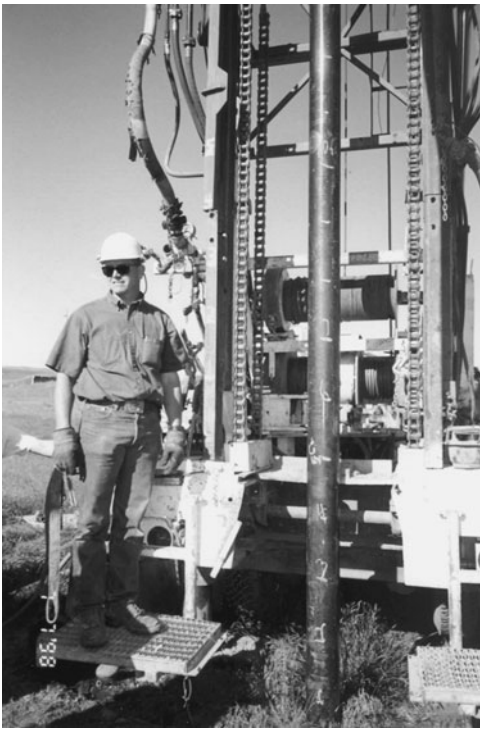

Figure 8.35 Depth markings on the steel casing.

Figure 8.36 Describing drill cuttings.

The driller nods and then starts pumping water along with the air to maintain circulation. It will be necessary to fill a 5-gal bucket (19-L) from the back of the water truck to rinse your cuttings now. What you observe in your sieve may represent a mixture of cuttings from the full length of the hole. What are we in? You communicate with the driller and get back on track. The hole seems to be making an increase in water, you ask the driller to stop at the end of the next joint and blow on it (only inject air) to see how much it is making (Figure 8.23).

Another 50 ft and the cuttings are not coming to the surface like before. The driller adds detergent to a mixing tank and begins to pump foam down the hole for added stability. It gets pretty messy around the base of the rig. The sieve fills up with mostly foam. You vigorously rinse the cuttings, but the operation is a bit more challenging.

Example 8.7 presents some issues worth discussing in more detail. How do you know what you are drilling in when the cuttings represent a mixture from the total length of the hole? As you drill deeper it takes longer for cuttings to reach the surface. How does one tell what the conditions of the subsurface are like?

Describing the cuttings

When drilling with air and at relatively shallow depths, cuttings arrive almost instantaneously at the surface. As drilling proceeds, cuttings from near the bit become mixed in with cuttings from "up-hole" as they are continuously blown to the surface. This yields a mixture of cuttings in your sieve. Generally, about half of what you see is from the current drilling depth. This needs to be evaluated along with the sound of drilling, drilling rate, and drilling depth. Shales and other softer materials will drill more quickly and quietly, while sandstone and limestone may be much louder and slower. Once again, consult with the driller in determining where a formation change took place or when you drilled through fractured rock.

In describing cuttings, it is helpful to find a representative large piece in the sieve and break it in half to obtain a fresh surface to look at with your hand lens. This will help you distinguish among the different lithologies, and more specifically among fine-grained materials. (Harder cuttings will not break in half.) A quick decision must be made when assessing the materials before writing something down. It becomes difficult at times to distinguish differences among mudstones, claystones, and siltstones. This is best evaluated from a field test, described in Table 8.1. Of course, don't try this if there is any danger of contaminated soils. This is mostly an exploration drilling technique, but can be very helpful.

Lag time

The time it takes cuttings to reach the surface from the drill bit is known as lag time. When drilling with air or foam, the fluids and air from the compressor must be able to lift all cuttings to the surface to

TABLE 8.1 Field Methodology for Distinguishing Finer-Grained Sediments

% Silt	Lithology	Taste test (rub against teeth)
0–33% Silt	Claystone or clay shale	Cuttings smear on teeth with little or no grit
33–67% Silt	Mudstone or mud shale	Very gritty on teeth, grit observable
67–100% Silt	Siltstone	Mostly grit observed

maintain circulation. There is turbulence during this process and cuttings may take quite a while to reach the surface after exceeding a depth of 300 ft (>100 m) or so. The best way to gauge lag time is to notice a distinctive formation and glance at your watch when you first hear it. Note the time and continue to log cuttings as they are blown out at the surface. Coal or some other marker bed is especially helpful. When the cuttings you noted appear at the surface, look at your watch again; this is the lag time. At depths greater than 100 m, the sound and chatter of the rig will be as helpful as the actual observed cuttings. By being able to have a marker bed or two every so often, the drill log can be adjusted to match the depths better. Adjustments can also be made on lithologic logs if geophysical methods are also available.

Example 8.8 While performing coal exploration in Wyoming, each coal bed had a particular "signature." It was easy to tell when you were in coal because of the chatter of the rig and rapid penetration, When drilling at depths of 500 ft or so, the lag times ran from between 15 and 20 min. The time depended on the drill hole diameter, volume of cubic feet per minute (cfm) of air being injected, and fluids being added.

As another example, lag times for cuttings mixed with mud from a 1,000-ft hole at the Big Sky Montana ski resort area required 30 min or so to reach the surface.

How much water is being made and where did it come from?

One of the objectives of drilling is to know when you first hit water and which zones the water was likely coming from. It may be that there is a significant difference between "first" water and where the static water level is. Confining units may be keeping the water from rising to its unrestrained levels. You can learn a lot about the hydrogeology of an area by observing which zones produce water and where the static water level is each day before you continue drilling.

You should make it a practice to take a level measurement (Chapter 5) in the hole at the beginning of each day and after periods of breakdown, where the hole has sat unperturbed for a significant length of time. This along with your notations of where producing zones are all tell part of the story.

TABLE 8.2 Production Estimates Based on Water Exiting the Hole

Production observed (gpm)	Possible from pump production (gpm)
3–5	5 +
5	7
7–8	10
10–12	12–15

If you suspect that the hole is producing water, ask the driller to stop at the end of the next joint or rod and inject air only. After 5 to 10 min, the water being produced from the hole will only be coming from the formation. Realize that this may represent minimum production, since not all of the water makes it out of the hole. Some may be going out into the formation. It is the author's experience that a hole will produce approximately 25 to 30% more than what is blowing out at the surface. This can have important implications for water production depending on whether water is being produced from the length of the hole or from a specific zone, because the upper zones are cased off. Table 8.2 gives a rough idea of the difference between volumes blowing from the hole and what could be produced with a pump.

Table 8.2 may be important because if drilling has proceeded for a couple of hundred feet (66 m) and total production is on the order of 2 to 3 gpm (0.13 to 0.19 L/s) one must evaluate the probability of success for additional production at deeper depths and the additional drilling costs.

Estimating the volume takes practice and can be solved a variety of ways. If the volume of water can all be channeled through a single place, the chances are greater of getting an accurate estimate. Using a bucket and timer, a weir, or flume are common methods (Figure 8.23) (see also Section 6.4). Most experienced drillers can estimate flow rates just by looking. If flow rate is an important issue, attempts to measure the volumes accurately are warranted. Figure 8.37 shows drillers filling 5-gal (19 L) buckets in sequence after waiting one minute to estimate yield.

8.5 Monitoring-Well Construction

Monitoring-well construction is ideally performed to provide a window into the aquifer at a given completion depth. The goal is to complete the well in such a way that you can have confidence in the hydraulic-head information and water-quality samples. Monitoring wells are usually not designed to evaluate aquifer hydraulics, although they are often used to do so. They are usable as observation wells, but not designed as production wells. Produetion wells, discussed in the next section, are designed to be pumped at a level that often stresses the aquifer.

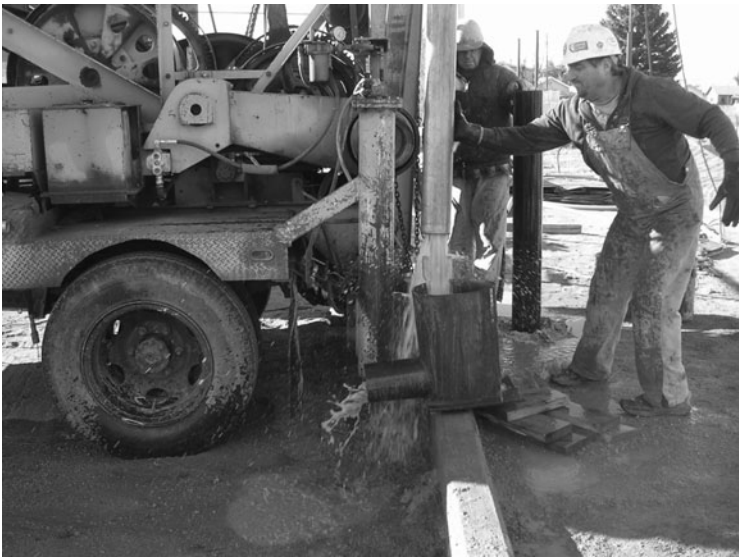

Figure 8.37 A driller helper guiding a bailer to a 5-gal (18.9-L) bucket to estimate well yield.

Objectives of a groundwater monitoring program

Monitoring-well programs require significant thought and planning to be able to accomplish their intended task. Table 8.3 lists some of the objectives associated with monitoring-well designs.

TABLE 8.3 Monitoring System Objectives

Objective	Discussion
Reconnaissance	This may be a regional study to see what is there. It may consist of a few sparsely placed wells. Shallow/deep pairs may be needed for head and quality data.
Fixed station	Long-term monitoring. Each station may have greater expense, such as a more secure access or a protective shelter.
Research	Temporary monitoring design that may have materials that need to be retrieved later on after research is completed.
Cause and effect	This is where monitoring is established to evaluate whether a process or procedure is effective. Usually there is a control area where the standard approaches or status quo is occurring, compared to a site where a treatment is being applied.
Compliance	These may be wells placed to make sure compliance requirements are being met according to some minimum or maximum standard.
Quality control	Monitoring may be occurring to check whether a process or remediation strategy is working properly.
Trend analysis	A monitoring system may be designed to determine whether a decreasing or increasing trend may be occurring.

From Table 8.3 it is apparent that the objectives must be well defined prior to achieving a successful program. Merely placing wells haphazardly is not an effective use of budget funds. Some of the objectives in Table 8.3 require that wells be placed with a certain component of randomness or the assumptions inherent in the analytical methods to be used will be violated. It is also important to have a knowledge of some of the following aquifer properties:

- Are there multiple aquifers?
- Are there perched zones?
- Is there contamination in the vadose zone?
- Is there more than one flow system? Local and regional?
- Recharge and discharge areas?
- What is the nature of a contaminant? Its solubility or density?

All of these issues complicate the monitoring design, since it may be necessary for multiple sampling ports at various depths. Are the wells being placed in the groundwater-flow path and at the appropriate depths to capture what is being monitored? Another consideration that seems to take precedence is what is the budget and how soon does the monitoring program need to be in place? Is the study being conducted "in-house" or is it under public scrutiny? All these things tend to complicate the process. In a public setting, there may be a negotiation process among regulators, the public, and the company, before the monitoring program can be implemented.

The philosophy regarding site assessment and monitoring designs at chemically contaminated sites has changed significantly in the past several years. Rather than taking a phased approach to site assessment and monitoring installation, there is a tendency to be more open about the process among the interested parties. The consultants, regulators, and responsible parties come together to work out a three-pronged method known as the Triad Approach (Crumbling 2004). The three basic areas of the Triad approach include: systematic planning, dynamic work strategies, and real-time measurement technologies. In this way the uncertainty regarding decision management is known and agreed upon during the aggressive process of locating and identifying the presence, fate, exposure, and transport of chemically contaminated sites. Here the most experienced persons are on-hand to make decisions in the field. It may be that you are called upon to assist in this process.

Since the first edition of this book an abundance of good information regarding site characterization and monitoring well design has come forth (Neilsen et al. 2006; and Sara 2006). In particular are discussions

and techniques for multilevel monitoring well completion using some new materials that result in a significantly improved understanding of the three-dimensional nature and heterogeneity of natural systems (Einarson 2006 and Neilsen and Schalla 2006). It is beyond the scope of this chapter to address all of these topics, but the intent is to give the newcomer facing monitoring-well installation a sense of the basics, before going into the field, and have a reference that is handy.

The method used to actually install monitoring wells depends on the geologic setting, the depth to be completed, diameter of borehole project goals, and so on. A common method for drilling and completing monitoring wells in unconsolidated materials is with hollow-stem augers (HSA) and a step-by-step procedure is presented next.

Installing a groundwater monitoring well

This example will be for a 2-in (5-cm) monitoring well to be used for hydraulic-head measurements and water-quality samples (Figure 8.38).

1. The casing materials and supplies for building the well have been laid out near the well site or are easily accessible from a vehicle nearby.
2. The bottom of the bit is fitted with a knock-out plate or a removable plug that slips down flush with the bit. The knock-out plate or plug serves to keep cuttings from passing up through the hollow stem and getting bound into the hole. This allows the cuttings to spiral

Figure 8.38 Water-quality testing from a monitoring well.

upward along the outside of the augers, similar to a solid-stem auger system. Once the desired depth has been reached, the knock-out plate can be dislodged so that the well can be constructed. The materials for the knock-out plate varies, but the author has seen from wood to polytetrafluoroethylene (PFTE, Teflon) used.

3. The drill hole penetrates through the first 5 ft (1.5 m). The helper loosens the two rod bolts, and the driller hoists up the kelly and drive sleeve up the mast. The helper slings over the next auger flight, fitting it on top of the one in the ground. Two bolts are pneumatically wrenched into place to secure the flights together (Figure 8.39). The driller lowers the kelly and drive sleeve over the new auger flight and the rod bolts are twisted on finger tight once again. The next 5 ft of drilling continues. As a hydrogeologist, you carefully describe the cuttings that spiral upward along the hollow stem. You record the information in the borehole log so that you know what all the critical depths are when constructing the well.
4. To meet the objectives of this study, you decide to penetrate the aquifer an additional 10 ft below the water table. Once there, you prepare to construct the well. A very important point will be made here. Before dislodging the knock-out plate it is important to **load the hole**. There may be a difference between the water level inside the bore hole and inside the hollow stem. "Loading the hole" means that water is added to the inside of the hollow stem to equalize the

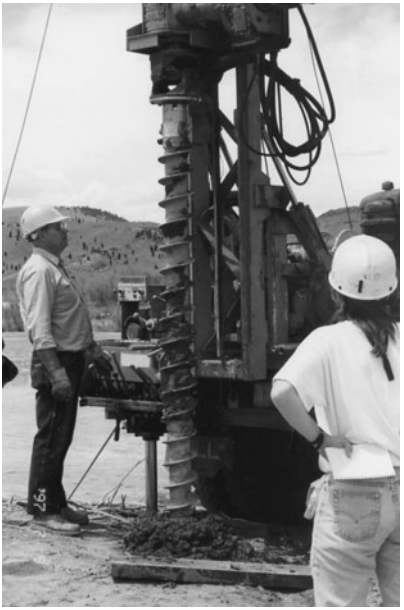

Figure 8.39 Adding additional auger flights.

two levels. If the hole is not "loaded," then muddy water from the borehole gushes up into the hollow stem chamber. This may produce a "skin" along the inside of the borehole that is difficult to remove during well development (Chapter 10). This is such a small step, but can make a great difference in well development. The author has seen wells become unusable by forgetting to "load the hole." Care must be taken to introduce clean water. You must know the source.

5. It is now time to remove the knock-out plate. This is done by lifting a heavy metal rod with a sand line and allowing it to "free-fall" inside the hollow stem to the bottom. This procedure is repeated several times. The driller checks the depth by lowering a cloth tape weighted with a heavy metal piece, so that it will fall freely to the bottom. The driller can also "feel" if the knock-out plate has been dislodged by distinguishing the difference between the bottom and the hard plate. In the case of the removable plug, it must be jarred loose and pulled out so that the well can be constructed.
6. It is time to start building the well (Figure 8.40). A bottom cap is secured onto the bottom of the well screen. It is important to make sure that when the well is constructed the screen is placed exactly where desired. Therefore, if the well penetrated into a confining layer, a sump consisting of blank casing will need to be added to the bottom so that the screen is positioned within the aquifer. Blank casing is added to the top of the screen until it extends a couple of feet (0.6 m) above the top of the hole, unless it is located in a street

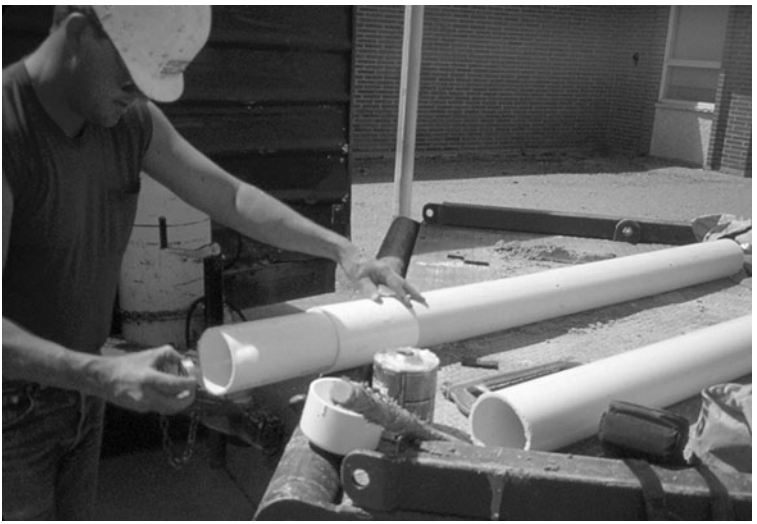

Figure 8.40 Monitoring well bottom cap, short sump, and well screen (knife in screen).

or pathway where one could trip on the casing. In this case, one should complete the well with a flush mounting (Chapter 5). A top cap is placed to keep the inside clean during the rest of the operation. Preferably this is all done with threaded pipe. Screens and pipe come manufactured in a variety of materials and lengths. This will be discussed later on.

7. Now that the casing is in the hole, it is time to "complete" the well. Typically, the next step is the placement of a filter pack around the screen. The packing material is poured down through the annulus between the hollow stem pipe and the casing. The filter packing materials should be larger than the screen slot size (<10% passing through the slots). Sieved silica sand is a good choice and these come in 50- and 100-lb (22.7- and 44.3-kg) bags (Figure 8.41). The 50-lb (22.7-kg) bags are much easier to handle if used directly, but the 100-lb (44.3-kg) bags may be more cost effective. The sand size should not be confused with the slot size. Sand sizes represent sieved intervals, for example, 10 to 20 sand was sized through a number 10 to 20 sieve (2 to 0.83 mm, very coarse sand). And a 20-slot screen size means that the openings are 20 thousandths of an inch (0.51 mm). This is a commonly used scenario. Another example would be to use 6 to 9 sieved (3.35 to 2.16 mm, very fine gravel) sand with a 40-slot (1.02-mm) screen (Figures 8.41, 8.42).
8. One effective way to add sand to the hole is to pour it from a 5-gal (18.9-L) bucket with a notched flap cut in the bottom and side. A 1-in

Figure 8.41 6 to 9 mesh sieved sand.

Figure 8.42 Stainless-steel screen.

(2.5-cm) cut is made on the side of the bucket, and then a 1-in (2.5-cm) cut is made to the bottom to make an L-shaped flap. This piece can be flipped up into place while sand is being added to the bucket and flipped down to allow the sand to pour in a controlled manner in the annulus between the hollow stem and the casing (Figure 8.43). This is a good way to keep sand or filter pack materials from spilling all over the place, and it allows the worker to use the more cost-effective 100-lb (44.3-kg) bags. While the sand is being added, the auger flights are being lifted upward to avoid creating a sand lock between the casing and the auger. This is checked by the driller with the weighted cloth tape in a tamping motion to "feel" the placement of the sand and make sure there is a space between the bottom of the auger and the top of the sand. This procedure is continued until the sand is at least a foot or two above the top of the well screen (this is different for a production well).

9. Once the sand is in place, depending on the stability of the hole, the rest of the auger flights may be pulled out for easier well completion. As each flight is raised up to where you can see the bolts, the helper shoves in a horseshoe-shaped plate to suspend the drill string below ground surface, while the connecting bolts are loosened with an air wrench. Once the bolts are loosened, the auger flight is pulled upward and the helper guides the auger flight away from the rig and lays it on the ground for cleaning. This process is repeated until all auger flights are out of the ground. If the hole is not stable, then the

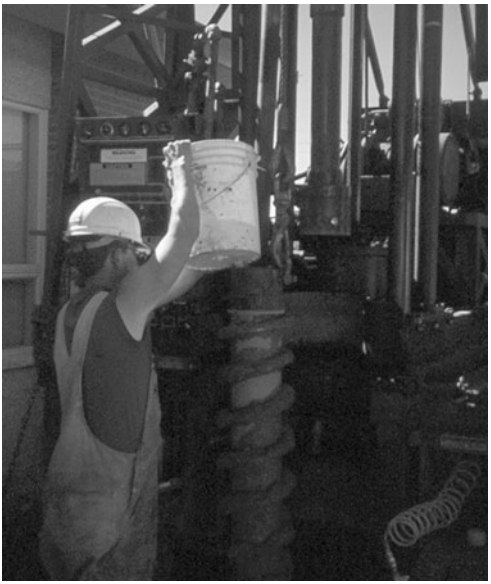

Figure 8.43 Adding sand using a bucket with a notch cut in the bottom.

bentonite sealing materials are added in a similar way, being poured through the annulus of the hollow stem and casing as the auger string is being incrementally raised.

10. A bentonite seal is placed on top of the sand-packing materials to isolate the zone that the monitoring well is sampled from and to protect this zone from contamination from above. There are a variety of methods to accomplish this. One method is to gradually pour 3/8-in (1-cm) bentonite chips around the casing. Care must be taken not to pour too quickly or a "bridge" can form that creates a void in the completion zone. Bentonite chips will fall through a water column if poured slowly (Figure 8.44). Deeper well completions may require the use of a tremie pipe. A tremie pipe is a smaller-diameter pipe that passes down the hollow stem to the desired depth. Bentonite also comes in pellet form. Both chips and pellets partially hydrate when they come in contact with water. The pellets can be placed with greater success if water is added to them in a bucket to make a slurry and then poured down the hole. If larger volumes are required, then grouting materials may need to be pumped into place with the drill rig. The length of the seal depends on regulations on a state-by-state basis. An expansive grouting material can be made by mixing cuttings with bentonite chips and then backfilled within approximately 2 ft (0.6 m) from the land surface.

Figure 8.44 Pouring bentonite chips to grout a monitoring well.

11. A top plug is made with concrete with framed sides to form a pad with sides sloping away from the casing. A metal locking security device can be shoved into the concrete to hold it tightly into place. This way the well could have a slip cap over the casing, with a locking painted metal security cover (Figure 8.45).
12. A drainhole should be drilled into the outer security casing to allow for condensation drainage (Fetter 1994). It is also a good idea to drill a hole below the cap of the monitoring well casing to allow for pressure changes to equilibrate easier, unless the site is for monitoring gases. This can be very important for widely fluctuating water levels (Chapter 5).

Well completion materials

Monitoring wells are supposed to provide hydraulic head and water-quality information representative of the aquifer. One of the most important criteria for selection of construction materials is water quality. For example, there is a tendency for chlorinated solvents to sorb onto polyvinyl chloride (PVC) and polytetrafluoroethylene PFTE (Teflon) from aqueous solutions (Reynolds and Gillham 1985). Stainless steel 304 and 316 may sorb heavy metals from aqueous concentrations as low as 50 to 100 μg/L (Parker et al. 1990). PVC glue, used for bell couplings, may also

Figure 8.45 Driller observing depth to water using reflected light off a mirror.

be leached into the monitoring well. This is one reason threaded couplings are desired over fitted couplings that require an adhesive.

Ranney and Parker (1997) performed tests on six different casing materials to see how they would react to 28 different pure "free product" organic chemicals and some acids and bases. PFTE and fluorinated ethylene propylene (FEP) casing showed good resistence to all chemicals, and stainless steel showed good resistence to the organic compounds. Stainless steel is less affected by organic compounds and is suitable for most geologic settings, except for acid rock drainage (ARD) sites where heavy metals may be present or where contamination with strong acids and bases has occurred. A reasonable casing material at an ARD site is PVC.

Some materials that may be the very best for chemical resistance may also be the most costly. The various pros and cons of different construction materials involve chemical resistance, weight, strength, and cost. A compromise may be required depending on the budget and site requirements. Table 8.4 lists some of the more common monitoring-well

TABLE 8.4 Well Construction Materials Comparison

Type	Advantage	Disadvantage	Relative cost
PVC	Lightweight, great for ARD acids, alkalies, alcohols, and oils	May adsorb VOC organics, react with ketones and esters	1.0
Stain less steel 304, 316 with varying amounts of nickel	Least reactive to organic materials, high strength, and temperature ranges	May corrode in heavy metal or ARD waters, higher cost than plastic, heavy to use	6.0, 11.2
Teflon	Resistant to many chemicals, lightweight	Lower wear resistence and tensile strength, expensive	20.7
Mild steel	Inexpensive, strong, lower temperature sensitivity	Heavy to use, not as chemically resistant as stainless steel	1.1
Polypropylene	Lightweight, resistant to acids, alkalies, alcohols, and oils	Weak, not very rigid, temperature sensitive, hard to make slots for screen	2.1

construction materials and lists respective advantages and disadvantages from Driscoll (1986) and Feter (1993).

Well development

One of the problems with monitoring wells, or production wells for that matter, is that they are often not properly developed. If the well-construction process goes as it should, and the water level recovers quickly after bailing the well a couple of times, these wells are often deemed completed, and the crew moves on to the next location. This may be adequate for establishing a connection with the aquifer to verify the hydraulic-head data but may not be adequate for water-quality sampling. The sediments from the drilling operation have not been properly mobilized from the borehole and may affect water-quality results. This can be kind of a dilemma because there is a tendency to limit well development at contaminated sites because of the need to handle the development water. There may also be a concern about disturbing the configuration of the plume. Decisions made about well development must be weighed with the objectives of the study.

If the monitoring well is to be used for slug testing (Chapter 11) or the evaluation of aquifer properties (Chapters 9 and 10), then proper well development is a must. This is done by pumping and surging the well to get the finer sediments to move back and forth through the screened interval. This may take an hour or more, but greatly improves the confidence in obtaining reliable water-level and water-quality data.

There are various techniques that can be used for developing monitoring wells. Many wells are simply overpumped until the water runs clear.

Using low-volume water-quality sampling pumps is a poor choice for well development because the impellers become clogged quickly and may seize the pump. It is better to use some form of surging action to mobilize the fines prior to using a pump designed to handle high sediment content. One good choice for development yields in the range of 10 to 15 gpm (0.63 to 0.95 L/s) is a converted chainsaw engine pump produced by Homelite. The pump needs to be primed, but does a great job of producing dirty water (Figure 8.46). Generally, it is *not* a good idea to add external water to the well, particularly if it is to be used for water-quality sampling. A couple of nonconventional well-development methods are given next.

Example 8.9 At one site a garden hose was within reach of a 2-in (5-cm) monitoring well. A successful well-development method was devised by using the garden hose with duct tape wrapped around it approximately 2 ft (0.6 m) below the nozzle to form a surging tool. The hose contributed clean water to the well as the surging tool was raised and lowered. The dirty water was lifted out of the well during the process for a successful completion.

In an another application a commercial hand pump was not working properly, so a water-bed venturi was attached to a hose connected to the handpump. This caused water to be produced from the well at a rate equal to production from the hose (Figure 8.47). These two examples violate the recommendation of not adding water to a well, but were justified because in both cases the wells were only being used for water-level and hydraulic property data.

Example 8.9 was not given as an example of standard practices, but as illustrations of the principles of surging and overpumping.

Figure 8.46 Using a converted chainsaw engine pump.

Figure 8.47 Using a garden hose and water-bed venturi to make a surging tool.

Completion of multilevel monitoring wells

The goal at many monitoring sites is to gain a detailed understanding of the vertical and horizontal distribution of water-quality parameters and hydraulic head. The best approach to this is by completing monitoring wells capable of sampling discrete vertical intervals. In shallow systems (less than 100 ft, 30 m) this can be a matter of drilling a larger diameter hole and placing several small diameter wells completed at different vertical depths within the borehole (Figure 8.48). This is known as a **nested well**. The deepest well is placed at the bottom of the borehole, with packing materials added to a foot above the screened zone followed by adding bentonite to the next desired depth. The process is repeated until several vertical zones have been established. Wells completed at different depths, but in close proximity to one another are known as **cluster** wells. Nested wells may have the problem of achieving a good seal occurs between desired intervals (vertical communication along the casing). Improvement in proper spacing between individual wells in a nest can be accomplished by using centralizers; however the U.S. EPA, and California Department of Water Resources discourage the use of nested wells (Einarson 2006).

Another approach to installing dedicated multilevel groundwater monitoring wells is by using the services or materials produced by commercially available systems. The four most prominent ones are: the Westbay MP, Solinst Waterloo, Solinst CMT, and Water FLUTe systems. These systems allow the vertical sampling of water quality and hydraulic head at 10 or more discrete positions in a single well. Ports

Figure 8.48 Constructed wetlands testing, using nested wells in the evaluation of the vertical distributions of dilute bromide in a tracer-test.

from individual vertical positions need to be established before placing the materials down-hole. A very good discussion of the peculiarities of installing multilevel monitoring wells along with additional references can be found in Einarson (2006).

8.6 Production-Well Completion

Production-well completion could easily comprise another chapter, but is included here as a comparison to monitoring-well completion. Proper production-well completion allows well yields to be maximized while maintaining efficiency. This also leads to confidence in the results from aquifer testing (Chapters 9 and 10).

A general question regarding well completion is: Are we testing the aquifer or the well? An aquifer capable of producing a fair amount of water may be hindered by drilling practices, choice of well-completion materials, or well-development technique. These may result in poor well

performance. Another type of problem arises when well-completion materials are preselected before there is a proper knowledge of the aquifer properties. A slot size or packing material is used that is similar to other wells in the area when they may not be appropriate. This is an inefficient use of resources. Just because a well may be designed to yield a particular quantity of water, the aquifer may be incapable of doing so.

The best way to tell what the aquifer is like is to drill a small diameter pilot or test hole. Larger-diameter production wells can then be drilled with a good knowledge of where the production zones are. If the cable-tool drilling method is used and the target aquifer is known to be productive, production diameter casing may be used from the beginning. This approach can also be used for "drill and drive" rotary methods. Samples from the production zone can be collected and analyzed to select the appropriate screen- and gravel-packing materials. The production zone can later be exposed by jacking up the casing to "expose" the screen.

Williams (1981) suggests that well-design criteria should include approach velocity and turbulence concepts rather than entrance velocity alone. This process begins with selecting the appropriate packing materials around the screen and selecting the right screen slot size. This is usually done by performing a sieve analysis on the formation materials. Well development around screens can be for "naturally" developed or artificial materials. Naturally developed wells are less expensive than gravel packed wells because of the additional steps involved in well completion. If the best production zone has a significant amount of stratified fines, then gravel packing allows for greater flexibility (Williams 1981).

Sieve analysis

Assuming the well has been drilled to a desired depth and is cased to the bottom, the hydrogeologist can take the formation cuttings to a lab for analysis or perform a sieve analysis, If the cuttings or formation materials have been bagged every 5 ft (1.5 m), a sieve analysis should be performed over every potential zone to be included within the screened interval. A way to evaluate the grain-size distribution is to plot them on a graph. Some graphs forms are prepared for this purpose and can be provided by any screen manufacturer (Figure 8.49). A general evaluation of grain-distribution or sorting is through the uniformity coefficient (C_u), Equation 8.1.

$$C_u = d_{60}/d_{10} \tag{8.1}$$

where d_{60} = diameter where 60% of the grain sizes are finer
d_{10} = diameter where only 10% of the grain sizes are finer, also known as the **effective grain size**

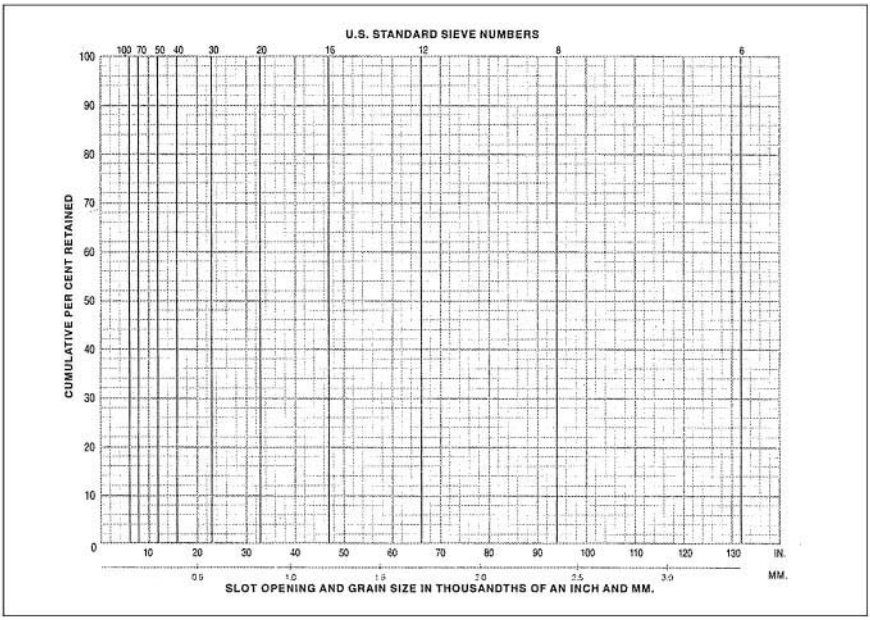

Figure 8.49 Grain-size analysis paper from Johnsons Well Screens.

If this ratio is less than 4 it is considered to be well sorted, and if it is greater than 6 it is considered to be poorly sorted (Fetter 1994). Walton (1962) suggests that in heterogeneous aquifer materials having a C_u greater than 6 the screen should retain 50% (allow 50% passing or use the d_{50} as the slot size) if the overlying materials are unconsolidated and collapsible, or as little as 30% (70% passing or use the d_{70} as the slot size) if the overlying materials are firm. In homogeneous materials that are well sorted, if the overburden is soft, the screen should retain 60% (allow 40% passing or use the d_{40} as the slot size), and if firm allow 40% (60% passing or use the d_{60} as the slot size). The reason for indicating percent retained or percent passing is because the graph paper is presented both ways. It is just as easy to plot the data using a spreadsheet program. A comparison of grain sizes versus sieve size is shown in Chapter 2.

Example 8.10 In southwestern Montana, an 8-in (0.2-m) irrigation well was drilled, and the driller wanted to know what size screen slot to recommend. He had collected representative samples every 5 ft (1.5 m) between 180 and 210 ft (56.1 and 64 m). Approximately 150 to 200 g of sample were placed into tins and cooked at 105°C until dry. Each sample was weighed and ran separately through a series of sieves in a ro-tap machine for 15 min. The results are shown in the partial spreadsheet of Table 8.5 and plotted in Figure 8.50.

TABLE 8.5 Sieve Analysis of Samples from an 8-in Irrigation Well Production Zone between 180 and 210 ft, from Figure 8.42

Screen #	Size mm	Size inch	180–185	185–190	190–195	195–200	200–205	205–210	185–210
5	4	0.157	0	6.22	10.548	10.862	27.272	23.673	10.887
10	1.981	0.078	1.354	9.94	19.605	10.866	17.045	17.618	11.987
18	0.991	0.039	4.426	20.96	31.14	15.104	32.77	29.175	19.004
40	0.425	0.0165	20.06	30.95	34.398	21.628	33.169	23.21	21.833
60	0.25	0.0097	23.38	9.31	14.365	14.02	12.387	7.502	8.831
100	0.149	0.0058	16.84	2.91	8.205	8.485	7.049	4.09	5.031
200	0.074	0.0029	7.568	1.783	5.233	3.184	4.727	2.578	2.851
<200			2.06	1.65	3.472	1.765	3.497	1.767	1.82
		Total	75.688	83.723	126.966	85.914	137.916	109.613	82.244
	Sample weight		76.76	86.13	127.16	85.85	138.04	110.16	82.36

Screen #	Cum. %	Cum. %	Cum. %	Cum. %	Cum. %	Cum. %	Cum. %
5	0.00	7.43	8.31	12.64	19.77	21.60	13.24
10	1.79	19.30	23.75	25.29	32.13	37.67	27.81
18	7.64	44.34	48.28	42.87	55.89	64.29	50.92
40	34.14	81.30	75.37	68.04	79.94	85.46	77.47
60	65.03%	92.42%	86.68%	84.36%	88.93%	92.30%	88.20%
100	87.28%	95.90%	93.14%	94.24%	94.04%	96.04%	94.32%
200	97.28%	98.03%	97.27%	97.95%	97.46%	98.39%	97.79%
<200	100.00%	100.00%	100.00%	100.00%	100.00%	100.00%	100.00%

Slot size	Screen #	% passing	% passing	% passing	% passing	% passing	% passing	% passing
157	5	100.00	92.57	91.69	87.36	80.23	78.40	86.76
78	10	98.21	80.70	76.25	74.71	67.87	62.33	72.19
39	18	92.36	55.66	51.72	57.13	44.11	35.71	49.08
16.5	40	65.86	18.70	24.63	31.96	20.06	14.54	22.53
9.7	60	34.97	7.58	13.32	15.64	11.07	7.70	11.80
5.8	100	12.72	4.10	6.86	5.76	5.96	3.96	5.68
2.9	200	2.72	1.97	2.73	2.05	2.54	1.61	2.21
	<200	0.00	0.00	0.00	0.00	0.00	0.00	0.00

The grain sizes for the sediments between 185 and 210 ft were more uniform, and the 180 to 185 sample was too small and different to be included in the production zone. The d_{60} ranges between 1.1 and 1.9 mm (coarse to very coarse sand) and the d_{10} ranges between 0.2 to 0.3 mm (fine to medium sand) with a C_u around 6. By evaluating Figure 8.50 at a 50% passing, a slot size of 40 was chosen.

Grain sizes with a d_{10} smaller than 0.25 mm and are fairly well sorted should probably have a gravel packing (Williams 1981). The well in Example 8.10 was successfully developed without a gravel packing because of the coarser fraction present.

When artificial gravel packing is introduced, a different philosophy is employed. Normally, the filter packing materials should be uniform

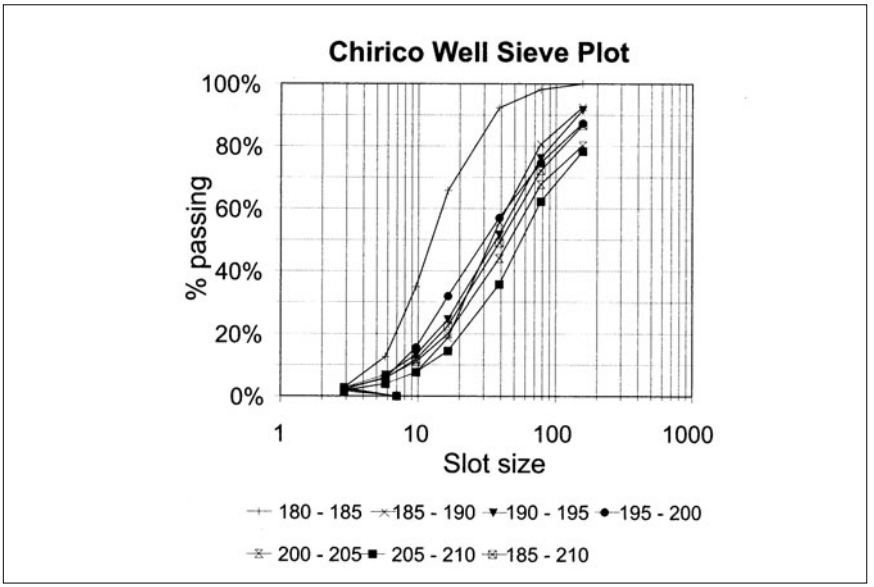

Figure 8.50 Graph of percent passing grain sizes versus slot size to evaluate the appropriate screen slot size, for an 8-in irrigation well in southwestern Montana.

in size with a uniformity coefficient less than 2. The aquifer grain-size distribution curves are evaluated to identify the finest grain-size interval in the screened zone. The d_{30} of the aquifer material is multiplied by a factor to obtain the d_{30} of the gravel packing materials (Williams 1981). The slot size is selected so that 90% of the filter pack material is retained (only 10% passes or the d_{10} slot size).

The thickness of gravel-packing materials measured between the borehole wall and the well screen should be at least 0.5 in (1.3 cm) thick, but not greater than 8 in (20 cm) (Williams 1981; Driscoll 1986). Greater thicknesses may actually hinder aquifer development because the energy required to develop the aquifer must be able to reach through the gravel packing to the aquifer. For most production wells, gravel pack thickness between 2 and 6 in around the well screen is a good target. Since well casing may not be placed dead center in the well bore, this can usually be accomplished.

Well screen criteria

The well screen is designed to facilitate entry of groundwater from the aquifer into the well bore. One of the greatest sources of well problems is from overpumping (Williams 1981). Overpumping causes fines from the aquifer to entrain and creates turbulence near the well bore.

Turbulence reduces well efficiency, enhances encrustation, and reduces well life. There is a limitation of how much water can be delivered from an aquifer, so the construction design should complement this maximum capacity. Sufficient funds should be invested for any production wells that are intended to be used for a long time. Temporary wells or monitoring wells may not require as high a level of design or expense. A list of the screen criteria and functionality is listed in Table 8.6 (modified from Driscoll 1986).

The slot size used in wells is measured in thousandths of an inch. For example, a 40-slot screen has a slot opening of 0.040 in (1 mm). A table of slot size versus millimeter equivalents is shown in Table 8.7.

As water moves toward a well, its velocity increases. If the velocity exceeds a critical limit, finer particles from the aquifer will become entrained and move into the gravel packing (Williams 1981). This critical limit is known as the **approach velocity** (V_a). This is not to be confused with the entrance velocity (discussed next). The entrance velocity is measured where water passes through the well screen into the well, and the V_a is measured at the borehole wall at the damage zone (Chapter 9). The V_a is significant because one should know the approximate pumping rate that would best develop the well once it is completed. Additionally, the V_a is a specific discharge and not a velocity where the specific discharge is divided by the effective porosity (Chapter 3). It can also be viewed as the discharge divided by circumferential area. For design purposes a conservative V_a (Huisman 1972) can be expressed as:

$$V_a = \sqrt{K}/30 \tag{8.2}$$

where: V_a and K are both in units of m/s.

TABLE 8.6 Criteria and Function of Well Screen [Adapted from Driscoll (1986)]

Criteria
Large open area
Nonclogging slots
Resistant to corrosion
Sufficient strength
Function
Easily developed
Minimizes incrustation
Low head loss
Control of sediment entry

TABLE 8.7 Slot Size in Inches and Millimeters

Slot Size	Inches	Millimeters
10	0.010	0.246
16	0.016	0.417
20	0.020	0.495
25	0.025	0.635
30	0.030	0.762
35	0.035	0.889
40	0.040	0.990
60	0.060	1.52
80	0.080	2.03
100	0.100	2.54
120	0.120	3.05
150	0.150	3.81
180	0.180	4.57
210	0.210	5.33
250	0.250	6.35

This can also be expressed in terms of grain size (Huisman 1972) from the aquifer materials as:

$$V_a < 2d_{40} \tag{8.3}$$

with similar units.

This assumes that the grain-size distribution is representative of the aquifer materials in the production zone (Williams 1981). Once the V_a is known, it can be multiplied by the circumferential area of the filter's outside area to estimate the maximum yield capacity (Q_c). If the distance (r_d) at which fines are removed during development can be estimated, the discharge (Q_d) necessary for proper development can also be estimated from the following relationship (Williams 1981).

$$\frac{Q_d}{Q_c} = \frac{V_a A_d}{V_a A_p} = \frac{r_d}{r_p} \quad \text{or} \quad \frac{Q_c r_d}{r_p} \tag{8.4}$$

where Q_c = capacity at the maximum approach velocity
Q_d = discharge during development
r_p = distance to outside edge of filter pack or screen diameter in naturally developed wells
r_d = distance of effective development
A_d = area at the outer effectiveness of development
A_p = area at the outside edge of filter pack or the outside of the screen for naturally developed wells

Williams (1981) points out that although the approach velocity cancels out in Equation 8.4, it is necessary for deriving the maximum yield capacity (Q_c).

Example 8.11 Referring to Example 8.10, the d_{40} (40% passing) is nearly equivalent to slot size 30. This yields a slot opening for the d_{40} of approximately 0.76 mm. From Equation 8.3 and Table 8.7 the maximum approach velocity is approximately:

$$V_a \leq 2 \times 0.000762 \text{ m} = 1.5 \times 10^{-3} \text{ m/s}$$

From pumping-test data, the hydraulic conductivity (K) is estimated to be 10 m/day. If this K value is plugged into Equation 8.2 and converted to m/s, another estimate of the maximum approach velocity is calculated to be:

$$V_a \leq (12 \times 10^{-4} \text{ m/s})^{0.5}/30 = 3.7 \times 10^{-4} \text{ m/s}$$

These are both within a factor of 5 of each other. By using an 8-in telescoping screen with outer diameter of 7.5 in (19 cm) we divide by 2 to obtain the (r_p) distance 0.095 m. The development distance is assumed to be an additional 4 in (10.2 cm) into the formation and the screen length is 25 ft (7.6 m). These can be plugged into Equation 8.4 to obtain a range of discharge values (Q_d). The two areas must first be converted into meters squared:

$$A_d = 2 \times \pi \times r_d \times \text{screen length} = 2\pi(0.197 \text{ m})(7.62 \text{ m}) = 9.43 \text{ m}^2$$

$$A_p = 2 \times \pi \times r_p \times \text{screen length} = 2\pi\,(0.095 \text{ m})(7.62 \text{ m}) = 4.55 \text{ m}^2$$

$$Q_c = V_a \times A_p = 1.5 \times 10^{-3} \text{ m/s} \times 4.55 \text{ m}^2 = 6.8 \times 10^{-3} \text{ m}^3\text{/s}$$

$$Q_d = \frac{Q_c r_d}{r_p} = \frac{(6.8 \times 10^{-3}\text{m}^3\text{/s})(0.197 \text{ m})}{0.095 \text{ m}} = 1.41 \times 10^{-2}\,\text{m}^3\text{/s}\ (224 \text{ gpm})$$

This means the developmental production rate Q_d should exceed 230 gpm (10 L/s) to mobilize formation fines within 4 in (10.2 cm) of the screen. If the r_p was 6 in (15.2 cm) instead of 4 in (10.2 cm) the Q_d would need to exceed 280 gpm (17.7 L/s).

Using the other approach velocity, a value of 3.5×10^{-3} m^3/s (55 gpm) was obtained. Actual production rates were approximately 180 gpm (1.1×10^{-2} m^3/s), which suggests the grain-size approach of Equation 8.3 may give a better approximation, *if* the production zone samples are representative or the factor in Equation 8.2 should be 10 instead of 30. This analysis can be performed if production-zone samples and sieve analyses are performed prior to a pumping test or well development.

Screen entrance velocity

Although the approach velocity is important for evaluating production rates for well development, the screen entrance velocity is probably one of the most frequently used criteria for sizing well screen. The volume of water pumped from a well is a function of percent open area and the entrance velocity. If the desired well discharge (Q) is known and a minimum entrance velocity is fixed in the design criteria, the only variable is the percent open area. The most commonly used entrance velocity for design purposes is 0.1 ft/s (0.03 m/s) (Williams 1981; Driscoll 1986); however, other screen manufacturers report acceptable entrance velocities as high as 3 ft/s (1 m/s) (Roscoe Moss 1994). A variety of different slot types are available, continuous, slotted, bridge-slot, and louvered (Figure 8.51), in as variety of materials. The continuous-slot screen has the largest percent open area per length, because a continuous wire spacing is welded to vertical supporting rods. The functions of well screen are listed in Table 8.6. As entrance velocities increase, the potential for turbulence and head losses also increase. This results in higher electrical costs, promotes encrustation, and enhances sediment mobilization.

The open area is increased by lengthening the screen or increasing its diameter. For thin aquifers the only choice may be increasing the diameter; however, only percentage gains are made by increasing the diameter. This can be evaluated by comparing some of the continuous slot

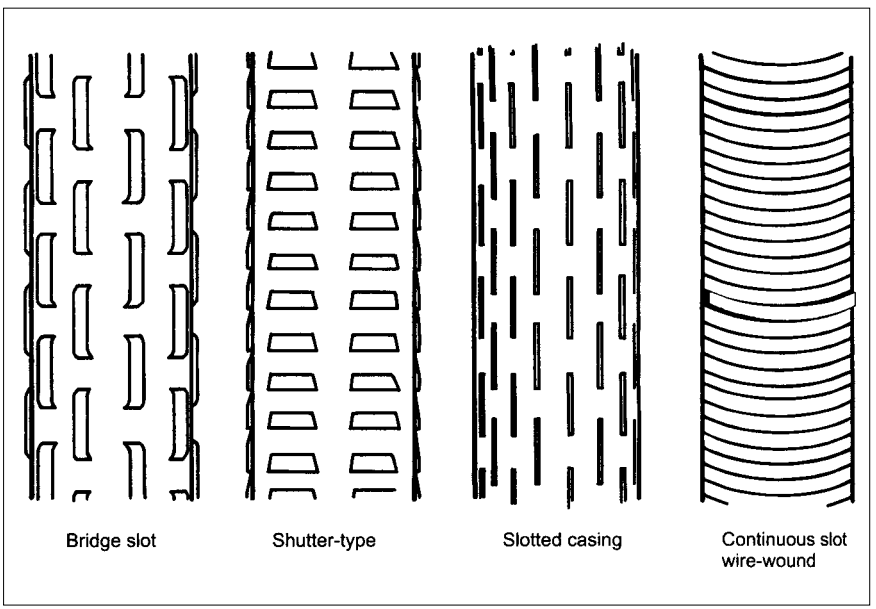

Figure 8.51 Various types of well screens. [*From NGWA (1989).*]

TABLE 8.8 Percent Open Area for Stainless-Steel Continuous-Slot Screens

	Slot size	in^2/ft	% Open area	Screen diameter	Slot size	in^2/ft	% Open area
4" ID	20	44	25	12" ID	20	69	14
	40	72	41		40	99	21
	60	90	52		60	135	28
	100	112	64		100	189	39
8" ID	20	45	18	16" ID	20	68	11
	40	77	31		40	124	21
	60	100	40		60	169	28
	100	131	53		100	238	40

values listed in Table 8.8. In unconfined aquifers, lengthening the screen may effectively reduce well yield by reducing the available drawdown. The opposite may be true for a confined aquifer, as long as the hydraulic head remains above the top of the aquifer (Chapter 5).

Bridge slotting runs one-fifth to one-third less percent open area than continuous slot screen for similar casing diameters. Louvered slot screen runs less than one-tenth to one-fifth of continuous slot screen (Driscoll 1986). Vertical slot screens generally yield a maximum of 3% open area. Other perforations that are handmade may be from torch-cut slots. These are usually used for monitoring deep wells but are known to be used in domestic well completions. This results in sediments coming into the well over the life of the well. Some perforations are made in situ in steel casing using a mill knife. This is a device placed downhole that hydraulically punches a hole outward in the casing like a can opener. This is commonly done on 6-in domestic wells, but once again may allow sediments to pass into the well.

Domestic wells may have their "pump liner" (described in the next section) perforated by a 1/16 -in (1.6-mm) or 1/8-in (3.2-mm) slot cut with a circular saw. Generally this is done by cutting a slot in length of approximately 6 in (15.2 cm) to 1 ft (30.5 cm) spaced every 1 ft or so. The casing is turned approximately 120° in successive rows that are staggered to make three rows that have a spiral pattern of perforations. This maintains a level of strength. The author recommends a maximum depth of 400 ft using this process for schedule 80 PVC screen. He has witnessed the collapse of vertically slotted screens at greater depths. Deeper wells should be completed with steel.

Example 8.12 This example will refer to the well discussed in Example 8.4, an 8-in production well designed to irrigate a 30-acre cemetery. The production yield was supposed to yield 250 gpm (15.8 L/s). The drilling method used was cable tool. Drilling would proceed 10 ft before welding on another section of casing. During drilling, a clay zone was encountered at approximately

90 ft (27.4 m) with "first water" at 25 ft (7.6 m). Drilling was hampered by heaving sands. The decision was made to continue looking for the next coarse-grained zone. A fine gravel zone was encountered between 148 and 165 ft (45.1 and 50.3 m) before encountering another clay zone. A sieve analysis was performed on samples collected from the production zone, assuming a natural gravel pack. The analysis indicated a 46-slot was appropriate for a 50% passing grain-size (Figure 8.52). If a 15-ft section of 46-slot screen was used in the production zone, would the entrance velocity be less than 0.1 ft/s? There are two ways to check, (1) either the entrance velocity calculated to be less than 0.1 ft/s using the desired Q or (2) the area and entrance velocity can be used to calculate a Q. As long as the Q exceeds 250 gpm, the design would be adequate. The percent open area from the chosen manufacturer's 46-slot continuous screen was 33%.

The surface area for the 15-ft screen was first determined

$$\begin{aligned}\text{Surface area} &= \pi \times d \times 12 \text{ in/ft (per ft of screen)}\\ &= \pi \times 7.5 \text{ in} \times 12 \text{ in/ft}\\ &= 282.7 \text{ in}^2\text{/ft (for 1 ft of screen)}\end{aligned}$$

Multiplying this by 15 ft yields: 283 in^2/ft × 15 ft of screen = 4,240 in^2
The percent open area is 33%, so:

$$4240 \text{ in}^2 \times 0.33 = 1399 \text{ in}^2, \text{ or}$$

$$1{,}399 \text{ in}^2/144 \text{ in}^2/\text{ft}^2 = 9.7 \text{ ft}^2$$

Q = 250 gpm, or 250 gpm/(448.8 gpm) per ft^3/s = 0.557 ft^3/s

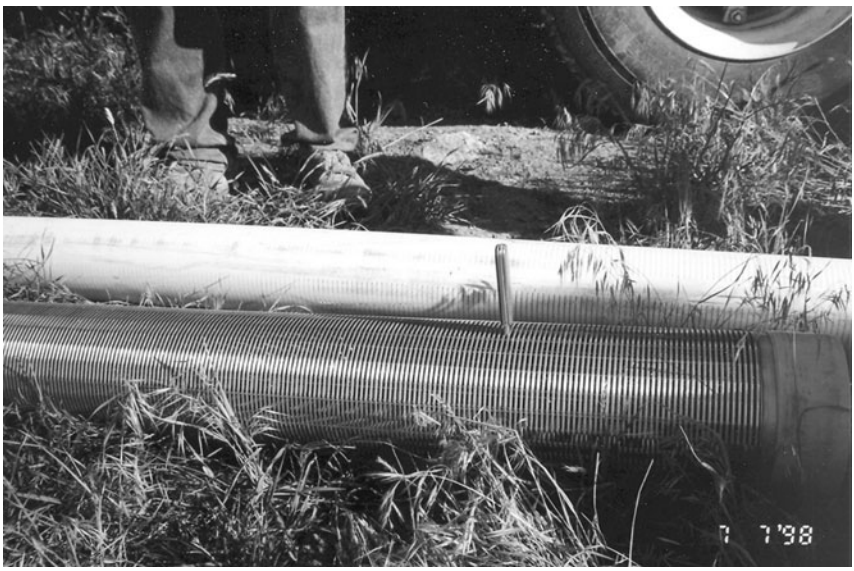

Figure 8.52 Stainless-steel, v-wire wrapped production screen.

From the relationship: $Q = V \times A$

We can estimate the velocity moving through the slots, where:

Q = flow in ft^3/s
V = velocity in ft/s
A = screen open area in ft^2

The velocity is calculated by: $V = Q/A = 0.557\ ft^3/9.7\ ft^2 = 0.057$ ft/s, which is well below 0.1 ft/s.

The maximum yield at 0.1 ft/s is given by:

$$Q = V \times A = 0.1\ \text{ft/s} \times 9.7\ ft^2/s = 0.97\ ft^3/s$$

$$0.97\ ft^3/s \times 448.8\ \text{gpm}/1\ ft^3/s = 435\ \text{gpm}$$

The well was over-designed, but the well owner wanted a well that would last more than 50 years, or many years beyond his lifetime. In this case, 10 ft of screen may have been adequate.

Well completion and development

Wells are either completed open-hole or through a packing procedure similar to the monitoring-well process. Domestic wells, if drilled in indurated materials, will be drilled open-hole and later have a plastic "pump liner" placed to protect the pump from materials that may slough off from the borehole wall. This is not desirable because of the increased potential for downward migration and cross contamination. Most well drillers realize this, but the competition of drilling by the foot results in well completions that are less than desired.

Larger production wells that require that the screen be the same diameter as the casing should be preconstructed before inserting into the drillhole (Driscoll 1986). The bottom plate, sump or tailpipe section, and screen should be welded together before being attached (welded) to the casing and lowered into the ground.

Wells that have been drilled and cased to the bottom have their production zones exposed later by hydraullically jacking up the casing using "spiders" and "slips," after the names of the jacking equipment used to grip the casing (Figure 8.53). The "spider" is a yoke-like feature that allows the casing to slide through the midst of it while resting on top of the jack lifts. The "slips" have grooved edges and a wedge shape that slips in between the "spider" and the casing to perform a friction grip on the casing during an 18-in (0.46-m) up-stroke (Figure 8.54). The slips are pulled out while the weight of the "spider" helps retract the jack heads for another stroke. A rhythm is established to jack the casing up to the desired position. Once the casing is at the desired position, the lifted portion is cut off with a torch.

Before the "jacking" step is taken a telescoping screen, about 1/2-in (1.2-cm) smaller diameter than the inside diameter of the casing is

Figure 8.53 Close-up of two sets of spiders (yoke-like piece) with four slips.

shoved down through the casing to the bottom. A tailpipe (sump) and bottom plate are welded to the bottom of the screen, along with a piece of blank casing extending upward that has a packer placed to form a seal between the inside of the driven casing and the extension piece (Figure 8.55). The whole package is dropped out of sight and followed in with the drillpipe to be held in place while the casing-jack assembly prys up the casing. The hydrogeologist is responsible for making sure that the screen has been exposed properly. If the telescoping screen package is not in the right place, it must be "fished" out and the hole cleaned out, and the process repeated.

Example 8.13 The 8-in well from Example 8.12 was drilled to a depth of 170 ft (51.8 m), having penetrated 5 ft (1.5 m) of clay. The telescoping package was designed with a 5-ft tailpipe, 15 ft of screen and a 5-ft extension equipped with a neoprene K-packer. The tailpipe would be located in the lower clay and the screen would fit in the 17 ft of available fine gravel. The package was dropped out of sight and came to a stop 5 ft short of the goal.

A steel fishing tool was constructed by the driller with two metal pieces that could rotate on a bolt that would flange outward to a maximum of 1/2 in (1.2 cm) smaller than the inside diameter of the telescoping screen (Figure 8.56). It could collapse inward but only flange outward to this maximum distance. This fishing tool was placed inside the well screen to hook onto the lip at the top of the screen. It worked beautifully on the first try.

Figure 8.54 Casing jacks fully extended, with spider and slips at top gripping the casing on the up-stroke. The driller is on the left-hand side of this reverse-circulation drill rig.

The hole was cleaned out, and the telescoping package was again dropped out of sight. This time the tailpipe was within 1 ft of the bottom, so the 15-ft screen was fitted exactly within the 17-ft gravel zone.

Well development in production wells is performed to correct the damage done during drilling and enhance the flow characteristics near the screen. With gravel-packed wells, the concepts of approach velocity should be used to determine maximum pumping rates (Williams 1981). Proper development pumping rates (Q_d) will mobilize the fines at an appropriate distance from the packing materials. In naturally packed wells, a significant portion of the fines near the screen are washed out during the development process to create a higher transmissivity zone next to the well screen. There are different methods used to accomplish this.

Overpumping is probably the simplest method of mobilizing fines within the screened zone. Pumping until the sediments cease to entrain

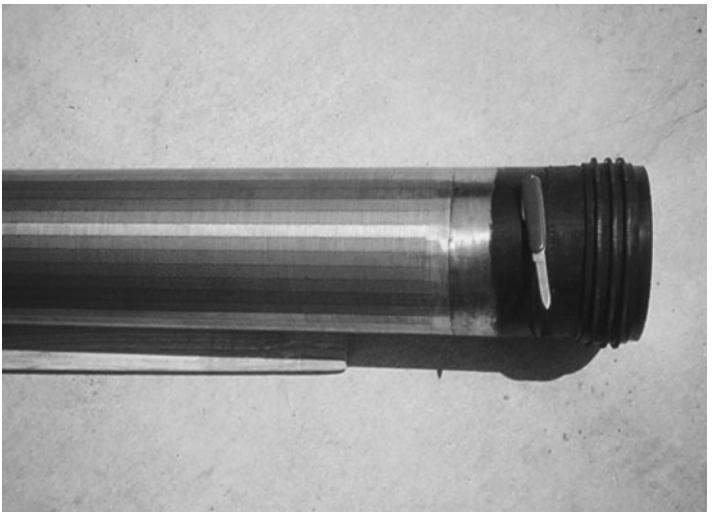

Figure 8.55 Neoprene K-packer indicated by a pencil.

works for pumping rates lower than the development rate. The problem with this method is that some fines become trapped from a one-way movement. When the pumping stops, the trapped sediments may become loosened and then remobilize again when the pump is turned back on. It is better to employ a back-and-forth motion, such as was described earlier in the monitoring-well section.

Figure 8.56 Fishing tool with flanged wings next to well screen.

One effective method of obtaining high volumes of water in a back-and-forth motion is known as **backwashing**. (This term is not to be confused with sharing a soda with a 2-year old). Using a forward rotary rig, the drill pipe is lowered to depth a few feet above the well screen. Air is injected into the well and displaces the water up to the surface. This is done for 15 min or so, and then the air is shut off, allowing the water column to rush back out through the screen into the formation. This process is repeated until the water rinses clean (Figure 8.57). This creates a back-and-forth motion in the production zone. It may take several hours to clean up the well, but it is effective. It is well worth the extra time and cost to make sure wells are properly developed. It should be mentioned that when injecting air from the drill pipe, it should not be within the screened interval because the air flow is too intense. If this occurs, the aquifer materials may become more damaged than from the drilling process.

Figure 8.57 Clean water using the backwashing development method after 6 h of development.

8.7 Water Witching

If there is to be section on water witching (or dowsing), it seems appropriate to be placed in this chapter since many well drillers and property owners use this service prior to drilling. There are individuals who claim to have incredible success rates and must therefore have certain divining powers. It seems appropriate that the author makes a few observations that represent his opinion.

The technique involves using welding rods (coat hangers or whatever) approximately 15 to 18 in (38 to 46 cm) long bent approximately 2 in down on one end. Forked hickory or willow sticks are also often used. The short lengths of the welding rods are held loosely in the hands while the long ends are allowed to rotate freely. In the case of the sticks, the two forked ends are held in the hands while the single end protrudes outward. The author's understanding is that when "water" is encountered the rods turn inward or outward and the hickory stick points downward. This has been used by many people to locate septic tanks or buried pipes on properties. There are mixed reviews on this process compared to technical methods (Mellet 2000). Some individuals use this for locating water on properties for a fee. The author is often asked by students and others what he thinks about this. A fairly complete history on this topic is found in U.S. Geological Survey Water Supply Paper Number 416.

Almost anywhere on the surface of the earth one will encounter water at depth. In an alluvial valley, almost anywhere in the valley would yield a productive well. The challenge comes when evaluating locations in solid rock formations or where the formations may be structurally tilted or disturbed. Even then, water will be eventually encountered; however, the yield may be very low. In hard-layered sedimentary, igneous, and metamorphic rocks, significant well yields may only be derived from secondary fracturing (Chapter 2). It may be that experienced water witchers use similar geologic principles as a scientist would. They may recognize structural trends and the orientations of fracture systems and have experience with other drill holes in the area. When this approach is taken, that is one thing; but when water witchers predict exact depths and yield rates, no matter how sincere and dedicated these folks may be, it is the author's opinion that this appears to be akin to consulting an Ouija board.

Example 8.14 The following true story took place in July 1993 in southwestern Montana. At the time, local ranchers had hired a driller to perform some wildcat drilling on the property at an hourly rate, prospecting for water. They owned 2,000 acres of land on either side of a small perennial stream. The property extends toward the mountains on either side of the valley. The thought was that they could run more cattle if there was more water available. Alluvial fans

coalesce and slope toward the center of the valley. Drill site locations were constrained to be within 0.25 mi (0.16 km) of a power source or a main road. A couple of drilling sites were selected and the lithologies encountered were alternating silty and gravelly materials, with yields only in the 30 to 40 gpm (1.9 to 5 L/s) range instead of the order of magnitude higher that was hoped for. We were just finishing the second, and last, hole when Elmer the neighbor came over.

Elmer was walking along the alluvial fan in a direction parallel with the mountains. As he walked the welding rods would move and cross at times. He was a larger man who said he couldn't always do this. He had worked for the U.S. Forest Service for about 20 years when an accident occurred that affected his neck. He was on disability and didn't charge for his services. He is a nice enough person with an interest in helping. He acknowledged that most people did not believe in "witching."

Elmer asked the rancher if he would like to try. The rods were placed in his hands and Elmer put his hand to the man's neck and wrist. The rancher exclaimed that no amount of squeezing his thumbs could keep the rods from moving. He was amazed and ran to get his daughter. It did not work for me. The daughter came and it worked for her. Elmer said, "ask how deep it is." The daughter said, "ask who?" (A significant question.) "The rods," Elmer replied. At that point the daughter handed the rods back to him.

Elmer proceeded to demonstrate his skills. He walked in a straight line, and the rods crossed where the water "started." They would cross and move back and forth where the "highest" flow was and then swing around pointing behind him when he walked "past" the water. He turned around and repeated the process. The "water" was approximately 20 ft (6.1 m) wide, the possible width of a gravel channel. He asked the rods, "How deep, how many gallons per minute, and how thick?" The rods crossed as he sequentially called out numbers. This was all pretty eerie, but what happened next was especially strange and didn't seem to have much to do with locating water.

Elmer asked, "Where does the water come from?" and the rods pointed toward the mountains, and when asked, "Where is the water going?", they pointed downslope toward the center of the valley. The final question was, "Where is [the rancher's name]?" and the rods swung around and pointed to him. About that time, I was making tracks for my pickup truck.

The author wishes to apologize to those who may have great faith in this process and may become offended by the above example, but he believes that there is a point where witchers take this process way too far. After all, they do refer to themselves as witches. Following geologic, hydrologic, or geophysical principles are still the only methods the author chooses to estimate drill sites for water production. People will have to decide what they will have faith in for themselves.

8.8 Summary

Selection of the appropriate drilling process requires an understanding of the geology and the objectives of the project. Rig safety and getting along with the drilling contractor can be done in a cooperative environment if

the hydrogeologist shows common courtesy and common sense. Well construction and development requires that accurate samples be collected in the production zone. If it is a monitoring well, then the construction materials need to be resistant to the contaminants involved. For production wells, a sieve analysis, screen design, and development strategy can be chosen that effectively produces a maximum yield.

References

Boothman, N., 2000. *How to Make People Like You in 90 Seconds or Less*. Workman Publishing Company, Inc. New York, N.Y. 171 pp.

Crumbling, D.M., 2004. *Summary of the Triad Approach*. US EPA, Office of Superfund Remediation and Technology Innovation. Washington D.C. http://www.triadcentral.org/ref/doc/triadsummary.pdf

Driscoll, F.G., 1986. *Groundwater and Wells*. Johnson Screens, St Paul, MN, 1108 pp.

Einarson, M., 2006. Multilevel Ground-Water Monitoring. In: *Practical Handbook of Environmental Site Characterization and Ground-Water Monitoring*, D.M Neilsen (ed.). Taylor and Francis Group, Boca Raton, FL pp. 807–848.

Fetter, C.W., 1993. *Contaminant Hydrogeology*, *2nd Edition*. Prentice-Hall, Upper Saddle River, NJ, 500 pp.

Fetter, C.W., 1994. *Applied Hydrogeology, 3*. Merrill, New York, 691 pp.

Geoprobe Systems, 1999. *The Probing Times*, Vol. 8, No. 1, Summer 1999, Salina, KS, www.geoprobesystems.com.

Huisman, L., 1972. *Groundwater Recovery*. Winchester Press, New York.

Mellet, J., 2000. GPR 5. Dowsers Zero. *Fast Times—The EEG Newsletter*, May 2000, 10 pp., The Environmental and Engineering Geophysical Society.

Midwest Drilling 2004. *The Rotasonic Drill*. A Division of Germac Enterprises Ltd. Winnipeg, Manitoba, Canada.

Neilsen, D.M., Neilsen, G.L., and Preslo, L.M., 2006. Environmental Site Characterization. In: *Practical Handbook of Environmental Site Characterization and Ground-Water Monitoring*, D.M Neilsen (ed.). Taylor and Francis Group, Boca Raton, FL pp. 35–205.

Neilsen, D.M., and Schalla, R., 2006. Design and Installation of Ground-Water Monitoring Wells. In: *Practical Handbook of Environmental Site Characterization and Ground-Water Monitoring*, D.M Neilsen (ed.). Taylor and Francis Group, Boca Raton, FL pp. 639–805.

NGWA, 1989. *Handbook of Suggested Practices for the Design and Installation of Ground-Water Monitoring Wells, EPA 600/4–89/034*. National Water Well Association, Dublin, OH and Environmental Monitoring Systems Laboratoty, Las Vegas, NV, 398 pp.

NGWA, 1998. *Manual of Water Well Construction Practices*, *2nd edition*. National Ground Water Association, Westerville, OH, pp.1–1 to 13–4.

NGWA, 1999. *Water Well Journal*, July. Westerville, OH, pp. 56–58.

NWWAA, 1984. *Drillers Training and Reference Manual*. National Water Well Association of Australia, St. Ives, New South Wales, 267 pp.

Parker, L.V., Hewitt, A.D., and Jenkins, T.F., 1990. Influence of Casing Materials on Trace-Level Chemicals in Ground Water. *Ground Water Monitoring Review*, Vol. 14, No. 2, pp. 130–141.

Precision sampling, 2006. www.precisionsampling.com

Ranney, T.A., and Parker, L.V., 1997. Comparison of Fiberglass And Other Polymeric Well Casings. Part I: Susceptibility to Degradation by Chemicals. *Ground Water Monitoring and Remediation*, Vol. 17, No. 1, pp. 97–103.

Reynolds, G.W., and Gillham, R.W., 1985. *Absorption Of Haloginated Organic Compounds by Polymer Materials Commonly Used in Ground-Water Monitors*. Proceedings of the Second Canadian/American Conference on Hydrogeology, Banff, Alberta, Canada, National Water Well Association, pp. 125–132.

Roscoe Moss, 1994. *Handbook of Ground Water Development*. John Wiley & Sons, New York, 493 pp.

Sara, M., 2006. Ground-Water Monitoring System Design. In: *Practical Handbook of Environmental Site Characterization and Ground-Water Monitoring*, D.M Neilsen (ed.). Taylor and Francis Group, Boca Raton, FL pp. 517–572.

Spellman, F., and Whiting, N., 1999. *Safety Engineering: Principles and Practices*, Government Institutes and ABS Group Company, Rockville, MD, 459 pp.

USGS, 1917. *The Divining Rod—A History of Water Witching*. U.S. Geological Survey Water Supply Paper No. 416, 59 pp.

Walton, W.C., 1962. *Selected Analytical Methods for Well and Aquifer Evaluation*. Illinois State Water Survey Bulletin 49, 81 pp.

Williams, E.B., 1981. Fundamental Concepts of Well Design, *Ground Water*, Vol. 19, No. 5, pp. 527–542.

This page intentionally left blank

Chapter

9

Pumping Tests

As a young person in high school, my friends and I would come to a stop at a red light, put the vehicle in park, open the doors, run around the vehicle, and then get back in before the light turned green. This silly activity was fun because of the chaotic flurry of confusion that took place, reminiscent of the Keystone cops, plus the bemused expressions of other drivers as they looked on. It was always a challenge to get everyone around the vehicle and back in so that traffic was not held up. This activity will be referred to as a wacky fire drill (WFD). The first few times one runs a pumping test, the chaotic flurry at the beginning of the test of synchronizing watches, obtaining manual readings every few tens of seconds, the management of a fairly long list of equipment, and the stress of being responsible to obtain meaningful data is much like a WFD.

Example 9.1 I can still remember my first experience in being involved with a pumping test back in the fall of 1980 in northern Wyoming. My job was to continue manual readings for the night shift and to radio in if there was trouble. At about 2 o'clock in the morning the pump started making a terrible noise and the radio had gone faint because the vehicle battery had run low from not restarting the engine to keep things charged up. I felt foolish and scared and wondered how long it would be before anyone found me. To my rescue came the hydrology supervisor, Jim Bowlby, who immediately realized the water level had drawn down to the pump intake, creating a potential cavitation situation. He also helped give me a jump-start to get the truck and the much needed heater going. We attempted to salvage the test, but the data were messed up. This was a WFD gone bad.

9.1 Why Pumping Tests?

There are many methods of obtaining hydraulic information from aquifers, but perhaps the most common and best is the pumping test or aquifer test. Please note that there is an industry-wide error in referring

Copyright © 2008, 2001 by The McGraw-Hill Companies, Inc. Click here for terms of use.

to these as "pump tests." Hopefully it will be the aquifer we are testing, *not* the pump. Without an estimate of the hydraulic properties of an aquifer, calculations of groundwater movement and contaminant transport cannot be performed with any level of confidence. Saying that pumping tests are the best method of obtaining hydraulic information presumes that the test has been designed properly and was run for an adequate period of time. This also includes setting the pump discharge at a sufficient rate to stress the aquifer and supposes that there is at least one observation well to obtain storativity values. By stressing the aquifer for a sufficient amount of time, a glimpse of the aquifer properties away from the pumping well can be obtained, including boundary conditions that may affect groundwater flow. Although less expensive point estimates can be obtained from specific capacity tests and slug tests, the insights gained from pumping tests can be far more meaningful. This, of course, depends on the objectives of the study. (Specific capacity tests and the evaluation of aquifer-test data are discussed in Chapter 10, and the field methodologies for slug testing and analysis are presented in Chapter 11).

Perhaps the most important reason for conducting an aquifer test is to obtain a picture of the general hydraulic properties of an aquifer. Well-hydraulic theory assumes that an aquifer is homogeneous and isotropic (Chapter 10), when in fact this is rarely the case. Another assumption that is often violated is that there are no boundary conditions, meaning that the aquifer is of infinite areal extent. To satisfy the condition of horizontal radial flow, the aquifer is supposed to be screened over the entire thickness of the aquifer. Geologic conditions and well completion costs often make this condition not practical. How can a pumping test be designed that will yield meaningful results? One that perhaps would reveal spatial variations in aquifer properties and the effects of boundary conditions either perceived or not? This is the topic of the next section.

9.2 Pumping-Test Design

Pumping-test design begins with establishing the objectives and conditions of the study. The objectives are usually to obtain hydraulic information; however, conditions may also correspond to circumstances that may exist in the field, for example:

- Is the pumping test being conducted near or within a contaminant plume? If so, where will the discharge water be stored and treated and how much will be produced? Or will the pumping test affect the configuration of a plume?
- Will pumping affect or impact other existing senior water users' wells?

- Will pumping occur near a construction site or downtown area where dewatered sediments may result in compaction and foundation stabilization problems?
- What size of pump will be necessary to adequately stress the aquifer? Will a sampling pump be adequate, or will a submersible or even a turbine pump be required? Think of equipment and costs.
- Is this well being tested for production purposes, such as for irrigation or public water supply, that would require long-term pumping? What impacts, if any, are expected to occur, and what additional personnel and equipment might be necessary?
- Is the aquifer being tested to check the requirements for a subdivision, or to perform dewatering estimates at a construction site or mining property?
- Is the test going to take place near a recharge or discharge area (Chapter 5)? Are vertical gradients or other components of groundwater flow important?
- Are multiple aquifers being affected?
- What are the potential boundary conditions in the area? Are there streams, faults, constructed barriers, or confining layers or discontinuities that may affect the shape of the cone of depression (Chapter 10)?

Sometimes there aren't any special conditions; it's just that a pumping test is needed to estimate the hydraulic properties for use in calculations for groundwater flow or for a groundwater-flow model or transport model. Maybe initial estimates are needed to estimate distance-drawdown relationships.

Geologic conditions

When designing a pumping test, it is imperative that a general background of the geology be known. Will this be a porous media test in unconsolidated or lithified sediments? What depositional environments are probably represented? Will this take place in fractured rock or karst conditions? Is this a dual or triple porosity system? For a general presentation on geologic conditions, see Chapter 2 and Chapter 13 for karst conditions.

General geologic information can be obtained from other wells drilled in the area. State agencies have well logs that are accessible by Section, Township, and Range (Chapter 1). For larger production wells, a small diameter pilot hole is advisable to anticipate the well construction design. In a monitoring-well field, it may be that all wells will basically be constructed the same. The pipe and screen will be fairly uniform. Details on monitoring-well construction and design are found in Chapter 8.

For the purposes of pumping tests and the analysis of results, the following geologic conditions are helpful to notice in advance of the pumping test:

- Do the sediments fine upward or downward? This may affect the rate of vertical contribution. Layered sediments will have an effect on the results in terms of potential delayed yield or other sources of recharge. These may also constrain the lateral contribution of water from course-grained sediments that may be confined or semiconfined above and below. This is especially important in determining the saturated thickness contributing water to partially penetrating wells during the pumping test (Chapter 10). To check the vertical connection of sediments, wells completed at various depths will be needed to observe any changes.
- What is the potential for lateral boundary affects? Are there surface water bodies, such as lakes, streams or ponds, that are hydraulically connected with the groundwater system (Chapter 6)? Or, could the aquifer be expected to thin or thicken or become coarser- or finer-grained in a particular direction? Are either recharge or barrier conditions anticipated? If so, it is advisable to locate an observation well away from the pumping well in the direction of anticipated impacts.
- Is the aquifer of low or high transmissivity? This will affect the spacing and distance of the observation wells. Cones of depression are steep in low-transmissivity aquifers and do not extend as far as in higher-transmissivity sediments.
- In fractured systems, what are the orientations of the major fracture zones? Observation wells drilled nearby may show little or no response if not connected to the main system. This is especially important in a forced gradient tracer test if a nearby monitoring well is to be used as the source well (Chapters 14 and 15).

Example 9.2 During the 1992 Montana Tech field camp a pumping-test site was selected with five observation wells (Figure 9.1). The students were to perform a 24-h pumping test and interpret the results of a preexisting site. The pumping well was sounded to check for depth and was found to be silted in within the entire 10-ft screened zone. The slot size of the screened interval during well completion was too coarse. Through bailing, the pumping well was cleaned out. Each of the three existing observation wells was also cleaned out, and two new ones were drilled and completed. The configuration of the aquifer test is shown in Figure 9.2. One thing that surprised the students was the rapid response of an observation well located much farther away than wells completed closer, until they considered the geologic conditions. After some thought, they realized that the completion depth and lithologies of the more distant well were very similar to the pumping well (Figure 9.3). Wells completed closer to the pumping well were completed more shallowly and screened in finer-grained sediments. Partial penetration effects were also a factor (Chapter 10).

Figure 9.1 Pumping test with five observation wells.

Observation well Ob-3 in Figures 9.2 and 9.3 responded sooner than Ob-2. Both the pumping well and northernmost observation well were completed at approximately 30 to 35 ft depths, while Ob-2 was only completed at 12 ft in finer-grained sediments. In time, all wells were impacted by drawdown. A schematic cross section is shown in Figure 9.3.

During a pumping test, the cone of depression expands in response to the requirements of the pump and the discharge constrictions.

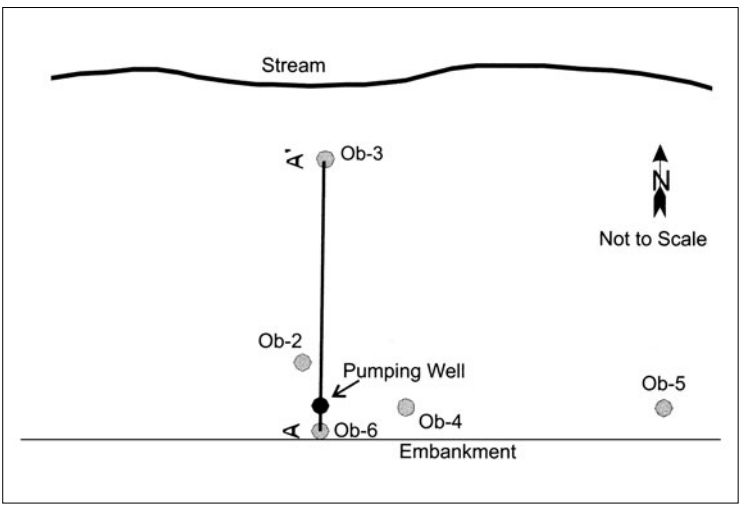

Figure 9.2 1992 Field camp pumping test layout. (Wells Ob-3 and Ob-5 are about 49 and 53 ft, respectively, from the pumping well.)

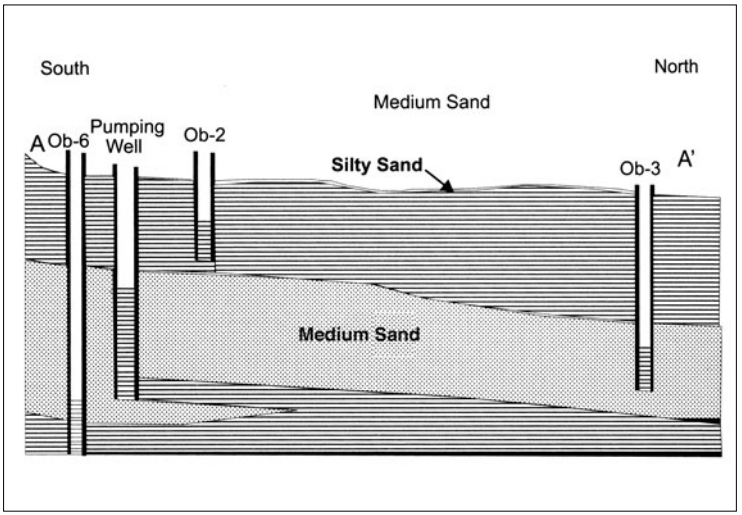

Figure 9.3 Cross-section view of Figure 9.2, from south to north.

Observation wells detect the aquifer response in the direction of the expanding cone. If a boundary exists, the observation well closest to the boundary will pick up the change reflected in the time/drawdown data first (Chapter 10). With more than one observation well picking up the same boundary, the distance to the boundary can be estimated (Heath and Trainer 1968).

Distance-depth requirements of observation wells

The depth of completion of observation wells should reflect the conditions of the aquifer to be developed or the hydraulic properties of the aquifer where calculations will be applied for the intended purpose of the study. If there are additional objectives, such as vertical connections or gradients between shallow and deep systems, then nested pairs are desirable.

The distance of observation wells from the pumping well should also reflect a basic understanding of the geologic conditions already mentioned above and whether the aquifer is confined or unconfined. Confined aquifers can have observation points literally miles (kilometers) away. It will also be a function of the time of pumping. Short-duration tests may require that monitoring wells be placed closer than those being tested at longer pumping times. If delayed yield is expected in the time/drawdown response curve, an observation well close enough to the pumping well to observe this will be necessary. This is usually on the order

of 10 ft (3 m) or so, but distances in excess of hundreds of feet have been observed by the author. Once again it depends on the duration of pumping and aquifer properties.

Example 9.3 In the Little Bitterroot Valley in northwestern Montana is an elongated N-NW trending intermontane basin (Figure 9.4). Before homesteaders arrived in the valley, water was only utilized at springs (Donovan 1985). The first developable water came from the Lone Pine aquifer.

Lone Pine aquifer consists of very permeable unconsolidated glaciofluvial gravels and sands of early Pleistocene age. These are overlain by about 200 ft (61 m) of silts and clays from Pleistocene Lake Missoula. A shallow surficial aquifer consisting of Pleistocene sand and gravel deposits and Holocene fluvial terrace gravels sits on top of the lacustrine sediments (Donovan 1985).

Drilling was accomplished through a jetting technique that cuts through the soft lacustrine deposits but was only able to penetrate a few feet into the Lone Pine gravels. The pressure head within the aquifer was sufficient to cause flowing artesian wells, with yields in excess of 1,000 gpm (3,790 L/min). The main use of developed water is for irrigation of approximately 3,000 to 3,500 acres, although some is used for domestic and stock watering purposes (Donovan 1983). Controversy arose over declines in flow from an increase in the number of wells. Additionally, the valley has warm water 25 to 53°C over approximately 600 acres of the Camp Aqua area (Figure 9.4). This resulted in problems with irrigation applications and with bath houses being developed (Donovan 1985).

Pumping tests were conducted during 1980–1983 to determine the aquifer characteristics of the Lone Pine aquifer. Measurable drawdown was observed in observation wells as far away as 9 mi (14 km)!

Ideally, any pumping test should have (at least) two observation wells. The two wells should be placed at different radial distances from the pumping well and at different compass orientations. The closer well would detect near-well conditions and be sure to pick up drawdown, and the other well would be helpful in evaluating the distance the cone of depression expands. It is also extremely important to have an understanding of the direction of groundwater flow. Drawdown will be detected in wells up gradient at farther distances than wells placed down gradient (Fetter 1993). In fact, wells down gradient may be out of the cone of influence of the radius of depression regardless of how long pumping takes place (Figure 9.5).

Figure 9.5 represents six cones of depression from pumping wells over the same duration. In each case there are two observation wells with one placed close to the pumping well and one located farther away. However, in cases C, E, and F, one or more wells do not detect drawdown at a given time t. It appears that the duration of pumping would have little effect on whether drawdown would be detected or not. In case B,

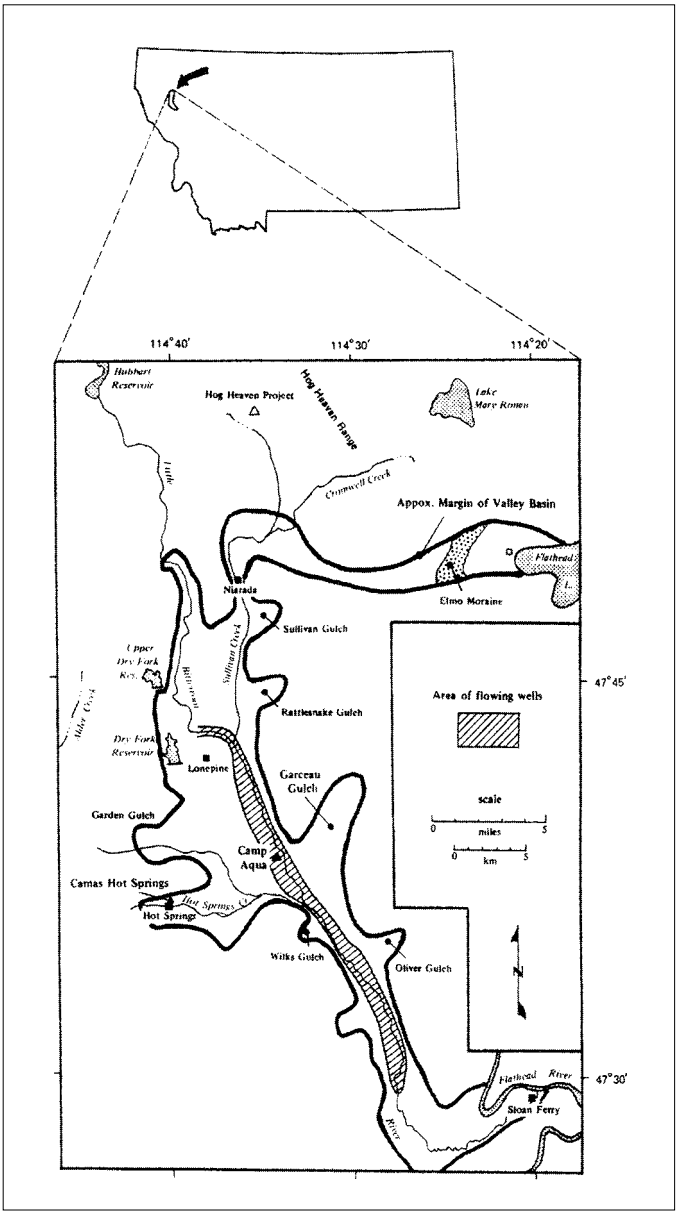

Figure 9.4 Location map of the Little Bitterroot Valley, northwestern Montana. [*Reprinted with permission from the MBMG (1985).*]

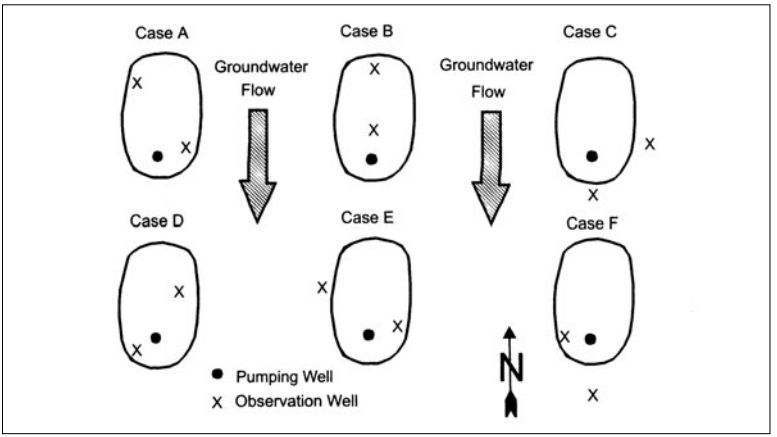

Figure 9.5 Configurations of pumping and observation wells and cones of depression with direction of groundwater flow at some time t. (Cases A, B, and D will detect drawdown in all wells, and Cases C, E, and F will not detect drawdown in one or more wells at time t.)

although both wells would detect drawdown, little information would be gained as to changes occurring east or west of the line of wells. There are not many advantages to a design like this. A schematic cross section of case B is shown in Figure 9.6 to illustrate the concept of a sloping water table and its respective cone of depression shape. This concept is significant to groundwater capture zones and remediation design. One of the assumptions in well hydraulic theory is that the potentiometric surface is flat.

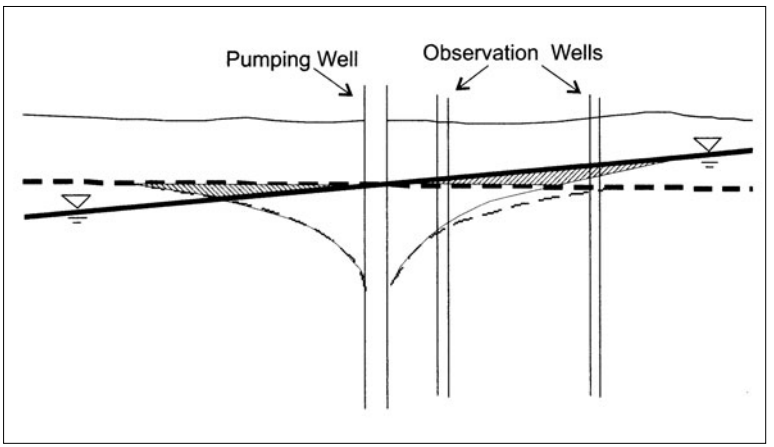

Figure 9.6 Cross section showing the difference between a cone of depression in a flat water table surface versus a sloping one in a capture zone scenario. (Note the asymmetry in the sloping cone.)

In Figure 9.6 the flat water table is indicated by a flat dashed line and the sloping surface is exaggerated for emphasis. A sloping water table yields an asymmetrical cone of depression. This is important in a capture-zone analysis. As one can see, this is also an important component in pumping-test design.

9.3 Step-Drawdown Tests

In order for pumping tests to effectively stress the aquifer, a proper pumping rate must be established. Even though the wells are properly placed and developed, if the pumping rate is too low, a small cone of depression will result and the drawdown in observation wells may not be detected. Conversely, if pumping rates are too high, then the test will not run very long because the pumping level will reach the pump, possibly causing cavitation. Another cause of cavitation occurs when the suction pipe is too small a diameter, producing turbulence and creating air bubbles. This is not a problem with submersible pumps unless the pumping level has reached the pump.

The procedure of changing pumping rates over a consistent time interval in a deliberate manner is known as a **step-drawdown test**. This is a single-well test where the initial pumping rate is lower than the maximum expected rate. After the drawdown stabilizes, then the rate is increased, or stepped up, to a higher rate for the same amount of time, usually 30 min to 2 h (Kruseman and de Ridder 1990). The key is to run each step for the same amount of time and to run at least three steps. This procedure is also done to check well performance. Step tests were first devised by Jacob (1947) to check what would happen to the drawdown if the pumping rate varied during a pumping test.

Well-hydraulics theory is based on the concept of laminar flow for groundwater. In the near vicinity of a well bore, velocities may increase to the point that turbulent conditions result. If the conditions are laminar, then the drawdown is proportional to the pumping rate (Q). If turbulence occurs, there are other well losses that also contribute resulting in a nonlinear relationship. Collectively these can be represented by the following relationship presented in Equation 9.1 (Roscoe Moss 1990).

$$s = ds + ds' + ds'' + ds''' \tag{9.1}$$

where s = total drawdown measured in the pumping well
ds = head loss in the aquifer (formation loss)
ds' = head loss in the damage zone (skin effect)
ds'' = head loss in filter pack
ds''' = well loss from water entering the screen

The total drawdown observed within a pumping well is the difference between the static water level and the pumping level, where the pumping

level is the level inside the well casing. The actual water level that exists outside of the casing varies according to a group of additional head losses that occur from other effects. Included are head losses that occur as water moves through the aquifer (*ds*), head losses as the groundwater encounters a skin effect or damage zone (*ds′*). The skin effect is a result of fine drill cuttings or films from fluids that remain on the borehole wall from drilling. Groundwater then passes through the filter pack material (*ds″*). Naturally developed wells may not have significant skin effects but will have the natural gravel packing materials. As groundwater enters the well screen and changes direction from horizontal to vertical flow toward the pump, additional wells losses take place (*ds‴*). A depiction of all these well losses is shown in Figure 9.7.

Well efficiency

Before continuing this is an appropriate place to present the idea of **well efficiency**. If the water level outside the casing matches the pumping level inside the casing, the well efficiency is said to be 100% efficient. This is one of the criteria assumed for aquifer hydraulic theory (Chapter 10). In reality the pumping level is usually much lower than the level outside the casing. The concept is illustrated in Figure 9.8 and defined in Equation 9.2, where: K represents the depth to the pumping level from static conditions and L represents the depth to the water level outside the casing from static conditions.

$$\% E = L/K \times 100\% \tag{9.2}$$

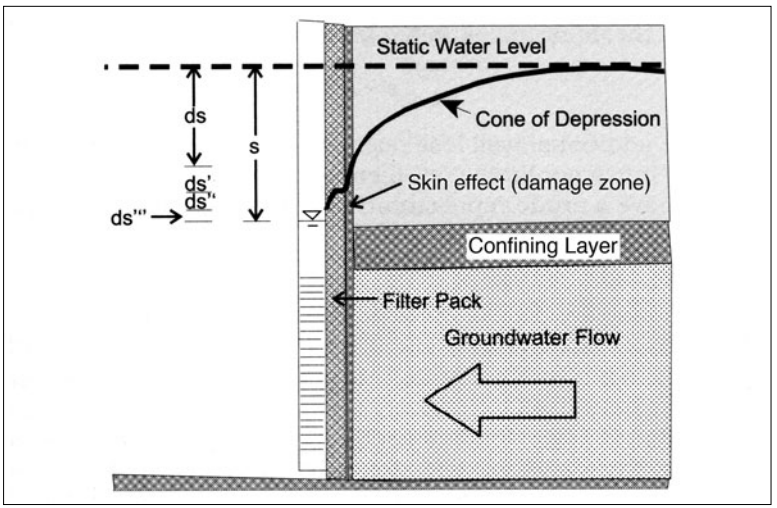

Figure 9.7 A schematic illustrating the individual contributing head losses to the total head loss observed at the pumping level. [*Modified after JAWWA (1985).*]

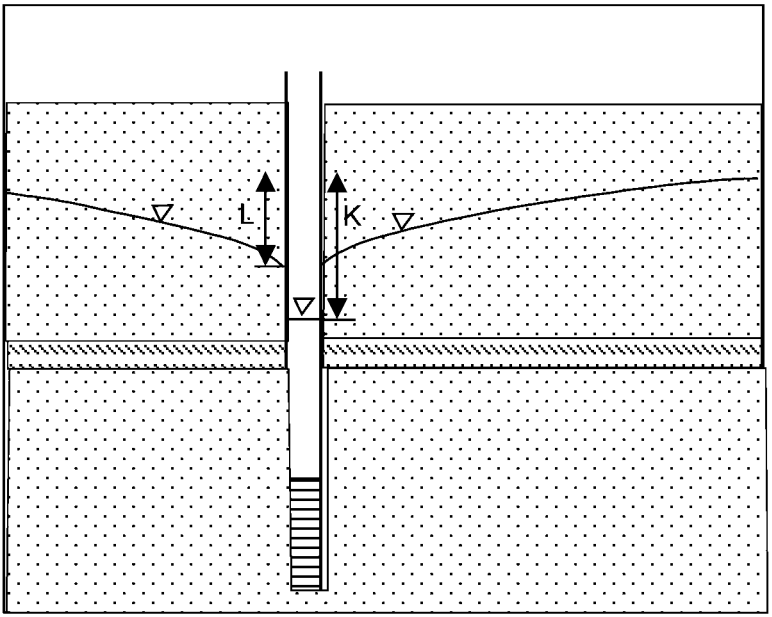

Figure 9.8 Concept of well efficiency, where K is the pumping level and L is the water level outside the casing and where all terms for % efficiency are presented in Equation 9.2.

Laminar versus turbulent flow

Laminar flow in a perfectly efficient well in a confined aquifer will yield the following relationship described as the modified nonequilibrium equation by Driscoll (1986):

$$B = \frac{264}{T} \log \left(\frac{0.3Tt}{r^2 S} \right) \tag{9.3}$$

where Q = pumping rate (gal/min)
T = transmissivity (gal/day · ft)
t = time (day)
r = radial distance of observation point (ft)
S = storativity (dimensionless)

This is also okay for unconfined aquifers if the drawdown (s) is small (the saturated thickness is within 90% of the original thickness) relative to the saturated thickness (b). The next step is to represent the laminar term by (B).

$$s = \frac{264Q}{T} \log \left(\frac{0.3Tt}{r^2 S} \right) \tag{9.4}$$

This yields the following simple relationship:

$$s = BQ \tag{9.5}$$

If all of the additional well loss terms shown in Equation 9.1 are combined together into a nonlinear turbulence factor (C) and added to the laminar term, we have a crude representation of the total drawdown (Equation 9.6).

$$s = BQ + CQ^2 \tag{9.6}$$

A more rigorous analysis of these processes and how they can be solved is presented by Driscoll (1986) and Kraseman and de Ridder (1990). A method on how to interpret variable-rate pumping test is also described by Birsoy and Summers (1980). However, a more simplified approach was presented by Walton (1970), which is useful for field approximations of maximum pumping rates and for selecting pumps. Walton (1970) provides a procedure where the turbulence factor (C) can be estimated from a step-drawdown test (Figure 9.9). The process involves conducting a step-drawdown test with successive increases in Q and plotting the results on a time-drawdown graph (Cooper-Jacob plot, Chapter 10). The first step should be within about 75% of the targeted Q followed by increases in Q on the order of 15 to 20%. Each step appears as a straight-line segment followed by a marked drop in drawdown between steps (Example 9.4b). Initially, during laminar flow, the slopes of the segments are approximately the same. As well efficiencies decrease and turbulence effects increase, the slopes of the straight-line segments will steepen. A rough estimate of well efficiency can be determined, and an appropriate maximum pumping rate can be estimated.

The turbulence factor can be approximated by:

$$C \approx \frac{\left(\frac{\Delta S_n}{\Delta Q_n}\right) - \left(\frac{\Delta S_{n-1}}{\Delta Q_{n-1}}\right)}{\Delta Q_n + \Delta Q_{n-1}} \tag{9.7}$$

where C = turbulence factor, in ft/(ft^3/s)^2
Δs_n = the change in drawdown from step n 1 to n, in ft
ΔQ_n = the change in pumping rate from step n 1 to n, in ft^3/s

Values of C also provide a qualitative measure of well efficiency. Walton (1970) gives the following groupings in Table 9.1.

The methodology will be illustrated with two examples: one from Walton (1970) with an efficient high-yield irrigation well followed by a bad example of how a step test should be done. The second example is useful in trying to make sense out of some actual field data, when the C-values don't make sense.

TABLE 9.1 Qualitative Values for Turbulence Factor C, in ft/(ft^3/s)^2 [From Walton (1970)]

Turbulence factors C	Comments
<5	Great
5–10	Good
10–40	Fair to poor
>40	Bad

Example 9.4a A 24-in (0.61-m) diameter irrigation well was tested and the data are summarized in Table 9.2.

From Equation 9.7 the respective C values are determined.

$$C_{1,2} \approx \frac{\left(\frac{1.59 \text{ ft}}{0.62 \text{ ft}^3/\text{s}}\right) - \left(\frac{5.40 \text{ ft}}{2.22 \text{ ft}^3/\text{s}}\right)}{2.22 \text{ ft}^3/\text{s} + 0.62 \text{ ft}^3/\text{s}} = 0.046 \text{ ft}/(\text{ft}^3/\text{s})^2$$

$$C_{2,3} \approx \frac{\left(\frac{0.72 \text{ ft}}{0.27 \text{ ft}^3/\text{s}}\right) - \left(\frac{1.59 \text{ ft}}{0.62 \text{ ft}^3/\text{s}}\right)}{0.62 \text{ ft}^3/\text{s} + 0.27 \text{ ft}^3/\text{s}} = 0.115 \text{ ft}/(\text{ft}^3/\text{s})^2$$

By using Equation 9.6 , one can determine the well losses from the turbulent factor at 1280 gpm (0.081 m^3/s) and 1,400 gpm (0.088 m^3/s), respectively.

$$s_{1280} = 0.046 \text{ ft}/(\text{ft}^3/\text{s})^2 \, (2.84 \, (\text{ft}^3/\text{s}))^2 = 0.37 \text{ ft}$$

$$s_{1400} = 0.115 \text{ ft}/(\text{ft}^3/\text{s})^2 \, (3.12 \, (\text{ft}^3/\text{s}))^2 = 1.12 \text{ ft}$$

The relative % losses can now be calculated:

$$\%\ \text{loss}_{1280} = 0.37 \text{ ft}/(5.4 \text{ ft} + 1.59 \text{ ft}) \times 100\% = 5.3\% \text{ very efficient!}$$

$$\%\ \text{loss}_{1400} = 1.12 \text{ ft}/(5.4 \text{ ft} + 1.59 \text{ ft} + 0.72 \text{ ft}) = 14.5\% \text{ still efficient}$$

At 1,400 gpm (0.088 m^3/sec), the well is still approximately 85% efficient.

Example 9.4b Near Three Forks Montana an irrigation well was drilled and completed and the drillers wanted to know what pumping rate to use for the

TABLE 9.2 Step-Drawdown Data from a 24-in Irrigation well [From Walton (1970)]

Step	Q (gpm)	ΔQ (gpm)	ΔQ (ft^3/sec)	Δs (ft)
1	1,000	1,000	2.22	5.40
2	1,280	280	0.62	1.59
3	1,400	120	0.27	0.72

constant-discharge test. They were optimistic and felt the well could yield 500 gpm (31.6 L/s). I suggested doing a step-drawdown test, starting near 200 gpm (12.6 L/s) and increasing the pumping rate approximately 50 gpm (3.2 L/sec) for the next five steps and each step be run for 30 to 45 min. There was approximately 200 ft of available drawdown. When I arrived the day after the step test the following data were given to me (Table 9.3).

As you can see the rates were variable and not run for the same length of time. The data were plotted so the drawdown response per step could be evaluated. It can be noted from Table 9.3 and Figure 9.10 the data stabilized after each step until the pumping rate was increased to 500 gpm (31.6 L/s). It is apparent from the data that 400 gpm (25.2 L/s) would be appropriate for the constant duration pumping test and the starting rate should have been 250 gpm (15.8 L/s). The constant-rate pumping test was began at 450 gpm (28.4 L/s) and had to be "valved" back to 375 gpm (23.7 L/s) after 2 h for the duration of the 72-h test. It was evident from the constant-discharge test that the step-discharge test was providing reasonable guidance to what the starting pumping rate should have been.

It is not always necessary to conduct a formal step-drawdown test prior to performing a pumping test. However, it is very helpful particularly if one is sizing a pump for production purposes and wishes to make a purchase. After one gains some experience, the appropriate pumping-discharge rates for a constant-discharge pumping test can be

TABLE 9.3 Step Test Data from the Jones Irrigation Well, Three Forks, Montana

Q in gpm	Time, min	Drawdown, ft	Q in gpm	Time, min	Drawdown, ft
170	1	60.78	400	55	126.61
170	2	65.4	400	60	130.08
170	3	65.4	370	65	130.08
170	4	65.4	370	70	130.08
170	5	65.4	370	80	130.08
250	6	79.26	370	90	130.08
250	7	81.57	500	91	150.87
250	8	83.88	500	92	162.42
250	9	83.88	500	93	167.04
250	10	83.88	500	95	171.66
250	15	83.88	500	98	173.97
250	20	86.19	500	99	179.75
250	25	88.5	500	100	178.59
250	30	88.5	480	105	179.75
250	35	88.5	480	110	180.9
250	40	88.5	480	120	181.48
250	45	88.5	480	125	182.05
250	50	88.5	480	135	183.21
400	51	106.98	480	145	184.94
400	52	111.6	480	155	185.52
400	53	116.22	480	165	186.65
400	54	123.15	480	175	187.25

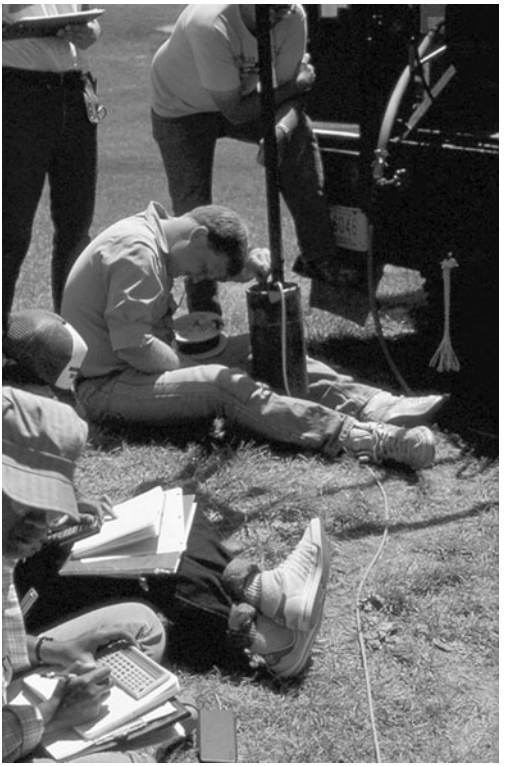

Figure 9.9 Students conducting a step-drawdown test.

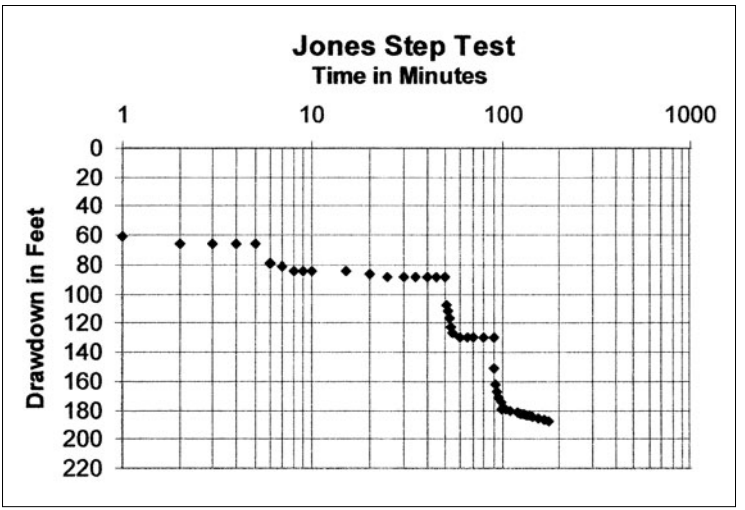

Figure 9.10 Step-drawdown test with four steps conducted on an irrigation well near Three Forks Montana. The step from 170 gpm (10.7 L/s) to 250 (15.8 L/s) is very subtle.

estimated by observing the drawdown in the pumping well after several minutes. Control of the discharge can be made over a fairly good range by constricting the outflow. However, one must start with a pump size that is within the appropriate range.

9.4 Setting Up and Running a Pumping Test

Setting up a pumping test can be frustrating if something is left off the equipment list and one must retrieve something back at the office. This section discusses the typical equipment that one should bring to have a successful experience. Discussion of the pitfalls that may occur are also presented. A discussion of the information that should be recorded in field books is given in Chapter 1.

The following is a list of equipment needed for a pumping test (items to bring are indicated in italics):

- *Power supply* (usually a generator, equipped with outlets that will allow the pump control box to be plugged in).
- *Extra fuel cans* for generator.
- *Control box* and pump.
- *Data logger*—for storing data and user's manual.
- *Transducers* (or well sentinels)—anticipate the drawdown expected in each well and have a transducer or well sentinel within range. Don't forget the *jumper cables* that connect the transducer to the data logger.
- *E-tapes*—for taking backup readings and to check conditions prior to setting up the test.
- *Laptop computer* or *field printer* with extra paper to view and plot the data *in the field*, with a flash drive as a backup.
- *Discharge system*—this may consist of a *garden hose* for small discharge rates or *riser pipe*, *elbows,* and *connectors* to convey the discharge away from the site. A means of measuring discharge is needed, either a *flow meter*, or a *calibrated container* (buckets) and a *stopwatch*. An in-line flow constrictor, such as a *gate valve* (preferred) or ball valve to put back pressure on the pump and control the discharge. *Teflon tape* may be needed for the threads when connecting the discharge lines and riser pipe.
- *Pipe wrenches*—to construct the discharge line (aluminum ones are much lighter).
- *Duct tape* (the most versatile tool in the box).
- *Electrical tape*.
- *Miscellaneous tools* (screwdrivers, wrenches, electrical tester, etc.).

- *Field books, field forms*, and *pens or pencils* (with refills).
- *Well logs* and *field map*.
- A way to plot the data for each observation well. (Data should always be plotted in the field to observe data behavior.)
- *Kitchen timers* (for timing readings).
- *Keys* (for gate locks or well access).
- *Shovel* and *rope*.
- Miscellaneous field equipment (such as water-quality equipment to check changes in pH, temperature, or specific conductivity).
- Hat, sunscreen, bug spray, and personal items.
- Rain clothing, tarp, and/or tent.

Power supply and pumps

In considering the appropriate power supply for a pumping test, one must have a knowledge of the pump and electrical feed requirements. Because many pumping tests are remote, a generator is often used, Buying the cheapest generator may be a big mistake. To run a small sampling pump system, it is necessary to provide a steady feed of voltage. Cheaper units will often sputter and surge. Unless the power feed is steady, trying to use these sensitive sampling pump systems will be a problem. Good results for small pumps have been obtained from Honda generators (Figure 9.11).

Figure 9.11 Pumping test conducted with a steady feed Honda generator.

These generators run smoothly and are relatively quiet. Some manufacturers overrate their products, so it is necessary to make sure there is sufficient capacity to start and run a pump. Other pumping systems may have their own recommended generator systems, so one should consult the user's manual.

In starting a generator, particularly if it has sat idle for several months, it may be necessary to activate a warmup switch for 15 to 30 s before switching the generator on. Changing the oil once a year is also a good idea, regardless of how little it may have been used. When the oil level gets low, many generators will shut down. It has been the author's experience, when the oil level has not been checked and is low, that the generator will make a couple of changes in sound (hiccups) from the normal purr of the engine approximately 1 h before it suddenly sputters and stops. Newer generators have a safety feature that shuts the engine off when the oil level is low.

Generators may require diesel or unleaded gasoline. No particular preference is recommended. Another maintenance item is the battery. It may be that everything else is working fine, but the battery cables are corroded. Sometimes after cleaning, one can give the generator a jump start, and then during the pumping test the battery will become charged (Figure 9.12). It is helpful to test the equipment before taking it out into the field.

Generators are usually distinguished by the number of kilowatts they are capable of. Pumps require a boost of electrical power to get started. A general rule of thumb is: A *kilowatt is required for every horse power* (*hp*). This is not entirely true, but will get one in the ballpark.

Figure 9.12 Jump-starting a generator battery.

For example, a 20-kW generator might get a 25-hp submersible pump started, but would require 220 V and 3-phase power. A 25-hp pump may need a 440-volt source. As another example, one driller was using a 150-kW generator for a 75 hp pump at 440 V producing 500 gpm (31.6 L/s). He commented that the generator could probably keep a 100 hp submersible pump going, but he wasn't sure whether it would start one. This is part of knowing what your electrical feed requirements are. Submersible pumps are wired to control boxes that are then plugged into the generators with 110-, 220-, or 440-V outlets. These pumps also come with quite a range of hp and electrical requirements, such as how many phases and amperage.

Smaller pumps (up to 1 hp) are usually single phase and have simple wiring requirements (Figure 9.13). From 1.5-hp on, submersible pumps may require 3-phase configurations. *Unless you are very adept at electrical wiring, this should be done by a professional.* This can cause all sorts of problems, such as the pump impellers going the wrong way or causing damage to the pump. The higher the horsepower rating, the greater the voltage needed. For example, in the 10- to 20-hp range, the electrical configurations may require a shift from 220 to 440 V. Pumps requiring 440 volts will yield hundreds of gpm (thousands of m^3/day) discharge range. At this level, it may be advisable to use a turbine pump system (Figure 9.14).

Example 9.5 A new 1-hp pump was purchased for use during a field camp. The wiring was done on the tailgate of a pickup truck. The pumping test was set up, and no water would come out. The pump was retrieved and placed in

Figure 9.13 Wiring a small 1-hp pump in the field.

Figure 9.14 Turbine pump yielding 375 gpm.

a 55-gal drum to test and see if it could pump water. It was determined that the wiring was done such that the impellers turned the wrong way. Once the wires were switched, the pump worked properly. Testing the pump in a drum is a quick way to see if the wiring is correct.

On another occasion, a sampling pump would not work. The impellers were seized up from sand (it is not a good idea to use a sampling pump for well development!) In this case, the pump impellers were cleaned and then put back in upside down. Again no water would come out and the pump got warm. After a careful inspection and comparison to diagrams in the user's manual, the impellers were placed properly and the pump worked once again (Figure 9.15).

Figure 9.15 Fixing the impellers on a small sampling pump.

The wire to the pump is usually spooled on a drum. The pump and wire can be lowered down the well if a broom handle or something like it is placed through the drum for unspooling. Pumps can be very heavy, and a security cable is recommended for retrieval in case it becomes hard to maneuver (Figures 9.16 and 9.17). For a sampling pump, the riser pipe or hose is already attached to the pump. In a submersible pump, lengths of riser pipe must be fitted into the top of the pump, extending upward. Each piece should be tightened with wrenches, with Teflon tape wrapped reverse style on the threading so it won't bunch up. Once the appropriate pumping depth is achieved, a 90° elbow fitting is needed to extend the discharge line away from the test site, preferably beyond the expected extent of the cone of depression or to a drain, if available (Figure 9.18).

Some pumps must be primed or have a chamber filled with water so they will produce water (Figure 9.19). This brings up a topic known as net positive suction head (NPSH). On the suction side of a pump, the NPSH is determined by subtracting the negative pressures (suction lift, friction loss, and vapor pressure) from the positive pressures (a function

Figure 9.16 Installing a 5-hp pump, with a security cable attached to prevent loss down the well.

Figure 9.17 Hoisting a 50-hp submersible pump.

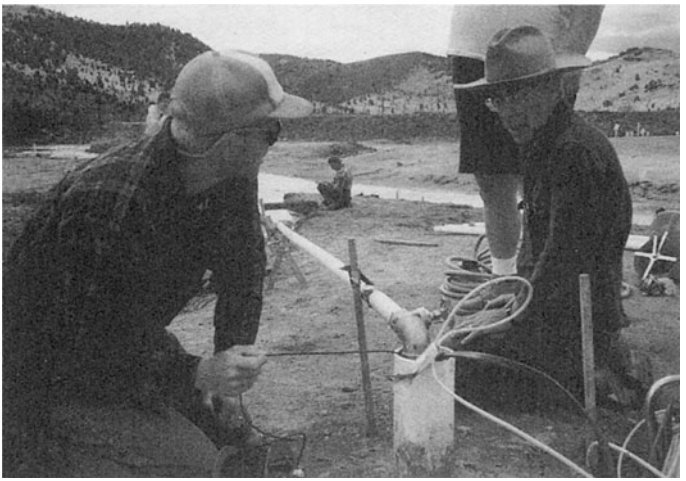

Figure 9.18 Using a 90° elbow on a discharge line directed away from the well.

Figure 9.19 Sump pump requiring priming before successful function.

of atmospheric pressure) (Figure 9.20). The atmospheric pressure is a function of altitude (Table 9.4). If the distance between the intake and the pump chamber is too great, the pump will never produce water, no matter how large the motor is. The vapor pressure requirement is not needed for temperatures greater than 60°F (Jacuzzi 1992). The pump design varies by manufacturer.

Data loggers, transducers, and well sentinels

Data loggers and well sentinels are a vast improvement over manual methods, but can cause some fieldworkers to become complacent and careless. It is always a good idea to collect manual backup measurements.

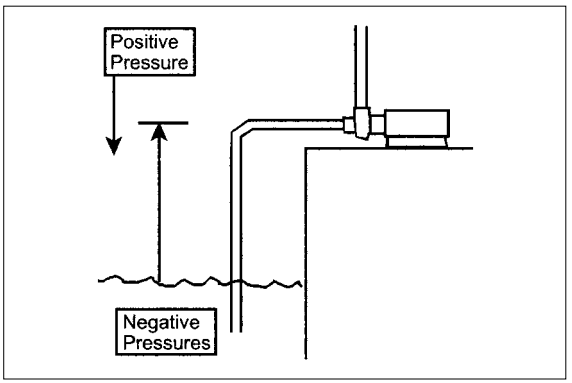

Figure 9.20 Schematic illustrating the concept of net positive suction head.

TABLE 9.4 Variation of Atmospheric Pressure as a Function of Altitude [From Jacuzzi (1992)]

Units	Sea level	2,000 ft	4,000 ft	6,000 ft	8,000 ft	10,000 ft	12,000 ft
lb/in^2	14.7	13.7	12.7	11.8	10.9	10.1	9.3
In · Hg	30.0	28.0	25.9	24.1	22.3	20.6	19.1
ft Water	34.0	31.7	29.4	27.3	25.2	23.4	21.6

One of the blessings of the data logger/transducer configuration is best illustrated by the effort required to collect single-well test data. In the "good old days," the trick was to finagle an E-tape down past the riser pipe and pump wiring in search of the pumping level. This would often result in hanging up the E-tape and missed data. The test would often have to be repeated several times with no guarantee of success.

Hydrogeologists should have access to data loggers and transducers or well sentinels to collect pumping-test data. Several companies have rental arrangements; however, if several pumping tests are expected to be run on a regular basis, it is wise to consider buying some equipment. The payback on the investment will take place in short order.

Transducers can come with a cable spool and extra cable lines greater than 350 ft (107 m) (Figure 9.21). The transducer or well sentinel should be lowered into the well within the depth range for the transducer and below the expected range of drawdown. The higher the transducer or well sentinel reading, the less sensitive (lower precision) they become. It doesn't make much sense to place a 100 psia transducer or well sentinel in a well that may only detect 1 ft (0.3 m) of drawdown. An example of typical ranges are shown

Figure 9.21 Transducers with cabled lines exceeding 300 ft (100 m).

TABLE 9.5 Transducer Ranges in psi Referenced from Atmospheric Pressure

Transducer range in psia	Range in ft	Range in m
5	11.5	3.5
10	23.1	7.0
15	34.6	10.6
20	46.2	14.1
30	69.3	21.1
50	115.5	35.2
100	231.0	70.4
200	462.0	140.7
300	693.0	211.1
400	924.0	281.4

in Table 9.5. Drawdown in the hundreds of feet range occur in mine shafts and large production wells. The principle here is to select a transducer or well sentinel based on water depth and the expected drawdown.

Once a transducer is lowered into a well, a loop (bite) greater than 1-in should be made to make sure that the cable's air line is not kinked. The cable should then be wrapped around the well casing one or more times and then secured in place with duct tape (Figure 9.22). The duct-tape loop may slip in hot weather, so a dowel or similar object can be placed to prevent kinking. The cable then is run to the data logger and connected. It is a good idea to lower the transducer down the well early in the setup phase to allow for stretching and straightening of the cable. The transducer in the pumping well should be attached tape with electrician's to the riser pipe or duct tape approximately 1 ft above the pump, with additional tape added every 5 ft (1.5 m) to the top of the well (Figure 9.23). If the cable must cross a road or a heavy traffic area, it is advisable to pass it under the road, if a culvert is available. Otherwise, two boards can be duct-taped to the road with the cable placed in a space between them, allowing for traffic to drive over the boards without impacting the cable directly.

The point of preventing a transducer cable from getting kinked is to enable any changes in barometric pressure to be sensed by the transducer. The cable is hollow and air pressure conditions are allowed to move freely through the line. Well sentinels on the other hand are self-contained and placed at depth down the well to sense changes in water level over time. If significant changes in barometric pressure are occurring at the surface, these will not be detected by the well sentinel. For this reason most manufacturers of well sentinel equipment also make "barologgers," whose purpose is to keep track of the barometric changes at the surface. Barologgers are placed in a protected place at the surface or a few feet down the well bore. The accompanying software will pull in the information from the well sentinel and the barologger and simultaneously adjust the data at a command prompt.

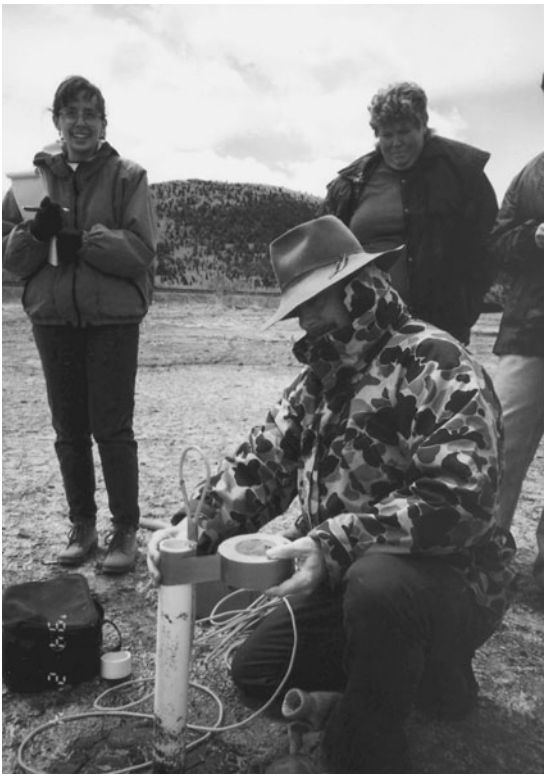

Figure 9.22 Transducer cable with greater than 1-in bite for airflow.

Well sentinels are communicated with via a cable with a USB connection to a laptop to facilitate the timing of when data are gathered and subsequently stopped. The parameters of the test are communicated through software to the sentinel unit including the option to synchronize with the time clock on the laptop computer. One must be careful to make sure the clock is current, for example with cell phone time.

Example 9.6 While performing a pumping test in southwestern Montana a client's production well was monitored while another pumping test was being conducted on a neighboring property. The question was whether the neighbor's well would impact the client's well. A starting time and synchronization was established with an older laptop with the appropriate software loaded. It was not noticed that the clock of the laptop was 4 years earlier than the existing time. Therefore, the well sentinel would not have started collecting data until 4 years hence from the date of the actual test! Fortunately manual readings had been taken before and during the test to confirm no impact had taken place. Without the manual readings the effort would have been completely wasted. This was also inspiration to retire the older laptop.

Figure 9.23 Taping transducer cable to a riser pipe in a pumping well.

Data loggers are usually capable of collecting data from multiple transducers. Each transducer needs to be registered and enabled. Transducer parameters, such as scale, offset, linearity, type, and ID number are required. The reference level is usually the last thing keyed in before starting the test. Extra care should be taken to ensure that the "jumper cables" are well connected to the data logger (please note that these are not the cables used to charge a dead vehicle battery). This can be checked by using the data logger to take a reading from the transducer. If "no signal" occurs or the reading is zero, check the connection and try again. The connections generally only work in one orientation. Look at the prongs of male and female connections to see if any wires may be bent. Many transducers have a strain gauge near the probe tip that has a screw on protective cap.

It is a good idea to unscrew the cap and make sure this area is clean. The following suggestions may explain why a transducer may be giving an improper signal or no signal at all:

- Check all connections.
- Check for cable damage—an unsecured cable can fall out of a truck and become damaged on the highway.
- Check the strain gauge end—strange field readings have been cleared up by unscrewing the end cap and washing the cap and strain gauge. This can happen if there is some muddy or silty material in the bottom of the well that is not cleaned off.
- Make sure the transducer is above the bottom of the well and free hanging.
- Some transducers have breather lines in their cables to sense changes in air pressure—transducer cables should have a loop of at least 1-in diameter, so that the cable does not become kinked. Kinked cables can result in strange readings. New transducers are vented to avoid this problem.
- The cable may be placed in water deeper than the range of the transducer—this will result in a reading of zero and may break the strain gauge.
- Check for damage to the probe—it may need to be shipped off to the manufacturer for recalibration.

Once the transducers are connected to the data logger and all the transducer information has been entered, it is time to set the reference level. This can be an elevation or an arbitrary point. It is *not* a good idea to use 0.0 as the reference level, since negative readings may occur. This does not bode well when plotting on log or semilog graphs (since negative log values are undefined). The user has the option of referencing all data from a positive downward or positive upward position. For example, top-of-casing (TOC) readings are referenced so that when water levels drop (like drawdown in a pumping test), the changes are recorded as positive downward. Surface referenced readings increase upward as they are often used in stage measurements to sense the increase in stage as levels rise. Readings can be set to log-cycle or linear-time scale. Usually after four log cycles have been recorded, a default linear scale is activated. Linear scales are useful for long-term monitoring or if readings for early-time details are not needed. Log-cycle scales allow one to obtain early-time data, which can capture the elastic response in unconfined aquifers (Chapter 11). Log cycles may have an interval sequence similar to those shown in Table 9.6.

In addition to pressure transducers, many companies provide additional probe types for collecting other kinds of data. For example, water-quality probes are available to collect pH, specific conductance, temperature, or specific ion data. Well sentinels often come with temperature, level, and

TABLE 9.6 Typical Log Configuration of Data-logger Readings

Log cycle	Time	Number of readings
1	0–2 s	20
2	2–20 s	20
3	20 s–2 min	20
4	2–20 min	20
4	20-memory limit	linear every 20 minutes

specific conductivity (TLC) capabilities. This can be helpful, along with the drawdown data, to detect sources of recharge or for other interpretations. Some self-contained units have multiple capabilities of level and water-quality data all in one. These can be programmed directly by attaching a cable to a laptop computer. Access to the data during the pumping test is also possible (Figure 9.24).

E-tapes

Electrical water-level meters or E-tapes have many uses at a pumping-test site. They are usually needed to take level measurements in all of the wells prior to lowering the transducers and the pump. They can be used to sound well depths for wells with missing well logs and even measure the distances between wells if a regular measuring tape is not available. One can determine the appropriate psia range for transducers

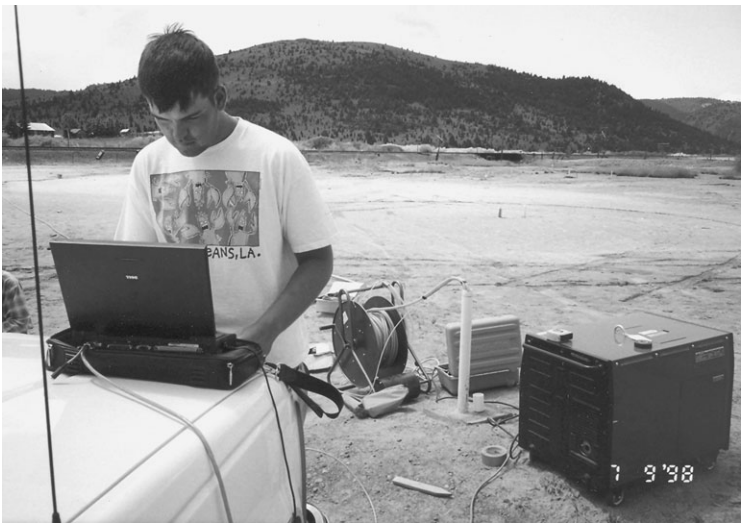

Figure 9.24 Evaluation of real-time data on a laptop computer.

from well logs and the depth to water. E-tapes are essential for backup readings. Backup readings are needed because they can "save" a test if the equipment malfunctions or the power supply unexpectedly shuts down (Example 9.6). E-tape measurements also help keep the field person focused and occupied. Kitchen timers are useful to alert the field person when the next reading should be taken. A discussion of E-tapes and their use and design is presented in Chapter 5.

Discharge system

The riser pipe provides a pathway for pump discharge. Once it reaches the well head and is connected with an elbow to convey the water away from the pumping well, it becomes the discharge line. The discharge line should extend far enough to not affect the cone of depression. Sometimes steady-state conditions are reached because the discharge line is too close to the pumping well. In this case, the pumped water recharges the aquifer by infiltrating back from the surface.

For smaller sampling pumps, the discharge line is essentially a garden hose. Additional hose can be attached to extend the line outward. Control of discharge can be made by attaching a spigot to the end of the hose. The spigot acts as a mini gate valve to control discharge. Pumps are designed to deliver a certain amount of flow per head loss. It is a good idea to have a pumping rate that is less than the maximum pump capacity. Back pressure can be placed on the pump by partially closing a gate valve or ball valve while maintaining a steady discharge rate. As drawdown continues during the test, the lift required by the pump may increase. Discharge can be maintained by opening the valve slightly. *There is much more control during this process with gate valves than with ball valves.*

One of the assumptions required for well hydraulic theory is that the discharge (Q) be constant (Chapter 10). One of the requirements of a pumping test is to configure the discharge system so that a constant discharge rate can be maintained. This requires frequent checks of pumping rates throughout the test. The first 15 minutes or so of the test are especially critical, until the drawdown stabilizes and valve adjustments are less frequent. For discharge rates up to 100 gpm (545 m^3/day) or so, a container and a stopwatch can be used. This can get the field person very wet if the container is too small. For higher discharges, a U.S. 5-gal (18.9-L) bucket will be too small. Just because the bucket is supposed to be 5 U.S. gallons (18.9 L), that doesn't mean that it is. From experience these have been observed to range from 4 to 5.5 gal (15.1 to 20.8 L). It is important to calibrate a bucket with a mark for every gallon, or some other desired volume, using a permanent marker. This way, there is some confidence in the readings. Time can be measured with a stopwatch or a watch with a second hand. The greater the discharge, the greater

TABLE 9.7 Reference of Time to Discharge Rates in gpm and L/s

Time to fill 5 gal in s	Discharge rate in gpm	Discharge rate in L/s	Time to fill 3 gal in s	Discharge rate in gpm	Discharge rate in L/s
2	150	9.47	1	180	11.36
3	100	6.31	2	90	5.68
4	75	4.73	3	60	3.79
5	60	3.79	4	45	2.84
6	50	3.16	5	36	2.27
7	42.9	2.71	6	30	1.89
8	37.5	2.37	7	25.7	1.62
9	33.3	2.10	8	22.5	1.42
10	30	1.89	9	20	1.26
12	25	1.58	10	18	1.14
14	21.4	1.35	12	15	0.95
16	18.8	1.19	14	12.9	0.81
18	16.7	1.05	16	11.3	0.71
20	15	0.95	18	10	0.63
22	13.6	0.86	20	8.2	0.52

the precision needed for time. Table 9.7 may be helpful in comparing time to particular volumes.

Another method to measure discharge is with an in-line flow meter. These are usually installed in the discharge line within 10 ft (3 m) or so of the pumping well. The flow meter is also placed between a control valve and the well (Figure 9.25). The control valve creates a back pressure

Figure 9.25 A discharge line for a pumping test equipped with an orifice weir (in the pipe) and an in-line flow meter with bubble read for flow. Notice the gate valve to the right allows for variable back pressure to maintain a constant discharge.

and fulfills the requirement of the pipe being full-flowing for readings to be accurate. In-line flow meters may have impellers that rotate to calculate a velocity and are calibrated to read a Q in gpm. They are accurate within a small percentage of the flow and are convenient because all you have to do is read the gauge.

For larger flow volumes, such as those from a high-capacity submersible or turbine pump, a different arrangement is often used. A circular orifice weir is fitted at least 6 ft from the gate valve within the discharge line (Driscoll 1986). An access nipple is fitted to the discharge line at midpipe, 2 ft (0.6 m) toward the gate valve from the orifice plate. To the nipple a manometer tube is attached that extends upward to be measured on a scale (Figure 9.26). The manometer measures the pressure (head) in the pipe and should be made of clear tubing so that its height can be observed next to a calibrated stick.

Duct tape

Duct tape is one of those essential items that is helpful in setting up a pumping test. Duct tape is used to attach transducers to the well casing. It can be used to hold braces together to support discharge lines, patch things together, and do a host of other jobs. Any serious user of duct tape should take a look at *The Duct Tape Book* by Berg and Nyberg (1995). As an example pertinent to hydrogeology work, consider Figures 9.27 and 9.28.

Setup procedure

Now that the essential equipment have been described, it may be useful to list the tasks generally associated with pumping tests. It is assumed

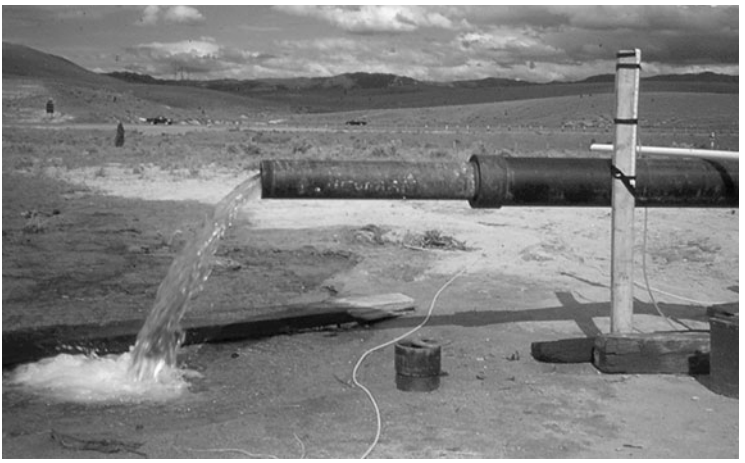

Figure 9.26 Manometer tube setup with circular orifice weir to measure flow.

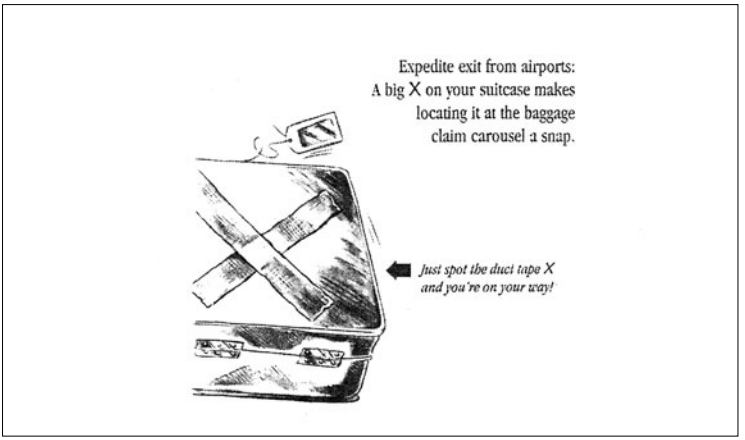

Figure 9.27 Hydrogeologists are always on the go. [*After Berg and Nyberg. Used with permission from Pfeifer-Hamilton Publishers (1995).*]

at this point that all observation wells have been drilled, completed, and developed, and permission to be on the property has been obtained. One should have a lamp or source of light that can be plugged into the generator for lighting and flashlights (with extra batteries) for taking manual readings during the night. Making the appropriate arrangements for food, supplies, and restroom facilities or designated areas will help make the time go smoother. A portable field table with chair and a tarp for inclement weather conditions are also recommended. Here is the list:

Figure 9.28 Duct fape holding a drill rig cab seat together.

1. Gather together the equipment listed at the beginning of this section. Obtain extra fuel.
2. Check the weather forecast and bring any essential clothing for the anticipated conditions.
3. Measure and record the water levels in all wells to be used in the test. Monitoring of wells for a few days prior to the test is helpful to determine if any regional trends are occurring (general decreases or increases in water levels).
4. If there are any nearby surface streams, establish the stage with a physical marker, so that it can serve as a gauging point should changes in stage occur.
5. Offload the equipment and begin placing the transducers or well sentinels in the wells and securing them in place with duct tape or clamps.
6. Place the pump and riser pipe in the well along with the transducer designated to measure levels in the pumping well. This transducer is needed to determine how close the pumping level is to the pump intake.
7. Attach and support the discharge line so that the discharge water is a suitable distance from the pumping well (Figure 9.29). Configure the discharge line for the appropriate discharge volume (e.g., in-line flow meter or manometer and scale), or get the discharge measuring device (calibrated bucket) and place it near the discharge point if another measuring system is not being used.

Figure 9.29 Discharge line away from pumping well. Manual backup readings with E-tape being collected.

8. Attach all transducers to the data logger with connecting cables. The data logger should be placed fairly close to the generator, so that they can both be activated simultaneously at start time.
9. Set up the test in the data logger by giving the test a name and enter all the transducer information. Make sure there is a good connection with each transducer by taking a reading of each one at the data logger. Do the readings make physical sense? If not, then check out why. In the case of well sentinels it may make sense to set readings to linear scale every 30 s with the same start time.
10. Run a step-drawdown test or test the pumping rate so that the gate valve or discharge control valve can be closed back to the appropriate discharge rate. Once there, leave it in the desired position.
11. Prepare field books for frequent readings (listed below) and synchronize all watches (Chapter 1, Section 1.8).
12. Prepare personnel with E-tapes for manual backup readings; one E-tape dedicated for each well (or two) is advised. If you are working alone, have an E-tape next to each well for ready use.
13. Make sure any safety issues are taken care of (listed below).
14. Prepare a signal so all parties can begin taking readings at the same time. The most critical is activating the data logger and the pump at the same time. A "1, 2, 3, go!" while dropping an arm system works well.
15. Once the test has begun, frequent manual readings are necessary. If there are two of you, it is helpful to have one call out the readings and the other keep track of time and record the numbers. The pumping rate in the calibrated bucket should also be measured or the discharge read from the flow meter or manometer tube. If manual readings coincide with data logger recordings "splash effects" may distort the data-logger value.
16. When the time spacing between readings gets longer (15 to 30 minutes), plot the data or graph it to see what is happening. One should never stop a test based on time alone. Look at the data and see whether boundary conditions or delayed yield or other effects are indicated in the data. When sufficient data have been collected, prepare for recovery mode.
17. If the data logger has a step function to go directly into recovery log mode, all that needs to be done is to synchronize the step-function button and deactivate the generator or pump. Some data loggers require that another test be defined and prepared beforehand to activate the recovery phase. By starting the "new" test, the "old" one is stopped automatically.

18. Once again, field books need to be prepared for frequent readings (listed below) and all watches synchronized.
19. The signal is given and the data logger is "stepped" while the pump is shut off. Immediately recovery mode manual readings are taken and recorded.
20. Make sure to plot the data during the test when time allows. There is a tendency to stop the recovery phase too soon. It is an excellent additional source of information, so it should be collected. Plan accordingly and be patient.

Frequency of manual readings

The majority of drawdown takes place during the first hour or so of the test. Continued drawdown does occur, especially if a barrier condition is encountered; however, changes are usually not as dramatic. The same is true for recovery mode. The initial hour after pumping stops is when recovery occurs most rapidly. At these times, if extra personnel can be on hand to help with manual readings, it can make a big difference in reducing stress. The flurry of activity at the beginning of the pumping test and the beginning of recovery is similar to a WFD.

The frequency of readings depends on the response of drawdown in the observation wells. Wells farther away may not "see" a response for several minutes. This depends on the completion depth of the wells and the geology (Example 9.2). It also depends on whether confining or semiconfining conditions are possible. Low (confined) storativities correspond to a rapid expansion of the cone of depression (Chapter 10). The key is to watch the changes in the data. Usually, 0.03 to 0.05 ft (0.91 to 1.5 cm) is a fair indication that the drawdown is real. When drawdown changes between readings drop to approximately 0.02 ft (0.6 cm) per reading, one should advance to the next time interval (Table 9.8). As a general guide, the schedule shown in Table 9.8 is

TABLE 9.8 Recommended Time Intervals for Manual Readings in a Pumping Test

Time since pump is turned on or off, in min	Length of time interval, in min	Comments
0–10	0.5	Readings can be staggered when observation wells are being measured.
10–15	1.0	
15–30	2.0	
30–60	5.0	
60–90	10.0	All later readings should be within 1–15 s of the appropriate time interval.
90–120	15.0	
120–360	30.0	
36–1,440	60.0	
1,440–end of test	240.0	

recommended, and then it should be adjusted according to what is observed.

Safety issues

As with any activity, there are always safety issues. Common sense will generally help one to be alert to most problems. A few specific items will be mentioned based on experiences by the author.

- Make sure the fuel containers are placed away from the exhaust of the generator. During one test, it was observed that part of the plastic fuel container was beginning to melt.
- Make sure vehicle exhaust is away from where people are working. Notice the wind direction and park in a safe orientation.
- Make sure the generator and data logger are protected from rain and placed on a surface with good drainage so that puddles of water do not accumulate.
- Secure the cables from the transducers so tripping hazards are avoided.
- Secure the area, if possible, to keep children and animals away from the working area (Figure 9.30).
- Use a funnel when refueling the generator during a test. Splashing fuel can be a problem.

Figure 9.30 If possible, children and animals should be kept away from the work area.

- Have lighting at night and a first aid kit on site.
- Don't panic.
- Don't work alone. This way someone can go for help.

Once again, common sense will help one to avoid most problems. The buddy system is always advisable for keeping each other alert or making runs for supplies. It is terrible to have a problem with no one around to help (Example 9.1).

9.5 Things that Affect Pumping Test Results

If none of the field conditions change from the beginning to the end of a pumping test, you are very fortunate. During the course of most pumping tests, some type of condition change may occur that affects the interpretation of the results. These changes should be recorded. If one is not paying attention to changes during the test and writing them down, they may not be accounted for during the interpretation phase (Chapter 10).

Weather and barometric changes

Consider the following scenario. At the beginning of a pumping test, it is sunny and clear. About 4 h into the test, a storm front moves through. The sky is dark and a steady rain falls. During the night, the storm passes over and the sky clears again. A nearby stream increases in stage to 1 ft (0.3 m) higher than at the beginning of the test and subsequently drops 2 ft.

If an aquifer is confined to semiconfined, the water levels in wells are affected by barometric changes. Sunny and clear weather accompanied by high barometric pressure presses harder on the water surface in wells, thus decreasing the relative water elevation. When a storm comes into the area, the relative air pressure decreases. Thus the air is not pressing as hard on the water surface, allowing the water level to rise. Personally, the author has observed water levels rise as much as 1 ft when a storm has come in. During a pumping test, the water levels are supposed to be decreasing if they do not encounter any recharge sources. It may be that a recharge source is being interpreted when it is really from a storm front affecting the data. This is where field notes come in handy.

Other apparent sources and sinks

Other physical phenomenon occurring in the field may affect the interpretation of pumping-test results. Nearby wells that were pumping and shut down during a pumping test may affect the drawdown

results. Since overlapping cones of depression are additive, the drawdown rates are accelerated when nearby wells are pumping. Here the interpretation of the transmissivity may be lower than the actual value. When a nearby well stops pumping, the time/drawdown curve will flatten, and the transmissivity may appear to be greater or the curve will suggest that a source of recharge has been encountered.

Example 9.7 A pumping test was being conducted to see whether a mining company supply well would impact other local residents. The geologic setting is depicted in Figure 9.31. The pumping well was completed within the granitic bedrock (granodiorite), and the residential wells were completed in both the granodiorite and in the surficial sediments. The sediments ranged in thickness from 30 to 55 ft (9.1 to 16.8 m) in the pumping-test area. In this instance, any resident within 2,000 ft (610 m) of the pumping well could have their wells monitored. Approximately seven residential wells were monitored by students. The instructions given to the residents were that no water use should take place during the test, which would begin at 8 a.m. on a Saturday morning. During the test, one of the observation wells seemed to be recovering the whole time. None of the wells completed within the sediments indicated a response except this well. After conferring with the well owner, it was discovered that someone used the bathroom earlier that morning and what was being observed was a recovery response from pumping. Wells completed within the granodiorite within 1,100 ft (335 m) did indicate a drawdown response.

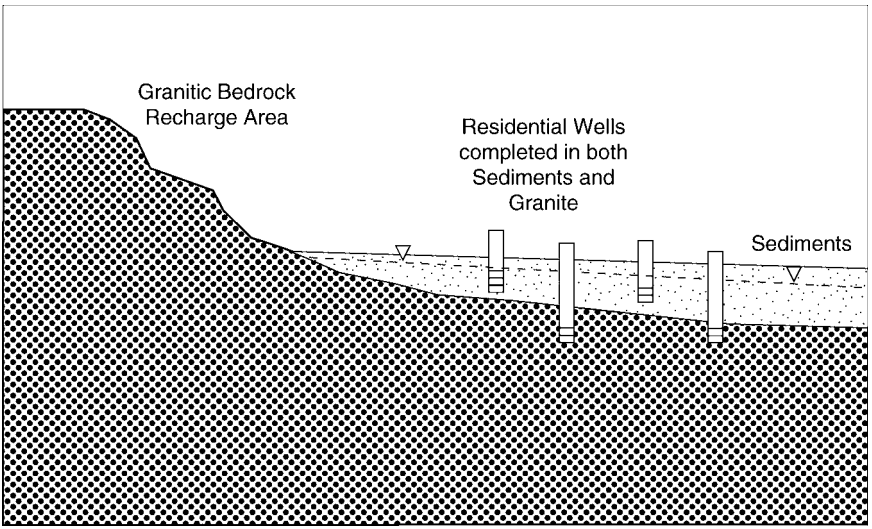

Figure 9.31 Geologic setting for Example 9.7. Residential wells are completed in both the granitic bedrock and the surficial sediments. (Not to scale.)

Another factor that can affect the drawdown response is a change in stage of a local stream. At the beginning of the test, the stage of the stream should be marked so that its stage is known. If changes in stage occur during the test, they can be noted.

Did it rain during the test? This could be a potential source of recharge in a shallow unconfined aquifer. Is the discharge line too close to the pumping test site? The author has observed a test reach steady-state conditions merely because someone failed to conduct discharge beyond the cone of depression.

Another consideration is the proximity of railroads and heavy traffic areas to shallow confined systems. A documented case in Long Island, NY, showed a hydrograph response near a train station (Jacob 1940). The weight of the train compressing the aquifer resulted in water-level rise, and when the train departed, the water level would drop once again. Be alert to physical changes that may occur during a pumping test. Write them down and use your field notes during the interpretation phase. Additional discussion on the interpretation of pumping-test results is presented in Chapter 10.

9.6 Summary

Pumping tests are valuable field methods in estimating the hydraulic properties of aquifers. The time and effort required to perform a pumping test can provide information about the aquifer that cannot be obtained from slug tests or specific capacity tests. Pumping tests can be stressful because they require a fairly large list of equipment and many things can go wrong. A check list is useful to remind field personnel what needs to be brought and tasks that need to be done.

It is important to have an understanding of the geology so that observation wells can be oriented appropriately and completed at the proper depths. Appropriate pumping rates are needed to stress the aquifer so that drawdown can be observed. Transducers and well sentinels should be selected that will be compatible with the water depths and the expected drawdown ranges. Discharge systems should be designed to maintain a constant discharge rate and obtain accurate information. The discharge line should be configured with a constricting device, so that it can be opened to accommodate more flow should drawdown conditions cause the flow rates to decrease. Extra personnel are helpful to have around at the beginning of a pumping test to help set up equipment and collect the early-time manual readings. This is also true at the beginning of the recovery phase. Changing weather and other field conditions that occur during the test should be recorded in the field books for use during the interpretation phase. The flurry of activity that can occur during a pumping test reminds the author of a WFD.

References

Berg, J., and Nyberg, T., 1995. *The Duct Tape Book*. Pfeifer-Hamilton, Duluth, MN, 64 pp.
Birsoy, Y.K., and Summers, W.K., 1980. Determination of Aquifer Parameters from Step Tests and Intermittent Pumping Data. *Ground Water*. Vol. 18, pp. 137–146.
Donovan, J.J., 1983. *Hydrogeology and Geothermal Resources of the Little Bitterroot Valley, Northwestern, Montana*. Montan Bureau of Mines and Geology Memoir 58, 60 pp. and two sheets.
Donovan, J.J., 1985. *Hydrogeologic Test Data for the Lonepine Aquifer, Little Bitterroot Valley, Northwestern Montana*. Montana Bureau of Mines and Geology, Open-file Report 162, 9 pp.
Driscoll, F.G., 1986. *Groundwater and Wells*. Johnson Screens, St. Paul, MN, 1089 p. 402
Fetter. C.W., 1993. *Contaminant Hydrogeology*. Prentice-Hall, Upper Saddle River, NJ, 500 pp.
Heath, R.C., and Trainer, F.W., 1968. *Introduction to Ground Water Hydrology*. Waterwell Journal Publishing, Worthington, OH, 285 pp.
Jacuzzi, 1992, *Jacuzzi Brothers Hydraulics Training Seminar Water Systems Workbook*. 40 pp.
Jacob, C.E., 1947. Drawdown Test to Determine Effective Radius of Artesian Well. *Trans American Society of Civil Engineers*, Vol. 112, Paper 2321, pp. 1047–1064.
Jacob, C.E., 1940. Correlation of Groundwater Levels and Precipitation in Long Island, NY, *Transcripts of American Geophysical Union*, Vol. 24, Pt.2, pp. 564–573.
Journal of American Water Works Association (JAWWA), Vol. 77, No. 9, September 1985.
Kruseman, G.P., and de Ridder, N.A., 1990. *Analysis and Evaluation of Pumping-Test Data. 2nd ed*. International Institute for Land Reclamation and Improvement, Wageningen, The Netherlands, Publication 47, 377 pp.
Roscoe Moss Company, 1990. *Handbook of Ground Water Development*. John Wiley & Sons, New York, 493 pp.
Walton, W., 1970. *Groundwater Resource Evaluation*. McGraw-Hill, New York, 664 pp.

Chapter

10

Aquifer Hydraulics

One of the key pieces of information hydrogeologists need to solve problems in the field of hydrogeology is an understanding of the hydraulic properties of an aquifer. Many questions, such as, how long will it take water from the recharge area to reach a production well? How long will it take a contaminant to move from point A to point B? If this production well is activated, how far will the cone of depression reach? And how many other wells will be affected? What distribution of hydraulic properties should be assigned to the layers within this groundwater-flow model? In order to answer such questions, it is necessary to perform pumping tests (Chapter 9) and slug tests (Chapter 11) to measure the aquifer stress response in wells over time. This chapter begins by discussing the traditional analytical methods followed by a discussion of applications when the data do not fit the ideal case. Unfortunately, the latter case is the more common scenario found in the field. It is beyond the scope of this chapter to provide an in-depth discussion of aquifer hydraulics, but it hoped that the presentation here will be useful. There are excellent discussions in Hantush (1964), Lohman (1979), Driscoll (1986), and Kruseman and deRidder (1991). Free microsoft Excel spread sheets for the analysis of aquifer tests and slug tests were created by Halford and Kuniansky (2002). Slug-test analytical methods are all presented in Chapter 11.

The Theis (1935) method is presented first to show what time-drawdown data look like. There may be a danger in immediately launching into a more complicated analytical method without first attempting a Theisian (1935) fit. Any pumping-test data set should probably be evaluated with a Theis (1935) analysis. If the graphical image does not fit or make sense, alternative methods may be needed. Pumping test data are also easily evaluated using the Cooper-Jacob method (1946) particularly if they are single-well tests (discussed later in Section 10.5); however, more assumptions are required. Additional topics covered in this chapter

Copyright © 2008, 2001 by The McGraw-Hill Companies, Inc. Click here for terms of use.

include distance-drawdown relationships, image-well theory, and a discussion of the application of pumping-test data to aquifer properties. Explanations for deviations from the Theis (1935) curve are offered along with field examples. Dual porosity and fracture-flow data sets have their own characteristic response. These are also presented with field examples.

10.1 Wells

Wells provide a point of access to the water-bearing materials, and are one of the most important features of groundwater studies. When properly designed and constructed (Chapter 8), wells provide useful information about the characteristics of an aquifer. Characterizing the physical properties of aquifers is the study of **aquifer hydraulics**.

The water level in a well, when no pumping is occurring, is known as the **static water level** (SWL). The SWL reflects the total head at the midpoint of screened intervals of a well (Chapter 5). (It is recommended that the reader refer to Chapter 5 in the interpretation of water-level data). If the well is an open-hole completion (open at the bottom with no screen) it is considered to be representative of the head at the bottom of the well. Typically, SWLs are measured from the top of the casing (TOC). Level surveys are then performed to determine the elevation of the TOC and the ground surface level (GSL) (Chapter 5). Once the reference level has been defined, the change in water level with time can be measured during a pumping or aquifer test to evaluate the hydraulic properties of an aquifer. The difference measured between the non-equilibrium water level at a particular time "t" and the initial SWL is known as **drawdown** (Driscoll 1986) (Figure 10.1).

Cone of depression

When pumping begins, the water level in the pumping well is lowered. This lowering (measured as drawdown) induces a gradient or slope all the way around the well bore known as the **cone of depression**. Flow proceeds radially toward the well, much like the spokes of a bicycle converge on the hub. The cone of depression extends outward until it can capture enough water to meet the demands of the pumping rate (Q). The shape of the cone of depression is estimated by observation wells that also show a drawdown response. If these are located in different azimuth orientations away from the pumping well (Chapter 9), one can evaluate anisotropy by plotting the drawdown at a specified time "t" and contouring it.

The cone of depression in a confined aquifer (Figure 10.1) occurs within the potentiometric surface above the top of the aquifer, whose position is determined by the SWL in cased wells. This means that the saturated thickness (b) is always maintained. Recall also that the

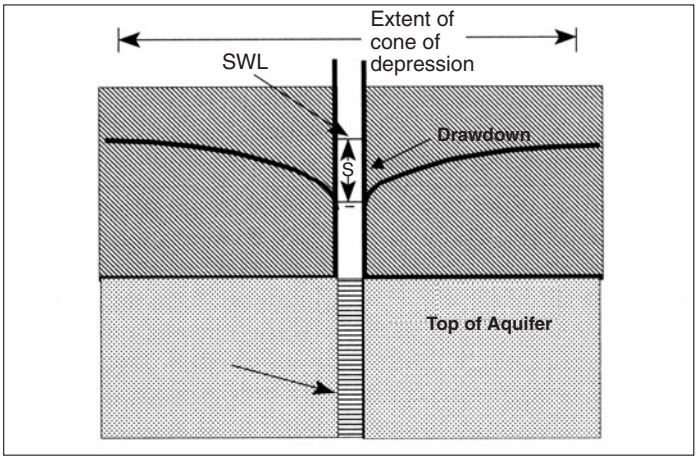

Figure 10.1 Schematic illustrating drawdown and cone of depression in a confined aquifer. Note the cone of depression is in the potentiometric surface while the aquifer remains fully saturated.

potentiometric surface is an imaginary surface that reflects both the pressure head and elevation head (Chapter 5).

The cone of depression in an unconfined aquifer represents a physical draining of the porous materials near the pumping well, creating an actual depression in the water-table surface (Figure 10.2). It is indicated by the respective drawdowns observed in nearby observation wells. The shape and extent of the cone of depression depends on the pumping rate (Q) and the nature of the geologic materials. Finer-grained materials

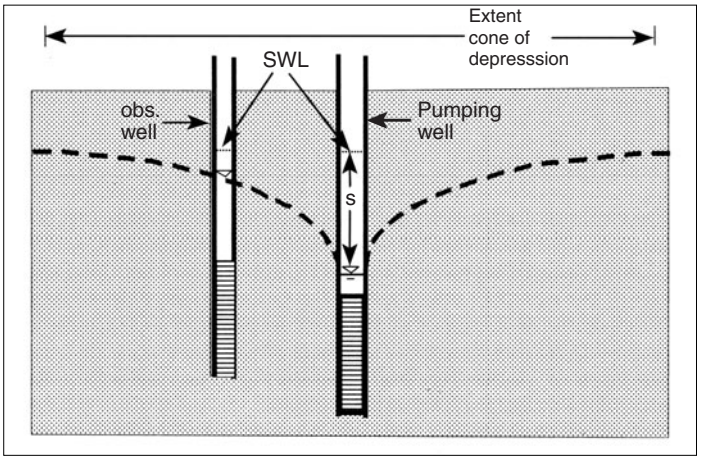

Figure 10.2 Schematic illustrating drawdown and cone of depression in an unconfined aquifer, with an observation well.

produce a steeper cone of depression because a steeper hydraulic gradient is required for gravity to move groundwater toward the pumping well. Pumping within transmissive materials produces a flatter cone of depression (Figure 10.3) that may extend further out. The relationship between the steepness of the cone of depression and the transmissivity is a proportional relationship between the hydraulic conductivity and the hydraulic gradient expressed in Darcy's law (Chapter 5). How this is applied can be illustrated in Example 10.1.

Example 10.1 Within the Butte, Montana, area are a number of Superfund operable units associated with mining operations. During the remediation design and subsequent construction phase, mine tailings were to be excavated and removed to another location. It was required that dewatering of the mine tailings and the underlying alluvial materials take place to perform the excavations.

Adjacent to the excavation operation is another Superfund operable unit associated with "organics" contaminated groundwater resulting from chemicals used in the timber treating process. The chemicals were used in treating support timbers used as underground mine supports. In this operable unit, the shallow groundwater system became contaminated with a mixture of diesel and pentachlorophenol (PCP). The concern with dewatering the mine tailings operable unit was that if the hydraulic conductivity was high, then the cone of depression from dewatering would extend sufficiently to the southeast, potentially mobilizing the organic plume.

The crux of the problem was centered in the estimated value for the hydraulic conductivity of the alluvium. The hydraulic conductivity for the alluvial materials was believed to be approximately 80 ft/day (24.3 m/day). This was based

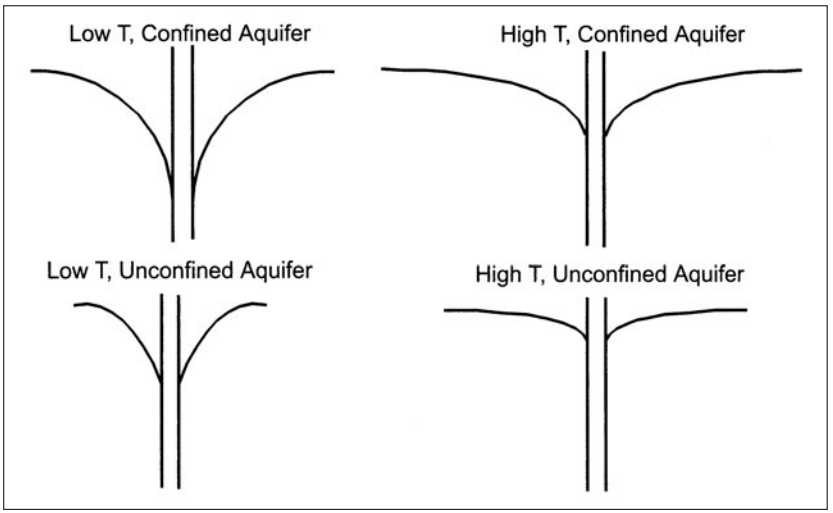

Figure 10.3 Schematic of the differences in the shapes of cones of depression based on aquifer properties.

upon groundwater models that could not reach calibration unless hydraulic conductivity numbers for the alluvium were this high. In the model, the alluvium was represented by a relatively thin package of sediments over impermeable bedrock. This layer could not allow sufficient water through it unless the hydraulic conductivity value was increased over the values found from pumping tests. Personnel from a local state agency (Montana Bureau of Mines and Geology) argued that the pumping tests suggest that the alluvial materials had a lower hydraulic conductivity. They pointed out that the required volume of water could move through the area using a lower hydraulic conductivity if an additional saturated thickness consisting of weathered granitic bedrock be used. The matter was settled by conducting a pumping test screened in the alluvial material. In the results, a hydraulic conductivity of 20 to 30 ft/day (6.1 to 9.1 m/day) was calculated for the alluvium, and a hydraulic conductivity for the weathered granite was estimated to be 1 to 5 ft/day (0.3 to 1.5 m/day). By adding an additional weathered bedrock layer to the model, calibration was reached with the lower hydraulic conductivity value more reflective of the local geology and pumping test results. This permitted the dewatering activities to take place (John Metesh personal communication, Butte, Montana, September 1995).

Figure 10.3 illustrates that a lower hydraulic conductivity results in a steeper, less extensive cone of depression, whereas a higher hydraulic conductivity results in a flatter, farther-reaching cone of depression. In example 10.1, the flatter cone from the higher estimated hydraulic conductivity would potentially reach the organic plume, mobilizing the contaminants. During the actual excavation and dewatering process, it was found that the lower hydraulic conductivity was correct.

Comparison of confined and unconfined aquifers

The size of the cone of depression is also affected by the storage coefficient and aquifer transmissivity. Typical ranges of storativity for a confined aquifer are between 10^{-3} and 10^{-6}. Unconfined aquifers have specific yields that range between 0.03 and 0.30 (Fetter 1993). Leaky-confined or semiconfined aquifers fall somewhere in between. The significance of the smaller storage value is that the cone of depression in a confined aquifer will extend faster and farther than in an unconfined aquifer. This is shown in Figure 10.3 and illustrated by the Example 10.2.

Example 10.2 While performing the technical analysis for a source-water protection plan in Ramsay, Montana, a pumping test was conducted on the local public water supply well (Figure 10.4) (O'Connell and Smith 1993). There are two production wells plumbed into a water tower pressurizing system. The wells were drilled in 1917, and the well logs are nonexistent. It was unclear whether the wells were drilled into younger layered sediments or deeper into the underlying Tertiary Lowland Creek Volcanics. The pump in each well can be activated manually or controlled by an automatic system. The well closest to the water

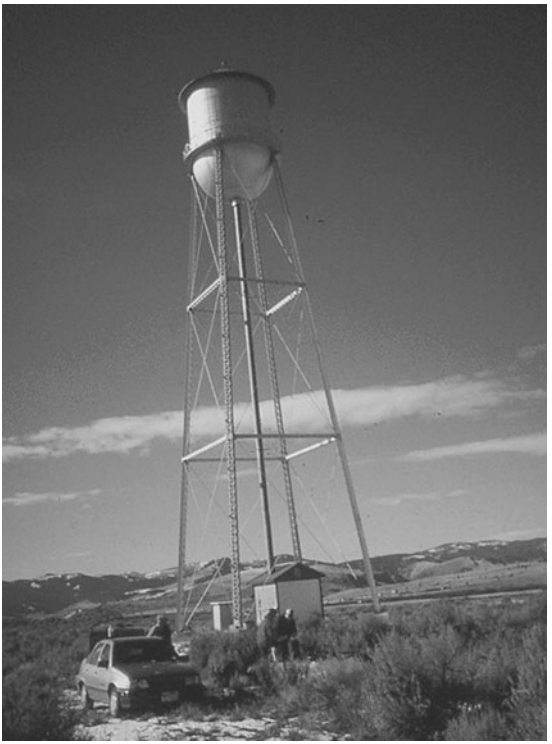

Figure 10.4 Water tower for the Ramsay, Montana, public water supply.

tower (the south well) was used as the pumping well, and the well 510 ft (155 m) to the northwest was used as the observation well. During the test, the pumping well was activated manually after instrumenting the wells with drawdown measuring equipment. The pumping rate was 210 gpm (13.2 L/s). The north observation well experienced 0.05 ft (1.5 cm) of drawdown within 30 s of pumping. This indicates that the cone of depression extended at a rate of at least 17 ft/s (5.2 m/s), which is at the rate of a very fast person running toward the well at full speed! A rapid expansion of the cone of depression implies the aquifer is confined!

Drawdown in a confined aquifer is from response to compression of the mineral skeleton and decompression of the water, and this occurs quickly. The cone of depression in an unconfined aquifer is a physical depression in the water table from drainage of the pores, is of more limited extent, and develops more slowly.

Example 10.3 To obtain a mental picture of what is occurring in a confined aquifer, imagine taking a household cleaning sponge (flat rectangular shapes). If this sponge is sandwiched between two pieces of plywood, then sealed with silicone around the sides, it could theoretically represent a confined aquifer.

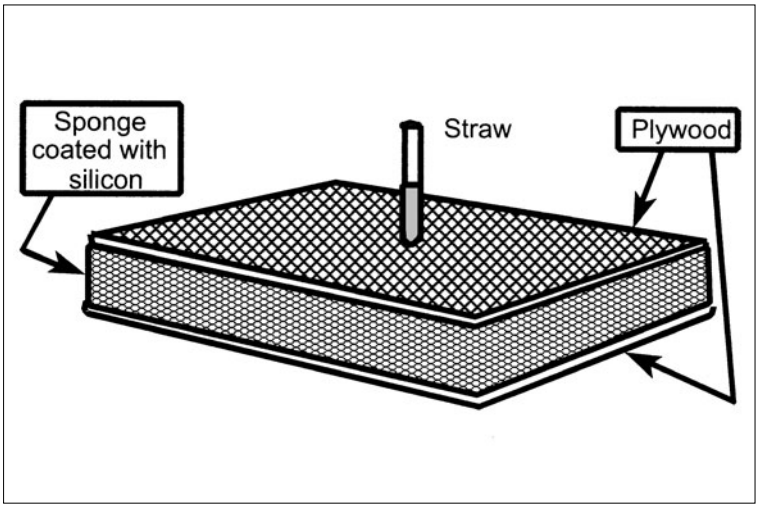

Figure 10.5 Model of a confined aquifer made with a sponge sandwiched between plywood and sealed with silicon calking. A hole is drilled and a straw inserted to represent a well.

The sponge represents the aquifer materials, and the plywood represents the confining layers. A hole is drilled through the top plywood piece into the sponge, and a soda straw is inserted to represent a well (Figure 10.5). The sponge is saturated and the elevation of the water level in the straw is visible above the top plywood piece. Any slight compression of the "aquifer" results in water rising quickly up the straw. The amount of compression would be almost imperceptible, even though a dramatic expulsion of water takes place. Lifting your hand off of the upper plywood piece results in the water level immediately dropping back to static conditions. This represents the elastic-like response of aquifers. A similar concept is illustrated by encased beverages that come sealed with a straw. The straw is inserted into the beverage and when the container is slightly squeezed, fluid emerges from the straw.

The equations describing nonequilibrium drawdown with time were first attributed to C.V. Theis (1935). In analyzing pumping-test data sets, the usual first step is to perform a Theis analysis to see what the data look like.

10.2 Traditional Pumping-Test Analytical Methods

In the early 1930s, C.V. Theis noticed that there was a relationship between drawdown and well yield with time. He approached a friend named Lubin, a mathematician at the University of Cincinnati, and described his problem (Bob Cleary, personal communication, San Francisco, CA, 1993). Lubin stated that he had a solution that was well known from the heat-flow literature. The analog to a well in an aquifer

was compared to a wire within a cube of steel, heated by a battery. Lubin said that the solution of the radial heat-flow equation being integrated was dependent upon the following assumptions:

- No edge effects (aquifer is of infinite areal extent).
- Uniform thickness (pumping well fully penetrates and receives water from the full thickness of the aquifer).
- Constant heat source (constant pumping rate).
- Homogeneous and isotropic (aquifer is uniform in character and the hydraulic conductivity is the same in all directions).
- No sources or sinks (water is discharged instantaneously from storage and not from external sources either adding or removing water).

Additional assumptions inherent in the Theis equations listed in Driscoll (1986) are:

- Pumping well is 100% efficient.
- Laminar flow (darcian) flow prevails throughout the well and aquifer.

The solution is known as the Theis equation:

$$h_o - h = s$$

$$= \frac{Q}{4\pi T}\left[-0.5772 - \ln u + u - \frac{u^2}{2 \times 2!} + \frac{u^3}{3 \times 3!} - \frac{u^4}{4 \times 4!} + - \cdots\right] \tag{10.1}$$

or simply

$$h_o - h = s = \frac{Q}{4\pi T} W_{(u)}$$

where Q = pumping rate (L^3/t)
T = transmissivity (L^2/t)
s = drawdown (L), $= h_o - h$, and
[ ] = $W_{(u)}$, part in brackets is known as the well function

Note: The units need to be worked out correctly to get the appropriate drawdown in units of length!

The well function is a function of u, where:

$$u = \frac{r^2 S}{4Tt} \tag{10.2}$$

Note: u is dimensionless!

where r = radial distance to the pumping well (L)
S = storage coefficient (unitless)
T = transmissivity (L^2/t)
t = time (in days or minutes)

The infinite series in the brackets of Equation 10.1 is known as the **well function ($W_{(u)}$)**. Interestingly enough, Theis (1935) published the solution of a partial differential equation (PDE) that did not exist until Jacob, a graduate student of his at the University of New Mexico, came up with it in 1941 (Bob Cleary, personal communication, San Francisco, CA, January 1993).

Considering the assumptions given, flow toward a well can be thought of as moving toward the well in a polar coordinate system. In the case where the aquifer is isotropic and homogeneous, with sources or sinks, the radial flow equation developed by Jacob (1950) can be expressed as:

$$\frac{\partial^2 h}{\partial r^2} + \frac{1}{r}\frac{\partial h}{\partial r} + \frac{W}{T} = \frac{S}{T}\frac{\partial h}{\partial t} \tag{10.3}$$

where r = radial distance from the well (L)
t = time (t)
h = hydraulic head (L)
S = storativity (dimensionless)
T = transmissivity (L^2/t)
W = source or sink term (L/t)

Instead of coming up with Equation 10.3 and solving it numerically, Theis (1935) solved it graphically. The method involves superimposing two curves. The first curve, laid on the bottom, called the **Normal type curve**, is a plot of the well function "$W_{(u)}$" (the bracketed part of Equation 10.1 along the ordinate) versus values of "u" (along the abscissa) given in Equation 10.2. Corresponding values for $W_{(u)}$ and "u" are given in Appendix D (Figure 10.6). Note how the plot of the Normal type curve, shown in Figure 10.6 is in log-log scale. The second curve, laid on top of the normal type curve, is from data from the pumping test. This plot, also in log-log scale, puts drawdown (expressed either as "s," or "$h_o - h$") in feet or meters (increasing upward in the y-axis) versus r^2/t along the x-axis. Care is taken to make sure the x and y axes are kept square (both the x and y axes are parallel to each other) as the data plot is slid along the Normal type curve, to obtain a "best" fit. An example showing a fit of the data and how to make the calculations is given in Example 10.4.

A convenient match point is usually selected where $W_{(u)}$ and u both equal 1.0. This simplifies the calculations using Equations 10.1 and 10.2 greatly. The corresponding matching value for drawdown (s or $h_o - h$) and r^2/t from the match point on the data plot can then be read

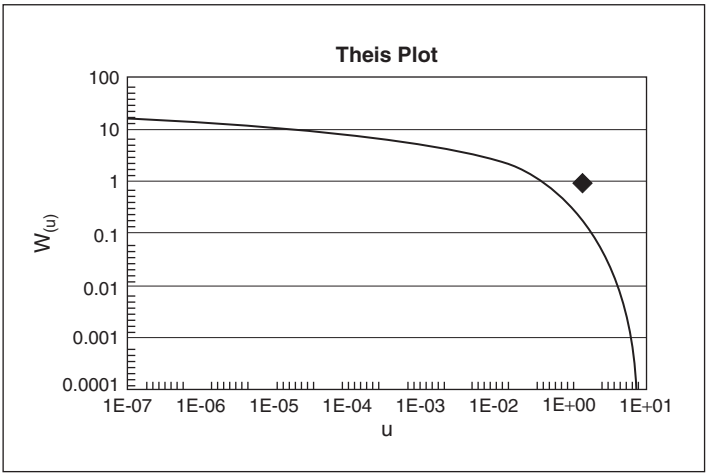

Figure 10.6 Theis Normal type curve. A plot of the well function $W_{(u)}$ versus values of "u." The diamond is the match point where $W_{(u)}$ and "u" (E + 00) both equal 1.0.

to solve for transmissivity from Equation 10.1 and then for storage by rearranging Equation 10.2.

Most hydrogeologists today use a **Reverse type curve** (Hereafter referred to as the Theis curve) (Figure 10.7). Both the type curve and field observed data curve are "reversed" by taking the inverse of the abscissa (x-axis) information. The reverse type curve is a plot of $W_{(u)}$ versus $1/u$, both

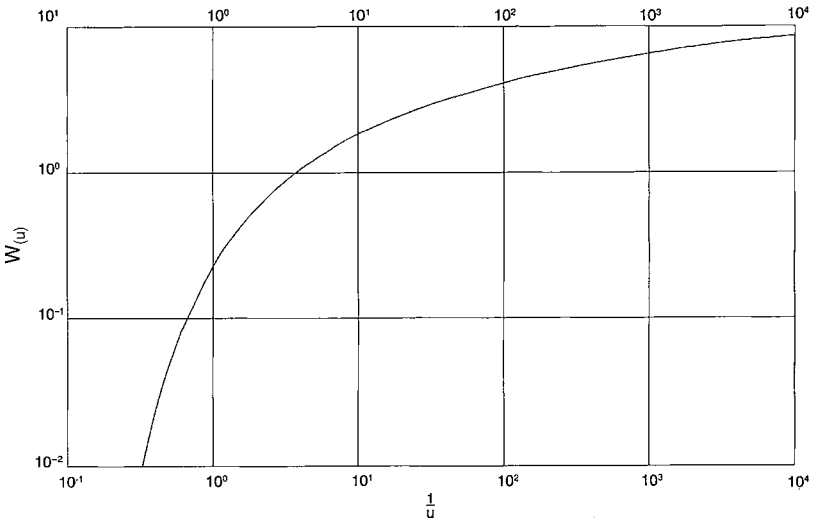

Figure 10.7 Plot of $W_{(u)}$ versus $1/u$ resulting in a reverse Theis curve. [*Modified after Lohman (1979).*]

on log scale. The data curve is a plot of drawdown (s) versus t/r^2, also on log-log scale. The reason for using the Reverse Theis curve is because any given observation well will have a constant radial distance (r). This means that the drawdown can be plotted directly with corresponding points in time (usually plotted in minutes). Plots of more than one observation well *on the same plot must use* the calculated t/r^2 values for the respective distances (r). The transmissivity is calculated from Equation 10.4.

$$T = \frac{Q}{4\pi s} W_{(u)} \quad \text{or} \quad \frac{Q}{4\pi(h_o - h)} W_{(u)} \tag{10.4}$$

where T = transmissivity (L^2/t)

And the calculation for storativity:

$$S = \frac{u4Tt}{r^2} \tag{10.5}$$

where S = storativity (dimensionless)

Remember to make sure all your units are consistent! Many errors occur in the calculations from not being careful with units! Calculations of transmissivity are usually in ft^2/min, ft^2/day, m^2/day, or gal/day · ft. Not being careful with your calculations can lead to erroneous interpretations and poor design. More applications will be given in Section 10.4. An example showing a data plot fit to a Reverse type curve with corresponding calculations is shown in Example 10.4.

Example 10.4 A pumping test for municipality was conducted for 70 days. The pumping rate was 350 gpm (22 L/s) and the data from the observation well located 450 ft (91 m) away were collected over the testing period. The time-drawdown data superimposed on the Reverse type curve yielded a drawdown of 0.4 ft and the time was 5 min at the match point ($W_{(u)} = 1/u = 1.0$). The data are plotted in Figure 10.8. Calculations of transmissivity and storativity were performed using Equations 10.4 and 10.5. The storativity suggests that the aquifer is confined.

$$T = \frac{350 \text{ gpm } (1 \text{ ft}^3/7.48 \text{ gal})}{4\pi(0.4 \text{ ft})} = 9.3 \text{ ft}^2/\text{min} = 13{,}400 \text{ ft}^2/\text{day}$$

$$S = \frac{4(9.3 \text{ ft}^2/\text{min})(5 \text{ min})}{(450 \text{ ft})^2} = 9.2 \times 10^{-4}$$

Example 10.5 One of the important requirements during a pumping test is that the pumping discharge rate be constant. This can affect the shape of the Theis curve. During a court case, a homeowner and a well driller were

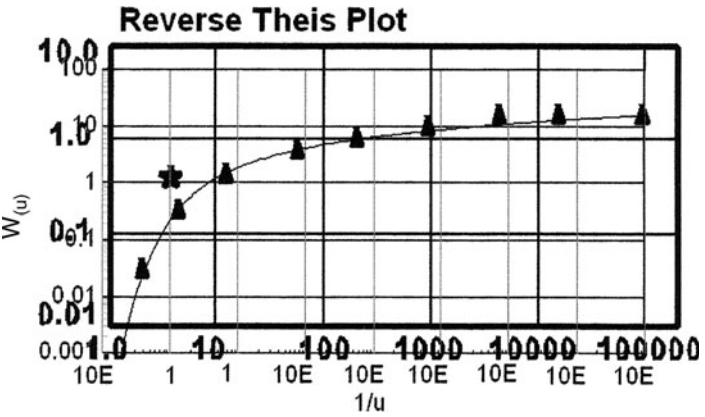

Figure 10.8 Theis method where data plot in drawdown versus time is superimposed on the reverse type curve. The match point is represented by the star, where $W_{(u)}$ and "1/u" equal 1.0.

at odds over drilling a well too deep (deep-holing). The total depth of the well was 325 ft (99 m).

At 200 ft (61 m) the well driller told the well owner they had 4 to 5 gpm (13.1 to 16.4 L/min) but were going to "chase it a bit." They chased it to 325 ft while the owner was at work and declared the well a success making 8 gpm (30 L/min). An argument led to the disagreement. The well owner was advised that if another driller came in and pulled the casing, backfilled the hole with gravel, and retested the well, achieving the same production yield, it would indicate the additional footage was unnecessary. The well owner was cautioned that there was great risk in doing this because he may lose the well from materials caving into the well. The well owner was mad enough to go ahead with it anyway. Another driller was hired, the casing was pulled, the well was backfilled with gravel to 212 ft, and then plugged with bentonite before reinstalling the well screen.

A pumping test was conducted by the other driller to see what kind of yield the well would make. The pump was set at 187 ft (57 m) and the pumping commenced at 10:00 a.m. The data collected are presented in Table 10.1.

The expert witness representing the driller used the data from Table 10.1 to generate a time-drawdown Theis plot. The shape of the drawdown curve was disjointed, caused by variations in the pumping rate, and the departure from the "type curve" was explained using fracture-flow theory to an uneducated jury. The author thought it prudent to visit the site and conduct his own brief pumping test at 8 gpm (30.2 L/min). A very characteristic Theis curve resulted when the pumping rate was constant. See Figure 10.10a for a good example of a Theis fit.

Cooper-Jacob straight-line plot

Cooper and Jacob (1946) recognized that if u in the Theis equation was sufficiently small, the nonequilibrium equation could be modified to a

TABLE 10.1 Pumping Test Data and Well Yield from Example 10.4

Time	Elapsed time (min)	Water level (depth)	Pumping rate (gal/min)
10:00	0	18′10″	7
10:25	25	61′5″	7
10:30	30	65′10″	7
10:35	35	69′8″	7
10:40	40	73′9″	5
10:45	45	79′0″	7
10:50	50	85′0″	7
10:55	55	89′10″	7
11:00	60	93′9″	7
11:05	65	98′7″	7
11:15	75	105′8″	6.5
11:25	85	115′	7
11:45	105	120′	5.5
11:55	115	140′	8.17
12:00	120	144′	7.5
12:12	132	164′	7.2
12:20	140	170′	7.2
12:35	155	174′	7.91
12:40	160	175′	8.3
12:45	165	175′	8.6
13:45	225	175	6

logarithmic term instead of an infinite series well function (Equation 10.6). Arguments arise as to when u is sufficiently small. Values range from 0.05 (Driscoll 1986; Fetter 1994) to 0.005 (Fletcher 1997). The software package AQTESOLV (Duffield 1991) indicates u is sufficiently small at 0.01. The smaller u is the less the error involved. The author believes 0.02 is sufficiently small. With u sufficiently small, Equation 10.1 can be rewritten as:

$$s = \frac{Q}{4\pi T}\left[-0.5772 - \ln(u)\right] \tag{10.6}$$

By substituting in the parameters from Equation 10.2 for u and finding a natural log value for $e^{0.5772}$, we obtain:

$$s = \frac{Q}{4\pi T}\left[-\ln(1.78) - \ln\left(\frac{r^2 S}{4Tt}\right)\right] \tag{10.7}$$

remembering that $-\ln A = \ln(1/A)$ and $\ln B \times C = \ln B + \ln C$:

$$s = \frac{Q}{4\pi T}\left[+\ln\left(\frac{1}{1.78}\right) + \ln\left(\frac{4Tt}{r^2 S}\right)\right] \tag{10.8}$$

Factoring out the natural log function and combining terms we obtain:

$$s = \frac{Q}{4\pi T} \ln \left[\frac{(2.25\ Tt)}{r^2 S} \right] \tag{10.9}$$

Since the relationship between $\log_{10} X$ and $\ln_e X$ is $\log_{10} X = 0.43429 \ln_e X$, we obtain:

$$s = \frac{2.3\ Q}{4\pi T} \log \left(\frac{2.25\ Tt}{r^2 S} \right) \tag{10.10}$$

where all units are assumed to be consistent

s = drawdown (L)
S = storativity (dimensionless)
T = transmissivity (L^2/t)
t = time (t)
Q = pumping rate (L^3/t)

When one plots drawdown (arithmetic scale on the "y" axis) versus time (log scale on the "x" axis) a straight line results if the conditions of "u" being small are met along with the other Theisian conditions (Figure 10.9). By evaluating Equation 10.2 one can see that u is small when r (the distance

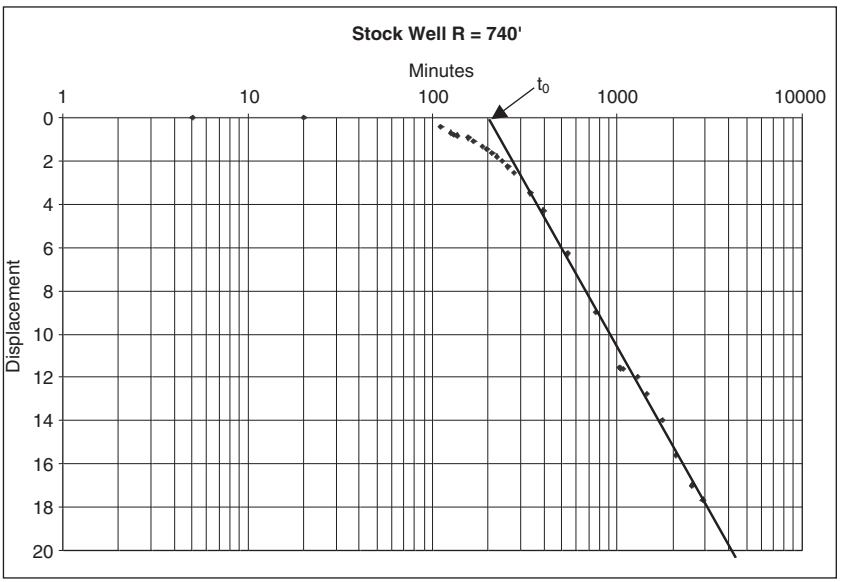

Figure 10.9 Cooper-Jacob plot showing straight-line behavior in drawdown in feet versus time. Zero drawdown ($h_o - h = 0$) occurs at time $t_0 = 200$ min.

of the observation point) is small or when the time t (time since pumping began) is large. This eliminates having to work with the well function ($W_{(u)}$). It should be noted that for a given pumping rate and observation well, located at a constant distance (r), drawdown (s) and time (t) are the only variables. By separating the variable (t) from the constant terms:

$$s = \frac{2.3\ Q}{4\pi T} \log\left(\frac{2.25\ T}{r^2 S}\right) + \frac{2.3\ Q}{4\pi T} \log(t) \tag{10.11}$$

Cooper and Jacob (1946) noticed that this could be compared to the equation for a line:

$$s = C_1 + C_2 \log(t), \quad \text{or} \quad y = b + mx \tag{10.12}$$

By selecting two times t_1, t_2, where: $t_2 > t_1$, then the drawdown at time t_1 is described by:

$$s_1 = \frac{2.3\ Q}{4\pi T} \log\left(\frac{2.25\ T t_1}{r^2 S}\right) \tag{10.13}$$

and the drawdown at time t_2 is described by:

$$s_2 = \frac{2.3\ Q}{4\pi T} \log\left(\frac{2.25\ T t_2}{r^2 S}\right) \tag{10.14}$$

The difference of the two drawdowns is expressed as:

$$s_2 - s_1 = \frac{2.3\ Q}{4\pi T} \log\left(\frac{2.25 T t_2}{r^2 S}\right) - \frac{2.3 Q}{4\pi T} \log\left(\frac{2.25 T t_1}{r^2 S}\right) = \frac{2.3\ Q}{4\pi T} \log\left(\frac{t_2}{t_1}\right) \tag{10.15}$$

By selecting time over one log cycle (a factor of 10), the (t_2/t_1) term simplifies to 1.0. The transmissivity is calculated using consistent units by the familiar expression in Equation 10.16:

$$T = \frac{2.3\ Q}{4\pi \Delta s} \tag{10.16}$$

where Δs is the drawdown over one log cycle.

The data, then, can be plotted in the field using a spreadsheet program on semi-logarithmic paper (arithmetic scale) s (ordinate) versus time (in log scale, usually in minutes). How do we get the storativity? The straight-line plot is extended to where the zero drawdown axis occurs

(Figure 10.9). The time where drawdown equals zero is known as t_0. Cooper-Jacob (1946) noticed that Equation 10.10 could be used to solve for the storativity. The first step is to move the constant portion to the other side:

$$\frac{s4\pi T}{2.3\ Q} = \log\left(\frac{2.25\ Tt_0}{r^2 S}\right) \tag{10.17}$$

By setting drawdown (s) = 0.0 and taking the exponent of both sides, we obtain:

$$10^0 = \frac{2.25\ Tt_0}{r^2 S} \tag{10.18}$$

Which simplifies to:

$$1.0 = \frac{2.25\ Tt_0}{r^2 S} \tag{10.19}$$

The storativity can be calculated by Equation 10.20:

$$S = \frac{2.25\ Tt_0}{r^2} \tag{10.20}$$

where T, r = as described previously
t_0 = straight-line projection of the time-drawdown curve up to where it intersects the zero-drawdown axis

When the results from the Theis curve are compared to the Cooper-Jacob method, the results are generally comparable; however, the Cooper-Jacob method is easier to plot in the field and does not require curve matching. If the conditions are not met, the Theis method is still viable for interpretation.

Example 10.6 A pumping test was conducted in July 1979 with a pumping rate of 1,200 gpm (75.6 L/s). The data are from an observation well located 850 ft away. The data are shown in Table 10.2 and plotted using the Theis (1935) and Cooper-Jacob (1946) methods, as shown in Figures 10.10a and 10.10b.

Notice the characteristic Theisian fit in Figure 10.10a. The calculated values for both methods are comparable, however the Cooper-Jacob straight-line fit is a least-squares best-fit, which is a characteristic of software programs. To identify where the data form a straight line the author advises that you hold the Cooper-Jacob plot away from you at a low angle. If you try this, you will note that the data after 180 min form a straight line. Another approach is to lay the plot on a table. Now get your face close to the table to

TABLE 10.2 Data from July 1979 Pumping Test

Time	Minutes	Water level	Drawdown
0700	0	40.0	0
0715	15	40.13	0.13
0730	30	40.5	0.5
0800	60	41.19	1.19
0830	90	41.7	1.70
0900	120	42.11	2.11
1000	180	42.78	2.78
1100	240	43.32	3.32
1300	360	44.01	4.01
1500	480	44.52	4.52
1700	600	44.89	4.89
1900	720	45.23	5.23
2100	840	45.55	5.55

evaluate the straightness of the data. The appropriate fit is slightly steeper than the best-fit line indicated on the plot and will result in the transmissivity value being slightly smaller than indicated but will better represent the data at later time.

Example 10.6 brings up a caution about aquifer testing software. These programs are wonderful for plotting the data, but tend to remove the thinking part of data analysis. If one accepts a best-fit line to the

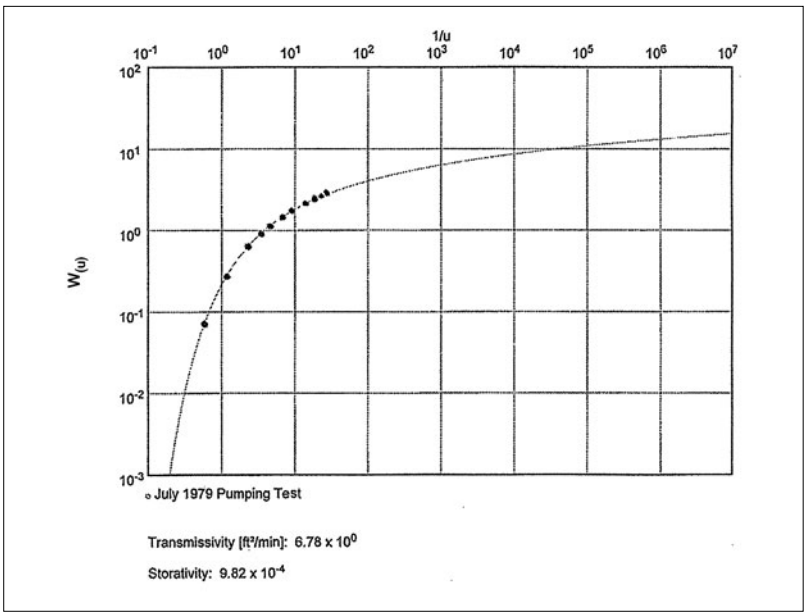

Figure 10.10a A typical Theis fit. The data are from a July 1979 pumping test, shown in Table 10.2.

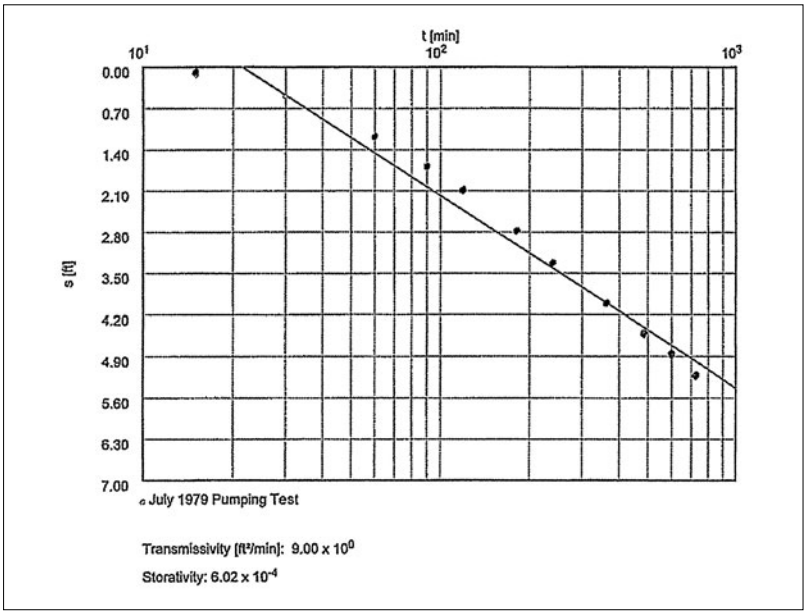

Figure 10.10b A least squares best-fit match. The data after 180 min form a straight line. (Straight line incorrectly fit by software.) The data are from Table 10.2.

data using the Cooper-Jacob (1946) method, and there are multiple slopes resulting from boundaries and other conditions, the interpretation will be wrong. Spreadsheet programs are useful for plotting data using the Cooper-Jacob (1946) method; however, plots using the Theis method are more involved. Errors result when the data plot and the well function characteristic curve are not at the same scale dimensions and curve matching is attempted. They should both have the same log-log spacing when overlaying and selecting a match point.

Once the Theis equation (Equation 10.1) has been used to obtain a transmissivity (T) and Equation 10.2 was used to solve for storativity (S) these aquifer properties are assumed to prevail throughout the entire aquifer. Therefore, these values can be used to evaluate drawdown for other pumping rates, radial distances (r), and different times of pumping (t). This is what the "nonequilibrium" part of the equation name means. This is assuming there are no boundary conditions (one of the assumptions of the Theis equation at the beginning of this section). How this is done is first a new value must be recalculated for "u" (Equation 10.2). (This allows taking into account a new position for the observation point "r" and any new time "t".) One then looks up a corresponding value for $W_{(u)}$ in Appendix D. The new drawdown is calculated using the Theis equation (Equation 10.1). Example 10.7 provides an illustration using the outcomes from Example 10.6.

Example 10.7 Assume that the aquifer properties of transmissivity and storativity are 8.8 ft^2/min and 9.8×10^{-4} respectively (obtained from Example 10.6). We want to estimate the drawdown at a distance 2000 ft away, after pumping at a rate of 1500 gpm (94.7 L/s) for 5 days. We adjust the transmissivity into units for ft^2/day:

$$8.8 \text{ ft}^2/\text{min} \times 1440 \text{ min}/1 \text{ day} = 12{,}670 \text{ ft}^2/\text{day}$$

Next, we use Equation 10.2 to recalculate a new value for "u":

$$u = \frac{r^2 S}{4Tt} = \frac{(2000 \text{ ft})^2 \, (9.8 \times 10^{-4})}{4(12670 \text{ ft}^2/\text{day}) \, (5 \text{ days})} = 0.015$$

From Appendix D the corresponding value for $W_{(u)}$ is 3.64. This is substituted into Equation 10.1, along with the new pumping rate and proper conversions (Appendix A) to make the units work out correctly:

$$s = h_o - h = \frac{Q}{4\pi T} W_{(u)}$$

$$= \frac{(1500 \text{ gal/min}) \, (1 \text{ ft}^3/7.48 \text{ gal}) \, (1440 \text{ min}/1 \text{ day})}{4\pi(12670 \text{ ft}^2/\text{day})} \, (3.64) = 6.6 \text{ ft.}$$

Single-well tests

Sometimes physical circumstances do not allow conducting pumping tests with observation wells. One reason may be that the aquifer is very deep (Belcher et al. 2001). In irrigation settings, such as in the Ogallala Formation of Kansas and Nebraska, wells are deliberately spaced far apart to reduce overlapping cones of depression. In this case neighboring wells do not make good observation wells.

In a study by Halford et al. (2006), 628 radial MODFLOW (McDonald and Harbaugh 1988) simulations of single-well pumping tests were conducted to see how well choices by analysts, using the Cooper-Jacob method (1946) compared with known transmissivities. Hydraulic properties were limited to plausible ranges. Transmissivities ranged from 10 to 10,000 m^2/day. Transmissivities of less than 10 m^2/day were excluded because here slug tests are more practical than pumping tests. A single specific storage of 5×10^{-6} m^{-1} was assigned to all aquifers because transmissivity estimates were insensitive to specific storage. Specific yields ranged from 0.05 to 0.3. Vertical anisotropies ranged between 0.02 and 0.2 and were assumed to represent a sedimentary system. Partial penetration (Section 10.5) effects in confined and unconfined aquifers were also included with penetrations ranging from 10% to 100% of the aquifer. All simulations were conducted for 2 days.

Pumping wells were simulated in column 1 and aquifer material was simulated with columns 2 through 99. Column 2 was 0.02-m wide and the remaining columns were 1.15 times the width of the previous column. The 100-m thick aquifers were uniformly subdivided into 100 rows. All models had no-flow lateral boundaries, initial heads of 0 m, and a single stress period of 50 time steps. The first time step was 0.1 s in duration. Each successive time step was 1.3 times greater than the previous one.

Cooper-Jacob transmissivity was estimated for each single-well test by a mechanistic approach (set up in an Excel spreadsheet) and separately by six analysts, including the three authors and three volunteers. A semilog slope was defined by the drawdowns at 0.5 and 2 days after pumping started. A minimum time of 0.5 day was selected as a compromise between avoiding the early-time complications due to wellbore storage, partial penetration, and water-table effects and assumed measurement sensitivity for actual aquifer tests. Experience guided analysts' best fit of semilog slopes.

Cooper-Jacob (1946) transmissivity estimates in confined aquifers were affected minimally by partial penetration, vertical anisotropy, and interpretative technique. Transmissivities of 100 m^2/day or greater were estimated within 10% of their value in all but one case (Halford et al. 2006). A steady additional drawdown from partial penetration and vertical anisotropy was established before 12 h of pumping had elapsed. Confined aquifer test results were unambiguous and transmissivity estimates varied little among analysts.

Transmissivities of unconfined aquifers were overestimated with a mechanistic application of Cooper-Jacob (1946). More than 75% of known transmissivity values between 10 and 1,000 m^2/day were overestimated. Estimates averaged twice known transmissivity values in this range. About 80% of known transmissivity values between 1,000 and 10,000 m^2/day were estimated within a factor of two (Halford et al. 2006). Transmissivity estimates were not improved by interpreting results with an unconfined analytical solution instead of using the Cooper-Jacob method (1946).

Hydraulic conductivity of confined aquifers was unambiguously determined as the transmissivity estimate divided by aquifer thickness, rather than the screen length, whenever transmissivity was 100 m^2/day or greater. At low transmissivity values (<10 m^2/day) hydraulic conductivity estimates using the screen length were believed to be appropriate. Hydraulic conductivity estimates ranged from 1.6 to 8 times known values where transmissivity estimates were divided by screen length (see Section 10.5).

Casing storage

Schafer (1978) pointed out that early-time pumping test data may lead to an erroneous interpretation of transmissivity. If the casing is of large diameter and the pumping rate is small, most of the water will

be coming from the casing (emptying the bucket, so to speak). For example, pumping an 8-in (20.3-cm) well at a rate of 5 gpm (18.9 L/min) will not result in much stress of the aquifer nor create much drawdown. In a single-well test, this can be especially important. A plot of the time-drawdown data may indicate a relatively steep-sloped pattern during the first 10 or 20 min (emptying the casing), followed by a flattening of the slope as water from the aquifer begins to come in through the screened interval. Fitting a slope to the early-time data to calculate transmissivity will result in under-estimating the appropriate value. Schafer (1978) suggested that a critical time (t_c) be calculated to indicate when casing storage is no longer contributing to the yield of a well. The t_c can be calculated by using Equation 10.21, sourced from Driscoll (1986):

$$t_c = \frac{0.6(d_c^2 - d_p^2)}{Q/s} \qquad t_c = \frac{0.017(d_c^2 - d_p^2)}{Q/s} \tag{10.21}$$

where t_c = time in minutes, when casing storage is negligible
d_c = inside diameter, in inches, of well casing
d_p = outside diameter, in inches, of pump riser pipe
Q/s = specific capacity of the well in gpm/ft at time t_c

where t_c = time in minutes when casing storage is negligible
d_c = inside diameter, in millimeters, of well casing
d_p = outside diameter, in millimeter, of pump riser pipe
Q/s = specific capacity of the well in m^3/day/m at time t_c

Being able to determine when t_c has occurred becomes an iterative process, because Equation 10.21 assumes that the drawdown at t_c is known. To begin one must start by selecting a drawdown and inserting this into Equation 10.21 to calculate t_c. The real drawdown at the calculated t_c is used to recalculate a new t_c. If the new t_c does not change much from the previous value, then the "true" t_c has been determined.

Example 10.8 A pumping test was conducted at 6 gpm in a 6-in (15.2-cm) domestic well near Yellowstone National Park. The time-drawdown data are shown in Figure 10.11. The inside diameter of the casing is 6 inches and the outside diameter of the riser pipe was 1.5 inches (3.8 cm). An iterative method to determine time critical was used to determine when the effects of casing storage were negligible.

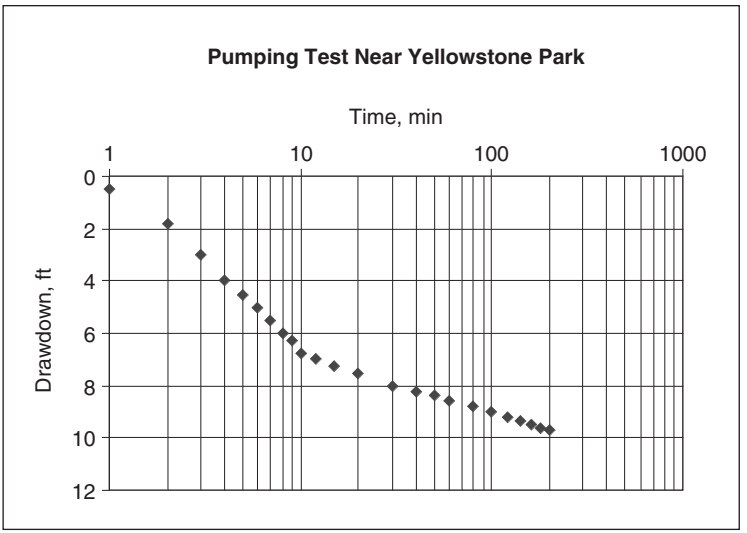

Figure 10.11 Time-drawdown data from a pumping test conducted near Yellowstone National Park.

The first guess for t_c is at a drawdown of 7 ft. Using Equation 10.21: $t_c = \dfrac{0.6(6^2 - 1.5^2)}{6/7} = 23.6$ min. The drawdown at 23.6 min is 7.6 ft. We substitute again this drawdown into Equation 10.21 and recalculate t_c. $t_c = \dfrac{0.6(6^2 - 1.5^2)}{6/7.6} = 25.7$ min. The process is repeated again and we obtain 26.1 min, which is a small change. The data before 26 min are not used in calculating the transmissivity.

Leaky-confined and semiconfined aquifers

Storativities between 0.001 and 0.03 suggest that the aquifer could be leaky-confined or semiconfined. The basic difference between a leaky-confined aquifer and a semiconfined aquifer is resolved through extending the time of pumping and recording the drawdown response. Reporting that an aquifer is confined or unconfined when the storativity falls between confined and unconfined values suggests a lack of understanding of the aquifer system, miscalculations, or errors in interpretation (Example 10.9).

Example 10.9 The following personal story may help illustrate an example of improperly reporting storativity values. Back in the mid-1980s the author participated in writing up a report of aquifer test data results on the Eocene Wasatch Formation for a coal gasification study (Borgman et al. 1986). Dr. Shlomo P. Neuman of the University of Arizona was one of the reviewers, and his pen

bled freely where I had incorrectly said that a particular unit was confined. In retrospect, the unit was semiconfined. A particular carbonaceous shale unit was confining a sandy aquifer unit where it existed; however, there were places where the shale unit pinched out and thickened once again, allowing the aquifer unit to become connected to another unconfined sandy unit above. Had the author been more experienced or aware, the data would have properly been interpreted.

Both leaky-confined and semiconfined aquifers initially follow the Theis type A curve (discussed soon) and then flatten, indicating a recharge condition (Figure 10.12). Physically, induced recharge may be through a leaky **aquitard**. The rate of **leakance** is determined by the hydraulic conductivity of the aquitard unit and the head differential. The hydraulic conductivity of the aquitard would normally be a couple of orders of magnitude lower than the aquifer unit. In this example, the stress caused by the pumping rate induces a change in head sufficient to cause groundwater to move from above or below the aquifer unit through the aquitard into the aquifer being pumped. Since all sources of recharge are moving through a semiconfining unit and is not releasing any storage, the flatness of the recharge effect on a Theis curve will continue in a horizontal manner (Lohman 1979) (Figure 10.12).

When the drawdown data over time fall below the Theis curve on a log-log plot and remains curved rather than becoming flat (a recharge effect),

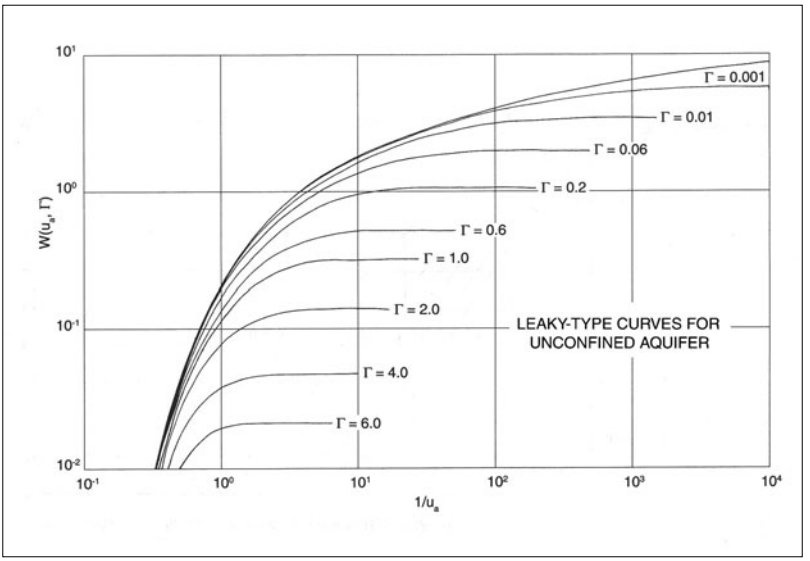

Figure 10.12 Leaky-type curves with the flat response being values of r/β. From bottom to top, r/β values are 2.0, 1.5, 1.0, 0.6, 0.4, 0.2, and 0.1. The smaller the r/β value, the closer the curve is to the reverse Theis type. (*Used by permission from Prentice Hall Publishing, Upper Saddle River, New Jersey*)

it is possible that the semiconfining layer is releasing water from storage. This occurs because the semiconfining layer is saturated and has a head higher than the head in the aquifer being pumped (Figure 10.13). This head differential may cause the aquitard to release water from storage, in an attempt to reach equilibrium. Type curves for this approach were created by Hantush (1960). The approach is to fit the field time and drawdown (s, or $h_o - h$) data to one of the beta (β) curves and select a convenient match point to obtain values for $H(u, \beta)$, $1/u$, time, and drawdown (s).

In a semiconfined aquifer scenario, aquitard units may pinch out laterally to encounter another part of the aquifer that is actually unconfined. The data are plotted and the flattening of the data below the Theis curve reflects a time delay of water from the aquifer yielding to the well as an apparent source of recharge or from an increased saturated thickness. Another source of recharge may come from the semiconfining layers themselves or through induced recharge from a layer above or beneath the aquifer being stressed. Most confining layers are leaky to one extent or the other. As in the leaky confined scenario, the initial drawdown tends to follow the confined Theis curve. As the aquifer becomes stressed and the head lowers in the pumping well, the head change stimulates leakage from above or below to act as recharge to the system. The result is a flattening of the curve rather than following the Theis curve. Hantush (1956) developed a whole suite of these curves. They are also given in Lohman (1979). If the semiconfining layer pinches out, the new saturated thickness becomes stressed again resulting in the

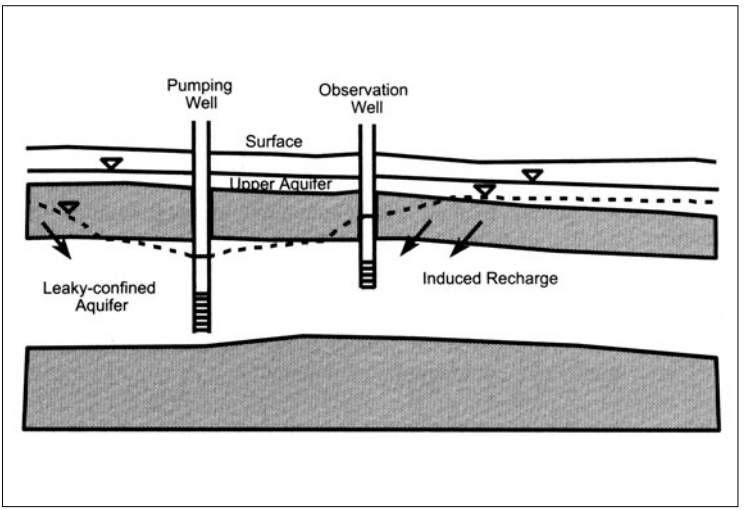

Figure 10.13 Pumping test conducted in a leaky-confined aquifer, with induced recharge through a silty layer, separating the upper and lower aquifer. The cone of depression is indicated by a dashed line.

data following a Theis nonequilibrium (Type B) curve once again. The "climbing" of the drawdown data back onto the Type B curve at a later time is known as **delayed yield** (Neuman 1972, 1975, 1979, 1987; Boulton 1973) (Figure 10.14). Fitting the later-time data results in roughly a two- to three-order of magnitude shift (increase) in the calculation of storativity. This puts the results closer to the unconfined range. If one only fits the early-time data, ignoring the later delayed-yield response, a lower than appropriate storage coefficient results.

Figure 10.14 shows the delayed yield type curves after curves developed by Boulton (1973), where the well function is a function of $W(u_A, u_B, \beta)$. On the left-hand side is a Theis curve, known as the Theis Type A curve. This curve represents the type curve for confined aquifers (like we have already discussed). The scale for "$1/u_A$" runs along the top (x-axis) of the graph, so the match point where $W(u_A)$ and $1/u_A$ both equal 1.0 is to the left of this curve. On the right-hand side is another Theis curve, known as the Theis Type B curve for unconfined aquifers. The scale for "$1/u_B$" for this curve runs along the bottom (x-axis) of the graph. The match point where $W(u_B)$ and $1/u_B$ both equal 1.0 is also to the left of this curve, but located three log scales (orders of magnitude) to the right of the confined Theis Type A match point.

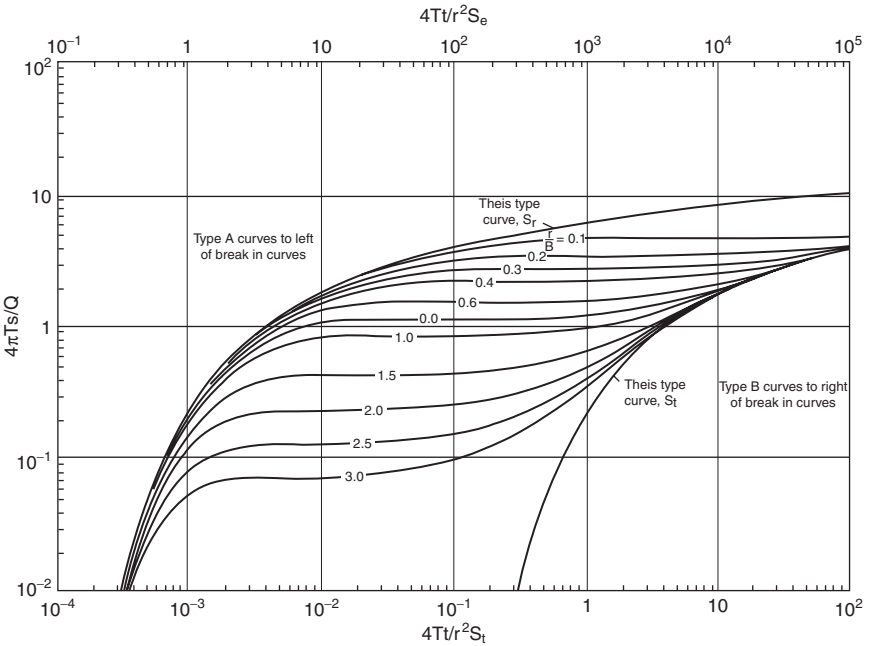

Figure 10.14 Delayed-yield type curves modified from Lohman (1979) after Boulton (1973). The scale for $1/u$ for Type A curves runs along the top and the scale for the Type B curves runs along the bottom. The numbered curves represent different β values. *(Used by permission from Prentice Hall Publishing, Upper Saddle River, New Jersey.)*

How does one fit the data? Early on, data follow the confined Theis Type A curve, because of the "confined environment" caused by the semiconfining unit. As the cone of depression extends outward into an area where the semiconfining unit "pinches out," the aquifer thickness increases. At this point in time the pumped aquifer thickness combined with the thickness of another unit above the "pinched out" semiconfining layer is "seen" as a source of recharge; hence, the flattening of the curve. Over time the new saturated thickness becomes stressed as pumping continues and the drawdown data begin to climb forming a Theis curve once again, where the second Theis curve represents the Type B curve. If a plot of the data (drawdown versus time in log-log scale) over time indicate this type of shape then it is appropriate to use the second (Type B) match point for calculations of transmissivity and storativity. With the shift to the right in match point from the confined (Theis Type A) to the unconfined (Theis Type B) the storativity will increase significantly. Why this is important will become more evident in the next section (distance-drawdown relationships).

The series of curves between the two Theis curves represent β-values. The β-value of the bottom-most curve is 3.0 and the β-value becomes smaller with successive curves in the upward direction. A curve with a β-value of 3.0 indicates that recharge from an increased thickness was detected almost immediately; while a β-value of 0.3 indicates that this process occurred much later in the test. The response observed is a function of the geologic setting (where the semiconfining unit pinches out), the pumping rate, and the position of the observation well relative to the pumping well and so forth.

A similar delayed-yield shape response can occur from at least a couple of other geologic settings. The geology of the first is described in Example 6.1 in Chapter 6. Here, an alluvial aquifer is overlain by silty (mine tailings) materials. The hydraulic head (Chapter 5) of the alluvial aquifer is approximately 6 in (15.3 cm) above the top of the alluvial materials (within the silty materials zone). Pumping of the alluvial aquifer results in lowering the head below the confining silty materials (see Example 10.9), thus allowing gravity drainage to occur. Another type of geologic setting is described in Section 10.6 (Fracture-Flow Analysis). Geologic materials that are fractured release water from the larger fractures readily. Over time and with increased aquifer stress from pumping, the smaller fractures and matrix materials of some rocks release water also from gravity drainage, at later time, reflected in the time-drawdown plot as a recharge response. Once the stress from pumping "catches up" with the recharge release a delayed-yield-like response occurs in the data as a resurgence of increased drawdown.

The question becomes, is this a leaky-confined aquifer or really a semiconfined aquifer with delayed yield? This question can only be

answered by running the pumping test sufficiently long (2 to 3 days, depending on the geologic setting). If the semiconfining layer extends far enough away, then the recharge effect will remain flat as in Figure 10.12, while one that pinches out within the reach of the cone of depression will show delayed yield if pumped long enough.

Understanding the significance of storativity values is important in evaluating aquifer conditions and the proper application of problem evaluation, such as the impacts of pumping wells on neighboring wells. The radial distance from the pumping well to zero drawdown in the cone of depression is known as the **range of influence**. This happens to be a sensitive parameter according to the storativity value (Example 10.10).

Example 10.10 A pumping test was conducted near Miles Crossing (Chapter 6, Figures 6.4 and 6.5) in a fluvial setting impacted by mine tailings from flooding. The pumping test was conducted during the Montana Tech hydrogeology field camp. Well MT97-2 is the pumping well, and the other three are observation wells. The pumping rate was approximately 4.5 gpm (17 L/min). The results of each log-log plot at the same scale are shown in Figures 10.15a, b, c, and d, from top to bottom, respectively. The direction of groundwater flow is generally from east-northeast to west-southwest.

One notes the immediate confined-like response followed by a recharge event (flattening of the curves). It appears that the static water level is up in the finer-grained silty materials and the initial response is confined, followed by a draining of the silty materials. Near the end of the test, it is apparent in the pumping well that delayed yield is beginning indicated by the upward trend (Figure 10.15b). It is interesting to see the same phenomenon with a different perspective in a Cooper-Jacob plot (Figure 10.16). Figure 10.16 represents the same time and drawdown for observation well MT97-3, but in semilog form. Notice the shift in t_0 from the early time to the position at late time where delayed yield is occurring. This results in a significant change in the estimate of storativity. Delayed yield did not occur until approximately 800 min. Had the pumping test been terminated at 600 min, this phenomenon would not have been observed. Notice also if a computer software package had selected a "best-fit" line through all the data, a very different interpretation would have resulted.

Specific yield and vertical hydraulic conductivity from unconfined aquifer tests

Unconfined aquifer tests lend themselves to making additional calculations of aquifer properties. The time-drawdown data have a tendency to follow two Theis Type curves (both A and B). Because of this there is an opportunity to evaluate the early-time data and the late time data, and obtain a beta (β) value for the data that follow one of the flattened curves between the Theis curves. In addition to calculating transmissivity values, one can also evaluate the changing values of storativity with time. Furthermore

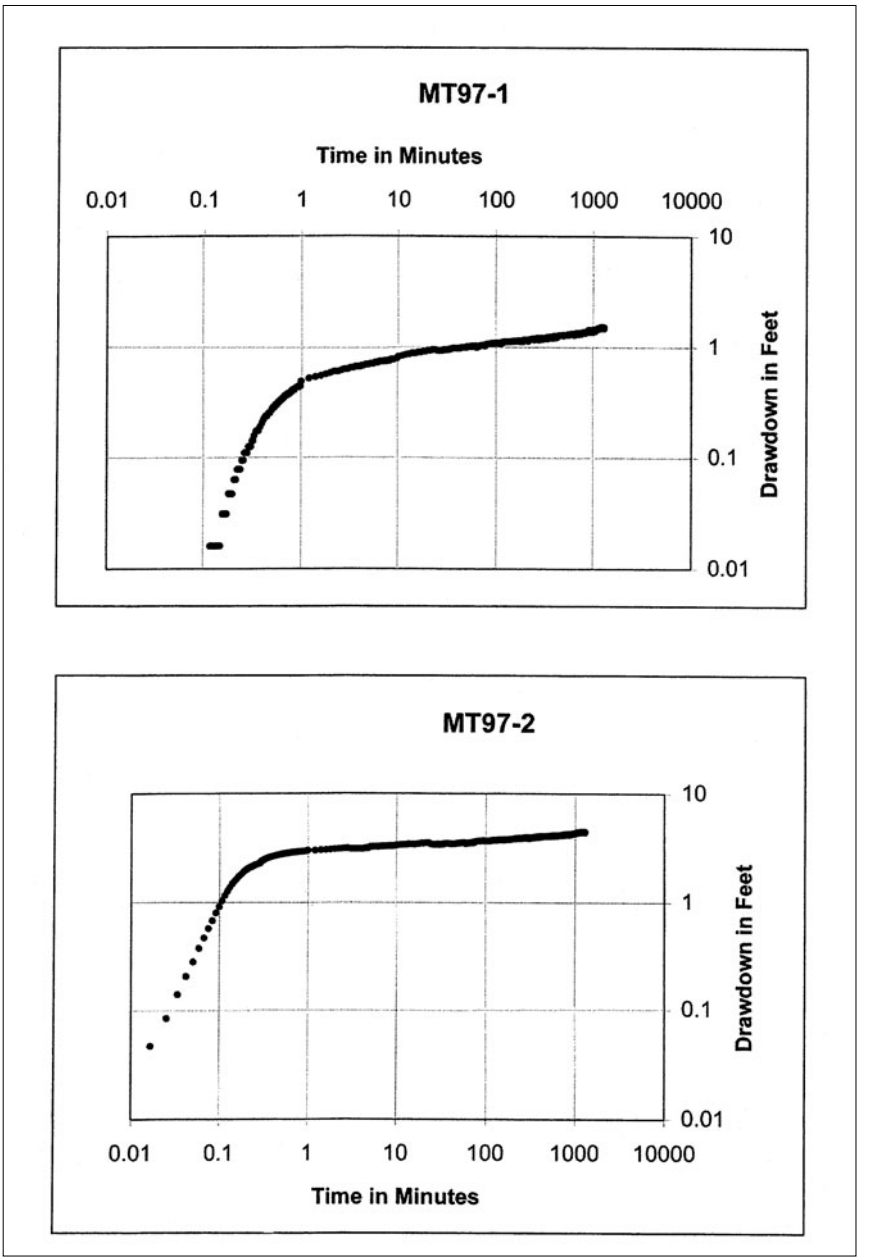

Figure 10.15a and b Theis plots for the pumping well MT97-2 and an observation wells, from top to bottom, respectively. Each indicate the beginnings of a delayed yield effect at time >800 min.

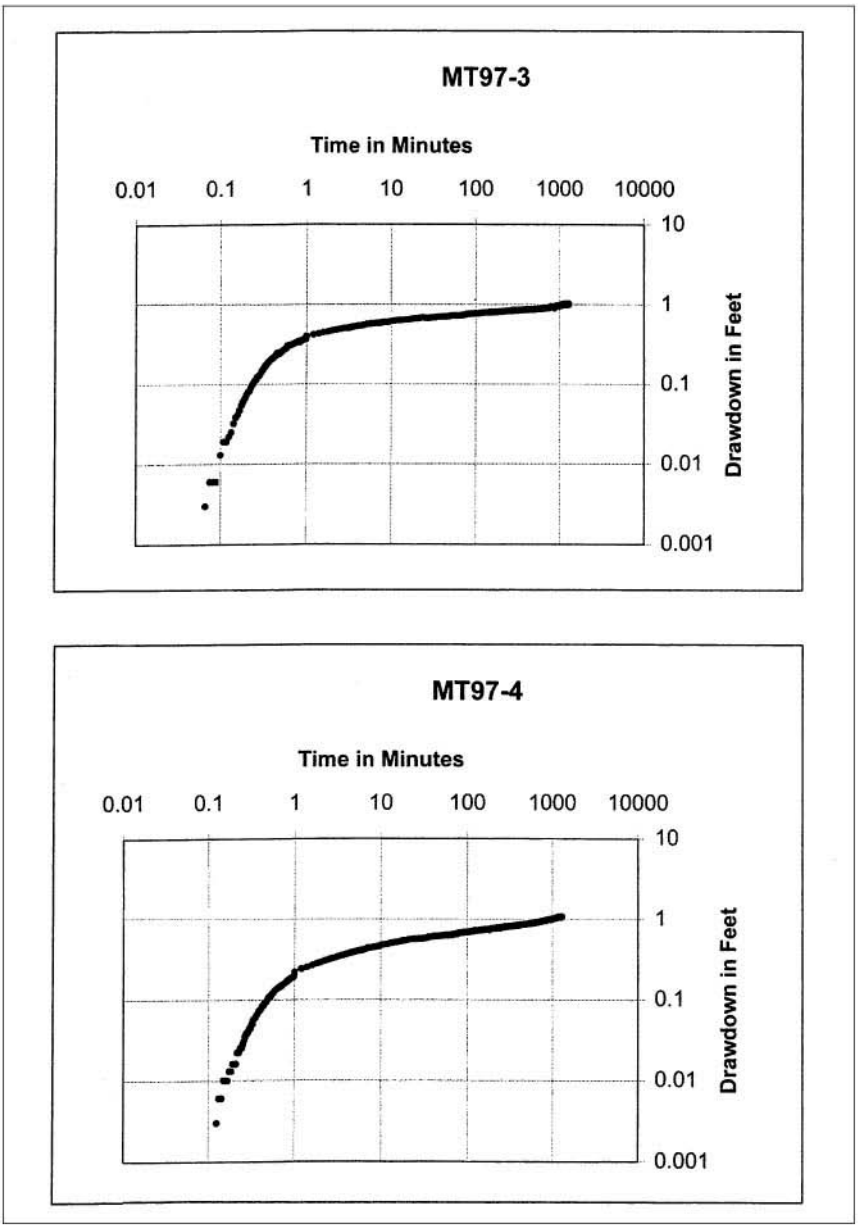

Figure 10.15c and d Theis plots for two observation wells from top to bottom, respectively. Each indicate the beginnings of a delayed yield effect at time >800 min.

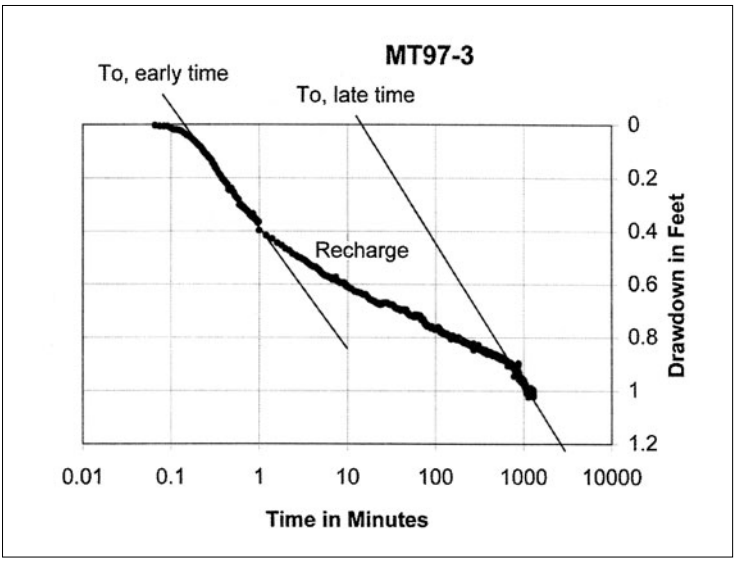

Figure 10.16 Copper-Jacob plot of observation well MT97-3 in Miles Crossing pumping test (compare with Figure 10.15c). Note how delayed yield is displayed as the second straight-line slope.

one can use the β-value to calculate specific yield and estimate the vertical hydraulic conductivity. How this is done is presented in Example 10.11.

In Chapter 3 the property of aquifer storativity is discussed. The low storativity of confined aquifers results in immediate changes in head with barometric pressure change or when a pumping stress is imposed. Decreases in pressure head from pumping cause the compressive stresses acting on the aquifer to increase. During the very early time of any aquifer test this confined-like response from changes in compressive stresses acting on the mineral skeleton accounts for the drawdown data following the Theis Type A curve. As gravity drainage begins (specific yield), a recharge response (flattening of the curve) is seen in the time-drawdown data plot. Once gravity drainage "catches up" with the pumping stress, the time-drawdown data begin to "climb" up on the Theis Type B curve. This means that even a very coarse-grained aquifer will display an initial confined-like response followed by a delayed yield pattern, even if the confined response is limited to the first minute of the aquifer test. This is discussed in more detail in Chapter 11 in Section 11.3 (the under-damped slug-test case).

When evaluating the early-time data the transmissivity and storativity are calculated using Equations 10.4 and 10.5 using the match point from the Theis Type A curve. As the time-drawdown data drop below the Type A curve they will follow a more flattened curve, with a particular β-value, that ultimately begins to follow the Theis Type B curve. The

drawdown at the match point associated with the late-time data following the Theis Type B curve is used along with Equation 10.4 to calculate transmissivity. However, a slight modification to Equation 10.5 is used to calculate the specific yield (Equation 10.22). We begin with defining u_B in Equation 10.22 and perform the algebra to obtain Equation 10.23.

$$u_B = \frac{r^2 S_y}{4Tt} \tag{10.22}$$

$$S_y = \frac{4Ttu_B}{r^2} \tag{10.23}$$

where all terms have been previously defined and "t" is the time at the Type B match point. Recall that at the match point one typically uses the point where $W(u_B, \beta)$ and $1/u_B = 1.0$, so if another point is used as the match point one must be aware that the value in Equation 10.21 may be smaller than 1.0. The relationship for β is used to obtain an estimate for the vertical hydraulic conductivity, where β is defined in Equation 10.24.

$$\beta = \frac{r^2 K_v}{b^2 K_h} \tag{10.24}$$

where r = radial distance to the observation well
b = saturated thickness, and
K_v and K_h are the vertical and horizontal hydraulic conductivities respectively

Remembering Equation 3.12, where $T = K_h \times b$ and rearranging Equation 10.24 we obtain a relationship to estimate the vertical hydraulic conductivity (Equation 10.25) (Fetter 1994).

$$K_v = \frac{K_h b^2 \beta}{r^2} \tag{10.25}$$

Example 10.11 A pumping test was conducted to estimate the aquifer properties for dewatering purposes at a mining operation in Florida. The relative coordinates for the pumping well (PW) and three observation wells (Obs1, Obs2, and Obs3) are shown in Table 10.3. The geologic setting is a quaternary sand aquifer, where each well was approximately 50 ft deep and the saturated thickness averaged 43 ft. The pumping rate was 82 gpm (5.2 L/s) and the test was run for 24 h. The time-drawdown data were plotted with Aqtesolv 3.5, where each curve was fit using the Neuman method as a solution (Figures10.17a, 10.17b, and 10.17c). Equally good fits can also be obtained using the Moench (1996) solution. The results are also listed in Table 10.3.

The transmissivities are remarkably uniform and all of the time-drawdown data plots indicate a delayed yield response. Obs1 and Obs3 are south and

TABLE 10.3 Locations of the Pumping Wells and Observation Wells for a Pumping Test Conducted in Florida

Well	Easting, ft.	Northing, ft.	Radial dist., ft.	Transm., ft^2/day	Storativity	Specific yield	Beta
PW	307.7	315.1					
Obs1	292.3	317.9	15.6	960	0.0015	0.14	0.058
Obs2	323.0	359.7	47.2	970	0.0005	0.025	0.075
Obs3	293.4	212.3	106.6	940	0.0007	0.085	3.26

southeast of the pumping well respectively, and indicate specific yields typical of an unconfined aquifer. Obs2 is located north-northeast of the pumping well and indicates a more semiconfined response, with a value at the low end of the unconfined range. From the relationship of saturated thickness (b) and transmissivity (T) above the horizontal hydraulic conductivity (K_h) is estimated to be 22 ft/day (6.7 m/day). Substituting the β-values from Table 10.3 and the other known quantities into Equation 10.24 we can estimate the vertical hydraulic conductivity (K_v). An example calculation is shown for well Obs1.

$$K_v = \frac{22 \text{ ft/day} \times 43 \text{ ft}^2 \times 0.058}{(15.6 \text{ ft})^2} = 0.44 \text{ ft/day}$$

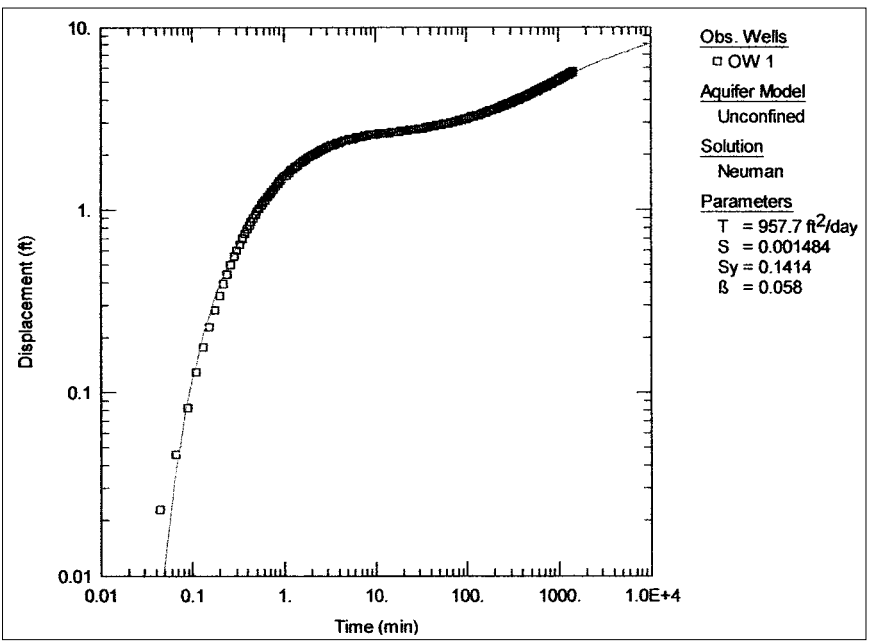

Figure 10.17a Florida pumping test at 82 gpm. Data are from observation well 1 located 15.6 ft (4.8 m) south.

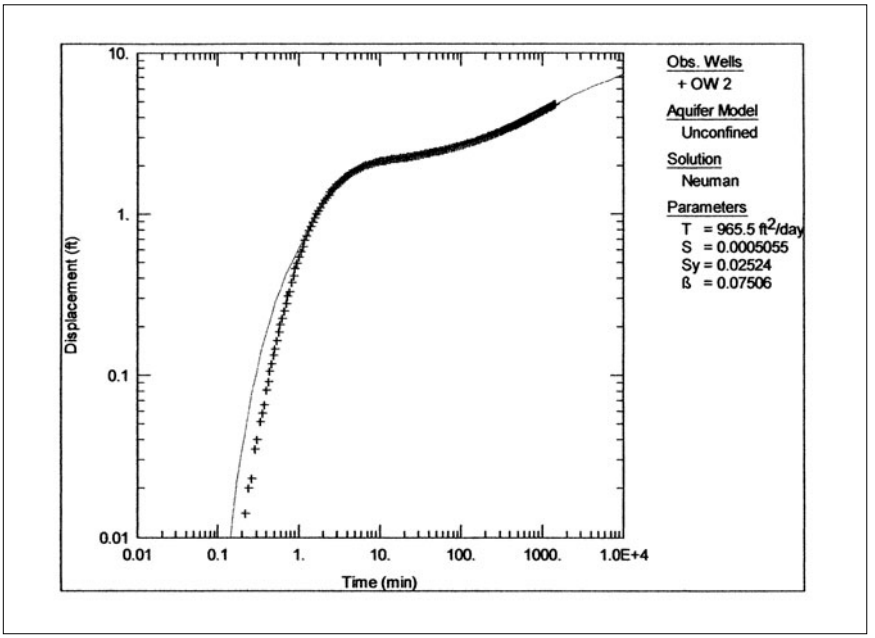

Figure 10.17b Florida pumping test at 82 gpm. Data are from observation well 2 located 47.2 ft (14.4 m) north northwest.

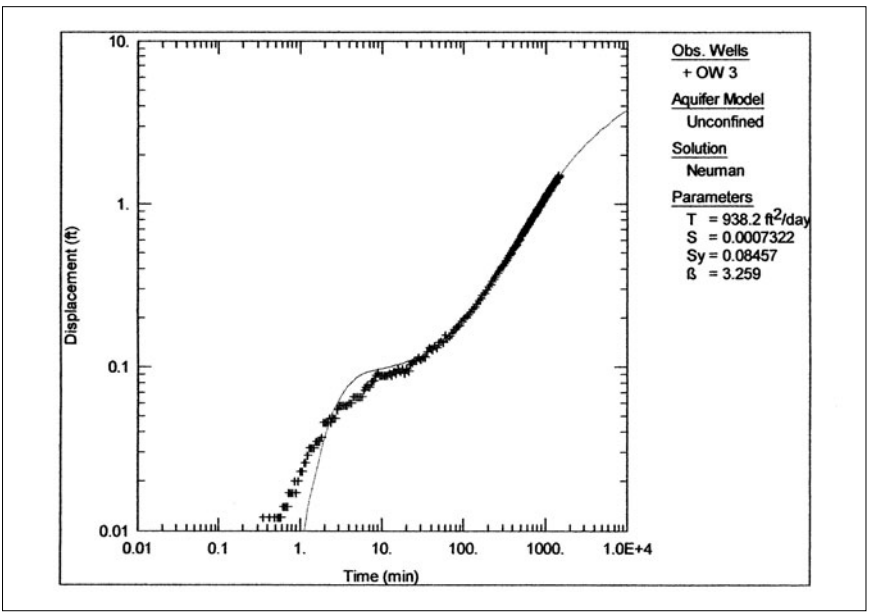

Figure 17c Florida pumping test 82 gpm. Data are from observation well 3 located 106.6 ft (32.5 m) southeast of the pumping well.

The K_v values for Obs2 and Obs3 are 0.062 and 0.53 ft/day, respectively. Notice how similar the K_v values are for the two wells with similar storativity values (Obs1 and Obs3) while Obs2 is indicating a K_v an order of magnitude less. Obs2 also showed a specific yield at the border of the unconfined range.

Distance-drawdown relationships

Back in 1906, G. Thiem developed a method of estimating transmissivity and storativity after steady-state conditions have been achieved (i.e., the cone of depression had stabilized). Once steady state occurs, time becomes inconsequential, and the hydraulic properties of an aquifer estimated from drawdown becomes a function of distance.

The Cooper-Jacob (1946) time-drawdown approach is modified to plot drawdowns at various radial distances from the pumping well at a chosen time "t." These plots are known as **distance-drawdown plots** (Jacob 1950). By graphing drawdown (arithmetic scale) versus distance (on a log scale) a straight-line fit results (Jacob 1950) if the aquifer is homogeneous and isotropic. Estimates of the hydraulic properties can also be made, if the assumption of u being sufficiently small (0.02, previous section) can be made. The intercept where the straight-line fit crosses the zero drawdown represents the range of influence of the cone of depression (Figures 10.1 and 10.2). In other words, the range of influence is the radial distance from the pumping well to zero drawdown.

There is a powerful relationship between the Cooper-Jacob (1946) time-drawdown plot and a distance-drawdown plot (Jacob 1950). The slope of the straight-line fit (drawdown per log cycle of distance) of the latter is exactly twice that of the time-drawdown plot (drawdown per log cycle of time). The reason for this can be seen by evaluating Equation 10.10. Within the "log" term notice that time (t) is to the first power and radial distance (r) is to the second power. The double slope results from the following relationship:

$$\log(r^2) = 2 \times \log(r) \tag{10.26}$$

This ratio is a fixed relationship. The approach is to choose a particular point in time. This "fixes" the shape of the cone of depression. From this an estimation of the radius of influence can be estimated with only one observation well. Clearly, more observation wells in different azimuth orientations and varying distances from the pumping well would improve the understanding of the "true" distance-drawdown effect. A comparative plot of drawdown versus distance can be made from several different observation wells during a pumping test to see if a straight-line plot results. If this is true, it indicates that the cone

of depression is symmetrical around the pumping well. If this is not true, there is likely some anisotropy to the shape of the cone. The equations used to calculate transmissivity and storativity analogous to Equations 10.16 and 10.20 using consistent units are (note the difference in the denominator):

$$T = \frac{2.3Q}{2\pi\Delta s} \tag{10.27}$$

$$S = \frac{2.25Tt}{r_0^2} \tag{10.28}$$

where T, t = as described previously
r_0 = range of influence, straight-line projection of the distance-drawdown curve up to where it intersects the zero-drawdown axis

Example 10.12 A mining operation producing railroad ballast required water to provide dust control for their operations (Figure 10.18). They spent two years preparing for the operation and had ignored the water issue until the end. A wildcat well drilled over 570-ft (173-m) deep near their operations failed to produce water. Approximately 0.8 mi (1 to 1.5 km) to the south is a small community of approximately 60 persons, including a recreational vehicle park. Each home or business has its own well and septic tank. The geology consists of approximately 50 ft of sediments overlying granitic rocks (see Figure 9.30). The production zones for wells are in fractures in granite that

Figure 10.18 Mining operation producing ballast.

parallel a creek flowing down from the mountains to the east and from the upper sandy sediment units. The mining company made a deal with a local resident to drill a well on his property that could pump water up the hill to the north. When the drill rig was set up in the yard, the residents started asking questions.

The author was asked to represent the mining company in answering a "few questions" at a public meeting. Unaware of the sensitive nature of the problems to be discussed, he agreed to be present. Before the meeting, the author obtained lithologic logs for each of the wells in the area. By evaluating the production testing performed on each well recorded on the well log, an estimate of the transmissivity and storativity were made. By manipulating Equation 10.28, an estimate of the range of influence for the proposed pumping rate could be performed. The transmissivity was estimated using a specific capacity equation for fracture flow (Section 10.3), and the storativity of the granite layer was estimated to be 0.001. A time of 100 days continuous pumping was used as a worst-case scenario.

$$r_0 = \sqrt{\frac{2.25(13 \text{ ft}^2/\text{day}) \times 100 \text{ days}}{0.001}} = 1{,}710 \text{ ft } (520 \text{ m})$$

At the meeting, the room was filled with angry residents. By the time the author was given the floor to speak, everyone was at peak irritation, similar to a hissing group of geese. (Ironically, the lady who was most upset did have geese that attacked us every time we took a water level in her well). This distance-drawdown analysis was used to tell all residents who lived more than 2,000 ft from the proposed well that they could go home. During the meeting, the mining company was committed to a pumping test and groundwater flow model to evaluate pumping and recovery scenarios. This solution appeased the residents and ultimately led to a practical solution.

Predictions of distance-drawdown from time-drawdown

As was mentioned, a powerful predictive tool results from the slope relationships between time-drawdown and distance-drawdown graphs. If a short-duration pumping test (less than 24 h) is conducted and a straight-line relationship develops, the straight line of the time-drawdown graph can be extended to longer periods of time (days, weeks). Once the drawdown at the longer period of time has been determined, a distance-drawdown graph (using twice the slope of the time-drawdown graph) can be used to estimate the range of influence of the cone of depression. This is useful when evaluating interference effects on other senior water users in the area.

If you have no pumping test data because you are trying to get a permit to drill a well, you can use Equation 10.28. Notice that if you estimate a value for T and S, you can obtain r_0 for a particular time (Example 10.13).

Example 10.13 Suppose there is a need to irrigate 30 acres (12.1 ha). You need to find out from your local state agency if any wells exist near the proposed well site. The well logs may give an idea of how deep it is to water and what lithologies the wells are completed in. They also may indicate how much water they make. Since $T = K \times b$, if an estimate for hydraulic conductivity can be obtained, and the saturated thickness (b) is known, a value for T can be estimated (Your estimate of T should be conservative). The storativity can be estimated from the lithologic conditions (Chapter 3) and whether the aquifer is confined (10^{-3} to 10^{-6}) or unconfined (0.03 to 0.30). In this example, a range for T and various times should be used to evaluate impacts to other wells (Table 10.4). By estimating the drawdown in the pumping well and the range of influence (distance to zero drawdown) one can perform a distance-drawdown plot to evaluate the impacts to neighboring wells. To produce Table 10.4, it was necessary to first use Equation 10.2 to calculate u. It was assumed for the pumping well, that the effective radius was 1 ft (0.3 m). A corresponding value for W_u was looked up in Appendix D. The drawdown was calculated using Equation 10.1. As a sample calculation, suppose the transmissivity is estimated to be 10,000 ft^2/day and the storativity is estimated to be 0.15, the range of influence after 30 days from rearranging Equation 10.28 is:

$$r_0 = \sqrt{\frac{2.25(10{,}000\ \text{ft}^2/\text{day}) \times 30\ \text{days}}{0.15}} = 2{,}121\ \text{ft}\ (647\ \text{m})$$

From Example 10.13, notice that the pumping rate Q was not used to evaluate r_0. The range of influence is dependent on T, S, and time (t). Since, the pumping rate does *not* affect the range of influence (see Equation 10.28), what is observed then is how the pumping rate affects the slope of the distance-drawdown plot. For a particular time t, the r_0 is fixed, but the slope of the distance-drawdown line drawn back to the vicinity of the pumping well depends on the pumping rate (Figure 10.19). Notice that the drawdown in Figure 10.19 at approximately 160 ft is expected to be 1.0 ft (0.3 m) for the pumping rate of 125 gpm (425 L/min).

TABLE 10.4 Comparison of Drawdowns, Transmissivity, and Time

Trans-missivity	1/3 day		30 days		60 days		180 days	
ft^2/day	Draw down @1 ft	radius of influ-ence ft	Draw down @1 ft	radius of influ-ence ft	Draw down @1 ft	radius of influ-ence ft	Draw down @1 ft	radius of influ-ence ft
1000	16.3	71	24.9	671	26.2	949	28.3	1643
3000	6.1	122	9.0	1162	9.4	1643	10.1	2846
5000	3.9	158	5.6	1500	5.9	2121	6.3	3674
10000	2.1	224	2.9	2121	3.1	3000	3.3	5196

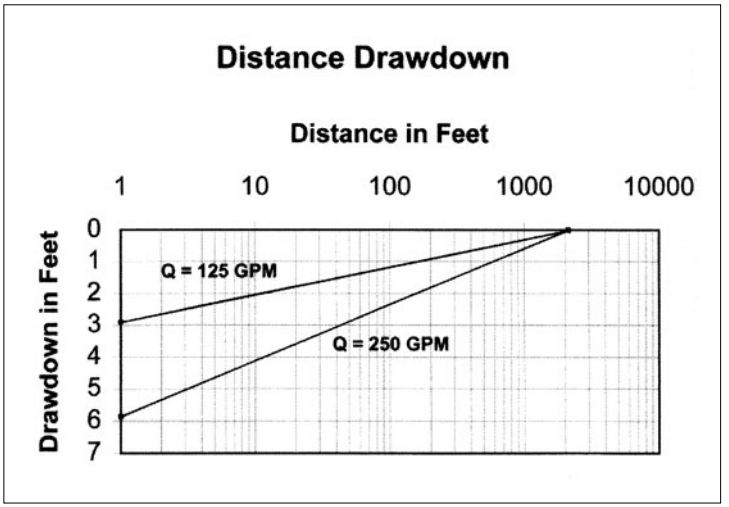

Figure 10.19 Distance-drawdown relationship assuming $T = 10{,}000$ ft^2/day, $S = 0.15$, and time = 30 days.

For most practical problems, the distance (r) at the pumping well is the **(effective radius, r_e)**, or the distance out to where the formation was disturbed during drilling (damage zone Figure 9.7, Chapter 9).

The Cooper-Jacob (1946) method of time-drawdown and Jacob (1950) method of distance drawdown are a modification of the Theis equation and assume that u is small. The Theis method is always a valid first approach to evaluating pumping-test data, and the Cooper-Jacob (1946) and Jacob (1950) methods are valid when the time (t) is sufficiently large or radial distance (r) is sufficiently small. It is useful to evaluate data using as many methods as possible. Each may help provide a different perspective and aid in a better interpretation.

Recovery plots

If you are running a pumping test, it makes a lot of sense to also collect the **recovery data** once the pump is turned off. There are a number of errors made in evaluating recovery data. There is a tendency to plot the recovery versus time in a similar manner as in a Cooper-Jacob (1946) plot. This does not work out. Instead the **residual drawdown** versus time should be plotted. Once the pump and generator are shut off, the data logger should be activated or "stepped" (Chapter 9) to collect recovery data. If this is being done manually, a similar frequency of data collection should be taking place as when the pumping test started (Chapter 9). As one might expect the early-time recovery data changes quickly at first and then slows down over time. One must be careful to

make sure there is a check valve in the pump *or* water from the discharge line and riser pipe will drain back into the well turning the impellers backward and giving a "false" recharge.

When performing a residual drawdown versus time plot the following information is needed: the time since pumping started (t), the time since pumping stopped (t'), and the residual drawdown (s') (The distance from static conditions to the actual water level). The plot is the residual drawdown versus the *ratio of* t/t', where residual drawdown is in arithmetic scale and the ratio of t/t' is in log scale. This produces a relationship where the early time data are indicated by large numbers and the late-time data become smaller as the ratio of t/t' gets closer to 2.0 more or less. If a straight-line relationship develops, then projecting the straight line to where the residual drawdown becomes zero represents the time at which full recovery will take place. Theoretically, this should occur at the projection to where the ratio of t/t' is 2. In a homogenous isotropic aquifer with no recharge sources, the time it took to generate the drawdown is the same time it will take to reach full recovery. Ratios less than 2 indicate slower recovery, and ratios greater than 2 indicate more rapid recovery. Once the pump is shut off, theoretically an imaginary injection well with a Q representative of the weighted average Q used during the pumping phase will cause the aquifer to recover. This is one reason data should be collected from all of the observation wells to provide a suite of recovery values for interpretation.

Example 10.14 A 72-h pumping test was conducted near Three Forks Montana on a new irrigation well. The desired pumping rate was 400 gpm (25.2 L/s), but over time the pumping rate decreased. The pumping rates and minutes pumped at each rate are given in Table 10.5. It was desired that a weighted average Q be calculated as an input parameter to evaluate the aquifer properties.

TABLE 10.5 Pumping Rates and Quantities Needed to Estimate a Weighted Average Pumping Rate

Q in gpm	Time pumped, min	Total, gal
450	65	29,250
430	15	6,450
415	100	41,500
390	120	46,800
375	1,300	487,500
360	300	108,000
375	1,100	412,500
330	1,328	438,240
	4328 total minutes	1,570,240 total gal

The total gallons divided by the total minutes pumped yields a weighted average pumping rate for the imaginary recovery well.

$$1570240 \text{ gal}/4328 \text{ min} = 363 \text{ gpm}$$

Example 10.15 During the recovery phase for the pumping test described in Example 10.10, recovery data were collected at 11, 20, and 36 h since pumping stopped. The duration of the pumping test was 12 h. A plot of these data is shown in Figure 10.20. Projected full recovery is at approximately $t/t' = 1.25$, or near 48 h. Time (t) keeps increasing after the pump shuts off, so for this example the following relationship occurs: $1.25 = (12 + x)/x$, or $1.25x = 12 + x$, therefore, $0.25x = 12$ and $x = 48$ h. A t/t' value of 1.25 indicates that the recovery is nearly four times greater than the drawdown part.

The time it takes for recovery becomes extremely important if you are evaluating pumping and recovery scenario impacts. Suppose, for example, that your distance-drawdown plot does show impact to other senior wells. It may be that by pumping and then letting the well recover before pumping again, it would provide a reasonable compromise to everyone's water use needs. The author's general experience is that many unconsolidated aquifers take 1 1/2 *times* the pumping rate time to fully recover and that fractured bedrock aquifers may take up to *four times* the pumping rate time to fully recover (Example 10.15). This is significant because in Example 10.15 a simple 12 h pumping–12 h recovery scenario may have a detrimental effect over

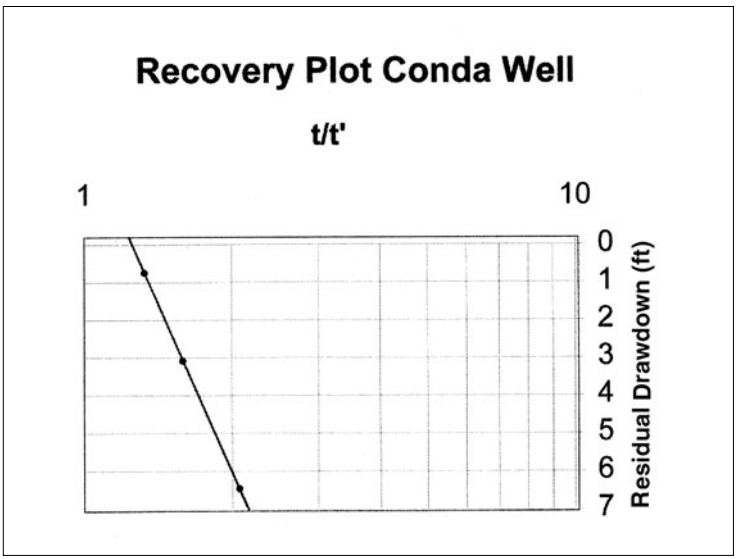

Figure 10.20 Recovery plot of well in fractured granite, with a pumping duration of 12 h.

time, while a 12-h pumping period followed by a 24-h recovery period may be acceptable.

10.3 Specific Capacity

One "first cut" approach to estimating transmissivity from drill logs is to use the **specific capacity** (S_c) relationship. Specific capacity is defined as:

$$S_c = \frac{Q}{s} \tag{10.29}$$

where Q = gpm
s = drawdown in feet after 24 h pumping

From the specific capacity equation, a rough rule of thumb derived from distance-drawdown relationships yields the following relationship for transmissivity (Driscoll 1986).

For confined aquifers:

$$T = S_c \times 2{,}000 \tag{10.30}$$

For unconfined aquifers:

$$T = S_c \times 1{,}500 \tag{10.31}$$

where T is in gal/day · ft.

A specific capacity approach applied to fractured bedrock aquifers was developed experimentally by Huntley and Steffey (1992), yielding the following relationship for bedrock aquifers:

$$T = 38.9\ (S_c)^{1.18} \tag{10.32}$$

where T is in ft^2/day. It should be noted that the units of the numerical factors 2000, 1500, and 38.9 in Equations 10.30, 10.31, and 10.32 convert the transmissivities into the given units.

For example, suppose that the lithology in the well log from a well drilled 300 ft (91.4 m) deep indicates several clay horizons above the production zone, suggesting that the aquifer may be confined. The production zone is screened over a 25-ft (7.6-m) thick sandstone. Suppose that the static water level (SWL) is at 20 ft (6.1 m) below ground surface. Through bailing, the production rate appears to be about 50 gal/min. Suppose further, that the measured drawdown is approximately 24 ft (7.3 m) from static conditions. This yields a specific

capacity of 50 gpm/24 ft = 2.08 gpm/ft. The transmissivity would be estimated to be 4200 gal/day · ft using Equation 10.30.

Something should be said about the drawdown reported in well logs by drillers. On many report forms the method of production is usually listed as pump, bailer, or air. When a pump is used the confidence in the pumping rate and drawdown is good. Estimates of production rates and drawdown using bailers are also pretty good. However, one should know what production by air means. The driller will first report the SWL, such as at 20 ft (6.1 m) below the surface. To produce water by air using a rotary rig (Chapter 8) means that the drill pipe is lowered to a depth near the screened interval, with the drill bit removed, and then injected with air to lift the water to the surface. The quantity of water discharging at the surface is estimated to be the production rate. In this case the reported drawdown then is the difference between the SWL and the depth to the end of the drill pipe. This leads to very low and strange specific capacity values. If all the wells drilled in a certain area are developed and tested in this a way a relative transmissivity can be obtained. An additional comment is that Equations 10.30, 10.31, and 10.32 normally assume that the measured drawdown is after 24 h of pumping (Driscoll 1986), when in most cases the development time for most domestic wells is 1 to 2 h. Recently, Jim Butler (personal communication, 2007) found that short developmental times still yield reasonable estimates for specific capacity. In either case, having an estimate for transmissivity is helpful.

In general the usefulness of the specific capacity can be summarized as follows:

- Gives a rough estimate of T (even with lousy data)
- Can be applied to confined, unconfined, or fractured bedrock aquifers
- Gives a rough idea of well completion (should the well yield more water than it is getting?)

If the specific capacity value is grossly smaller than expected, the following reasons could explain the results:

- Poorly completed, not screened in the right zone, or not screened at all.
- Well screen is clogged, either poor well development, precipitation of minerals in the screen, or biofouling.
- All well development was performed by air.
- Contractor fraud? It may be that if there is a pattern to poorly completed wells in an area where specific capacity values are noticeably higher in adjacent wells. If the poor wells were all completed by the same contractor, you could be suspicious of fraud.

Equation 10.32 was used in Example 10.12 to perform the distance-drawdown relationship needed for the public meeting.

10.4 Well Interference and Boundary Conditions

When the drawdown cones of multiple wells overlap at a particular point, the net affect is the *sum of the drawdowns* from all of the wells. This can be determined either graphically, using distance-drawdown methods, or mathematically, using Equations 10.1 or 10.10. Equation 10.1 can be used anytime, whereas Equation 10.10 can only be used if u is small (i.e., less than 0.02). It is the author's opinion that using Equation 10.1 after using Equation 10.2 to obtain a value for "u," and looking up a value for W_u in Appendix D is the easiest way. The reason the effect of neighboring wells is additive is because the LaPlace equation is linear.

$$\frac{\partial^2 h}{\partial x^2} + \frac{\partial^2 h}{\partial y^2} = 0 \tag{10.33}$$

Drawdown can be positive (downward, s) or negative (with groundwater mounding, $-s$). When there are injection or recharge wells (the pumping term becomes negative, $-Q$), instead of creating a cone of depression, there is a **cone of impression**. A cone of impression can be thought of as an upside-down cone of depression, creating a mound in the potentiometric surface at the location of the injection well (Figure 10.21). The net drawdown affect of pumping and injection wells can be evaluated independently and added at a particular point of interest (Example 10.16).

Example 10.16 Suppose we wish to evaluate the net drawdown at point A from the effect of three wells. Two of these wells are pumping wells, and one of the wells is an injection well (Figure 10.22). The pumping rates (500 and 600 gpm)

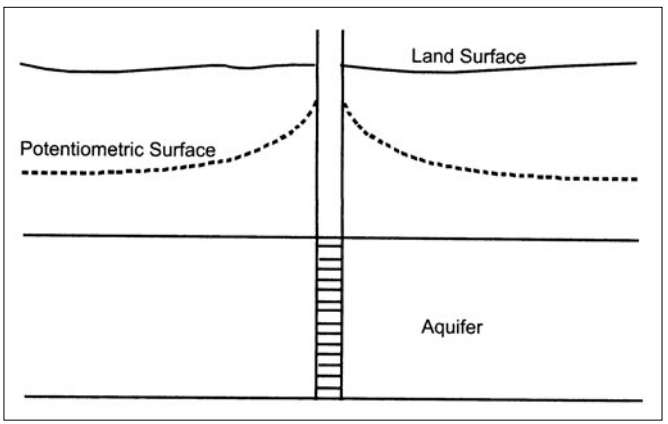

Figure 10.21 Schematic illustrating a cone of impression (mounding of the potentiometric surface).

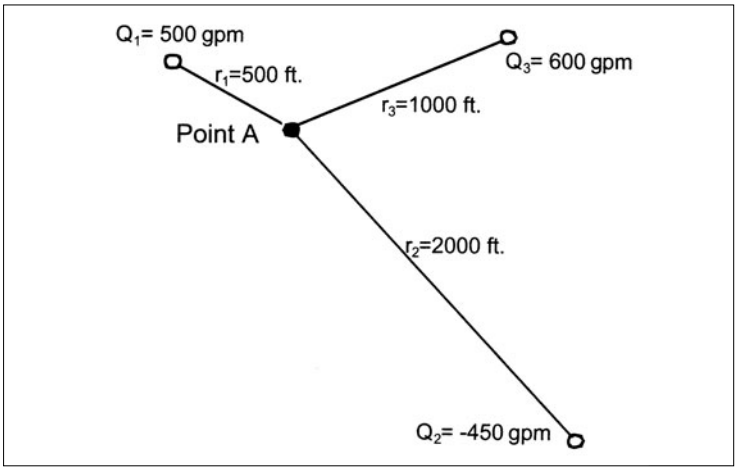

Figure 10.22 Schematic for Example 10.16.

and injection rate (450 gpm) in Figure 10.22 are shown, and the duration of pumping is one year (365 days). The transmissivity is 5,000 ft^2/day, and the storage coefficient is 0.20. The steps are to calculate u and then look up a corresponding value for $W_{(u)}$ in Appendix D and apply Equation 10.1. If u is small, Equation 10.10 can be used, but requires more effort. It is usually easiest to look up a $W_{(u)}$ for a calculated value of u and apply Equation 10.1. The results are shown in Table 10.6.

The net value is 10.0 ft of drawdown. The values for W_u are given in Appendix D. A sample calculation follows.

$$s = \frac{Q}{4\pi T} \times W_u$$

$$= \frac{500 \text{ gal/min}}{4\pi(5{,}000 \text{ ft}^2/\text{day})} \times \left(\frac{1 \text{ ft}^3}{7.48 \text{ gal}} \times \frac{1{,}440 \text{ min}}{1 \text{ day}}\right) 4.413 = 6.76 \text{ ft}$$

Graphically, a distance-drawdown graph should be created separately for each pumping or injection well in Example 10.16 (Figure 10.23). The injection well would be treated the same way as the pumping well except

TABLE 10.6 Parameters Associated with Drawdown Calculations

Well	r (ft)	u	$W_{(u)}$	Q gpm	Drawdown (ft)
1	500	0.00685	4.413	500	6.76
2	2,000	0.1096	1.737	−450	−2.39
3	1,000	0.0274	3.044	600	5.60
				Net	9.97 (10 ft)

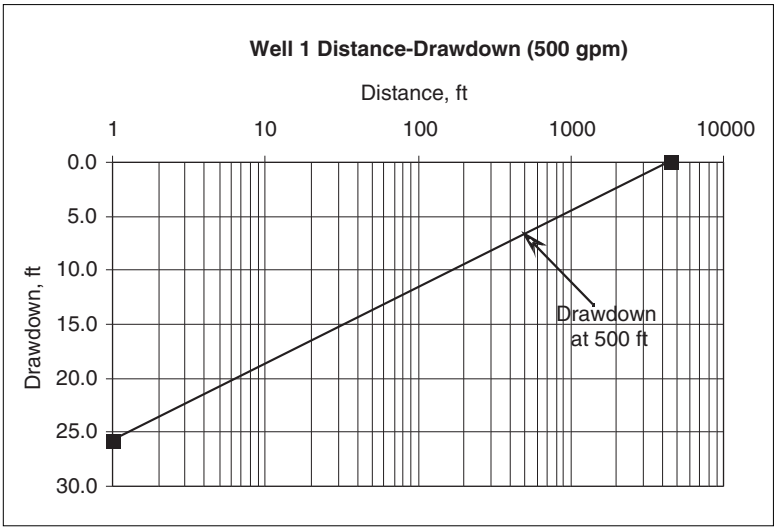

Figure 10.23 Distance-drawdown graphic for well 1 in Example 10.15, where Q = 500 gpm, r_0 = 4531 ft using Equation 10.27, and u = 2.74E-08, W_u = 16.84 and the drawdown at r = 1.0 ft is 25.8 ft. Compare the drawdown at 500 feet with the calculated value in Table 10.6.

that the drawdown would be negative. The drawdowns (plus or minus) at the respective distance from the point of interest (point A) would be picked from the distance-drawdown graph and then summed up.

In the case of well 1 in Example 10.16 one can use Equation 10.28 and the given T and S to calculate the radius of influence (r_0). The drawdown at a distance of 1 ft (0.3 m) would represent the position of a given pumping or injection well. With r = 1 ft, calculate "u" using Equation 10.2 and look up the corresponding value for $W_{(u)}$ from Appendix D. Finally, calculate the drawdown at a distance of r = 1 ft using Equation 10.1. A graph is made at r = 1 ft and at r_0 using the two drawdowns. This process is repeated for every pumping or injection well. The results should be pretty much the same.

This brings up a point regarding the power of a numerical groundwater model because the drawdown is determined not only at a single point A, but every cell on a grid. If the aquifer is not of infinite aerial extent, boundary conditions must also be considered.

Aquifer boundary conditions

Up to this point, we have been considering the aquifer to have infinite areal extent. This means that the cone of depression continues outward forever. The cone of depression will stop if it

- Becomes large enough to capture enough water demanded by the pumping rate from recharge and leakage, thus reaching steady-state conditions
- Reaches a hydrogeological recharge boundary

In reality, most hydrogeologic settings rarely have aquifers that are of infinite areal extent; rather they change laterally in grain size, shape, or lithology. These changes affect the shape of a time-drawdown curve in characteristic ways. Some boundaries that are encountered are less permeable than the aquifer unit being pumped. These are known as barrier boundaries. Time-drawdown data are affected by a steepening of the straight-line plot in the Cooper-Jacob (1946) method and a rising of the drawdown data above the reverse Theis (1935) curve. Examples of **barrier boundaries** include:

- Decrease in aquifer thickness from thinning or erosion
- Decrease in aquifer permeability from decreasing grain size (e.g., facies change)
- Encountering a fault plane, bedrock contact, or some other barrier
- Startup of a nearby pumping well, or effect of another nearby pumping well

Some cases occur where the boundaries encountered are more permeable than the aquifer unit being pumped. These are known as recharge boundaries. The time-drawdown data are affected by a flattening of the straight-line plot in the Cooper-Jacob (1946) method and the drawdown data dropping below the reverse Theis (1935) type curve. Examples of **recharge boundaries** include:

- Increase in aquifer thickness (thus an increase in T)
- Increase in aquifer permeability from increasing grain size (e.g., facies change)
- Encountering a recharge source, such as a lake, stream, or gravel channel
- Shutdown of a nearby pumping well, or the effect of another nearby pumping well shutting off
- Leakance from adjacent aquifers

The effects of boundaries are usually seen when the drawdown is plotted, either by the Theis (1946) or Cooper-Jacob methods (1946) (Figures 10.24 and 10.25). Notice how in a barrier boundary the drawdown increases with time, and in a recharge boundary the drawdown decreases with time. The way boundaries are accounted for in drawdown calculations is by applying both well interference and **image well theory**.

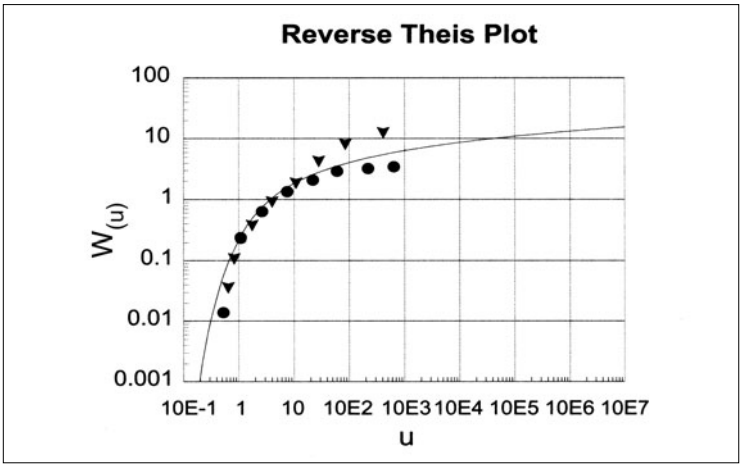

Figure 10.24 Reverse-type curve with data illustrating recharge (dots) and barrier (triangle) conditions.

Image well theory

When a boundary is encountered, its effects are simulated by use of an image well. Perhaps it would be better to explain with an example. Suppose a pumping well begins pumping. After 100 min, the cone of depression hits a bedrock barrier boundary. The effect on a time-drawdown plot is a steepening of the slope; thus the drawdown is now increasing more rapidly with time. To simulate this effect, an *imaginary well* is placed at an equal distance on the other side of the boundary the same distance the pumping

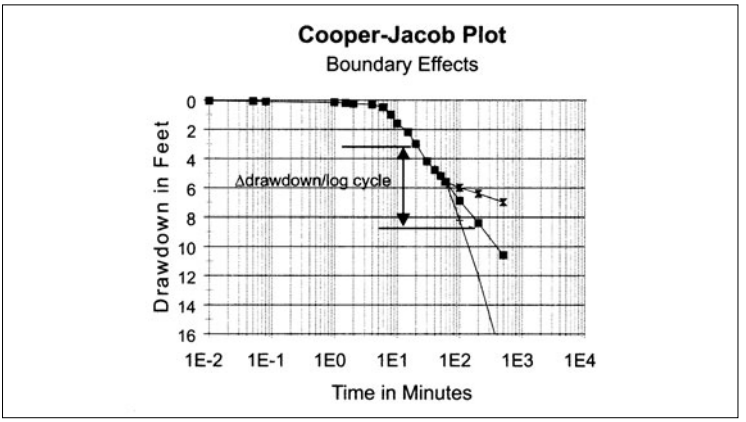

Figure 10.25 Cooper-Jacob plot of three wells: Hourglass pattern indicates recharge, boxes represent straight-line pattern (no boundary effects), and crosses represent a barrier condition. Deviations take place at 60 min.

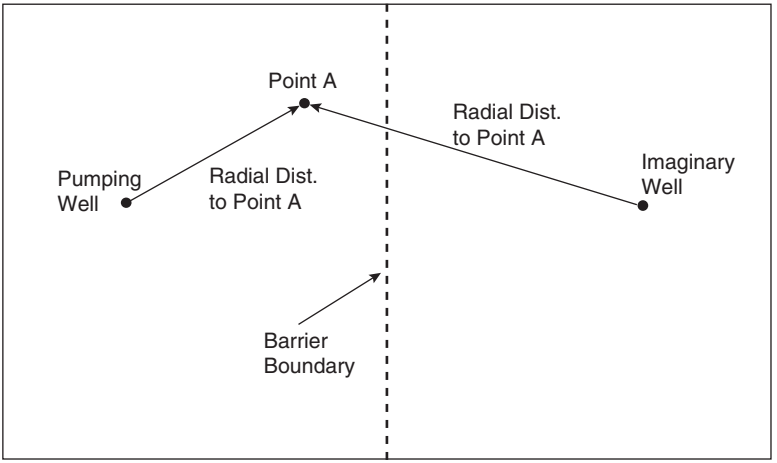

Figure 10.26 Schematic of pumping well and associated image well and distance from a barrier boundary (note the distances to the barrier boundary are equal). Also shown are the respective distances "r" to a point of evaluation of drawdown (Point A).

well is to the boundary and at the same pumping rate (Figure 10.26) (This is like a mirror image). Since the boundary is a barrier boundary, the imaginary well is also acting as a pumping well (barrier boundaries result in the pumping rates of the image wells having the same sign). The drawdown effects at the boundary, or anywhere within the radius of influence of the imaginary well, are added together with the effects of the real pumping well according to the principles explained previously.

If the boundary is a recharge boundary, the image wells are located in the same way except that the "sign" of pumping for the imaginary well is opposite that of the real well. The drawdown from pumping becomes negated by the recharge effect from the imaginary well with the opposite sign. These effects are seen in Figures 10.24 and 10.25. If two boundaries are encountered, the resulting effect would be to have an image well for each boundary. You would likely have to have more than one observation well during a pumping test to "see" two boundaries.

10.5 Partial Penetration of Wells and Estimates of Saturated Thickness

Wells that fully penetrate the aquifer and are fully screened have radial (horizontal) flow toward the well bore. If the well only partially penetrates the aquifer, the flow paths have a vertical component to them (Figure 10.27). The flow paths are, therefore, longer and converge on a shorter well screen, resulting in an increase in head loss and decrease in well efficiency (Driscoll 1986).

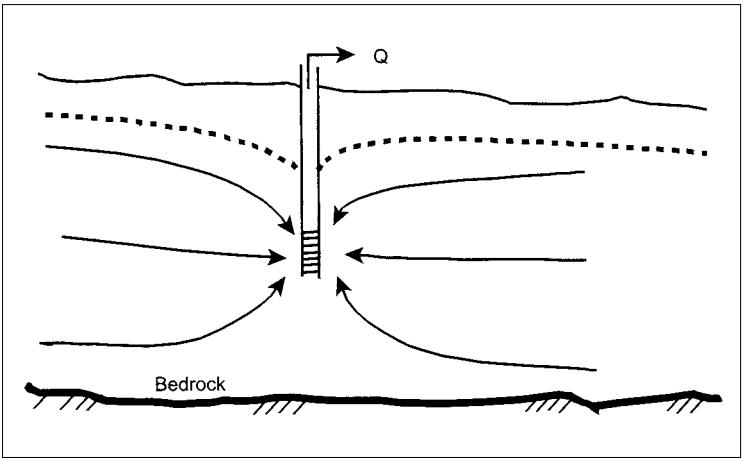

Figure 10.27 Schematic of partial penetration effects illustrating horizontal and vertical flow components.

Many times it is not possible or desirable to design a well that fully penetrates an aquifer. This is particularly true in an unconfined aquifer (Figure 10.27) that may be hundreds of meters thick; hence these wells are partially penetrating. In the Helena, Montana, Valley, many domestic wells only have an "open-hole" completion or have a few circular saw slots in PVC casing or torch-cut slots in steel casing, while partially penetrating hundreds of feet (meters) of aquifer. These limited openings provide the only access to the aquifer to retrieve water. In an unconfined aquifer, it is practical to place screen in the lower one-third of the aquifer to allow maximum drawdown in the production zone. (It is much easier for water to move downward than upward.) Observation wells for pumping tests should be placed far enough away from the pumping well to avoid partial penetration effects.

When is an observation well in a pumping test far enough away from the pumping well to avoid the effects of partial penetration? Hantush (1964) indicates that if the observation well fully penetrates the aquifer or if it is partially penetrating and more than $1.5b\ (K_h/K_v)^{0.5}$ away from the pumped well, the effects are negligible. In the distance equation, b is the saturated thickness, K_h and K_v are the horizontal and vertical hydraulic conductivities (discussed earlier). The vertical hydraulic conductivity is approximately an order of magnitude less than the horizontal hydraulic conductivity. Driscoll (1986) suggests than at a distance of $2b$, horizontal flow prevails.

Before continuing on perhaps it is appropriate here to mention a correction that may be needed when conducting pumping tests in unconfined

aquifers. The Theisian theory associated with pumping test assumes that the saturated thickness b is maintained (Section 10.2). This assumption is often violated when conducting pumping tests in unconfined aquifers. If the saturated thickness drops below 90% of the starting saturated thickness a correction factor must be applied to the data before plotting the time-drawdown data. The relationship is shown in Equation 10.34.

$$s' = (h_o - h)' = (h_o - h) - \frac{(h_o - h)^2}{2b} \tag{10.34}$$

where s' or $(h_o - h)'$ = corrected drawdown
$(h_o - h)$ = observed drawdown
b = saturated thickness

Estimates of the saturated thickness in unconfined aquifers

In the preceding discussion, there is a big question about the saturated thickness b. In this section we explore the practical applications of estimating b for confined and unconfined aquifers and explore an appropriate method of assignment of the horizontal hydraulic conductivity K. A common characterization method for estimating horizontal hydraulic conductivities is by deriving transmissivity estimates from pumping tests and then dividing by saturated thickness. There is a tendency in practice to assume that saturated thickness is equal to the screen length. This is appropriate if the screen fully penetrates the aquifer and horizontal flow prevails. However, this ideal situation is not often accomplished because most pumping wells are completed with partially penetrating screen settings or "open holes." Where, an open hole is just that a un-bottom-capped casing with no perforations. Groundwater flowing toward the screened interval or open hole has vertical components, resulting in an effective saturated thickness that can differ significantly from the screened (or open hole) interval. Depending upon the length of time of pumping and the existing geologic conditions, horizontal hydraulic conductivities can be significantly overestimated. Rules of thumb for estimating "effective saturated thickness" were proposed as a function of pumping time (Figure 10.28) and the characterization of vertically heterogeneous geology (Figure 10.29) in the first edition of this book (Weight and Sonderegger 2001). The two general principles are presented again followed by results from a numerical analysis of the problem.

Time. When a pumping test is being conducted in relatively homogenous sediments and time is short (to be defined later), then the contributing

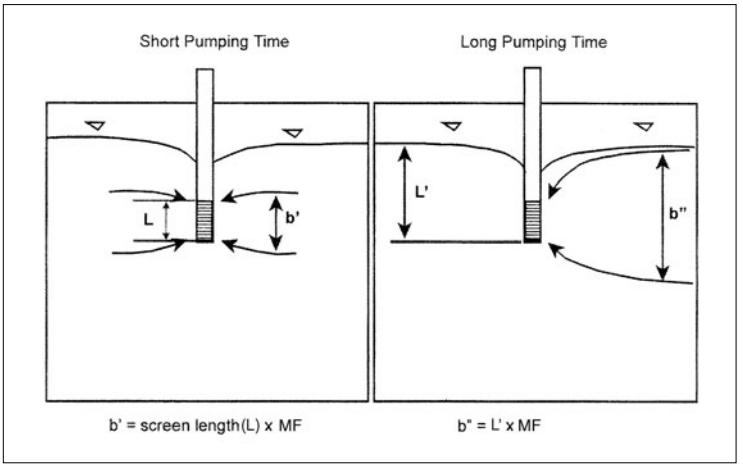

Figure 10.28 Contributing thickness of an aquifer depending on time for a relatively homogeneous hydrogeologic setting. Where MF = Multiplication Factor.

saturated thickness b' is approximately the screen length (L) times a multiplication factor (MF) (Figure 10.28). When the pumping time is longer (24 h or so) the reference thickness (L′) in an unconfined aquifer becomes the distance from the water table to the bottom of the screen (Figure 10.28). The estimated effective saturated thickness is L′ times MF. In the first edition (Weight and Sonderegger 2001) the MF was suggested to be 1.3 based upon our years of experience performing pumping tests.

Geology. When lithologic units are layered or interbedded with units of significantly differing physical properties in the vertical direction, then the transmissivity assigned to the saturated thickness must be evaluated according to the contributing hydrogeologic units. If the hydraulic conductivity of a hydrogeologic unit is one order of magnitude or greater than other units, the majority of water will be produced from the higher K unit (Example 10.17). Water seeks a path of least resistance. It will be easier for water from the lower hydraulic conductivity units to find a pathway up or down to a higher hydraulic conductivity unit rather than take the relatively longer pathway to the well screen (Figure 10.29). This may result in water being primarily produced from an aquifer thickness less than the screen length in shorter duration pumping tests in heterogeneous aquifers.

Example 10.17 Layered sedimentary units may be somewhat homogenous within layers, with a production screen that spans more the one layer. In this example we consider four sedimentary layers that contribute to a production well. Each layer has a known horizontal hydraulic

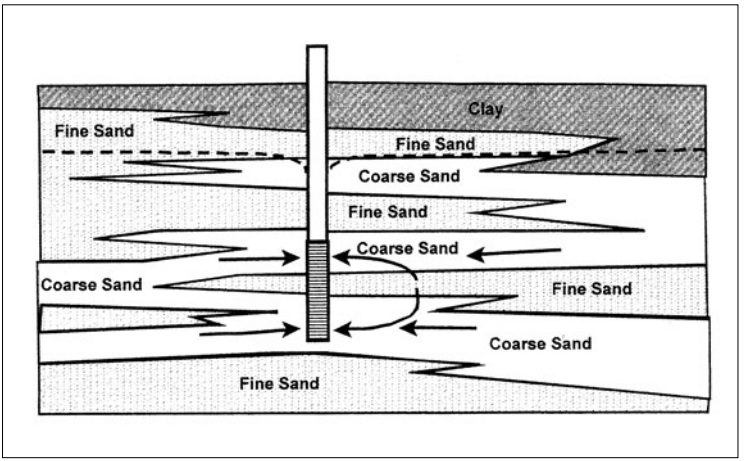

Figure 10.29 Pumping test in variable hydrogeologic units. In short duration tests, the actual contributing thickness may be less than the screen length.

conductivity (K_h) and the vertical hydraulic conductivity (K_v) is assumed to be a factor of 15 less than K_h. In this case the averaged horizontal (K_{hAve}) and vertical (K_{vAve}) hydraulic conductivities are computed using Equations 10.35 and 10.36.

$$K_{hAve} = \sum_{i=1}^{k} \frac{K_{hi} \times b_i}{b} \tag{10.35}$$

and,

$$K_{vAve} = \frac{b}{\sum_{1=i}^{k} \frac{b_i}{K_{vi}}} \tag{10.36}$$

where K_{hi} = the horizontal hydraulic conductivity of the ith layer, (length/time)
b_i = the thickness of the ith layer, (length)
K_{vi} = vertical hydraulic conductivity of the ith layer, (length/time)
b = total aquifer thickness, (thickness)

The described four-layer scenario is depicted in Figure 10.30. The four contributing sedimentary layers from top to bottom are: Unit A–limestone 8 m thick, with K_h = 5 m/day; Unit B–siltstone 15 m thick, with K_h = 0.5 m/day; Unit C–medium-grained sandstone 5-m thick, with K_h = 10 m/day; and Unit D conglomerate 3 m thick, with K_h = 65 m/day.

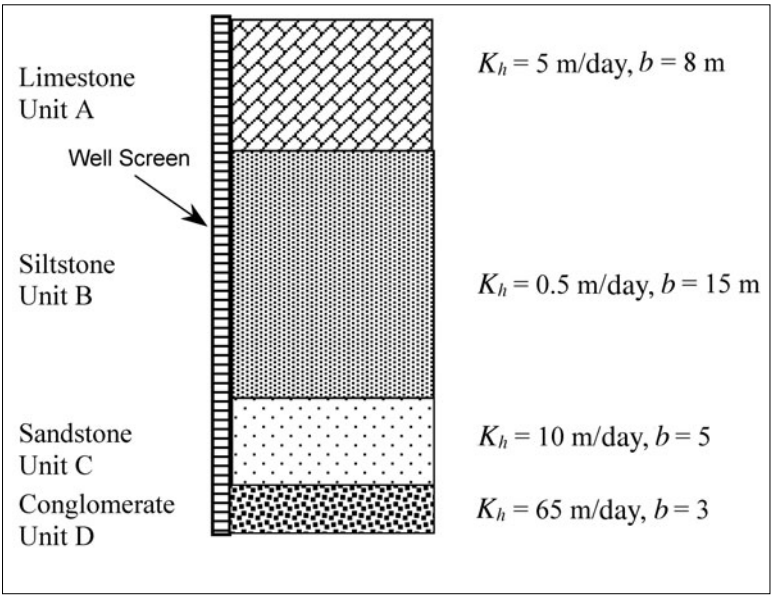

Figure 10.30 Four-layer sedimentary unit spanned by a production well screen.

Equation 10.35 is used to estimate the average horizontal hydraulic conductivity:

$$K_{hAve} = \left[\frac{(5\,\text{m/day}) \times 8\,\text{m} + (0.5\,\text{m/day}) \times 15\,\text{m} + (10\,\text{m/day}) \times 5\,\text{m} + (65\,\text{m/day}) \times 3\,\text{m}}{31\,\text{m}}\right]$$

$$= 9.4\ \text{m/day}$$

One can observe that the relative weighting from each unit is 13.7%, 2.6%, 17%, and 66.7% respectively. Notice how Unit D contributes 2/3, even though it is the thinnest of all the units. The averaged vertical hydraulic conductivity is found using Equation 10.36:

$$K_{vAve} = \left[\frac{31\ \text{m}}{(8\ \text{m}/5\ \text{m/day}) + (15\ \text{m}/0.5\ \text{m/day}) + (5\ \text{m}/0.5\ \text{m/day})(3\ \text{m}/65\ \text{m/day})}\right]$$

$$= 1\ \text{m/day}$$

Numerical analysis. After additional feedback from other professionals it made sense to evaluate the original rules of thumb numerically as a

cost-effective method of analysis. The numerical scenarios were conducted using USGS finite-difference model MODFLOW (McDonald and Harbaugh 1988), supplemented with commercially available pre- and post-processing software. The MODFLOW model grid is 1,000 ft by 1,000 ft with 10 ft by 10 ft grid spacing. Twenty layers of equal thickness were needed to evaluate vertical flow without significant "boundary effects." The top of the model domain is at an elevation of 100 ft and the bottom datum is 0 ft. A pumping well was placed in the exact center of the grid, spanning layers 4 and 5 (elevations 75 to 85 ft) to represent a screened section of 10 ft. Transient conditions were established over one stress period with 30 time steps. An accelerator parameter of 1.2 was used to spread out the influences of pumping over a time frame of 5 days (Weight et al. 2003).

Pumping rates were varied from 50 to 200 gpm. A horizontal hydraulic conductivity (K_h) of 200 ft/day was fixed throughout all of the simulations to represent coarse sand to sandy gravels, representative of public supply wells. The vertical hydraulic conductivity (K_v) was varied from 200 to 20 ft/day to represent a typical range of stratification-caused anisotropy, and storage coefficient values were alternated between 15 and 30%.

Drawdowns, heads, and streamlines from each simulation run were evaluated. All drawdown values were contoured at an interval of 0.1 ft. It was reasoned that 0.1′ to 0.2′ of drawdown could be used to define "significant hydraulic influence," and thus the vertical extent of significant flow to the pumping well. For each run, six numerical values were visually estimated to establish hydraulic response curves over the first 2 days of pumping. The two "depth" results represent the model-elevations reached by the 0.1′ and 0.2′ drawdown contours below the bottom of the well screen, and the two "width" results are the corresponding radial distances from the pumping well. The two "top" results are the model elevations, above the top of the well screen, where the 0.1′ and 0.2′ contours have reached. The maximum value for each of these results was determined for each time step and plotted. The curves were evaluated to determine the sensitivity of simulated hydraulic responses to variations in the basic parameters and to reevaluate the two rules of thumb discussed above and what the appropriate MF value should be. A summary of the modeling scenarios and results are shown in Table 10.7.

Graphical depictions of each modeling scenario were performed to look for trends and patterns, used in reevaluating the rules of thumb. An example is shown in Figure 10.31.

Two columns in Table 10.7 indicate when the influence of pumping reached or exceeded 1.5 times the screen length. Most of these results are less than an hour. Additionally, the last 2 columns of Table 2 indicate the

TABLE 10.7 Summary of Results from Modeling Scenarios and Times in Hours to Reach the Water Table or Specified Depths from, Weight et al. 2003

Run	$K_h : K_v$ ratio	Pumping rate (gpm)	Storage coefficient (%)	Maximum drawdown (ft)	Time (hours) for drawdowns (0.1′ and 0.2′) to reach water table or certain depths					
					Water table		1.5 × screen		1.5 × well bottom	
					0.1′	0.2′	0.1′	0.2′	0.1′	0.2′
PP5	1	100	15	0.9	0.6	1.0	0.2	0.4	0.6	1.7
PP6	5	100	15	1.6	2.1	4.0	0.3	0.4	2.0	5.0
PP7	10	100	15	2.0	4.9	8.9	0.3	0.6	3.5	9.0
PP8	5	200	15	3.2	1.7	2.1	0.1	0.3	1.0	2.0
PP9	10	200	15	4.0	3.3	4.0	0.2	0.3	2.0	3.5
PP10	5	200	30	3.0	3.3	4.0	0.3	0.5	2.1	3.9
PP11	10	200	30	3.8	6.0	8.9	0.5	0.7	4.0	7.3
PP12	5	100	30	1.5	4.0	7.3	0.5	0.9	4.0	10.8
PP13	10	100	30	1.9	8.9	15.7	0.7	1.3	7.3	19.0
PP14	5	50	30	0.7	7.3	22.9	0.9	2.6	10.8	>48
PP15	10	50	30	0.9	15.7	47.9	1.2	3.3	19.0	>48

time required for detecting the influence of water movement within 1.5 times the distance from the water table to the bottom of the screen. This is achieved in less than half a day, except for scenarios with the lowest pumping rate simulated. This suggests that using the screen length could significantly overestimate "*b*" and underestimate K_h. The rules of thumb

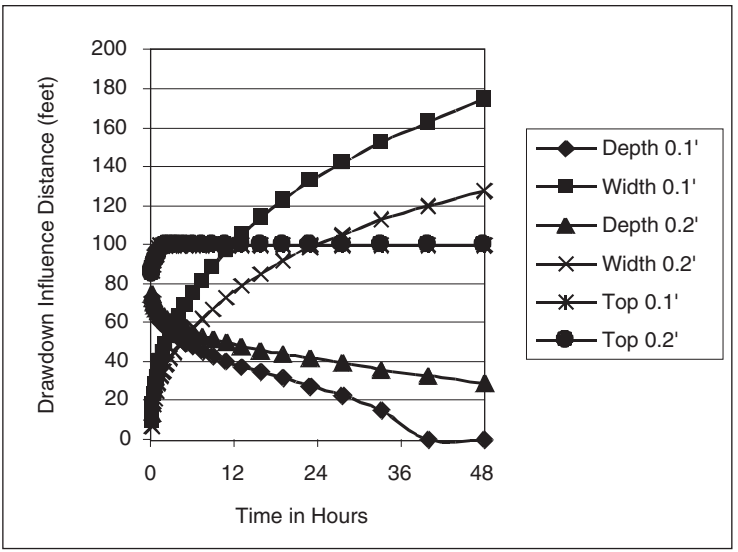

Figure 10.31 Graphical representation of one modeling scenario from Table 10.7. [*After Weight et al.* (*2003*)].

suggested by Weight and Sonderegger (2001) should be updated based on the numerical results. Instead of an MF factor of 1.3, an MF more like 1.5 or 2.0 should be used for the examples shown in Figure 10.28.

The issue concerning the saturated thickness b is an important one that is not given enough attention. It has been the author's experience that many hydrogeologists working for consulting companies are mainly concerned with obtaining a transmissivity value during the pumping test and divide by the screen length to obtain a hydraulic conductivity value without regard whether the K value matches the lithology. Worse yet is the case where hydraulic conductivity values are used in calculations, along with reported transmissivity values from pumping tests, and the calculated saturated thicknesses make no sense whatsoever. It is as though the pumping tests were performed because they were necessary to estimate the hydraulic properties of an aquifer, and then in the analysis the hydraulic conductivity didn't come out as expected so the field results were ignored.

Example 10.18 While performing a technical analysis of a consultant's report of a flow and transport model for a landfill, the author noticed that a very careful analysis was performed during the site characterization phase. A significant amount of expense, time, and effort was made to establish a conceptual model based upon drill hole information and constructed cross sections. Additionally, pumping tests were performed with both transmissivity and hydraulic conductivity values reported that were used in the numerical model. The hydraulic conductivity values used in the groundwater-flow model were inconsistent with the lithologic units and reported transmissivities. (Also, the length of pumping was on the order of a few minutes to a few hours.) The respective saturated thicknesses were calculated at 50 to 60 ft (15.2 to 18.3 m) thick, when the screen length was only 10 ft (3 m) and pumping-test duration was short. It was as though a list of field exercises were performed to fulfill certain requirements, with little effort made to be consistent when it came time for the numerical model. Calibrating the model to yield a particular flow scenario seemed to be more important than reality.

10.6 Fracture-Flow Analysis

The previous section has been primarily concerned with pumping tests in porous media. Pumping tests in fractured porous media have a very different time-drawdown behavioral response. The physical setting is one where high conductivity fractures drain quickly, while smaller fractures and block media drain at later time. Diagrammatically there is a different flow-path length for groundwater in fractures compared to porous media. The flow-path length compared to lateral distance is known as the **tortuosity** factor. In fractured media, the tortuosity factor can be significantly less (Figure 10.32).

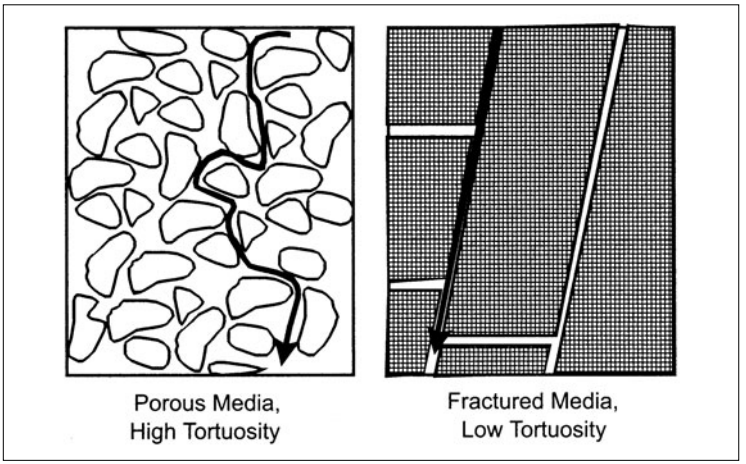

Figure 10.32 Differences in tortuosity (flow-path length) in porous versus fractured media.

The distances over which groundwater moves are more direct and therefore can result in significant velocities. As the velocity of groundwater flow increases, it begins to gain kinetic energy and become turbulent. Turbulent flow in fractured aquifers is a common phenomenon (Carriou 1993). Once turbulent flow dominates, then Darcy's law is no longer valid and a different equation for hydraulic gradient is used (Bear 1979).

$$\frac{dh}{ds} = A_L q + B_T q^n \tag{10.37}$$

where dh/ds = hydraulic gradient (L/L)
q = specific discharge (L/t) = $K \times dh/ds$
A_L = laminar flow constant (t/L)
B_T = turbulent flow constant (t/L)
n = turbulent flow exponent
K = hydraulic conductivity (L/t)

Turbulence increases the drawdown within the pumping well by a factor of $B_T q^n$, where n increases with the degree of turbulence, which has experimentally been found to range from 1.6 to 2.0 (Bear 1979).

The dynamics of groundwater flow to a pumping well in fractured media was first considered by Barenblatt et al. (1960). They gave the following equation for describing flow in a fractured aquifer to a pumping well:

$$\Delta s_f = \frac{Q}{4\pi T} \int J_0(xr) \left[1 - \exp \frac{ktx^2}{1 + x^2 \eta_f} \right] \frac{\partial x}{x} \tag{10.38}$$

where s_f = drawdown in the fractured aquifer (L)
Q = pumping rate (L^3/T)
T_f = transmissivity of fractured aquifer (L^2/t)
J_0 = Bessel function of the first kind, or zero order
r = radial distance from the pumping well (L)
t = time since pumping began
κ = ratio of fractured aquifer transmissivity to aquifer storativity, or $T_f/S_p(L^2/t)$
η = fissure characteristic (dimensionless)
S_p = porous block storativity (dimensionless)
d_x = differential $\times$ operator (radial distance from center of well to the limit of integration (L)

The part after the integral sign in Equation 10.38 is the well function associated with a discretely fractured aquifer. The type curve was plotted by Carriou (1993) and is shown in Figure 10.33. Notice the linear early-time portion of the curve. This represents water yield from discrete fractures crossing the well bore coming from fracture storage (Carriou 1993). As more water is withdrawn, the hydraulic gradient within the bedrock induces water from the bedrock and smaller fractures to move to the larger fractures, thus transitioning to a more Theisian-like response at later time. Additional type curves are shown in Streltsova (1976). Field studies in petroleum settings indicate that fractures greater than 0.05 mm are large enough to contribute significantly to fluid extraction volume while contributing very little to overall aquifer block storativity (Gringarten et al. 1974; Streltsova 1976).

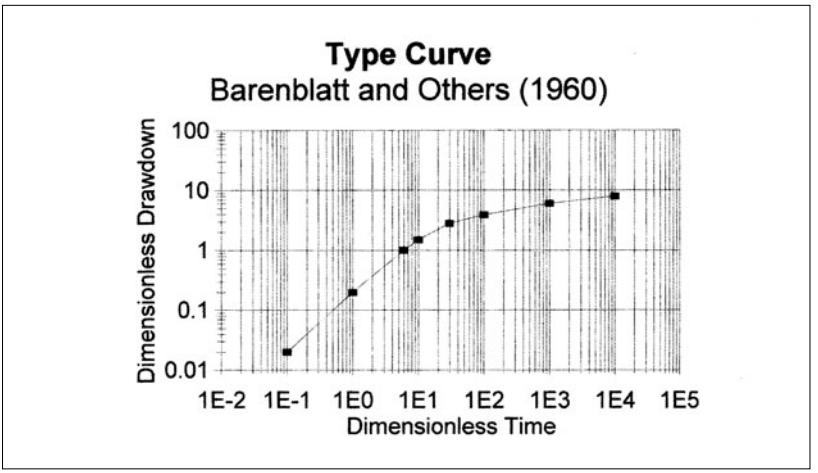

Figure 10.33 Type curve for discrete fractures.

The analytical approach for pumping tests in discrete fractures is to plot field values of drawdown (s) versus time (t) in log-log scale. This plot is overlain on top of the type curve for dimensionless fracture drawdown (s_{df}) versus dimensionless time, also in log-log scale (Figure 10.33). The axises are kept square similar to the Theis curve-matching approach (Section 10.2), except that both the linear pattern (representing fracture dewatering) and the late time are both included in the Barenblatt et al. (1960) solution. This means that there is no need to emphasize early- or late-time in the "fit." The transmissivity and storativity are solved using Equations 10.39 and 10.40 from Barenblatt et al. (1960).

$$T_f = \frac{Qs_{df}}{4\pi\Delta s} \tag{10.39}$$

$$S_p = \frac{4T_f t}{t_d r^2} \tag{10.40}$$

where Q = withdrawal rate (ft^3/min)
S_{dr} = dimensionless fracture drawdown from match point
T_f = fracture transmissivity (ft^2/min)
S_p = aquifer storativity (dimensionless)
t = time from match point (minutes)
t_d = dimensionless time from match point
r = radial distance from pumping well to observation well (ft)

The pumping test described in Example 10.12 resulted in some of the observation wells indicating a fracture response (Figure 10.34). The test was only run for 12 h, so only the linear (fracture dewatering) response is observed.

Additional fracture responses are possible from fractured media depending on the physical properties of the block materials. For example, if there is a fractured sandstone being stressed by pumping, both the fractures and the blocks will yield water in a dual porosity model. The dual porosity model is similar to a delayed yield response in porous media (Neuman 1979), where the fractures behave linearly; once the blocks begin to yield water, a recharge effect (flattening of the drawdown curve) occurs. Later on when the blocks become stressed, another curvilinear response occurs, indicated by increased drawdown once again (Figure 10.35).

Pumping tests in flowing wells

Pumping tests can also be conducted in flowing (artesian) wells if the "pumping well" can be controlled with a shutoff valve. At start time, the

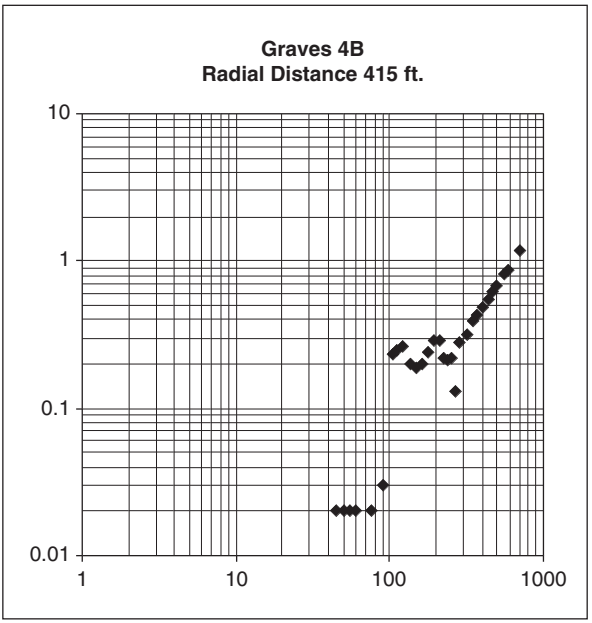

Figure 10.34 Observation well drawdown response from Example 10.12.

pumping well is opened up, allowing the free flow of water. A flowing observation well is plumbed with a transducer to measure the reduction in head over time (Figure 10.36). If the flow does not decrease more than 10% or so, a reasonable fit can be made to the pumping-test data. "Pumping" times should be similar to conventional pumping tests.

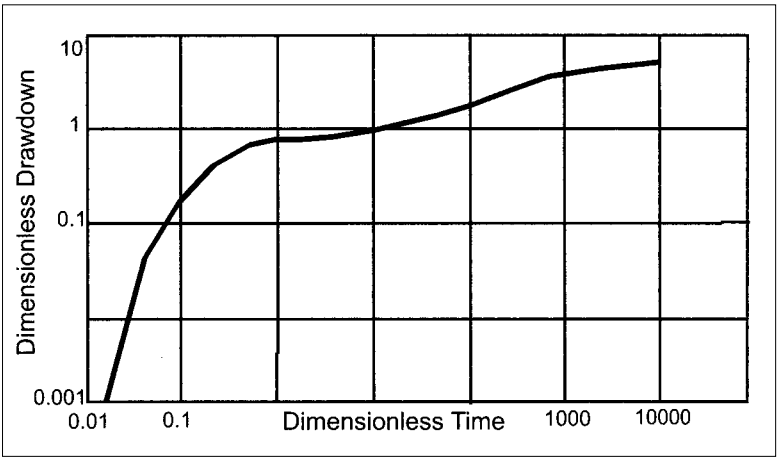

Figure 10.35 Dual porosity type curve indicating a delayed yield-like response.

Figure 10.36 Plumbing a transducer in a flowing well used as an observation well.

Example 10.19 In Petroleum County, in central Montana, are several flowing wells from differing Cretaceous hydrogeologic units. In a study performed by Brayton (1998), pumping tests were conducted in the basal member of the Cretaceous Eagle Formation. A flowing pumping well was shut down, while the flowing observation well was plumbed with a pressure transducer (Figure 10.36). The pumping test was conducted by opening the valve on the "pumping well" and allowing the data logger to record the decrease in pressure over time. Decreased pressure was converted to drawdown in feet over time. An example plot of the data is shown in Figure 10.37, indicating a dual porosity fracture-flow response.

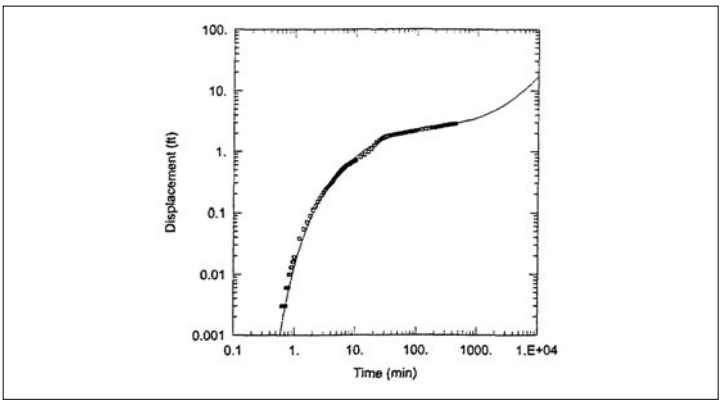

Figure 10.37 Dual porosity fracture-flow response from a pumping test in the Cretaceous Eagle Formation, central Montana. [*After Brayton (1998).*]

10.7 Summary

One of methods of evaluating the hydraulic properties of aquifers is through conducting pumping tests. How to conduct a pumping test is described in Chapter 9, while helpful suggestions on what to record in your field book are found in Chapter 1. This chapter addressed several of the analytical methods used to analyze pumping-test data. The most common approach is to perform a Theis analysis or do a Cooper-Jacob plot *in the field during the test* to see how the data behave. Boundary conditions and other effects are observed directly in the plot. Care must be taken to ensure that the pumping rate was kept constant, or strange patterns may occur that are an artifact of varying pumping rates.

One must also make sure the pumping test was conducted long enough when a recharge response was observed early on. Does the recharge response reflect a leaky confined setting, or is delayed yield occurring? This can only be resolved through recording additional time-drawdown responses.

Direct relationships exist between time-drawdown and distance-drawdown plots. These can be used to evaluate the impacts of a longer duration pumping test on neighboring wells with senior water rights.

The analysis of pumping-test data is closely connected with having an understanding of the geologic setting and a knowledge of the well-completion details. Pumping tests yield an estimate for transmissivity (T) and storativity (S). These are two-dimensional parameters, in which the vertical dimension is averaged. When estimating the hydraulic conductivity (K) from the transmissivity value, it is important to consider test duration and geology, particularly in a partial penetration scenario.

Fracture-flow responses have their own characteristic behavior. Type curves for discrete-fracture or dual-porosity models are very different. A common aspect of both is the early-time linear response on a log-log plot of drawdown versus time. Care must be taken to make sure the analysis method, field observations, and geologic setting all make sense.

References

Barenblatt, G.I., Zheltov, I.U.P., and Kochina, I.F., 1960. Basic Concept in the Theory of Seepage of Homegenous Liquids in Fissured Rocks. *Journal of Applied Mathematical Mechanics*, Vol. 24, No. 5, pp. 1286–1303.

Bear, J., 1979. *Hydraulics of Groundwater*. McGraw-Hill, New York, 569 pp.

Borgman, L.E., Weight, W.D., and Quimby, W.F., 1986. *Geological and Hydrological Characteristics of the Hoe Creek Underground Coal Gasification Site*. Technical Report 86-2. Prepared for the United States Environmental Protection Agency EMS Laboratory, Las Vegas, NV, 71 pp.

Boulton, N.S., 1973. The Influence of The Delayed Drainage on Data from Pumping Tests in Unconfined Aquifers. *Journal of Hydrology*, Vol. 19, pp. 157–169.

Brayton, M., 1998. *Recovery Response From Conservation Methods in Wells Found in the Basal Eagle Sandstone, Petroleum County, Montana.* Master's Thesis, Montana Tech of the University of Montana, Butte, MT, 68 pp.

Carriou, T.M., 1993. *An Investigation into Recovering Water Levels in the Butte, Montana, Bedrock Aquifer*. Master's Thesis, Montana Tech of the University of Montana, Butte, MT. 160 pp.

Cleary, B., 1993. *Personal Communication*. San Francisco, CA.

Cooper, H.H., Jr., and Jacob, C.E., 1946. A Generalized Graphical Method for Evaluating Formation Constants and Summarizing Well-Field History. *Transactions of the American Geophysical Union*, Vol. 27, pp. 526–534.

Driscoll, F.G., 1986. *Groundwater and Wells*. Johnson Screens, St. Paul MN, 1108 pp.

Duffield, G.M., and Rumbaugh, J.O., III, 1991. *AQTESOLV, Aquifer Test Solver Software. Version 1.00*, Geraghty and Miller Modeling Group, Reston, VA., 90 pp.

Fetter, C.W., 1993. *Applied Hydrogeology*, *3rd Edition*. Macmillan, New York, 691 pp.

Fletcher, F.W., 1997. *Basic Hydrogeology Methods: A Field and Laboratory Manual with Microcomputer Applications*. Technomic, Lancaster, PA, 310 pp.

Gringarten, et al., 1974. Unsteady-state Pressure Distributions Created by a Single Infinite-Conductivity Vertical Fracture. *Society of Petroleum Engineers Journal*, Vol. 14, No. 4, 347 pp.

Hantush, M.S., 1956. Analysis of Data From Pumping Tests in Leaky Aquifers. *Transactions of the American Geophysical Union*, Vol. 37, pp. 702–714.

Hantush, M.S., 1960. Modification of the Theory of Leaky Aquifers. *Journal of Geophysical Research*, Vol. 65, pp. 3713–25.

Hantush, M.S., 1964. Hydraulics of Wells. In *Advances in Hydroscience*, *Vol. 1*, V.T. Chow, (ed.) Academic Press, New York, pp. 281–432.

Huntley, D.R., and Steffey, D., 1992. The Use of Specific Capacity to Assess Transmissivity in Fractured-Rock Aquifers. *Ground Water*, Vol. 30, No. 3, pp. 396–402.

Jacob, C.E., 1950. Flow of Ground-Water. In *Engineering Hydraulics*, H. Rouse (ed.), John Wiley, New York, pp. 321–386.

Kruseman, G.P., and deRidder, N.A., 1991. *Analysis and Evaluation of Pumping Test Data*, *2nd Edition*. International Association for Land Reclamation and Improvement, Publication 47, Wageningen, The Netherlands, 377 pp.

Lohman, S.W., 1979. *Ground-Water Hydraulics*. U.S. Geological Professional Paper 708, Washington, DC, 70 pp.

Metesh, J., 1995. *Personal Communication,* in Butte, Montana.

Neuman, S.P., 1972. Theory of Flow in Unconfined Aquifers Considering Delayed Response to the Water Table. *Water Resources Research*, Vol. 8, pp. 1031–1045.

Neuman, S.P., 1975. Analysis of Pumping Test Data from Anisotropic Unconfined Aquifers Considering Delayed Gravity Response. *Water Resources Research*, Vol. 11, pp. 329–342.

Neuman, S.P., 1979. Perspective on "Delayed Yield". *Water Resources Research*, Vol. 15, No. 2, pp. 989–998.

Neuman, S.P., 1987. On Methods of Determining Specific Yield. *Ground Water*, Vol. 25, No. 6, pp. 679–684.

O'Connel, W.T., and Smith, T.C., 1993. Aquifer Characterization for the Well-Head Protection Plan for Ramsay, MT. Senior Design Project, Department of Geological Engineering Montana Tech of the University of Montana.

Streltsova, T.D., 1976. Hydrodynamics of Groundwater Flow in a Fractured Formation. *Water Resources Research*, Vol. 12, No. 3, pp. 405–414.

Theis, C.V., 1935. The Lowering of the Piezometer Surface and the Rate and Discharge of a Well Using Ground-Water Storage. *Transactions of the American Geophysical Union*, Vol. 16, pp. 519–524.

Thiem, G., 1906. *Hydrologische Methoden*. Gebhardt, Leipzig, 56 pp.

This page intentionally left blank

Chapter

11

Slug Testing

Slug testing has been used over the years to obtain a cost-effective quick estimate of the hydraulic properties of aquifers. Slug testing has gained in popularity since the 1980s since it can be used to obtain hydraulic property estimates in contaminated aquifers where treating pumped waters is not desirable. Slug-testing analysis methods were first developed during the 1950s (Hvorslev 1951; Ferris and Knowles 1954). The simple method devised by Hvorslev (1951) led to its wide use for both confined and unconfined aquifers as an estimate of the hydraulic conductivity within the screened interval. Improvements of the methods by Ferris and Knowles (1954) were made by Cooper et al. (1967) and Papadopulos et al. (1973) for confined aquifers. Later, Bouwer and Rice (1976) and Bouwer (1989) developed a method for analysis in confined, semi-confined, or unconfined aquifers that takes into account aquifer geometry and partial penetration effects. Campbell et al. (1990) summarizes the various methods used and their relative merits with an extensive list of references. An article by Butler et al. (1996) describes the protocol that should be used in the field to reduce errors of estimation. A recent book by Butler (1998) presents a fairly comprehensive summary on slug-test methodology and analysis. If this chapter does not satisfy the reader on the topic of slug testing, the book by Butler (1998) is highly recommended, which is in a second edition.

Constant-discharge pumping tests are a better method of analyzing the physical properties of aquifers (Chapter 9), since their influence goes beyond the immediate vicinity of the borehole, although in high-transmissivity aquifers the influence can be detected several hundred feet away (Bredehoeft et al. 1966). Slug tests are especially useful in locations where handling the discharge of contaminated pumping waters is prohibited, and yet a rough estimate of the hydraulic properties of the aquifer is needed. Another great thing about slug tests is that they can be conducted relatively quickly, so that several point estimates of

Copyright © 2008, 2001 by The McGraw-Hill Companies, Inc. Click here for terms of use.

hydraulic conductivity can be collected within a day's work. The chances of a hydrogeologist needing to perform slug tests are pretty high. The intent of this chapter is to discuss the methodology of performing slug tests in the field followed by methods used to analyze the data. This is done for both the overdamped and underdamped cases. Discussion of the problems that can occur in the field will also be presented along with the typical mistakes that are made when performing the analysis.

11.1 Field Methodology

Slug testing involves lowering a "slug" (a cylinder of known volume, usually constructed of PVC pipe or some other suitable material filled with sand or gravel that is capped at both ends) tied to a rope or cable, down a well bore to displace the static water with an equivalent volume (Figure 11.1). A pressure transducer, previously placed below the slug level, senses the water-level responses, and the data are recorded in a data logger (Figure 11.2). The slug remains in place until the water level equilibrates. Once at equilibrium, the data logger is activated and the slug is briskly retrieved above the static water level (Figure 11.3). The displaced water recovers to the original static level. The time required for static conditions to occur once again is proportional to the hydraulic conductivity of the aquifer materials. Graphical methods are used to obtain parameters that are used to calculate the hydraulic conductivity values.

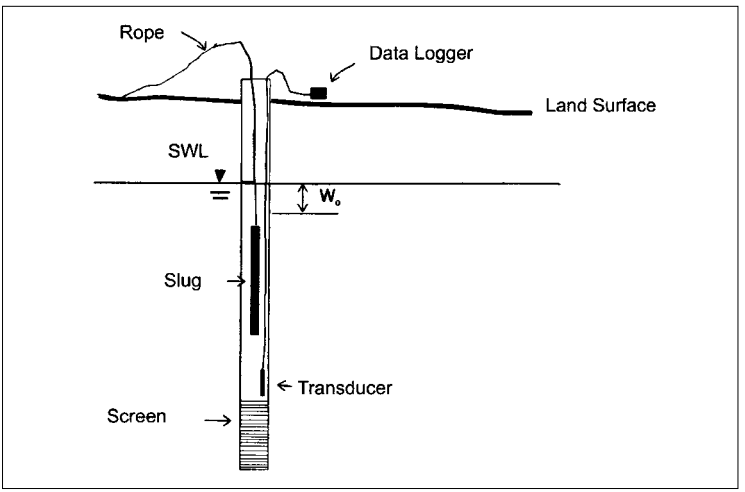

Figure 11.1 Slug testing schematic. [*Weight and Wittman (1999). Used with permission of Groundwater Publishing Co.*]

Figure 11.2 Using the data logger in the field to gather slug-test data.

Figure 11.3 Lowering a slug down a well.

In the pre-1990s, water-level changes during slug tests were measured using steel tapes or electrical tapes (E-tapes). This only allowed slug tests to be conducted on relatively low hydraulic conductivity materials. Therefore, this was applicable when water levels slowly recovered over a matter of minutes to several hours. With the current wide use of high-speed data loggers, pressure transducers, and well sentinels, slug-test analysis may be conducted on materials over a wide range of hydraulic conductivities.

How to make a slug

It is important that the size of the slug be appropriate to the amount of water desired to be displaced. For example, 1 1/4-in PVC works well for 2-in wells, and 3-in PVC works well in 6-in wells (larger-diameter slugs can be used, but become difficult to handle). The lengths should be designed so that at least 1 ft (0.3 m) or more of displacement can occur. One can calculate the approximate volume of the slug before going into the field. Typical slug lengths are 3 ft (1 m), 6 ft (2 m), or 10 ft (3 m). The general procedure for constructing slugs is described next:

- Take a blank piece of PVC casing and cut it to the desired length, allowing for the top and bottom caps to contribute to the total length.
- The bottom of the casing is capped, and either glued with PVC glue or screwed together, or both. Preferably, this is reinforced with duct tape.
- Sufficient sand or gravel is added, so that when the slug is capped at the top, it will sink.
- A hole is made in the top cap, large enough for the rope or cable to thread through. A large knot, like a figure eight, can be tied to keep the rope or cable from pulling back through.
- The top cap is then secured into place. Once again, this should have duct tape wrapped *around the cap and rope* or cable for additional security.
- Make a variety of sizes and have additional materials with you in the vehicle to make additional slugs or in case adjustments are needed.

Example 11.1 While performing several slug tests in the Beaverhead Valley, near Dillon, Montana (Figure 11.4), in 1996, a supposedly secure top cap separated from the slug and we helplessly watched the rest of the slug drop out of sight. It had been held on with PVC glue. Reinforcing each slug, top and bottom, with duct tape became standard procedure ever since and even after several tens of more tests, this security step proved itself again and again.

In another setting, a heavy pump was to be lowered down a well, via a braided stainless-steel cable. A loop through the top of the pump was used to link the cable, and a purchased clamp that was wrenched tight

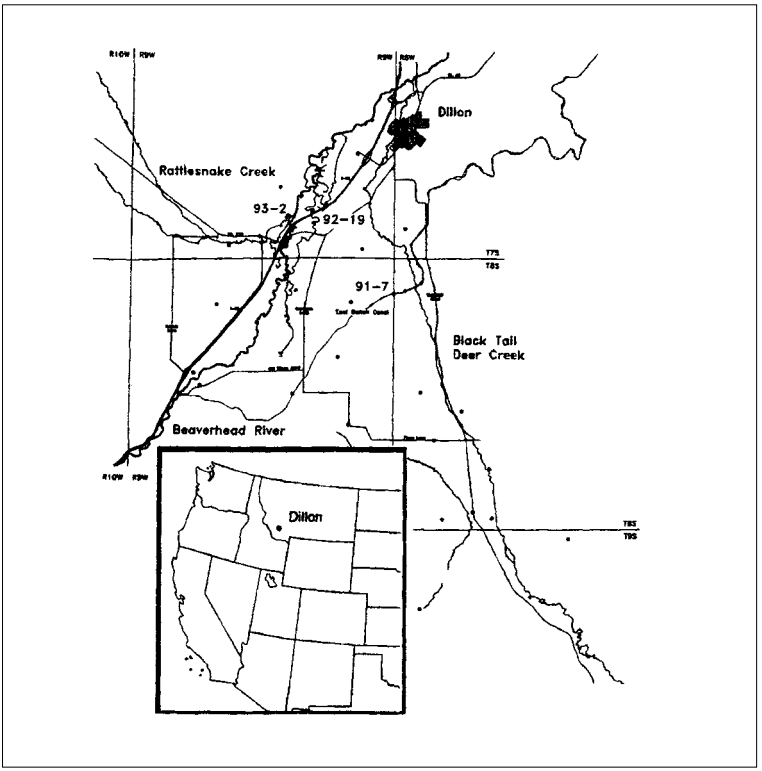

Figure 11.4 Slug test area, Beaverhead Valley, Dillon, Montana.

was supposed to hold the loop. Fortunately, after raising the pump, the faulty clamp slipped, revealing its inability to hold the cable before it was positioned over the well. A new approach of tying a knot and duct taping the knot, in addition to the clamp, worked beautifully. It is much easier to cut away duct tape than "fish out" lost equipment.

Performing a slug test

Performing a slug test is fairly straightforward and should take less than a half-hour per well, unless the hydraulic conductivity is very low. The following steps are presented to help the field person remember what to do:

- Obtain general information about the well, such as well completion information, total depth, location of screen, diameter, height of water column above the screen. This is important to select an appropriately sized slug, and to know the transducer range that will be necessary (Chapter 9).

- Remove the well cap and take a static water-level measurement. This should be checked a few times before starting the test to see if changes or trends are occurring.
- Select the appropriate transducer and lower it *below* the location where the bottom of the slug will be placed. Note that if the transducer is rated at 10 psi and if it is lowered into more than 23 ft of water, it may become damaged and not take a reading (Chapter 5). Allow the transducer to stretch and hang for a few minutes, so that vertical movement is not occurring during the test.
- Create a loop (bite) of at least 1-in diameter in the transducer cable and secure it with duct tape or electrical tape. The loop rests on the top of the well casing, and an additional wrap of the transducer cable is made around the well casing. This is all secured into place with duct tape so that the transducer doesn't move during slug retrieval (Figure 11.3).
- Connect the transducer to the data logger, establish the transducer parameters, and prepare for the starting of the test. Before lowering the slug and setting the reference level, take a reading from the data logger to see if the water depth looks reasonable. Reasons for strange readings on transducers are discussed in Chapter 9.
- Lower the slug with a rope or cable below the water level and tie it off until the water level equilibrates. Note that if the slug floats, it needs to be retrieved and filled with more sand and gravel to make sure it sinks.
- Once the water level has equilibrated, the test is ready. Recheck the data logger and establish the reference level to be some value greater than the maximum expected displacement (a value of 10 or 100 is usually what the author uses).
- While holding the line, carefully untie the slug rope and be ready for the signal to retrieve the slug. Start the data logger in log mode, and with only a second or two delay, briskly retrieve the slug. One way to think of it is to count to four and on three start the data logger.
- Check the data logger to see whether the water level has equilibrated and stop the test. This process should be repeated three times to make sure the data behave similarly.
- Decontaminate the slug and make sure well caps are replaced and the site is left the way you found it.

What was just described is a **rising-head test.** Theoretically, one could get the same results by suspending the slug above the static water level and lowering the slug into the water. This would cause the water level to be displaced upward and gently return down to the original level (a **falling-head test**). Another way to perform a falling-head test

is to pour a known volume of water down a well and record the "fall" in water level to equilibrium. This assumes that adequate well development has occurred. The author prefers the rising-head test because the water that is displaced must come from the aquifer, rather than pushed out into the aquifer as is done in a falling-head test.

The reason for turning the data logger on just a few seconds before the slug is "instantaneously" retrieved is to make sure that the slug clears the water. If the slug hasn't cleared the water surface, "splash effects" and an erroneously large reading will occur (Table 11.1). One must look for the maximum displacement (h_o or w_o in Figure 11.1) in the data. This is presumed to occur at time zero. All other data (h) are adjusted and referenced from the maximum displacement point. In Table 11.1, the measurement at time 0.0133 min represents where the slug did not break the water surface yet, thus creating an erroneously large displacement value. The subsequent oscillation downward represents the splash effect. Time zero has been adjusted from 0.0266 min. Displacement versus time plots are used to estimate the hydraulic properties. Slug testing is also performed pneumatically by plumbing the well so that a "blast" or pulse of air instantaneously displaces the water surface (Butler, 1998). The datalogger records the displaced water-level data over time. The collected data are plotted and form the basis for estimating aquifer hydraulic properties.

TABLE 11.1 Slug Test Illustrating a Slug not Clearing the Water Surface with Initial Reference of 100 ft (3-ft Slug in 2-in Well)

Time (min)	Displacement (ft)	Time (min)	Displacement (ft)
0.0	99.984	0.12	101.218
0.0033	99.984	0.14	101.155
0.0066	99.984	0.16	101.91
0.01	100.095	0.18	101.033
0.0133	107.954	0.20	100.947
0.0166	101.392	0.30	100.767
0.02	101.423	0.40	100.623
0.0233	101.55	0.50	100.509
0.0266	101.566	0.60	100.442
0.03	101.534	0.70	100.378
0.0333	101.518	0.80	100.316
0.0366	101.502	0.90	100.269
0.04	101.487	1.00	100.236
0.05	101.455	1.20	100.175
0.06	101.408	1.40	100.148
0.07	101.376	1.60	100.116
0.08	101.329	1.80	100.092
0.09	101.297	2.00	100.079
0.10	101.265	2.50	100.042

Slug tests using well sentinels

Well sentinels are uniquely suited to obtaining slug-test data. The parameters of the well sentinel are established prior to the test communicated via a USB cable and laptop computer. The author has found it convenient to set the well sentinel to collect data in linear mode every 0.5 s. This is usually sufficient to capture the aquifer response. The protocol differs only slightly from what was described in the previous section. A brief synopsis of the appropriate steps to take is presented.

- After the static water level has been measured, attach the well sentinel to a secure cable on the spool (Figure 11.5). The parameters should have previously been established with the laptop and the sentinel may already be collecting data.
- Lower the sentinel below the "active depth" of where the slug will be raised and lowered, but not below the PSI rating of the sentinel. The cable can be secured in place with a strong spring-tensioned clip.
- Lower the slug into the water and tie it off for 10 min or so (depending on the expected recovery time) then briskly retrieve the slug out of the well and wait for another 10 min or so (once again depending upon the expected time needed for recovery). The well sentinel should have collected the first falling head and rising head test.
- Repeat the process twice more to obtain three falling-head tests and three rising-head tests. (Figure 11.6)

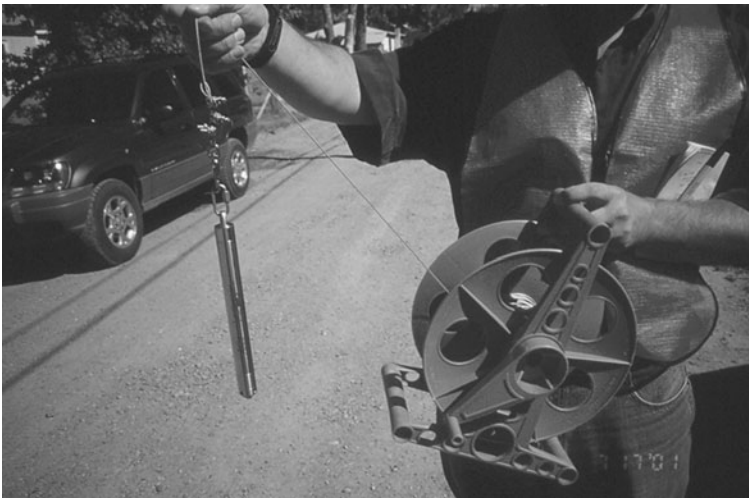

Figure 11.5 Well sentinel attached to airline cable on a spool.

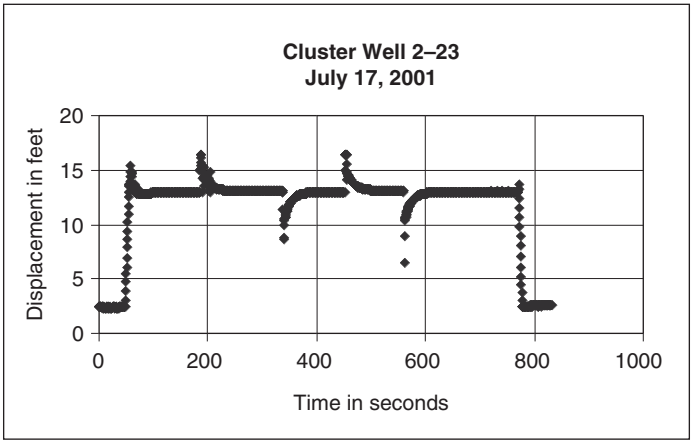

Figure 11.6 Data set showing lowering of the well sentinel down the well followed by lowering and retrieving a slug several times and finally lifting the well sentinel back to the surface. A data set like this would be cut and pasted into separate spreadsheet pages for individual analysis.

- The well sentinel will need to be reconnected with the laptop to upload the data and configure before moving on to the next well.
- Any decontamination should also be performed before transferring the well sentinel to another well.

11.2 Common Errors Associated with Performing Slug Tests

There are two topics the author would like to emphasize about the hydrogeologic setting where slug tests are typically performed, that of performing slug tests in monitoring wells. The other topic has to do with equipment problems. Most of this information was taken from a short course taught by the author at a field conference in Florida (Weight 2006).

Monitoring well completion issues

Everything mentioned in the previous section about the slug-testing procedures sounds fine until one considers a few things about monitoring wells. Monitoring wells tend to be placed quickly and methodically to establish a monitoring network to estimate the spatial distribution of hydraulic head and of water-quality constituents. Hopefully, by the time the wells are installed the connection with the aquifer is good enough to believe those data. Monitoring wells are usually not drilled or developed with the objective of estimating aquifer properties. Slug testing, therefore, can be seen as an afterthought or as "Hey let's

estimate the aquifer properties too while we are collecting field data." Nevertheless slug testing can be performed to obtain useful relative information. To explore some of the problems with monitoring wells it is useful to consider the many ways monitoring wells are drilled and completed:

- What is being tested, the well completion or the aquifer? What kinds of screen and sand packing materials were used?
- Is the well an "open-hole" completion? Or is the bottom cap missing?
- Does the screen extend above the static water level?
- What is the position and length of the screen?
- Is sand packing material present or is the well naturally developed? If so over what length?
- Which drilling methods were used and were any problems encountered during drilling?
- How long and to what extent was well development performed? What "skin effect" issues might there be?
- Was grouting used and if so where?
- If the well is surged using a slug does it produce sediment? When doing this does surging develop or clog the sand packing?
- Was slug testing performed multiple times on each well?

The list above is by no means exhaustive but serves to get the reader thinking. There are some general principles that can be derived from posing the above questions. First of all if the screen and packing materials are of a smaller diameter than the aquifer materials the hydraulic properties of the aquifer *is not* what will be tested. Many times "in stock" monitoring screens of a given slot size or packing materials are used on every monitoring well, regardless of the aquifer's physical properties. In this case monitoring wells should only be used for static head and water-quality parameters.

Slug-testing analysis procedures require that one know the length and diameter of the screen, the distribution of packing materials, and the moment in time of maximum water-level displacement. Water in wells with screens that extend above the static level surface is being displaced within the casing *and* the packing materials. Screens and packing materials that are *not* wet should not be included in the calculations. As obvious as this statement sounds the author has seen this occur.

Skin effects represent places where the borehole wall is disturbed or damaged and not well connected with the aquifer. This can occur from a sudden gush of water entering a hollow-stem drill string once a "knockout

plate" is removed (Chapter 8). During this event, muddy water in the drill hole "slimes" or coats the borehole wall, making it difficult to remove the fines during development. Another example of borehole wall damage occurs when the drill bit encounters a larger cobble and wobbling of the drill string extends the disturbed zone out farther than usual. Any of these mishaps may render the monitoring well useless, even with extra time that may be used during well development. When problems like the ones explained and others happen during drilling and well completion it may be more appropriate to abandon the well and start another hole.

Equipment problems

While performing slug tests there are some unique problems that may occur in the field which may affect the data. As one arrives in the field and removes the well cap the first step should be to measure the static water level. This should be done a few times before starting any test. Without the static water level measurement there is no reference point to know when equilibrium has been reached. If one is sensing water-level changes with pressure transducers using cables with "breathable" (hollow) barometric lines, care must be made to watch for kinks in the line. Kinks may result in the data not being accurately transmitted to the data logger. Usually a minimum-sized loop of 2.5 cm (1 in) in the line is enough to prevent kinking. Allow 10 to 15 min of time to allow the cables to be stretched straight so they aren't moving with time. Duct tape is usually a good medium to secure cables to the well bore. It should be noted that in the hot sun duct tape may "loosen its grip" and slippage or kinking of the line may result.

Another equipment problem results from idiosyncrasies associated with pressure transducers. For example, one of the last steps taken before one lowers the slug is to set the transducer reference level. All subsequent levels recorded by the data logger will be added or subtracted from the established reference level. If this is set before one allows cables to stretch or the transducer is secured, adjustments in the displacement data will be required. If one is performing a series of slug tests, one must reset the reference position for each well, as it will likely vary from well to well and contribute to confusion in interpretation of the data from several wells later on.

Also, before performing a slug test using pressure transducers, one should "read" the level sensed by the transducer at the data logger. If the unit was not lowered sufficiently below the water surface the slug will probably disturb it. If the pressure transducer level reads zero, then there may be a couple of explanations. First, check the cable connections with the data logger. Are any of the small wires in the connecting

junctions bent? Was the transducer or down-hole data logger stressed beyond its capacity? If you lower a 10-psi transducer into 35 ft of water, you may damage the unit and most likely the reading of head at the data logger will be zero (this is the voice of experience here).

With down-hole data loggers or well sentinels, the pressure level sensor and data logger are contained within the same unit. In this case the unit is programmed by a USB connection attached to a laptop computer to be programmed prior to lowering the unit down the well. With the down-hole data logger secured in place, a common scenario may be to program the time readings in linear scale every 0.5 or 1.0 s and then perform three falling-head tests and rising-head tests. When the data are read back unto the laptop one can tell when the slug displaced the static water level and reached equilibrium and was subsequently retrieved, repeating the process three times. The question comes up, how long does one wait between tests? This can be evaluated by measuring the static water level with an E-tape (this needs to be noted in a field book for possible corrections, as the E-tape may disturb the displacement data). In high transmissivity aquifers a linear time setting of 0.5 or 1.0 s may allow too much time to pass between measurements to provide sufficient detail needed for under-damped analysis. In this case the slug test would need to be redone with log cycle time settings and the down-hole data logger reread or re-programmed each time.

11.3 Analyzing Slug Tests—The Damped Case

Slug-testing methods and other topics in well hydraulics presume that Darcy's law is valid. Specifically, this means that viscous forces or frictional effects during groundwater flow predominate over inertial forces, which are usually considered to be negligible. The viscous forces allow sufficient friction to keep the water column from oscillating. This is known as the damped case. When the water column is displaced to the maximum (h_o), recovery occurs quickly at first and then tapers off. This is viewed in a data plot as a flattening in the slope. In high-transmissivity aquifers, water-level responses recover quickly and may have sufficient momentum to overcome the viscous forces and oscillate as an under-damped spring. What to do in this situation is discussed in Section 11.4.

This section presents how to analyze slug tests using the most common methods of slug test analysis, the Hvorslev (1951) and Bouwer and Rice (1976) methods. Frequently these are used for analysis in unconfined aquifers, but they have been used in analyzing partially penetrating and confined aquifers if the screen is well below the confining layer (Fetter 1994). Both methods provide an estimate of the hydraulic conductivity, but have no means for estimating storativity. Papadopulos et al. (1973)

provide a set of type curves that data can be matched to calculate transmissivity and storativity for confined aquifers. The data are plotted on semilog paper as the ratio of displacement (h) over maximum displacement (h_o) as h/h_o (log scale) versus time in arithmetic scale. A description of this method is summarized in Fetter (1994). Additional discussion and methodologies are presented by Butler (1998) in his book.

Hvorslev method

One of the most popular methods of analyzing slug-test data is known as the **Hvorslev** (1951) method (pronounced horse-loff). It is probably the quickest and simplest method. It is restricted to estimates of hydraulic conductivity within the screened zone of a well and can be applied to confined and unconfined aquifers. The maximum displacement value (h_o) is identified in the data. This is presumed to occur at time zero. The ratio of all other displacement data (h) to h_o or h/h_o are plotted on the ordinant (y-axis) in log scale, and time is plotted arithmetically along the abscissa (x-axis). There are no type curves with which to match the data. The plot is needed to identify the parameter (T_o) or the time it takes the water level to rise or fall to 37% of the initial maximum, h_o. This 37% is derived from the inverse of the natural log e. The value e is 2.7182818…, and the inverse of this number is 0.368 or roughly 0.37, hence the 37%. (It will be shown after the Bouwer and Rice (1976) section how to analyze these data without using a ratio approach to obtain T_o. There is an easier way). Hvorslev (1951) developed several equations to meet certain conditions, but the most commonly used equation is:

$$K = \frac{r^2 \ln(L/R)}{2LT_o} \tag{11.1}$$

where K = hydraulic conductivity
r = radius of well casing
R = radius of borehole (i.e, effective radius)
L = length of well screen plus filter packing if it extends above the top of the screen
T_o = time to reach 37% of H_o

Equation 11.1 is good for any case where $L/R > 8$. This is easily satisfied unless the well screen and packing interval are very short. The other parameters are derived from the well completion information (Figure 11.7). The radius of the well casing r is straightforward unless the displacement water level drops within the range of the screened interval. In monitoring wells that are completed to monitor LNAPLs such as gasoline, the screen typically extends above the static water level (Figure 11.8). In this case, the casing radius becomes an effective casing radius. If the

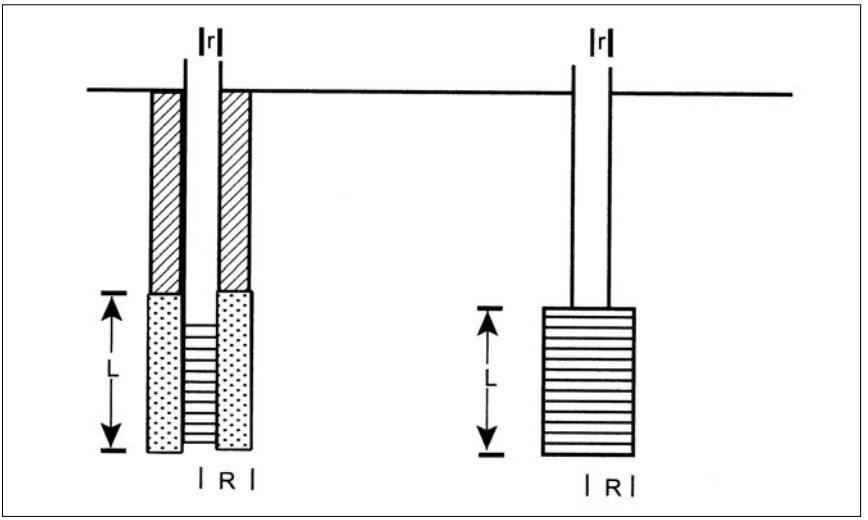

Figure 11.7 Well completion information used to obtain parameters used in the Hvorslev (1951) method in Equation 11.1. [*Modified from Fetter (1994).*]

gravel-packing material also extends above the top of the screen, the porosity of the gravel-packing material is taken into account to obtain an adjusted casing radius (r_A) by using Equation 11.2 (Bouwer 1989). The parameter η represents the porosity of the packing materials.

$$r_A = [(1.0 - \eta)r^2 + \eta R^2]^{1/2} \tag{11.2}$$

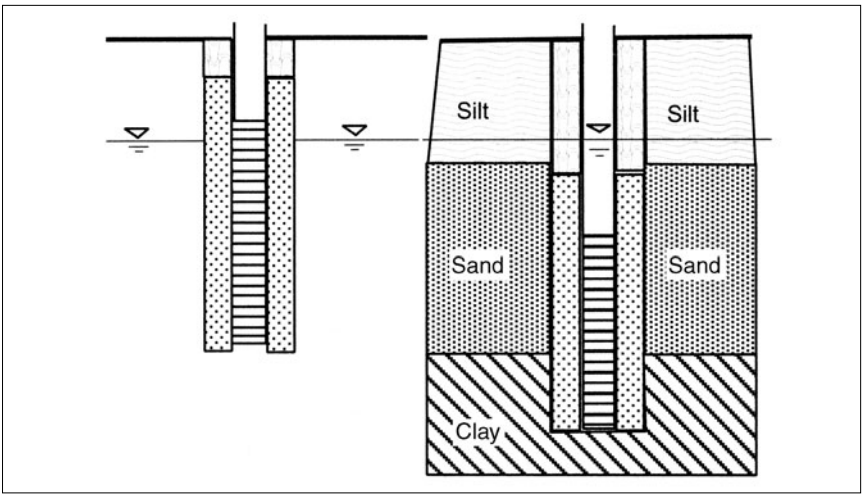

Figure 11.8 Examples of well completion showing gravel pack above the water table and the screen and gravel pack partially completed in clay.

Example 11.2 As an example to this adjustment for r_A, suppose the radius of the well screen is 0.167 ft (5.1 cm) and there is a gravel-packing material extending an additional 0.25 ft (7.6 cm) to the edge of the borehole with a porosity of approximately 25% all around the well screen. The radius of the borehole is 0.42 ft (12.7 cm). The adjusted radius of the casing using Equation 11.2 would be:

$$r_A = [(1.0 - 0.25)(0.17 \text{ ft})^2 + 0.25(0.4167 \text{ ft})^2]^{1/2} = 0.253 \text{ ft}$$

If the water level is affected within the packing materials, then the height or magnitude of displacement is proportionally less than would be seen if all displacement changes occurred solely within the casing. The parameter R is the effective radius of the borehole. The diameter of the borehole may vary, according to problems encountered during drilling. If the borehole is damaged or coated with drilling fluids, then a "skin effect" will separate the borehole from the aquifer and the hydraulic conductivity may reflect the "skin" and not the aquifer. The parameter L *includes* the gravel-packing materials. It is a common error to use only the screen length. The full saturated gravel-pack length is capable of allowing water from the aquifer to enter the packing material and thus the screen. One must properly apply the well completion information to perform the calculations. For example, Figure 11.8 shows an example of a well completed with screen above the static water level and an example of a well partially screened within a clay unit. It doesn't make much sense to extend the parameter L above the water table or into the clay unit if they are not contributing water. Example 11.2 shows how to adjust for the radius of the casing when displacement levels drop within the screen interval.

The author is aware of cases where the driller wishes to complete a monitoring well with packing materials at a lower hydraulic conductivity than the aquifer. If this is true and the well is supposed to be used for estimating hydraulic properties, then the driller should be "slapped up the side of the head." The hydraulic parameters that will be estimated will only reflect the gravel pack and not the aquifer. It is the hydrogeologist's responsibility to make sure that well completion reflects the purposes of the well.

Example 11.3 The data plotted in Figure 11.9 comes from a well completed in a streamside mine tailings area in southwestern Montana. Monitoring wells were installed to learn about the flow characteristics in the impacted area. The raw data are found in Table 11.1. The adjusted time zero is at 0.0266 min. All data previous to this time are presumed to be attributed to splash effects and are not used. The reference of 100 ft (30.5 m) is subtracted from all the displacement data before plotting.

If one looks at the data from a low angle (now get your face near the table surface), roughly three straight-line segments can be identified. The first

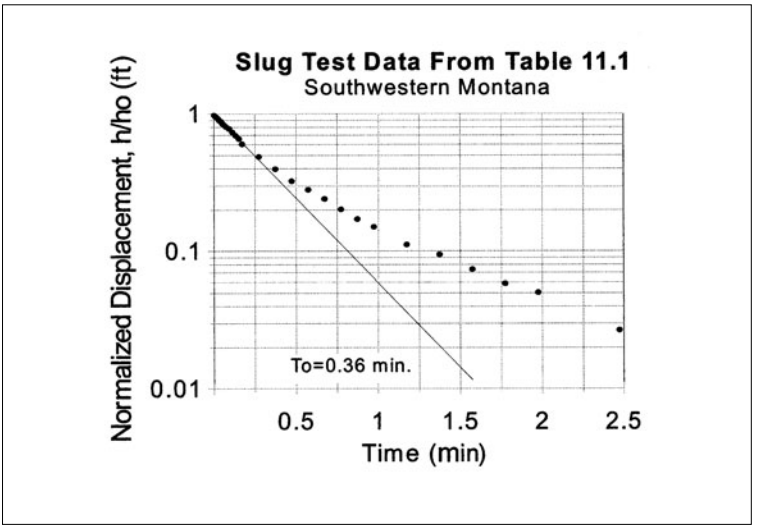

Figure 11.9 Slug test illustrating the Hvorslev slug test method. Flattening of the curve shows the tailing effect.

break is at approximately 0.25 min (15 s) and the second break is after 1.0 min. Approximately 50% of the total recovery took place during the first straight-line segment. The second and third segments are collectively referred to by the author as a "tailing effect" as a tapering recovery takes place. This is described in the paper by Bouwer (1989). From the diagram, a T_o of approximately 0.36 min is identified and used in Equation 11.1. The diameter of the casing is 2 in (5.1 cm), $r = 0.083$ ft, and the diameter of the borehole is approximately 8 in (22.8 cm), radius of $R = 0.33$ ft. The length of the screen (L) is 5 ft (1.5 m) and the packing materials are 7 ft (2.1 m).

$$K = \frac{r^2 \ln(L/R)}{2LT_o} = \frac{(0.083\text{ ft})^2 \times \ln(7\text{ ft}/0.33\text{ ft})}{2 \times 7\text{ ft} \times 0.36\text{ min}}$$

$$= 4.2 \times 10^{-3}\text{ ft/min} \times 1440\text{ min/day} = 6\text{ ft/day}$$

Bouwer and Rice slug test

Another commonly used slug-test method was developed by Bouwer and Rice (1976) that would estimate the hydraulic conductivity of aquifer materials from a single well. It was designed to account for the geometry of partially penetrating or fully penetrating wells in unconfined aquifers (Bouwer 1989). Many software packages provide the Hvorslev (1951) and Bouwer and Rice (1976) methods as the only choices for slug test analysis. Having more than one method to calculate the hydraulic conductivity is helpful. It is especially useful for cross-checking values for

comparison purposes. If the results of one method differ significantly from the other, then this is helpful in detecting calculation errors.

The slug-test data are collected, as before, except that Bouwer and Rice (1976) use a slightly different notation. They prefer to call the maximum displacement y_o instead of h_o and refer to the other displacement values as y_t instead of h. There is also no ratio of the data from y_o. Instead, y_o is chosen from the plot at time zero, unless there is a double-line effect (discussed later on in this section). The geometry of the variables used in the analysis is shown in Figure 11.10.

The variables are defined as:

h = depth from bedrock to water table
L_w = length from bottom of screen to the water table
L_e = length of well screen plus any packing materials
R_w = effective radius of well bore
y = displacement interval (shown as H in Figure 11.10)
r_c = radius of the casing where the rise of the water level is measured

As was mentioned earlier, Bouwer (1989) suggested that if the water level rises within the open or screened portion of the well, an adjusted r_c value needs to be calculated that accounts for the porosity of the packing material. This adjustment is not necessary if the rise in water level back to static water level is confined within the well casing. The hydraulic conductivity is calculated from:

$$K = \frac{r_c^2 \ln(R_e/R_w)}{2L_e} \frac{1}{t} \ln \frac{y_o}{y_t} \tag{11.3}$$

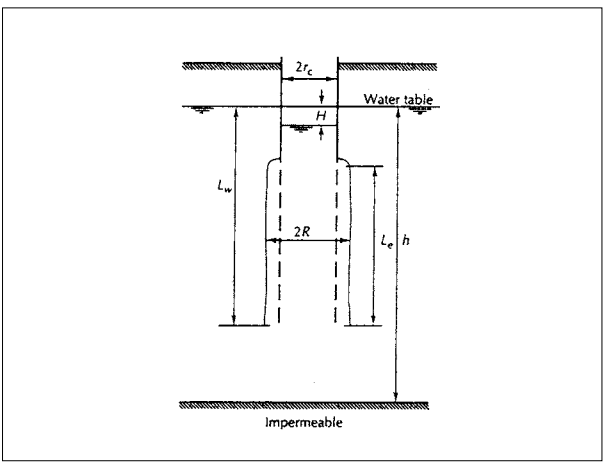

Figure 11.10 Geometry and parameters for a partially penetrating well screen in an unconfined aquifer. [*Bouwer (1989). Used with permission of Ground Water Publishing.*]

where y_o = the maximum displacement at time zero
y_t = displacement at a chosen time t
$\ln(R_e/R_w)$ = dimensionless ratio that is evaluated from analog curves (R_e is the effective distance over which the head displacement dissipates away from the well)

The analog data in Bouwer and Rice (1976) are used to fit one of two equations, one for the case that $L_w < h$ (i.e., partial penetration), and one for $L_w = h$ (i.e., fully penetrating). The equation for the partial penetration case is:

$$\ln \frac{R_e}{R_w} = \left[\frac{1.1}{\ln(L_w/R_w)} + \frac{A + B \times \ln[(h - L_w)R_w}{L_e/R_w} \right]^{-1} \tag{11.4}$$

and the equation for the fully penetrating case is:

$$\ln \frac{R_e}{R_w} = \left[\frac{1.1}{\ln(L_w/R_w)} + \frac{C}{L_e/R_w} \right]^{-1} \tag{11.5}$$

where: A, B, and C are dimensionless numbers plotted as a function of L_e/R_w.

The plots of A, B, and C are shown in Figure 11.11. One possible benefit of the Bouwer and Rice (1976) method is that the aquifer geometry is taken into account. A problem arises in using this method if the depth to bedrock is not known or cannot be estimated.

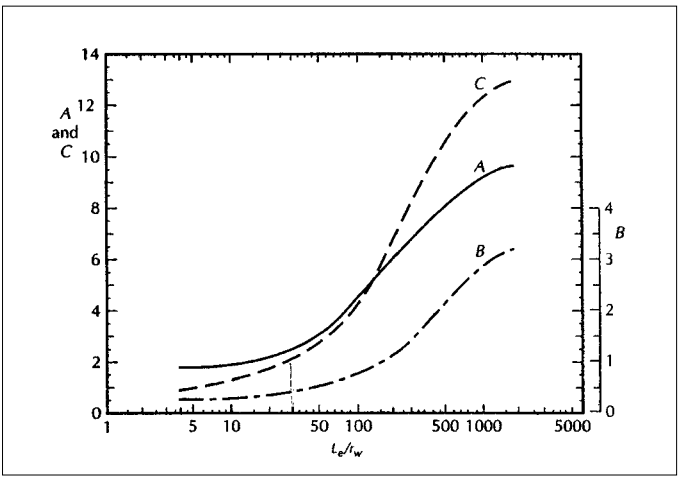

Figure 11.11 Parameters A, B, and C (dimensionless) plotted as a function of L_e/R_w used in Equations 11.4 and 11.5. [*Bouwer (1989). Used with permission of Ground Water Publishing.*]

Another phenomenon that may be observed in pumping tests is what is known as the double straight-line effect (Bouwer 1989). During initial displacement, the water in the gravel-packing material drains quickly into the well, thus showing a steep slope in the displacement data (Figure 11.12). When the water level in the packing materials equals the water level in the casing, then the water level slows to reflect the contribution of the aquifer materials, thus forming a second straight line. Any deviations after the second straight line may be attributed to the "tailing effect" described earlier in the Hvorslev (1951) method. The steep first-line portion of the curve usually takes place over a matter of a few seconds. In Example 11.3, one may argue that a double-line effect is observed; however, the first straight line takes place over 15 s, and the calculated value is consistent with the lithology (fine to medium sand). It is the author's experience that steep first-line segments reflecting drainage from the gravel pack occur over a few seconds or a very small proportion of the total time of recovery.

Since the first (very steep) straight line is representative of the gravel-packing materials, the second straight line is used in performing the calculations. Notice that y_o is projected back to time zero (Figure 11.12). The straight line for the aquifer response is projected below the tailing effect. Any time t can be chosen along the aquifer response line for the calculations. In Equation 11.3, the selected time t is matched with a corresponding displacement value y_t that is used when calculating the hydraulic conductivity. Since there are no requirements concerning 37% of the recovery, as in the Hvorslev method, it is convenient to select a time and displacement that are most easily read from the plot.

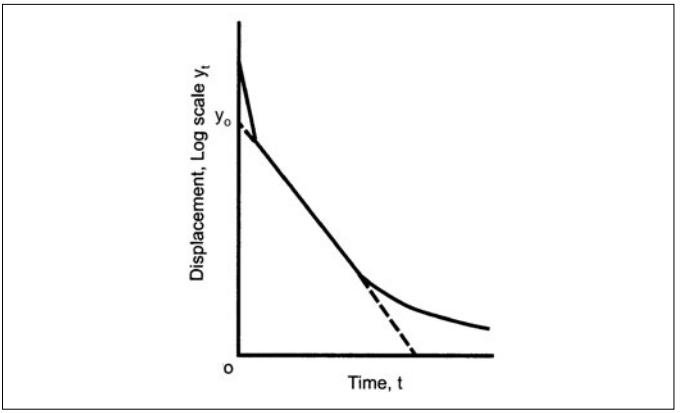

Figure 11.12 Displacement of head in a well versus time, showing the double straight-line effect. The first segment represents drainage of the gravel pack, the second segment the aquifer response, followed by the curved tailing effect. [*Modified from Bouwer* (*1989*).]

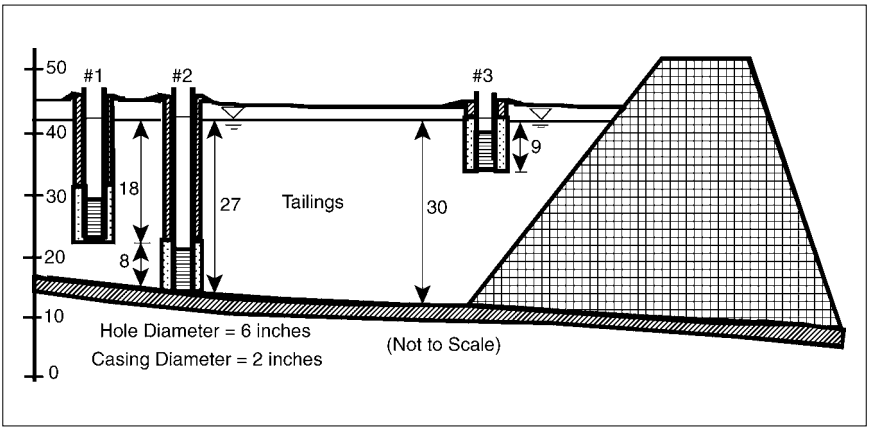

Figure 11.13 Cross-section view of the tailings pond with monitoring well completion information for Example 11.4.

TABLE 11.2 Slug Test Data from a Tailings Pond Site

Well 1		Well 2		Well 3	
Time (s)	Displacement (ft)	Time (s)	Displacement (ft)	Time (s)	Displacement (ft)
0	1.00	0	2.00	0	3.00
1	0.78	1	1.76	1	2.10
2	0.61	2	1.54	3	1.37
3	0.48	3	1.34	5	1.05
4	0.37	4	1.18	7	0.98
5	0.29	5	1.00	9	0.90
6	0.22	6	0.88	14	0.78
7	0.17	7	0.78	19	0.69
8	0.13	8	0.68	24	0.60
9	0.10	9	0.60	29	0.54
10	0.081	10	0.54	34	0.48
11	0.062	11	0.48	39	0.43
12	0.049	12	0.41	44	0.38
13	0.039	14	0.35	49	0.34
14	0.03	16	0.30	59	0.30
		18	0.28	69	0.28
		20	0.263	79	0.26
		22	0.248	89	0.24
		24	0.236	99	0.22
		26	0.224		
		28	0.213		
		30	0.205		

Example 11.4 Three students were sent out to a tailings pond site to conduct slug tests. Figure 11.13 shows a cross section of the setting. Each student selected a slug that would displace the same amount of water (in feet) as the well number. All students evaluated the data using the Bouwer and Rice (1976) method. Notes on the lithologic materials were misplaced. Implications concerning the nature of the tailings were to be evaluated from the slug test results. The data are shown in Table 11.2, and the plots and calculations are shown below.

Well 1 Since well 1 is partially penetrating, Equation 11.4 is used, where:

$$L_e = 9 \text{ ft}, L_w = 18 \text{ ft}, r = 0.083 \text{ ft}, R_w = 0.25 \text{ ft}, h = 26 \text{ ft},$$

$$A = 2.6, B = 0.45, t = 9 \text{ s}, y_t = 0.1 \text{ ft}, y_o = 1.0 \text{ ft}$$

$$\ln \frac{R_e}{R_w} = \left[\frac{1.1}{\ln(18 \text{ ft}/0.25 \text{ ft})} + \frac{2.6 + 0.45 \times \ln[(26 \text{ ft} - 18 \text{ ft})/0.25 \text{ ft}]}{9 \text{ ft}/0.25 \text{ ft}} \right]^{-1}$$

$$= 2.683$$

$$K = \frac{(0.083 \text{ ft})^2 (2.683)}{2(9 \text{ ft})} \frac{1}{9 \text{ s}} \ln \frac{(1.0 \text{ ft})}{(0.1 \text{ ft})} = 2.63 \times 10^{-4} \text{ ft/s} = 23 \text{ ft/day}$$

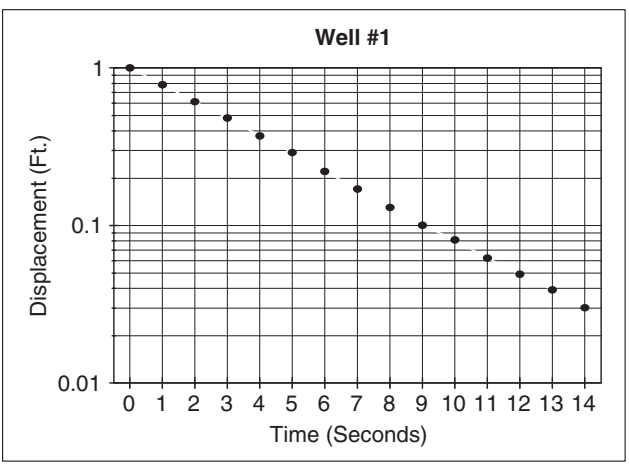

Well 2 Since well 2 is fully penetrating, Equation 11.5. is used, where:

$$L_e = 8 \text{ ft}, L_w = 27 \text{ ft}, r = 0.083 \text{ ft}, R_w = 0.25 \text{ ft}, h = 27 \text{ ft}, C = 2.2$$

$$t = 5 \text{ s}, y_t = 1.0 \text{ ft}, y_o = 2.0 \text{ ft}$$

$$\ln \frac{R_e}{R_w} = \left[\frac{1.1}{\ln(27 \text{ ft}/0.25 \text{ ft})} + \frac{2.2}{8 \text{ ft}/0.25 \text{ ft}} \right]^{-1} = 3.29$$

$$K = \frac{(0.083 \text{ ft})^2 (3.293)}{2(8 \text{ ft})} \frac{1}{5 \text{ s}} \ln \frac{(2.0 \text{ ft})}{(1.0) \text{ ft}} = 1.98 \times 10^{-4} \text{ ft/s} = 17 \text{ ft/day}$$

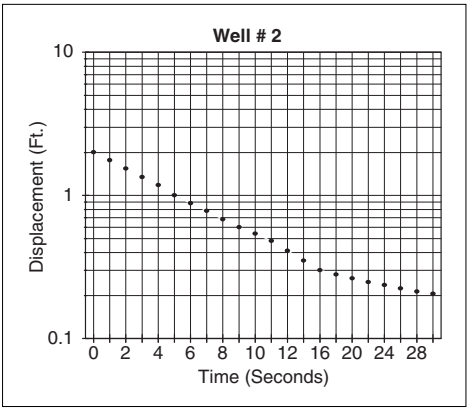

Well 3 Since well 3 is partially penetrating, Equation 11.4. is used, where:

$L_e = 9$ ft, $L_w = 9$ ft, $r = 0.083$ ft, $R_w = 0.25$ ft, $h = 30$ ft

$A = 2.6$, $B = 0.45$, $t = 9$ s, $y_t = 0.9$ ft, $y_o = 1.12$ ft

$$\ln \frac{R_e}{R_w} = \left[\frac{1.1}{\ln(9 \text{ ft}/0.25 \text{ ft})} + \frac{2.6 + 0.45 \times \ln[(30 \text{ ft} - 9 \text{ ft})/0.25 \text{ ft}]}{9 \text{ ft}/0.25 \text{ ft}} \right]^{-1} = 2.3$$

$$K = \frac{(0.083 \text{ ft})^2 (2.30)}{2(9 \text{ ft})} \frac{1}{9 \text{ s}} \ln \frac{1.12 \text{ ft}}{0.9 \text{ ft}} = 2.14 \times 10^{-5} \text{ ft/s} = 2 \text{ ft/day}$$

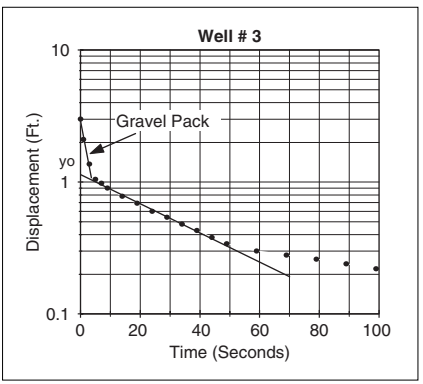

Even though the lithologic logs were lost, one can make some inferences concerning the hydraulic and lithologic properties of the tailings sediments from the location of the wells and the calculations. It is evident that the hydraulic conductivity decreases toward the dam. This is something that might be expected. As the tailings are slurried toward the dam, the coarsest fraction would likely settle out first. The finer materials would continue toward the dam. It appears that the coarsest fraction lies near the bottom with a fining upward sequence to the sediments. This suggests that higher hydraulic conductivities may be found nearer the bedrock in a direction away from the dam.

Common errors made in analyzing slug test data

There are some common ways that individuals make errors in performing calculations of slug tests. The most routine ones are presented below with an example with discussion following (Example 11.5).

- One uses the diameter of a casing or borehole instead of the radius in the calculations. All of the methods require the radius instead of the diameter.
- Forgetting to include the gravel-packing materials above and below the screen as the contributing length L. Many have only used the screen interval, which leads to inaccurate results.
- Be careful not to average the data to make a single "best fit" line. If the data are roughly in a straight line, then this is no problem, but including the tailing effect portion along with the aquifer response data will result in underestimating the hydraulic conductivity. Get your face close to the table to evaluate the plot to detect the appropriate straight-line section from which to draw the line.
- Don't forget to square the casing radius value. In both methods described above, the radius of the casing is squared in the calculations. In the Bouwer and Rice (1976) method, it is important to take the inverse of the bracketed quantity in Equations 11.4 and 11.5.
- In the Bouwer and Rice (1976) method, in the partial penetration case, make sure that the constants A and B are picked from the appropriate scales (the B scale is on the opposite side of the graph as the A scale.

Example 11.5 The author has observed numerous examples of "poor fits" from data plots performed by consultants, resulting in hydraulic parameters that make no physical sense compared to the aquifer materials. A typical example of one of these plots is shown in Figure 11.14. The displacement data are in feet and the selected time scale is in days. Notice that the maximum displacement occurs at about 4.2 ft (1.3 m) and much of the recovery data

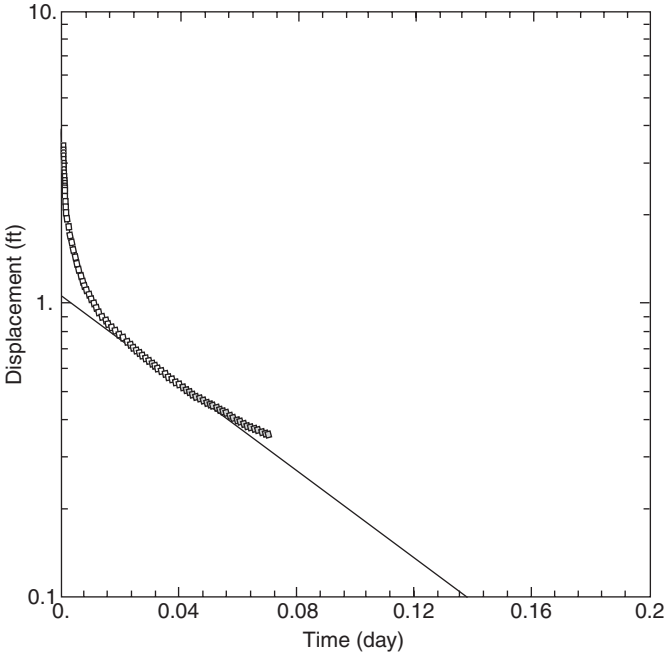

Figure 11.14 Example of a "poor fit" of the data from a slug test performed by a hydrogeologic consulting company.

(down to about 1.5 ft is a nice straight line) followed by a curved tailing effect. The presumed aquifer response was fit to the tailing effect (between 0.8 and 0.4 ft.), where less than 10% of the recovery data occur. The time scale of days was a poor choice and compressed the data where the aquifer response was occurring. The scale is also confusing because each tick mark on the x-axis represents 0.008 days (not exactly a convenient scale to work with). From the data fit the consultants arrived at an estimate of hydraulic conductivity of approximately 0.03 ft/day (0.001 m/day) for fine sand. If one fits the steep slope of the curve, one obtains a value closer to 2 ft/day (0.6 m/day). The author did not have confidence in the consultants work and redid the slug tests obtaining values of approximately 10 ft/day (3 m/day). It was unknown whether the consultants wished to skew the data to the lower side, as they had contamination issues and did not want to show much impact.

How to analyze slug tests for both damped methods from a single plot

Now that the Hvorslev and Bouwer and Rice methods have been presented, it is useful to see how to perform the calculations for both methods from a single plot. The simplest way of dealing with slug-test data is to plot displacement versus time. Recall that in the Hvorslev (1951)

method the data were normalized with h_o so that at time zero the value would be near 1.0. From this plot, the time at 37% was selected as T_o to be used in the calculations. Any displacement versus time plot can be used for the Hvorslev (1951) method. One only needs to determine what h_o or y_o is and then take 37% of this value for the corresponding T_o value.

For example, in well 3 in Example 11.4, if the projected h_o in the tailings pond is 1.12 ft, then 37% of this is 0.41 ft. T_o would be approximately 40 s. This would be used in Equation 11.1 to obtain:

$$K = \frac{(0.083 \text{ ft})^2 \ln(9 \text{ ft}/0.25 \text{ ft})}{2(9 \text{ ft})40 \text{ s}} = 3.4 \times 10^{-5} \text{ ft/s} = 3 \text{ ft/day}$$

In comparing the calculated values between the two damped case methods, the Hvorslev (1951) method yields a larger number, although both values are smaller than those of the other two wells. The reader is invited to make a comparison of well 1 and well 2 using the Hvorslev (1951) method (taking 37% of y_o to determine T_o) to recalculate the hydraulic conductivity. Similar trends to the Bouwer and Rice (1976) method should be observed; however, the numbers are not exactly the same. This is typical of aquifer hydraulics (Chapter 10); in some cases, one method may yield a higher or lower value than another method, but should yield similar trends.

The author noticed that when the well was fully penetrating (the case of well 2) the numbers from the two methods were almost the same. The Hvorslev (1951) method produces a higher hydraulic conductivity value for wells 1 and 3. In both of these cases, the wells are partially penetrating. The Bouwer and Rice (1976) method takes into account partial-penetration effects by including the aquifer geometry and may more accurately reflect the conditions. This is a subject for additional study and debate.

11.4 Analyzing Slug Tests—Underdamped Case

Unlike the previous sections where the methodologies for the damped case have been presented, there are occasions in high-transmissivity aquifers where the water-level response during slug tests behaves like an under-damped spring. The water level literally oscillates back and forth above and below the static equilibrium level in a methodical motion. This behavior is unexpected by many field personnel, since slug tests were primarily developed for low-transmissivity aquifers (Lohman 1972). Although different methods for analyzing these data sets exist, it is the author's experience that many individuals who encounter oscillatory water-level data during slug tests deem the data either "confusing

or unsolvable" or simply assign a "high" hydraulic conductivity. Analytical methods for oscillatory data in the literature are mathematically complex and challenging to use (van der Kamp 1976; Uffink 1984; Kipp 1985; Butler 2004).

Simplifying methods for practitioners have been developed for spreadsheets for the van der Kamp (1976) method (Wylie and Magnuson 1995) and for the Kipp (1985) method (Weight and Wittman 1999). One potential drawback is that both methods assume there is no skin effect, although the equations in the Kipp (1985) method do allow for skin effects. It is known that both positive and negative skins can occur (Yang and Gates 1997; Butler 1998); however, the impact of skin effects is often evaluated with lower hydraulic conductivity formations and can be reduced with proper well development. The author believes that a skin effect is a "fudge factor" associated with poor well completion and is difficult to quantify.

A relatively small group of researchers and practitioners have published information on water-level responses that indicate inertial effects resulting in oscillations. van der Kamp (1976) presented the first significant paper leading to the analysis of oscillatory data using a sinusoidal approximation method. In 1985, Kipp expanded the theory presented by Bredehoeft et al. (1966) to produce a series of type curves. Butler and Garnett (2000) have developed a spreadsheet method for slug tests performed on partially penetrating unconfined and confined aquifers respectively, which has been adopted into software packages. There are other underdamped methodologies that have been developed by Uffink (1984), Springer and Gelhar (1991), McElwee et al. (1992) and Butler and Garnett (2000). Some of these are also similar to the method by Kipp (1985) in that they also estimate a damping parameter (ζ) and the effective water-column height (L_e) and have been tested in the field.

Nature of underdamped behavior

The first significant explanations of underdamped oscillatory behavior were offered by Bredehoeft et al. (1966). They were intrigued by a couple of examples that occurred in Florida and Georgia. In Florida, a 12-in well completed in a cavernous limestone aquifer (transmissivity approximately 120,000 ft^2/day) responded in an underdamped oscillatory fashion when a float was periodically raised and lowered. This behavior was picked up by a pressure transducer within the well. In Georgia, a recorder located 200 ft from a city supply well showed an oscillatory response every time the city well's pump kicked on (Bredehoeft et al. 1966). Additional geologic field settings are described by Butler (1998). According to Bredehoeft and others (1966), systems are said to be:

- Overdamped or damped, where no oscillations occur following initial disturbance, indicating that viscous forces or Darcian conditions dominate the system,
- Underdamped, where oscillations occur as a damped sine wave, indicating that inertial forces are significant, and
- Critically damped, where the system is in transition between the two.

Bredehoeft et al. (1966) first studied inertial effects by simulating an oscillatory system using an electric analog, but did not develop a method of slug-test analysis. They present a relationship between transmissivity and effective column height (roughly the distance from the midpoint of the screen to the static water level surface.) for a given transmissivity and storativity (Figure 11.15). The fit line in Figure 11.15 represents where the critically damped transition takes place. A sinusoidal approximation to the underdamped oscillatory slug test response was presented by van der Kamp in 1976. Another sinusoidal approximation,

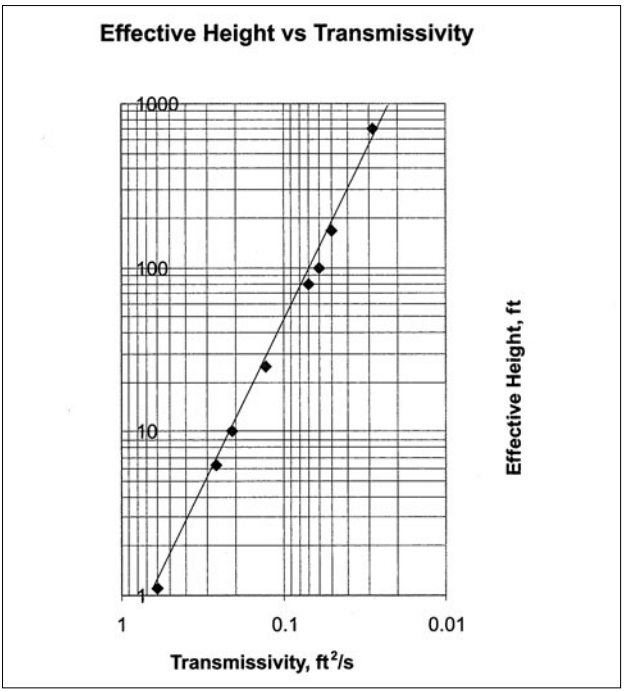

Figure 11.15 Relationship of transmissivity to effective water column height. Area above the plotted points represent the underdamped case, area below represents the damped case, and modified fitted line represents the critically damped transition. [*Modified after Bredehoeft et al. (1966.)*]

using a pneumatic procedure, is described by Uffink (1984) in Kruseman and de Ridder (1990). Kipp (1985) was later able to develop a method of slug-test analysis with type curves. The van der Kamp (1976) approximation method is easily performed using a spreadsheet solution developed by Wylie and Magnuson (1995). The type curves of the Kipp (1985) method along with a spreadsheet solution were developed by Weight and Wittman (1999).

Example 11.6 During the 1988 Hydrogeology Field Camp of Montana Tech of the University of Montana, underdamped oscillatory responses from slug tests were observed in wells west of Butte, Montana (Manchester 1990). Matching oscillations were noticed from two wells located 40 ft apart, although the observation well was significantly dampened. Follow-up pneumatic slug tests were performed, including one in a well "completed" in the swimming pool on the Montana Tech campus to simulate "infinite" transmissivity. A spectacular oscillatory response was observed (Manchester 1990).

Another "infinite" transmissivity example was observed in a 12-in production well after a blasting charge was set off. The 12-in well was supposed to be drilled into a mine adit that was encountered by two adjacent wells A and B (Figure 11.16). The adit was believed to be missed by only 1 to 3 ft. A blasting charge was set off to breach the connection (Figure 11.17). A pressure transducer in well B was destroyed during the process so no data were collected; however, a reflected beam of light from a mirror revealed a clear oscillatory response for over 7 min. The production well was subsequently tested at 200 gpm with 0.6 ft of drawdown observed, indicating that an excellent production well was achieved.

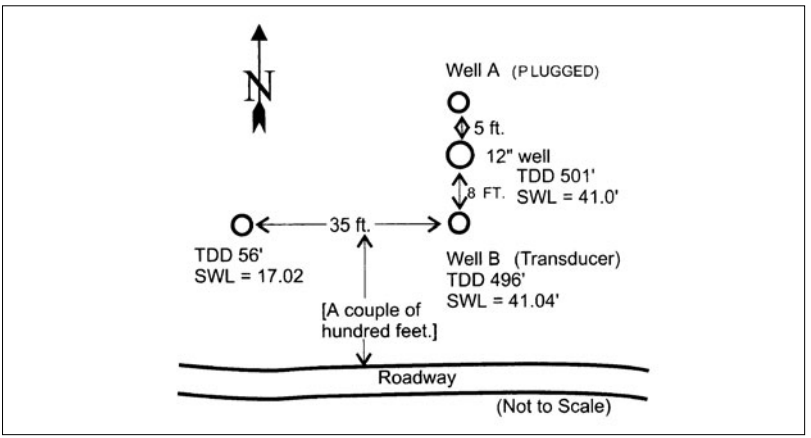

Figure 11.16 A 12-in production well missed a mine adit encountered by wells A and B. A blasting charge successfully breached the adit as oscillatory behavior occurred in the water level for over 7 min.

Figure 11.17 Constructing explosives pack.

Weight and Wittman (1999) describe oscillatory water-level responses while collecting slug-test data from wells scattered within the Beaverhead Groundwater Project Area (BGPA) in southwestern Montana (Figure 11.4). Point estimates of hydraulic conductivity values within the BGPA were needed to provide additional hydraulic control within a large area that was to be numerically modeled. These data would augment other hydraulic parameter estimates from pumping tests and previous slug tests. Of the 30-plus wells that were tested, over half of the wells showed an underdamped oscillatory response. It became necessary to analyze these data or have significantly less hydraulic control within the model domain.

Example 11.7 Perhaps one of the more spectacular oscillatory data sets collected by the authors occurred west of Butte, Montana, in July 1996, during the Hydrogeology Field Camp at Montana Tech of the University of Montana. The slug test was conducted prior to a constant discharge rate test (Figure 11.18). The normalized oscillatory response data are shown in Table 11.3 and illustrated in Figure 11.19. The effective column height was approximately 190 ft (58 m).

Effective stress and elastic behavior

Physically, the oscillatory behavior phenomenon can be partially explained by the concept of effective stress and inertia, resulting in an elastic wave propagation. The effective stress is the difference between

Figure 11.18 Constant discharge pumping test, Hydrogeology Field Camp, July 1996.

the total stress and the fluid pressure. Within an aquifer, the total load from the water and geologic materials is "felt" above a given plane (Fetter 1994). The load carried by the mineral skeleton is somewhat offset by the fluid pressure, resulting in an effective stress.

$$\sigma_t = \sigma_e + P_f \tag{11.6}$$

where σ_t = total stress
σ_e = effective stress
P_f = fluid pressure

In confined aquifers, changes in pressure can occur with very minute changes in actual thickness (Fetter 1994). In this condition, there is very little change in the total stress; however, the effective stress increases as the fluid pressure decreases and vice versa. The exchange back and forth in stresses produces an elastic-like response in a confined aquifer from being under pressure. The inertial effects of the displaced water column eventually balance out with the frictional forces of the geologic media and well completion materials (van der Kamp 1976).

The phenomenon of elastic behavior does not appear to be restricted to confined aquifers only. It is the author's observation that *any* aquifer that is being stressed during the first few seconds to a minute or so produces water from compression of the mineral skeleton or expansion of water (Chapter 10), even in unconfined aquifers (Prickett 1965; Neuman 1979; and Moench 1993). This essentially describes the specific storage (S_s) or

TABLE 11.3 Normalized Oscillatory Response Data, Sand Creek Well, West of Butte, Montana

Time (s)	Displacement (ft)	Time (s)	Displacement (ft)
4.0	−0.019	25.0	−1.471
4.5	−0.529	26.0	−1.377
5.0	−1.011	27.0	−1.112
5.5	−1.458	28.0	−0.718
6.0	−1.846	29.0	−0.252
6.5	−2.158	30.0	0.223
7.0	−2.384	31.0	0.642
7.5	−2.529	32.0	0.954
8.0	−2.583	33.0	1.121
8.5	−2.548	34.0	1.134
9.0	−2.438	35.0	0.995
9.5	−2.249	36.0	0.734
10.0	−1.997	37.0	0.390
10.5	−1.682	38.0	0.012
11.0	−1.320	39.0	−0.344
11.5	−0.923	40.0	−0.636
12.0	−0.510	41.0	−0.832
12.5	−0.095	42.0	−0.907
13.0	0.315	43.0	−0.863
13.5	0.696	44.0	−0.712
14.0	1.039	45.0	−0.476
14.5	1.335	46.0	−0.189
15.0	1.571	47.0	0.107
15.5	1.741	48.0	0.375
16.0	1.845	49.0	0.576
16.5	1.880	50.0	0.693
17.0	1.849	51.0	0.715
17.5	1.754	52.0	0.639
18.0	1.603	53.0	0.485
18.5	1.398	54.0	0.277
19.0	1.152	55.0	0.044
19.5	0.872	56.0	−0.186
20.0	0.573	57.0	−0.375
21.0	−0.044	58.0	−0.510
22.0	−0.621	59.0	−0.570
23.0	−1.081	60.0	−0.551
24.0	−1.373		

elastic storage viewed on a type A Theis (1935) curve (the early-time data, Chapter 10). Higher-transmissivity aquifers tend to propagate perturbations within an aquifer faster, indicating significant inertial effects over lower-transmissivity aquifers. An example of the quick transition of confined to unconfined conditions is presented in Example 11.8.

Example 11.8 Near Kalispell, in northwestern Montana, is a glacio-fluvial setting where a shallow coarse gravel aquifer (less than 30 ft or 9.1 m) overlies lacustrine clays. A constant discharge rate pumping test at 350 gpm

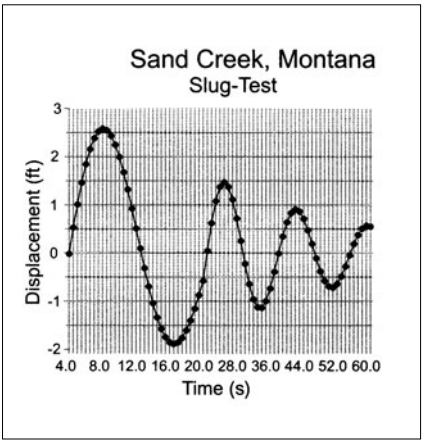

Figure 11.19 Slug test illustrating oscillatory behavior (data from Table 11.3).

(1,908 m^3/day) was conducted in a 10-in well to evaluate the hydraulic properties of the aquifer (King 1988). A plot of the data from an observation well located 37 ft away from the pumping well is shown in Figure 11.20. No transducer was on hand to collect the earliest time data (less than 1 min); however, delayed yield is evident within a couple of minutes. Delayed yield indicates the aquifer is unconfined and that the elastic response of the aquifer must have occurred within a minute or less, the approximate time of a slug test in a high-transmissivity aquifer. The transmissivity calculated was very high for a porous media aquifer, 70,000 ft^2/day.

During an instantaneous removal of a slug, the fluid pressure suddenly decreases, causing an increase in the effective stress. The mineral

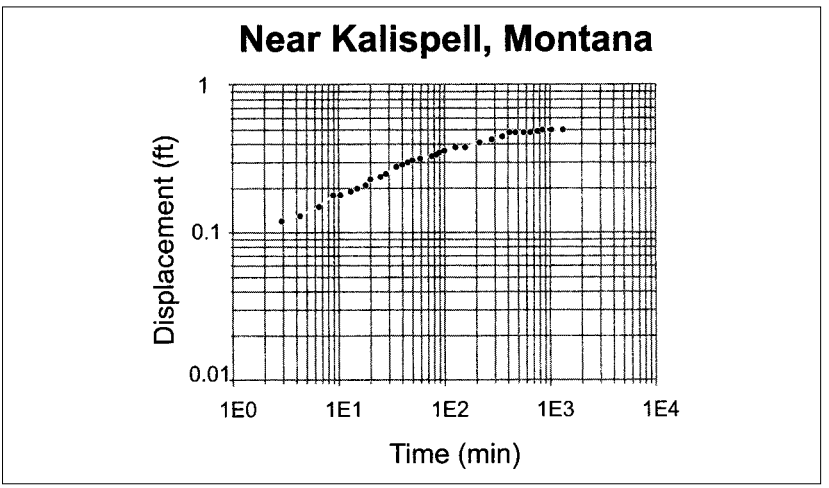

Figure 11.20 Displacement (ft) versus time (min) with pumping rate of 350 gpm, in a pumping test near Kalispell, Montana.

skeleton has to take more of the load, and this squeezes the aquifer slightly. Water from the aquifer then gushes into the well bore past the original "preslug" equilibrium position resulting in an upward oscillation. The inertial effects, that is, rate of change of momentum of the water column, pulled downward by gravity, gushes back out into the aquifer, increasing the fluid pressure once again during the downward oscillation. This can occur because the water column height is sufficiently high or the transmissivity is sufficiently large to overcome the critically damped transition zone (Bredehoeft et al. 1966). This process repeats itself until the aquifer materials and well completion materials finally dampen the process. It can be thought of as an elastic response created by a pressure wave propagating radially from the well. The higher the transmissivity, the easier it is for the pressure wave to propagate outward. Wylie and Magnuson (1995) draw the analogy of a mechanical system of a spring in a viscous medium, where the water column is the mass and the aquifer is the spring. In the "infinite" aquifer scenario of a cavernous limestone, swimming pool, or mine adit, eventually the well completion materials and boundary effects of the cavity cause damping to finally occur. In the above discussion, it is assumed that there were no skin effects.

Two methods will be presented on how to analyze data that behave in an underdamped fashion, the van der Kamp (1976) and Kipp (1985) methods. Each of these will incorporate spreadsheet algorithms developed by Wylie and Magnuson (1995) and Weight and Wittman (1999) to facilitate the process. All underdamped methods adjust the maximum displacement to time zero. Commercial software is available to describe the method by Butler and Garnett (2000).

van der Kamp method

Garth van der Kamp (1976) developed a sinusoidal approximation method to underdamped slug-test data. A brief theoretical development is presented, followed by the use of a spreadsheet analog with an example. The geometry needed to discuss the analysis of the well response is shown in Figure 11.21.

The effective length of the water column (L), as defined by Cooper et al. (1967) with the terms in the equation shown in Figure 11.21 is:

$$L = L_c + 3/8L_f \tag{11.7}$$

The equation for the balance of forces within the well filter, including inertial effects, is given in Equation 11.8.

$$\frac{d^2w}{dt^2} + \frac{g}{L}w = \frac{g}{L}h_f \tag{11.8}$$

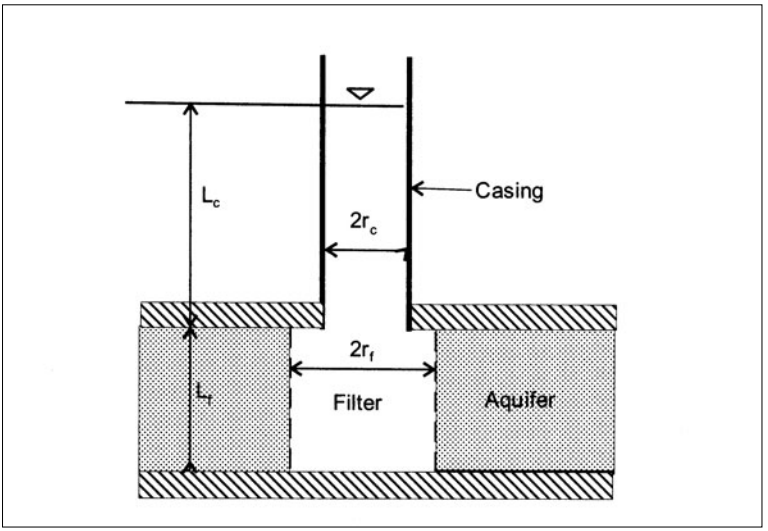

Figure 11.21 Geometry of slug test. [*Modified from van der Kamp (1976).*]

where w = transient water level in the well (L)
g = acceleration due to gravity (L/T^2)
h_f = hydraulic head of water in the filter (L)
L = length of the effective water column (L)

If the transient part of the hydraulic head can be assumed to be governed by the standard equation for radial flow and h_f is assumed to be the same everywhere inside of the filter pack an approximate solution can be used to simulate an exponentially damped cyclic fluctuation (Wylie and Magnuson 1995):

$$\omega(t) = \omega_o e^{-\gamma t} \cos(\omega t) \tag{11.9}$$

where γ = damping constant (gamma) (T^{-1})
ω = angular frequency of the oscillation (omega) (T^{-1})
ω_o = initial water-level displacement from slug removal (L)
T = time from the start of the test (T).

The field data are fitted to the approximation equation to determine values for γ and ω. It is presumed that Storativity (S) and the filter radius (r_f) are known or can be estimated. In the spreadsheet program created by Wylie and Magnuson (1995) the transmissivity values are estimated by fitting the field data to the approximation algorithm. Access to the spreadsheet program can be done by contacting the author at: wweight@mtech.edu. Essentially, once the spreadsheet is loaded,

one must follow the format of setting up the field data and then manually make adjustments to γ until there is a good match to the approximation algorithm. These are graphed as two different plot series whose patterns overlay once the appropriate γ and ω are chosen. The following suggestions will help one to quickly evaluate the data.

- Retrieve the spreadsheet program from the Internet created by Wylie and Magnuson (1995).
- Copy this spreadsheet to another worksheet so your field data can be evaluated, using the first spreadsheet as a reference.
- On the reference sheet notice that the *maximum* displacement value is used as the time zero position. If the maximum displacement value is not used at time zero, the graph of the algorithm approximation will not make sense.
- Increasing the gamma (γ) values narrows the frequency of the field data, and decreasing them will cause them to spread out more.
- Increasing the omega (ω) values tends to decrease the amplitude height of the field data.
- Decreasing the storativity values tends to increase the transmissivity significantly.

Example 11.9 An example of a sequential fit to the data from Table 11.3 is shown in Figure 11.22. As in the Kipp (1985) method, the storativity values are somewhat sensitive to the transmissivity outcomes. A discussion about this follows the presentation of the Kipp (1985) method.

Kipp method

Another method that can be used to estimate transmissivity values for aquifers was developed by Kenneth Kipp (1985). He was the first to expand the earlier theory developed by Bredehoeft et al. (1966) that takes into account both well-bore storage and inertial effects and produces a series of type curves that allow for oscillatory responses to be analyzed (Figure 11.23).

A summary of the basic assumptions given by Kipp (1985) was summarized by Manchester (1990) with additional discussion by Weight and Wittman (1999).

- Confined aquifer, bounded on the top and bottom
- Uniform aquifer thickness
- Well fully penetrates the aquifer
- Aquifer of infinite areal extent

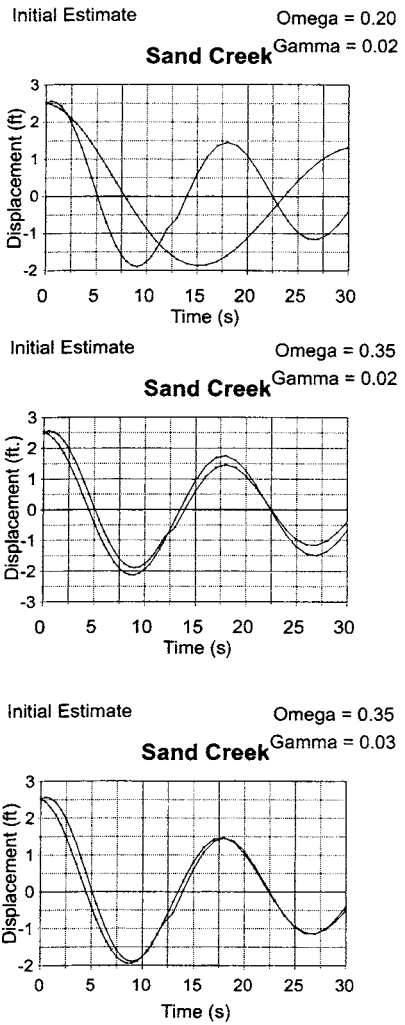

Figure 11.22 Sequential adjustments of omega and gamma in fitting the Sand Creek field data (Table 11.3) using the sinusoidal approximation spreadsheet algorithm by Wylie and Magnuson (1995).

- Homogeneous porosity (η) and matrix compressibilities
- Flat potentiometric surface
- Delayed yield not considered (Chapter 10)
- Constant water density in the well bore and a constant compressibility in the aquifer

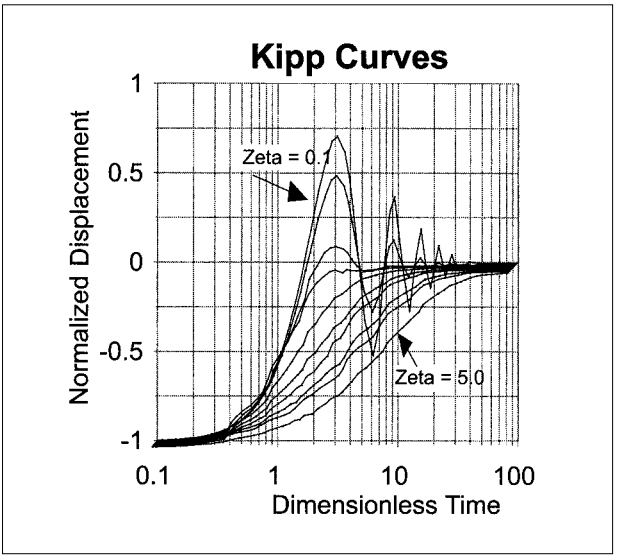

Figure 11.23 Type curves for normalized oscillatory slug-test data sets. Damping parameters Zeta are 0.1, 0.2, 0.5, 0.7, 1.0, 1.5, 2.0, 3.0, 4.0, and 5.0, with the smallest value representing the most oscillatory responses.

Kipp (1985) was able to generate dimensionless variables and parameters which were plotted into a series of type curves (Figure 11.23). For example, there is a dimensionless inertial parameter (β) that can be held constant while different values of the storage parameter (α) are used to produce the dimensionless damping parameter (ζ). The tabled values from the Kipp (1985) paper were entered into a spreadsheet (Weight and Wittman 1999). Field data can appropriately be scaled to fit the type curves to yield a value for transmissivity. A copy of this file is available via the Internet by contacting the author through the home page of the Department of Geological Engineering at Montana Tech (www.mtech.edu).

Methodology

The steps of the Kipp methodology will first be described from the paper by Weight and Wittman (1999) along with examples. To be able to follow along, it is assumed that the data collected in the data logger (displacement versus log time) have been uploaded to a PC or notebook computer into a spreadsheet program.

1. The uploaded data should first be converted into time units of seconds (x-axis) and displacement values in meters (y-axis) to match the type curves. Please read step 2 before this step is completed.

2. Evaluate the raw data and determine the reference point that the oscillations eventually dampen out to. This should compare closely to the original static water level or transducer reference point. For example, if the reference point in the raw data is 10.0 ft (3 m) and the data eventually dampen out to 10.019 ft, then 10.019 ft becomes the reference point. This also becomes the zero displacement reference level (w). All other displaced data are referenced to this final damped value so that differences will oscillate above and below the zero displacement line.
3. Determine the maximum displacement (w_o). Note: sometimes there is some confusion here if the data logger is turned on *before* the slug has been pulled. The authors have seen cases where the data logger records data as the slug is being pulled from the well bore and has not broken the water surface yet. This results in an abnormally large maximum displacement value (Table 11.1). If this occurs, use the next largest displacement value as w_o. This is also the reason for activating the data logger a few seconds before pulling the slug. Furthermore, it is important to also rescale the time value back to zero at the chosen w_o value.
4. Calculate $-w/w_o$ values for the displaced data. The minus sign is there because the type curves are viewed from a negative displacement perspective (i.e., rising-head test). Graph time in seconds (x-axis in log scale) versus $-w/w_o$ (y-axis in arithmetic scale).
5. Match the type curves with the graphed data. As you do this you will determine three values: the damping parameter (ζ), the first peak $\hat{t}$, and the subsequent inflexion point t. Highly oscillatory systems, with parameters smaller than 0.5, should be matched to the first largest inflexion point or peak to select time $\hat{t}$. Time t is picked at the second inflexion point (where the displaced data first change from concave downward to concave upward, usually near where it crosses the displacement axis; see the examples that follow). For oscillatory systems with a parameter greater than 0.7, use the lower inflexion point (where concave upward just begins, again consult the example).
6. Calculate the effective column length (L_e) using $\hat{t}$ and t using Equation 11.9 (Kipp 1985):

$$\hat{t} = \frac{t}{(L_e/g)^{1/2}} \tag{11.10}$$

where L_e = effective static water length (m)
g = acceleration of gravity (m/s^2)
$\hat{t}$ = dimensionless time
t = time

7. Calculate the dimensionless storage parameter (α). This takes into account well-bore storage by considering the radius of the casing. It is presumed that storativity S is known or can be estimated (Kipp 1985).

$$\alpha = \frac{r_c^2}{2 \times S \times r_s^2} \tag{11.11}$$

where α = dimensionless storage parameter
r_c^2 = radius of the casing (m)
S = storage
r_s^2 = radius of the screen (m)

8. Solve for the dimensionless inertial parameter (β), (Equation 28 in Kipp 1985). The critical damping parameter (ζ) is selected or estimated from the fit of the data to the type curves. This will also include additional discussion following step 9.

$$\zeta = \frac{\alpha(\sigma + 1/4 \times \ln(\beta))}{2 \times \beta^{1/2}} \tag{11.12}$$

where ζ = dimensionless damping factor
α = dimensionless storage parameter
β = dimensionless inertial parameter
σ = dimensionless skin factor

9. Calculate the transmissivity (T) in m^2/s, using the previously derived parameters (Kipp 1985).

$$\beta = \frac{L_e}{g}\left(\frac{T}{S \times r_s^2}\right)^2 \tag{11.13}$$

Equation 11.12, used to solve for β, is most easily derived by setting up an iterative solver on a spreadsheet. The solver can be set up from the following logic also presented by Weight and Wittman (1999). Assuming the dimensionless skin factor (σ) is zero, Equation 11.12 can be rewritten in the following form:

$$\zeta = \frac{\alpha \times \ln(\beta)}{8 \times \beta^{1/2}} \tag{11.14}$$

Equation 11.14 can be rearranged to:

$$\beta \times C^2 = (\ln \beta)^2 = 2 \times \ln \beta \tag{11.15}$$

where:

$$\zeta \times 8/\alpha = C \tag{11.16}$$

and C = a constant

$$\frac{\beta \times C^2}{2} = \ln \beta \tag{11.17}$$

Steps 6 through 9 are performed on the spreadsheet developed by Weight and Wittman (1999), including an iterative solver for Equation 11.14. The solver uses a fixed cell for the constant (C) and another cell is assigned to β. Three columns with formulas are set up to compare order of magnitude changes in β with the two sides of the equation expressed in Equation 11.14. When the values in the two columns match closely, the appropriate value for β can be identified. The following examples will illustrate the spreadsheet approach developed by Weight and Wittman (1999). In spite of the assumptions ball-park estimates for transmissivity can be made. It is recommended that estimates be compared to the method by van der Kamp (1976) and Butler and Garnett (2000).

Example 11.10 This example describes the step-by-step process to evaluate the data in Table 11.3 as a comparison to Example 11.8.

Key in the data from Table 11.3 onto a spreadsheet. The displacement values in feet need to be converted to meters (multiply by 0.3048 m/ft), the time data in seconds are already in the appropriate format.

Evaluate the data to determine a reference point where the data dampen to. In this case, assume this is at 0.0 ft since the time/displacement data stop before full dampening takes place.

The maximum observable displacement w_o is 0.787 m (2.583 ft). The data previous to 4 s are clouded by splash effects, this makes it difficult to determine where to rescale time zero. The author subtracted 6 s from the time data to rescale the data back to time zero.

A column on the spreadsheet is set up for the $-w/w_o$ values. A plot of time versus $-w/w_o$ values is shown in Figure 11.24.

From the plot, the values for $\hat{t}$ and t are estimated to be 10.1 and 13.8 s, respectively. The zeta value appears to be less than 0.1 (Figure 11.24), so a value of 0.09 is estimated.

The radius of the screen is 0.0254 m, and the radius of the casing is 0.0762 m, so alpha is calculated to be 4500 using Equation 11.11.

The value for beta from the spreadsheet matches well at 1.66×10^9, yielding a transmissivity of 0.01924 m^2/s (17,900 ft^2/day). This compares with an estimated value of 9600 ft^2/day using the van der Kamp method (1976) developed on the spreadsheet by Wylie and Magnuson (1995). Both suggest a high transmissivity.

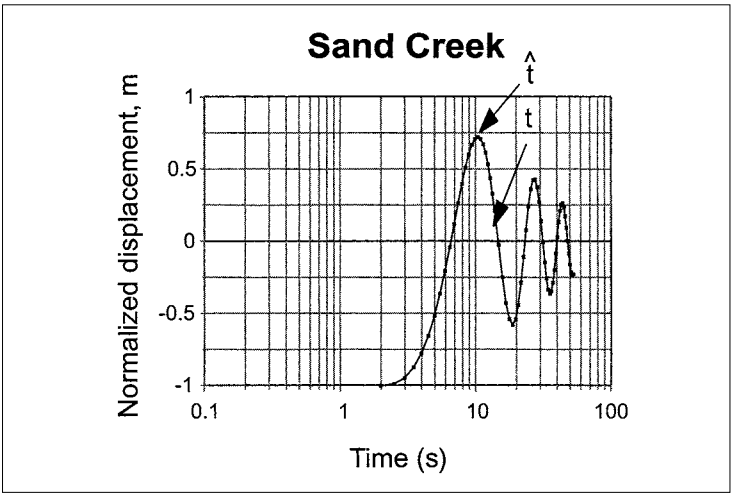

Figure 11.24 Plot of normalized displacement $-w/w_o$ versus time, illustrating how $\hat{t}$ and t are estimated in the Kipp Method (1985) for the Sand Creek data (Table 11.3).

Example 11.11 To illustrate an example of a larger damping parameter zeta, here is a data set from Well 93-2 south of Dillon, Montana, along Blacktail Deer Creek (Figure 11.4). The data are shown in Table 11.4.

Key in the data from Table 11.4 onto a spreadsheet. The displacement values in feet need to be converted to meters (multiply by 0.3048 m/ft); the time data in seconds are already in the appropriate format.

Evaluate to reference point where the data dampen to. In this case, dampening takes place near 0.0 ft (0.003 ft).

The maximum observable displacement w_o is 0.417 m (1.367 ft). The data previous to 1.8 s are clouded by splash effects. The author subtracted 1.8 s from the time data to rescale the data back to a new time zero.

A column on the spreadsheet is set up for the $-w/w_o$ values. A plot of time versus $-w/w_o$ values is shown in Figure 11.25.

From the plot, the values for $\hat{t}$ and t are estimated to be 2.2 and 8.5 s, respectively. The zeta value appears to be about 4.0 (Figure 11.23).

The radius of the screen is 0.0254 m and the radius of the casing is 0.0762 m, so alpha is calculated to be 45000 using Equation 11.11.

The value for beta from the spreadsheet matches well at 7.15E+07, yielding a transmissivity of 0.0192 m^2/s (130 ft^2/day). This compares with an estimated value of 0.0095 m^2/s (64 ft^2/day) using the van der Kamp method (1976) using an omega value of 0.05 and a gamma value of 0.08 from the spreadsheet developed by Wylie and Magnuson (1995). Both suggest a relatively low transmissivity. Data like these would more likely be analyzed with the Hvorslev (1951) or Bouwer and Rice (1976) method, but are presented here for comparison purposes.

TABLE 11.4 Data Set from Well 93-2 South of Dillon, Montana

Time (s)	Displacement (ft)	Time (s)	Displacement (ft)	Time (s)	Displacement (ft)
0.20	0.213	4.8	0.980	20.0	0.194
0.4	2.261	5.2	0.948	21.0	0.171
0.6	0.546	5.6	0.914	22.0	0.149
0.8	0.371	6.0	0.875	23.0	0.133
1.0	0.476	6.4	0.844	24.0	0.114
1.2	1.082	6.8	0.812	25.0	0.102
1.4	1.183	7.2	0.780	26.0	0.089
1.6	1.316	7.6	0.749	27.0	0.076
1.8	1.367	8.0	0.72	28.0	0.067
2.0	1.348	8.6	0.679	29.0	0.054
2.2	1.297	9.2	0.638	30.0	0.048
2.4	1.266	9.8	0.600	31.0	0.041
2.6	1.234	10.4	0.565	32.0	0.035
2.8	1.202	11.0	0.533	33.0	0.029
3.0	1.186	12.0	0.479	34.0	0.026
3.2	1.158	13.0	0.431	35.0	0.019
3.4	1.129	14.0	0.387	36.0	0.016
3.6	1.113	15.0	0.346	37.0	0.013
3.8	1.085	16.0	0.311	38.0	0.007
4.0	1.066	17.0	0.276	40.0	0.007
4.4	1.037	18.0	0.247	42.0	0.003
		19.0	0.219	44.0	0.003

Comparison of two methods and discussion of storativity

Weight and Wittman (1999) provide a table illustrating a comparison of 16 slug tests using the two spreadsheet algorithms presented above. In most cases the results are comparable (within a factor of 2 or 3). The author's experience is that one method does not necessarily yield a higher

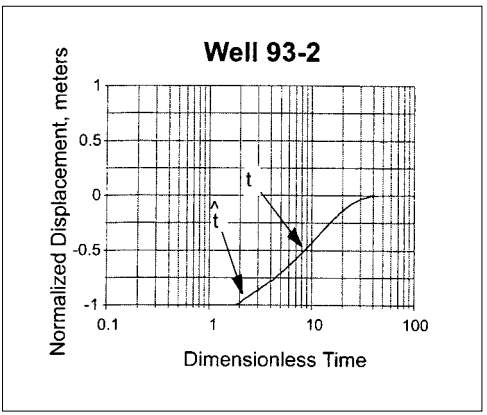

Figure 11.25 Plot of normalized displacement $-w/w_0$ versus time, illustrating how $\hat{t}$ and t are estimated in the Kipp Method (1985) for Well 93-2 in the Beaverhead, Montana, area.

or lower value on a consistent basis. Sometimes the van der Kamp (1976) method yields a higher value than the Kipp (1985) method, with the reverse also being true. The benefit of having two methods is to get a range of transmissivity values that may be representative of the aquifer.

Generally, the more oscillatory the data are, the smaller the damping parameter (ζ) and the higher the transmissivity. Wells with larger water columns also tend to have higher transmissivities (Figure 11.15). Butler (1998) points out that the water-column length is usually measured from the midpoint of the screen to the static water level. Wells with estimated damping parameters greater than 1.0 can probably be analyzed using the Hvorslev (1951) or Bouwer and Rice (1976) methods (Weight and Wittman 1999).

Both methods require an estimate of storativity. If the aquifer is confined, values between 10^{-3} and 10^{-5} are typical. However, as was discussed earlier with Example 11.8, both spreadsheet algorithms can be applied to leaky-confined or even unconfined aquifers (Weight and Wittman 1999). In all cases, it is necessary to use a confined storativity value or the results will not match the lithologies represented. Wells that are more shallowly completed and have less confining materials should begin evaluation using storativities of 0.001, and wells completed deeper or have semiconfining materials present should be evaluated using a storativity of 0.0001 (Weight and Wittman 1999). Storativity values can be adjusted by a factor of 5 to see where both underdamped methods agree best. Decreasing the storativity value results in an increase in the calculation of β and subsequently a larger transmissivity value. It is the author's experience that the Kipp (1985) method appears to be more sensitive to changes in storativity than the van der Kamp (1976) method. One should use the same storativity for both methods for a particular data set.

11.5 Other Observations

It is the author's experience that the results from slug testing tend to underestimate hydraulic conductivity values compared with constant duration pumping tests. This is based upon field experience where the author has observed data from wells that have been tested by both pumping tests and slug tests and from discussions with other colleagues. The amount of underestimation may range from approximately 30 to 100% to over an order of magnitude. This may be a function of well development and, therefore, skin effects and a reduced effective radius of influence for slug testing.

Within contaminated plume areas, where monitoring wells are installed, wells are not designed to produce much water and are not likely well developed. Monitoring wells completed in high-transmissivity

aquifers are installed with the intention of providing hydraulic head values and estimates of hydraulic properties. It is in high transmissivity aquifers where monitoring wells that are slug tested may also show underdamped behavior. The methods described in the this chapter can be used to evaluate slug-test data.

References

Bouwer, H., and Rice, R.C., 1976. A Slug Test for Determining Hydraulic Conductivity of Unconfined Aquifers with Completely or Partially Penetrating Wells. *Water Resources Research*, Vol. 12, pp. 423–428.

Bouwer, H., 1989. The Bouwer and Rice Slug Test—An Update. *Ground Water*, Vol. 27, No. 3, pp. 304–309.

Bredehoeft, J.D., Cooper, H.H., Jr., and Papadopulos, I.S., 1966. Inertial and Storage Effects in Well-Aquifer Systems: An Analog Investigation. *Water Resources Research*, Vol. 2, No.4, pp. 697–707.

Butler, J.J., Jr., McElwee, C.D., and Liu, W., 1996. Improving the Quality of Parameter Estimates Obtained from Slug Tests. *Ground Water*, Vol. 34, No. 3, pp. 480–490.

Butler, J.J., Jr., 1998. *The Design, Performance, and Analysis of Slug Tests*. Lewis Publishers CRC Press, Boca Raton, FL.

Butler, J.J., Jr., and Garnett, E.J., 2000. Simple Procedures for Analysis of Slug Tests in Formations of High Hydrualic Conductivity Using Spreadsheet and Scientific Graphics Software. *KSG Open-File Report 2000-40*. http://www.kgs.edu/Hdro/Publications/OFR00_40/index.html

Butler, J.J. Jr., and Zhan, X., 2004. Hydraulic Tests in Highly Permeable Aquifers. *Water Resources Research*, Vol. 40, W12402, 12 pp.

Campbell, M.D., Starrett, M.S., Fowler, J.D., and Klein, J.J., 1990. Slug Tests and Hydralulic Conductivity. *Proceedings of Petroleum Hydrocarbons and Organic Chemicals in Groundwater*, October 31–November 2, Houston, TX, NWWA, Dublin, OH, pp. 85–99.

Cooper, H.H., Jr., Bredehoeft, J.D., Papadopulos, I.S., 1967. Response of a Finite-Diameter Well to an Instantaneous Charge of Water. *Water Resources Research*, Vol. 3, pp. 263–269.

Crump, K.S., 1976. Numerical Inversion of Laplace Transforms Using a Fourier Series Approximation. *Journal of ACM*, Vol. 28, No. 1, pp. 89–96.

Driscoll, F.G., 1986. *Groundwater and Wells*, *2nd edition*. Johnson Division. St. Paul, MN, 891 pp.

Ferris, J.G., and Knowles, D.B., 1954. *Slug Test for Estimating Transmissibility*. U.S. Geological Survey, Note 26, 7 pp.

Fetter, C.W., 1994. *Applied Hydrogeology*, *3rd edition*. Macmillan, New York, 691 pp.

Hvorslev, M.J., 1951. *Time Lag and Soil Permeability in Ground Water Observations*. U.S. Army Corps of Engineers Waterway Experimentation Station, Bulletin 36.

King, J.B., 1988. *Hydrogeologic Analysis of Septic-System Nutrient-Attenuation Efficiencies in the Evergreen Area, Montana*. Master's Thesis, Montana College of Mineral Science and Technology, Butte, MT, 91 pp.

Kipp, K.L., Jr., 1985. Type Curve Analysis of Inertial Effects in the Response of a Well to a Slug Test. *Water Resources Research*, Vol. 21, No. 9, pp. 1397–1408.

Kruseman, G.P., and de Ridder, N.A., 1990. *Analysis and Evaluation of Pumping-Test Data*. International Institute for Land Reclamation and Improvement, Publication 47, 377 pp.

Lohman, S.W., 1972. *Well Hydraulics*. U.S. Geological Survey Professional Paper 708.

Manchester, K.R., 1990. *Oscillatory Responses Due to Inertial Effects and Observation Well Water Level Fluctuations Induced by Pneumatic and Vacuum Slug Test Methods*. Master's Thesis, Montana College of Mineral Science and Technology, Butte, MT, 85 pp.

McElwee, C.D., Butler, J.J., Jr., and Bohling, G.C., 1992. *Nonlinear Analysis of Slug Tests in Highly Permeable Aquifers Using a Hvorslev-Type Approach*, Kansas Geological Survey, Open-File Report 92–39.

Moench, A.F., 1993. Computation of Type Curves for Flow to Partially Penetrating Wells in Water-Table Aquifers. *Ground Water*, Vol. 31, No. 6, pp. 966–971.
Neuman, S.P., 1979. Perspective on "Delayed Yield". *Water Resources Research*, Vol. 15, pp. 899–908.
Papadopulos, I.S., Bredehoeft, J.D., and Cooper, H.H., Jr., 1973. On the Analysis of "Slug-Test" Data. *Water Resources Research*, Vol. 9, pp. 1087–1089.
Prickett, T.A., 1965. Type-Curve Solution to Aquifer Tests under Water-Table Conditions. *Ground Water*, Vol. 3, No. 3, pp. 5–14.
Springer, R.K., and Gelhar, L.W., 1991. *Characterization of Large-Scale Aquifer Heterogeneity in Glacial Outwash by Analysis of Slug Tests with Oscillatory Responses, Cape Cod, Massachusetts*, U.S. Geological Survey Water Resource Investigation Report 91–4034.
Theis, C.V., 1935. The Relation between the Lowering of the Piezometric Surface and the Rate and Duration of Discharge of a Well Using Ground-Water Storage. *Transactions of the American Geophysical Union*, Vol. 16, pp. 519–524.
Uffink, G.J.M., 1984. *Theory of the Oscillating Slug Test*. National Institute for Public Health and Environmental Hygiene, Bilthoven. Unpublished research report, 18 pp.
van der Kamp, G., 1976. Determining Aquifer Transmissivity by Means of Well Response Tests: The Underdamped Case. *Water Resources Research, American Geophysical Union*, Vol. 12, No. l, pp. 71–77.
Weight, W.D., and Wittman, G.P., 1999. Oscillatory Slug-Test Data Set: A Comparison of Two Methods. *Ground Water*, Vol. 37, No. 6, pp. 827–835.
Weight, W.D., 2006. Field Performance and Errors in the Analysis of Slug Tests. Conference Proceedings of the 2006 North American Environmental Field Conference and Exposition, Tampa, Florida. Presented by the Nielson Environmental Field School, 15 pp.
Wittman, G.P., 1997. *Computer Simulated Flow Model of the Groundwater Resources of the Beaverhead Valley in the Dillon Area, Beaverhead County, Montana*. Master's Thesis, Montana Tech of the University of Montana, Butte, MT, 101 pp.
Wylie, A., and Magnuson, S., 1995. Spreadsheet Modeling of Slug Tests Using the van der Kamp Method. *Groundwater*, Vol. 33, No. 2, pp. 326–329.
Yang, Y.J., and Gates T.M., 1997. Wellbore Skin Effect in Slug-Test Data Analysis for Low-Permeability Geologic Materials. *Ground Water*. Vol. 35, No. 6, pp. 931–937.

This page intentionally left blank

Chapter

12

Vadose Zone Hydrogeology: Basic Principles, Characterization, and Monitoring

The vadose zone is generally defined as the geologic media between land surface and the regional water table (Figure 12.1). The upper part of the vadose zone commonly includes the plant root zone and weathered soil horizons. Within the vadose zone, soils and bedrock are usually unsaturated, that is, their pores are only partially filled with water.

In places, however, the vadose zone may become water saturated; consequently, the vadose zone is not synonymous with the unsaturated zone. One obvious location where this occurs is just above the regional water table where capillary rise causes water to fill the pore spaces. Here, the pores are saturated but the water is held under tension, that is, the fluid pressure is less than atmospheric pressure. Saturated regions with positive pressures may also be found in the vadose zone; such as above a low permeable layer where perched conditions may develop (Chapter 3). A perched aquifer occurs within and is part of the vadose zone, and it is separated from the regional water table below by an unsaturated zone. These unsaturated zones above and below the perched aquifer are critical to the definition and field identification of a perched aquifer. In the vadose zone, saturated conditions also may develop locally beneath surface impoundments and drainages, as well as over more extensive areas near land surface during infiltration following precipitation events or flood irrigation.

To many hydrogeologists, groundwater occurs at a depth where water first enters a well. This is not uncommon for definitions set for various groundwater related regulations. But, Figure 12.1 shows that, by our preferred definition, the groundwater system includes the vadose zone as well. The groundwater system also includes the geologic medium below the regional water table, the phreatic zone, which will be an aquifer, aquiclude, or aquitard.

Copyright © 2008, 2001 by The McGraw-Hill Companies, Inc. Click here for terms of use.

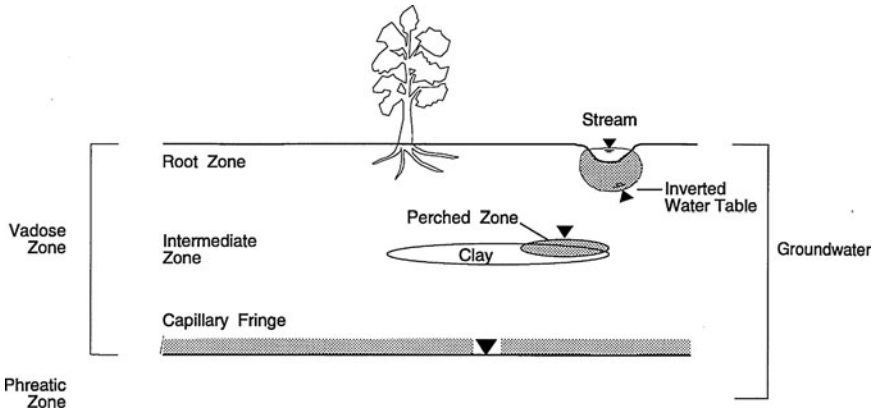

Figure 12.1 Conceptual model of the vadose zone. (*From Stephens, 1996. With permission of Taylor & Francis Group LLC.*)

12.1 Energy Status of Pore Water

What causes water to flow in the vadose zone? Just as in aquifers, the vadose zone water flows from areas of high potential energy to areas of low potential energy. To determine the direction of the driving force acting on water in the vadose zone, one needs to quantify the total potential energy of the soil water. The gradient of this total soil-water potential (the change in potential energy with direction in space) determines the magnitude of the driving force acting on the fluid. Mathematically, the total soil-water potential, ϕ_T, is expressed as:

$$\phi_T = \phi_{sw} + \phi_G \tag{12.1}$$

Notice that there are two primary components to the total soil-water potential, just as there are for the total hydraulic head in an aquifer (Chapter 5). The first component is the soil-water potential, ϕ_{sw}, and the second is simply the gravitational potential, ϕ_G.

The soil-water potential accounts for soil-water movement due to gradients in capillarity, pressure, temperature, chemical, and electrical potential. These components of the soil-water potential have been derived from fundamental thermodynamic principles. We will avoid these details here and summarize the main components of the soil-water potential:

$$\phi_{sw} = \phi_{\text{matric}} + \phi_{\text{pressure}} + \phi_{\text{osmotic}} \tag{12.2}$$

The matric component, ϕ_{matric}, recognizes that the energy state of water, relative to the reference state of an open body of pure water at 20°C, is influenced by the mutual attraction between the liquid, gas, and solid phases of the soil. In the definition of matric potential, we assume

that the other components, such as air pressure and chemistry of the pore fluids, are the same as those in the reference reservoir. Matric potential is attributed to capillary forces which predominate in wet soils and adsorptive forces which are more important in dry soils. Water held by capillarity occurs in the main pore bodies, whereas adsorbed water occurs where the polar water molecules coat the charged surfaces of the solid soil particles (Figure 12.2). In clayey soils, water can also be bound to soil particles in the electrostatic double layers. Where the soil is fully saturated and no air-water interface is present, $\phi_{\text{matric}} = 0$.

In the relatively wet range, which is generally at matric potentials greater than about -1 bar, the matric component is expressed by the capillarity equation:

$$\phi_{\text{matric}} = \frac{2\sigma}{r} \tag{12.3}$$

where σ is the interfacial tension of the liquid (MT^{-2}), and r is the radius of curvature on the air-water meniscus. Ideally, the surface tension of water is 72 dyn/cm. If the meniscus is concave toward the air, r is negative by convention. Therefore, the matric potential is negative as referenced to a free water surface at zero potential. Equation 12.3 can be written in terms of the radius of a capillary tube, r_t by recognizing that $r = r_t/\cos \alpha_c$:

$$\phi_{\text{matric}} = \frac{2\sigma \cos \alpha_c}{r_t} \tag{12.4}$$

where α_c is the contact angle made by the liquid-gas interface where it contacts the solid.

The osmotic component, ϕ_{osmotic}, takes account of the chemical concentration differences that may influence the energy state of the water.

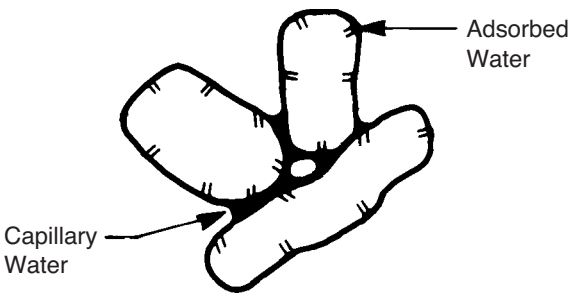

Figure 12.2 Matric potential is due to water held in soil by capillary and adsorptive effects. (*From Stephens, 1996. With permission of Taylor & Francis Group LLC.*)

Increasing the chemical concentration of the pore fluid will lower the potential energy of the liquid relative to the pure water reference state.

After considering all the components of total soil-water potential in the vast majority of practical vadose zone problems, matric potential remains as the most important to characterize, inasmuch as gradients of the other components of the soil-water potential are usually small relative to the soil-water potential gradient and gravitational gradient.

For computations, it is most convenient, however, to express soil-water potential as the potential energy per unit weight, so that the gravitational potential can be expressed in units of length and calculated simply as the elevation of the measurement point above some datum (Chapter 5). When the soil-water potential is expressed as a potential energy per unit weight, the soil-water potential is called the pressure head, ψ. Many soil scientists and engineers use different units of pressure to express soil-water potential, so it is useful to be familiar with some unit conversions:

$$1\text{bar} \approx 0.99\ \text{atm} \approx 100\ \text{kPa} \approx 1017\ \text{cm}\ H_2O \tag{12.5}$$

To convert the volume-based soil-water potential, ϕ_{sw}, to pressure head, ψ, the following equation is used:

$$\psi = \frac{\phi_{sw}}{\rho g} \tag{12.6}$$

where ρ is the fluid density and g is the gravitational constant. When the potential energy of water in soil is expressed on a per unit weight basis, the total potential energy Equation 12.1 becomes:

$$H = \psi + z \tag{12.7}$$

where H is the total hydraulic head and z is the elevation head relative to an arbitrary datum. This is exactly the same equation routinely used by hydrogeologists to compute hydraulic head and hydraulic gradients in aquifers, except that this form is more general in that, with our definition of ψ, water movement can occur under unsaturated as well as saturated conditions.

One of the key characteristics of the vadose zone is that the soil-water potential in partially saturated soil pores is less than zero, relative to a free water surface. The soil-water potential, including pressure head, would be positive within perched zones and below the water table, whereas at the water table, the soil-water potential would be essentially zero (where zero represents atmospheric pressure). Elsewhere, the soil-water potential is negative. There is a continuum of pressure in the vadose zone and this continuum extends into the underlying phreatic zone as well.

12.2 Water Content

The water content of a soil is probably the easiest property of the vadose zone to understand. However, different disciplines deal with this property in different ways. Three common expressions for water content are:

$$\text{Volumetric water content: } \theta = \frac{\text{volume water}}{\text{bulk volume soil}} \ (\text{cm}^3\ \text{cm}^{-3}) \quad (12.8)$$

$$\text{Gravimetric water content: } \theta_g = \frac{\text{mass water}}{\text{mass dry soil}} \ (g\ g^{-1}) \quad (12.9)$$

$$\text{Saturation percentage: } S = \frac{\theta}{n} \times 100 \ (\text{cm}^3\ \text{cm}^{-3}) \quad (12.10)$$

Most hydrologists and soil scientists prefer the volumetric water content, while geotechnical engineers generally use gravimetric water content, and petroleum engineers often work with saturation percentage. The volumetric water content is typically 40 to 60% greater than the gravimetric water content because of the following relationship:

$$\theta = \frac{\rho_b}{\rho_w} \theta_g \quad (12.11)$$

where the dry bulk density, ρ_b, is typically 1.4 to 1.6 g/cm^3, and the density of water, ρ_w, is 1.0 g/cm^3.

12.3 Soil-Water Retention Curves

There is a very important relationship that exists between the soil-water potential and the water content which is illustrated in the so-called soil-water retention curve or **soil-water characteristic curve** (Figure 12.3).

One way to illustrate the relationship between tension (soil-water potential) and water content is to represent the variable pore sizes of a field soil as a bundle of vertical capillary tubes having different diameters. If this bundle of tubes is inserted into the water table, water will be drawn up into the tubes until a static equilibrium condition is achieved (Figure 12.4b). The equation to compute the height of water rise in a capillary tube (Figure 12.4a) reveals that the smaller the tube radius, the greater the height of capillary rise. Up to a certain distance above the water table, all the tubes are filled with water. This height above the water table defines the upper limit of the capillary fringe. For clayey soils, the height of the capillary fringe may exceed 2 m in clay, and in gravel, it may only rise 10 cm. At greater distances above the water table, notice that fewer tubes are filled with water. By looking at the proportion of the tubes which are water-filled at progressively greater elevations, it is evident

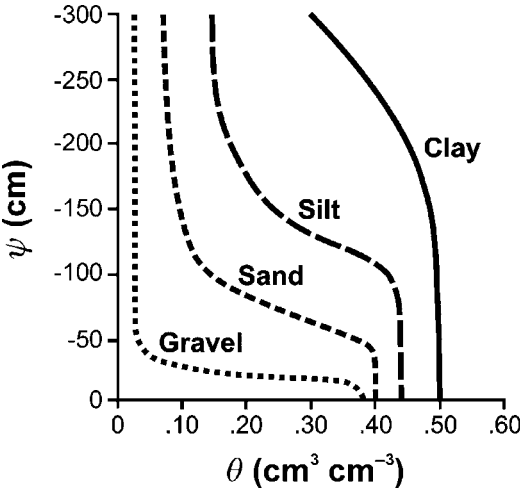

Figure 12.3 Effect of texture on the soil-water characteristic curve. (*From Stephens, 1996. With permission of Taylor & Francis Group LLC.*)

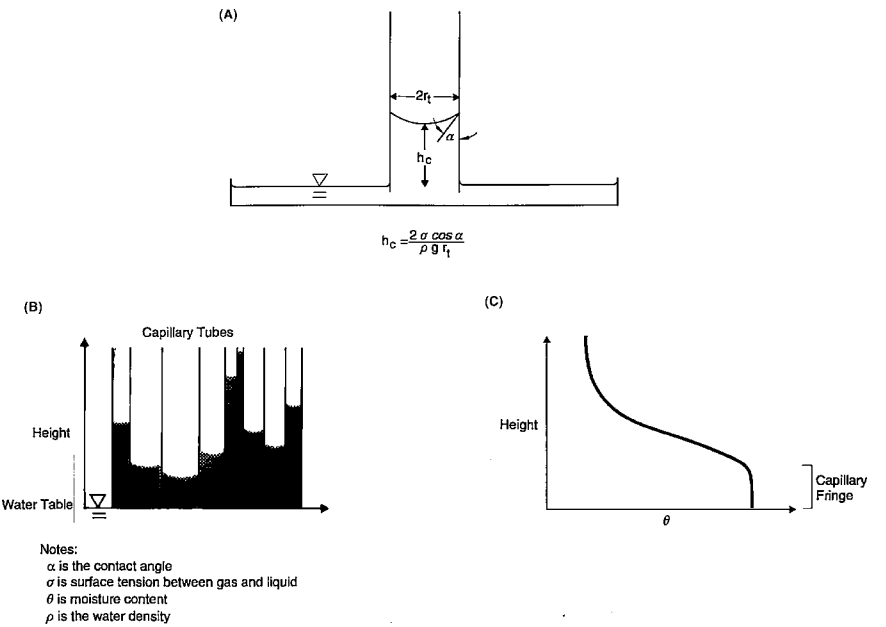

Figure 12.4 (A) Height of water rise in a capillary tube, (B) water rise in a bundle of capillary tubes representing a range of pore sizes, and (C) soil-water content above a static water table. (*From Stephens, 1996. With permission of Taylor & Francis Group LLC.*)

that the mean water content within the bundle of tubes decreases with increasing height above the water table (Figure 12.4b).

Thus, by analogy to the capillary tube bundle, the amount of water held in the soil at a prescribed pressure head or tension is dependent upon soil texture, as shown in Figure 12.3. If a soil is saturated and begins to drain (e.g., water table falls), coarse soils drain faster than fine-textured soils.

There are several features of a soil-water characteristic curve which are commonly referenced or measured (Figure 12.5). During drainage, the pressure head at which the air first begins to enter the previously saturated soil is called the air-entry value. Sand and gravel lose a large portion of their water just after the pressure head decreases below the air-entry value, whereas clay tends to lose much less water with decreasing pressure head.

Another term associated with soil-water characteristic curves is the **field capacity**. After 2 or 3 days of drainage following a thorough rain or irrigation, the rate of gravity drainage slows considerably, and the water content at this stage of drainage is called the field capacity. Although there is no good alternative for measuring field capacity other than in the field, field capacity often is arbitrarily quantified in laboratory tests as the water content corresponding to −100 or −300 cm pressure head (about −1/10 to −1/3 bars; Figure 12.5).

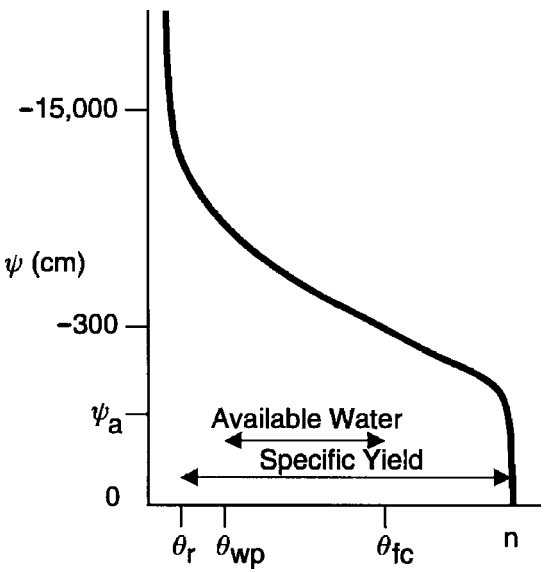

Figure 12.5 Indices describing the soil-water characteristic curves: θ_r is residual water content, θ_{wp} is permanent wilting point, θ_{fc} is field capacity, n is porosity and ψ_a is air-entry value. (*From Stephens, 1996. With permission of Taylor & Francis Group LLC.*)

With additional slow drainage or evapotranspiration to a very dry condition, the water content may become so low that many plants wilt. By convention, the water content corresponding to −15,000 cm pressure head (about −15 bars) is called the **permanent wilting point**, although the soil-water potential near many desert plants is even less, in places −40 to −80 bars or less. The water content difference between field capacity and permanent wilting (or −1/3 bar minus −15 bar water contents) is called the available soil water (to plants) (Figure 12.5).

As the soil dries below the permanent wilting point, the water content approaches an asymptote, so that with decreasing pressure head no further water drains from the soil. This is called the **residual water content**.

12.4 Darcy's Equation and Unsaturated Flow Parameters

Perhaps the most widely recognized equation among soil scientists, hydrologists, and petroleum engineers is Darcy's equation. Buckingham (1907), a soil scientist, demonstrated that Darcy's equation could be extended to unsaturated conditions as well.

If only water is the fluid of interest, then Darcy's equation is written as:

$$q_i = -K(\theta)_{ij}\left(\frac{\partial \psi}{\partial x_i} + \frac{\partial z}{\partial x_i}\right) \tag{12.12a}$$

where z is positive upward. Where the soil is homogeneous and isotropic and flow is vertical, then Darcy's equation becomes:

$$q_z = -K(\theta)\left(\frac{\partial \psi}{\partial z} + \frac{\partial z}{\partial z}\right) = -K(\theta)\left(\frac{\partial \psi}{\partial z} + 1\right) \tag{12.12b}$$

Darcy's equation simply states that fluid flow is a function of the driving force called hydraulic gradient (pressure and gravity terms in brackets) and a constant of proportionality called the hydraulic conductivity, K. The hydraulic conductivity accounts for the viscous flow and frictional losses that occur as a fluid moves through the porous medium.

Hydraulic gradient

The hydraulic gradient in the vadose zone exhibits interesting characteristics that contrasts markedly with those hydrogeologists are accustomed to in aquifers. In aquifer systems, flow is primarily horizontal and the regional hydraulic gradient is often in the range of 10^{-4} to 10^{-3}; it is rare that the hydraulic gradient ever exceeds 0.01, although there are exceptions such as at seepages faces, where groundwater flows across

faults and aquitards, and very close to pumped wells. But in the vadose zone, hydraulic head gradients near 1.0 (unit gradient) are common. Near unit hydraulic gradients may occur in deep vadose zones with uniform texture where the soil-water content is constant with depth. A unit hydraulic gradient indicates that the soil water is flowing vertically downward. When the gradient is unity, the magnitude of the flux, q, equals the hydraulic conductivity, $K(\theta)$.

Although the hydraulic gradient is often near unity, the hydraulic gradient can be many orders of magnitude larger near sharp wetting fronts in dry soils. On the other hand, the hydraulic gradient may also be much less than unity and, in fact, is zero where no flow occurs.

Unsaturated hydraulic conductivity

The following equation further explains how the hydraulic conductivity is a function of the fluid properties, the media properties, and the water content, θ:

$$K(\theta) = \left(\frac{k\rho g}{\mu}\right) k_r(\theta) \tag{12.13}$$

where k = intrinsic permeability of the medium (L^2), ρ = fluid density (ML^{-3}), g = gravitational constant (LT^{-2}), μ = dynamic viscosity of fluid ($MT^{-1}\,L^{-1}$), and $k_r(\theta)$ = relative permeability (dimensionless, ranges from 0 to 1). In Equation 12.13, the quantity in brackets represents the familiar saturated hydraulic conductivity for isotropic conditions. The relative permeability, sometimes called relative hydraulic conductivity, is a dimensionless parameter which accounts for the dependence of the hydraulic conductivity on pressure head or water content, as shown in Figure 12.6.

The relative hydraulic conductivity decreases rapidly with decreasing water content. As drainage progresses, smaller and smaller pores are left holding water. As the water content decreases, the path of water flow becomes more tortuous and the cross-sectional area of water in the pores decreases. In the dry range, the relative hydraulic conductivity becomes very small, so at low water content, the hydraulic conductivity may be perhaps more than a million-fold smaller than the saturated hydraulic conductivity.

The hydraulic conductivity of variably saturated media is highly dependent upon soil texture (Figure 12.7). Hydrogeologists and engineers are well aware of the nature of spatial variability in saturated hydraulic conductivity that is attributed to variability in the intrinsic permeability (Equation 12.13) of the geologic material (Chapter 3). For instance, well-sorted sand typically has a saturated hydraulic conductivity of about 10^{-2} cm/s, whereas clay may have a saturated hydraulic

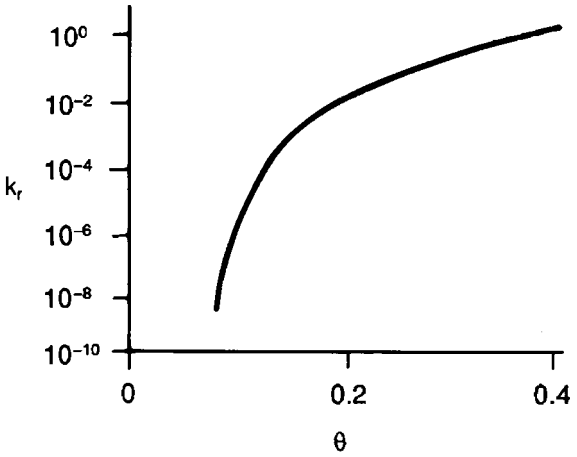

Figure 12.6 Relative hydraulic conductivity, K_r, versus water content, θ. Porosity is 0.4 cm^3/cm^{-3}. (*From Stephens, 1996. With permission of Taylor & Francis Group LLC.*)

conductivity of about 10^{-6} cm/s. But over the range of water contents likely to be encountered in the vadose zone, the unsaturated hydraulic conductivity of a single soil sample may change by one-million- or one-billion-fold or more.

It is especially important to recognize that at low pressure head or water content, the unsaturated hydraulic conductivity of a fine-textured soil may be greater than that of a coarse soil. For most hydrogeologists and engineers, this is a paradox, in that the soil with the highest intrinsic permeability (Equation 12.13) can have the lowest hydraulic conductivity. However, this fact can be very important in forming conceptual models about vadose zone processes of flow and transport, particularly in heterogeneous or layered media.

The concepts of unsaturated flow presented thus far are summarized in Example 12.1.

Example 12.1 The hypothetical problem is to determine the direction and rate of soil-water flow from in situ measurements of pressure head and hydraulic conductivity in a soil having a uniform texture. Figure 12.8 shows the location of two tensiometers (discussed in Section 12.7) for measuring pressure head. Table 12.1 indicates the pressure head measurements at the two depths. It has already been determined from laboratory analyses of cores that the saturated hydraulic conductivity is 1 cm/day. We assume that the unsaturated hydraulic conductivity fits the exponential model:

$$K(\psi) = K_s \exp(\alpha\psi) \tag{12.14}$$

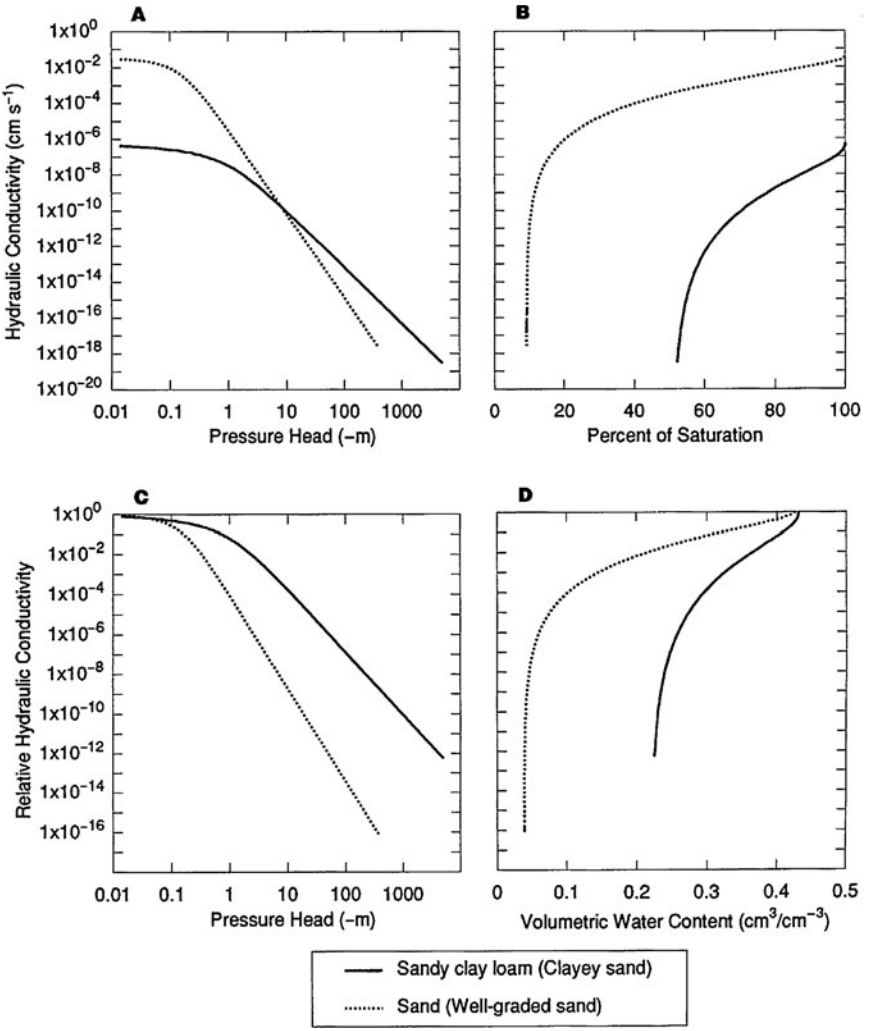

Figure 12.7 (A) Hydraulic conductivity, K, versus pressure head, ψ, for sand and sandy clay loam; (B) hydraulic conductivity versus water content; (C) relative hydraulic conductivity versus pressure head; and (D) relative hydraulic conductivity versus percent saturation. (*From Stephens, 1996. With permission of Taylor & Francis Group LLC.*)

with $\alpha = 0.02$ cm^{-1} for this soil. (The exponential model means that on semi-logarithmic paper, ln K-ψ fits a straight line having a slope α and an intercept K_s)

To solve this problem, we assume that the flow is vertical and apply a form of Darcy's equation (Equation 12.12b). We also set the vertical axis as positive upward. The first step to compute the Darcy velocity, q_z, is to determine the hydraulic head gradient from the sum of the pressure head and total head gradients. In our problem, the pressure head decreases upward, so at

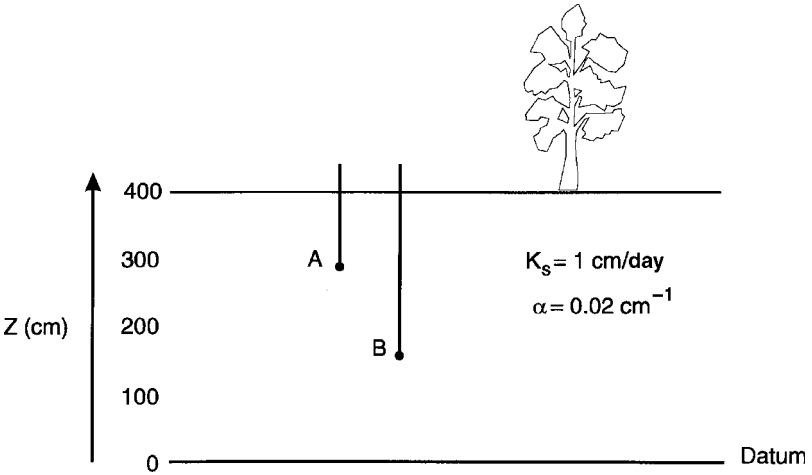

Figure 12.8 Example to calculate hydraulic gradient, flow direction, and flow rate. (*From Stephens, 1996. With permission of Taylor & Francis Group LLC.*)

first glance it may appear that flow is upward. But when the gravitational gradient is added to the pressure head gradient, the total hydraulic head decreases downward (Table 12.1). Recall it is the gradient of total head, not pressure head, which is the water driving force. Consequently, the flow is downward and the magnitude of the total hydraulic head gradient is:

$$\frac{dH}{dz} \cong \frac{H_2 - H_1}{Z_2 - Z_1} = \frac{200 - 110}{100} = 0.9 \tag{12.15}$$

Note that by our choice of sign convention, the higher subscript refers to the location farthest from the origin.

The second step is to compute the unsaturated hydraulic conductivity. To do this, we will determine the mean pressure head in the region between the tensiometers:

$$\frac{\psi_1 + \psi_2}{2} = -95 \text{ cm} \tag{12.16}$$

TABLE 12.1 Pressure Head and Total Head Measurements at Two Depths

	Measured pressure head ψ (cm)	Elevation Head Z (cm)	Total head H (cm)
A	−100	300	200
B	−90	200	110

Next, substitute this mean pressure head into Equation 12.14 above, along with our previously determined values of K_s and α. The result is $K = 0.15$ cm/day. The third step is to multiply the hydraulic head gradient by the unsaturated hydraulic conductivity to obtain the Darcy velocity.

$$q_z = -K\left(\frac{dH}{dz}\right) = -(0.15)(0.9) = -13 \text{ cm/day} \tag{12.17}$$

The negative sign indicates flow is in the opposite direction in which z increases, that is, downward.

12.5 Soil-Water Budget

The general equation for the soil-water budget is derived by considering the mechanisms by which water can enter, exit, or be stored in a predefined region of the vadose zone. For many problems, the inflow across the upper boundary of the vadose zone is infiltration, while outflow from the upper boundary is evaporation and transpiration, and outflow from the lower boundary is groundwater recharge. Net inflow (inflow minus outflow) must equal the change in soil-water stored in the vadose zone:

$$I - E - T - R = \Delta S \tag{12.18}$$

where I is cumulative infiltration, E is evaporation, T is transpiration, R is deep percolation or recharge (all four variables in units of L^3T^{-1}), and ΔS represents the change in water storage over the time interval Δt. Now we will briefly describe each of the principal soil-water budget components, and present some of the methods to obtain them.

Infiltration

Perhaps the most widely studied subsurface hydrological process has been infiltration. Infiltration is the process whereby water enters the soil from surficial sources, such as rainfall, snowmelt, flooding, irrigation, liquid waste spills, etc. Infiltration is usually regarded as a process which occurs predominantly in the vertical direction when water is applied over extensive areas of the land surface. The infiltration process in any geometry is controlled by many factors, such as the precipitation characteristics, rate of water application, antecedent moisture in the soil, soil hydraulic properties, topography, and others.

First consider a thick, uniform-textured, permeable soil that is subject to a gentle but constant rainfall rate over a flat-lying terrain (Figure 12.9a). In this case, we are describing a one-dimensional

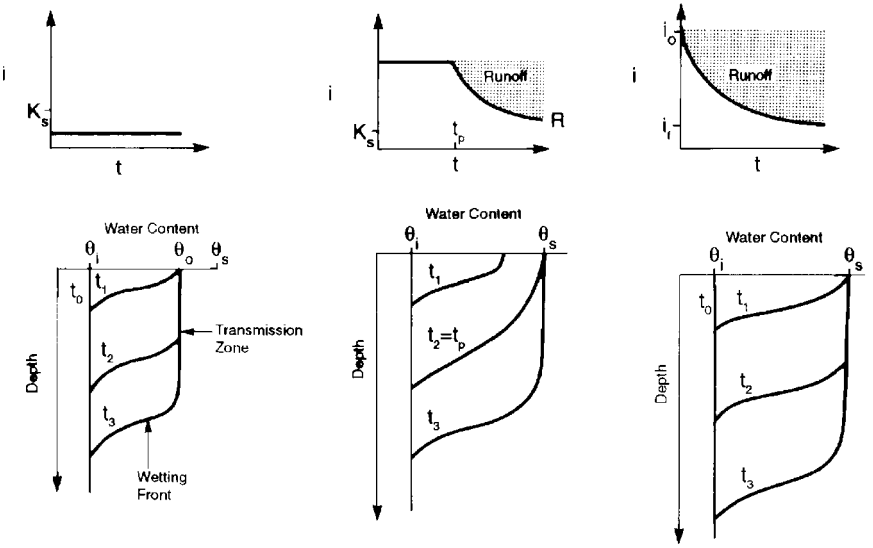

Figure 12.9 Infiltration rate dependence on rain intensity, *i*, and water content profiles during (A) low, (B) moderate, and (C) intense precipitation. (*From Stephens, 1996. With permission of Taylor & Francis Group LLC.*)

infiltration process in which the rainfall intensity of the rain is less than the magnitude of the saturated hydraulic conductivity of the soil. All the water supplied is free to infiltrate, so none is available for runoff. Because the capacity of the soil to conduct water is greater than the rate of supply, the soil will be unsaturated. And, if the rain continues for a prolonged period at this rate, the unsaturated hydraulic conductivity of the soil will approach the rain intensity. Next consider the case in which a constant rainfall rate in excess of the saturated hydraulic conductivity is applied to initially dry soil. The soil initially takes up the rain water as rapidly as it falls (Figure 12.9b), owing to the strong capillary forces in the dry soil. As the soil pores fill with water, the influence of the capillary forces on infiltration diminish gradually. Therefore, as the soil becomes wetter and as the depth to the wetting front increases, the hydraulic head gradient decreases. Consequently, the infiltration rate decreases over time. If the rain persists, ponding on the soil surface will occur at time, t_p, when the soil cannot transmit water at a rate greater than the rainfall rate. When ponding occurs, the soil surface layer is saturated, except perhaps for entrapped air. After ponding, the infiltration rate continues to diminish and approaches the field-saturated hydraulic conductivity of the soil. Finally, for the case where storm intensities which are high relative to the saturated hydraulic conductivity, it is probable that ponding will begin almost instantly (Figure 12.9c).

Figure 12.9 also illustrates the water content profiles associated with the low and moderate intensity rain infiltration as well as ponded infiltration into a uniform soil.

Infiltration is usually quantified in one of three ways: by the residual from a surface water budget analysis, by field measurements, or by calculation based on soil hydraulic properties. In a surface water budget, infiltration may be computed by measurements of precipitation, applied irrigation, and surface run-on, and subtracting from this sum the surface runoff, interception of water on plant canopies, direct evaporation, and increases in surface water storage. Methods to quantify each of these components of a surface water budget can be found in standard engineering hydrology texts and reference books.

In the field, infiltration from precipitation as rainfall can be measured by weighing and totaling in precipitation gages, estimated from surrounding recording stations (e.g., Daymet) or it is simulated by using a rainfall simulator to quantify infiltration over an area of roughly 1 to 10 m^2 for controlled duration and intensity storms (e.g., Zegelin and White 1982). Under ponded-conditions a ring infiltrometer, a short cylinder approximately 0.1 to 1 m^2 in cross section driven into the soil, can be used to determine the infiltration rate by measuring flow through the cylinder under equivalent ponded head conditions. Beneath impoundments, lakes, or reservoirs, seepage meters (Chapter 6) may provide reliable infiltration measurements (e.g., Stephens et al. 1985). Infiltration from stream channels, where evaporation can be neglected, is most readily obtained by subtracting discharges measured at stream gaging stations along the reach of the channel. Infiltration can also be calculated from hydraulic properties of the soil using mathematical expressions which describe the infiltration process, such as Darcy's equation.

To describe the one-dimensional vertical infiltration process, Green and Ampt (1911) developed the following simple but very useful equation:

$$i = K_o\left[\frac{(H_p + L) - \psi_f}{L}\right] \tag{12.19}$$

where K_o is the hydraulic conductivity behind the wetting front, H_p is depth of ponding, L is depth to the wetting front, and $\psi_f < 0$. This equation is virtually identical to Darcy's equation, with the term in brackets representing the hydraulic gradient. Unlike the usual application of Darcy's equation to flow in soil columns or aquifers, L is time dependent in the Green-Ampt equation. Inspection of Equation 12.19 shows that for a constant depth of ponding, as the depth to the wetting front increases, the gradient eventually approaches one regardless of the magnitude of the ponding depth. Consequently, the late time, steady infiltration rate is independent of the ponding depth.

Undoubtedly, the most widely referenced mathematical equation on infiltration is that by Philip (1957). Where the depth of ponding is very thin, the simplified form of Philip's transient infiltration equation is:

$$i = \frac{1}{2} St^{-1/2} + K_o \tag{12.20}$$

where S is called the sorptivity of the soil, t is time since infiltration began, and K_o is the hydraulic conductivity of the soil's upper layer. Sorptivity is a soil hydraulic property that embodies several factors describing the capacity of the soil to imbibe water at early time, such as the initial dryness of the soil (e.g., Brutsaert 1977). Note that as $t \rightarrow \infty$, the late time infiltration rate approaches K_o, just as we discussed previously for the Green-Ampt equation. Solutions to Philip's equation can be used to predict not only the transient infiltration rate, but also water content profiles.

Evaporation and transpiration

Evaporation refers to the water lost from the vadose zone by vapor phase transport from the soil directly to the atmosphere. Transpiration is the water depleted from the vadose zone by plant root uptake. For most practical problems it is both difficult and unnecessary to separate these two processes, so the two are combined and called evapotranspiration. There are two different approaches to determine evapotranspiration, by measurement and by estimation.

Soil lysimeters provide the most accurate method to measure evapotranspiration, and in fact most estimation methods for evapotranspiration have been verified by comparing the estimates to measured lysimeter data. Unfortunately, soil lysimeters are usually cumbersome, in some cases expensive to construct, and require rather long periods of data collection. There are three types of lysimeters used for water balance analysis: weighing, non-weighing and floating. All soil lysimeters share the same concept. A small monolith of soil with vegetation is placed in a container and is returned to its original position in the landscape. Instrumentation is emplaced to allow measurements of precipitation, soil-water storage, and deep drainage. From these components, one can compute evapotranspiration by simple arithmetic using the water balance equation (Equation 12.18). In a weighing lysimeter, the lysimeter is placed on a scale (Figure 12.10). In a non-weighing lysimeter, evapotranspiration from the soil monolith is determined by measuring the rate of water supply to the monolith container that is necessary to maintain a constant depth to water in the base of the container. And in a floating lysimeter, the soil monolith is placed on a liquid-filled pillow so that water gains and losses can be obtained by measuring fluid pressure through a manometer tube.

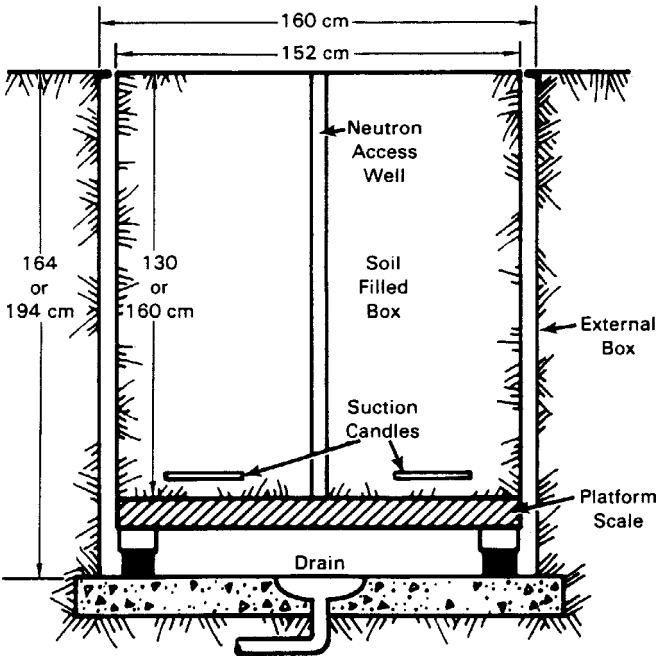

Figure 12.10 Cross-sectional view of weighing lysimeter. (*From Kirkham et al. 1984. With permission of ASA, CSSA and SSSA.*)

Another approach to measure evapotranspiration is to place a canopy over the plant and measure air flow rate and water content of the inflowing and outflowing air (Sebenik and Thomas 1967).

Methods for making micrometeorological measurements above a vegetated surface have been developed over the past 50 years or so to determine the actual evapotranspiration (Rosenberg et al. 1983). Two such methods are the Bowen ratio method (e.g., Tanner 1960) and the eddy-correlation method (Swinbank 1951). The Bowen ratio method is based upon a simplified energy-budget equation (e.g., Marshall and Holmes 1992).

Instrumentation requirements include a net radiometer, soil heat flux, and temperature and vapor pressure at two elevations above the surface. The eddy correlation method is based on the principle that water vapor flux across the land surface can be measured by correlating the vertical variations of wind speed, w, with variations of vapor density, q_v (Tanner et al. 1985). The instrumentation requirements include an anemometer, hygrometer, and thermocouples which are connected to a data logger.

The so-called eddy correlation-energy budget method (e.g., Czarnecki 1990) is used to determine the actual evaporative flux when field instrumentation accounts for net radiation and heat conduction into the ground, as in the Bowen ratio method, and when sensible heat flux is determined by the eddy correlation technique.

Because of the obvious logistical difficulties associated with measuring evapotranspiration over extensive areas, estimates of evapotranspiration are usually preferred. There are two broad approaches to estimate this component of the soil-water budget, climatological and micrometeorological methods. Among the climatological methods, some are based on air temperature (e.g., Thomthwaite 1948; Blaney and Criddle 1950); others are derived from solar radiation measurements (e.g., Jensen and Haise 1963), and others incorporate both energy supply data and turbulent transfer of water vapor away from the surface (e.g., Penman 1948). A study by Jensen et al. (1990) concluded that these combination energy balance-aerodynamic methods provide the most accurate estimates.

While actual evapotranspiration (ET) is the quantity we seek, it is important to recognize that the above climatological methods calculate the potential evapotranspiration (PET), that is, the amount of evapotranspiration that would occur from a short green crop that fully shades the ground, exerts negligible resistance to the flow, and is always well supplied with water.

To compute the ET from PET when the water supply is limited requires an additional calculation based upon plant type, water availability, and vegetation coverage on the landscape:

$$\mathrm{ET} = K_c\,(\mathrm{PET}) \tag{12.21}$$

where K_c is a crop coefficient. The crop coefficient is usually obtained by establishing an experimental relationship between ET (measured with lysimeters) and PET (calculated by a specific method) for some brief period. Crop coefficients for agricultural crops are summarized by Doorenbos and Pruitt (1975) and values for selected native vegetation are presented in Table 12.2 from McWhorter and Sunada (1977). The dependence of the crop coefficient upon available water (AW) is described by a wide variety of formulations (Moridis and McFarland 1982). Perhaps currently the most widely used method is that published as Food and Agriculture Organization (F.A.O) Irrigation and Drainage Paper 56

TABLE 12.2 Estimated Plant-Water-Use Coefficients K_{co} for Native Vegetation

	K_{co}							
Vegetation	Nov to Mar	Apr	May	Jun	Jul	Aug	Sep	Oct
Sagebrush-grass	0.50	0.60	0.80	0.80	0.80	0.71	0.53	0.50
Pinyon-Juniper	0.65	0.70	0.80	0.80	0.80	0.80	0.69	0.65
Mixed mountain shrub	0.60	0.67	0.81	0.85	0.82	0.74	0.65	0.60
Coniferous forest	0.70	0.71	0.80	0.80	0.80	0.79	0.75	0.71
Aspen forest	0.60	0.67	0.85	0.90	0.86	0.75	0.65	0.60
Rockland and miscellaneous	0.50	0.60	0.65	0.65	0.65	0.60	0.50	0.50
Phreatophytes	1.00	1.00	1.00	1.00	1.00	1.00	1.00	1.00

From McWhorter and Sunada, 1977. With permission.

(Allen et al. 1998). Allen et al. (1998) also describe the application of remote sensing techniques to obtain crop coefficients.

12.6 Water Storage and Deep Percolation

To quantify water storage changes requires repeated measurements of water content within the soil-water budget volume. Over a year or several years, the water content change is usually small, and for some sites and climatic conditions, the long-term change is negligible.

Neutron probe logging affords a means to nondestructively measure water content changes at the same depths without introducing the sampling bias accompanying destructive soil sampling techniques. From the discrete water content measurements, θ, the volume of water in storage is calculated as:

$$\Delta S = \frac{1}{\Delta t}\left[\int_0^D \theta dz\right]\cdot(\text{area}) \tag{12.22}$$

The rate of change in water storage is calculated by subtracting the water storage to depth D at two different time periods and dividing this by the time between monitoring events. In weighing soil lysimeters, the change in water storage within the monolith can be simply obtained from the change in mass divided by the water density.

Deep percolation is the water which moves downward below the root zone. Often the deep percolation below the root zone will become groundwater recharge when it reaches the water table. Groundwater recharge is water which enters either a perched aquifer or the phreatic zone. One of several ways water can enter aquifers is by migration of deep percolation through the vadose zone. In the following discussion, we summarize methods to calculate deep percolation and recharge to an aquifer from the vadose zone by physical and chemical methods.

12.7 Physical Methods

Soil lysimeters

Soil lysimeters for the purpose of collecting deep drainage and estimating recharge are constructed by excavating soil to the desired depth, installing casing with a sealed base, and repacking the casing with soil to the in situ bulk density. Water percolating under tension can be collected at the bottom of the lysimeter by extracting it from porous ceramic cups or tubes which are subject to a vacuum that exceeds the soil-water potential. Alternatively, the water accumulated at the base of the lysimeter can be obtained by measurements of water content change with a neutron probe or by piezometers to measure the depth of saturation.

Water balance

One of the most widely adopted approaches to determine deep percolation or groundwater recharge is the water balance method. In this approach, recharge is calculated as the residual in the water-budget equation (Equation 12.18). Gee and Hillel (1988) point out that precision in precipitation is seldom less than ±5%, and the precision for evapotranspiration is typically greater than ±10%. Because of the propagation of errors in the water balance analysis, there is large uncertainty in the calculated recharge when recharge is a small fraction of precipitation. They conclude that in arid climates, the error in recharge calculated by water balance methods could exceed the calculated value of recharge itself. Hence, water-budget methods to quantify deep percolation and recharge are more appropriate in humid climates.

Darcy flux in the vadose zone

Darcy flux calculations also comprise a physical means to calculate recharge from the vadose zone. The components in Darcy's equation for unsaturated vertical flow include the hydraulic conductivity at the field water content (or potential) and the hydraulic gradient. In soils below the root zone where the matric potential is nearly constant with depth, it is a good assumption that the hydraulic gradient is approximately unity, and flow is downward. Consequently, where this assumption is reasonable and where vapor phase transport downward is negligible, the recharge rate is approximately equal to the in situ vertical, unsaturated hydraulic conductivity.

Numerical models of soil-water flow

There are two types of numerical models relevant to calculating deep percolation and recharge: water balance models and the models based on the Richards' equation. Richards' equation for unsaturated flow can be written as:

$$\nabla \cdot K(\psi)\nabla H = C(\psi)\frac{\partial \psi}{\partial t} \tag{12.23}$$

where C is the specific water capacity, which is the slope of the soil-water retention curve.

The water balance models include codes such as HELP (Schroeder et al. 1984), GLEAMS (Leonard et al. 1989), PRZM-2 (Mullins et al. 1993) and INFIL (Flint, et al. 1996).

All these vadose zone water balance models partition precipitation into runoff and infiltration. Infiltration is further separated into components such as evapotranspiration, lateral drainage or interflow, soil

water storage, and deep percolation by applying deterministic and empirical equations which describe each of the processes. Actual evapotranspiration is computed from climatic data (e.g., precipitation, temperature, solar radiation), input from on-site measurements or from default daily historic data for the nearest location stored in the program library. Other factors such as the vegetation cover and rooting characteristics also enter into the evapotranspiration analysis. Water which cannot be held in storage or extracted by the plants becomes available for deep percolation. Some models such as PRZM-2 and INFIL3 (Hevesi et al. 2003) take the deep percolation output from the water balance in the root zone and also route this through the deeper vadose zone using Darcy's equation for one-dimensional, unsaturated flow.

One of the algorithms often used to compute recharge in the soil-water budget models is based on the concept of field capacity. Percolation below any soil layer is allowed in the models only if the water content exceeds the field capacity.

There are a large number of numerical models for simulating soil-water processes, including finite difference and finite element forms, based on one-, two-, or three-dimensional forms of Richards' equation (e.g., HYDRUS, VS2D, and TOUGH2). To account for infiltration and evapotranspiration in these codes, in lieu of detailed meteorological information, the upper boundary of the model and/or the root zone is usually specified as either a constant or time varying flux or pressure head. In contrast to some of the water balance models, the numerical models allow the user to more realistically represent the physical properties of the porous medium, including complex geology with spatially varying hydraulic conductivity and water retention characteristics. When the lower boundary of the model is specified as the water table, the water flux out the base of the model represents the groundwater recharge.

Chemical methods in the vadose zone

Among the chemical methods for calculating recharge, there are stable and radioactive isotopes which serve as a means to compute recharge, including tritium, chlorine-36, chloride, and oxygen-18 and deuterium. One advantage of some of these methods is that the analysis may represent an integration of hydrologic events over decades or even tens of thousands of years. Another advantage is that the data are derived from in situ sampling, without need for field instrumentation for monitoring.

Tritium. Tritium, a radioactive isotope of hydrogen with a half life of about 12.4 years, is well suited as a hydrologic tracer because it is part of the water molecule. During the atmospheric nuclear testing beginning in the 1950s, the tritium in the atmosphere increased substantially over a relatively short time, culminating in the period 1963–1964

(Phillips et al. 1988). The record of tritium has been preserved in atmospheric water that infiltrated the soil profile. Recharge, or more precisely, net infiltration, is obtained from the depth to the center of mass of the tritium pulse, L, with the following equation:

$$R = \theta \frac{L}{\Delta t} \tag{12.24}$$

where θ is the mean water content through depth L.

Chlorine-36. Another tracer of soil-water flux or recharge is chlorine-36. This is a radioactive isotope with a half life of about 300,000 years, produced as a by-product of thermonuclear testing near the oceans in the 1950s (Bentley et al. 1982). Chloride is very stable in the environment and enters the hydrologic cycle as the chloride ion dissolved in water and as a component of dust fallout. Because it is soluble and nonvolatile, chloride is an excellent tracer for liquid-phase transport. Recharge can be determined from the depth of the chlorine-36 peak, in the same manner as described above for tritium.

Chloride mass balance. The chloride mass balance method relies upon the slow accumulation in the soil profile of natural chloride that dissolves in precipitation and infiltrates. The concentration of chloride typically decreases with increasing inland distance from the coasts. The expected chloride pattern in the soil profile, at least in areas of modest precipitation, is that chloride is concentrated with increasing soil depth, as water is extracted by the plant roots; and below the root zone the chloride concentration is expected to be constant where the deep percolation migrates toward the water table.

To interpret chloride distribution in the vadose zone, three fundamental assumptions are made: all chloride in the vadose zone originates from atmospheric deposition, the only long-term sink for chloride is downward advection or dispersion, and chloride behaves conservatively during soil-water transport. If dispersion and macropore flow are neglected, a simple piston-displacement model is derived in which the chloride concentration increases in proportion to the ratio of precipitation to recharge (Allison and Hughes 1978):

$$R = \frac{PCl_p + D}{Cl_s} \tag{12.25}$$

where P is the average precipitation rate, Cl_p is chloride concentration in precipitation and D is dry fallout, and Cl_s is the average soil chloride concentration in pore water below the root zone.

Chloride patterns which depart from this model may produce a bulge in the chloride concentration at some depth in the profile, and below this the concentration decreases to approach a near constant value. Phillips (1994) discussed possible explanations for this behavior in desert soils such as preferential or bypass flow in macropores, but suggested that the low concentration of chloride at depth most likely reflects greater recharge during a wetter paleoclimatic period when the indigenous plants were less efficient at capturing the soil moisture.

12.8 Characterizing Hydraulic Properties

In this section, we present some of the field and laboratory techniques that are available for obtaining parameters which can be used in quantitative analyses and model simulations of vadose zone processes. For additional details, refer to Stephens (1996).

Soil-water characteristic curve

To obtain the moisture retention or soil-water characteristic curve, laboratory methods are most often chosen. There are essentially two types of laboratory methods for measuring soil-water characteristic curves. The first is the hanging water column method in which the soil water in the sample is subjected to a tension, and the second is the family of pressure plate techniques. In both techniques, the hanging water column apparatus uses a Büchner funnel (available from scientific glassware suppliers), a glassware which contains a fritted glass, porous plate (Figure 12.11). The pore size of the plate is so fine that after the plate is saturated, the water tension must decrease to -0.1 or -0.3 bars before the air will displace water from the pores of the plate.

The soil sample is placed in the Büchner funnel on the upper side of the porous plate. A plastic tubing and burette assembly control the tension on the underside of the Büchner funnel which causes water to drain from the soil. After equilibrium is achieved, the amount of drainage is recorded in the burette, and then the burrette is lowered again and the process continues to a mean negative pressure head equal to the distance between the center of the sample and the water level in the burette. Additionally, the distance between the center of the soil sample and water level in the burette is recorded as a measure of the pressure head in equilibrium with the water still held in the soil. Upon completion, the final water content of the sample is determined. The water content associated with all other previous "tensions" achieved in the test is calculated by adding to the final water content the incremental volumes of water drained or imbibed from each step. In this way, one obtains pairs of water content and pressure head data.

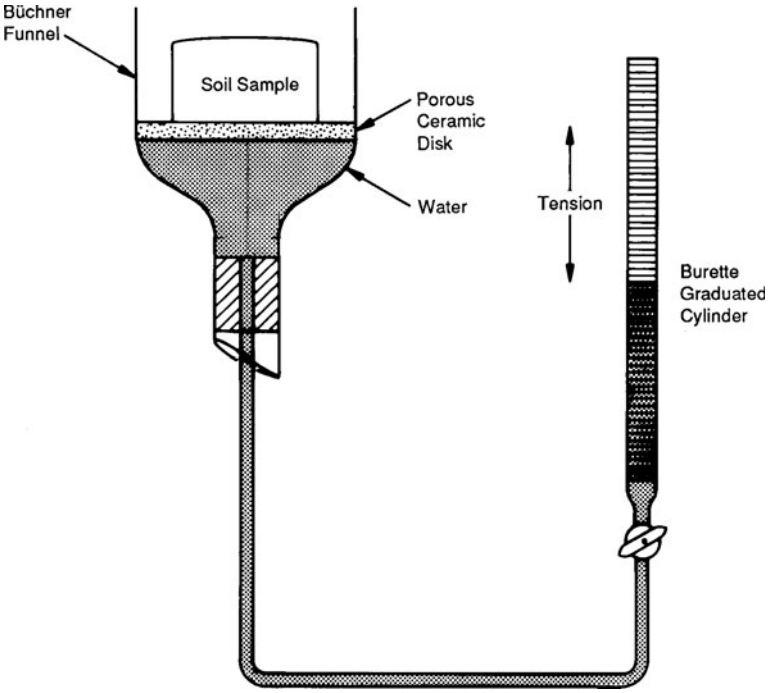

Figure 12.11 Hanging water column (Büchner funnel) apparatus. (*From Stephens, 1996. With permission of Taylor & Francis Group LLC.*)

The hanging water column method is practical for relatively wet conditions to pressures as low as about −0.3 bars, depending upon the air-entry value of the porous plate in the Büchner funnel.

The pressure cell methods include Tempe cells (Figure 12.12a), pressure plate apparatus, and pressure membrane apparatus (Figure 12.12b). Tempe cells have ceramic plates which remain saturated to approximately −2 bars; the pressure plate apparatus uses ceramic plates with a range to about −15 bars, and pressure membranes of cellulose acetate are useful to about −150 bars.

The basic assembly contains a pressure chamber comprised of a rigid cylinder fitted tightly on the top by a lid or removable plate. Attached to the bottom of the pressure chamber is another removable or fixed end plate. Above the bottom plate is a water-saturated porous disc (ceramic plate, cellulose acetate, or visking membrane), which is seated tightly against the wall of the cylinder by a rubber gasket or O-ring. A wet-soil sample in a sample ring is placed on the porous plate and the top and bottom plates are tightly attached. A nitrogen gas is applied at constant pressure to the sample chamber through a fitting in the cylinder wall. Water is forced out of the sample through the porous disc and into a collection tube, until

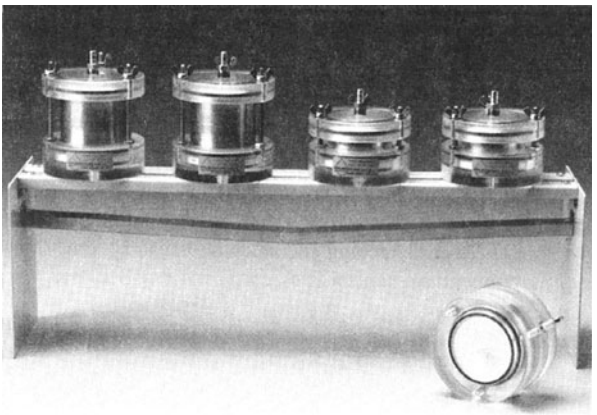

A

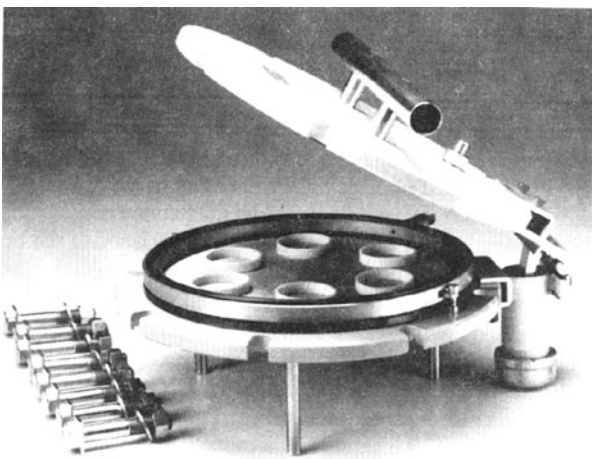

B

Figure 12.12 Water retention apparatus: (A) Tempe cells and (B) pressure membrane apparatus. (*Courtesy of Soilmoisture Equipment Corp.*)

water outflow ceases. The moisture content still retained in the soil sample is presumed to be in equilibrium with the applied pressure.

For the very dry range, psychrometric and centrifuge methods are also useful.

Saturated hydraulic conductivity

Laboratory methods. Because saturated hydraulic conductivity is one of the most widely characterized hydraulic properties of soils, representative values have been published for a wide range of soils (Figure 12.13).

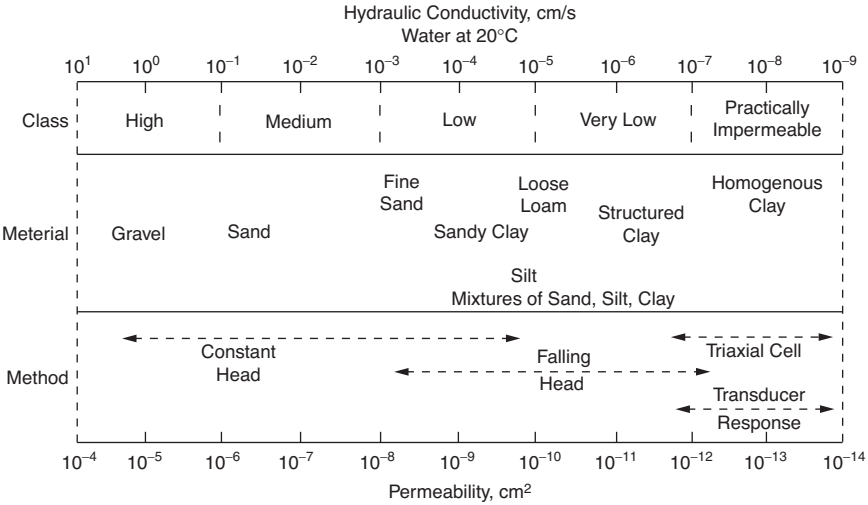

Figure 12.13 Hydraulic conductivity of various materials at saturation. (*From Klute and Kirksen 1986. With permission of ASA, CSSA, and SSSA.*)

Laboratory tests involve removing a small sample of soil and testing it in the laboratory under controlled conditions. Because of concern for problems of sample disturbance and representativeness of the relatively small sample, field methods are often preferred. Although field methods may overcome the limitations of the laboratory methods, they often suffer from lack of control on the experimental conditions and other logistical problems.

There are in general two types of laboratory tests for saturated hydraulic conductivity: constant head and falling head permeameters. In a constant head permeameter, water is introduced into the sample by maintaining inflow and outflow reservoirs at constant positions relative to the sample (Figure 12.14). The steady flow rate, sample length and cross-sectional area, difference in reservoir elevations, and water temperature are used to calculate hydraulic conductivity according to Darcy's equation (Equation 5.1, Chapter 5). In a falling head permeameter, water is introduced to a water-saturated sample by gravity drainage from a standpipe, while the head on the downstream end of the sample remains constant (Figure 12.15). There are standards published by the American Society for Testing and Materials (ASTM) for laboratory tests on granular and fine-textured soils (ASTM D-2434-68 and D-5084-90). For compressible soils in particular, such as clay liner material, it is also important to conduct the tests under confined conditions which reproduce the overburden pressures. Soil engineers use fixed wall and flexible wall cells (e.g., triaxial cells) to accomplish this (e.g., Daniel, 1989; Daniel, 1993). For additional guidance refer to appropriate ASTM standards or reference materials such as Klute and Dirksen (1986).

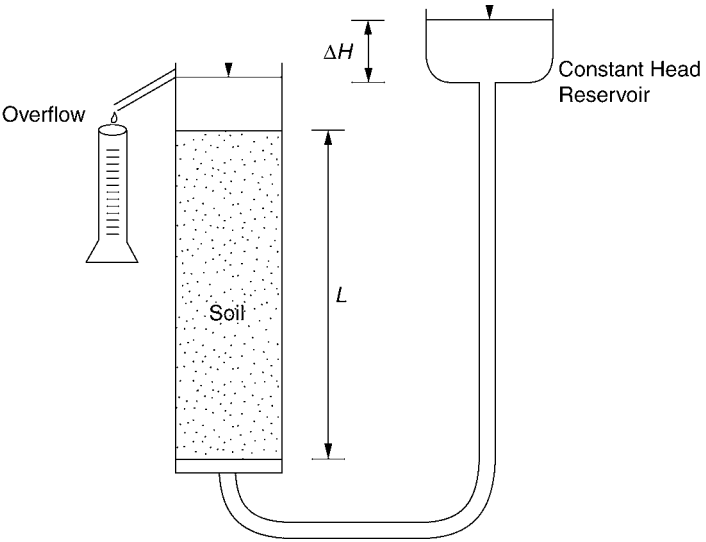

Figure 12.14 Constant head permeameter. (*From Stephens, 1996. With permission of Taylor & Francis Group LLC.*)

Field methods. Here we discuss only the air-entry permeameter and borehole permeameter, although the disc permeameter and sealed double-ring infiltrometer are other viable approaches, as discussed in Stephens (1996).

Air-entry permeameter. The air-entry permeameter (Figure 12.16) was first proposed by Bouwer (1966) as a means to determine the vertical,

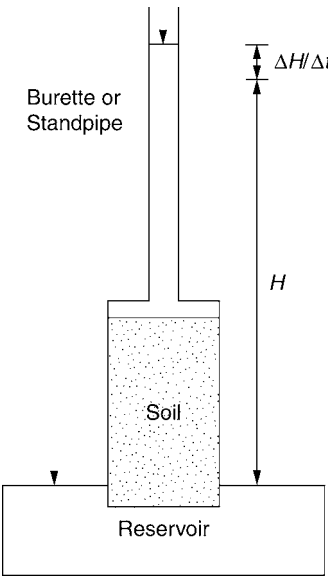

Figure 12.15 Falling head permeameter. (*From Stephens, 1996. With permission of Taylor & Francis Group LLC.*)

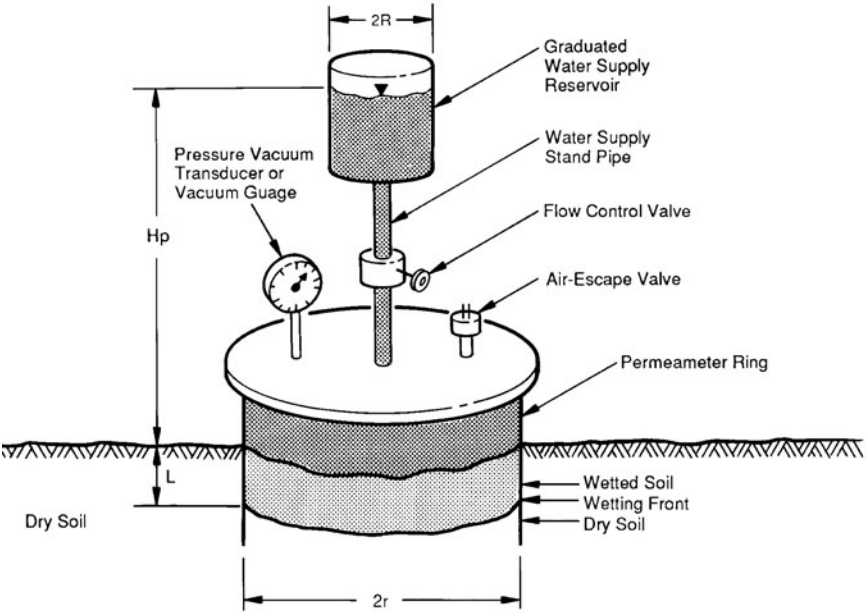

Figure 12.16 Air-entry permeameter. (*From Havlena and Stephens 1991. With permission of ASTM.*)

field-saturated hydraulic conductivity of geologic materials above the water table. The air-entry permeameter consists of a single ring, typically 30 cm in diameter and 25 cm deep, which is driven vertically into the material to be tested. A water supply reservoir is mounted on top of an adjustable standpipe. To begin the test, the air-entry permeameter reservoir is filled and water is allowed to infiltrate into the ring. When the water displaces the air between the soil and top plate, the air-escape valve is closed. The rate of decline of head applied at the soil surface is then recorded, either through the use of a transducer set within the ring at the soil surface or by observing the decline of water in the graduated supply reservoir (ASTM D-5126). Infiltration continues until the wetting front approaches the bottom of the ring, as indicated usually by a change in soil tension monitored by a tensiometer or the change in electrical conductivity at buried resistance probes, or as inferred by a mass balance approach using an assumed fillable porosity of the soil. The water supply valve is closed, and the soil water is allowed to redistribute. The negative pressure created by the redistributing soil water is monitored by a vacuum gauge or pressure transducer mounted at the top of the ring. When air begins to enter into the saturated soil from below the wetting front, the gauge will have recorded a minimum pressure. The minimum pressure achieved during this portion of the test is

used to calculate the air-entry pressure of the soil, ψ_a. The field saturated hydraulic conductivity, K_{fs}, is calculated using the following equation:

$$K_{fs} = \frac{(R_r/r)^2 \, L \, (dH/dt)}{(H_p + L - \psi_a)} \tag{12.26}$$

where R is the radius of the reservoir, r is the radius of the cylinder, L is the depth to the wetting front when dH/dt is measured, dH/dt is the rate of decline in head in the reservoir, and H_p is the depth of ponding when dH/dt is measured.

Borehole permeameters. The vadose zone borehole permeameter is a method to determine in situ saturated hydraulic conductivity, K_s, of unfissured, homogeneous, isotropic soil and rock above the water table. The borehole is constructed utilizing an auger (or drilling) to the desired depth, and, if the soil contains fines, the sides of the borehole must be scraped to remove any smear zone. In caving formations, well screen and a coarse sand or gravel pack must be placed in the borehole. In a typical borehole permeameter, a constant head of water is maintained in the borehole until the infiltration rate is steady. The borehole testing equipment typically consists of a water supply reservoir and a means of controlling the head of water within a 5- to 15-cm-diameter borehole.

There are two types of equations to compute hydraulic conductivity: deep and shallow water table conditions, as descried by the U.S. Bureau of Reclamation (1977). In general, deep water-table conditions exist when the distance between the water level in the borehole and the water table is greater than three times the depth of water in the borehole (U.S. Bureau of Reclamation, 1974). Most of the steady-state solutions are valid where $H/r > 10$. Analytical solutions for the deep water table case were derived by Nasberg (1951), Glover (1953), Terletskaya (1954), Cecen (1967), and Reynolds et al. (1983). All these formulae neglected capillarity. Stephens and Neumann (1982), Stephens et al. (1987), Philip (1985), and Reynolds et al. (1985) developed approximate analytical solutions to compute K, which take capillarity into account. Shallow water-table conditions exist if the distance between the water table and the water surface in the borehole is less than three times the depth of water in the borehole. An equation for K_s under shallow water table conditions was developed by Zanger (1960). For additional discussion on borehole permeameters refer to Stephens and Neuman (1982), ASTM Standard D-5126, and Elrick and Reynolds (1992).

Example 12.2 To illustrate the borehole permeameter method in a loam soil under deep water table conditions, a cased and screened borehole, 5 cm in diameter (r) was set at a depth of about 110 cm below ground surface and the

hole was filled with water to 76 cm depth (H). This depth was maintained constant with a carburetor valve and styrofoam floats. Prior to water delivery, carbon dioxide gas was pumped into the borehole to minimize entrapped air. Figure 12.17 illustrates the infiltration rate. For simplicity, capillarity is ignored and the equation of Glover (1953) is selected:

$$K_s = \left(\frac{Q_s}{C_u r H}\right) \tag{12.27}$$

where:

$$C_u = \frac{2\pi(H/r)}{\sin h^{-1}(H/r) - 1} \tag{12.28}$$

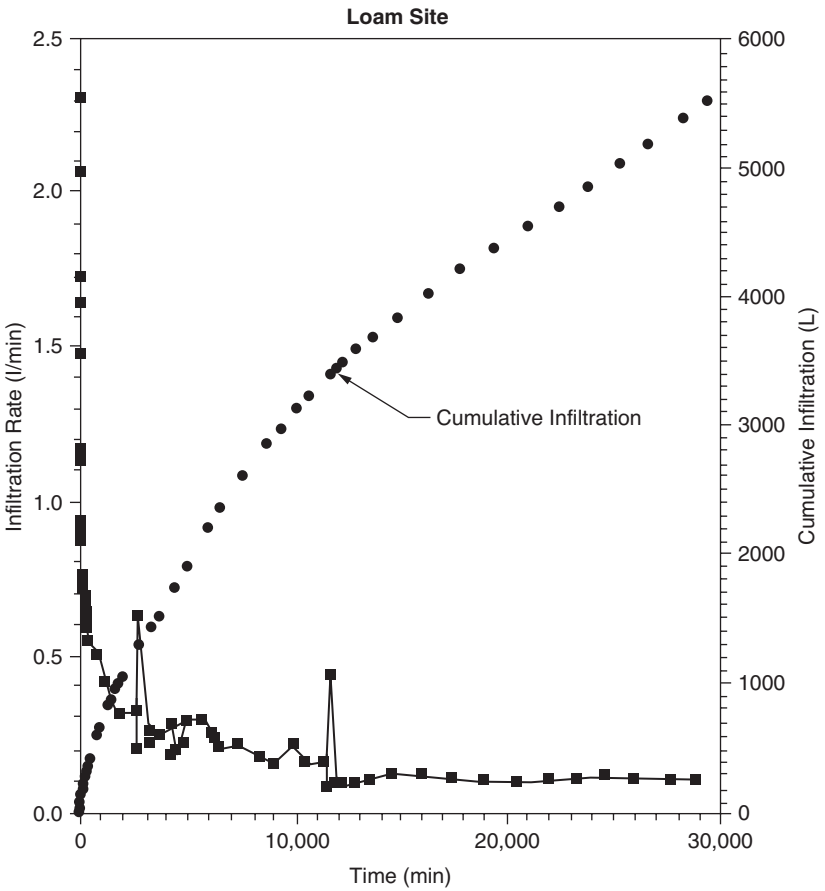

Figure 12.17 Infiltration rate and cumulative infiltration at the M-mountain loam site. (*From U.S. Department of Agriculture, ed. M. Th. van Genuchten, F. J. Lei, L. J. Lund, 1989.)*

and Q_s is the steady infiltration rate. For $Q_s = 0.12$ L/min (Figure 12.17), $H = 76$ cm, $r = 5$ cm, and Glover's solution gives $K_s = 1.3 \times 10^{-4}$ cm/s (as described in more detail in Stephens, 1996).

Unsaturated hydraulic conductivity

The purpose of this section is to review methods to measure unsaturated hydraulic conductivity in the field and laboratory. For additional detail on many of the methods discussed here, refer to Dirksen (1991) and Stephens (1993).

Laboratory methods. Laboratory methods have been grouped into two general categories: steady-state flow methods and transient flow methods. In most cases, the transient techniques offer comparable accuracy with considerably less time to complete testing.

Steady, unsaturated flow can be introduced into vertical laboratory columns under constant head or constant flux conditions. By whatever plumbing apparatus this is achieved, the unsaturated hydraulic conductivity is calculated from Darcy's equation as simply the ratio of steady flow rate per unit cross-sectional area to the hydraulic gradient (Equation 12.12). The hydraulic conductivity is associated with the mean water content and/or pressure head established in the column. Tensiometers (see Subsection Tensiometers) are often installed through the wall of the soil column at two different positions to measure soil-water pressure head for computing both the hydraulic gradient and the mean pressure head at steady state. A series of steady state tests are run to obtain a sequence of conductivity measurements, beginning with a nearly saturated column and ending with a low water content column.

Transient laboratory techniques to measure unsaturated hydraulic conductivity include: instantaneous profile method, Bruce-Klute method, pressure plate method, one-step outflow method, and the ultracentrifuge method. Refer to Stephens 1996 for additional details.

Field methods. Field methods include the instantaneous profile method, flux control methods, flow net method, borehole point source method, and air permeameter method as described in Stephens (1996). The instantaneous profile method is probably the most widely used of the field techniques.

In the instantaneous profile method, a square plot, approximately 3 to 10 m on a side, is prepared at a level site and a berm is made on the perimeter. Tensiometer nests and a neutron probe access tube are emplaced inside the plot, near the center where the flow field is likely to be unaffected by lateral flow beyond the perimeter of an unbounded plot. The "bermed" area is filled with water until the profile is saturated to the depth of interest. Usually this depth is within 2 to 3 m of the surface, but

for clay soils the practical depth of testing may be much less. During infiltration, the tensiometers and neutron probe measurements show when the soil has reached maximum saturation. Either the infiltration rate at constant ponding when the soil is saturated, or the rate of decline in ponded depth upon cessation of water application, may be used to estimate the field saturated hydraulic conductivity if lateral seepage is negligible.

To obtain the unsaturated hydraulic conductivity by the instantaneous profile method, the water supply is shut off, the plot is covered to prevent evaporation, and pressure head and water content are measured as the profile drains. The transient data are used to calculate the unsaturated hydraulic conductivity at some depth below the top of the soil profile, L, according to the following equation:

$$K(\overline{\theta}) = \int_0^L \frac{\partial \theta}{\partial t}\, dz \div (dH/dz) \tag{12.29}$$

At discrete depths, simultaneously, the hydraulic gradient is calculated from tensiometric data, and the rate of change in moisture content is calculated from the slope of the moisture content versus time plot.

Example 12.3 Figure 12.18 shows an excellent example of an instantaneous profile test conducted on fine sandy loam at Sandia National Laboratory in Albuquerque, NM (Bayliss et al. 1996; Goering et al. 1996).

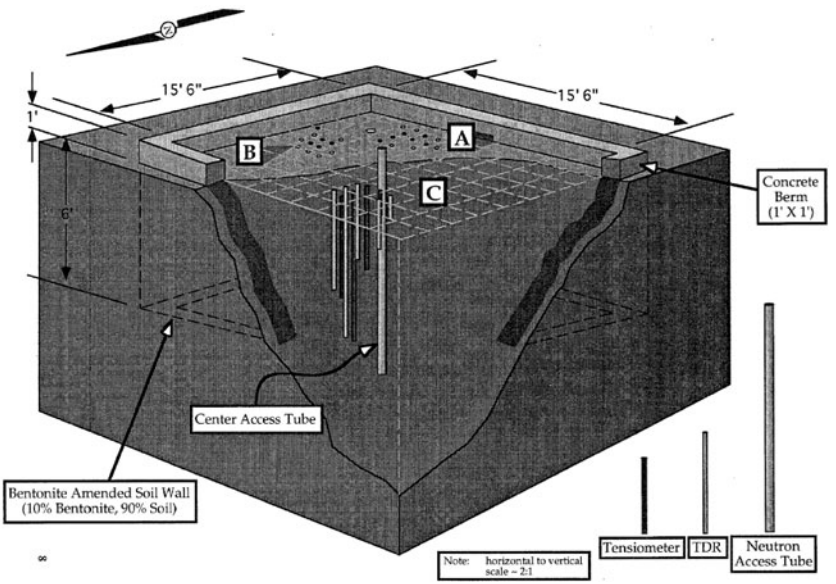

Figure 12.18 Cross section of IP plot showing instrument Cluster C. (*Bayliss et al. 1996, Sandia National Laboratories.)*

The 15.5 m × 15.5 m bermed area was flooded with water to a constant depth of about 5 cm until the infiltration rate was constant (Figure 12.19) and the soil profile was thoroughly wetted, as indicated by periodic measurements with neutron probe measurements to 3 m, tensiometer measurements to 1.8 m, as well as time domain reflectometry probes, and frequency domain reflectometry probes. After about 1.5 days, the profile was satiated to the 2 m depth. Water content profiles show the rapid initial rate of drainage and much slower drainage until the test was terminated after 400 days (Figure 12.20). The hydraulic head data (Figure 12.21) indicate near unit gradient conditions. Unsaturated hydraulic conductivity was calculated by discretizing Equation 12.29 and using data in Figures 12.20 and 12.21; the results are shown in Figure 12.22. Note that hydraulic conductivity changes by nearly 1000 fold over a water content change of only about 15%. The results also show the nature of heterogeneity in hydraulic conductivity with depth.

Estimating unsaturated hydraulic conductivity

Field and laboratory methods to characterize unsaturated hydraulic conductivity are either tedious, time consuming, or have other logistical difficulties. It is more convenient to estimate unsaturated hydraulic conductivity in lieu of measuring it in the laboratory or in the field. There are two general approaches for estimation. The first is called a pedotransfer function approach and the other is to calculate conductivity from moisture retention data.

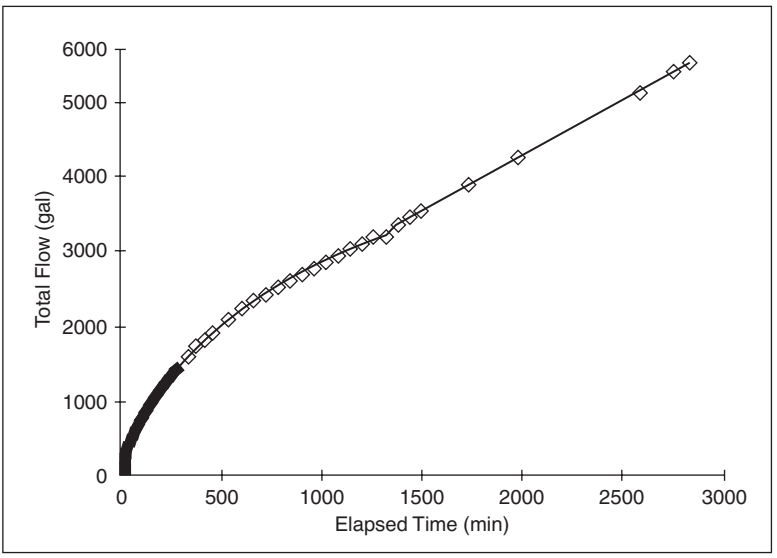

Figure 12.19 Cumulative flow applied to the IP test plot. (*Goering et al. 1996, Sandia National Laboratories.*)

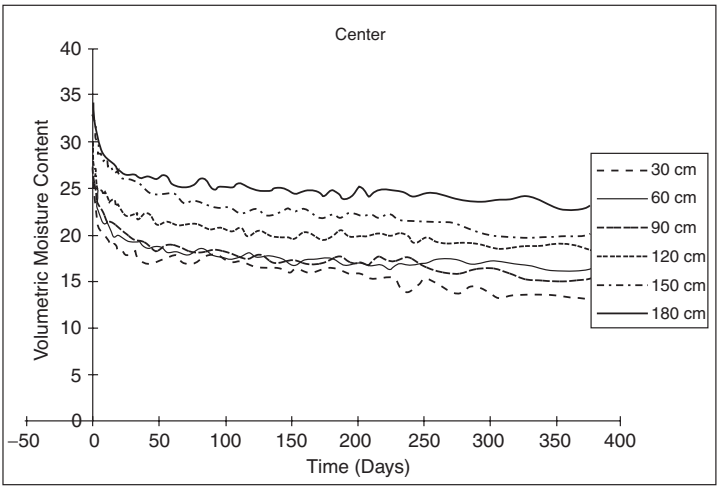

Figure 12.20 Moisture content data over the duration of the IP test. (*Goering et al. 1996, Sandia National Laboratories.*)

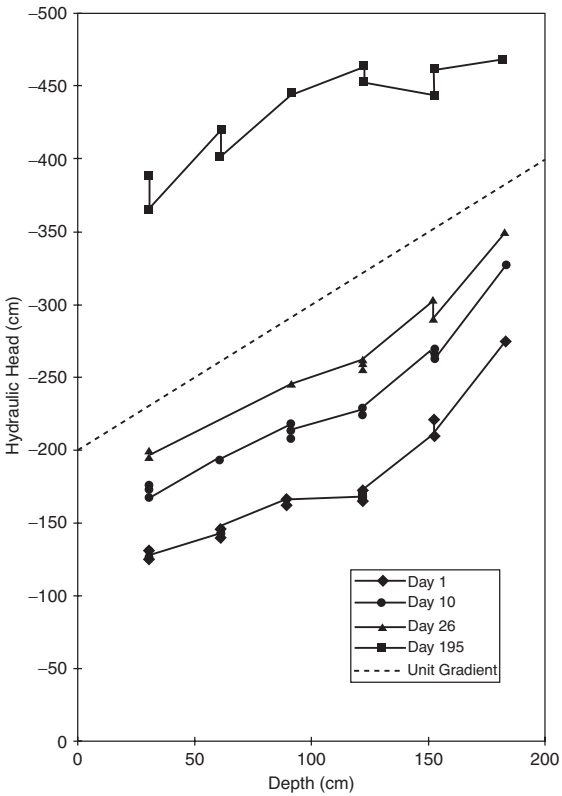

Figure 12.21 Hydraulic head profile changes with time. (*Goering et al. 1996, Sandia National Laboratories.*)

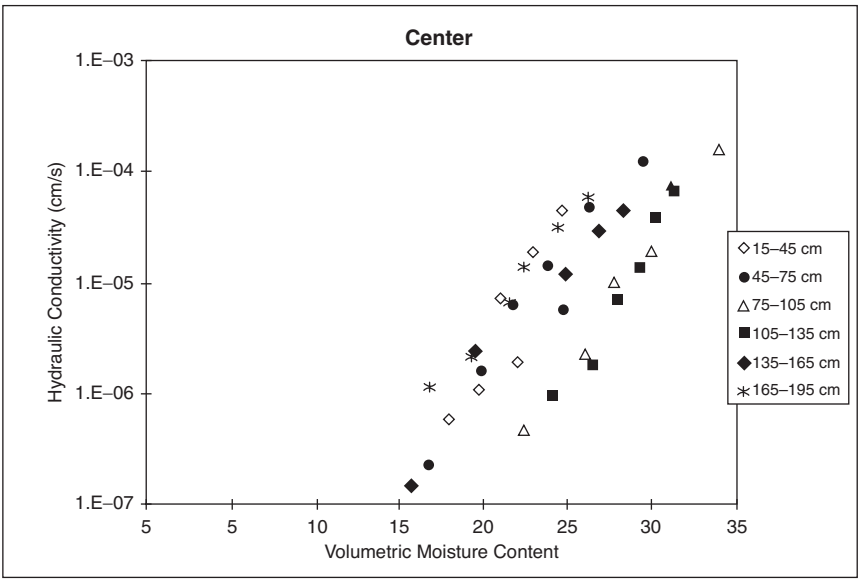

Figure 12.22 Unsaturated hydraulic conductivity as a function of moisture content. (*Goering et al. 1996, Sandia National Laboratories.*)

Pedotransfer function approach. Unsaturated hydraulic conductivity can be estimated by assuming that the soil follows a particular model or relationship between conductivity and pressure or moisture content. For example, Brooks and Corey (1964) proposed the equation:

$$K_r = (\psi/\psi_{cr})^{-\lambda} \tag{12.30}$$

where ψ_{cr} is the critical pressure or bubbling pressure $\psi \leqslant \psi_{cr}$, and λ is the pore size distribution index. These two parameters can be estimated from the relative percentages of sand, silt, and clay, as shown in Figure 12.23 from McCuen et al. (1981).

Calculating hydraulic conductivity ($K - \psi$) from moisture retention ($\theta - \psi$) curves is perhaps the most popular of all means in current use, in part because it is based on measured hydraulic properties (porosity, saturated hydraulic conductivity, and moisture retention). Based upon theoretical models of the porous medium, van Genuchten (1978; 1980) developed a convenient, closed-form analytical solution for calculating conductivity which is based on the following equation that must be fitted to the measured moisture retention curve:

$$S_e = \left[1 + |\alpha_v \psi|^N\right]^{-m} \tag{12.31}$$

where α_v and N are fitting parameters, and S_e is effective saturation $(\theta - \theta_r) \div (n - \theta_r)$. A nonlinear least-squares computer routine

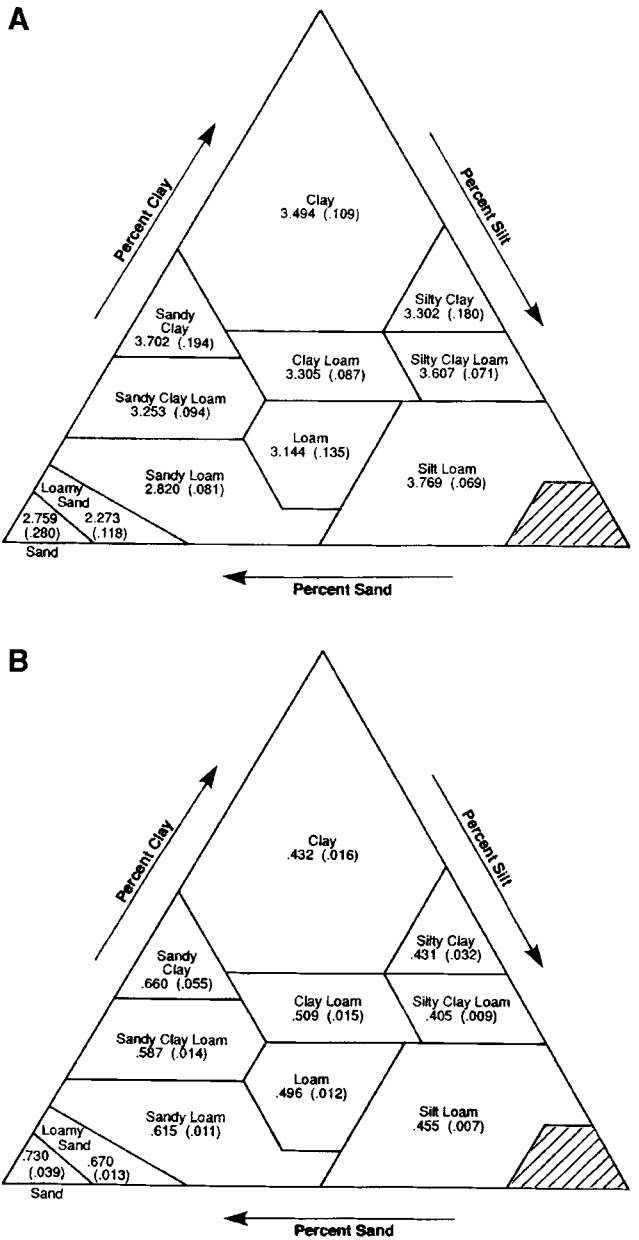

Figure 12.23 Mean and (standard error) of Brooks and Corey parameters: (A) in ψ_b and (B) $\lambda^{1/2}$. (*From McCuen et al. 1981. With permission of American Geophysical Union.*)

(RETEC; van Genuchten) automatically finds α_v and N by determining the best fit of Equation 12.31 to observed moisture retention ($\theta - \psi$) data. These fitting parameters are used to compute relative unsaturated hydraulic conductivity from the following equation for Mualem's model:

$$K_r(\psi) = \frac{\{1 - |\alpha_v \psi|^{N-1}[1 + |\alpha_v \psi|^N]^{-m}\}^2}{[1 + |\alpha_v \psi|^N]^{m/2}} \qquad (12.32)$$

The so-called van Genuchten parameters used to predict relative hydraulic conductivity can also be obtained by pedotransfer function approaches developed by Carsel and Parrish (1988) and Shaap et al. (2001).

12.9 Vadose Zone Monitoring

Vadose zone monitoring includes methods to measure pressure head and moisture content, as well as methods to sample pore liquids and soil gas. Some of these have been in use for many decades, primarily in applications to agricultural problems. For additional details, refer to Stephens (1996).

Pressure head soil-water potential

Pressure head is an important measure of the energy status of soil water. In the vadose zone, spatial differences in the potential determine the direction of soil-water movement.

Tensiometers. A tensiometer consists of a porous cup, usually composed of a moderately permeable ceramic, which remains saturated under significant tensions (Figure 12.24). Tensiometers are commercially available from Soilmoisture Equipment Corp. in Santa Barbara, California, for example. The cup is attached to a small diameter water-filled pipe that is sealed on the upper end with a removable cap. The purpose of the removable cap is to allow for filling of the tensiometer with water and for purging of air accumulations. A manometer installed through the top part of the water-filled pipe measures the pressure of the water in the tensiometer. When the tensiometer is inserted into the soil, the soil imbibes water from the tensiometer, and as this occurs, the water tension in the tensiometer increases until the tensiometer fluid pressure is in equilibrium with soil water outside the cup. The principal differences among tensiometers are attributable to the types of manometers used to measure pressure (Figure 12.24).

All tensiometers share a variety of problems. Care must be taken to use de-aired water in the tensiometer and maintain tight fittings to minimize air accumulation in the system. A small amount of air is

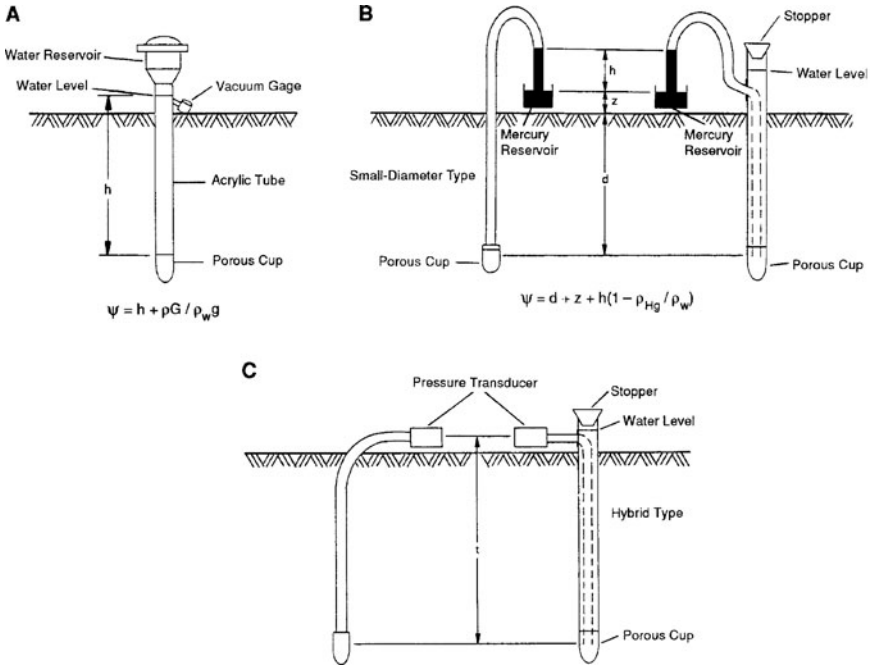

Figure 12.24 Tensiometer systems using the following pressure sensors: (A) bourdon gage, (B) mercury manometer, and (C) pressure transducer. (*Modified from Stannard 1990. USGS.*)

tolerable, but as the air accumulates, the response time of the system decreases. Consequently, air must periodically be removed from the system. The most significant limitation is that tensiometers cannot measure soil-water potentials less than about −0.8 bars, because near −1 bar at sea level, the water in the tensiometer would vaporize. For most irrigated soils as well as for uncultivated coarse, uniform textured soils this is not a severe limitation. In fact, tensiometers have functioned quite well even in semiarid climates in sand dunes where the moisture content is only about 5% (Stephens and Knowlton 1986). Freezing conditions can create severe problems for some systems unless antifreeze is used as the solution in the tensiometer (McKim 1976).

Psychrometers. A soil psychrometer measures the relative humidity within the soil atmosphere from the difference between the wet bulb and dry bulb temperature. The lower the relative humidity, the faster will be the rate of evaporation, and the lower will be the temperature of an evaporating liquid relative to the dry bulb temperature. In contrast to tensiometers, the pressure head determined from psychrometers includes both the matric (capillary plus adsorbed water) and osmotic (solute)

potential components, as presented in Equation 12.2. The contribution of osmotic potential to the soil-water potential is usually small and is generally ignored. Figure 12.25 illustrates the general features of a Spanner (1951) psychrometer, which is the common design used in field applications. Psychrometer calibration is accomplished by using the sensor to determine the output voltage (temperature depression) from a series of sodium or potassium chloride solutions of known different concentrations. These aqueous solutions have known osmotic potentials likely to be encountered in the field (e.g., Lang 1967). This calibration curve is used

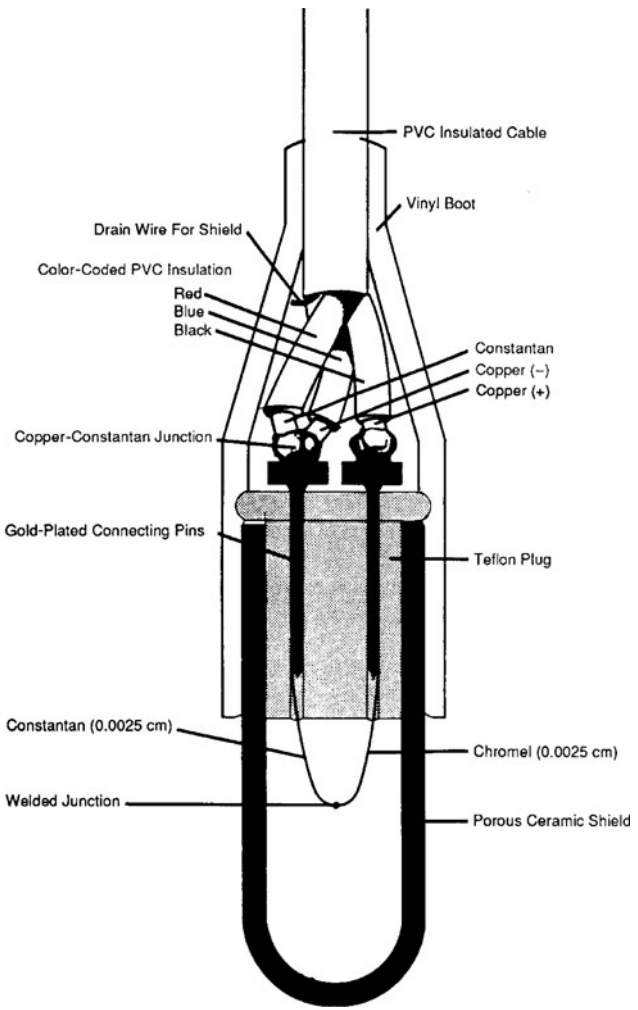

Figure 12.25 Peltier psychrometer/hydrometer with porous ceramic thermocouple shield. (*From Briscoe 1986. With permission.*)

to compute the in situ soil-water potential from the measured field output voltage. One of the potentially serious problems with all psychrometers is that the calibration can change over time due to microbial growth on the thermocouple wires (Merrill and Rawlins 1972) or corrosion (Daniel et al. 1981). Psychrometers are used only for dry conditions, usually where soil-water potential is in the range of about −2 to −70 bars or even lower.

Indirect methods

Indirect methods include electrical resistance blocks, heat dissipation sensors, and filter paper method. All indirect methods share the same general operational principles. When the sensor is placed in firm contact with the soil, water flows into or out of the sensor due to the hydraulic gradient between the potential in the sensor and the soil-water potential, until there is equilibrium. The water content of the sensor depends on the pore-size distribution of the sensor as well as the soil-water potential. To relate the measured water content of the sensor to the soil-water potential requires calibration in a pressure plate apparatus or an independent laboratory determination of the soil-water characteristic curve for the porous sensor.

Electrical resistance blocks. Electrical resistance blocks consist of porous gypsum, nylon, or fiberglass within which is embedded an electrode with leads connected to a wheatstone bridge to measure resistance (Figure 12.26). As the water content of the resistance block decreases, the electrical conductivity of the block decreases. The solubility of the gypsum blocks limits their longevity to perhaps a couple years in wet soils. Daniel et al. (1992) found that wet gypsum blocks disintegrated when repeatedly installed and retrieved. Although the nylon and fiberglass blocks are not readily soluble, Campbell and Gee (1986) report that in some cases these units may fail in 2 to 3 years because of corrosion of the welds. According to Campbell and Gee (1986), gypsum blocks are most sensitive in the dry range at potentials below about −0.3 bars, whereas nylon and fiberglass blocks are most sensitive in the range of 0 to −1 bars.

Heat dissipation sensors. Heat dissipation sensors are comprised of a porous material (ceramic in the commercially available ones) that surrounds a heating element and thermal detector (Phene et al. 1971) (Figure 12.27). The principle is based on the dependence of the thermal diffusivity (thermal conductivity + heat capacity) on moisture content of the porous material in the sensor. Current is passed into a coil of copper wire in the center of the porous material, and after the heating phase,

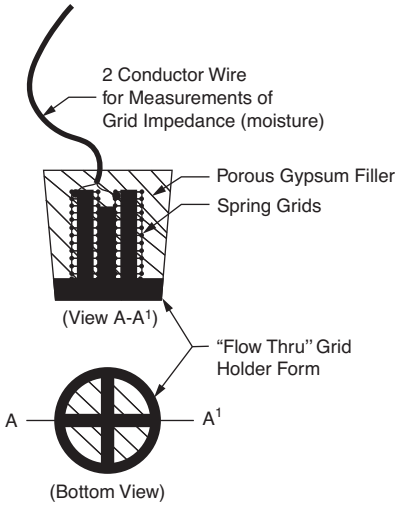

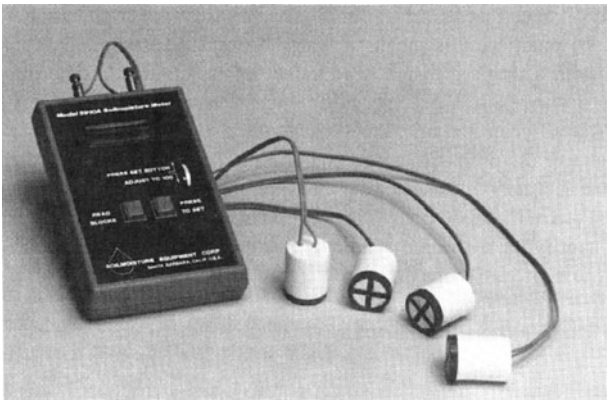

Figure 12.26 Gypsum block. (*Courtesy of Soilmoisture Equipment Corp.*)

the rate of temperature decline is determined with a diode circuit located inside the heating element. As the moisture content of the porous material increases, the thermal diffusivity increases, and the voltage output from the diode circuit decreases (Campbell and Gee 1986). The output voltage is related to the potential of the soil by a laboratory calibration curve. The heat dissipation sensor is insensitive to changes in soil salinity. Table 12.3 compares the range of sensitivity of the heat dissipation sensor with electrical resistance blocks and the portable salinity probe.

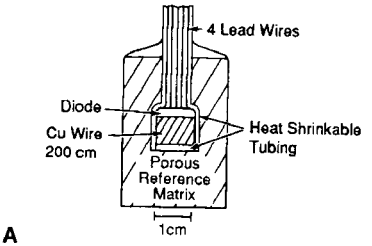

A

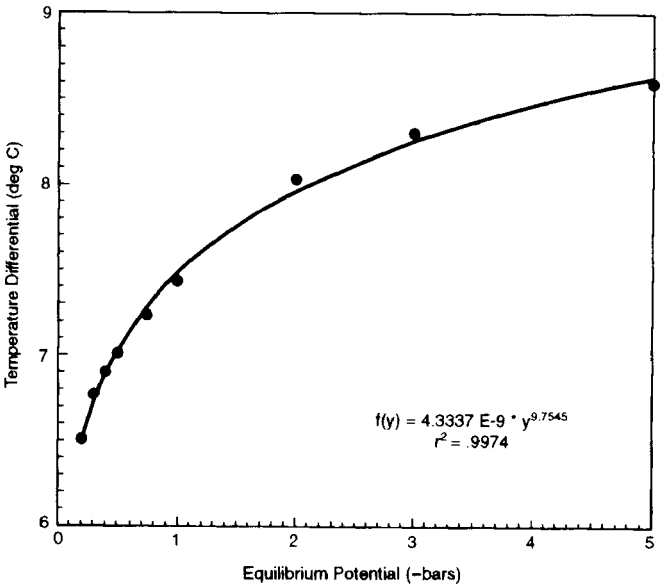

B

Figure 12.27 (A) Cross-sectional sketch of the Phene heat-dissipation sensor (*modified from Phene et al. 1971a, 1971b, with permission of ASA, CSSA, and SSSA*), and (B) heat dissipation probe calibration.

TABLE 12.3 Comparison of Calibration Tests Conducted on Four Vadose-Zone Monitoring Probes in a Kaolin Clay

	Range over which probe exhibited maximum sensitivity of response	
Type of monitoring probe	Volume water content (%)	Soil suction (bars)
Gypsum block	20–50	0–15
Fiberglass res. device	40–55	0–4
Heat dissipation sensor	30–50	0–10
Resistivity probe	20–35	5–15

From Daniels et al., 1992. With permission of ASTM.

Moisture content

Gravimetric method. The gravimetric method derives its name from the fact that moisture content is determined by weighing. There are two approaches that are commonly in use to express water content. The first is volumetric water content and the second is the mass-based or gravimetric water content. The volumetric moisture content represents the water volume in a known volume of soil, whereas the gravimetric water content represents the mass of water in a known dry mass of soil. For typical soils, the volumetric water content (% cm^3/cm^3) will be roughly 20 to 50% larger than the gravimetric water content (% g/g).

To determine moisture content by either approach, a sample of soil is collected from a particular depth by hand auger, power auger, or drilling rig. If the sample is undisturbed and collected so that the bulk volume of soil can be quantified, such as in a known volume of a ring sample (100 cm^3 and 250 cm^3 sizes are common), then the volumetric water content can be determined. Undisturbed samples are usually obtained by carefully pushing a sampling ring in to the soil by hand, hydraulic press, or weight of drill rig. In the laboratory, the testing process is almost identical for gravimetric or volumetric water content determinations. After removing the field wrapping, the samples are placed in a tare dish and weighed. The samples are then dried at a temperature of about 105°C in either a conventional convection oven (for 24 h), forced draft oven (for 10 h) or household microwave oven (for 6 to 20 min) (Gardner 1986). The samples are removed from the oven, and after cooling in a desiccator, they are reweighed to determine the loss of water. This loss on a mass basis, or on a volume basis if converted by dividing by the water density, is directly used to compute the gravimetric or volumetric water content, respectively.

Subsurface geophysical methods. For many applications, it is important to monitor moisture content profiles over time. This necessitates a nondestructive measurement which can be made repeatedly. Geophysical techniques are well-suited to this purpose, both subsurface and surface techniques.

Time domain reflectometry (TDR). TDR is based on measuring the dielectric constant of soil. Topp et al. (1980), who first proposed the method for soil-water investigations, showed that the dielectric constant of soil is dependent primarily upon the water content through a nearly universal calibration equation that is very insensitive to soil type. Most soil minerals have a dielectric constant of less than 5, whereas water has a dielectric constant of about 78. Thus, water content variations should be easily detectable from measured variations in dielectric constant.

To measure the dielectric constant in situ using TDR requires determining the rate of travel of electromagnetic energy through the soil along two parallel metallic conductor rods pushed into the soil (Figure 12.28). The TDR source introduces a voltage pulse and an oscilloscope maps the travel time for the wave to propagate along the transmission lines and reflect back to the source. From this velocity, one can calculate the apparent dielectric constant, K_{ad}, and then use the generic calibration equation (Topp et al. 1980) to compute the water content:

$$\theta = -0.053 + 0.029\,K_{ad} - (5.5 \times 10^{-4})\,K_{ad}^2 + (4.3 \times 10^{-6})\,K_{ad}^3 \tag{12.33}$$

This calibration equation reportedly has an accuracy of $\pm 0.02\ \text{cm}^3/\text{cm}^3$.

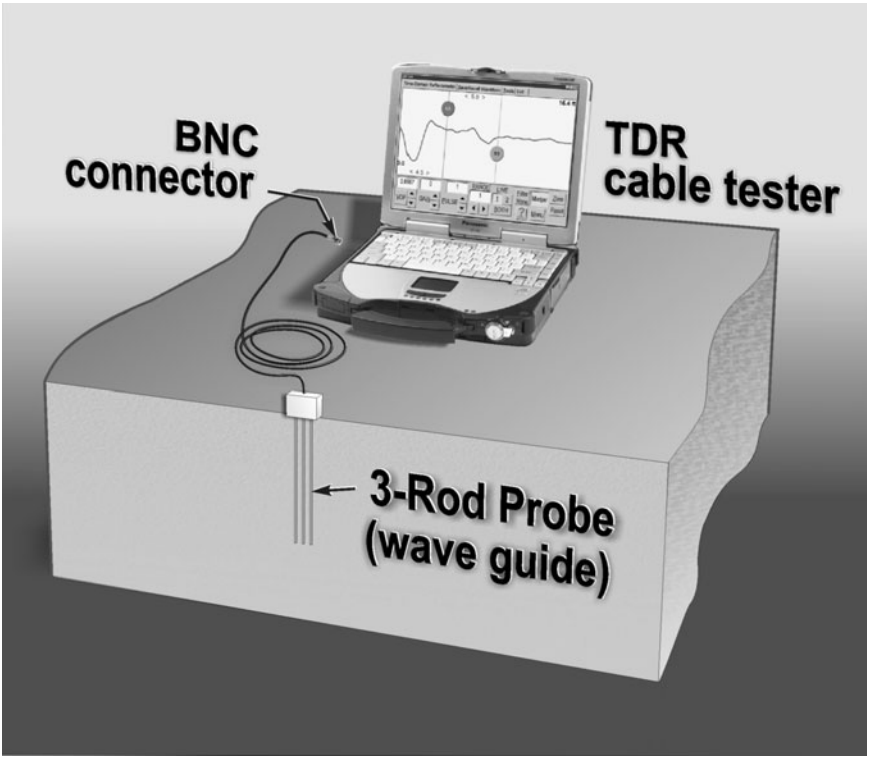

Figure 12.28 Time-domain reflectometry (TDR) equipment setup. (*Adapted from Greenlee Textron, Inc., with permission.*)

Neutron probe. The neutron probe is a geophysical logging tool that is lowered into a cased borehole on a cable which connects the neutron source with electronic readout equipment on the surface (Figure 12.29). The principle is based upon the neutron thermalization process, in which a radioactive source (e.g., amerecium–241) emits high energy neutrons into the soil where, through collisions primarily with hydrogen atoms, the energy of the neutrons is reduced to lower (thermal) energy levels (Gardner 1987). The neutrons are emitted more or less radially and form a sphere around the source within which the fast neutrons are attenuated. For dry soils the diameter of the sphere is approximately 70 cm, and at saturation the diameter is only about 16 cm; this diameter is unaffected by the

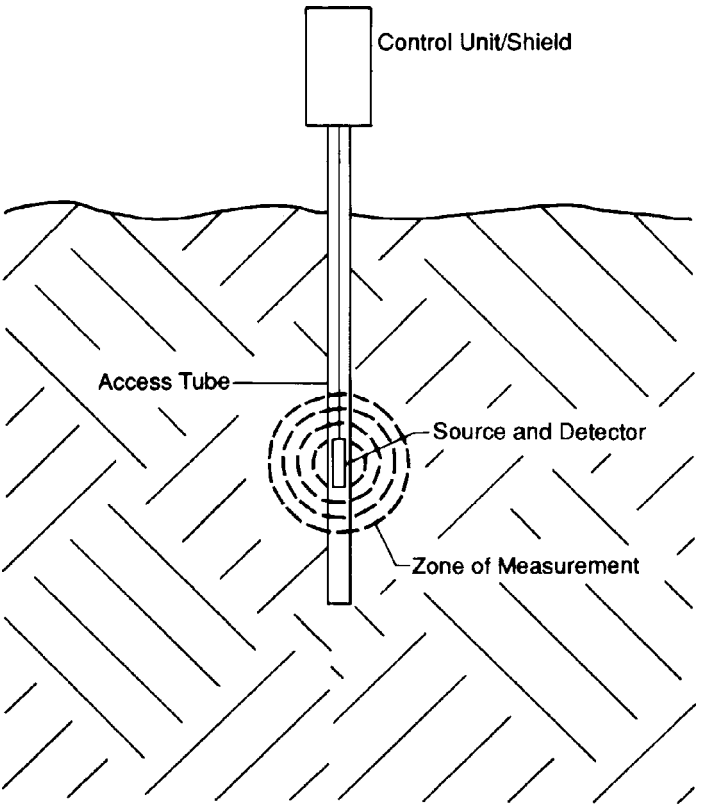

Figure 12.29 Schematic diagram of water content measurement by the neutron depth probe method. (*From ASTM D-5220-92, 1992. With permission of ASTM.*)

strength of the radioactive source (Gardner 1987). The detector of thermal neutrons commonly consists of a boron trifluoride gas, which when encountering a thermal neutron, emits an alpha particle as it decomposes to lithium-7 (Goodspeed 1981); this causes an electrical pulse to be released within the detector. In other words, the number of electrical pulses counted by the detector is proportional to the number of thermal neutrons it encountered.

If hydrogen is the only variable affecting the density of slow or thermal neutrons, then a calibration curve can be developed to relate count rate to water content. The calibration of a neutron probe can be done in the field or in the laboratory.

The preferred borehole construction for shallow vadose zone investigations calls for 5-cm-diameter (2-in-diameter), thin-walled aluminum tubing within which the slightly smaller diameter neutron probe can be easily raised and lowered. The tubing fits tightly in a smooth-walled borehole to minimize air pockets outside the casing. Other casing materials, such as polyvinylchloride and steel, tend to absorb the slow neutrons, but it is possible to prepare a separate calibration curve for each different casing material, with some loss of sensitivity.

Soil gas sampling and monitoring

Soil gas monitoring is a technique that is applicable to highly volatile organic chemicals which partition into the air-filled soil voids. There are both passive and active types of soil gas monitoring techniques. The passive devices are tubes containing absorbent material, usually activated carbon, which are placed in the soil for a period of time and later retrieved for chemical analysis (e.g., Bisque 1984) (Stutman 1993). The absorbing material picks up volatile and semi-volatile chemicals as they diffuse from the soil and are adsorbed. The passive absorbers must be buried for approximately several days to 2 weeks before retrieval. The active type of soil gas sampler is still by far the most popular. It uses vacuum to pump soil vapor from an in situ sampling probe directly into a chemical analyzer for a more rapid turnaround compared to the passive systems. There are several different installations for collecting soil gas in active sampling systems, including permanent soil gas monitor wells, a semipermanent monitoring system, soil gas surveys, and soil gas profiles. Depth profiling for soil gas is accomplished by either the permanent or semipermanent installations described above or by driving probes and sequentially sampling as the drive point is advanced to greater depths. For most unconsolidated soils a cone penetrometer rig (Chapter 8) can collect soil gas samples

as the cone is advanced by the hydraulic jack system. An advantage of the cone penetrometer method is that other information on soil texture can be collected continuously with depth at the same time and location as the soil gas sample is collected. This approach can lead to improved interpretations and more rapid decisions in the field program which may follow.

Pore liquid sampling

Pore liquid sampling includes extracting liquids from the matrix of soil cores and in situ samplers to collect liquids from the vadose zone. Samples of soil can be collected from the soil by hand tools or mechanical drilling equipment. Conventional drilling equipment such as the hollow stem flight auger with core sampling generally produces excellent results, except in very loose dry soils, and cemented or stony soils. In most solid or hazardous waste site sampling projects, soil cores are sent to a laboratory for chemical analysis, under strict preservation and quality assurance/quality control procedures. The main point to recognize in considering soil cores for pore liquid sampling is that this is a destructive technique. For time series monitoring, repeated coring to collect samples from the same general location potentially introduces significant bias which may preclude distinguishing chemical changes attributable to contaminant migration from changes due to spatial variability in fluid chemistry.

Porous cup samplers, also referred to as suction lysimeters or porous suction samplers, consist of a porous tip attached with an air-tight seal to the lower end of a thin plastic casing. The upper end is also tightly capped, so that a vacuum can be applied and maintained to the casing through connections in the upper cap. The sampler cup is designed with pores sufficiently fine that they remain saturated with water while the vacuum is applied to the casing section. The principle of operation is to place the sampler in a boring so that there is good communication with the formation. Usually a slurry of soil cuttings or 200 mesh silica flour is placed around the sampler (in a thin pancake batter consistency), and bentonite seals are set above this interval to prevent channeling of runoff or perched fluids. A vacuum is applied to the sampler with the intent that it will establish a hydraulic gradient between the formation and the sampler. This system may fail for a variety of reasons, for example, if the applied vacuum exceeds the air-entry value for the porous cup or if the soil tension exceeds the air-entry pressure of the cup. In all these instances, consequently, the porous cup will dewater partially, the air in the sampler casing will be in communication with the soil air, and vacuum on the liquid phase will be lost.

Porous cup samplers differ in two general ways, by the material used to construct the cup and by the design of the component. Most of the cups consist of porous ceramic or Teflon, although Alundum and nylon have been used (Creasey and Dreiss 1985). In the simplest design of the porous cup sampler, the cup is located at the bottom of the sampler tube. A two-hole rubber stopper caps the upper end of the casing so that a short tube inserted through the stopper can be used to apply a vacuum to collect the liquid in the sampler. Then a vacuum is applied to the long discharge tube which is set to the base of sampler to bring the liquid to the surface (Figure 12.30). This design,

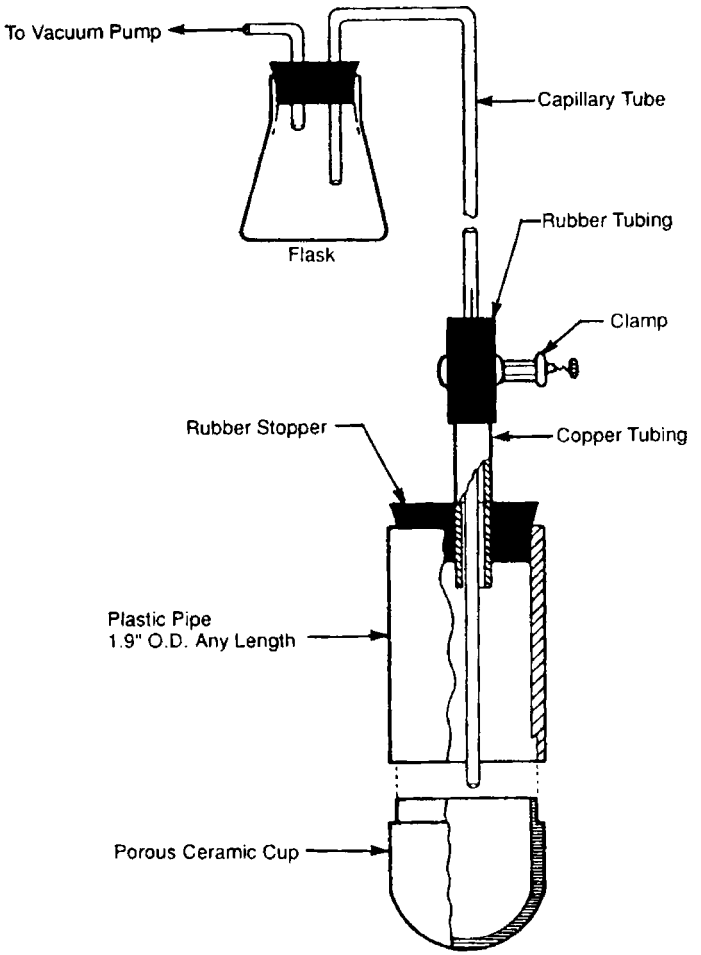

Figure 12.30 Pore liquid sampling with porous cup vacuum sampler (lysimeter). *Note*: Capillary tube is only inserted to recover the water sample. (*From Parizek and Lane 1970. With permission from Elsevier.*)

referred to as the vacuum sampler, is usually used at depths of less than 2 m but potentially could be installed at depths less than about 8 m, the maximum practical suction lift. For deeper sampling, a pressure-vacuum sampler (Parizek and Lane 1970) is required. When vacuum is applied a check valve opens and the sample is drawn from the cup to an upper chamber within the sampler. Then positive pressure is applied as the check valve closes to prevent liquid from the upper chamber from falling back into the cup and the sample is forced to the surface (Figure 12.31). A type of porous cup sampler called the BAT system (Torstensson 1984) is a unique design to allow sampling of volatile chemicals and constituents involved in redox reactions (Figure 12.32). Perhaps the greatest problem with porous cup samplers is that they simply do not function if the soil-water potential is less than about 1 bar. In humid climates, this may not be a problem, except at shallow depths after prolonged dry conditions. But in semiarid and Mediterranean climates, many fine-textured soils are too dry for these samplers to function.

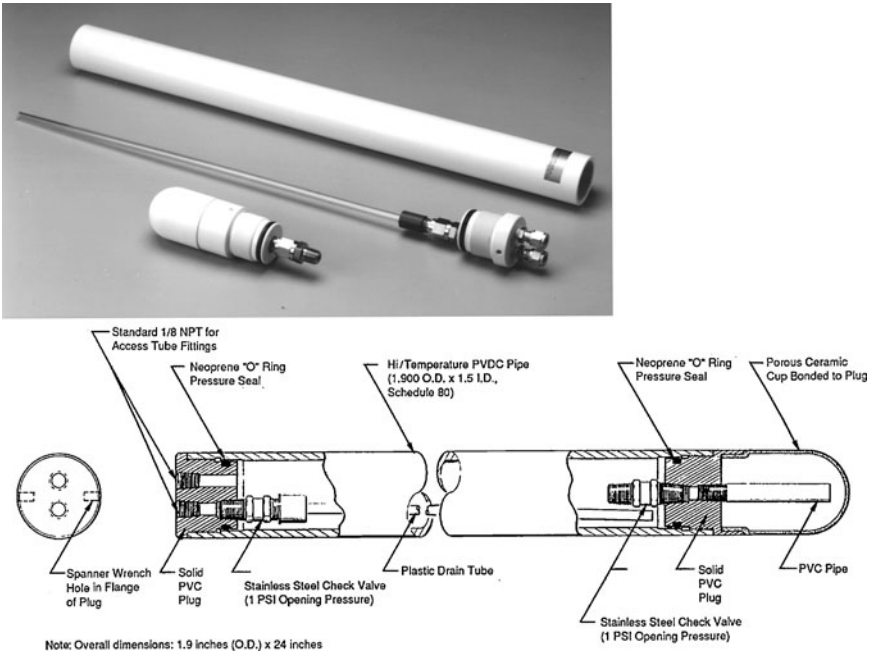

Figure 12.31 Model 1940 high-pressure-vacuum soil water sampler. (*Courtesy of Soilmoisture Equipment Corp.*)

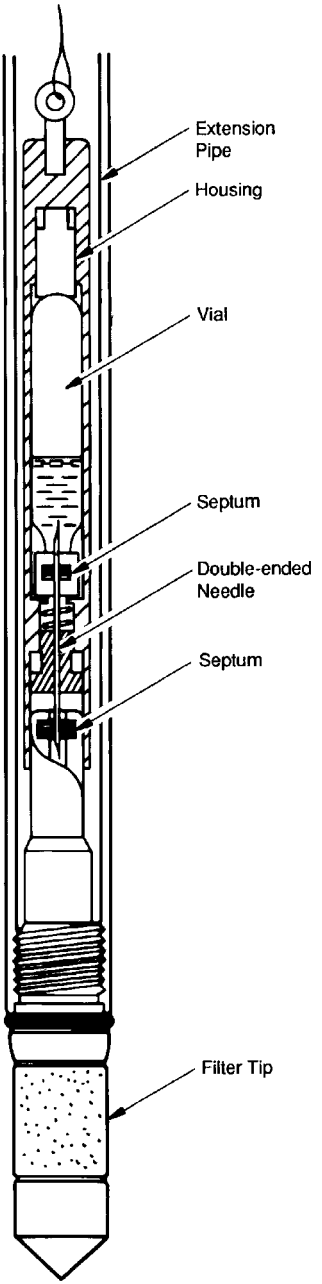

Figure 12.32 BAT system. (*From Torstensson 1984. With permission of the National Water Well Association.*)

12.10 Summary

The vadose zone is an integral part of the hydrogeologic system consisting of the porous or fractured media above the regional water table. Understanding the processes governing flow through the vadose zone are highly relevant to hydrogeologic applications including quantifying natural and artificial recharge, assessing impacts from chemical spills and leaching from waste sources such as landfills for instance. Characterizing the hydraulic properties of the vadose zone is more complex than characterizing aquifer properties, because in the vadose zone properties such as unsaturated hydraulic conductivity not only varies spatially but they exhibit large variations with water content. Fortunately, there is a wide array of field and laboratory methods to characterize vadose zone hydraulic properties and to monitor water and chemical movement, most of which have been in wide use for many decades.

References

Allen, R.G., Pereira, L.S., Raes, D., and Smith, M. 1998. Crop evapotranspiration, Guidelines for computing crop water requirements. FAO Irrigation and Drainage Paper 56, Food and Agriculture Organization of the United Nations, Rome, Italy.

Allison, G.B., and Hughes, M.W. 1978. The use of environmental chloride and tritium to estimate total local recharge to an unconfined aquifer, *Australian Journal Soil Research*, 16, 181.

American Standards for Testing and Materials. 1992. D-5220-92 Method for water content of soil and rock in-place by the neutron depth probe method. ASTM International, West Consohoken.

Bayliss, S.C., Goering, T.J., McVey, M.D., Strong, W.R., and Peace, J.L. 1996. Preliminary data from an instantaneous profile test conducted near the mixed waste landfill, Technical Area 3, Sandia National Laboratories, NM, SAND96-0813.

Bentley, H.W., Phillips, F.M., Davis, S.N., Gifford, S., Elmore, D., Tubbs, L.E., and Gove, H.E. 1982. Thermonuclear C1-36 pulse in natural water, *Nature* 30 (23/30), 737–740.

Bisque, R.E. 1984. Migration rates of volatiles from buried hydrocarbon sources through soil media *in* Proceedings of the National Conference on Petroleum Hydrocarbons and Organic Chemicals in Groundwater—Prevention, Detection, and Restoration, National Well Water Association, Worthington, OH.

Blaney, H.F. and Criddle, W.D. 1950. Determining water requirements in irrigated areas from climatological and irrigation data, Technical Paper No. 96, U.S. Department of Agriculture Soil Conservation Service, Washington, DC.

Bouwer, H. 1966. Rapid field measurement of air-entry value and hydraulic conductivity of soil as significant parameters in flow system analysis, *Water Resources Research*, 2, 729.

Briscoe, R.D. 1986. Thermocouple psychrometers for water potential measurements, in *Advanced Agricultural Instrumentation: Design and Use, NATO ASI Series,* Gensler, W. G., Ed., Martinus Nijhoff, Dordrecht, Netherlands.

Brookings, D.G., and Thomson, B.M. 1992. Geochemical considerations for disposal facilities: waste disposal in desert playas, in *Deserts as Dumps,* Reith, C. C. and Thomson, B.M., Eds., University of New Mexico Press, Albuquerque, NM, 199.

Brooks, R.H., and Corey, A.T. 1964. Properties of porous media affecting fluid flow, *ASAE Journal of Irrigation Drainage Division*, IR2, 61.

Brutsaert, W. 1977. Vertical infiltration in dry soil, *Water Resources Research*, 13, 363.

Buckingham, E. 1907. Studies on the movement of soil moisture, U.S. Department of Agriculture Bureau Soils, 38.

Campbell, G.S., and Gee, G.W. 1986. Water potential: miscellaneous methods, in *Methods of Soil Analysis, Part 1, 2nd ed.* Klute, A., Ed., Agronomy Monograph No. 9, ASA, CSSA, and SSSA, Madison, WI, 619.

Carsel, R.F., and R.S. Parrish. 1988. Developing joint probability distributions of soil water characteristics. *Water Resources Research* 24:755–769.

Cecen, K. 1967. *The Investigation of the Coefficient of Permeability in Connection with Construction Engineering Soil Investigations,* Verlag Wasser and Boden, Hamburg, Germany.

Creasey, C.L., and Dreiss, S.J. 1985. Soil water samplers: do they significantly bias concentrations in water samples?, *in* Proceedings of the Conference on Characterization and Monitoring of the Vadose (Unsaturated) Zone, National Well Water Association, Dublin, OH, 173.

Czarnecki, J.B. 1990. Geohydrology and evapotranspiration at Franklin Lake Playa, Inyo County, California, Open-File Reptort 90-356, U.S. Geological Survey, Denver, CO.

Daniel, D., Hamilton, J., and Olson, R. 1981. Suitability of thermocouple psychrometers for studying moisture movement in unsaturated soils, in *Permeability and Groundwater Contaminant Transport, ASTM STP 746,* Zimmie, T.F., and Riggs, C.O., Eds., ASTM, Philadelphia, PA, 84.

Daniel, D.E., Burton, P.M., and Hwang, S.D. 1992. Evaluation of four vadose zone probes used for leak detection and monitoring, in *Current Practices in Ground Water and Vadose Zone Investigations, ASTM STP 1118,* Nielsen, D.M., and Sara, M.N., Eds., American Society for Testing and Materials, Philadelphia, PA.

Daniel, D.E. 1989. In situ hydraulic conductivity tests for compacted clay, *ASCE Journal of Geotechnical Engineering*, 115, 1205.

Daniel, D.E., State-of-the-art: laboratory hydraulic conductivity tests for saturated soils, in *Hydraulic Conductivity and Waste Contaminant Transport in Soils, ASTM STP 1142,* Daniel, D.E., and Trautwein, S.J., Eds., ASTM, Philadelphia, PA, 1993.

Dirksen, C. 1991. Unsaturated hydraulic conductivity, in *Soil Analysis: Physical Methods,* Smith, K.A., and Mullins, C.E., Eds., Marcel Dekker, New York, NY, 209.

Doorenbos, J., and Pruitt, W.O. 1975. Crop water requirements, in Irrigation and Drainage Paper, FAO, Rome, Italy.

Elrick, D.E., and Reynolds, W.D. 1992. Infiltration from constant-head well permeameters and infiltrometers, in *Advances in Measurement of Soil Physical Properties: Bringing Theory into Practice,* SSSA Special Pub. No. 30, Topp, G.C., Reynolds, W.D., and Green, R.E., Eds., ASA, CSSA, and SSSA, Madison, WI, 1.

Flint A.L, J.A. Hevesi, and L.E. Flint. 1996. Conceptual and numerical model of infiltration for the Yucca Mountain area, Nevada. Milestone Report 3GUI623M, U.S. Geological Survey, Denver, CO.

Gardner, R. 1955. Relation of temperature to moisture tension of soil, *Soil Science,* 79, 257.

Gardner, W H. 1986. Water content, in *Methods of Soil Analysis, Part I, 2nd ed.,* Klute, A., Ed., Agronomy Monograph No. 9, ASA, CSSA, and SSSA, Madison, WI, 493.

Gardner, W.R. 1987. Water content: An overview, *in* International Conference on Measurement of Soil and Plant Water Status, Vol. 1, Soils, Utah State University, Logan, UT, 7.

Gee, G., and Hillel, D. 1988. Groundwater recharge in arid regions: review and critique of estimation methods, *Hydrological Processes*, 2, 255.

Glover, R.E. 1953. Flow for a test hole located above groundwater level, in *Theory and Problems of Water Percolation*, Engineering Monograph No. 8, Zangar, C.N., Ed., U.S. Bureau of Reclamation, 69.

Goering, T.J, McVey, M.D., Strong, W.R., and Peace, J.L. 1996. Analysis of instantaneous profile test data from soils near the mixed waste landfill, Technical Area 3, Sandia National Laboratories, NM, SAND95-1637.

Goodspeed, M.J., 1981. Neutron moisture meter theory, in *Soil Water Assessment by the Neutron Method,* Greacen, E.L., Ed., CSIRO, East Melbourne, Australia, 17.

Green, W.H., and Ampt, G.A. 1911. Studies in soil physics, I. The flow of air and water through soils. *Journal of Agricultural Science*, 4, 1–24.

Havlena, J.A., and Stephens, D.B. 1991. Vadose zone characterization using field permeameters and instrumentation, in *Current Practice in Ground Water and Vadose Zone*

Investigations, ASTM STP 1118, Nielsen, D.M., and Sara, M.N., Eds., ASTM, Philadelphia, PA.
Hevesi, J.A., Flint, A.L., and Flint, L.E. 2003. Simulation of net infiltration and potential recharge using a distributed-parameter watershed model of the Death Valley Region, Nevada and California. U.S. Geological Survey Water-Resources Investigations Report 03–4090.
Jensen, M.E., and Haise, R. 1963. Estimating evapotranspiration from solar radiation, *ASCE Journal of Irrigation and Drainage Division*, 89, 15.
Jensen, M.E., Burman, R.D., and Allen, R.G. 1990. Evapotranspiration and irrigation water requirements. Engineering Practice Manual No. 70, American Society of Civil Engineers, New York, NY, 332 pp.
Kirkham, R.R., Gee, G.W., and Jones, T.L. 1984. Weighing lysimeters for long-term water balance investigations at remote sites, *Soil Science Society of America Journal,* 48(5), 1203–1205.
Klute, A., and Dirksen, C. 1986. Hydraulic conductivity and diffusivity: laboratory methods, in *Methods of Soil Analysis, Part I, 2nd ed.,* Klute, A., Ed., Agronomy Monograph No. 9, ASA, CSSA, and SSSA, Madison, WI, 687.
Lang, A.R.G. 1967. Psychrometric measurement of soil water potential in situ under cotton plants. *Soil Science* 106, 460–464.
Leonard, R.A., Davis, F.M., and Knisel, W.G. 1989. Groundwater Loading Effects of Agricultural Management Systems (GLEAMS): A tool to assess soil-climate-management-pesticide interactions, U.S. Department of Agriculture, Tifton, GA.
Marshall, T.J., and Holmes, J.W., *Soil Physics*, Cambridge University Press, London, 1992.
McCuen, R.H., Rawls, W.H., and Brakensisk, D.L. 1981. Statistical analysis of the Brooks-Corey and the Green-Ampt parameters across soil textures, *Water Resources Research*, 17(4), 1005–1013.
McKim, H.L., Berg, R.L., McGaw, R.W., Atkins, R.T., and Ingersoll, J. 1976. Development of a remote reading tensiometer/transducer system for use in subfreezing temperatures, *in* Proceedings of the second Conference on Soil-Water Problems in Cold Regions, AGU, Edmonton, Alberta, Canada.
McWhorter, D.B., and Sunada, D.K. 1977. *Ground-Water Hydrology and Hydraulics,* Water Resources Publication, Ft. Collins, CO.
Merrill, S.D., and Rawlins, S.L. 1972. Field measurement of soil water potential with thermocouple psychrometers, *Soil Science*, 113, 102.
Moridis, G.J., and McFarland, M.J. 1982. Modeling soil water extraction from grain sorghum, in *Proceedings Winter Meeting*, ASCE, St. Joseph, MI.
Mullins, J.A., Carsel, R.F., Sarbrough, J.E., and Ivery, A.M. 1993. PRZM-2, A Model for Predicting Pesticide Fate in the Crop Root and Unsaturated Soil Zones, User's Manual for Release Version 2.0, U.S. Evironmental Protection Agency, Environmental Research Laboratory, Athens, GA.
Nasberg, V.M. 1951. *The Problem of Flow in an Unsaturated Soil or Injection under Pressure,* Izvestja Akademia Nauk, SSSR odt tekh Nauk. No. 9, translated by Mr. Reliant, 1973, B.R.G.M., France.
Parizek, R.R., and Lane, B.E. 1970. Soil-water sampling using pan and deep pressure-vacuum lysimeters, *Journal of Hydrology*, 11, 1.
Penman, H.L. 1948. Natural evapotranspiration from open water, bare soil and grass, *Proceedings of the Royal Society London*, 193A, 120.
Phene, C.J., Hoffman, J., and Rawlins, S.L. 1971. Measuring soil matric potential in situ by sensing heat dissipation within a porous body: I. Theory and sensor construction, *Soil Science Society of America Proceedings,* 35, 27.
Philip, J.R. 1957. The theory of infiltration. 1. The infiltration equation and its solution, *Soil Science*, 83, 345.
Philip, J.R. 1985. Approximate analysis of the borehole permeameter in unsaturated soil, *Water Resources Research,* 21, 1025.
Phillips, F.M., Mattick, J.L., Duval, T.A., Elmore, D., and Kubik, P.W. 1988. Chlorine 36 and tritium from nuclear weapons fallout as tracers for long-term liquid and vapor movement in desert soils, *Water Resources Research*, 24, 1877.

Phillips, F.M. 1994. Environmental tracers for water movement in desert soils: a regional assessment for the American Southwest, *Soil Science Society of America Journal*, 58(1), 15–24.
Reynolds, W.D., Elrick, D.E., and Topp, G.C. 1983. A reexamination of the constant head well permeameter method for measuring saturated hydraulics conductivity above the water table, *Soil Science,* 136, 250.
Reynolds, W.D., Elrick, D.E., and Clothier, B.E. 1985. The constant head well permeameter: effect of unsaturated flow, *Soil Science,* 139, 172.
Rosenberg, N.J., Blad, B.L., and Verma, S.B. 1983. *Microclimate: The Biological Environment, 2nd ed.,* Wiley-Interscience, John Wiley & Sons, New York, NY.
Schroeder, P.R., Gibson, A.C., and Smolen, M.G. 1984. The hydrologic evaluation of landfill performance (HELP) model, USEPA Doc. No. EPA/530-SW-84-010, U.S. Environmental Protection Agency, Office of Solid Waste and Emergency Response, Washington, DC.
Sebenik, P.G., and Thomas, J.L. 1967. Water consumption by phreatophytes, Progessive Agriculture in Arizona, 19, 10.
Shaap, M.G., Lei, F.J, and van Genuchten, M.Th. 2001. ROSETTA: A computer program for estimating soil hydraulic parameters with hierarchical pedotransfer functions. *Journal of Hydrology*. 251:163–176.
Spanner, D.C. 1951. The Peltier effect and its use in the measurement of suction pressure, *Journal of Experimental Botany,* 11, 145.
Stannard, D.I. 1990. Use of a hemispherical chamber for measurement of evapotranspiration, Open-File Report 88-452, U.S. Geological Survey, Denver, CO.
Stephens, D.B., Lambert, K. 1987. and Watson, D., Regression models for hydraulic conductivity and field test of the borehole permeameter, *Water Resources Research*, 23, 2207.
Stephens, D.B., and Neuman, S.P. 1982. Free surface and saturated-unsaturated analysis of borehole infiltration tests above the water-table, *Advances in Water Resources*, 5, 111.
Stephens, D.B., Knowlton, R.G., Jr., Stanfill, M., and Hirtz, E. M. 1985. Field study to quantify seepage from a fluid impoundment, *in* Proceedings of the Conference on Characterization and Monitoring of the Vadose (Unsaturated) Zone, NWWA, Dublin, OH, 283.
Stephens, D.B., and Knowlton, R., Jr. 1986. Soil water movement and recharge through sand at a semi-arid site in New Mexico, *Water Resources Research*, 22, 881.
Stephens, D.B. 1992. Application of the borehole permeameter, in *Advances in Measurements of Soil Physical Properties: Bringing Theory into Practice,* SSSA Special Publication No. 30, Topp, G.C., Reynolds, W.D., and Green, R.E., Eds., SSSA, Madison, WI, 43.
Stephens, D.B. 1993. Hydraulic conductivity assessment of unsaturated soils, in Hydraulic Conductivity and Waste Contaminant Transport in Soils, ASTM STP 1142, Daniel, D.E., and Trautwein, S.J., Eds., ASTM, Philadelphia, PA.
Stephens, D.B. 2006. *Vadose Zone Hydrology*. CRC Press, Boca Raton, FL.
Stutman, M. 1993. A novel passive sorbent collection apparatus for site screening of semivolatile compounds, *in* Proceedings of the Third International Conference on Field Screening Methods for Hazardous Waste and Toxic Chemicals. Las Vegas, NV. Feb. 24–26, 1993.
Swinbank, W. C. 1951. A measurement of vertical transfer of heat and water vapour and momentum in the lower atmosphere with some results, *Journal of Meteorology,* 8, 135.
Tanner, C.B. 1960. Energy balance approach to evapotranspiration from crops, *Soil Science Society of America Proceedings*, 24:1–9.
Terletskaya, N.M. 1954. Determination of permeability in dry soils, Hydroelectric Waterworks No. 2, February, Moscow.
Thornthwaite, C.W. 1948. An approach toward a rational classification of climate. *Geographical Review,* 38(1):55–94.
Topp, G.C. 1987. The application of time-domain reflectometry (TDR) to soil water content measurement, in International Conference on Measurement of Soil and Plant Water Status, Vol. 1, Soils, Utah State University, Logan, UT, 85.
Topp, G.C., Davis J.L., Annan A.P. 1980. Electromagnetic determination of soil water content: measurements in coaxial transmission lines. *Water Resources Research,* 16, 574–582.
Torstensson, B.A. 1984. A new system for groundwater monitoring, *Ground Water Monitoring Rev*iew, 4, 131.

U.S. Bureau of Reclamation. 1974. *Earth Manual*, 2nd ed., U.S. Government Printing Office, Washington, DC.
U.S. Bureau of Reclamation. 1977. Ground Water Manual, First edition. U.S. Government Printing Office, Washington, DC.
van Genuchten, M.T. 1978. Calculating the unsaturated hydraulic conductivity with a new closed-form analytical model, Research Report 78-WR-08, Princeton University, Princeton, NJ.
van Genuchten, M.T. 1980. A closed-form equation for predicting the hydraulic conductivity of unsaturated soils, *Soil Science Society of America Journal*, 44, 892.
Zanger, C. N. 1953. Theory and problems of water percolation, Engineering Monograph No. 8, U. S. Bureau of Reclamations, Denver, CO.
Zegelin, S.J., and White, I. 1982. Design for a field sprinkler infiltrometer, *Soil Science Society of America Journal*, 46, 1129.

This page intentionally left blank

Chapter

13

Karst Hydrogeology

David M. Bednar, Jr.

Eagle Environmental Consulting, Inc. Fort Smith, Arkansas and Vinita, Oklahoma

13.1 Introduction

Karst is an area of land, predominantly underlain by carbonate rocks, where unique surface and subsurface landforms and hydrology are created by the reaction of water with the bedrock. Carbonate rocks consist of limestone and dolostone. Calcite ($CaCO_3$) is the dominant mineral in limestone and dolomite ($CaMg(CO_3)_2$) is the dominant mineral in dolostone. Water that falls as precipitation to the earth contains dissolved carbon dioxide (CO_2) that produces a weak carbonic acid (H_2CO_3). The weak acidic water dissolves the calcite and dolomite in the rock and transports the mineral matter into and through the groundwater-flow system (Figure 13.1). Water that moves through the soil increases in acidity by further absorption of CO_2 from microorganisms living in the soil and decayed plant matter. Once groundwater reaches the bedrock, it passes through bedding planes, joints, and fractures in the rock and openings become wider through time.

Distinctive surface landforms that form in karst include sinkholes, sinking steams and many types of sculpted bedrock surfaces. Distinctive subsurface features include caves and the unique formations that develop in them. Some karst terrains are a rough and jumbled land of deep depressions, isolated towers, and pointed hills while others may be gently rolling plains with only the slightest number of depressions to label them as karst (White 1988). For example, some karst areas such as the Mitchell Sinkhole Plain of Indiana and the Pennyroyal Sinkhole Plain in Kentucky show obvious signs of karst while other areas are not so obvious.

Copyright © 2008, 2001 by The McGraw-Hill Companies, Inc. Click here for terms of use.

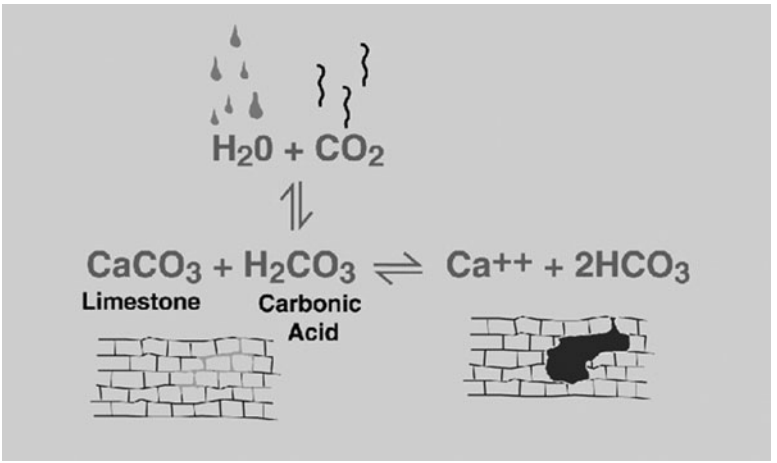

Figure 13.1 The generalized chemical reaction that occurs when carbonic acid flows over limestone in areas of karst. (*Used with permission, North Carolina Geological Survey*.)

Karst landscapes are found in many areas from tropical to colder alpine settings. About 25% of the United States is karst with 40% located east of the Mississippi River (Figure 13.2). About 25% of the world's population depends on freshwater from karst aquifers (Ford and Williams 1989). Some of the karst areas in the United States include the Great

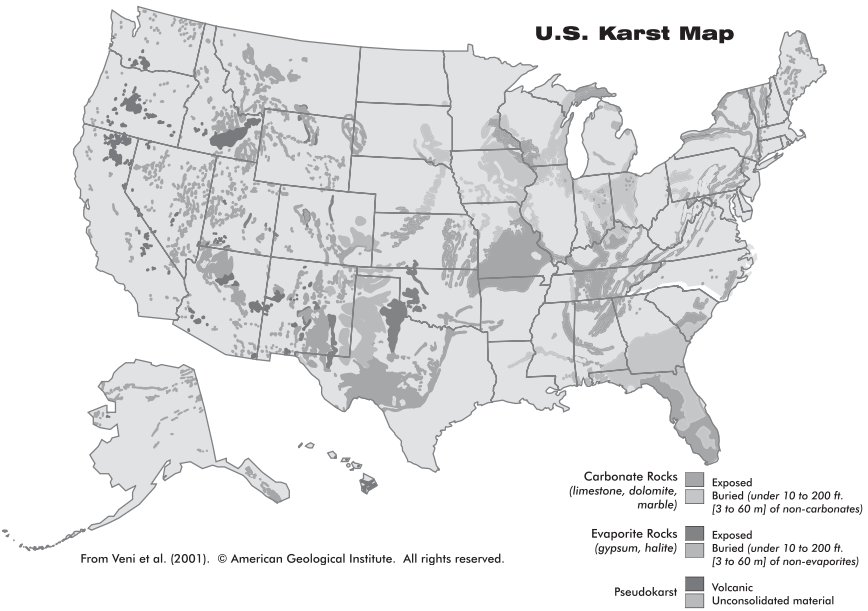

Figure 13.2 General representation of karst and pseudokarst areas in the United States. (*Used with permission, American Geological Institute*.)

Valley of the Appalachian Mountains, the Ozark Plateau of southern Missouri and northern Arkansas, the Pennyroyal Plain of western Kentucky, the Mitchell Plain of Indiana, the Edwards Plateau in southwestern Texas, the Nashville and Lexington Plains in Tennessee and Kentucky, the Black Hills of western South Dakota, and Florida. Karst areas are found in other countries some of which include Slovenia, Russia, the Southern and Western Alps of Italy, Grand Causses and Jura Mountains in France, Franconian Alps in Germany, the Padis Karstic Plateau in the Bihor Mountains of the western Carpathians in Rumania, the Carboniferous Limestone, Peak District, Yorkshire Dales, North Wales, Northern Pennies, and the Mendip Hills of Great Britain, Cockpit Plateaus of Jamaica, Lunan in Yunnan, China, the Nullarbor Plain in Australia, and the Bonito karst region in Midwestern Brazil (Figure 13.3).

Karst is the Germanized word for Kras. In Slovene language, Kras is a plateau region underlain by limestone, now a part of Slovenia and Croatia, along the northernmost part of the Adriatic Sea. The plateau stretches in a northwest-southeast orientation and is 25 mi long and up to 8 mi wide, covering about 170 mi^2 (Kranjc 1997). The earliest origin of the word Kras means "stony ground." The land was left stony and barren because deforestation and overgrazing led to the loss of most soil into sinkholes and caves (Gams 1994). It is not yet completely documented how the name Kras became the general term for land with

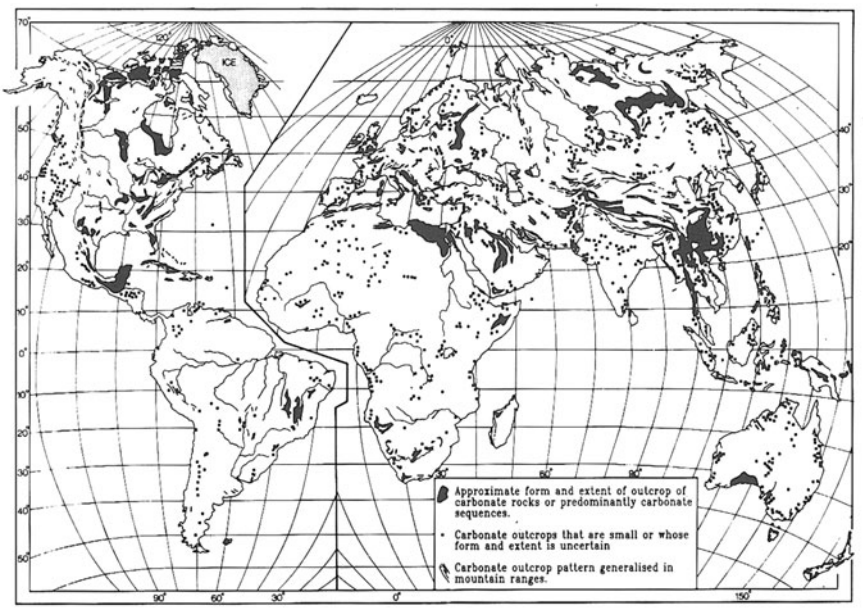

Figure 13.3 Global distribution of major outcrops of carbonate rocks. (*Used with permission of Springer Science and Business Media.*)

karstic characteristics and who was the first or the most important to make the transition (Kranjc 1998). In the 1800s, geologists and geographers entered the Slovene term "Kras" into the geologic and geographic literature. Jovan Cvijic's 1893 composition of Das Karstphaenomen is still considered a landmark investigation on the geomorphology (study of landforms) of karst areas. Some considered Cvijic to be the Father of karst geomorphology.

13.2 Karst Types

Not all karst landscapes look identical. The degree to which karst forms is dependent on several factors, some of which include climate type, the amount of rainfall, the depth of groundwater circulation, amount of soil cover, the structure of the rock and its solubility. Some karst areas are easily recognizable based on surface landforms while other areas may show no surface expression of karst development, but contain solution caves beneath the surface.

Covered and exposed karst

Geoscientists have distinguished karst landscapes from one another by the degree to which sediment covers the karst and by the karst feature that dominates the landscape. Quinlan (1967, 1978) developed a classification scheme for karst landscapes according to what covers the karst and placed them into two major types: covered karst and exposed karst. Covered karst represents areas where the soluble rock is covered by some material and not exposed at the surface. Five subcategories within this type include: subsoil karst, mantled karst, buried karst, interstratal karst, and subaqueous karst.

Subsoil karst occurs when the karst surface is covered with soil either transported or its own sediment (White 1988). A karst area that is covered by a thick deposit of unconsolidated sediments is known as mantled karst. Buried karst, also known as paleokarst, occurs when a karst surface is completely filled within sediments and buried with younger rocks. Interstratal karst refers to soluble rocks buried by less soluble rocks prior to karstification. Even though these rocks are not exposed at the surface, soluble rocks can still develop karst features if located within the groundwater-flow system. Subaqueous karst forms beneath bodies of water such as rivers and lakes, or within tidal zones.

Exposed karst refers to areas of soluble rock that are exposed at the surface. Four subcategories occur within this type and include: naked karst, denuded karst, exhumed karst and relict karst. Naked karst occurs primarily in alpine regions where soils are poorly developed (White 1988). Denuded karst occurs when an insoluble rock located above the soluble rock has been removed by erosion and the soluble rock is exposed

at the surface. Exhumed karst refers to karst that was once buried and later exposed by erosion. Relict karst is soluble rock that has been removed by erosion without any trace of topographic expression.

Cone and tower karst

The requirements for cone and tower karst (Figure 13.4) seem to be a thick massive limestone, high relief, and a well-developed fracture system (White 1988). Cone and tower karst, sometimes called tropical karst, develops in tropical regions where the greater amount of rainfall aids in the dissolution of the vertical fracture system. Cone and tower karst is found in Central America and the South Pacific (White 1988). The classic tower karst can consist of isolated or nested towers that are often relatively narrow with vertical sides while cone karst refers to more rounded or conical hills. The Yangshuo Region of Guangxi, China provides an excellent example of cone and tower karst.

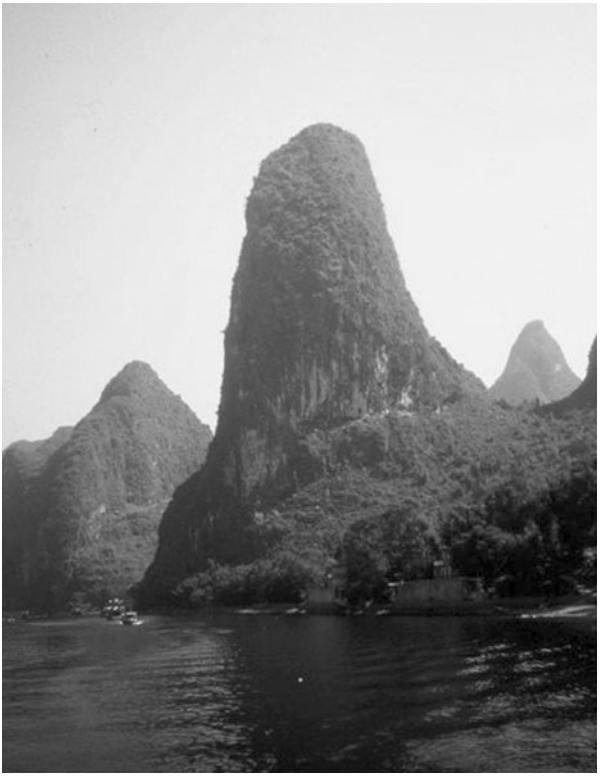

Figure 13.4 Cone and Tower Karst of China. (*Photo courtesy of Andrej Kranjc.*)

Cockpit karst

The type area for well-developed cockpit karst lies in Jamaica (Figure 13.5). Additionally known as polygonal karst, the depressions are a series of touching polygons. The topography of the cockpit karst resembles an egg carton consisting of large star-shaped closed depressions or sinkholes surrounded by cone-shaped hills. The cockpits are steep sided and surrounded by ridges and many cockpits are connected to each other (Day and Chenoweth 2004).

Pavement karst

Pavement karsts (Figure 13.6) occur in high latitude or alpine terrains were soils are thin or stripped (White 1988). Sometimes called bare karst, the lack of soils and vegetation exposes vertical or nearly vertical fractures in the rock and dissolution creates wide crevices in the rock known as kluftkarren. Sweeting (1973) preferred the term glaciokarst. A fine example of pavement karst is found in the Burren Plateau in Ireland.

Fluviokarst

A karst landscape that shows evidence of a past drainage system is called fluviokarst. Many karst features occur in fluvial karst such as swallow holes, sinkholes, blind valleys, and caves. Limestone surfaces in fluviokarstic areas tend to be more soil covered due to the presence of soil washing and debris caused by fluvial processes (Sweeting 1973).

Figure 13.5 Cockpit karst of Jamaica. (*Photo courtesy of Mick Day.*)

Figure 13.6 Limestone pavement, Pyrenees Mountains, Spain. (*Photo courtesy of John Mylroie.*)

Much of the karst in the eastern United States is fluviokarst; some of the best examples occur along the Cumberland Plateau in Tennessee and northern Alabama (White 1988). Other examples of fluviokarst are located in the Mendip Hills and the Peak District in Britain and the Causses of Quercy in central France.

Sinkhole karst

The dominant surface feature in this type of karst is the sinkhole. Bedrock underlying sinkhole karst is relatively flat. Examples of sinkhole karst can be found in northern Florida, south central Kentucky, and in southern Indiana (Figure 13.7).

Karst in the literature

The geology, hydrology, and geomorphology of karst landscapes have been studied for over 100 years and resulted in an extensive amount of literature including textbooks, encyclopedias, conference proceedings volumes, and original papers. Textbooks on karst written within the last 35 years include those by Herak and Stringfield (1972), Sweeting (1973), Jakucs (1977), Bogli (1980), Jennings (1985), Dreybrodt (1988), White (1988), Bosak, et al. (1989), Ford and Williams (1989), Drew and Hotzl (1999), Klimchouk et al. (2000), Waltham et al. (2005), Palmer (2007), Klimchouk (2007) and Milanovic (1981 and 2004). The Encyclopedia of Cave and Karst Science (Gunn 2004) and the Encyclopedia of Caves (Culver and White 2005) provide some of the most recent knowledge on

Figure 13.7 Sinkhole plain, Indiana, USA. (*Photo courtesy of Samuel S. Frushour.*)

karst landscapes. Ford and Williams (2007) is the second edition prepared by the authors that presents a systems oriented approach and integration of geomorphology and hydrology.

Probably the most recognized conferences held within the last 25 years on sinkholes and the engineering and environmental impacts of karst have been those sponsored by P.E. LaMoreaux and Associates, Inc. and recently by the Geo Institute of the American Society of Civil Engineers. Additionally, original karst research has been published by several mainstream professional journals some of which include the Journal of Hydrology, Groundwater, and Environmental Geology.

13.3 Carbonate Rocks

Carbonate rocks are those rocks that contain more than 50% by weight of the minerals calcite, aragonite, or dolomite. To be considered pure, carbonate rocks must have at least 90% of such minerals (Jennings 1985). A carbonate rock that predominantly contains the minerals calcite is called limestone. There are over 100 uses for carbonate rocks in industry; some of these include filler material for asphalt, fertilizer, cement, building stones, roadstone, and for the manufacture of glass and paper (Siegel 1967).

The color of a carbonate rock is due to such factors as the environment of deposition, variations in the size of grains within the rock, mineral content, and the amount of organic material. Carbonate sediments buried in shallow water in an environment with low amounts of oxygen

with organic material would likely produce a gray or black color. Sediments buried with traces of iron and exposed to the atmosphere and weathering are usually a buff or faded yellow or cream color. Carbonates formed in deeper water may be red, pink, or purple through preservation of iron and manganese oxide pigments (Wilson 1975).

Carbonate rocks commonly form in shallow marine areas known as carbonate platforms. Carbonate platforms are known to occur attached to landmasses such as south Florida and the south coast of the Persian Gulf (Blatt 1982), but also can occur in deep ocean basins, non-marine environments in lake depressions, and as isolated accumulations of carbonate producing organisms that rise from greater depths like the Pacific atolls. Currently, carbonate sediments are forming in shallow waters in the Bahama-Florida platform, Gulf of Batabanno off southern Cuba, Campeche Bank off Yucatan Peninsula, the continental shelf of British Honduras, the Trucial coast of the Persian Gulf, the coasts of Western Australia and Queensland (Bathurst 1975).

The Bahama Platform represents a well studied and excellent example of a modern isolated carbonate depositional area (Blatt 1982). The northwestern Bahama Islands consist of isolated masses that rise above sea level from two carbonate platforms, Little Bahama Bank and Great Bahama Bank (Onac et al. 2001). This platform consists of 20 major islands with a surface area of 434 mi (698 km) by 186 mi (299 km) (Tucker and Wright 1990). It is generally submerged to a depth of less than about 30 ft (9.1 m), the greater part of the seafloor being covered by less than about 21 ft (6.4 m) of water (Bathurst 1975). Drilling on the islands has encountered about 15,000 ft (4572 m) of shallow carbonate and associated rocks.

Much has been written about the origin and occurrence of carbonate depositional environments and rocks that comprise them. Some of these works include Chilingar et al. (1967), Lippman (1973), Bathurst (1975), Wilson (1975), Cook and Enos (1977), Boggs (1987, 2001), Tucker (1981), Blatt (1982), Blatt and Tracey (1999), Scholle et al. (1983), Tucker and Wright (1990), Braithwaite (2005), and Moore (2001).

Limestone

Limestone ($CaCO_3$) commonly forms in shallow marine environments within 30° of the equator. These rocks are composed of calcite grains along with visible or microscopic shells from marine organisms. To completely understand the formation of limestone one must have knowledge of the biochemical interactions between marine organisms and the waters in which they live (Blatt 1982).

Several classification schemes have been developed over the years to describe the differences in particles or grains that appear in limestones. The classification schemes developed by Robert Folk (1959, 1962) and

Robert Dunham (1962) are the most widely used by geologists that study carbonate sediments. Folk's scheme has been widely used, but Dunham's classification is recommended for practical use (Braithwaite 2005).

Folk classification

Folk (1959, 1962) developed a classification that was based on the size and shape of grains within the rock and the crystals that hold or cement the grains together. Folk defined these particles as allochems and orthochems (Figure 13.8). Allochems consist of the particles in the rock and are subdivided into four categories: fossils, peloids, ooids, and intraclasts. All four constituents listed above may be mixed in a wide range or proportions to form limestone beds (Folk 1962).

Intraclasts are fragments of existing limestone that were disturbed and redeposited within the area of deposition. Intraclasts may be of any shape or size. Ooids are small spherical grains coated with calcium carbonate that have formed around small shell fragments or quartz

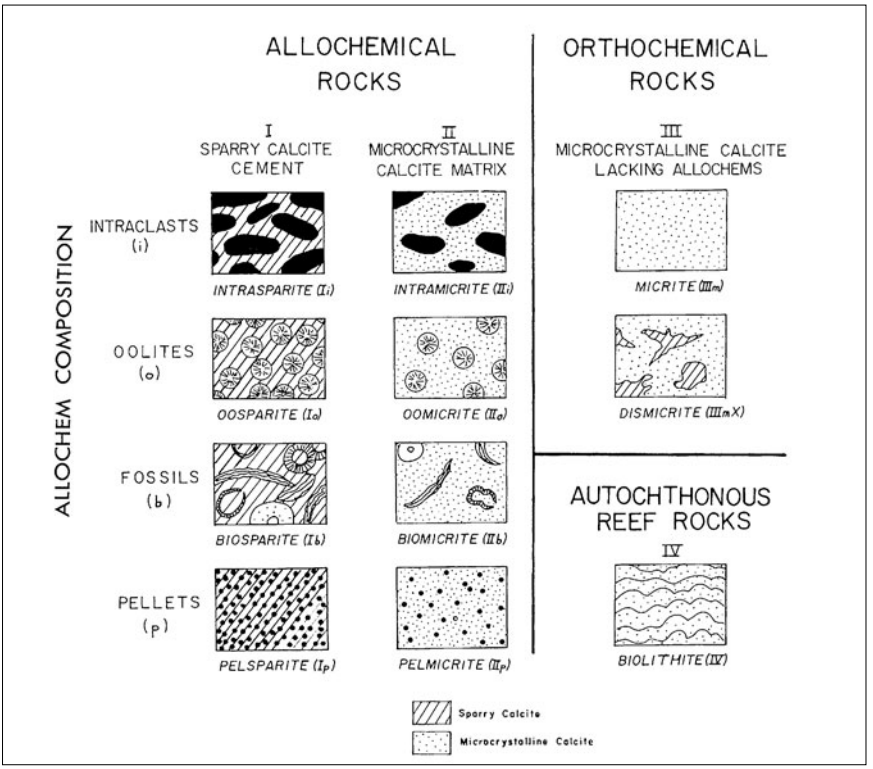

Figure 13.8 Folk classification for limestones. Folk 1962. (*Courtesy of the American Association of Petroleum Geologists.*)

grains. The carbonate coating is chemically precipitated from agitated water which is evident of being transported by strong currents (Blatt 1982) in high energy environments such as tidal channels. Larger ooids are called pisoids.

Pellets are muddy carbonate grains that have no apparent internal structure (Braithwaite 2005). They are thought to be of fecal origin excreted by marine organisms (Selley 2000) such as gastropods and worms. Some pellets harden over time while others weather and fall apart. Pellets are smaller than ooids and range in size from silt to fine sand and are characteristic of low energy environments such as lagoons.

Fossil skeletal particles, also known as bioclasts, consist of broken fragments of or whole marine organisms such as pelecypods, brachiopods, and ostracods. Skeletal particles are by far the most common allochem in carbonate rocks and are so abundant that in some limestones they make up the entire rock (Boggs 1987).

Orthochems are the smaller grains that holds or acts as a cement to hold the larger grains together. Microcrystalline calcite or micrite are smaller particles that are deposited at the same time as the allochems. Micrite is composed of very small carbonate crystals deposited under quiet water conditions. It can be present as matrix material among larger carbonate grains or it may make up most or all of the limestone (Boggs 1987). Carbonate sediments are accumulating in many modern environments from tidal flats and shallow lagoons to the deep sea floor. Spar or sparry calcite cement infiltrates the deposit of allochems after deposition and cements the allochems in place. Sparry calcite cement fills the pore spaces within the carbonate particles.

A limestone can exhibit various amounts of allochems and orthochems. To name the rock, Folk developed a prefix for each allochem and a suffix for each orthochem. Fossil was replaced by the prefix bio; pel replaced peloid; oo replaced ooid; intra replaced intraclast; mic replaced micrite; and spar replaced sparite. For example, a limestone composed of ooids within a micrite matrix is identified as an oomicrite.

Dunham classification scheme

The classification developed by Dunham was also based on the depositional texture of the rock with an additional subdivision based on the abundance of grains (Figure 13.9). Grains are carbonate particles found in the rock. The grains can be composed of skeletal particles or nonskeletal particles. A limestone with less than 10% of the rock composed of grains with a mud matrix are named mudstones, mudstones with greater than 10% grains but still with a mud matrix are wackstones. Grain supported muddy carbonate rocks are termed packstone. Those rocks that are mud free and grain supported are grainstones.

DEPOSITIONAL TEXTURE RECOGNIZABLE					DEPOSITIONAL TEXTURE NOT RECOGNIZABLE
Original Components Not Bound Together During Deposition				Original components were bound together during deposition... as shown by intergrown skeletal matter, lamination contrary to gravity, or sediment-floored cavities that are roofed over by organic or questionably organic matter and are too large to be interstices.	Crystalline Carbonate
Contains mud (particles of clay and fine silt size)			Lacks mud and is grain-supported		
Mud-supported		Grain-supported			(Subdivide according to classifications designed to bear on physical texture or diagenesis.)
Less than 10 percent grains	More than 10 percent grains				
Mudstone	Wackestone	Packstone	Grainstone	Boundstone	

Figure 13.9 Dunham classification for limestone. Dunham 1962. (*Courtesy of the American Association of Petroleum Geologists.*)

Dolomite

Dolomite $CaMg(CO_3)_2$ is a rock that is composed of greater than 50% of the mineral dolomite. Some researchers prefer to use the term dolostone to refer to the rock composed of dolomite. However, both terms have been used to identify the rock.

Dolomite has been known to be precipitated directly from water such as some lagoons and lake settings. However, this is a rare event in the geologic record. Predominantly, dolomite forms when existing limestone rocks are chemically altered after deposition by magnesium-rich water that infiltrates the rock. Reasons to suggest dolomite forms after deposition is that it has irregular boundaries within the rock strata and lacks even bedding (Selley 2000).

Dolomites form at low latitudes in shallow marine water just as limestones. Recent dolomite deposits are known to form in arid hypersaline coasts termed sabkha—Arabic for salt marsh. Dolomite crusts occur on tidal flats of Andros Island in the Bahamas, Sugarloaf Key, Florida, Bonaire Island of the Venezuela mainland, Netherland Antilles; in the high intertidal sediments of the Trucial Coast and within coastal evaporitic lakes of the Coorong, South Australia; in saline lakes of Victoria, Australia; and in hypersaline lagoons of Baffin Island, Texas and Kuwait (Tucker and Wright 1990).

Dolomite is rare in modern carbonate environments and more abundant in older rocks. Investigators have called this "the dolomite problem." Dolomite has been intensely studied throughout the century and remains one of the most thoroughly researched, but poorly understood problems in sedimentary geology (Boggs 2001; Arvidson and MacKenzie 1997). Although authors agree that the source of magnesium in the rock must come from seawater, the mechanism required to precipitate dolomite is still up for debate. This inability of scientists to agree on a single mechanism for dolomite formation has resulted in the development of several models of deposition and there are critics and supporters of each. All current models of dolomite formation are primarily physical descriptions of how to move seawater, or modified seawater, through calcium carbonate sediments (Burns et al. 2000).

13.4 Recharge Areas

The karst landscape and its subsurface are sculpted by flowing water. Over time, water slowly dissolves the rock away as it works its way through joints and bedding planes. Eventually, surface and groundwater flow function as one continuous unit. In a true karst landscape, no water exists on the surface, all water is circulating through fissures underground (Sweeting 1973). This section discusses the various types of features that commonly develop on karst landscapes.

Surface water that infiltrates the karst surface through openings in the bedrock is known as recharge. Several terms have been used in the karst literature to describe recharge water that enters the karst landscape. The four terms that are commonly used included allogenic, autogenic, diffuse and concentrated recharge. Allogenic recharge refers to surface water that flows from adjacent non-karst areas onto the karst landscape and sinks into the subsurface. Allogenic recharge enters the subsurface through concentrated areas of the bedrock that have been dissolved out or solutionally enlarged. This commonly occurs along stream segments and through the bottoms of sinkholes. Autogenic recharge is defined as infiltration supplied by precipitation that falls directly on the karst landscape and enters the subsurface through smaller openings in the bedrock, spread out over the entire area of karst landscape. Diffuse recharge refers to the water that enters the subsurface through small openings in the bedrock at less volume. Concentrated recharge enters the subsurface through larger openings and has greater flow volume. Concentrated recharge and diffuse recharge represent the maximum ends of a continuum and most karst landscapes exhibit both types of recharge.

Gunn (1985) developed a conceptual model for flow in karst aquifers and introduced four additional terms to describe recharge: diffuse autogenic, concentrated autogenic, diffuse allogenic, and concentrated allogenic. Diffuse autogenic recharge falls directly on the karst landscape and enters the subsurface through small openings in the bedrock. Concentrated autogenic recharge is recharge that falls on the karst landscape and flows toward closed depressions such as sinkholes. Diffuse allogenic recharge falls onto non-permeable rocks that overlie the karst. Concentrated allogenic recharge falls on non-karst lands and flows to the karst where it enters the subsurface through sinking streams not far from the non-karst/karst boundary.

Ewers (1992) conducted a study with data loggers to closely monitor the physical and chemical reactions of karst springs during storm events in Kentucky. Two additional terms were used to describe recharge. Quickflow recharge described relatively rapid movement of water into the subsurface and seepage recharge was used to identify the movement of water that flowed slower.

Recharge water can move into the subsurface at various speeds which is dependent on the size of the opening in the bedrock. Eight terms have been introduced in this section to describe water flow into the karst subsurface. More terms have been developed in the literature to describe the difference between slow and faster recharge into the karst subsurface. The beginner to karst investigations needs to be aware of the differences in these terms, use caution and not confuse terms. All terms can be appropriate depending on the objective of the study.

13.5 Surface Karst Features

Surface landforms come in a variety of sizes and shapes ranging from small dissolutional grooves on exposed rock surfaces, shallow to deep circular depressions to large isolated towers of rock that can be seen at great distances. In some areas, karst landforms are overly abundant at the surface and easily recognizable while in other areas they are not so easy to find.

Sinkholes

One of the most recognizable surface karst landforms is the sinkhole. Sinkholes are circular or enclosed depressions of various sizes. The Serbian word doline meaning a little dole or valley, is commonly used as the equivalent of sinkhole in karst areas (Stringfield et al. 1979), especially outside of North America. In some karst areas like the Mitchell Plain in Indiana and Pennyroyal Plain in Kentucky, sinkholes are very obvious with the use of aerial photography and topographic maps and from viewpoints on the surface that are much higher in elevation that surround the valley. Sinkholes can be broad, shallow, and barely noticeable to tens or hundreds of feet in diameter. Depths of sinkholes can range from a few feet to several hundreds of feet.

Sinkholes have been classified into different types several times in the literature (Sweeting 1973; Bogli 1980; Jennings 1985; Beck and Sinclair 1986; White 1988; Ford and Williams 1989; Lowe and Waltham 2002; Williams 2004; Waltham et al. 2005). Beck (2005) provides a process oriented definition of a sinkhole: Sinkholes are the surface and near surface expressions of the internal drainage and erosion process in karst terrane, usually characterized by depressions in the land surface. Beck (2005) classifies sinkholes into five types which include: solution sinkholes, cover-collapse sinkholes, bedrock or cave collapse sinkholes, cover-subsidence sinkholes, and buried sinkholes. These five sinkhole types are the result of two different processes: the transport of surface material downward along solutionally enlarged channels, or collapse of the rock roof over large bedrock cavities (Beck 2005) and dissolution of the

limestone is most rapid at the surface. The complexity of natural processes often results in more than one mechanism being involved in the formation of sinkholes such that they can be considered as having a poly-genetic origin (Williams 2004).

Solution sinkholes develop when the rock is exposed at the surface or very close to the surface. Water drains downhill and enters the rock where the water can easily enter the subsurface and begins to enlarge vertical pathways. Over time, soil slowly drains into the enlarged openings in the underlying limestone bedrock. Eventually, these sinkholes provide a direct connection to the underlying groundwater-flow system. A number of these sinkholes may in time coalesce, or join, by lateral enlargement and form into a uvala (Stringfield et al. 1979).

Cover-subsidence sinkholes (Figure 13.10) develop in areas where unconsolidated material such as alluvium, glacial moraine, or sand overly the karst bedrock (Williams 2004) and is called a mantled karst (Beck 2005). Soils slowly wash down through the vertical drain within the limestone. Soil piping is the term used to describe the slow upward erosion of soils within the sinkhole. European investigators split subsidence sinkholes into two types based on the amount of time it takes for the sinkhole to form and includes suffusion and dropout sinkholes. Suffusion sinkholes form from subsidence that occurs over a period of months or years while dropout sinkholes are the result from an instantaneous failure (Waltham et al. 2005).

Figure 13.10 Sinkholes on Greenbrier County, West Virginia. (*Photo courtesy of John Mylroie.*)

Buried sinkholes are sinkholes that have been filled in over time by natural processes and are no longer visible at the surface. Although no longer visible at the surface, it still functions as a drain for water to enter the groundwater-flow system (Beck 2005).

Cover-collapse sinkholes cause the most amount of damage whether they occur in residential or urbanized areas (Figure 13.11). Cover-collapse sinkholes can develop in a relatively short period of time and are typically the result of the collapse of an underlying soil arch above the limestone drain or the collapse of an underlying cavity roof within the bedrock. A cover-collapse sinkhole is a subtype of subsidence sinkholes.

Cenotes (a Spanish word meaning well) (Figure 13.12) are collapse sinkholes that form from the collapse of flooded underlying caves especially found in the Yucatan. Blue holes are similar collapse features that form on the carbonate islands in the Bahamas and represent steep vertical openings in the carbonate rock. The largest and best known blue holes are found on North Andros, South Andros, and Grand Bahama Islands in the northwestern Bahamas (Mylroie 2004). Blue holes (Figure 13.13) are subsurface voids that are developed in carbonate banks and islands; are open to the earth's surface; contain tidally influenced waters of fresh, marine, or mixed chemistry; and extend below sea level for a majority of their depth (Mylroie et al. 1995). Blue holes differ from cenotes in that the cave water the blue holes are connected to is tidally influenced groundwater and creates strong current within the caves.

Figure 13.11 Collapse sinkhole, Trigg County, Kentucky. (*Photo courtesy of John Mylroie.*)

Figure 13.12 Cenote taken near Mayan ruins in Yucatan Mexico. (*Photo courtesy of John Mylroie*.)

Figure 13.13 Dean's Blue Hole on Long Island, Bahamas, the world's deepest blue hole at over 200 m deep. (*Photo courtesy of John Mylroie*.)

Bedrock or cave collapse sinkholes occur in rocks that overly cavities in limestone. The roof of a cave continuously or suddenly collapses and extends upward into the overlying non-karst rock until ground failure eventually occurs at the surface to develop a sinkhole. An example of this type of sinkhole is found in the Namurian Sandstone in South Wales where the overlying conglomeritic sandstone has collapsed into the underlying limestone caves (Williams 2004).

Sinking streams

Stream valleys underlain by less permeable non-karst rocks like shale maintain their flow across the landscape. In karst areas, this is not always the case and internal drainage dominates. In places, usually at or near the contact of the karst and non-karst rocks, all the water is lost or sinks through the streambed or along the stream bank into the subsurface through dissolved openings in the underlying limestone and are called sinking, losing, or disappearing streams. Large volumes of concentrated recharge from losing and sinking rivers are central to the evolution of most of the world's largest and most significant caves and springs in karst (Ray 2005).

Swallow holes, additionally known as swallets and ponors, represent the openings in the bedrock where the surface water enters the subsurface in large volume which vary in shape and size. Some swallow holes are pits and open cave entrances (White 1988). Downstream from the swallow hole, the stream bed is mostly dry and this segment of the stream is typically known as a lost stream, disappearing stream, or sinking stream. Eventually, these waters reappear at the surface further downstream at springs or a series of springs. One example is the Lost River in Hardy County, West Virginia, USA (Figures 13.14a and 13.14b).

The Lost River loses surface water continuously to the groundwater-flow system at a portion in the river known as the "sinks." In this stretch, the river is underlain by the limestone of the Helderberg Formation. During the dry season, river flow decreases and the entire discharge of the river sinks underground and reappears at a series of springs on the bank 2 mi (3.2 km) downstream. Throughout the summer, the Lost River stream channel is dry except for some springs that drain the surrounding ridges. However, as precipitation increases later in the year, the groundwater-flow system can no longer handle the entire discharge of the river and flow continues downstream. Sinking streams represent one mode of recharge to the underlying karst aquifers.

Karst valleys

Three distinctive types of valleys can occur in karst: dry valleys, blind valleys, and poljes. In dry valleys, the entire discharge from the river basin

Figure 13.14a Lost River, Hardy County, West Virginia photographed during high flow conditions.

Figure 13.14b Lost River, Hardy County, West Virginia photographed during low flow conditions.

is lost to the subsurface. Overland flow will only occur during major flood events. A blind valley occurs when water is able to flow across the karst for some distance and then terminates into a cliff of soluble rock. The River Rak entering Tkalca Cave in Slovenia represents a good example.

Poljes are another form of a karst valley (Figure 13.15). Meaning "field" in Slovene, poljes are large closed depressions with a well-developed underground drainage system bounded by steep-sided uplands. The best occurrence of poljes is in the Adriatic karst. Runoff from the surrounding uplands discharges at springs in the polje to form alluvial streams. These streams sink into caves or swallow holes on the opposite side during periods of low to moderate flow and discharge from them when the groundwater system is at full capacity during periods of high flow.

Karren

Karren refers to the variety of small to larger scale grooves, pits, or channels carved into the rock through controlled flowing water on the karst rock. The name karren was originally used to describe solution channels or runnels cut into limestone, but it is used for the whole complex of microforms that occur on outcrops of karst limestones (Sweeting 1973). Karren develops best in massive, thick bedded pure limestone (White 1988). Factors that affect the formation of karren include amount of precipitation, slope of the bedrock, nature of the bedding, texture of the rock, and the presence or lack of vegetative cover. Sweeting (1973),

Figure 13.15 Cerknisko polje seen from Mt. Slivica in Slovenia. (*Photo courtesy of Martin Knez.*)

White (1988), and Ford and Williams (1989) provide lengthy discussions on the variety of karren types.

Rillenkarren is the smallest karren type and forms on steep to nearly vertical slopes and consists of small, rounded troughs with sharp ridges produced by direct rainfall and was the first type of karren to be described in the Alps and Dianaric Karst (Sweeting 1973). Rinnenkarren is similar to rillenkarren but at a larger scale. They are found on limestone surfaces of all slopes and on bare as well as soil covered surfaces (White 1988). The crests between the troughs on rinnekarren are sharp and the troughs are generally rounded and can contain pits and scallops. When the crests are peaked they are called spitzkarren (Sweeting 1973). On shallower slopes the solution channels take on the appearance of a meandering river channel and are called meanderkarren.

Kluftkarren develops along near vertical-to-vertical joints in the exposed bedrock surface and represents one of the largest forms of karren in karst. Through time the rock dissolves away and the solution channel widened joints can become wider and deeper depending on the structure of the rock. As water flows down the vertical joint it can come into contact with a horizontal bedding plane in the rock at depth. The water can then flow along the fracture and dissolve the rock adjacent to the bedding plane. Examples of kluftkarren are found in the limestone areas in Counties Clare and Galway in Ireland (Sweeting 1973). Trittkarren, also known as stepped karren, forms on near flat surfaces and takes on the appearance of heel prints. As water flows down the rock in repeated waves, a stepped surface is formed. Once started, the steps stabilize and enlarge into a step-like form with a nearly flat tread and a nearly vertical riser (White 1988).

Epikarst

The epikarst can be generally defined as the uppermost portion of the weathered bedrock surface or the interface between the soil and bedrock in karst landscapes and is typically about 30 ft (9.1 m) deep (Williams 2003) (Figure 13.16). Mangin (1975) and Williams (1972, 1983) are commonly referred to in the literature as calling attention to this area of the karst bedrock. Mangin referred to the karst zone near the surface as the epikarst while Williams called it the subcutaneous zone (Williams 2004). The development of the epikarst is controlled by several factors which include the structure of the bedrock, lithology, climate, time since the last glaciation, solubility of the rock, vegetal cover, and depth of groundwater circulation (Aley 1997). As a result, the nature of the epikarst is highly variable with location (Williams 2003).

The top portion of the epikarst is dominated by vertical infiltration of water from the karst surface. With depth, the vertical movement of

Figure 13.16 An epikarst exposure of the Boone formation in northcentral Arkansas along U.S. 65. (*Photo courtesy of Debbie Burris Bednar*.)

water decreases as openings in the rock gets narrow and becomes less abundant. The path of water begins to move laterally, then becomes increasingly concentrated to form shafts (Klimchouk 1996). A limited number of vertical drains cause a backup in the flow of water through the groundwater-flow system and cause the water to be stored there temporarily. Results from hydrochemical and isotopic studies from various regions demonstrate that such a delay can last from several days to a few months (Gunn 1983; Williams 1983). However, as the number of vertical shafts and their ability to transmit water increases with time, the ability of the epikarst to retain water diminishes despite an increasing porosity of the epikarstic zone (Klimchouk 2000).

Aley (1997) recognized three types of epikarstic zones in unconfined carbonate aquifers based on results from about 30,000 quantitative dye analysis samples and about 1,000 positive groundwater traces. These include: rapidly draining, seasonally saturated, and perennially saturated epikarsts. These epikarst types were categorized based on the capacity of the epikarst to retain water.

Rapidly draining epikarsts typically develop in areas of high topographic relief in bedrock with high solubility, negligible sediment infiltration, little water storage, and are saturated with water for short periods of time, especially after storm events. Seasonally saturated epikarsts develop in areas of moderate relief where the solubility of the bedrock has resulted in the development of soil and residuum thickness at elevations greater than local perennial streams. Water is typically

stored seasonally and after major storm events lasting periods of weeks to months. Perennially saturated epikarsts occur in areas of low to moderate relief along perennial streams and are mostly saturated with water.

In 2003, the Karst Waters Institute sponsored a symposium about the epikarst that was attended by hydrologists, biologists, and geoscientists. The purpose of this interdisciplinary group of professionals was to gain a better understanding of the physical, chemical, and biological processes of the epikarst and to compose a better definition. As the conference proceeded, it was apparent that the epikarst was difficult to characterize and its properties remain unpredictable (Jones et al. 2004).

Karst springs

The location where groundwater appears at the surface is called a spring. Karst springs are some of the largest springs in the world and provide substantial quantities of water for human consumption and commercial enterprises (Figure 13.17). Big springs rather than small

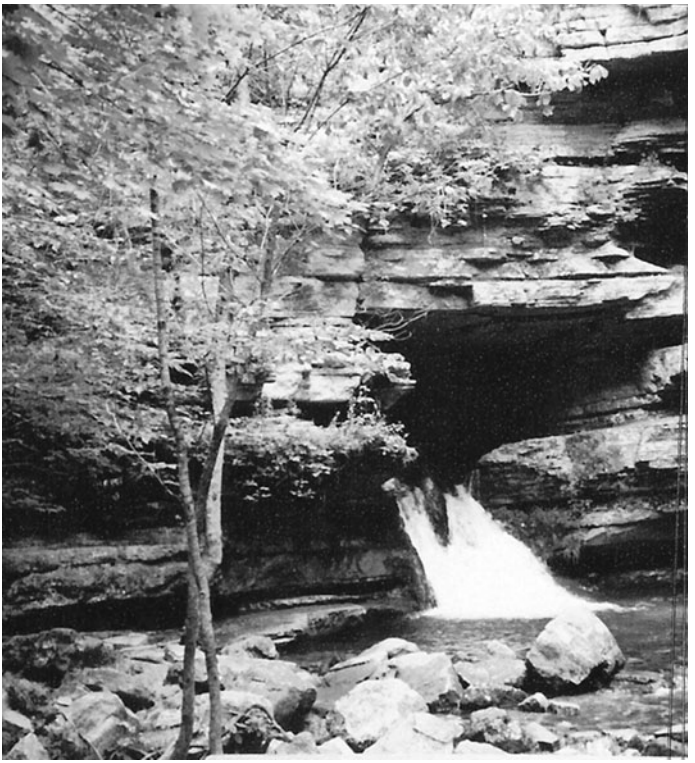

Figure 13.17 Blanchard Springs located at Blanchard Springs Caverns in Arkansas.

springs are the general rule in mature karst regions (LeGrand 1983). The largest reported karst springs are located in Papua New Guinea where several large rivers flow directly from caves (White 2005). Figeh Spring, in Syria, which is the 3rd largest spring in the world, on average discharges 63,200 gal/min (3,990 L/s) and supplies the entire city of Damascus with water (Veni et al. 2001). Several spring types have been recognized by geologists and the name given for the spring is dependent on where the spring appears at the surface, and the characteristics of the flow rate and chemistry of the water. The following paragraphs provide a few examples of studies conducted to learn more about karst springs and the general conclusions about them.

White (2005) recognized two broad types of karst springs: conduit flow springs and diffuse flow springs which were named after the work done by Shuster and White (1971) from a study of 14 springs that discharged from the Ordovician dolomites and limestones in central Pennsylvania. They suggested that flow type within the aquifer controlled the chemical character of the springs and used the statistical variation in water hardness (the amount of dissolved carbonate in the water) to distinguish between the two types. The first group of springs that discharged from the fractured dolomites had a constant hardness with a variation of less than 5%, displayed a nearly constant chemical character regardless of season or storm event and were recharged by diffuse recharge and White called them diffuse flow springs. Diffuse flow springs discharge from many fractures and areas of high permeability and are considered to be non-flashy and groundwater flow moves slower and can take months to travel short distances.

The second group of springs discharged from karstic limestones with concentrated recharge water from sinkholes. Hardness was found to be very variable throughout the year with a variation of greater than 10% and these are called conduit flow springs. Jacobson and Langmuir (1974) produced similar results regarding chemical variation at carbonate springs. Springs that discharge from conduits are known to be flashy based on the high ratios between maximum discharge and base flow discharge. Base flow is the lowest discharge from the spring. Flow is turbulent while water hardness is low but highly variable. The variation in hardness ranges from 10 to 25% or more (Quinlan, 1989; Quinlan and Ewers, 1985). Groundwater flow velocities are commonly rapid and can travel up to a mile per day (1.6 km/day).

The use of statistical variations in water hardness to distinguish between spring flow types appeared to work well for the study conducted by White for small drainage basins in temperate climates. However, larger drainage basins showed less variation when springs are fed by conduits (White 1988). Subsequent studies found that the binary classification developed by Shuster and White (1971) was not applicable for all karst settings.

Aley (1978) applied different terms for spring types in Missouri. He used the terms high transit springs and high storage springs. High transit springs derive water from areas of discrete recharge and are similar to conduit flow springs. High storage springs are similar to diffuse flow springs where water is derived from areas of diffuse recharge.

Scanlon and Thrailkill (1987) conducted a study in the relatively flat lying limestones and shales of the Inner Bluegrass karst region of central Kentucky. The physical and chemical characteristics of springs from the Inner Bluegrass were compared with those from the study conducted by Shuster and White (1971). Results from their study showed that seasonal water chemistry variation in major springs did not correspond with the physical characteristics of the springs over time. Chemical similarities were attributed to the mode of recharge. Bedrock type and structure between the two studies were considered to be controlling factors regarding the relationships between physical and chemical attributes of the springs.

Worthington et al. (1992) performed a statistical analysis using data from 39 springs in six countries with temperate climates taken from the literature. Results from their study demonstrated no evidence that hardness variation was an indicator of flow conditions within an aquifer as suggested by Shuster and White (1971) and that greater than 75% of hardness variation was explained by recharge type.

Smart and Worthington (2004) stress that recharge and the conduit network within the karst aquifer result in the water quality and quantity variations we experience at karst springs and named two broad spring types. Resurgences are springs that have variable flow rates, high variations in water quality, and receive most of their flow from allogenic recharge. Springs that receive most of their discharge from autogenic recharge are called exsurgences and show less variability in water chemistry and flow rate.

13.6 Caves

A cave can be defined as a natural opening formed in the rocks below the surface of the ground large enough for a human to enter (Field 1999). The scientific study of caves is known as speleology, derived from the Greek word spelaion, meaning cave, and logos, meaning study. The study of caves to determine how and why they originate and develop is known as speleogenesis. Of the several different types of natural caves that have been identified, those that form in soluble rocks are known as solution caves. Solution caves exist in the vadose zone (above the water table) and the phreatic zone (below the water table) and several theories on cave formation have been proposed to explain how they develop.

The most cavernous states in the United States, ranked by the number of known caves, are in Tennessee, Missouri, Virginia, Alabama, Kentucky, West Virginia, Arkansas, and Indiana (Palmer 2005). Gulden (2006) provides a list of the longest and deepest caves in the United States and the World and the longest and deepest caves in Canada. Krubera (Voronja) Cave is the deepest cave in the world. It is located in the alpine glaciokarst of the Arabika limestone Massif in the Western Caucasus Mountains in Abkhazia, a republic within Georgia with a depth of 7021 ft (2140 m). An open shaft was first documented by Georgian researchers in the early 1960s who named it after Alexander Kruber, a founder of karst science in Russia (Klimchouk 2005).

Mammoth cave is the longest cave in the world and is located about 100 mi (160 km) south of Louisville, Kentucky near Park City and Cave City, Kentucky. All passages combined total about 367 mi (591 km). Most of the cave lies within Mammoth Cave National Park and is developed within Mississippian limestone rocks in an area known as the central Kentucky karst (Brucker 2005). Mammoth Cave is a great tourist attraction and scientists have used the cave for many decades to understand how caves are formed. The cave formed within the Girkin Formation, St. Genevieve Limestone, and the Upper St. Louis Formation. The Girkin Formation is primarily composed of limestone; the St. Genevieve of limestone and dolomite with chert beds, and the St. Louis Formation with limestone, dolomite, chert, and gypsum. The stratigraphy and structure of the bedrock have influenced the regional groundwater flow patterns while bedding planes appear to have greater influence on passage orientation than do variations in rock type (Deike 1989).

The deepest limestone cave in the Unites States and fifth longest in the world is Lechuguilla Cave. Lechuguilla Cave is located within the Guadalupe Mountains in Carlsbad Caverns National Park in southeastern New Mexico. Lechuguilla Cave represents one of the world's best documented examples of a cave formed by the dissolution of carbonate rocks by sulfuric acid and is being used for important studies in geology, cave microbiology, microclimatology, geomicrobiology, and geochemistry (Kambesis 2005). Over 300 caves have been documented in the Guadalupe Mountains, the most widely known of these caves are Carlsbad Caverns and Lechuguilla Cave.

The origin of the sulfuric acid that dissolved the carbonate rock that formed Lechuguilla Cave was hydrogen sulfide gas. Evidence to support the generation and migration of gas is from water analysis of oil wells within the nearby Delaware Basin. The hydrogen sulfide ascended through the rock strata into the overlying carbonate rocks of the Guadalupe Mountains. Hydrogen sulfide mixed with the descending groundwater at the water table to form sulfuric acid which dissolved the carbonate rocks. Other evidence to support dissolution by sulfuric acid

is the presence of gypsum blocks and native sulfur not commonly found in caves developed by carbonic acid dissolution and isotopic evidence from cave deposits similar to that of petroleum reservoirs.

Twentieth century theories on cave formation

European and American geoscientists have studied caves for over 100 years. By 1900, caves were thought to have formed in the vadose zone, shallow phreatic zone, or the deep phreatic zone. European geomorphologists were concerned with active drainage systems and saw caves only as conduits through which the water moved while most American geomorphologists studied dry caves (White 1988). Americans focused on whether caves formed above or below the water table. A summary of some of the theories and models proposed on the formation of caves in the twentieth century will be presented by the author in a forthcoming beginners guide to karst.

The Ford and Ewers model forms the common ground of most current international speleogenetic thinking (Lowe 2004a). Although no model is perfect, the Ford and Ewers model was the first model to provide an explanation that caves could form above, at, and below the water table. In 1978, their paper, *The Development of Limestone Cave Systems in the Dimensions of Length and Depth*, presented a model of speleogenesis derived from detailed field studies in southwest England, the Rocky and Mackenzie Mountains of Canada, and other general observations elsewhere.

Controlling factors in cave formation

Several factors influence or control the development of cave passageways. These controls include the interaction of chemically aggressive groundwater within the openings in the bedrock, the structure of the bedrock, and the elevation or base level of nearby rivers. Within individual caves, the fundamental passage pattern is controlled mainly by the nature of the groundwater recharge to the karst aquifer (Palmer 2000). Early in the dissolution process, recharge enters the subsurface through many flow paths in the rock and the widest openings in the rock throughout their lengths are the ones that enlarge into caves (Palmer, 1987). Cave development by diffuse recharge generally takes longer due to the large surface area which takes the water a longer time to dissolve the rock. However, over time, the water manages to find the best route through the rock and dissolve larger openings with depth which increases the water's ability to dissolve the rock.

Concentrated recharge is the most effective recharge type to develop large conduits in the subsurface. At least 60% of all caves of explorable size are fed by small point sources (sinkholes) or concentrated recharge (Palmer 2000). Through time, conduits grow larger where the rock is at

or close to the surface and sinkholes will develop to provide a direct connection to the subsurface. As additional sinkholes form in the recharge area, more water is added to the groundwater-flow system to increase the cave development process.

The structure of the bedrock has an influence on passage development. In bedded strata, groundwater in the vadose zone follows pathways in the most down gradient direction by following the openings in the rock along vertical joints and along the horizontal bedding plane partings. Once the groundwater reaches the water table or phreatic zone, the groundwater will generally follow the strike of the geologic formation and form a tubular passage. Regardless of the inclination or dip of the rock, the vadose dip orientation and phreatic strike orientation are most probable in well-bedded rocks regardless of dip (Palmer 2000). Additionally, Palmer (1987) recognized that beds resistant to dissolution, such as shale of chert, can control cave development by perching or confining groundwater flow.

The elevation or base level of nearby rivers exerts an influence on cave development. The longer the base level remains static, the longer caves have the opportunity to become more developed. As base level falls, cave passages that were saturated will soon become abandoned and dry as the water moves to the lower base level.

Cave passageways

Cave passageways reflect the local hydrogeologic setting (Palmer 1991). Palmer and Audra (2004) identified several distinctive cave patterns: branchwork, anastomotic mazes, network mazes, spongework mazes, and ramiform patterns (Figure 13.18). Branchwork caves are similar to dendritic surface water drainage. Concentrated recharge from sinkholes contribute water to form these cave passageways. Early in cave formation, passages are isolated and not hydraulically connected. However, over time, these passages are forced to converge due to the intersection of structural features in the bedrock. Several cave passageway geometries are encountered in branchwork caves. Passages influenced by bedding plane partings are sinuous and curvilinear (Palmer 1991). Single conduit caves can exhibit linear, angulate or sinuous passageways. Linear passages are straight without any bends. Angulate passages have sharp bends and straight segments. Sinuous passages meander like surface streams. Examples of branchwork caves include Mammoth Cave and the caves in the Mendip Hills of England (Palmer and Audra 2004).

Palmer (1975) performed an exhaustive study of maze caves and identified two types. Network maze caves can form where permeable insoluble rock such as sandstone overlies limestone. The network pattern arises when all joints, regardless of their original permeability are dissolved at a uniform rate, so that all possible mechanical openings enlarge into

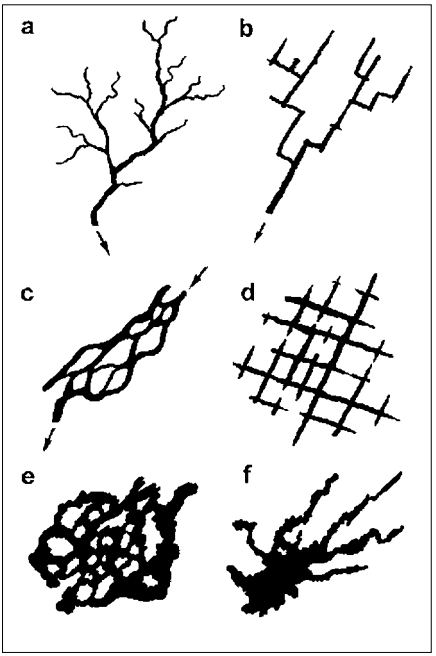

Figure 13.18 Types of cave passageways. (*Used with permission from Arthur N. Palmer.*)

the cave (White 1988). Clifty Cave in Indiana and Anvil Cave in Alabama are examples of this type of cave.

Anastomotic maze passages look like a braided stream on the surface. Spongework passages are random, interconnected passageways that vary in size and consist of a three-dimensional pattern. Parts of Carlsbad Caverns exhibit a spongework maze. Ramiform caves resemble ink plots in plan view and passageways grade from spongework to network caves (Palmer 1991). An example of a ramiform cave is Carlsbad Caverns.

Sometimes a cave will exhibit several layers or tiers of nearly horizontal cave passageways. Tiered caves are developed as the regional groundwater table lowers over time. As the water level in adjacent streams erodes to lower elevations, the water flowing through the cave will seek that same elevation and eventually abandon the higher level cave. The Mammoth Cave-Flint Ridge Cave System is an exceptionally large and complex tiered cave (White 1988).

Speleothems

Speleothems represent secondary mineral deposits that form along the roof, walls, and floors of caves as carbon dioxide rich waters enter the cave atmosphere. The cave environment has influenced the mineral's deposition (Hill and Forti 1997). Over 200 caves minerals have been

documented. Calcite is the most important and, together with aragonite, constitutes perhaps 95% of all cave minerals (Gillieson 1996). Speleothems are rarely composed of dolomite. Hill and Forti (1997) provided a comprehensive book on the cave minerals of the world and recognize thirty eight types, subtypes, and varieties of speleothems.

Stalactites and stalagmites are the most known types of speleothems. Stalactites grow as water drips from the cave ceiling. They commonly develop in lines along joints or bedding planes through which the water percolates (Jennings 1985). Calcite crystals deposit around the circumference of the water drop to form a hollow ring of calcite. Through time, successive rings of calcite are deposited. Usually young stalagmites are called soda straws. Drops of water that reach the floor of the cave accumulate and form calcite crystals. These crystal deposits grow vertically and are called stalagmites. A column is formed when a stalactite and stalagmite meet and form a single vertical speleothem. Figure 13.19 shows an example of a stalactite, stalagmite, and a column formed in Mystic Caverns in central Arkansas.

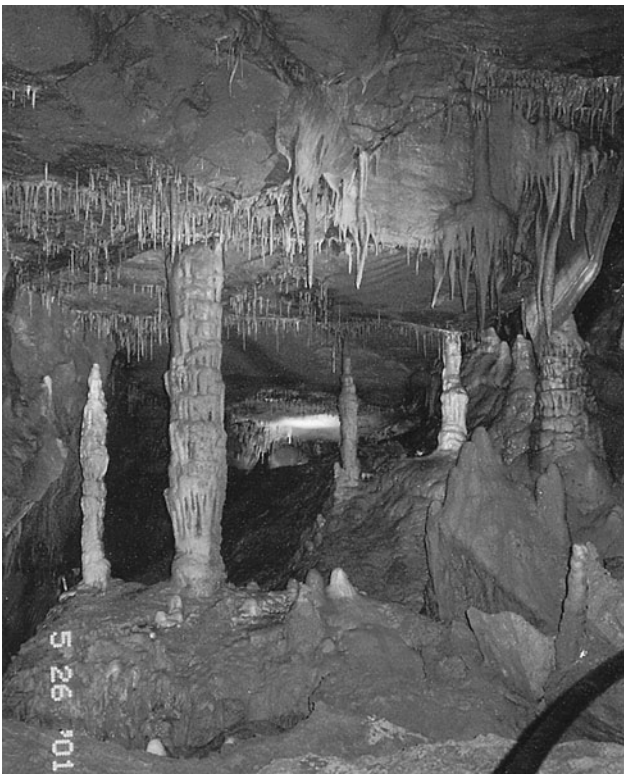

Figure 13.19 Speleothems at Mystic Caverns in central Arkansas.

13.7 The Karst Aquifer

During the last 40 years, several researchers proposed generalized conceptual models of groundwater flow through karst aquifers. Investigative methods primarily used to collect data to support models included results from groundwater dye tracing studies, spring hydrograph and chemograph analysis on karst springs, water budgets, cave mapping, and quantitative mathematical analysis. As more data became available from research conducted throughout the world, conceptual models were revised and improved. The following paragraphs provide summaries of some of the studies and critical thinking conducted over the years to develop a better understanding of how groundwater flows through karst aquifers. The models proposed by various authors to characterize karst aquifers are based on their own interpretation and have been collectively used to further the knowledge of groundwater flow through karst.

Because the entire groundwater-flow system cannot be observed physically, emphasis is placed on understanding the differences in the water as it enters and exits the subsurface. Chemical and flow characteristics of recharge water and spring water are examined in detail. The storage characteristics or volume of water within the karst aquifer is of importance. Water that moves quickly through the aquifer by large passageways, called conduits, are considered to have low storage while water that moves slower through small openings expressed a higher storage capacity or volume. Conduits are a feature of karst aquifers that makes them distinctive from other aquifers because they act as networks of pipes carrying water rapidly through the aquifer (White 2005).

White (1969) developed conceptual models for flow in carbonate aquifers. His models were based on hydrogeology and included diffuse flow aquifers, free flow aquifers, and confined flow aquifers; each flow type included subtypes. Diffuse flow and conduit flow represented end members along a flow continuum and most carbonate aquifers contain characteristics of both while being more toward the conduit flow type. Diffuse flow exhibits laminar to slightly turbulent flow through a system of widened joints or bedding planes that are being dissolved very slowly. Diffuse flow was thought to commonly occur in less mature or developed karst areas.

Conduit flow refers to water that enters the groundwater system and is transported quicker through a network of interconnected passageways or conduits to discharge at big springs or spring systems. Conduit flow is more turbulent in larger passageways where velocity is greater. Pollutants can travel rapidly and can have catastrophic effects on water quality more than 10 mi away (16 km) in just a week during base flow (Vandike 1982) and even sooner during flood flow. White (1977) revised his conceptual model from 1969 to consider what effect relief, geologic structure, and the aerial extent of the aquifer had on its development.

LeGrand and Stringfield (1971) recognized three types of karst aquifers based on the uneven distribution of permeability. Fine-textured karst aquifers were defined by closely spaced openings in the bedrock and were of young geologic age. Coarse textured karst aquifers were characterized by larger openings spaced farther apart in the bedrock as displayed in areas of mature karst. Reactivated karst aquifers are the oldest of the three aquifers that have undergone submergence by an advancing sea and buried by younger sediments.

Atkinson and Drew (1974) performed a 7-year detailed hydrological study using water budgets and measurements from several limestone springs in the Mendip Hills of England to determine the nature of a limestone aquifer. Results indicated that conduits provide a direct connect from swallets to springs and that recharge to underlying conduits from swallets accounted for less than 30% of discharge to springs. Recharge from percolation water accounted for greater than 70% of the discharge to springs and that percolation water ultimately reaches water-filled conduits. Atkinson (1977) studied the Cheddar Spring catchment area within the carboniferous limestone of the Mendip Hills in Great Britain. His study was conducted to determine the proportions of conduit flow and diffuse flow within an aquifer. Atkinson used the terms quick flow for conduit flow and base flow for diffuse flow. Quick flow includes water derived from sinking streams and percolation water while base flow obtains water from slow percolation from groundwater leakage and areas not drained by closed depressions. Results from the study indicated that limestone aquifers are a two-component system where the majority of water in storage comes from narrow fissures (base flow) while most of the water is transported through the solutionally enlarged conduits (Atkinson 1977).

Gunn (1983) recognized that closed depressions were an important source of concentrated recharge to limestone aquifers dominated by conduit flow. He proposed a six component depression hydrology model within the polygonal karst of the Oligocene Te Kuiti Group limestones in New Zealand. Storage was derived from the overlying soil and surface deposits, the epikarst, phreatic conduits, and the saturated rock mass. Additionally, Gunn's model provided for ten types of distinctive flow regimes to the aquifer that consisted of overland flow, infiltration, throughflow, percolation, epikarstic flow, shaft flow, vadose flow, vadose seepage, diffuse flow, and conduit flow. Gunn believed that storage in the soil and epikarst zone and autogenic concentrated recharge was not sufficiently recognized while diffuse flow and storage in the bulk rock mass was overemphasized.

Worthington (1991) conducted a study of the karst springs at Crowsnest Pass in the Canadian Rocky Mountains. His analysis of the discharge and hydrochemical variations of the springs resulted in the development of a

new conceptual model regarding the development and function of karstic aquifers. The model enables predictions to be made of sink to resurgence flow velocities, of conduit depth below the water table, of the ratio of beds and joints used by conduits, of the spacing between cave tiers, and of the depth of vauclusian springs (Worthington 1991). Additionally, he provided the catalyst toward a new view on flow in carbonate aquifers. Worthington proposed, based on documented discharge rates of springs, that all karst springs discharge from conduits and that the idea of a diffuse karst aquifer is a contradiction in terms (Worthington 1991).

Quinlan et al. (1992) developed a conceptual model that used recharge, flow, and storage as a measure of the aquifers susceptibility to groundwater contamination and proposed four dominant aquifer types: hypersensitive aquifers, very sensitive aquifers, moderately sensitive aquifers, and slightly sensitive non-karst aquifers. Hypersensitive aquifers are the most karstic, thus most susceptible to contamination, and are characterized by discrete recharge, conduit flow, and low storage. Any contaminants that enter this type of aquifer will most likely pass through the aquifer relatively quickly to discharge at springs.

Very sensitive aquifers are characterized by discrete recharge, conduit flow, and low to moderate storage. Moderately sensitive aquifers would have recharge somewhere between discrete and dispersed through epikarstic drains, intermediate flow through dissolutionally enlarged fissure networks, and moderate to high storage. Slightly sensitive aquifers are not karst aquifers, but some carbonate aquifers are similar in character to clastic aquifers in which flow is via intergranular pores or fractures developed during unloading or exposure in the near surface environment (Quinlan et al. 1992).

Worthington et al. (2000, 2001) provided support for a triple porosity/triple permeability model for unconfined carbonate aquifers. Four contrasting carbonate aquifers were studied in Ontario, Canada, Kentucky, USA, Great Britain, and the Yucatan Peninsula in Mexico to approximate the porosity, permeability, storage, and proportions of flow within the rock matrix, fractures, and channels. Matrix permeability refers to the pore spaces in the bedrock, fracture permeability refers to all joints and bedding plane partings that have not been enlarged by dissolution and channels refer to all joints, faults, and beddings planes that have been enlarged by dissolution. Channel and conduit permeability are synonymous terms used in the literature to refer to pathways enlarged by dissolution within the karst aquifer. Aquifers were chosen to provide a mixed range of rock type (limestone and dolostone), recharge, (allogenic and autogenic), and age (Paleozoic, Mesozoic, and Cenozoic) (Worthington et al. 2000).

Investigative methods included results from analysis of bedrock core samples, packer tests, pumping tests, videos of fractures in boreholes, dye trace tests, cave passage geometries, geochemical studies, and numerical

models and demonstrated that at least 96% of the storage or volume of groundwater in all four karst aquifers was in the matrix portion of the rock (Worthington et al. 2001). In all four cases it was shown that the enhancement of permeability caused by dissolution created efficient dendritic networks of interconnecting channels that are able to convey 94% or more of the flow in the aquifer (Worthington et al. 2001). Today it is widely accepted that carbonate aquifers should be classified as "triple porosity" or "triple permeability" aquifers (White 1999; Worthington et al. 2000; White and White 2000, 2001; Martin and Screaton 2001), where water flow exists within the rock matrix, fractures, and dissolutional channels.

13.8 Land Use Problems in Karst

Approximately 20% of the earth's land surface is located in karst areas (White 1988). Karst represents areas of land that are highly vulnerable to groundwater contamination due to the ease at which surface waters can move into the subsurface and through the groundwater-flow system. Improper land use planning on karst areas can result in the contamination of private and public water supplies and potential impact to sensitive cave species. Additionally, development can and has resulted in substantial damage to private property and local infrastructure. Unfortunately, development on karst will continue, but with proper land use planning strategies and construction practices, impacts to the vulnerable landscape can be minimized. The following paragraphs provide a few examples of problems that have occurred in karst areas.

Human impact on karst groundwater resources

Many people depend on karst groundwater resources for their source of water. It is estimated the 25% of the world's population, including many large cities and extensive rural areas depend on karst water supplies to sustain their daily activities (Ford and Williams 1989). Springs serve as natural outlets from karst aquifers and are used as water supplies. Groundwater can travel through large open conduits in the karst aquifer quicker than non-karst aquifers with extreme velocities of 7,500 ft per hour (2,286 m/h) while a range of 30 to 1,500 ft/h (10 to 460 m/h) is typical (Quinlan and Ewers 1985). As a result, any type of contamination that enters recharge waters that feed springs can impact water supplies within days or weeks (Examples 13.1 and 13.2).

Example 13.1 Rubin and Privitera (1997) reported on the construction of a 107 acres (43.3 ha) industrial park site located in New York east of the Catskill Mountains and slightly west of the Hudson River. The park was designed to be located along the top of a narrow forested ridge underlain by carbonate

rocks. The karst aquifer beneath the park is within the dolostone and limestone of the Upper Silurian Rondout Formation and the limestones of the Lower Devonian Group. A storm water drainage system was designed to direct runoff into an unroofed deep vertical mine. Once in the mine the stormwater would flow through a mound of newly blasted rock and through a short horizontal adit where it would drain into a sinkhole (Rubin and Priniterra 1997). This project consisted of a major federal action which by law required an environmental impact analysis. Consulting engineers and geologists hired by the development company denied the presence of sinkholes, caves, and sinking streams. No site specific karst investigations were conducted (Rubin and Priniterra 1997).

Example 13.2 In Indiana, two sinkholes were used as a municipal dump, known as the Lemon Lane Landfill, from 1933 to 1964 on the west central edge of the city of Bloomington, Indiana. Bloomington is located in the Mitchell Plain, a low plateau underlain with carbonates of Mississippian age on which a characteristic karst terrane has developed (McCann and Krothe 1992). A large number of electrical capacitors containing polychorinated biphenyls (PCBs) were dumped at the Lemon Lane Landfill. Within one mile of the landfill there are approximately 90 homes that obtain drinking water from private wells and several drinking water wells have been found to be contaminated with PCBs (EPA 2006). Several local springs have been contaminated with PCBs as a result of contaminant migration from the landfill. Currently, the landfill is listed as a Superfund site.

George et al. (1999) provided the results of a multiphase characterization study at an industrial site in central Alabama. The site is underlain by the Ketona Dolomite and preliminary investigative results showed releases of coal tar and light oils into the groundwater system. It was concluded that slow groundwater flow rates keep the contaminants onsite.

Berry et al. (2001) report on the accidental release of 900 gal of gasoline at a convenience store in Bulverde, Texas. The site is underlain by the karst Trinity aquifer located 300 ft beneath the surface. A few days later residents that lived down slope of the spill detected a gasoline odor in their drinking water. Results for groundwater sampling indicated unacceptable levels of MTBE and BTEX.

Improper agricultural and industrial activities have impacted groundwater in karst areas. Huntoon (1992) reported on deforestation of the uplands above the stone forest aquifers within the south China karst belt from 1958 to the mid 1970s. The karst uplands were left barren which resulted in an alternation of the hydrologic conditions of the area. Before deforestation, the uplands temporarily stored the groundwater which was slowly released to the stone forest aquifers in the valley during the dry season. After deforestation, the uplands could no longer retain the water that resulted in less discharge to springs and decreased water levels during the dry season.

13.9 Investigative Methods in Karst

Groundwater dye tracing

Groundwater dye tracing has been used in karst areas to determine groundwater flow routes and velocities from sinking points in recharge areas to springs. Springs serve as excellent sampling locations to monitor for dye that has been introduced into the karst groundwater system. A successfully designed dye trace study should determine all possible discharge points to be sampled and also some unlikely ones. A few examples are given below, however an expanded discussion of this is found in Chapter 15.

Dye tracing is used on a wide variety of projects, some of which include proposed highway corridor studies, delineation of springhead protection areas, recharge areas and subsurface basins, leakage in sewage disposal systems, identification of sources of potential pollution from hazardous waste sites, and detection of leakage from dam sites. Nontoxic fluorescent dyes have been used in karst since the late 1800s. The first reported use of a fluorescent dye as a tracer was conducted in southwestern Germany in 1877 where dye was injected at infiltration points in the bed of the Danube River and reappeared two days and 7.5 mi (12 km) away at the Aach Spring (Jones 2005). The location of dye introduction points, the manner in which the dyes are introduced into the subsurface, and the sampling strategy and analytical approach used must be tailored to the hydrogeologic setting, the issues of concern, and the quality and credibility of the data needed for the study (Bednar and Aley 2001).

Example 13.3 Groundwater dye tracing is an effective tool to use during the highway development process to avoid or minimize impacts to karst groundwater resources. Detailed hydrologic studies must be employed when planning highway projects through karst because underlying karst aquifers are highly vulnerable to contaminants. Contaminants can enter the groundwater-flow system and reach important springs used for human consumption or recreation activities relatively quickly.

Spangler (2002) conducted a study of the Dewitt Spring near Logan, Utah. Dye trace studies determined travel times ranging from 22 to 31 days from losing stream segments located approximately 7 mi from the spring. Results indicated that groundwater velocities ranged from 530 to 1,740 ft/day. In the southern Missouri karst, travel times for dye arrival from surface sinks to springs took 16 days to travel 39.5 mi (Aley 1997).

Example 13.4 Bednar and Aley (2001) provided the results of studies conducted along highway corridors in Arkansas, Tennessee, and West Virginia. In West Virginia, three dye traces were conducted along the preferred alignment for the Corridor H Highway project near Greenland Gap in Grant County. Greenland Gap was formed from the down-cutting of New Creek Mountain by Patterson Creek. Patterson Creek was considered a high quality

trout stream that received discharge from a karst spring upstream from the gap. The preferred alignment crossed the mountain upslope of many sinkholes. Sinkholes that contribute water to the groundwater-flow system could adversely impact the spring. Results demonstrated that water derived along the preferred alignment would discharge at two springs along Patterson Creek within 7 days.

Example 13.5 Duwelius et al. (1995) described a dye trace study that was conducted for the Indiana Department of Transportation during the State Route 37 Bedford to Mitchell highway improvement project. The project area was located in the Mitchell Plain of Indiana and was characterized by numerous sinkholes. Semi-quantitative dye tracing involved injection of fluorescent dyes into 15 sinkholes along the highway right-of-way as part of an underground drainage assessment. Results form the study demonstrated that all sinkholes along the project alignment were hydrologically interconnected.

Example 13.6 Dye tracing was conducted at Sulphur Springs Pool in Hillsborough County, Florida, in response to unsafe levels of coliform bacteria in the water (Wallace 1993). The pool had been used as a swimming and recreational area since the 1920s. Dye testing was conducted on several occasions since 1958 to determine the source of the problem. Results from the dye tracing showed that the source of contamination was from a sinkhole that was located within a stormwater basin adjacent to Interstate 275 that provided a direct connection to Sulphur Springs Pool.

Hydrographs and chemographs

Spring hydrograph and chemograph analysis have been widely used in concert with dye tracing to gain insight about groundwater flow through karst. A hydrograph shows a plot of spring discharge versus time in the shape of a curve. Discharge is plotted on the vertical axis and time on the horizontal axis. The hydrograph is used to gain information as how the spring responses to storm events. A spring hydrograph is divided into three segments for analytical purposes and include: lag time, the rising limb, and the falling limb (Figure 13.20). The lag time portions of the curve shows the spring discharge before the recharge event reaches the spring. The rising limb portion shows the first arrival and increase of discharge at the spring. The peak of the graph indicates the maximum amount of spring discharge from the storm event. The peak discharge reflects older water that is already within the aquifer in the most downstream direction and not the recharge water that enters the subsurface from the storm event (Huntoon 2000). The falling limb, more commonly called the recession curve, shows the spring discharge as it returns to prestorm conditions.

A chemograph (Figure 13.21) can show several characteristics of the water chemistry, sediment content, and discharge rates of spring water

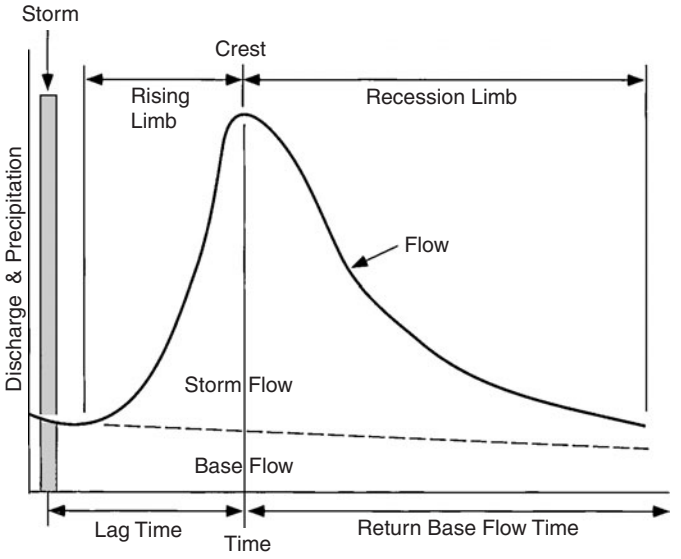

Figure 13.20 A spring hydrograph. (*Used with permission, Karst Waters Institute.*)

over time. Although many parameters can be used to characterize the chemistry at karst springs, common parameters include: turbidity, dissolved oxygen, hardness, stable isotopes, specific conductance, and temperature (Ford and Williams 1989).

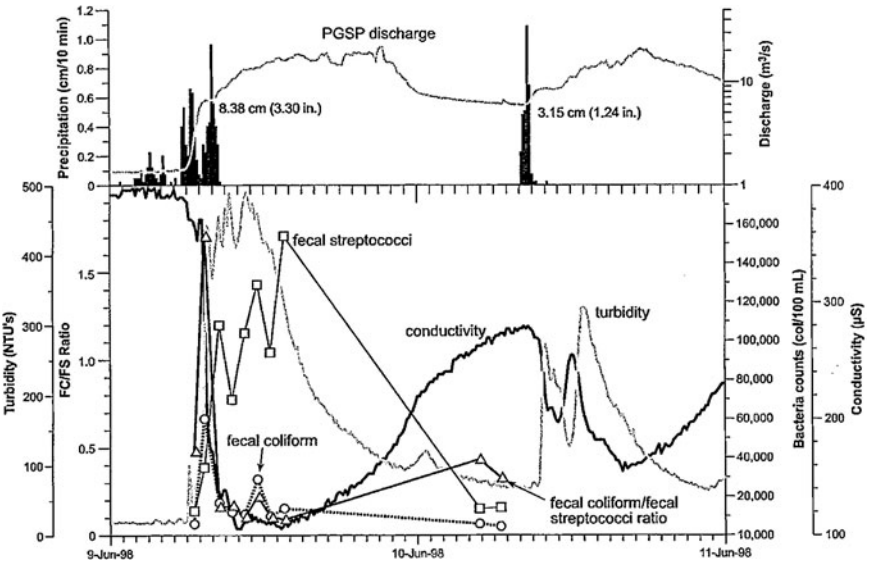

Figure 13.21 Chemograph of Pleasant Grove Spring. Currens 2005.

Geophysical techniques

Geophysical methods measure the physical, electrical, and chemical properties of soil, rock, and pore fluids (ASTM 1999; Benson 2000). The bedrock-soil interface in karst areas is commonly composed of an irregular surface consisting of high and low points from the dissolving action of the groundwater. As a result, geophysical surveys have been used to better define the bedrock soil boundary and aid in the interpretation of subsurface karst features, cavities, and potential groundwater flow routes. Common geophysical surveys used in karst include: seismic, electrical resistivity, electromagnetic, ground penetrating radar, and gravity. More examples and theory on these methods can be found in Chapter 4.

Electrical survey

The electric resistivity survey measures the resistance to flow of electricity in subsurface materials (EPA 1993). Electrodes are inserted into the soil and the electrical resistance between them is measured (White 1988). As the resistance to current flow varies vertically and horizontally, changes in the electrical potential reflect these differences (Nowak 1999).

Frequency domain electromagnetic survey

Frequency electromagnetic (EM) surveys measure the electrical conductivity or the ability of the subsurface materials to react to an induced electromagnetic field produced by a transmitter coil. A receiver coil then intercepts the electromagnetic fields created by the transmitter coil. Measurements are made as an operator walks along the ground carrying an instrument and results are typically presented in map form (Hoover 2003).

Ground penetrating radar

The ground penetrating radar (GPR) geophysical method is a rapid, high resolution tool for noninvasive investigation (Cardimona 2002). This method involves the transmission of ultra high frequency radio waves into the subsurface by a transducing antenna. When the subsurface signal encounters a boundary between the media with different electrical properties a portion of the signal is reflected back to the surface, detected by the antenna, and recorded on a graphical recorder (Smith 2002). Results of the survey are shown as a profile of the subsurface.

Gravity survey

Microgravity surveys measure differences in the density of the underlying soil and rock and can be used to characterize geologic conditions. It is a powerful tool for establishing the presence of karst features which

often give rise to measurable negative anomalies (McDonald et al. 1999). Identification of underlying material of high and low density can aid the investigators to determine the characteristics of the subsurface. Characteristics include the depth to bedrock, extent and shape of a collapse area below the surface, location of the crevice or crevices into which regolith (all earth material that includes soil and rock fragments above the bedrock) is collapsing, and locations of additional regolith voids in the vicinity of a collapse (Crawford et al. 1999). Low density zones can identify the location of cavities and buried sinkholes.

Seismic survey

Seismic surveys are regularly used in karst terrain to answer geotechnical questions about the soil and bedrock (Smith 2005). There are two types of seismic surveys: seismic reflection and seismic refraction. Seismic reflection measures the amount of time that a sound wave takes to bounce off rocks in the subsurface. Seismic refraction measures the velocity of the energy that is transmitted through the subsurface. Seismic methods were developed out of the pioneering earthquake studies in the mid to late nineteenth century (Reynolds 1997). Since the early twentieth century, seismic methods have been used often for hydrocarbon exploration. Seismic methods have been used for engineering site investigations, groundwater exploration, location of faults and fractures zones and rock types, geologic studies of aquifers, and shallow coal exploration. Seismic methods can also be used to determine subsurface cavities.

Example 13.7 In May 2000, the United States Geological Survey (USGS) conducted a survey at the Gregg Chemical waste landfill site in northwestern Arkansas, an area underlain by the karst limestone of the Boone Formation, to locate filled pits where glass containers of laboratory chemicals were buried (Stanton and Schrader 2001). Electromagnetic conductivity, magnetometer, and electrical resistivity surveys were used to locate the glass containers. The use of these geophysical methods in concert helped to determine the location of five potential areas of concern where hazardous materials may be found.

Example 13.8 Styles and Thomas (2001) conducted a microgravity survey to detect cavities beneath the surface in an area under construction for a container Port in Freeport, Grand Bahama, Bahamas. The survey resulted in the delineation of a large cave system beneath the site. Jansen et al. (1993) used electrical resistivity and seismic refraction surveys to determine the location of bedrock pinnacles for the expansion of a landfill site in Monroe County, Wisconsin. Results from the survey demonstrated that the geophysical methods employed were generally successful in detecting bedrock pinnacles but an extensive boring program was necessary to confirm the geophysical results.

Example 13.9 Seismic methods were used at the Oak Ridge Reservation in Tennessee to assess karst features (Doll et al. 2005). Seismic refraction and seismic reflection surveys were used to determine the depth to bedrock and karst features that could direct contaminants to the site. Daniel et al. (1999) reported on this use of gravity, electromagnetic, and electrical resistivity surveys to evaluate karst features for roadway design in association with a maximum security prison in Lee County, Virginia. Gravity, electrical resistivity, ground penetrating radar, and seismic refraction surveys were used to detect subsurface cavities in a karst area along a proposed highway alignment in Logan County, Ohio (Nowak 1999). A geological investigation, including the use of electrical resistivity surveys, was conducted as part of a comprehensive engineering design study for a planned highway widening project south of Front Royal, Virginia (Rehwoldt and Reed 2001). A concern of the Virginia Department of Transportation was to protect Skyline Caverns from the effects of roadway construction.

13.10 Summary

Karst landscapes are unique geologic environments formed from the dissolving of the rock by natural water. Sinkholes and sinking streams serve to transmit the water into the subsurface at greater velocities. As openings in the rock grow larger and larger, so does the amount of water that can travel into and through the groundwater-flow system to eventually discharge at springs. Karst springs used for public water supplies or recreational activities are highly vulnerable to contamination due to the relatively quick speeds at which water can move through the groundwater-flow system as demonstrated in this chapter.

Proper land use planning must be used when residential, commercial, and transportation development occurs in karst areas. Investigative techniques such as groundwater dye tracing and geophysical surveys are essential tools for use to help avoid or minimize impacts to karst environments. The more we learn about karst the more we can reduce pollution of its natural waters. Appendix E provides a list of agencies and organizations where the beginner can learn about cave and karst science.

References

Aley, T. 1978. Ozark Hydrology: A Predictive Model. *Journal of the Missouri Speleological Survey*. 18, 185.

Aley, Thomas. 1997. Groundwater Tracing in the Epikarst. In: *The Engineering Geology and Hydrogeology of Karst Terranes*, Beck and Stephenson (eds.). Balkema, Rotterdam. 207–211.

Aley, Thomas. 1999. *The Ozark Underground Laboratory's Groundwater Tracing Handbook*. The Ozark Underground Laboratory. 35.

Arvidson and MacKenzie. 1997. Tentative Kinetic Model for Dolomite Precipitation Rate and Its Application to Dolomite Distribution. *Aquatic Geochemistry* 2, 273–298.

ASTM. 1999. Standard Guide for Selecting Surface Geophysical Methods, Standard Method D-6429. ASTM. 753–763.

Atkinson, T.C., and D.P. Drew. 1974. Underground Drainage of Limestone Catchments in the Mendip Hills. *Fluvial Processes in Instrumental Watersheds*, Special Publication 6. The Institute of British Geographers. 87–106.

Atkinson, T.C. 1977. Diffuse Flow and Conduit Flow in Limestone Terrain in Mendip Hills, Somerset (Great Britain). *Journal of Hydrology*. 35, 93–110.

Bathurst, R.G.C. 1975. Carbonate Sediments and Their Diagenesis. *Developments in Sedimentology 12.* Elsevier Scientific Publishing Company. 658.

Beck, B.F., and W.C. Sinclair. 1986. Sinkholes in Florida: An introduction. *Florida Sinkhole Research Institute Report 85-86-4*, 16.

Beck, B.F. 2005. Soil Piping and Sinkhole Failures. In: *Encyclopedia of Caves*, Culver, D.C. and W.B. White (eds.). Elsevier. 521–526.

Bednar, D., and Thomas Aley. 2001. Groundwater Dye Tracing: An Effective Tool to Use During the Highway Development Process to Avoid or Minimize Impacts to Karst Groundwater Resources. In: Beck, B and J. G. Herring (editors). *Geotechnical and Environmental Applications of Karst Geology and Hydrology*. A.A. Balkema Publishers. 201–207.

Benson, R.C. 2000. Case Histories of Six Roadway Investigations in Karst Combining Geophysical and Conventional Methods. In: *51st Annual Highway Geology Symposium Proceedings*. Washington State Department of Transportation. 3–10.

Berry, R, Long R., and T.M. Baer. 2001. Operation and Maintenance of Vadose Zone and Groundwater Remediation Systems in a Karst Aquifer. In: Beck, B.F., and J.G. Herring (eds.). *Geotechnical and Environmental Applications of Karst Geology and Hydrology. Balkema Publishers*. 287–291.

Blatt, H. 1982. *Sedimentary Petrology*. W.H. Freeman and Company. 564.

Blatt, H., and R.J. Tracey. 1999. *Petrology, Igneous, sedimentary, and Metamorphic*. W.H. Freeman and Company. 529.

Boggs, S. 1987. *Principles of Sedimentology and Stratigraphy*. Merrill Publishing Company. 784.

Boggs, S. 2001. *Principles of Sedimentology and Stratigraphy*. Prentice Hall.

Bogli, A. 1980. *Karst Hydrology and Physical Speleology*. Springer-Verlag. 284.

Bosak, P. et al., 1989. *Paleokarst, a Systematic and Regional Review*. Elsevier Publishing Co. 725.

Braithwaite, C. 2005. *Carbonate Sediments and Rocks*, *A Manual for Earth Scientists and Engineers*. Whittles Publishing. 164.

Brucker, R.W. 2005. Mammoth Cave System. In: Culver and W.B. White (eds.). *Encyclopedia of Caves*. Elsevier. 351–355.

Burns, S.J., McKenzie, J.A., and C. Vasconcelos. 2000. Dolomite formation and biogeochemical cycles in the Phaserozoic. *Sedimentology*, 47 (Suppl. 1), 49–61.

Cardimona, S. 2002. Electrical Resistivity Techniques for Subsurface Investigation. In: *Geophysics 2002,* The 2nd Annual Conference on the Application of Geophysical and NDT Methodologies to Transportation Facilities and Infrastructure. Federal Highway Administration, FHWA-WRC-02-001.

Chilingar, G.V., H.J. Bissell, and R.W. Fairbridge. 1967a. *Carbonate Rocks, Physical and Chemical Aspects, Developments in Sedimentology 9B.* Elsevier Publishing Company. 413.

Cook, H.E., and P. Enos. 1977. Deep-Water Carbonate Environments. *Society of Economic Paleontologists and Mineralogists*, Special Publication 25. 336.

Crawford, N.C., Lewis, M.A., Winter, S.A., and J.A. Webster. 1999. Microgravity Techniques for Subsurface Investigations of Sinkhole Collapses and for Detection of Groundwater Flow Paths through Karst Aquifers. In: Beck, B.F., Pettit, A.J. and J.G. Herring (eds.). *Hydrogeology and Engineering Geology of Sinkholes and Karst*. A.A. Balkema. 203–218.

Culver and White. 2005. *Encyclopedia of Caves*. Elsevier. 654.

Currens, J.C. 2005. Changes in Groundwater Quality in a Conduit Flow Dominated Karst Aquifer as a result of Best Management Practices, Report of Investigations 11. Kentucky Geological Survey. 72.

Daniel, J.C., Benson, R.C., and A.M. Samford. 1999. Use of Geophysical Techniques to Evaluate Karst Features for Roadway Design. In: *50th Annual Highway Geology Symposium Proceedings*. Radford University. 32–41.

Day, M., and S. Chenoweth. 2004. Cockpit County Cone Karst, Jamaica. In: *Encyclopedia of Caves and Karst Science*. Gunn, J. (ed.). Fitzroy-Dearborn, 233–235.
Deike, G.H. 1989. Fracture Controls in Conduit Development. In: White, W.B. and White, E.L (eds.). *Karst Hydrology: Concepts from the Mammoth Cave Area.* Van Nostrand. 259–293.
Doll, W.E., B.J. Carr, J.R. Sheehan, and W.A. Mandell. 2005. Overview of Karst Effects and Karst Detection in Seismic Data from the Oak Ridge Reservation, Tennessee. In: Kuniansky, E.L. (ed.). *U.S. Geological Survey Karst Interest Group Proceedings*, Rapid City, South Dakota, September 12–15, 2005, Scientific Investigations Report 2005–5160. 20–28.
Drew, D., and H. Hotzl (ed.). 1999. *Karst Hydrogeology and Human Activities*, *Impacts*, *Consequences, and Implications*. A.A. Balkema. 322.
Dreybrodt, W. 1988. *Processes in Karst Systems*. Springer-Verlag. 288.
Dunham, R.J. 1962. Classification of Carbonate Rocks. In: Ham, W.E. Classification of Carbonate Rocks, a Symposium. *American Association of Petroleum Geologists,* Memoir 1. 108–121.
Duwelius, J. et al. 1995. Application of Fluorescent Dye Tracing Techniques for Delineating Sinkhole Drainage Routes, Highway 37 Improvement Project Lawrence County, Indiana. In: Beck, B. (ed.). *Karst Geohazards*. Balkema, Rotterdam. 227–233.
Environmental Protection Agency. 1993. Use of Airborne, Surface, and Borehole Geophysical Techniques at Contaminated Sites. A Reference Guide. *Environmental Protection Agency*, EPA/625/R-92/007. 304.
Ewers, R.O. 1992. The Use of Digital data-Loggers in Defining Groundwater Transport Mechanisms in Karst Aquifers.
Field, Malcolm S. 1999. The QTRACER Program for Tracer-Breakthrough Curve Analysis for Karst and Fractured-Rock Aquifers. *U.S. Environmental Protection Agency*. 137.
Folk, R.L. 1959. Practical Petrographic Classification of limestones. *Bulletin of the American Association of Petroleum Geologists*. 43, 1–38.
Folk, R.L. 1962. Spectral Subdivisions of Limestone Types. In: Ham, W.E. Classification of Carbonate Rocks, Memoir 1. American Association of Petroleum Geologists, 108–121.
Folk, R.L. 1962. Spectral Subdivisions of Limestone Types. In: Ham, W.E. (ed.). Classification of Carbonate Rocks, American Association of Petroleum Geologists. Memoir 1. 62–84.
Ford, D., and P. Williams. 1989. *Karst Geomorphology and Hydrology*. Chapman and Hall. 701.
Gams, I. 1994. Types of Polges in Slovenia, Their Inundation and Land Use. *Acta Carsologica,* 23, 285–302.
George, S., Aley, T., and A.L. Lange. 1999. Karst System Characterization Utilizing Surface Geophysics, Borehole Geophysics, and Dye Tracing Techniques. In: Beck, B.F., Pettit, A.J., and J.G. Herring (eds.). *Hydrogeology and Engineering Geology of Sinkholes and Karst*. A.A. Balkema. 225–242.
Gillieson, D. 1996. *Caves: Processes, Development and Management*. Blackwell Publishers. 324.
Gunn, J.A. 1983. Point Recharge of Limestone Aquifers: A Model from New Zealand Karst. *Journal of Hydrology*, 61, 19–29.
Gunn, J.A. 1985. A Conceptual Model for Conduit Flow Dominated Karst Aquifers. Karst Water Resources, No. 161. *International Association of Hydrological Sciences*. 587–596.
Gunn, J.A. (ed.) 2004. *Encyclopedia of Caves and Karst Science*. Fitzroy and Dearborn.
Gulden, B. 2006. Website. http://www.cavediggers.com/Main_Page/LongandDeep/longanddeep.html
Herak, M., and V.T. Stringfield. 1972. *Karst, Important Karst Regions of the Northern Hemisphere*. Elsevier Publishing Company. 551.
Hill, C.A., and P. Forti. 1997. *Cave Minerals of the World, 2nd edition*. National Speleological Society. 463.
Hoover, R. 2003. Geophysical Choices for Karst Investigations. In, Beck, B.F. (ed.), *Sinkholes and the Engineering and Environmental Impacts of Karst*, Geotechnical Special Publication No. 122. American Society of Civil Engineers. 529–538.
Huntoon, P. 1992. Chairman Mao's Great Leap Forward and the Deforestation Ecological Disaster in the South China Karst Belt. In: *Proceedings of the Third Conference on Hydrogeology, Ecology, Monitoring, and Management of Ground Water in Karst Terranes*. Water Well Journal Publishing Company. 149–159.

Huntoon, P.W. 2000. Variability of Karstic Permeability between Unconfined and Confined Aquifers, Grand Canyon Region, Arizona. *Environmental and Engineering Geoscience*, 6, 2, 155–170.
Jacobson, R.L., and D.L. Langmuir. 1974. Controls on the Quality Variations of Some Carbonate Spring Waters. *Journal of Hydrology*. 23, 247–265.
Jakucs, L. 1977. *Morphogenetics of Karst Regions*. Halsted Press. 268.
Jansen, J., Ankam, J., Goowin, C., and A. Roof. 1993. Electromagnetic Induction and Seismic Refraction Surveys to Detect Bedrock Pinnacles, In: Beck, B.F. (ed.). *Applied Karst Geology*. A.A. Balkema. 115–130.
Jennings, J.N. 1985. *Karst Geomorphology*. Blackwell Publishers. 293.
Jones, W.K., Culver, D.C., and J.S. Herman. 2004. Introduction. In: *Epikarst*. Special Publication 9. Karst Waters Institute. 1–2.
Jones, W.K. 2005. Karst Water Tracing. In: Culver, D.C, and W.B. White. (eds.). *Encyclopedia of Caves*. Elsevier. 321–329.
Kambesis, P. 2005. Lechuguilla Cave, New Mexico. In: Culver and W.B. White. (eds.), *Encyclopedia of Caves*. Elsevier. 339–346.
Klimchouk, A.B. et al. 1996. "Hidden" Shafts at the Base of the Epikarstic Zone: A Case Study from the Sette Communi Plateau. Venetian Pre-Alps, Italy. *Cave and Karst Science, Transactions of the British Cave Research Association*. 23(3), 101–107.
Klimchouk, A. 2000. The Formation of the Epikarst and its Role in Vadose Speleogenesis. In: *Speleogenesis, Evolution of Karst Aquifers*. Klimchouk et al. (eds.). National Speleological Society, Inc. 91–99.
Klimchouk, A. 2005. Krubera (Voronja) Cave. In: Culver and W.B. White (eds.), *Encyclopedia of Caves*. Elsevier. 335–338.
Klimchouk, A. 2007. Hypogene Speleogenesis: Hydrogeological and Morphogenetic Perspective. National Cave and Karst Research Institute, Special Paper No. 1. Carlsbad, NM. 106.
Klimchouk, A., Ford, D.C., Palmer, A.N., and W. Dreybrodt (eds.). 2000. *Speleogenesis: Evolution of Karst Aquifers*. National Speleological Society. 527.
Kranjc, A. (ed.). 1997. *Slovene Classical Karst-Kras*, ZRC SAZU. Ljubljana. 254.
Kranjc, A. 1998. Kras (The Classical Kras) and the Development of Karst Science. *Acta Carsologica*, 27, 151–164.
LeGrand, H.E., and V.T. Stringfield. 1971. Development and Distribution of Permeability in Carbonate Aquifers. *Water Resources*, 7(5), 1284–1294.
LeGrand, H.E. 1983. Perspective on Karst Hydrology. *Journal of Hydrology*, 61. 343–355.
Lippman, F. 1973. *Sedimentary Carbonate Minerals*. Springer-Verlag. 228.
Lowe, D., and T. Waltham. 2002. *Dictionary of Karst and Caves*. British Cave Research Association, 10. 40.
Lowe, D.J. 2004a. Speleogenesis Theories: Post-1890. In: *Encyclopedia of Caves and Karst Science*. Fitzroy and Dearborn. 670–674.
Mangin, A. 1975. Contribution a l etude hydrodynamique des aquifers kartiques. *Ann Speleol.*, 29(3/4), 283–601; 30(1), 21–124.
Martin, J.B., and E.J. Screaton. 2001. Exchange of Matrix and Conduit Water with Examples from the Floridian Aquifer. In: *U.S. Geological Survey Karst Interest Group Proceedings*, Water Resources Investigations Report 01-4011. 38–44.
McCann and Krothe. 1992. Development of a Monitoring Program at a Superfund Site in a Karst Terrane near Bloomington, Indiana. In: *Proceedings of the Third Conference on Hydrogeology, Ecology, Monitoring, and Management of Groundwater in Karst Terranes*. Water Well Journal Publishing Company. 349–372.
McDonald, R., Russill, N., and R. Davies. 1999. Integrated Geophysical Surveys Applied to Karstic Studies. In: Beck, B.F., Pettit, A.J., and J.G. Herring. *Hydrogeology and Engineering Geology of Sinkholes and Karst*. Balkema Publishers. 243–246.
Milanovic, P. 1981. *Karst Hydrogeology*. Water Resources Publications. 434.
Milanovic, P. 2004. *Water Resources Engineering in Karst*. CRC Press. 312.
Moore, C.H. 2001. *Carbonater Reservoirs: Porosity Evolution and Diagenesis in a Sequence Stratigraphic Framework*. Elsevier. 444.
Mylroie, J., Carew, J.L., and A.I. Moore. 1995. Blue Holes: Definition and Genesis. *Carbonates and Evaporites*. 10(2), 225–233.

Mylroie, J. 2004. Blues Holes of the Bahamas. In: *Encyclopedia of Caves and Karst Science*. Fitzroy Dearborn. 155–156.
Nowak, E. 1999. Near Surface Cavity Detection—Logan County, Ohio. In: *50th Annual Highway Geology Symposium Proceedings*. Radford University. 68–84.
Onac, B.P., Mylroie, J.E., and W.B. White. 2001. Mineralogy of Cave Deposits on San Salvador Island, Bahama. *Carbonates and Evaporites*. 16(1), 8–16.
Palmer, A.N. 1975. The Origin of Maze Caves. *National Speleological Society*. 37, 56–76.
Palmer, A.N. 1987. Cave Levels and Their Interpretation. *National Speleological Bulletin*. 49(2), 50–66.
Palmer, A.N. 1991. Origin and Morphology of Limestone Caves. *Geological Society of America. Bulletin*. 103(1), 1–21.
Palmer, A.N. 2000. Hydrogeologic Control of Cave Patterns. In: *Speleogenesis: Evolution of Karst Aquifers*, Klimchouk et al. (ed.) National Speleological Survey, Inc. 77–90.
Palmer, A.N. 2005. Solution Caves in Regions of Moderate Relief. In: Culver, D.C. and W.B. White (eds.). *Encyclopedia of Caves*. 527–535.
Palmer, A.N. 2007. Cave Geology. Cave Books, Dayton Ohio. 454.
Palmer, A.N., and P. Audra. 2004. Patterns of Caves. In: Gunn (ed.), *Encyclopedia of Caves*. Elsevier. 573–575.
Quinlan, J. 1967. Classification of Karst Types: A Review and Synthesis Emphasizing the North American Literature, 1941–1966. *National Speleological Society Bulletin*, 29, 107–109.
Quinlan, J. 1978. Types of Karst, with Emphasis on Cover Beds in Their Classification and Development. *PhD Thesis, Geology*, University of Texas, Austin.
Quinlan, J.F., and O.E. Ralph. 1985. Ground Water Flow in Limestone Terranes: Strategy Rationale and Procedure for Reliable, Efficient Monitoring of Ground Water Quality in Karst Areas. In: *Proceedings of the National Symposium and Exposition on Aquifer Restoration and Groundwater Monitoring*. National Groundwater Association. 197–234.
Quinlan, J.F., and R.O. Ewers. 1985. Ground Water Flow in Limestone Terranes: Strategy Rationale and Procedure for Reliable, Efficient Monitoring of Ground Water Quality in Karst Areas. In: *Proceedings of the Fifth National Symposium and Exposition on Aquifer Restoration and Groundwater Monitoring*, May 21–24, 1985. 197–234.
Quinlan, J.F. 1989. Ground-Water Monitoring in Karst Terranes: Recommended Protocols and Implicit Assumptions. *U.S. Environmental Protection Agency*. 79.
Quinlan, J.F. et al. 1992. Recommended Administrative/Regulatory Definition of Karst Aquifer, Principles for Classification of Carbonate Aquifers, Practical Evaluation of Vulnerability of Karst Aquifers, and Determination of Optimal Sampling Frequency at Springs. In: Quinlan J. and Stanley, A., (eds.), *Conference on Hydrogeology, Ecology, Monitoring, and Management of Groundwater in Karst Terranes Proceedings*. National Groundwater Association. 573–635.
Ray, J.A. 2005. Sinking Streams and Losing Streams. In: *Encyclopedia of Caves*, Culver, D.C. and W.B. White (eds.). Elsevier. 509–514.
Rehwoldt, E.B., and R.E. Reed. 2001. Characterization of Karst Systems for a Highway Widening Study in Warren County, Virginia. In: *The 52nd Annual Highway Geology Symposium*. Maryland State Highway Administration. 50–59.
Reynolds, J.M. 1997. *An Introduction to Applied and Environmental Geophysics*. John Wiley and Sons, Inc. 796.
Rubin, P.A., and J.J. Privitera. 1997. Engineered and Unregulated Degradation of Karst Aquifers: Two Case Studies in New York, USA. In: Beck, B.F., and J. Brad Stephenson. *The Engineering Geology and Hydrogeology of Karst Terranes*. A.A. Balkema/Rotterdam/ Brookfield. 467–478.
Scanlon, B.R., and T. Thrailkill. 1987. Chemical Similarities Among Physically Distinct Spring Types in a Karst Terrain. *Journal of Hydrology*, 259–279.
Scholle, P.A., Bedout, D.G., and C.H. Moore (eds.). 1983. *Carbonate Depositional Environments*. American Association of Petroleum Geologists, AAPG Memoir 33. 708.
Selley, R.C. 2000. *Applied Sedimentology, 2nd edition*. Academic Press. 523.
Shuster, E.T., and W. White. 1971. Seasonal Fluctuations in the Chemistry of Limestone Springs: A Possible Means for Characterizing Carbonate Springs. *Journal of Hydrology*, 14, 93–128.

Siegel, F.R. 1967. Properties and uses of the carbonates. In: Chilingar, G.V., Bissell, H.J. and R.W. Fairbridge (eds.). *Carbonate Rocks: Origin, Occurrence and Classification, Developments in Sedimentology*, Series No. 9A, Chapter 9. Elsevier Publishing Company. 471.
Smart, C., and S.R.H. Worthington. 2004. Springs. In: *Encyclopedia of Cave and Karst Science*. 699–703.
Smith, D.V. 2005. The State of the Art of Geophysics and Karst: A General Literature Review. In, Kuniansky, E.L. (ed.). *U.S. Geological Survey Karst Interest Group Proceedings*, Rapid City, South Dakota, September 12–15, 2005. 10–16.
Smith, R. 2002. GPR and EM Surveys to Detect and Map Peat and Permafrost: A Pilot Study. In: *Geophysics 2002, The 2nd Annual Conference on the Application of Geophysical and NDT Methodologies to Transportation Facilities and Infrastructure*. Federal Highway Administration, FHWA-WRC-02-001.
Spangler, L.E. 2002. Use of Dye Tracing to Determine Conduit Flow Paths Within Source Protection Areas of a Karst Spring and Wells in the Bear River Range, Northern Utah. In: Kuniansky, E.L. (ed.). *U.S. Geological Survey Karst Interest Group Proceedings*, Shepherdstown, West Virginia, Water Resources Investigations Report 02-4174. 75–80.
Stanton, G.P., and T.P. Schrader. 2001. Surface Geophysical Investigation of a Chemical Waste Landfill in Northwestern Arkansas. In: Kuniansky, E. (ed.). *U.S. Geological Survey Karst Interest Group Proceedings*, St. Petersburgh, Florida, February 13–16, 2001. U.S. Geological Survey. 107–115.
Stringfield, V.T., Rapp, J.R. and R.B. Anders. 1979. Effects of Karst and Geologic Structure on the Circulation of Water and Permeability in Carbonate Aquifers. *Journal of Hydrology*, 43, 313–332.
Styles, P., and E. Thomas. 2001. The Use of Microgravity for the Characterization of Karstic Cavities on Grand Bahama, Bahamas. In: Beck, B., and J. G. Herring (eds.). *Geotechnical and Environmental Applications of Karst Geology and Hydrology*. A.A. Balkema Publishers. 389–396.
Sweeting, M.M. 1973. *Karst Landforms*. Columbia University Press. 362.
Sweeting, M.M. 1973. *Karst Landforms*. Columbia University Press.
Tucker, M.E. 1981. Sedimentary Petrology: An Introduction. *Geoscience Texts Volume III*. John Wiley and Sons. 252.
Tucker, M.E., and V.P. Wright. 1990. *Carbonate Sedimentology*. Blackwell Science Publishing. 482.
U.S. Environmental Protection Agency. 2006. Website.
Vandike, J.E. 1982. The Effects of the November 1981 Liquid Fertilizer Pipeline Break on Groundwater in Phelps County, Missouri. Unpublished report on file with Missouri Department of Natural Resources, Division of Geology and Land Survey. 27.
Veni, G., et al. 2001. *Living With Karst: A Fragile Foundation*. American Geological Institute. 64.
Wallace, R.E. 1993. Dye Trace and Bacteriological Testing of Sinkholes Tributary to Sulphur Springs, Tampa, Florida. In: Beck, B.F. (ed.). *Applied Karst Geology*. A.A. Balkema. 89–98.
Waltham, T., Bell, F., and M. Culshaw. 2005. *Sinkholes and Subsidence*. Springer/Praxis Publishing. 382.
White, W. 1969. Conceptual Models for Carbonate Aquifers. *Groundwater*. 7(3).
White, W. 1977. Conceptual Models for Carbonate Aquifers: Revisited. In: Dilamarter, R.R. and S.C. Csallany. *Hydrologic Problems in Karst Regions*. Western Kentucky University. 176–187.
White, W. 1988. *Geomorphology and Hydrology of Karst Terrains*. Oxford University Press. 464.
White, W., and E. White. 2000–2001. Conduit Fragmentation, Cave Patterns, and the Localization of Karst Groundwater Basins: The Appalachians as a Test Case. *Theoretical and Applied Karstology*, 13–14, 9–23.
White, W.B. 2005. Hydrogeology of Karst Aquifers. In: Culver, D.C. and W.B. White (eds.). *Encyclopedia of Caves*, Elsevier. 293–300.
White, W.B. 2005. Springs. In: Culver, D.C. and W.B. White (eds.). Encyclopedia of Caves. Elsevier. 565–570.
Williams, P.W. 1972. Morphometric Analysis of Polygonal Karst in New Guinea. *Geological Society of America Bulletin*. 83, 761–796.

Williams, P.W. 1983. The Role of the Subcutaneous Zone in Karst Hydrology. *Journal of Hydrology*. 61, 45–67.
Williams, P.W. 2003. The Epikarst: Evolution of Understanding. In: Jones, et al. Epikarst, Special Publication 9. Karst Waters Institute. 8–15.
Williams, P.W. 2004. Dolines. In: Gunn (ed.). *Encyclopedia of Cave and Karst Science*. Fitzroy and Dearborn. 304–310.
Wilson, J.L. 1975. *Carbonate Facies in Geologic History*. Spring Verlag. 471.
Worthington, et al. 1992. Geochemistry of Springs in Temperate Carbonate Aquifers: Recharge Type Explains Most of the Variation. In: *Colloque d'Hydrologie en pays Calcaire et en Millieu Fissure (5th Neuchatel Switzerland), Proceedings*. Annales Scientifiques de l'Universitie de Besancon, Geologie—Memoires Hors Series, No. 11, 341–347.
Worthington, et al. 2000. Porosity and Permeability Enhancement in Unconfined Carbonate Aquifers as a Result of Solution. In: *Speleogenesis: Evolution of Karst Aquifers*. Klimchock, et al., (eds.). National Speleological Society, Inc. 463–471.
Worthington, et al. 2001. Characteristics of Porosity and Permeability Enhancement in Unconfined Carbonate Aquifers Due to the Development of Dissolutional Channel Systems. In: Present State and Future Trends of Karst Studies Proceedings. Gunay, G, Johnson, K, Ford, D, and A.I. Johnson, editors. *Technical Documents in Hydrology*, 1, 49, UNESCO, 13–29.
Worthington, S. 1991. *Karst Hydrology of the Canadian Rocky Mountains: Unpublished Ph.D. Dissertation*. Department of Geography, McMaster University. Hamilton, Ontario, Canada. 227.

This page intentionally left blank

Chapter

14

Tracer Tests—General

Marek Zaluski

MSE Technology Applications
Butte, Montana

A tracer test is a field method used in hydrogeology to quantify selected hydraulic or hydrochemical parameters. In its most common form, a tracer test is conducted by emplacing a defined quantity of traceable substance or a heat source within the aquifer and tracking it down hydraulic-gradient, where at certain points of space and time, its quantity is measured. This form of a tracer test can be viewed as a positive-displacement slug test or an injection test in which stress to the aquifer is delivered in the form of chemical substance or a heat source, rather than by injecting a known volume of water. Dissipation of such a stress with respect to time and the aquifer space provides a data set from which many hydrogeologic conditions may be concluded. Quantification of the groundwater flow direction and rate, aquifer porosity, anisotropy, dispersivity, retardation factor, and other physicochemical characteristics are the most common results of the tracer-test interpretation.

Other types of tracer tests deal with quantifying the dissipation of elements that naturally occur in groundwater and/or injection of certain substances that react with hydrocarbon contaminants, allowing determination of the contaminant concentration. These two types of tracer tests, as well as a large family of surface-water tracer tests (Chapter 6), are not discussed in this chapter.

Tracer tests, their objectives, theory, performance, and interpretation have been addressed in relatively broad literature. Information provided in this chapter is based on these sources as well as actual field experience of the author; it does not, however, aspire to be a handbook for all or any selected method or application. It summarizes practical guidelines for

Copyright © 2008, 2001 by The McGraw-Hill Companies, Inc. Click here for terms of use.

planning and performing tracer tests for common applications. For details on specific application and a comprehensive review of the subject, the reader is referred to the references included at the end of this chapter.

A particular importance reference is a 581-page book entitled *Tracing Technique in Geohydrology* by W. Käss (1998). This book seems to be the most comprehensive source of information on the tracer technology for groundwater and surface water, and includes approximately one thousand references on tracer tests and related topics.

14.1 Tracer Test Objectives

In many cases, a tracer test is part of site-characterization efforts. The appropriate tracer test procedure is selected depending on questions remaining after all other information has been collected. For example, if the dispersivity value is all that is needed, then a single-well tracer test may be performed. However, if the isotropic conditions of the aquifer are questioned, a more time-intensive tracer test, which may involve numerous wells, would need to be considered. Therefore, the kind of the tracer test that needs to be conducted depends upon its objectives as specified in Table 14.1.

For all methods, the retardation coefficient may be obtained if adsorptive and conservative tracers are injected simultaneously and the results compared. The only exception is a recirculating test, with the pumped water recirculated to the point-source.

14.2 Tracer Material

There are quite a variety of substances that may be used as tracers for groundwater investigations. Detailed information regarding these tracers and the application methods can be found in Davis (1985), Käss (1998) or other publications. Table 14.2 summarizes information on various tracers, but should not be used exclusively for the final selection of the trace material. Readers are encouraged to look for case studies that would include information on the use of the particular tracer in the given hydrogeologic setting. The statement "one size and kind fits all" is not applicable for the tracer test technology, as a tracer that might be excellent for certain geological conditions might be unusable for other subsurface environments as shown in the following example.

The Rhodamine WT dye was developed by DUPONT (Käss, 1998) especially for water, as signified by the WT (Water Tracer) abbreviation. This dye that has a reputation as one of the most conservative (minimal adsorption) tracers with a very low detection limit was successfully used in limestone—karstic environments and for some

TABLE 14.1 Most Common Tracer Tests for Groundwater Investigations

Test	Subcategory	Source duration	Information obtained	Hydraulic stress	Comments
Single well	Borehole dilution	Instantaneous	Flow direction, seepage velocity	Natural flow conditions	Special instrumentation needs to be installed in the well, e.g., thermistors
	Injection/pumping	Instantaneous	Seepage velocity dispersion coefficient	Injection period precedes pumping period	
Point-source/ one sampling well	Natural flow	Instantaneous or continuous	Seepage velocity dispersion coefficient	Natural flow conditions	Wells must be located at the same flow line
	Diverging test	Instantaneous	Porosity, dispersion coefficient	Injection in the point-source; sampling well is not pumped	
	Converging test	Instantaneous	Porosity, dispersion coefficient	Pumping from the sampling well; point-source well is not stressed	Pumping at discrete intervals enables vertical differentiation
	Recirculating test	Continuous	Porosity, dispersion coefficient	Both wells are stressed. Injecting well receives pumped water or "clean" water from other source	Tests a considerable larger portion of the aquifer, than a converging test
Point-source/ two sampling wells	Recirculating tests	Continuous	Porosity, dispersion coefficient, anisotropy	All wells are stressed. Injecting well receives pumped water or "clean" water from another source	
Point-source/ multiple sampling wells		Instantaneous	Flow direction, seepage velocity, anisotropy*	Natural flow conditions	

*Only if contours of hydraulic head are known

TABLE 14.2 Most Common Tracers Used for Groundwater

Tracer	Subcategory	Permeable medium	Detection		Advantages	Disadvantages	Comments
			Field method	Limit			
Ions						At high concentrations tend to sink	Anions are more conservative than cations
	Br^-	Any kind	Bromide electrode, Hach kit	1 ppm	(1) Low [<1 ppm] background concentration in ground-water (2) Very low toxicity (3) No MCL*	At low pH may be adsorbed by clay	(1) May be the most common tracer used (2) Common source: NaBr
	Cl^-	Any kind	Chloride electrode, Hach kit	1 ppm	Availability	High background concentration drinking water standard** = 250 ppm	Very conservative
	I^-	Any kind	Iodine electrode, Hach kit	1 ppm	Very low [<0.01 ppm] background concentration in ground-water	May be affected by micro-biological activity	Radioactive isotope of iodine was used as a radioactive tracer
Dyes		Perform best in fracture rock and karst					(1) Maybe the oldest tracer used (2) Less conservative than anions
	Fluorescein	Karst rock, clean sand, sandstone, basalt Works better in porous medium than rhodamine WT and eosine	Fluorimeter	0.3 ppb over back-ground	(1) Less expensive than other dyes (2) Visually detected if >40 ppm	(1) High natural background fluorescence (2) Adsorbs strongly to organic matter (3) Loses color at pH <6	Green opalescent color

	Rhodamine WT	Fracture and karst rocks	Fluorimeter	0.013 ppb over background	Low detection limit	(1) Biologically not as safe as fluorescein (2) May strongly adsorb to certain sediments	Red color
Radionuclides	^{131}I, ^{82}Br,	Any kind	Radiation meters	Extremly low	(1) Short half life [8 & 1.5 days] in comparison to other radionuclides (2) Very mobile	Despite the demonstrated safety, public perception, and regulations often prohibit the field usage of these tracers	Superior tracers
Heat		Any kind	Thermistors	0.05°C	Direct measure of groundwater flow direction		(1) Used in a single well (2) Feasible for multiwell tracer test, if a point or line sink of warm water is active for long time
Bacteria	Variety	High permeable media	None, requires laboratory procedure			(1) Regulatory concerns (2) Strain used must be mobile	Bacteria must be nonpathogenic
Virus	Variety	High permeable media	None, Requires laboratory procedure			(1) Regulatory concerns (2) May move faster than advection (preferential path due to large size)	Virus must be nonpathogenic

*MCL = Maximum contaminant level
**National secondary drinking water regulations

nonconsolidated porous deposits. However, its transition to sediments deposited between lava flows present in Idaho is an example of a mismatch of the tracer material and subsurface environment. After an unsuccessful series of tracer tests, batch tests were conducted to determine sorption and desorption isotherms for rhodamine WT, eosine and fluorescein to clastic sediments present between lava flows. The result of the investigation demonstrated that a Freundlich adsorption isotherm for rhodamine WT could be expressed by the following equation:

$$C_{ad} = 19.083 \times C_{aq}^{0.915} \tag{14.1}$$

where C_{ad} is rhodamine WT adsorbed by sediment (μg/kg) and C_{aq} is rhodamine WT present in solution (μg/L). A very high, 19.083, coefficient indicates that rhodamine WT was very strongly adsorbed to sediments, thus could not be considered a tracer. For comparison, the Freundlich adsorption isotherm for fluorescein was expressed as

$$C_{ad} = 0.535 \times C_{aq}^{0.890} \tag{14.2}$$

A coefficient 0.535 in Equation 14.2 indicates that fluorescein was a much better tracer than rhodamine WT as its retardation coefficient ranged from 3.65 to 1.64 for concentrations of 1.92 μg/L and 750 μg/L, respectively.

This example illustrates the importance of an appropriate match of a tracer with the given hydrogeological condition and/or tracer test objectives and the danger of making inadequately researched assumptions.

14.3 Design and Completion of Tracer Test

There are several components of a tracer-test procedure that, if considered, planned, and carefully implemented, will usually lead to a successful completion of the project. These are:

- Conceptual design
- Selection of the initial mass of the tracer or its concentration
- Point-source infrastructure
- Observation wells
- Sampling schedule
- Monitoring
- Equipment used

Conceptual design

This preliminary phase includes

- Review of site hydrogeologic information available
- Setting the objectives for the tracer test
- Selection of the kind of the tracer test to be conducted
- Selection of the tracer material and its cost evaluation
- Preliminary costing of a necessary infrastructure
- Assessment of operational costs

If the predicted expenses are within the available budget, the tracer concentration may be assessed in detail. Otherwise, it may be necessary to revise (limit) the objectives of the tracer test and choose a less expensive method as presented in Example 14.1.

Example 14.1

Initial Conceptual Design

Hydrogeologic information

A contaminated site in question is located between two perennial creeks. An unconfined aquifer beneath the site is formed in alluvial deposits. A 2-in diameter monitoring well is located in the center of the reported incidental gasoline spill and two 2-in diameter monitoring wells are located adjacent to each creek. There is no information regarding the site location with respect to the groundwater divide.

Objectives of the tracer test:

Determination of the flow direction at the spill location
Defining seepage velocity
Defining anisotropy ratio

Tracer test initially selected:

Point source (an existing central well) and multiple (six) sampling wells located in hexagonal pattern around the point source well.

Tracer material selected:

One kilogram of bromide provided as NaBr NaBr is available in 50 Lb bags @ $70 a bag	$ 70

Necessary infrastructure:

Six 2-in diameter observation wells @ $600	$ 3,600

Operational costs:

Technician 12 h @ $60	$ 720
Measuring equipment (bromide electrode and a meter)	$ 1,200
Miscellaneous expenses (containers, glassware, & incidentals)	$ 500

Total expenses	$ 6,900
Available budget	$ 4,000

The deficit of $2,900 could be offset by decreasing the number of observation wells from six to two. Such a reduction, however, would jeopardize the accomplishment of the three objectives for the tracer test. However, dropping the objective of anisotropy-ratio determination and changing the multiwell tracer test to a borehole dilution test would allow for achieving two remaining objectives within the budgetary requirements. Moreover, it would be possible to determine these parameters for three separate locations as demonstrated below.

Revised Conceptual Design

Objectives of the tracer test:

Determination of the flow direction at the spill location
Defining seepage velocity

Kind of tracer test:

Single well borehole dilution test

Tracer material selected:

Heat stress delivered by a down-hole instrument with a central heat electrode and six thermistors

Rental fee: @ $400 a field-day (shipment cost and time covered by vendor)	$ 400

Necessary infrastructure:

Three 4-in diameter test wells @ $900	$ 2,700

Operational costs:

Technician 9 h (3 h per well) @ $60	$ 540
Measuring equipment, included in the rental fee	
Miscellaneous expenses (incidental)	$ 300
Total expenses	$ 3,940

Selection of the initial mass of the tracer or its concentration

As stated in Table 14.1, a tracer can be introduced into the hydrologic system either in an instantaneous (slug) or a continuous manner. Depending on the type of the tracer test and the method of interpretation, either an initial mass of the tracer or its initial concentration needs to be considered to secure appreciable concentration of the tracer at the receptor point. For a continuous injection of a tracer, its initial concentration is to be evaluated. For an instantaneous placement, depending on the tracer test method, either the tracer mass or its concentration needs to be considered. An inherent contradiction of the successful tracer test is that it is necessary to assume the results of the tracer test before

it is actually conducted. To do so, the effect of the tracer dilution, dispersion, adsorption, and reactivity need to be preevaluated to predict the expected peak concentration at the receptor and to compare it with the detection limit and operational range of available instruments.

The peak concentration at the receptor point can be estimated by using an appropriate closed-form equation, which can be found, for instance, in Javandel et al. (1984), Sauty (1980), Bear (1979), Domenico and Schwartz (1990), and Freeze and Cherry (1979), or using a public domain program SOLUTE (a proprietary version compiled by Paul K.M.van der Heijde is distributed by International Ground Water Modeling Center) or any other solute transport model. In this process, an assumed mass or an initial concentration is plugged into an appropriate method, and the tracer concentration at the receptor can be calculated for the given time and at its maximum.

At this point, however, it is necessary to emphasize that spending extensive time for premodeling of a tracer test is usually not a good time investment. This is because there are too many unknown variables at that stage of the hydrogeologic investigation. Had those variables been known, there would not have been any need to conduct the tracer test. Nevertheless, a good match of the hydrogeologic conditions and the kind of the tracer test with the stipulations set for applicability of the given formula is of prime importance. For example, for a simple case of a two-well tracer test conducted at natural flow regime with a instantaneous release of the tracer, the following formulas may be used.

For a three-dimensional flow regime (Freeze and Cherry 1979):

$$C_{(x,y,z,t)} = \frac{M}{8(\pi t)^{3/2}\sqrt{D_x D_y D_z}} \exp\left(-\frac{X^2}{4D_x t} - \frac{Y^2}{4D_y t} - \frac{Z^2}{4D_z t}\right) \quad (14.3)$$

For a two-dimensional flow regime (Bear 1979):

$$C_{(x,y,t)} = \frac{M}{4\pi t\sqrt{D_x D_y}} \exp\left(-\frac{X^2}{4D_x t} - \frac{Y^2}{4D_y t}\right) \quad (14.4)$$

For a one-dimensional flow regime (Bear 1979):

$$C_{(x,t)} = \frac{M}{2\sqrt{\pi D_x t}} \exp\left(-\frac{X^2}{4D_x t}\right) \quad (14.5)$$

In Equations 14.3, 14.4, and 14.5:

C = Contaminant concentration at location x, y, z at time t (M/L^3, M/L^2, M/L) for three-, two-, and one-dimensional flow, respectively, where

L is the linear dimension

x, y, z = Coordinates (L) of the receptor with respect to the point source

M = Mass (M) of contaminant introduced at the point source—It can be expressed as the product of initial concentration C_0 and initial volume V_0.

t = Time elapsed (t) from the instantaneous injection of the tracer.

D_x, D_y, D_z = Dispersion coefficient (L^2/t) in longitudinal, transversal, and vertical (transversal in the vertical plane) direction, respectively

X, Y, Z = Distance (L) to the receptor from the center of gravity of the contaminant mass

For the specific case where the point source and the receptor are at the same flow line, the position of the center of gravity of the contaminant mass at time t will lie along the flow path in the x direction at coordinates x_t, y_t, z_t (L). Consequently $y_t = z_t = 0$, but $x_t = vt$ where $v(L/t)$ is the average velocity (seepage velocity) and n (dimensionless) is the effective porosity. Thus, in Equation 14.3, 14.4, and 14.5, $X = x - vt$ and Y, Z = zero.

Formulas 14.3, 14.4, and 14.5 are valid for calculation of the tracer concentration until it reaches its maximum (the rising limb of the bell-shaped curve). Thus, they may be used for prediction of the time for first arrival of the tracer at the receptor point. Certain modification of the definition for the time term (t) is needed to have these formulas valid for times longer than this, which correspond to the maximum concentration.

For the prediction of the maximum concentration (C_{max}) at the receptor point, that is, when $x = vt$ and consequently $X = 0$, these formulas simplify to contain only their first member. Such formulas reflect a condition that for a nonreactive transport the maximum concentration of tracer coincides with the time t, which equals an advective travel time from the injection source to the receptor point. For a two-dimensional flow, the maximum concentration at the receptor point is expressed as:

$$C_{(\max)} = \frac{M}{4\pi t\sqrt{D_x D_y}} \tag{14.6}$$

An example of a spreadsheet for prediction of the maximum concentration of a tracer at the receptor point is presented in Example 14.2. For the tracer-test configuration as defined in the spreadsheet, the maximum concentration of 116.7 mg/L will be recorded after 1.93 days in the monitoring well located 12 ft from the point source. Using the same spreadsheet, one can calculate that the maximum concentration in a well located twice as far, that is, at the distance of 24 ft, would be only 29 mg/L and would be recorded after 3.86 days.

Example 14.2 Spreadsheet software can be used to estimate maximum solute concentration at the receptor (two-dimensional, advective-dispersive transport, and instantaneously released tracer at natural hydraulic gradient). The following information is entered in the spreadsheet cells, represented by the table shown in this example:

hydraulic conductivity [ft/day]

*d*20 [mm] if used to estimate hydraulic conductivity

effective porosity [dimensionless fraction]

distance [ft] between the injection and receptor points

hydraulic gradient [dimensionless fraction]

hydraulic head (*H*) difference [ft] at the injection and receptor locations if used for hydraulic gradient calculation

tracer mass [mg]

tracer initial concentration [mg/L] and volume of water injected with tracer [L] if used for calculating mass of the tracer

Assumptions:

Injection and receptor points are on the same flow line.

Lateral extent of the aquifer does not limit transversal spread of the tracer.

Longitudinal dispersivity is 0.1 of the distance between the injection and receptor points.

Transversal dispersivity is 0.01 of the distance between the injection and receptor points.

Hydraulic conductivity (*K*) may be estimated based on sieve analysis using the U.S. Department of Agriculture formula:

$$K = 0.36 \times d20\text{^}2.3 \text{ cm/s} \tag{14.7}$$

where *d*20 = Particle diameter (mm) that together with smaller particles constitutes 20% of weight of the sample

Hydraulic conductivity value	91.23 ft/day
*d*20	0.35 mm
K	0.03 cm/s 91.23 ft/day
Effective porosity	0.25
Distance from injection point	12 ft
Hydraulic gradient	0.02
Del *H*	0.20 ft
Calc. hydraulic gradient	0.02
Tracer mass, *M*	10,000 mg
Co	5.000 mg/L
Vo	2.00 L
M	10,000 mg

Formula:

$$C\text{max} = M/[4 * \text{PI} * t * (DxDy)\text{^}0.5 * 9.29] \tag{14.8}$$

where $C\text{max}$ = maximum concentration at the receptor point [mg/dec^2, an equivalent of mg/L for 3-D flow]
Co = tracer initial concentration [mg/L]
Vo = volume of injected water with the tracer [L]
t = travel time for advective flow from the injection point to the receptor point [d]
Dx = coefficient of hydrodynamic dispersion in direction X [ft^2/day]
Dy = coefficient of hydrodynamic dispersion in direction Y [ft^2/day]
9.29 = conversion factor from ft^2 to dec^2

Calculation

v = 6.20 ft/day
t = 1.93 days
Dx = 1.20 ft^2/day
Dy = 0.12 ft^2/day
$C\text{max}$ = 117 mg/dec^2

After the initial mass of the tracer or its concentration is calculated, it needs to be reevaluated with respect to uncertainty of the values used for calculation. It is common to use a safety factor and increase the calculated initial concentration or its mass one order of magnitude for tracer tests that will involve hydraulic stress at the point source or at the observation well. Depending on hydrogeologic conditions, a safety factor of 1,000 may be used for tracer tests that are conducted under the natural hydraulic gradient of groundwater. Conversely, a recirculating tracer test is the least vulnerable to miscalculations of the initial concentration.

There are two main reasons for using a safety factor:

- Intensive and costly efforts may be undertaken for tracer test preparation and its monitoring. Thus, it is hardly possible to imagine a more embarrassing scenario than the one with a no-show of the tracer at the receptor point.
- It is practically impossible to repeat the tracer test after an apparent failure of an earlier attempt and still have confidence regarding the origin of detected concentration of the tracer at the receptor point. Either a long time (relatively to the seepage velocity) has to separate two attempts or the second tracer needs to be different.

Point-source infrastructure

Injection wells. In most cases, a tracer is introduced to the hydrogeologic system using an injection well. Construction requirements for such a well depend on the source duration.

For a continuous injection of the tracer a well should have some characteristics similar to a pumping well, that is:

- The well needs to have an appropriate transmitting capacity to accommodate the designed injection rate without excessive well loss.
- Its screen should not straddle the water table, otherwise water will be injected directly to the unsaturated zone.

Conversely, if a tracer is to be injected between two packers that are placed within the screened interval, the well must not be gravel packed and it should be poorly developed to disallow a shortcut of water through the gravel pack back to the well.

One also needs to realize that for an unconfined aquifer, even if the screen does not straddle the water table, mounding of groundwater will occur. Therefore, the injection rate should be slow enough to accommodate the mass injected. Groundwater mounding might affect the dynamics of the tracer test, especially at the beginning when the transient phase groundwater "invades" the vadose zone whose hydraulic conductivity is always lower until it reaches full saturation (Chapter 12). This is one of the reasons why, for a recirculating test with a continuous tracer injection, the tracer should not be introduced to the system until a steady-state flow is approached.

For most tracer tests with an instantaneous release of the tracer, the injection well should be designed so that:

- Its screened interval and its diameter are large enough to allow for placement of the tracer solution as one slug. Otherwise, the requirements of the instantaneous release will not be satisfied.
- Its screened interval and its diameter are small enough to disallow or minimize the effect of dilution of the tracer in the well before it enters the aquifer.
- Its construction allows for placement of the tracer with no or minimal changes in the natural flow regime in the aquifer. Otherwise the requirement of point-source release will not be satisfied, and the calculated values will include additional errors. For instance, values of transversal dispersivity in horizontal and vertical planes will be exaggerated. Needless to say, this requirement is not important for a single well–injection/extraction test or the diverging test for which a radial flow pattern is a designed feature.
- Its screened interval coincides with the section of the aquifer to be tested by the tracer test.
- The screen has high transmitting capacity, and the well is well developed (Chapter 8).

A design that satisfies the above requirements would allow for placing in the well a tightly fitting and closed container with the entire volume of the tracer. After the natural flow regime has recovered, that

is, the water table in the well has returned to its initial level, the bottom valve is opened and the container removed from the well exposing the tracer to a screened portion of the well. This method of releasing a tracer to a hydrogeologic system is especially recommended for a test that is conducted at natural flow conditions.

For such a case, a common recommendation of "pushing" the tracer by injecting a three-well-volume slug of clean water is in error. If a well is screened over the tested interval, the tracer does not need to be "pushed" out of the well, because it will leave the well itself being "pushed" by the flowing groundwater that actually converges in the well. The convergence is caused by the principle of streamlines refraction (tangent law) at the interface of the aquifer material and a circular object, the well, of an infinite hydraulic conductivity. Specifically, twice as much of the groundwater will flow horizontally through a circular cross section of the well than through an equally wide section of the aquifer.

Sometimes, however, in a real field situation, some of the above recommendations are difficult to implement and the tracer test is conducted with several simplifications, as described in Example 14.3. While analyzing the results of such a test, it is necessary to limit the conclusions to only those whose correctness was not jeopardized by the deficiencies of the field procedure.

Example 14.3 A tracer test was conducted as an experiment to see whether a forced gradient setting (the hydraulic stress) could mobilize a NaBr tracer approximately 15 ft from an injection point toward a pumping well. The pumping well was pumped at a constant rate of 5 gpm (18.9 L/min) for 2.5 h prior to the introduction of a NaBr solution. The solution was mixed in a 13-gal (49-L) container and pumped via a peristaltic pump over a period of 1 h and 45 min (Figure 14.1). The solution was released at the screen depth and was supposed to be observed at the pumping well at some time in the future.

Figure 14.1 Delivery of bromide trace via a peristaltic pump.

The concentration of the solution at the pumping well was desired to be approximately 100 mg/L. An estimate of the starting concentration was devised through a simplified version of a pie approach (Domenico and Robbins 1985). The starting concentration at the pumping well was assumed to be 0 mg/L, and the starting concentration at the injection point was the unknown. The pumping rate (Q) was 5 gpm, and the proportion of the contributing Q for the pie shaped area near the injection point was estimated by assuming that it would take 1 h to pump in the 13-gal (49-L) solution. The mixing equation was used to estimate the unknown initial concentration to be used in the field test. Schematically this is illustrated in Figure 14.2.

Because of unavailability of a bromide electrode in the field, the pH electrode was used instead. Standards were made up in the lab in mg/L and brought out into the field (Figure 14.3). Table 14.3 lists the values measured in the field.

The injection solution was estimated to be near 2,300 mg/L. The effluent discharge remained at pH 7.05 for 2 1/2 h, and it occurred to the participants that it could take many hours before the plume moved 14.9 ft. Thus a piezometer was hand-drilled along the pathway at a distance of 6.9 ft from the injection point, and a reading of pH = 8.36 was obtained at 3 h. The gradient was 4/15, the effective porosity was assumed to be 0.15, and the movement 7 ft in 1/8 of a day yielded a seepage velocity of 56 ft/day. The hydraulic conductivity was calculated to be 31 ft/day. This correlated well with estimates from constant discharge pumping tests, yielding an estimate between 25 and 40 ft/day.

Nonwell injections. In special cases like investigating surface water/groundwater relationship or groundwater recharge conditions, it is necessary

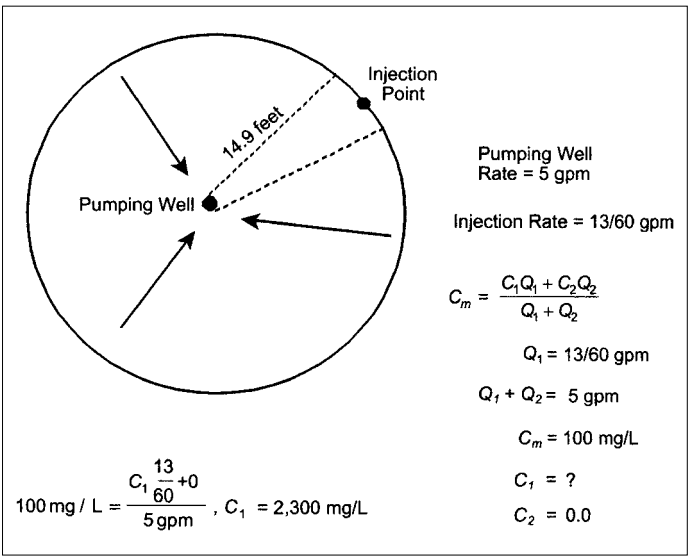

Figure 14.2 Schematic of forced gradient tracer test, showing initial concentration calculations.

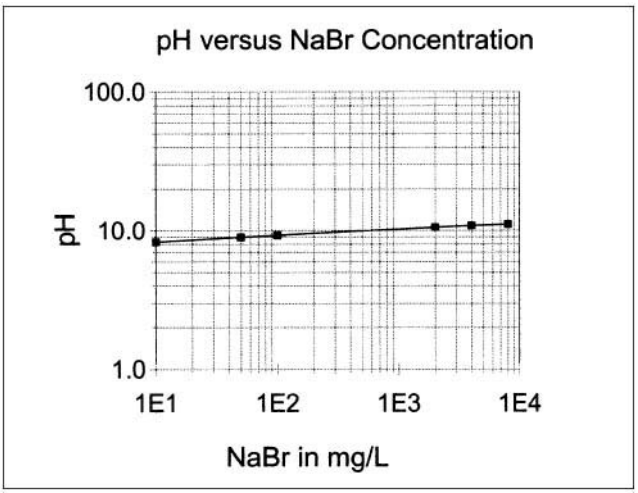

Figure 14.3 Plotted field measurements from Table 14.3.

to introduce a tracer at the location where the recharge is assumed to take place (Chapter 6). In many cases, especially in areas with well-developed morphology, it is a body of surface water that recharges groundwater system. An example of such a case may be a stream, flowing through a karst area, that may be losing a portion of its water through a sinkhole located in the stream bottom. Another case might be an artificial pond created either for landscaping or industrial purposes. In such situations, there is hardly a standard method for emplacement of the tracer, leaving investigators to their own inventiveness. This is illustrated in Example 14.4.

Example 14.4 The photograph in Figure 14.4 depicts the emplacement of the bromide tracer in a flow-through settling pond located on the top of a waste rock pile accumulated in front of an adit of the abandoned mine. The pond contained relatively good quality water. The water balance of that pond indicated that approximately 10% or 2 gpm of water flowed through the pond leaks and through the pond bottom to presumably reappear at the toe of

TABLE 14.3 Field Measurements for Example 14.3

Concentration NaBr in mg/L	pH units (10^{-n})
Distilled water	7.09
10	8.27
50	8.97
100	9.26
Solution	10.64
4000	10.93
8000	11.18

Figure 14.4 Placing a bromide tracer in a flow-through settling pond.

the rock pile heavily contaminated (enriched) with heavy metals. To confirm and quantify this stipulation, a tracer test was conducted using bromide as the tracer. The following procedure was used to emplace the bromide.

The required initial concentration of bromide (Br) in the pond was determined as 2,000 mg/L. Depth of the pond was surveyed, and volume of water in the pond was determined to be 46,550 L (12,300 gal). Thus, 93 kg (205 lb) of bromide was needed for the tracer test. This amount of bromide was provided in 120 kg (264 lb) of dry sodium bromide (NaBr). Mine water usually flowing into the pond was diverted, and the outflow was dammed to create a standing body of water in the pond.

Dry NaBr, 120 kg (264 lb), was dissolved in a plastic container to make 465 L (123 gal) of solution that contained 258 g/L of NaBr, an equivalent of 200 g/L of Br. This solution had a specific gravity of 1.193. A battery-powered, boat-trolling motor was used to mix dry NaBr in the container with water.

A 50-ft length of 1.5-in diameter hose was attached to the bottom of the NaBr solution container. The other end of the hose was extended to a small pontoon floating on the pond. A trolling motor was attached to the pontoon to be used for mixing NaBr solution in the pond water. Ropes were attached to the pontoon, so that two people standing on the shore could pull the pontoon across and along the pond.

Another person boarded the pontoon and directed the outlet of the hose with gravity-flowing bromide solution to the propeller of the trolling motor, while the pontoon was dragged back and forth across the pond. This procedure provided good 1:100 mixing of the bromide solution with water in the pond, preventing stratification of the heavy bromide solution in the bottom. Upon mixing, samples of pond water were collected, and the concentration of bromide was checked using a bromide electrode.

An approximately 2,000 mg/L bromide solution was left in the pond to leak through its bottom. After four days, approximately 90% of the pond water

leaked through its bottom, and the natural flow condition through the pond was restored to maintain constant hydraulic head over the moving tracer.

Observation wells

For a recirculating tracer test, a sampling well should have some characteristics similar to a pumping well to accommodate required discharge. For all other tracer tests, the diameter of a sampling well should be small to minimize the effect of the dead water residing in the well above the sampling interval. More important, however, is to screen the well over the entire investigated interval and have no blank casing (sump) below the screen (Chapter 8).

Sampling schedule

The sampling schedule is usually a by-product of the preliminary calculation of the tracer's initial concentration. Theoretically, first sampling should be scheduled for the calculated time of arrival of the front portion of the dispersed tracer. Then, the sampling and measurements of the tracer concentration need to be continued until the tracer test is terminated. For a continuously injected tracer, the test may be terminated when there is no change of the tracer concentration as measured in the real time at the receptor point. For an instantaneously injected tracer, which should yield a bell-shaped curve of the concentration versus time, it is best to terminate the test when the measurements are again close to the detection limit.

Prediction of the time for an earliest sampling may be done using Equations 14.3, 14.4, 14.5, or other formulas whose applicability match a configuration of the given test. A spreadsheet for determination of the tracer concentration versus time for a two-dimensional flow at natural hydraulic condition is given in Example 14.5. In this case, because of an assumption that the point source and the receptor point are placed at the same flow line, Equation 14.4 simplifies to:

$$C_{(x,y,t)} = \frac{M}{4\pi t\sqrt{D_x D_y}} \exp\left(-\frac{x^2}{4D_x t}\right) \tag{14.9}$$

This simplification is possible because $Y = y = 0$, as explained earlier in this chapter, and there is no movement of the tracer with respect to the y coordinate, except for the transversal dispersion. Example 14.5 uses the same tracer-test configuration assumed for Example 14.2. The final result of the calculation shown in Example 14.5 is a predicted time for the first measurable record of the tracer at the receptor point if the instrument detection limit is 0.005 mg/L. This time of arrival is 0.21 day. Maximum concentration of 116.7 mg/L will be recorded at 1.93 days.

Example 14.5 Spreadsheet software can be used to predict the tracer concentration versus time (two-dimensional, advective-dispersive transport, and instantaneously released tracer at natural hydraulic gradient). The following information is entered in the spreadsheet cells, represented by the table shown in this example:

Limitation: Values are calculated for a valid time (t) not greater than the time ($t$max) corresponding to the maximum concentration.

Time (t) [day] for the calculated concentration of the tracer

Hydraulic conductivity [ft/day]

$d20$ [mm] if used to estimate hydraulic conductivity

Effective porosity (dimensionless fraction)

Distance (x) [ft] between the injection and receptor points

Hydraulic gradient (dimensionless fraction)

Hydraulic head (H) difference [ft] at the injection and receptor locations if used for hydraulic gradient calculation

Tracer mass [mg]

Tracer initial concentration [mg/L] and volume of water injected with tracer [L] if used for calculating mass of the tracer

Assumptions:

Injection and receptor points are on the same flow line.

Lateral extent of the aquifer may not impact transversal spread of the tracer.

Longitudinal dispersivity is 0.1 of the distance between the injection and receptor points.

Transversal dispersivity is 0.01 of the distance between the injection and receptor points.

Instrument detection limit is 0.005 mg/L.

Hydraulic conductivity (K) may be estimated based on sieve analysis using the U.S. Department of Agriculture formula:

$$K = 0.36d20\text{^}2.3 \text{ cm/s} \tag{14.10}$$

where $d20$ = particle diameter (mm) that together with smaller particles constitutes 20% of weight of the sample

time (t)	0.21 day
Hydraulic conductivity value	91.23 ft/day
$d20$	0.35 mm
K	0.03 cm/s 91.23 ft/day
Effective porosity	0.25
Distance from injection point	12 ft
Hydraulic gradient	0.02
Del H	0.20 ft
Calc. hydraulic gradient	0.02
Tracer mass, M	10,000 mg
Co	5,000 mg/L
Vo	2,00 L
M	10,000 mg

Formula:

$$Ct = M/[4 * \mathrm{PI} * t * (Dx * Dy)\text{^}0.5 \times 9.29] \exp(-X\text{^}2/(4 * Dx * t * 9.29)) \quad (14.11)$$

where Ct = concentration of the tracer at the receptor point at time (t) [mg/dec^2, an equivalent of mg/L for 3D flow]
Co = tracer initial concentration [mg/L]
Vo = volume of injected water with the tracer [L]
t = time for calculated concentration of the tracer at the receptor point [d]
Dx = coefficient of hydrodynamic dispersion in direction X[ft^2/day]
Dy = coefficient of hydrodynamic dispersion in direction Y[ft^2/day]
9.29 = conversion factor from ft^2 to dec^2
$X = x - vt$

Calculation

Seepage velocity	v = 6.20 ft/day
	X = 10.70 ft
Max. concentration time	$t$max = 1.93 days
	Dx = 1.20 ft^2/day
	Dy = 0.12 ft^2/day
	Ct = 0.005 mg/dec^2, for t = 0.21 day

The time of arrival calculated in Example 14.5, however, needs to be adjusted (shortened) proportionally to the uncertainty of dispersivity values used for calculations. The frequency of measurements may also be determined through preliminary calculation to ensure that a reasonably smooth curve can be obtained.

Monitoring

Results of the tracer test must be monitored at real time as soon as a sample is collected. The monitoring equipment used depends on the kind of tracer. For instance, for dye tracers, a fluorimeter is required; for a radioactive tracer (currently very seldom used), an appropriate radiation meter is used. If bacteria are used as a tracer, it is necessary to provide an appropriate analytical field kit. Unfortunately, field kits for bacteria are notorious for unreliable performance.

For most popular tracers like bromide or iodine, a single ion electrode is commonly used. Such electrodes have certain operational range, usually starting from one part per million (ppm), and a very specific calibration procedure. If several samples a day are collected, an electrode must be calibrated at least twice a day, otherwise an electrode drift may remain unnoticed. It is a common mistake to save little time for a field calibration of the measurement instrument, only to end up spending excessive time later during the data-reduction process for removing a guesstimate drift portion of the field measured values.

Maintaining detailed notes of the recorded noise (i.e., measurements below the detection limit) is also strongly recommended especially for tracer tests with multiple observation wells and large vertical component of hydraulic gradient. It happened once to the author that the flow direction was traced only by recording consistent noise at one of many observation wells.

Equipment

Equipment used for a tracer test depends of the procedure used. The least equipment-intensive tracer tests are those conducted at natural flow conditions. Conversely, recirculating tracer tests usually include a lot of equipment that amplify proportionally to the rate of recirculated fluid. Figure 14.5 depicts a setup for a recirculating tracer test conducted with two sampling/extraction wells and an injection well operated at 7-gpm injection rate over a 4-day period. Two 1,000-gal tanks, electrical mixers, a battery of flowmeters, submersible and centrifugal pumps, and the like, were used for this project, which included needs for anisotropy ratio determination. The list of equipment may include the following.

General equipment

- First-aid kit
- Safety gloves
- Safety goggles
- Emergency telephone

Figure 14.5 Setting up equipment for a recirculating tracer test.

- Weather radio
- Good supply of paper, notebooks, and pencils
- Paper towels
- String, duct tape, and insulation tape
- Measuring tape
- A kit with pH, specific conductance and temperature meters and probes
- Shelter for rainy or hot weather (e.g., a pickup with a topper)

Tracer-test implementation equipment

- Appropriate amount of a tracer
- Material safety data sheet (MSDS) of the tracer used
- Tarp or waterproof boxes to store supply of a tracer (if continuous injection)
- Weighing scale to weigh bulk tracer while preparing the tracer solution
- Containers for preparing and storing the tracer solution
- Stir or mechanical mixer for tracer solution preparation
- Calibrated bucket for discharge measurements, if applicable
- Flowmeters (for a recirculating tracer test)
- Submersible pumps (for a recirculating tracer test)
- Centrifugal pumps for transfer tracer solution (for a recirculating tracer test)
- Hoses and valves
- Generator, if applicable
- Data logger with pressure transducers (for recirculating tracer test)
- Water-level indicator E-tape (Chapter 5)
- Stopwatch
- Alarm clock
- Good source of light for night sampling
- A tool box with tools appropriate for the infrastructure used

Tracer test monitoring equipment

- Measuring instrument(s) for monitoring of tracer concentration
- Instruments' instruction manuals

- Weighing scale for preparation of a set of calibration solutions
- Calibrated cylinders and pipettes for preparing calibration solutions
- Tissues for blotting electrodes, etc.
- Deionized water
- An icebox with ice for cooling calibration solutions if temperature-sensitive
- A propane/butane stove for heating water to warm calibration solutions if temperature-sensitive
- Bottles (containers) to store calibration solutions
- Bottles (containers) to store and keep electrodes hydrated between measurements
- Boxes with lids to store measuring equipment and calibration solutions between measurements
- Forms for keeping records of instruments calibrating
- Forms for recording measurements
- A laptop computer with a spreadsheet allowing real-time plotting of the concentration curve

14.4 Common Errors

A tracer test justifies the expression "those who do nothing make no errors." A variety of tracer-test procedures, tracer-test materials, and diversity of hydrogeologic conditions make each tracer test a unique task for which no standard operating procedure exists. It is thus inevitable that mistakes will be made despite all efforts undertaken to avoid them. The key issue is to minimize the number of mistakes. Some common field errors are listed below.

- The receptor was located too far from the injection point.
- Monitoring of the tracer test was terminated prematurely because:

  Assumed effective porosity was too low.
  Assumed hydraulic conductivity was too high.
- Monitoring of the tracer started too late because:

  Assumed effective porosity was too high.
  Assumed hydraulic conductivity was too low.
- Measured concentrations were too low to be used for quantitative interpretation because:

  Dispersivity values were underestimated.
  Tracer was less conservative than expected.

Ratio of anisotropy and/or principal directions of anisotropy were "misevaluated."
Location of the receptor was incompatible with the actual flow pattern.
Vertical component of hydraulic gradient was neglected or "misevaluated."
Instrument detection level was too high.

- A continuous-injection tracer test was initiated before steady-state conditions for flow had been established.
- Emplacement of the tracer significantly altered natural flow conditions while the conditions supposed to be undisturbed.
- Calibration check of the instruments used for measuring tracer concentrations at the receptor point were not frequent enough.

Errors committed during the test design or its result interpretation are usually related to inappropriate match of the formula or the method used with the hydrogeologic setting or the tracer test conducted. An example of such an error would be using a formula developed for a three-dimensional flow to design a tracer test in a shallow flow system with a long distance between injection and receptor points.

References

Bear, J., 1979. *Hydraulics of Groundwater*. McGraw-Hill, New York.
Davis, S.N., Cambell, D.J., Bentley, T.J, Flynn T.J., 1985. *Ground Water Tracers*. National Water Well Association. National Ground Water Association, Westerville Ohio.
Domenico, P.A., and Robbins, G.A., 1985. A New Method of Contaminant Plume Analysis, *Ground Water*, Vol. 23, No. 4, pp. 476–485.
Domenico, P.A., and Schwartz, F.W., 1990. *Physical and Chemical Hydrogeology*. John Wiley & Sons, New York.
Freeze, R.A., and Cherry, J.A., 1979. *Groundwater*. Prentice-Hall, Upper Saddle River, NJ.
Javandel, I., Dughty, C., Tsang, C.F., 1984. *Groundwater Transport: Handbook of Mathematical Models*. American Geophysical Union. Water Resources Monograph Series 10. American Geophysical Union, Washington, DC.
Käss, W., 1998. *Tracing Technique in Geohydrology*. A.A. Balkema/Rotterdam/Brookfile.
Sauty, J.P., 1980. An Analysis of Hydrodispersive Transport in Aquifers. *Water Resources Research*, Vol. 16, No. 1, pp. 145–158.
van der Heijde, P.K.M., 1997. *Solute, Analytical Models for Solute Transport in Ground Water*. IGWMC-BAS 15, International Ground Water Modeling Center, Colorado School of Mines, Golden, CO.

Chapter

15

Tracer Tests—Dye

Thomas Aley

Ozark Underground Laboratory
Protem, Missouri

15.1 Utility of Groundwater Tracing

Groundwater tracing is a fundamental tool for hydrogeology work in karst areas and in many fractured rock settings. Tracing agents, and particularly fluorescent tracer dyes, have a well established track record for demonstrating flow directions and travel times from both surface and subsurface points to wells, springs, and surface streams fed by groundwater. Fluorescent dyes have also been used to trace water through talus and landslide debris, glacial deposits, through permeable zones in earth-fill dams, and into and through both active and abandoned mines. Dyes are also used to trace inflow into pipes (infiltration) and leakage out of pipes (exfiltration).

At waste sites tracer dyes have demonstrated connections and travel times between contaminant source areas and monitoring and recovery wells (Figure 15.1). They have been introduced into aquifers immediately prior to the addition of groundwater remediation compounds to delineate the portion of the aquifer that will be affected and to characterize travel times. At sites where hazardous waste leaks have been discovered and repaired the tracer dyes have been used to demonstrate that the repaired leaks can account for all monitoring wells where contaminants of concern have been detected. They are also used to verify the credibility of groundwater modeling at waste sites.

Groundwater tracing with fluorescent tracer dyes has been used to delineate groundwater protection zones for municipal wells and to help

Copyright © 2008, 2001 by The McGraw-Hill Companies, Inc. Click here for terms of use.

Figure 15.1 Dye introduction into a shallow trench dug to bedrock. Solvents had previously been dumped on the ground in this area. Dye infiltrating through the trench was subsequently detected in 13 monitoring wells and piezometers and at two off-site groundwater monitoring stations about 4,000 ft (1219 m) from the dye introduction trench.

delineate Zones of Influence for quarries pumping appreciable quantities of groundwater. They have also been used to delineate the recharge areas for caves, springs, and wetlands that provide habitat for threatened and endangered aquatic species and to help assess the potential impacts of proposed road construction and timber harvest on groundwater systems supplying water to salmon and trout streams.

With modern analytical equipment and protocols the detection limits for the more useful tracer dyes are in the parts per trillion range. Successful groundwater traces can be conducted with even smaller concentrations of dye by using activated carbon samplers that adsorb and accumulate tracer dyes until those dyes are eluted from the activated carbon in the laboratory. These samplers will be discussed under the Section 15.6 “Sampling and Analysis for Dyes.”

A wide range of tracing agents in addition to fluorescent dyes has been used. These have included soluble salts, radioactive isotopes, sulfur hexafluoride, and minute biological agents including bacteriophage and *Lycopodium* spores. Kass (1998) provides an excellent compendium of information on almost every tracing agent ever used in groundwater tracing. However, this chapter places primary emphasis on tracer dyes since the author estimates that about 90% of all professionally directed groundwater traces in the United States have used these dyes and the use of these tracers is simple, practical, and routinely effective. Tracer dyes in the amounts used for professionally directed groundwater tracing work do not pose health or environmental risks that should limit or preclude their use (Field et al. 1995; Smart 1984).

Three basic questions commonly encountered in groundwater hydrology are:

- Where does the water go?
- How long does it take to get there?
- What happens along the way?

Tracing agents are very good for answering the first two questions and in some cases they can address the third question. For example, *Lycopodium* spores have a mean diameter of 33 microns and vary only slightly from this mean size. The spores are an order of magnitude larger than many pathogenic bacteria, so if spores can be traced through a groundwater flow route one can credibly conclude that smaller bacteria could also be transported through the same flow route. As another example, fluorescein dye experiences less adsorption onto soil particles than the commonly used herbicides Alachlor and Atrazine, but these herbicides experience more adsorption onto soils than does rhodamine WT dye (Sabatini 1989). One could thus use these dyes to bracket the performance of these herbicides in an aquifer.

Much hydrogeologic work is based on equations and calculations that presume homogeneous and isotropic groundwater conditions. Tracers are particularly useful where these conditions are not met or may not be met. In karst and fractured rock aquifers modeling premised on presumed homogeneous and isotropic conditions can yield estimates of travel times that are orders of magnitude in error, and these errors can have serious implications as indicated in Example 15.1.

Example 15.1 Walkersville, Maryland, is underlain by a limestone aquifer. A well field with three municipal wells supplies public water. As part of a wellhead protection study, the aquifer was modeled and lines were drawn on maps indicating 5- and 10-year "time of travel" borders. City officials were concerned that the delineations might be substantially in error and funded

a groundwater tracing investigation to verify or refute the credibility of the time of travel modeling. One dye introduction made almost on the 5-year time of travel line reached town wells in less than 17.5 h. A few years after the groundwater tracing work a construction accident resulted in a release into the groundwater system of 900,000 gal of raw municipal sewage (Figure 15.2). Based on the previous mathematical modeling the travel time to wells from the spill area would have been approximately 8 years. Bacterial sampling and tracer dye introduced at the spill site showed that the actual travel time for first arrival of bacteria and dye at the wells was between 4 and 5 days. Fortunately, because of the earlier dye tracer study, the city responded immediately to the spill and took effective and comprehensive actions to obtain alternate emergency water supplies and protect their residents. There were no resulting cases of waterborne illness. The lesson for the hydrogeologist is that the assumptions of uniformity used in the modeling were inappropriate for a soluble rock aquifer and resulted in travel rate estimates that were two to three orders of magnitude too low.

Fractured rock aquifers commonly provide preferential flow routes where travel rates are substantially greater than estimated by groundwater modeling. A tracer test (hereafter referred to as trace) conducted by the author in fractured basalt over a distance of several hundred feet from an injection well to a recovery well resulted in the first arrival of dye within 20 min of introduction. Modeling had predicted first arrival times of 20 to 28 days, a travel rate three orders of magnitude too slow. While this and the Walkersville cases may be extreme examples they illustrate the utility and necessity for tracer studies in aquifers where preferential flow routes exist or are likely to exist.

Figure 15.2 Site of the Walkersville Maryland sewage spill. Fluorescein dye was introduced into the pit in the foreground. It was first detected between 4 and 5 days later in the Walkersville municipal well field about 5,300 ft (1615 m) from the spill site.

15.2 Characteristics of Ideal Tracing Agents

The following list of characteristics of ideal tracing agents is slightly modified from Ford and Williams (1989, p. 229). To be suitable for groundwater tracing artificial tracers should be:

- Nontoxic to the handlers, to the ecosystem, and to potential consumers of the labeled water
- Soluble in water with the resulting solution having approximately the same density as water
- Neutral in buoyancy and, in the case of particulate tracers, sufficiently small to avoid excessive losses by natural filtration
- Unambiguously detectable in very small concentrations
- Resistant to adsorptive loss, cation exchange, photochemical decay, and quenching by natural effects such as pH change and temperature variation
- Susceptible to quantitative analysis
- Quick to administer and technologically simple to detect
- Reasonably inexpensive and obtainable

Few tracers fully satisfy all of these criteria, but several do to a significant extent or can be used in such a manner as to overcome limitations. The absence of toxicity is a very important characteristic, and this requirement is adequately met by the principal fluorescent tracer dyes used in groundwater tracing work.

15.3 Common Misconceptions about Tracer Dyes

One common misconception is that dyes may be harmful or that large amounts of dye must be used and that this will visibly color water throughout an area. There is extensive technical literature (such as Field et al. 1995 and Smart 1984) demonstrating that the dyes discussed in this chapter present no health or environmental problems at concentrations five orders of magnitude or more above the detection limits of modern analytical protocols. Dye tracing does not require large quantities of dyes, and the dyes are not harmful in the amounts needed for groundwater tracing.

Most adequately designed and conducted tracer studies will not result in visibly colored off-site water unless this condition is inherent in the design of the tracer study. There are cases where dyes at visible concentrations need to be detectable in the field. This is best done by working in a dark room and shining a flashlight into a glass jar containing

the test water at a right angle to the viewer. If fluorescent dye is visually detectable it will be seen in the light beam. This test should obviously not be conducted by a person who is color-blind. All dyes discussed in this chapter have their maximum fluorescence in the visible wavelength range. *The idea that the best way to detect the discussed dyes is with an ultraviolet light is a myth.*

A second common misconception is that dye tracing works only in well-developed karst areas of limited size where one is tracing from features such as sinkholes to springs. While tracing is often needed for investigating water related issues in such settings, successful groundwater tracing can routinely be conducted in almost any soluble bedrock aquifer as well as in many other hydrogeologic settings. Fluorescein dye has been used to trace from sinking surface streams through the groundwater system for almost 40 mi to Big Spring, Missouri at a time when the flow rates of the spring were 400 to 650 cubic feet per second (cfs). The amount of dye equivalent in the dye mixture used for this trace was 5.6 lb. Fluorescent dyes have also been successfully used in many traces in high-yield limestone aquifers including the Edwards Aquifer in Texas and the Floridan Aquifer. Hauwert et al. (2002) discusses an extensive tracing program in the Austin, Texas, area of the Edwards Aquifer.

A third common misconception is that tracer dyes will not work in acidic waters such as those commonly encountered in metal or coal mines. While not all of the dyes are suitable for such conditions, many successful traces into and/or through both active and inactive mines have been conducted with fluorescent dyes. Mine waters present unique challenges and bench tests lasting a few weeks with mine water and/or representative rock units are prudent for selecting the most appropriate type and quantity of dye for the planned trace. Groundwater traces of up to 1.6 mile with mean travel rates of greater than 100 ft/day have been conducted into mines using fluorescein and eosine introduced along normal faults in sedimentary rocks including sandstone, shale, and coal.

A fourth common misconception is that dyes are rapidly destroyed by sunlight and this precludes their use for tracing water into or out of surface streams. Rhodamine WT and sulforhodamine B are not rapidly destroyed by sunlight. Dyes introduced into a surface stream late in the day usually have adequate time to enter the groundwater system prior to being exposed to appreciable sunlight. Dyes discharged from groundwater into a surface stream at night can be detected with activated carbon samplers or in water samples collected with an automatic sampler programmed to collect samples during the hours of darkness.

A fifth common misconception is that groundwater tracing is impractical because it requires substantial experience, the purchase of hard to find materials, and analytical work necessitating instruments not normally found in water testing laboratories. There are firms that routinely

provide these services and assist others in designing and conducting groundwater traces. You can find them on the internet. Since there is no EPA or ASTM standard protocol for tracer dye analysis each of these firms has its own protocols and they are not all of equal quality. Desirable analytical protocols are discussed later in this chapter.

15.4 Dye Nomenclature and Properties

There are a number of fluorescent dyes that have been used in groundwater tracing with varying degrees of success. This chapter focuses on five of the most useful and most commonly used dyes. All five of these dyes present negligible adverse health and environmental problems when used with the protocols needed for effective groundwater tracing when modern sampling and analytical approaches are used (Field et al. 1995; Smart 1984). Color index names and numbers are the technical identifiers for the dyes and should be included in reports in addition to the more common names (such as eosine, fluorescein, etc.).

All of the dyes are sold as mixtures. The dye equivalent in a dye mixture is the percent of dye in the mixture. The rest of the mixture is a diluent. Diluents are used to standardize the product and facilitate mixing with water. Dye mixtures that are liquids routinely contain lower dye equivalents than powder mixtures. Liquid mixtures are usually easier to use than powders that must be mixed with water. Unfortunately, dye equivalent values are seldom shown on labels and most retail suppliers of dyes do not know the dye equivalent percent in the mixtures they sell, regardless of whether the mixtures are liquids or powders. Many tracing efforts have failed because mixtures used were assumed to be almost 100% dye when in reality the dye equivalent was only a few percent. Firms that provide analytical services for dye tracing studies often supply dye mixtures of known dye equivalent percentages to minimize problems for clients and as part of their quality assurance programs. The dye equivalent percent of dye mixtures used should be included in reports in addition to the amount of the dye mixture introduced.

Eosine is also known as Eosin, Eosine OJ, and Drug and Cosmetic (D&C) Red 22. Eosine is Acid Red 87 and its color index number is 45380. Its CAS number is 17372-87-1. The approximate percent of dye in "as sold" mixtures ranges from about 2 to 75%. Eosine is a pink to green dye depending upon concentration and whether it is viewed in sunlight or shade. When mixed in water this dye is the least noticeable to the general public of the five dyes discussed in this chapter.

Fluorescein is also known as Uranine, Uranine C, sodium fluorescein, fluorescein LT, D&C Yellow 8, and fluorescent yellow/green. The fluorescein used in dye tracing is a sodium salt of fluorescein and one

should always ensure that the fluorescein mixture being used is the sodium salt of fluorescein. Fluorescein is Acid Yellow 73 and its color index number is 45350. Its CAS number is 518-47-8. The approximate percent of dye in "as sold" mixtures ranges from 2 to 80%. Fluorescein has a green color and is the distinctive coloring agent in most automotive coolant solutions. Fluorescein from vehicle coolants can sometimes be detected in wells, springs, and streams downstream of large parking areas and busy roads due to leakage of coolants from vehicles. Fluorescein is also common in landfill leachates and has been used as an indicator of such waters. Fluorescein is present in some household products and thus is routinely present in municipal sewage. Groundwater heavily impacted by municipal sewage discharge commonly has detectable concentrations of fluorescein since this dye is not removed by sewage treatment plants except to the extent that this occurs by photodegradation. Fluorescein performs well in sea water and was the dye used for the tracing work shown in Figure 15.3.

Pyranine is also known as Solvent Green 7 (SG 7). Its color index name is D&C Green 8 and its color index number is 59040. Its CAS number is 6358-69-6. The approximate percent of dye in "as sold" mixtures undoubtedly varies among suppliers but is commonly about 77% when sold as D&C Green 8. Pyranine is present in some household products but to a lesser extent than is fluorescein. A major limitation of pyranine is that its emission peak fluorescence and fluorescence intensity varies with pH values in the range normally encountered in groundwater. While pyranine can be used effectively in some settings its use and analysis requires more technical sophistication than is

Figure 15.3 View of a National Park Service center in Sitka, Alaska. A tracer dye was introduced into the on-site sewage treatment system at the visitor center to determine if it contributed to springs (dark areas in the foreground) within the inter-tidal zone. No dye was detected in the springs.

required for the other four dyes discussed, and one of the other dyes is likely to be more suitable for the tracing work.

Rhodamine WT is sometimes sold as Fluorescent Red, but this name has also been applied to Rhodamine B (Basic Violet 10) which has potential carcinogenic properties, a dramatically different chemical structure, and is not a suitable dye for groundwater tracing. The color index name for Rhodamine WT is Acid Red 388; no color index number has been assigned. The CAS number is 37299-86-8. The approximate percent of dye in "as sold" mixtures ranges from about 3 to 20%; this dye is almost always sold in a liquid form. Rhodamine WT is a dark red dye. Emission fluorescence peak wavelengths for rhodamine WT and sulforhodamine B are very close together and these two dyes should generally not be used concurrently in situations where both might appear at a particular sampling station. Dyes with fluorescent characteristics similar to rhodamine WT and sulforhodamine B are used as the coloring agents in some hydraulic fluids and thus may be present at some industrial sites.

Sulforhodamine B is also known as Sulfo Rhodamine B, Pontacyl Brilliant Pink B, Lissamine Red 4B, Kiton Rhodamine B, Acid Rhodamine B, Amido Rhodamine B, and Fluoro Brilliant Pink. This dye is sometimes sold simply as "red fluorescent dye" and may be confused with rhodamine WT if only common names are used. The color index name for sulforhodamine B is Acid Red 52, and its color index number is 45100. The CAS number is 3520-42-1. The approximate percent of dye in "as sold" mixtures range from about 3 to 75%. Sulforhodamine B is a dark red dye.

Table 15.1 summarizes data on dye degradation in sunlight as measured by fluorescence magnitude. The values are for pans containing 0.5 in of water that were allowed to sit in bright sunlight for periods of 1, 3, and 5 h. As should be expected larger dye concentrations last longer

TABLE 15.1 Dye Degradation in Sunlight as Measured by Fluorescence Magnitude

Dye	Initial dye concentration (ppb)	1 hour	3 hours	5 hours
Eosine	1,000	2%	<1%	—
Eosine	100	1%	<1%	—
Fluorescein	1,000	19%	<1%	—
Fluorescein	100	7%	<1%	—
Pyranine	1,000	68%	3%	—
Pyranine	100	55%	1%	—
Rhodamine WT	1,000	100%	100%	83%
Rhodamine WT	100	97%	49%	32%
Sulforhodamine B	1,000	100%	97%	95%
Sulforhodamine B	100	81%	70%	60%

Table from Aley (2002); courtesy Ozark Underground Laboratory, Inc.

NOTE: Water depth 0.5 in. Percentages reflect amount of initial dye remaining.

than smaller concentrations. Dyes will experience slower photodegradation in deeper streams, streams that are well shaded, and in streams where turbidity limits sunlight penetration. Fluorescein and eosine dyes can be used to trace groundwater into most surface streams if sampling stations are placed at intervals where the mean travel time between stations is 6 h or less. Such sampling stations are able to detect dyes discharging into the stream at night and when the sun is at low angles to the earth. Placing sampling stations on surface streams at about 0.5 to 1.0 mi intervals works well in many landscapes, and in many urban and suburban areas road access makes this general interval possible. When sampling a large stream where dilution is a major concern the intervals should be shorter. In many cases sampling near the bank of a large stream and on the same side as the dye introduction point will also be more likely to detect the tracer dyes than will sampling further out into the stream.

Table 15.2 summarizes the influence of pH on the fluorescence magnitude of the five tracer dyes. Despite the values in Table 15.2, fluorescein dye is still an effective tracing agent in many acidic waters. Low pH values alter the fluorescein from a fluorescent to a nonfluorescent molecule. If the pH of a water sample containing fluorescein is pH adjusted to basic values prior to analysis, fluorescein will again fluoresce. However, the nonfluorescent molecules of fluorescein have a greater tendency to be adsorbed onto earth materials than is the case for fluorescein at neutral to basic pH values. Activated carbon samplers (discussed in Section 15.6) effectively adsorb fluorescein from both acidic and basic waters. Based on field studies Aley (2002) ranked the general suitability of the five tracer dyes for use in tracing acidic mine waters as follows: Fl > Eos > SRB > RWT. Pyranine is not suitable for this use.

Table 15.3 compares tracer dye adsorption onto various mineral and organic materials. Note that all dyes are subject to some adsorption and that the amount of adsorptive loss increases as the amount of the adsorbing material increases. Adsorptive losses can be overcome in groundwater tracing work by increasing the amount of dye used. There are no data

TABLE 15.2 Influence of pH on Fluorescence Intensity

Dye	Fluorescence substantially decreased at pH less than:	Fluorescence mostly eliminated at pH less than:
Eosine	4.0	2.5
Fluorescein	6.5	5.5
Pyranine	9.5	6.5
Rhodamine WT	5.0	2.5
Sulforhodamine B	3.5	2.0

Table from Aley (2002); courtesy Ozark Underground Laboratory, Inc.

TABLE 15.3 Comparison of Tracer Dye Adsorption onto Mineral and Organic Materials

Material	Sediment concentration, g/L	FL	PY	RWT	SRB
		Mineral			
Kaolinite	2	98	95	89	88
Kaolinite	20	93	95	67	51
Bentonite	2	98	100	92	98
Bentonite	20	87	98	79	—
Limestone	2	98	96	93	97
Limestone	20	94	85	66	76
Orthoquartzite	2	98	100	98	—
Orthoquartzite	20	98	87	90	—
		Organic			
Sawdust	2	86	70	81	92
Sawdust	20	11	30	42	—
Humus	2	83	76	82	92
Humus	20	17	31	11	63
Heather	2	41	74	81	—
Heather	20	0	18	18	—

Table from Aley (2002); courtesy Ozark Underground Laboratory, Inc. Adapted from Smart and Laidlaw (1977).

NOTE: Values are percent of dye remaining in solution from a 100-ppb initial solution. FL = Fluorescein; PY = Pyranine; RWT = Rhodamine WT; SRB = Sulforhodamine B.

presented for eosine since this dye was not studied by Smart and Laidlaw (1977). Based upon field experience eosine typically experiences similar, but somewhat greater, sorptive losses than does fluorescein.

Based upon laboratory test (which did not include eosine) Smart and Laidlaw (1977) ranked the resistance of the dyes to adsorption onto inorganic material as follows: Py > FL > RWT > SRB. They ranked the resistance of the dyes to adsorption onto organic material as follows: Py > SRB > FL = RWT.

Behrens (1986) ranked the resistance of a number of tracer dyes to adsorption. His data were largely based upon field work in Europe and were based mostly on water samples. His rankings were: Py = FL > Eos > RWT > SRB. Aley (2002) reported similar findings for sampling based on activated carbon samplers although he noted that his data on pyranine were limited.

Table 15.4 shows typical detection limits for the five tracer dyes. Instrument analysis values are derived from method detection limits currently used in analysis work at the Ozark Underground Laboratory and values for other laboratories may be somewhat different.

TABLE 15.4 Detection Limits for Five Tracer Dyes under Different Conditions

Method	EO	FL	PY	RWT	SRB
Dye in water, instrument analysis	0.015	0.002	0.015*	0.015	0.008
Dye in charcoal elutant, instrument analysis	0.050	0.015	0.010	0.170	0.080
Dye in water; field conditions, experienced person	135	7	175*	125	50
Dye in water; field conditions, general public	13,500	140	3,500*	2,500	1,000
Dye in water; dark room with flashlight, experienced person	10	2	3*	50	5

Table slightly modified from Aley (2002); courtesy Ozark Underground Laboratory, Inc.
*pH adjusted water with pH of 9.5 or greater.

NOTE: Concentrations are in parts per billion (ppb) and are based upon the as-sold weights of the dye mixtures. Dye equivalent values for the mixtures were 75% for eosine, fluorescein, and sulforhodamine B; 77% for pyranine, and 20% for rhodamine WT. EO = Eosine; FL = Fluorescein; PY = Pyranine; RWT = Rhodamine WT; SRB = Sulforhodamine B.

15.5 Designing a Dye Tracing Study

The following are key issues that should be addressed in designing a dye trace:

- What questions do you wish to answer with the tracing work and how precisely do you need to have the answers? The latter question will, in part, determine how frequently samples must be collected and analyzed.
- What is the hydrogeologic setting? At a minimum, what geologic units are involved? To what extent must preferential flow pathways be expected?
- Where will the dye or dyes be introduced? It is often possible to conduct two or three concurrent traces for only a slightly greater cost than a single trace because samples can often be analyzed for multiple dyes at little or no additional analytical cost.
- How much water will be introduced with the dye? This is specific to each trace. Before introducing dye add sufficient water to moisten all surfaces if they are not already wet. As a general rule the more water used to flush the dye into and through the groundwater system the better the tracing effort will be. However, in some cases one does not wish to distort water elevations in the aquifer. In groundwater sampling it is common to extract a volume of water equal to three to five well volumes within the saturated zone prior to collecting a water sample. For dye introductions one can moisten well surfaces, introduce the dye as a pulse, and then add three to five well volumes to move most of the dye out of the well bore and into the aquifer.

- Can chlorinated tap water be used for the dye introduction? In many cases the answer is yes and it is generally more desirable to use tap water than water from ponds and streams. In some cases it may be desirable to dechlorinate the tap water before introducing it; activated carbon is one way of doing this. Historically much groundwater tracing has used stormwater runoff or waters naturally sinking into the groundwater system in a localized area. Chlorinated tap water will not destroy much of the introduced dye because of the high dye concentrations at the dye introduction point.
- How will the dye be introduced? In general it is easier and better for tracing purposes to introduce the dye as a short-duration pulse rather than adding it with introduced water at a constant rate for a prescribed period of time.
- How much background sampling will be done prior to dye introduction? Background sampling determines if one or more dyes or compounds with fluorescence characteristics similar to dyes may already be present at some of the sampling stations. Even in remote areas one should usually have at least one set of background samples collected and analyzed from most or all sampling stations prior to any dye introduction. In areas where previous tracing may have been done or in urban or industrial areas two or three sets of background samples that have been analyzed are desirable.
- What dye or dyes will be used and in what quantities? As will be discussed later different dyes have different properties, and as a result a pound of one dye is not equivalent to a pound of another dye. The selection of dye type and quantity is very important to successful groundwater tracing. A study plan should include a preliminary determination of the dye type(s) and quantity(s) to be used, but the final determination of both type and quantity must be made after at least one set of background samples. Laboratories that routinely assist in tracer studies can usually analyze background samples and identify potential dye interferences within a week of the time the background samples are collected.
- Where are all of the potential sampling points? In most cases you should not limit sampling to the points where you expect to detect dyes. It is often important to identify points where the dye is not detectable. Control stations to demonstrate that dyes you did not introduce are not moving into your study area are often desirable, especially in urban settings. Maintain flexibility in the study plan to permit adding or modifying sample locations based upon conditions discovered in the field. As an example, major precipitation or snow melt runoff during a trace may create additional sampling points that should be tested.

- Are there any data or calculations indicating likely travel times for the trace? If such data exist they should be used to the extent reasonable. A common approach is to design the study to continue for 1.5 times the estimated travel time to the most distant sampling station where dyes may be detected.
- What is the pH of waters that will be encountered in the trace? If the pH is less than about 6.8 it may affect the type and/or quantity of dye that should be used.
- Develop a good site map showing hydrogeologic features that may be of significance plus all dye introduction and dye sampling locations. Developing a good site map should not be deferred until the report phase of the study.
- Develop a rationale for the conditions under which the study can be ended. A common approach is to identify a tentative study duration but then state that sampling will not be ended until certain conditions have been met. Common criteria for ending sampling include: (1) no new dye detection sites in the last 3 weeks of sampling unless the new detection sites are in areas near previous dye detection points, (2) dye concentrations are decreasing at most (and preferably all) sampling stations where dye has been detected, and (3) no other factor(s) warrant extending the sampling period. Sampling can be discontinued earlier than the tentative study duration at some sampling stations where dye has been detected in multiple samples or it can be discontinued if there have been at least two positive dye detections at each of the dye sampling stations and it is reasonable to conclude that no additional sampling stations are likely to receive the tracer dye. Bear in mind that the credibility and utility of many dye traces have been compromised because sampling was ended prematurely; this is bad science and a false economy.
- Gain concurrence from all relevant parties for the study plan prior to beginning the study. Be aware that many regulatory agencies are often staffed by people with limited experience and that their experience may not include tracer studies. Providing copies of toxicity papers such as Field et al. (1995) and Smart (1984) can be helpful to reviewers.
- Determine if there are any other site-specific conditions that should be addressed in the study plan.
- Few consulting firms or universities have the analytical equipment needed for conducting modern dye traces. An old filter fluorometer in a storage room will not be adequate for most tracing work. Additionally, few of these entities have personnel with expertise in designing and conducting dye traces. Most consulting firms, and a few universities, offset the lack of equipment and experience by contracting with a

firm that specializes in the analysis of tracer dyes and has expertise in the design of tracer studies. Such firms can be found through an internet search; as should be expected the quality and level of expertise of the firms varies. If this approach is to be used then, before you start a trace, get the outside analytical service on board with the project. In addition to analyzing samples, a quality firm can assist in the design of the study, provide activated carbon samplers and certified dye-free sample containers, and provide dye mixtures of known dye equivalent percentages.

- Specify the details of sample collection, shipping, and analysis. Identify the laboratory that will do the analysis work and provide the details on how that work will be done. Firms that routinely assist in tracer studies usually have detailed procedures and criteria documents that can be incorporated as an appendix in the study plan if their services are involved.
- Identify what reports will be prepared and when they will be submitted.
- Determine if the tracing work is to be conducted in a state or an area where a short-term authorization, permit, or some other type of official notification or authorization may be required. Where such permitting or notification is required it is usually simple. A little time on the phone can find the person responsible for dealing with any required permits and that person can help you determine exactly what information is needed and what procedure should be followed. Even when a permit or notification may not be required it is good protocol to inform agencies responsible for water quality protection about the planned dye tracing work. Extending that informing to entities that might receive a phone call from the public about colored water (if that is a possibility) is also a prudent action. If you are not required to obtain a permit from a particular agency then do not ask for their permission; instead, simply inform them.

15.6 Sampling and Analysis for Dyes

Grab samples of water and activated carbon samplers can both be used to detect the tracer dyes. In addition, there are some flow-through fluorometers that can be used in the field to provide a continuous graph of fluorescence intensity at a sampling station. While these instruments are useful for some purposes, they are most useful for time of travel studies in surface waters where there is no question as to where the dyed water will appear.

Grab samples of water can either be collected by hand or with a programmable automatic sampler. The automatic samplers fill bottles at

selected time intervals or can collect composite samples. The analytical laboratory should be queried as to the quantity of sample they require; the quantities are typically 40 mL or less, although for some tracing in the vadose zone samples as small as 2.5 mL have been used. For most dye tracing involving monitoring wells it is not necessary to pump and purge the wells prior to sampling; this greatly simplifies the sampling and field and wastewater disposal costs.

Analysis of water samples provides a known dye concentration at a particular point in time. Since a dye pulse reaching a sampling station may last only a relatively short period of time, sampling that places primary reliance upon water samples routinely requires a large number of samples. Automatic samplers can be advantageous if there are only a few sampling stations where this equipment must be used. The typical automatic sampler holds 26 bottles. The automatic samplers cost several thousands of dollars each and this routinely limits their use. Also, the samplers must be set on the surface of the ground and can only lift water from relatively shallow monitoring wells. As a result of these conditions, traces that rely primarily or exclusively on grab samples of water are expensive in terms of field time and analytical costs. There are some monitoring wells that are equipped so that they can only be sampled with grab samples of water. In such cases if these wells are to be monitored it must be with grab samples of water.

Activated carbon samplers are fiberglass screen packets partially filled with a laboratory grade of coconut shell activated carbon. Firms providing tracer dye analysis and assistance routinely provide the activated carbon samplers. The typical samplers contain about 4.25 g of activated carbon, but the amount varies among the firms with some entities not using a standard amount of carbon. Appropriate activated carbon is capable of adsorbing and retaining all five of the tracer dyes discussed in this chapter. Activated carbon samplers can be left in place in the water being sampled for periods ranging from a day to a few weeks. A common sampling interval is about 1 week. Longer sampling intervals may be used for tracing in remote areas especially if the water being sampled is of high quality. At waste sites sampling intervals should generally not be longer than about a week since the longer the sampler is in place the fewer available activation sites remain on the carbon. The author has found that sampling intervals of 1 week have worked well even in wells with free product petroleum or high concentrations of solvents.

Aley (2002) found that an activated carbon sampler in place for a week in water that has detectable movement will adsorb and then release to the eluting solution in the laboratory a dye concentration that is roughly 400 times greater than the mean dye concentration present in the associated water. The magnification factor varies with the type of dye and is lower in monitoring wells where water circulation is

minimal. Aley (2002) indicates that the ability of activated carbon to adsorb dye in field situations and then release it to the eluting solution is as follows: FL > EO > RWT > SRB > PY.

In monitoring wells activated carbon samplers are often attached to the top of dedicated disposable bailers and suspended in the middle of the screened interval or in the middle of the saturated zone. In some studies it is desirable to learn what zones in the well are contributing most of the dyed water. In such cases a weighted line can be used with an activated carbon sampler attached at each zone of interest (Example 15.2).

Example 15.2 In a tracer test to determine the point where contaminants of concern were entering a city storm sewer, a cord was run through the sewer for a city block with carbon samplers placed every 50 ft. This identified the area where contaminants were entering the sewer and minimized the amount of street that needed to be excavated to repair the pipe.

Activated carbon samplers placed in springs or surface streams are anchored to stakes, rocks, or bricks and placed where there is visible current. At such stations a minimum of two independently anchored samplers should be placed in the event one is lost and to permit analysis of some duplicate samplers for statistical analysis of the precision of analytical results. The activated carbon is *adsorbing the dye, not filtering it* out of the water, so the velocity of the water makes relatively little difference in the amount of dye that will be adsorbed in the sampler so long as the water in contact with the activated carbon is not appreciably depleted in dye due to adsorption.

If the bottom of the spring or stream is loose sediment, the samplers should be placed so they do not become submerged in the sediment. If pumping wells are sampled, a continuous stream of water equal to about 1 gal/min should pass through the sampler. This can often be achieved by running water continuously through a bucket and having the sampler suspended in the bucket.

When activated carbon samplers are collected they are placed in sterile labeled plastic bags. Most firms that do dye analysis work will supply such bags and will have done quality assurance work to ensure that the bags are free of any tracer dyes. The bags are labeled as to station number, name, and date and time of collection. The labeling must be on the outside of the bags and with an indelible black-felt marker. Do not use red felt markers since many of these contain eosine dye as the coloring agent.

Even if primary sampling reliance is placed on activated carbon samplers it is commonly good protocol to also collect a grab sample of water each time a sampling station is visited. If dye is detected in the charcoal sampler for the station the water sample can also be analyzed to determine the dye concentration at that time. You should know that you have not maintained continuous custody for activated carbon samplers

"in place" at sampling stations such as springs and surface streams. You have maintained custody of grab samples of water from these stations and these results add credibility to your sampling results and verification that the results from the carbon samplers are reasonable.

Table 15.5 summarizes advantages and disadvantages of designing traces where sampling reliance is placed on water samples, on activated carbon samplers, or with primary reliance on activated carbon samplers with secondary reliance upon water samples. The table indicates that sampling which places primary reliance on activated carbon samplers with secondary reliance upon water samples is commonly the best strategy for a problem-solving project that must be conducted for reasonable budgets. It is also the best strategy for minimizing the amount of dye that is needed.

TABLE 15.5 Advantages and Disadvantages of Sampling Reliance Based on Water Samples Only, Activated Carbon Samplers Only, or Primary Reliance on Activated Carbon Samplers with Secondary Reliance on Water Samples

Sampling based on water samples only. *Advantages:* Generally best suited to research projects. Accurate determinations of dye concentrations at known times. Data suitable for developing a mass balance (i.e., accurately knowing how much of the introduced dye was detected at particular sampling stations). Maintains chain of custody of all samples except possibly automatic pumped samplers. Can accurately identify time of first dye arrival and time of peak dye arrival at a sampling station. *Disadvantages*: Requires more sampling time and more analytical costs than is the case with activated carbon samplers. Because samples must be collected frequently, this method is not well suited to traces with a large number of sampling stations. One may miss detecting dye at stations reached by only small concentrations of dye; this can be especially important for monitoring wells at hazardous waste sites. Likely to miss dyes rapidly destroyed by sunlight in surface streams since more sampling is done during daylight hours when the dyes would have been destroyed. Requires the use of substantially more dye than if sampling utilizes activated carbon samplers.
Sampling based on activated carbon samplers only. *Advantages*: Minimizes amount of dye needed for the tracing since activated carbon samplers accumulate dyes. Permits continuous sampling of all sampling sites. Excellent approach for identifying all sampling stations reached by the tracer dye. Excellent approach for traces with a large number of sampling stations and stations in remote locations. Minimizes field time since sampling can typically be done once per week or sometimes at longer intervals. Minimizes analytical costs. Suitable for sampling at multiple levels in the same well. Ideal for detecting dyes that may discharge into surface stream during nighttime when they are not destroyed by sunlight. *Disadvantages*: Time of first dye arrival and time of peak dye arrival at sampling stations is known only within a sampling period that is likely to be several days long; precision in this information is often not critical. No quantitative dye concentration data for water at sampling stations. Good chain of custody only for stations (such as wells) that are locked.
Sampling based on primary reliance on activated carbon samplers with secondary reliance on water samples. *Advantages*: Generally best suited to problem-solving projects. Same advantages as sampling with activated carbon samplers plus quantitative dye concentration data for water at sampling stations where dyes are detected. Permits good chain of custody for water samples. Good method for enhancing the credibility of tracing results. *Disadvantages*: Increases analytical costs over use of activated carbon samplers alone by 15 to 30%; insignificant increase in field expenses and no increase in dye costs.

Collected samples, both as grab samples of water and activated carbon, should be kept in the dark (to prevent photodecomposition) and in a cooler after collection. While the tracer dyes are reasonably stable in the activated carbon samplers they can degrade or be destroyed in water samples that are not refrigerated. It is a good protocol to ship samples by overnight courier to an analytical laboratory in coolers packed with "Blue Ice." There is no established "hold time" for dye samples, but it is good protocol to have them analyzed as soon as possible.

In the laboratory activated carbon samplers are washed in strong jets of unchlorinated and dye-free water to remove sediment and debris that can interfere with the analysis. The samplers are then eluted in a solution consisting of a strong base, alcohol, and water. There is no standard ASTM or EPA protocol for dye analysis and different laboratories use somewhat different eluting solutions. The different solutions are typically designed to best elute the mixture of dyes that the particular laboratory routinely uses, and all of the eluting solutions work reasonably well. The activated carbon is typically left in the eluting solution for a standard time period; one hour is common.

The quality of the reagent water used for washing samplers is critical and should be considered in selecting a laboratory for use in a study. A few laboratories use tap water without any treatment. This presents two quality control problems. First, at times public water supplies (and especially those using surface waters) may contain small concentrations of tracer dyes or similar fluorescent compounds that have the potential to contaminate samples. Secondly, public water supplies are chlorinated and the chlorine can destroy some of the adsorbed dye. *This problem is most severe for activated carbon samplers that contain only a small amount of dye.*

After the activated carbon sampler has been eluted for a standard time period, the eluting solution is poured off and a sample of it is then available for analysis. Water samples can be analyzed directly. Various fluorometric instruments can be used to conduct the analysis but the most sensitive and the ones best suited to discriminating between dyes and other fluorescent materials are spectrofluorophotometers that can synchronously scan excitation and emission wavelengths and print out a graph of the emission fluorescence. Figure 15.4 shows an example of such a graph for an activated carbon sampler that contained fluorescein, eosine, and rhodamine WT dyes. The emission wavelengths of the fluorescence peaks are a function of the particular dye, its matrix, and various instrument settings. The emission wavelength ranges of the dyes are sufficiently separated that traces can often be conducted concurrently with two or three dyes. These dyes are typically fluorescein, eosine, and rhodamine WT. Rhodamine WT and sulforhodamine B should generally not be used concurrently if there is any chance that both of the dyes might appear at the same sampling station.

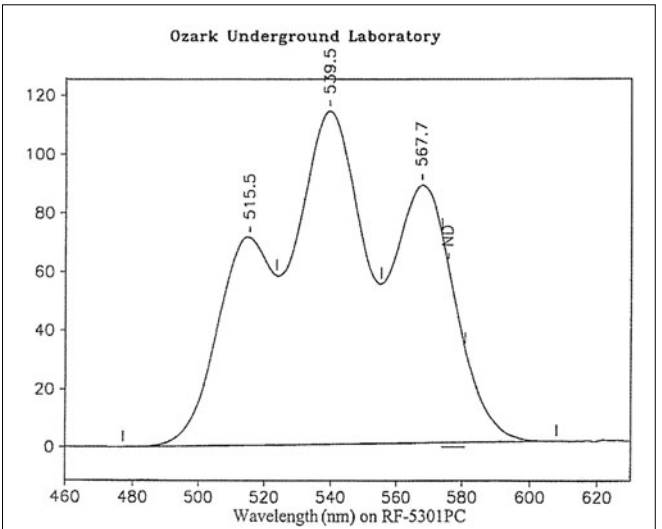

Station 1: Left Drain @ Weir
OUL number: N2546
Matrix: Elutant
Placed: 04/30/04 1430
Analyzed: 05/07/04
Collected: 04/30/04 1500

Peaks within the normal range of tracer dyes:

Peak nm	Left X	Right X	Height	Area	H/A	Conc.
515.5	477.1	523.5	70.76	1,330.52	0.05	32.4
539.5	523.6	555.1	113.43	2,623.59	0.04	113
567.7	555.2	607.9	87.60	1,928.86	0.05	191
575.7	573.8	580.8	0.00	0.00	0.00	ND

Peaks close to the normal range of tracer dyes:

Figure 15.4 Emission fluorescence graph from a synchronous scan of an activated carbon sampler that contained fluorescein (peak on the left, concentration 32.4 ppb); eosine (peak in the middle, concentration 113 ppb); and rhodamine WT (peak on the right, concentration 191 ppb). Traces were through an earthfill dam from three different points on the upstream side of the dam.

Table 15.6 summarizes some of the fluorescence characteristics of the five dyes. The maximum excitation and emission wavelengths of each of the dyes are from Ford and Williams (1989). The normal acceptable wavelength ranges for the dyes in water and in the standard elutant used by the Ozark Underground Laboratory are also shown to illustrate how the values differ among the dyes and between water and elutant samples. The normal acceptable wavelength range is derived from a data base of positive dye detections from actual traces. The acceptable range equals the mean wavelength plus and minus two standard deviations. All synchronous scan values for eosine, fluorescein, rhodamine WT and sulforhodamine B are from synchronous scans with a bandwidth separation of 17 nanometers (nm) and standard excitation and emission slit settings. The pyranine scan values are from synchronous scans with a bandwidth separation of 35 nm.

TABLE 15.6 Fluorescence Characteristics of Five Dyes

Dye	Maximum excitation	Maximum emission	Normal acceptable wavelength range for water samples	Normal acceptable wavelength range for elutant samples
Eosine	515	535	529.6–538.4	533.0–539.6
Fluorescein	490	520	505.6–510.5	510.7–515.0
Pyranine	455	515	501.2–505.2*	500.4–504.6
Rhodamine WT	555	580	569.4–574.8	561.7–568.9
Sulforhodamine B	565	590	576.2–579.7	567.5–577.5

*Adjusted to a pH of 9.5 or greater.

NOTE: See text for explanations. All values in nanometers (nm).

15.7 Detection Limits for Tracer Dyes

Detection limits for tracer dyes are commonly expressed as the concentration of the dye mixture in the water or elutant sample rather than as the dye equivalent. The wider the excitation and emission slit settings in a spectrofluorophotometer the lower the detection limits, but the less discrimination there is among fluorescent compounds. Spiked laboratory samples provide lower detection limits than spiked field samples; the latter are the more appropriate since they represent "real world" conditions. One must never assume that the best analytical protocol is the one with the lowest reported detection limits. Table 15.4 (presented earlier) indicates detection limits for the five tracer dyes in samples analyzed at the Ozark Underground Laboratory; the concentrations are based upon typical as-sold dye mixtures rather than dye equivalents. The dye mixtures were 75% dye equivalent for fluorescein, eosine, and sulforhodamine B; 20% dye equivalent for rhodamine WT; and 77% dye equivalent for pyranine.

The reason that the detection limits are smaller for water samples than for carbon elutant samples is that the slit widths under which carbon elutant samples are analyzed are narrower than the slit widths for water samples. Activated carbon can adsorb many compounds and the narrower slits provide more discrimination for carbon elutant samples than is deemed necessary for water samples.

Remember that activated carbon samplers are continuous and accumulating samplers. Depending upon how long they are in place in the water being tested they routinely yield dye concentrations at least one and often two orders of magnitude larger than the mean dye concentration in the water. As a result, detection limits alone do not adequately represent the small concentrations of dye in the tested water that can be effectively sampled with these samplers.

Detection limits vary among the dyes because of variations in dye equivalents in the dye mixtures and also because fluorescence intensity also varies among the dyes. *The important point here is that a pound of one dye mixture is not equivalent to a pound of another dye mixture.*

Quantification of the concentrations of each of the dyes present in a sample is obviously information that any good quality dye analysis laboratory will provide. This applies to both water samples and elutants from activated carbon samplers. Quantitative analysis with a spectrofluorophotometer operated under a synchronous scan protocol is more accurate than with a fluorometer.

15.8 Determining Dye Quantities

As will be demonstrated in this section, experience in groundwater tracing with fluorescent dyes is the best general method for estimating the quantity of dye needed for particular traces. Determining the quantity of dye needed for a particular trace cannot be accomplished by using any simple equation. Appreciable amounts of dye can be lost to various processes including adsorption and decomposition. Substantial dilution occurs in many aquifers including some of those with significant preferential flow routes. While there are over 20 equations that have been developed for calculating dye quantities, none is recommended for routine use.

Aley (1997) summarized data from about 1,000 positive groundwater traces in the epikarst. The epikarst (Chapter 14) is the weathered upper portion of the bedrock in carbonate rock landscapes and is commonly about 33 ft thick, but there is a large range in thickness. Based on data from the 1,000 traces Aley (1997) reported that dye recovery rates for traces conducted in the permanently saturated epikarstic zones are from 0.1 to 1.0% of the amount introduced into the groundwater system. The percentages are typically 1 to 10% for the seasonally saturated epikarstic zone. Recovery rates reported in the literature for other traces in karst areas (often along major solutionally widened conduits from sinkholes or losing streams to springs) are typically in the range of 20 to 50% of the introduced dye. In the author's experience dye recovery rates from traces in fractured rock aquifers are commonly in the range of 1%, but are also highly variable.

The amount of dye needed for successful tracing is also a function of the sampling and analytical approaches being used. Traces where primary sampling reliance is placed on grab samples of water and dye detections are likely to occur at multiple sampling stations are likely to require at least an order of magnitude more dye than would be necessary if primary sampling reliance were based on activated carbon samplers.

Filter fluorometers are sometimes used for dye analysis work. These instruments are not capable of separating fluorescence intensity measurements into background fluorescence and fluorescence due to a tracer dye. Background fluorescence can vary by an order of magnitude over the course of a week so dye pulses at a sampling station can readily be masked by background fluorescence. This problem does not affect spectrofluorophotometers operated under a synchronous scan protocol. As a result, if dye analysis is to be dependent upon a filter fluorometer then the amount of dye needed for a trace will typically be 5 to 10 times greater than the amount needed with a spectrofluorophotometer operated under a synchronous scan protocol. Additionally, while groundwater traces using two or three dyes concurrent can readily be done using a spectrofluorophotometer operated under a synchronous scan protocol, traces dependent upon filter fluorometers for analysis should use only one dye at a time.

The amount of dye needed for a trace is also a function of the type of dye. In a setting where all of the five tracer dyes are potentially useful a trace that could be done with about one pound of fluorescein would typically require about 1.5 lb of eosine for similar results or about 4 lb of rhodamine WT or about 5 lb of sulforhodamine B. If all of these dyes could be used pyranine would not be a reasonable selection. If it were selected, the trace would require about 3 lb of pyranine. The above quantity estimates presume that all of the dye mixtures contain about 75% dye equivalents except for rhodamine WT which is assumed to have a dye equivalent of 20%.

Based on the author's experience and estimates for fluorescein mixtures with a 75% dye equivalent many groundwater traces can be done with 5 lb or less of the dye mixture. This presumes that sampling places primary reliance on activated carbon samplers and analysis with a spectrofluorophotometer operated under a synchronous scan protocol. Traces in fractured rock aquifers typically require at least three times as much dye as traces in karst aquifers and the amount may be more than this. Traces in the epikarstic zone of a karst aquifer require three to five times more dye than traces below this zone, and this is especially true for perennially saturated epikarstic zones. Traces through alluvial and glacial deposit aquifers typically require about three times more dye than traces in karst aquifers with finer textured materials requiring more dye than courser materials.

The best approach for making a final selection of dye type and quantity is to seek the advice of a person with extensive dye tracing experience. Their advice is typically based upon personal experience with similar tracing projects. Such persons are often associated with a firm capable of providing design assistance and analytical services for tracer tests.

15.9 Summary

Groundwater tracing with fluorescent dyes is a cost-effective method for determining flow paths and travel rates through aquifers. Tracing with the fluorescent dyes is particularly useful in karst and fractured rock aquifers, but can be used effectively in other types of aquifers.

Successful groundwater traces require the selection of a dye appropriate for the site; all dyes are not equal in performance and detectability. Sampling for the dyes can be done with water or activated carbon samplers. For most problem solving tracing work primary sampling reliance should be based upon activated carbon samplers and secondary reliance upon water samples. This minimizes costs, the quantity of tracer dyes needed, and the risk that sites receiving only small amounts of dye will not be identified as detection locations.

For most tracing work the analysis should rely on spectrofluorophotomers operated under a synchronous scan protocol. These instruments are vastly superior to filter fluorometers for tracing work. There are several commercial firms that routinely provide analytical services, supplies, and assistance in the design of tracer studies.

References

Aley, T., 1997. Groundwater Tracing in the Epikarst. Proceedings of the 6th Multidisciplinary Conference on Sinkholes and the Engineering and Environmental Impacts of Karst. A.A. Balkema, pp. 207–211.

Aley, T., 2002. *The Ozark Underground Laboratory's Groundwater Tracing Handbook*. Ozark Underground Laboratory, Protem, MO 35 pp. Available on-line from www.ozarkundergroundlab.com or in hard copy from the laboratory.

Behrens, H., 1986. Water Tracer Chemistry: A Factor Determining Performance and Analytics of Tracers. *Proceedings of the 5th International Symposium on Water Tracing*, Institute of Geology and Mineral Exploration, Athens, pp. 121–133.

Field, M.S., Wilhelm, R.G., Quinlan, J.F., and Aley, T.J., 1995. An Assessment of the Potential Adverse Properties of Fluorescent Tracer Dyes Used for Groundwater Tracing. *Environmental Monitoring and Assessment*, Vol. 38, pp. 75–96. Kluwar Academic Publishers.

Ford, D.C., and Williams, P.W., 1989. *Karst Geomorphology and Hydrology*. Unwin Hyman. Gulf Coast of Geological Societies, Corpus Christi, TX, pp. 229.

Hauwert, N.M., Johns, David A., Sansome, J.W., and Aley T.J., 2002. Groundwater Tracing of the Barton Springs Edwards Aquifer, Travis and Hays Counties, Texas. *Gulf Coast Association of Geological Societies Transactions*, Vol. 52, pp. 377–384.

Hotzl, H., and Werner, A. (eds.). 1992. Tracer Hydrology. *Proceedings of the 6th International Symposium on Water Tracing*. Karlsruhe, Germany. A.A. Balkema. 464 pp.

Kass, W., 1998. *Tracing Technique in Geohydrology* (translated from German). A.A. Balkema. Rotterdam, Netherlands, 581 pp.

Kranjc, A. (ed). 1997. Tracer hydrology 97. *Proceedings of the 7th International Symposium on Water Tracing*. Portoroz, Slovenia. A. A. Balkema. 450 pp.

Sabatini, D.A., 1989. Sorption and Transport of Atrazine, Alachlor, and Fluorescent Dyes in Alluvial Aquifer Sands. *PhD Dissertation*, Iowa State University. 216 pp.

Smart, P.L., 1984. A Review of the Toxicity of Twelve Fluorescent Dyes Used for Water Tracing. *National Speleological Society Bulletin*, Vol. 46, pp. 21–33.

Smart, P.L., and Laidlaw, I.M.S., 1977. An Evaluation of Some Fluorescent Dyes for Water Tracing. *Water Resources Research*, Vol. 13(1), pp. 15–33.

Appendix

A

Unit Conversions Tables

Copyright © 2008, 2001 by The McGraw-Hill Companies, Inc. Click here for terms of use.

TABLE A.1 Unit Conversions for Length

Unit	Inch	Feet	Yard	Mile	mm	cm	m	km
1 in	1	0.08333	0.02777	1.5783e-05	25.40	2.54	0.0254	2.54e-05
1 ft	12	1	3	5280	304.8	30.48	0.3048	3.048e-04
1 yd	36	3	1	5.682e-04	914.4	91.44	0.9144	9.144e-04
1 mi	63,360	5280	1760	1	1.609e-06	1.609e-05	1609.3	1.609
1 mm	0.03937	3.2808e-03	1.0936e-03	6.2137e-07	1	0.1	0.001	1e-06
1 cm	0.3937	0.03281	1.0936e-02	6.2137e-06	10	1	0.01	1e-05
1 m	39.37	3.2808	1.0936	6.214e-04	1000	100	1	0.001
1 km	39.370	3280.8	1093.6	0.621	1e-06	100,000	1000	1

TABLE A.2 Unit Conversions for Area

Unit	$Feet^2$	$Mile^2$	Acre	$Meter^2$	km^2	Hectare
1 ft^2	1	3.587e-08	2.296e-05	0.09291	9.291e-08	9.291e-06
1 mi^2	2.788e-06	1	640	2.59e-06	2.59	259
1 acre	43,560	1.5625e-03	1	4047	4.047e-03	0.4047
1 m^2	10.764	3.861e-07	2.471e-04	1	1e-06	0.0001
1 km^2	1.0764e-07	0.3861	247.1	1e-06	1	100

TABLE A.3 Unit Conversions for Volume

Unit	mL	Liters	Meter^3	Feet^3	Gallons	Acre · ft	Million gal
1 mL	1	0.001	1e-06	3.531e-05	2.6414e-04	8.107e-10	2.6414e-10
1 L	1000	1	0.001	0.03531	0.2641	8.107e-07	2.641e-07
1 m^3	1e-06	1000	1	35.31	264.14	8.107e-04	2.641e-04
1 ft^3	28,317	28.317	2.8317e-02	1	7.481	2.2957e-05	7.481e-06
1 gal	3785.9	3.7859	3.786e-03	0.1337	1	3.0691e-06	1e-06
1 acre · ft	1.2335e-09	1.2335e-05	1233.5	43560	3.2583e-05	1	0.32583
1e-06 gal	3.7859e-09	3.7859e-06	3786	1.3367e-05	1e-06	3.0691	1

TABLE A.4 Unit Conversions for Time

Unit	Seconds	Minutes	Hours	Days	Years
1 s	1	0.01667	2.778e-04	1.1574e-05	3.171e-08
1 min	60	1	0.01667	6.944e-04	1.9026e-06
1 h	3600	60	1	0.04167	1.1416e-04
1 day	86,400	1440	24	1	2.74e-06
1 year	3.1536e-07	5.256e-05	8760	365	1

TABLE A.5 Unit Conversions for Hydraulic Conductivity

Multiply	By	To obtain
1 gal/day/ft^2	0.1337	ft/day
1 cm/s	2835	ft/day
1 m/day	3.2808	ft/day
1 gal/day/ft^2	4.72×10^{-5}	cm/s
1 ft/day	3.53×10^{-4}	cm/s
1 m/day	1.16×10^{-3}	cm/s
1 gal/day/ft^2	4.07×10^{-2}	m/day
1 cm/s	864	m/day
1 ft/day	0.3048	m/day
1 cm/s	21203	gal/day/ft^2
1 ft/day	7.48	gal/day/ft^2
1 m/day	24.54	gal/day/ft^2

TABLE A.6 Unit Conversions for Flow

Unit	m^3/sec	m^3/day	L/sec	ft^3/sec	acre · ft/yr	gal/min	million gal/day
1 m^3/s	1	86,400	1000	35.31	6.255e-07	15,849	22.822
1 m^3/day	1.1574 e-05	1	0.01157	4.087e-04	0.2959	0.1834	2.641e-04
1 L/s	0.001	86.4	1	0.03531	25.57	15.849	0.02282
1 ft^3/s	0.02832	2446.6	28.32	1	724.2	448.8	0.6463
1 acre · ft/year	1.5987e-08	3.3795	0.03911	1.381e-03	1	0.612	8.927e-04
1 gal/min	6.31e-05	5.4526	0.0631	2.228e-03	1.613	1	1.44e-03
1 million gal/day	0.04382	3786	43.816	1.5473	1120.2	694.4	1

TABLE A.7 Conversion of Pressure

Pressure mm Hg	Feet	Meters	Calibration
760	0	0	100
752	278	85	99
745	558	170	98
737	841	256	97
730	1126	343	96
722	1413	431	95
714	1703	519	94
707	1995	608	93
699	2290	698	92
692	2587	789	91
684	2887	880	90
676	3190	972	89
669	3496	1066	88
661	3804	1160	87
654	4115	1254	86
646	4430	1350	85
638	4747	1447	84
631	5067	1544	83
623	5391	1643	82
616	5717	1743	81
608	6047	1843	80
600	6381	1945	79
593	6717	2047	78
585	7058	2151	77
578	7401	2256	76
570	7749	2362	75
562	8100	2469	74
555	8455	2577	73
547	8815	2687	72
540	9178	2797	71
532	9545	2909	70
524	9917	3023	69
517	10293	3137	68
509	10673	3253	67
502	11058	3371	66
495	11455	3492	65

TABLE A.8 Other Combinations

1 miner's inch = 11.22 gal/min
1 ft^3/sec (cfs) = 40 miner's inches
1 cubic centimeter (cm^3) = 0.061 cubic inch (in^3)
1 cubic meter (m^3) = 6.290 barrels (bbl)
1 bbl = 42 gallons
1 gram (g) = 0.002205 pounds (lb)
1 gram (g) = 0.0352 ounce (oz)
1 short ton = 2000 lb
1 long ton = 2240 lb
1 kg = 2.2046 lb
1 kg/cm^2 = 0.96 atmospheres (atm)
1 kg/cm^2 = 0.98 bar
1 atm = 1.01325 bar
1 g/cm^3 = 62.4 lb/ft^3
1 degree Celsius = [(1.8°C) + 32] °F
1 grain of Hardness per gallon = 17.1 mg/L in Total Dissolved Solids

Appendix

B

Relationship of Water Density and Viscosity to Temperature

Temp (°C)	Density (g/cm^3)	Viscosity (g/s · cm)
0	0.99984	0.01782
2	0.99994	0.01673
4	0.99997	0.01567
6	0.99994	0.01473
8	0.99985	0.01386
10	0.99970	0.01308
12	0.99950	0.01236
14	0.99924	0.01171
16	0.99894	0.01111
18	0.99860	0.01056
20	0.99820	0.01005
22	0.99777	0.00958
24	0.99730	0.00914
25	0.99704	0.00894
26	0.99678	0.00874
28	0.99623	0.00836
30	0.99565	0.00801
35	0.99403	0.00723
40	0.99221	0.00656
45	0.99021	0.00599
50	0.98805	0.00549

SOURCE: *Handbook of Chemistry and Physics,* CRC Press, Boca Raton, FL, 1990.

Copyright © 2008, 2001 by The McGraw-Hill Companies, Inc. Click here for terms of use.

This page intentionally left blank

Appendix

C

Periodic Table

Copyright © 2008, 2001 by The McGraw-Hill Companies, Inc. Click here for terms of use.

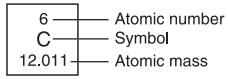

Periodic Table of the Elements

Atomic masses are based on ^{12}C. Atomic masses in parentheses are for the most stable isotope.

Periods	Groups IA	IIA	IIIB	IVB	VB	VIB	VIIB	VIIIB			IB	IIB	IIIA	IVA	VA	VIA	VIIA	VIIIA
1	1 H 1.0079																	2 He 4.00260
2	3 Li 6.941	4 Be 9.01218											5 B 10.81	6 C 12.011	7 N 14.0067	8 O 15.9994	9 F 18.998403	10 Ne 20.179
3	11 Na 22.98977	12 Mg 24.305											13 Al 26.98154	14 Si 28.0855	15 P 30.97376	16 S 32.06	17 Cl 35.453	18 Ar 39.948
4	19 K 39.0983	20 Ca 40.08	21 Sc 44.9559	22 Ti 47.90	23 V 50.9415	24 Cr 51.996	25 Mn 54.9380	26 Fe 55.847	27 Co 58.9332	28 Ni 58.70	29 Cu 63.546	30 Zn 65.38	31 Ga 69.72	32 Ge 72.59	33 As 74.9216	34 Se 78.96	35 Br 79.904	36 Kr 83.80
5	37 Rb 85.4678	38 Sr 87.62	39 Y 88.9059	40 Zr 91.22	41 Nb 92.9064	42 Mo 95.94	43 Tc (98)	44 Ru 101.07	45 Rh 102.9055	46 Pd 106.4	47 Ag 107.868	48 Cd 112.41	49 In 114.82	50 Sn 118.69	51 Sb 121.75	52 Te 127.60	53 I 126.9045	54 Xe 131.30
6	55 Cs 132.9054	56 Ba 137.33	57 La 138.9055	* 72 Hf 178.49	73 Ta 180.9479	74 W 183.85	75 Re 186.207	76 Os 190.2	77 Ir 192.22	78 Pt 195.09	79 Au 196.9665	80 Hg 200.59	81 Tl 204.37	82 Pb 207.2	83 Bi 208.9804	84 Po (209)	85 At (210)	86 Rn (222)
7	87 Fr (223)	88 Ra 226.0254	89 Ac 227.0278	† 104 Unq (261)	105 Unp (262)	106 Unh (263)												

*Lanthanide series

58 Ce 140.12	59 Pr 140.9077	60 Nd 144.24	61 Pm (145)	62 Sm 150.4	63 Eu 151.96	64 Gd 157.25	65 Tb 158.9254	66 Dy 162.50	67 Ho 164.9304	68 Er 167.26	69 Tm 168.9342	70 Yb 173.04	71 Lu 174.967

†Actinide series

90 Th 232.0381	91 Pa 231.0359	92 U 238.029	93 Np 237.0482	94 Pu (244)	95 Am (243)	96 Cm (247)	97 Bk (247)	98 Cf (251)	99 Es (252)	100 Fm (257)	101 Md (258)	102 No (259)	103 Lr (260)

Appendix

D

Values of $W(u)$ and u for the Theis Nonequilibrium Equation

Copyright © 2008, 2001 by The McGraw-Hill Companies, Inc. Click here for terms of use.

Values of *W*(*u*) and *u* for the Theis Nonequilibrium Equation

N\u	N × E-12	N × E-11	N × E-10	N × E-09	N × E-08	N × E-07	N × E-06	N × E-05	N × E-04	N × E-03	N × E-02	N × E-01	N
1.0	27.054	24.751	22.449	20.146	17.844	15.541	13.238	10.936	8.633	6.332	4.038	1.823	0.219
1.5	26.648	24.346	22.043	19.741	17.438	15.135	12.833	10.530	8.228	5.927	3.637	1.465	0.100
2.0	26.361	24.058	21.756	19.453	17.150	14.848	12.545	10.243	7.940	5.639	3.355	1.223	0.049
2.5	26.138	23.835	21.532	19.230	16.927	14.625	12.322	10.019	7.717	5.417	3.137	1.044	0.024
3.0	25.955	23.653	21.350	19.047	16.745	14.442	12.140	9.837	7.535	5.235	2.959	0.906	0.013
3.5	25.801	23.499	21.196	18.893	16.591	14.288	11.986	9.683	7.381	5.081	2.810	0.794	0.007
4.0	25.668	23.365	21.062	18.760	16.457	14.155	11.852	9.550	7.247	4.948	2.681	0.702	0.0038
4.5	25.550	23.247	20.945	18.642	16.339	14.037	11.734	9.432	7.130	4.831	2.568	0.625	0.0021
5.0	25.444	23.142	20.839	18.537	16.234	13.931	11.629	9.356	7.024	4.726	2.468	0.560	0.0011
5.5	25.349	23.047	20.744	18.441	16.139	13.836	11.534	9.231	6.929	4.631	2.378	0.503	0.00064
6.0	25.262	22.960	20.657	18.354	16.052	13.749	11.447	9.144	6.842	4.545	2.295	0.454	0.00036
6.5	25.182	22.879	20.577	18.274	15.972	13.669	11.367	9.064	6.762	4.465	2.22	0.412	0.0002
7.0	25.108	22.805	20.503	18.200	15.898	13.595	11.292	8.990	6.688	4.392	2.151	0.374	0.00012
7.5	25.039	22.736	20.434	18.131	15.829	13.526	11.223	8.921	6.619	4.323	2.087	0.340	0.000066
8.0	24.974	22.672	20.369	18.067	15.764	13.461	11.159	8.856	6.555	4.259	2.027	0.311	0.000037
8.5	24.914	22.611	20.309	18.006	15.703	13.401	11.098	8.796	6.494	4.199	1.971	0.284	0.000022
9.0	24.857	22.554	20.251	17.949	15.646	13.344	11.041	8.739	6.437	4.142	1.919	0.260	0.000012
9.5	24.803	22.500	20.197	17.895	15.592	13.290	10.987	8.685	6.383	4.089	1.870	0.239	0.000007

Appendix

E

Sources of Cave and Karst Information

Several organizations, societies, conferences, and government entities throughout the world are associated with the study of cave and karst science. The following pages provide a brief overview of some of these organizations and societies, in addition to, many Internet sites that serve as convenient sources of information about cave and karst science.

American Sources

The National Speleological Society: http://www.caves.org/

In 1941, the National Speleological Society (NSS) was founded for the purpose of advancing the study of caves with regard to exploration and conservation. Several internal organizations exist within the NSS. Approximately 200 local chapters or grottos have been established across the county. The NSS is split into about 17 sections that concentrate on various topics such as cave conservation and management, cave diving and cave rescue, paleontology, surveying and cartography, and geology and geography. The Geology and Geography section publishes an infrequent newsletter titled *Geo*^{2} that focuses on matters related to cave science. Two publications offered to society members include the NSS News and the Journal of Cave and Karst Studies. The NSS News predominantly features articles on cave exploration and conservation. The journal includes articles more of the scientific aspect of caves and karst. You can also access the online bookstore which contains many recently published material related to caves.

Copyright © 2008, 2001 by The McGraw-Hill Companies, Inc. Click here for terms of use.

The Karst Waters Institute: http://www.karstwaters.org/

The main goal of the Karst Waters Institute (KWI) is to improve the understanding of karst groundwater resources and to educate the public and professionals through the scientific study of these systems. Recent publications available of the KWI focus on cave management, epikarst, hydrogeology and biology of carbonate aquifers, and karst modeling. Conferences about aspects of cave and karst science are advertised at the KWI Web site. Karst education, employment notices, and links to several other karst resource related sites are provided.

Cave Research Foundation: http://www.cave-research.org/

The Cave Research Foundation (CRF) is a "private nonprofit organization dedicated to facilitating research, management and interpretation of caves and karst resources, forming partnerships to study, protect, and preserve cave resources and karst areas, and promoting the long-term conservation of caves and karst ecosystems." The CRF has a publishing partner known as Cave Books that can be found at http://www.cavebooks.com/.

National Cave and Karst Management Symposia: http://www.nckms.org/

The National Cave and Karst Management Symposia (NCKMS) hosts a symposium every two years that provides an opportunity for those with interest in cave and karst science to meet and discuss topics related to the protection and conservation of caves, cave ecosystems, water resources and karst lands. The first NCKM symposium was held in 1975 and has been held every two years since 1978. A proceedings volume is routinely published after the symposium.

National Caves Association: http://www.cavern.com/

The National Caves Association (NCA) was "founded in 1965, is a nonprofit organization of publicly and privately owned show caves developed for public visitation in the United States." Over 80 show caves are listed at the Web site and many links are provided for most that are included in the list.

National Cave and Karst Research Institute: http://www2.nature.nps.gov/nckri/

In 1998, the National Cave and Karst Research Institute (NC&KRI) was established by the U.S. National Park Service as the result of The

National Cave and Karst Research Institute Act of 1998—Public Law 105-325. The purpose of the Institute is to "further the science of speleology, to encourage and provide public education in the field, and to promote environmentally sound cave and karst management."

U.S. Geological Survey:
http://water.usgs.gov/ogw/karst/index.htm

In 2000, The Water Resources Division of the U.S. Geological Survey developed the Karst Interest Group (KIG). The KIG consists of U.S.G.S. employees that are interested in and conduct karst hydrology studies. Conferences were held in 2001, 2002, and 2005 and the proceedings volumes can be found at the USGS Web site.

American Cave and Conservation Association
http://www.cavern.org/acca/accahome.html

The American Cave Conservation Association (ACCA) is "a national, nonprofit association dedicated to the protection of caves, karstlands and groundwater and operates the American Cave Museum and Karst Center, an educational center that includes the American Cave Museum and Hidden River Cave." This Web site describes several professional services conducted by the ACCA such as the design and construction of gate caves. A vast technical library is available for those who require information about karst. Education workshops have been conducted with regard to land management for caves. Additionally, the Hidden River Cave can be utilized to research with respect to the cave and water quality. The ACCA provides an irregularly published magazine called American Caves.

Highway Geology Symposium:
http://www.highwaygeologysymposium.org/

Since 1950, the Highway Geology Symposium has been held in the United States every two years as a medium to promote a better understanding between the geologic and engineering professions with regard to the construction of our nation's highways. "The governing body of the symposium consists of about 25 engineering geologists and geotechnical engineers from state and federal agencies, colleges and universities, as well as private service companies and consulting firms throughout the country." Papers on karst issues are routinely contained to some degree in the proceedings volume. A cumulative index to each proceedings volume is provided at the Web site.

Non-American Sources

Speleogenesis and Evolution of Karst Aquifers: The Virtual Scientific Journal
http://www.speleogenesis.info/

This virtual scientific journal provides a nonprofit Web site dedicated to the study of speleogenesis—the origin and development of solution caves. Now in its seventh issue, many of the recent papers that deal with speleogenesis of karst can be found in this journal. Additional features at the site include a bibliographic search, book reviews, recent news about the karst community, and links to 10 Web sites that show international journals on cave and karst science.

British Cave Research Association:
http://www.bcra.org.uk/index.html

The British Cave Research Association (BCRA) was established to "promote the study of caves and associated phenomena and supports research on cave and karst research by encouraging original exploration in the United Kingdom and on expeditions overseas and by collecting and publishing speleological information." Recent books available at the BCRA include Cave Surveying by Day, a Dictionary of Karst and Caves by Lowe and Waltham, and Sediments in Caves by Ford. Additionally, BCRA publishes Cave and Karst Science, a peer reviewed journal, and Speleology, a magazine that covers popular science and technology related to caving, as well as expedition reports and the activities of BCRA's special interest groups.

Karst Dynamics Laboratory:
http://www.karst.edu.cn/

The Karst Dynamics Laboratory (KDL) was established in 1997 and is affiliated with the Ministry of Land and Resources in Guilin, China. KDL supports research in basic theory in karstology, rehabilitation of rocky desertification, and development of karst water resources and geological hazards prevention. The Director of the laboratory is Prof. Yuan Daoxian who has published extensively in the field of karst processes.

Limestone Research Group: http://
www.hud.ac.uk/sas/geog/lrg/purpose.htm

In 1985, Professor John Gunn of the University of Huddersfield, UK, founded the Limestone Research Group (LRG). "The mission of the LRG is to provide a high quality, multidisciplinary capability for research, consultancy and teaching in the applied earth and environmental sciences

with particular reference to limestone terrain." The Web site provides a list of current research conducted by the LRG in addition to a list of papers and reports prepared by the group members since 1996.

Karst Research Institute:
http://www.zrc-sazu.si/izrk/

The Karst Research Institute (KRI) is located in Slovenia, the type area where karst studies were initially conducted. The institute's sole purpose is to study the hydrology, geomorphology, speleology, and microbiology of the classical karst landscape. In association with KRI, ZRC Publishing, a unit of the Scientific Research Centre of the Slovenian Academy of Sciences and Arts, Ljubljana, Slovenia, publishes a journal titled Acta Carologica. The contents of this journal can be viewed at the Web site.

Theoretical and Applied Karstology:
http://www.geocities.com/karstology/

The Theoretical and Applied Karstology Web site or TAK-online, is a yearly publication of the Romanian Academy's Publishing House dedicated to cave and karst science. TAK publishes the contributions with regard to the study of karst such as physical speleology, karst geomorphology, cave management, engineering and environmental problems in karst, karst hydrology, and chemical and physical processes in karst. The contents of each of the 15 volumes published from 1984–2002 are available for review on the Web site in abstract in French and English. Some full length articles are available to download.

The Canadian Cave and Karst Information Server:
http://www.cancaver.ca/

Since 1996, this Web site has provided a wealth of information related to cave conservation in Canada. Some features found at this site include a list of Canada's longest and deepest caves and caving organizations by province, and cave rescue. One page is devoted to Canadian karst resources and issues. Items of interest include karst resource management of Vancouver Island and case histories and associated impacts with regard to forest management on karst. Several reports are provided at the Web site. The Stokes report examines cave and karst issues that relate to forestry activities on Vancouver Island. The Blackwell report was prepared to summarize all existing literature that pertained to the management of forested cave and karst ecosystems to aid land managers

in British Columbia. Other useful features include a multipage glossary of karst related terms and a list of over 20 Web sites, both Canadian and international, that provides information about karst resources and conservation.

Karst Link Page:
http://www.sgp.org.pl/spec/linkk.html

This Web site is maintained by the Association of Polish Geomorphologists and contains over 70 links of Web sites located mostly from North America and Europe.

Appendix

F

Water Quality Parameters and Their Significance

(Information you may wish to provide homeowners)

Constituent or physical property	Source or cause	Significance
Calcium (Ca) and Magnesium (Mg)	Dissolved from almost all soils and rocks but especially from limestone, dolomite, and gypsiferous sediments. Ca and/or Mg are found in large quantities in some brines; Mg is present in large quantities in sea water.	Cause most of the hardness and scale-forming properties of water; soap consuming. Waters low in calcium and magnesium are desired for electroplating, tanning, dyeing, textile, and electronics manufacturing.
Sodium (Na) and Potassium (K)	Dissolved from almost all rocks and soils. Found in ancient brines, some industrial brines, sea water, and sewage.	Large amounts give a salty taste when combined with chloride. Moderate quantities have little effect upon usefulness of water for most purposes. Sodium may cause foaming in steam boilers, and a high sodium adsorption ratio may limit the water for irrigation. Concentrations greater than 270 mg/L may be harmful to persons on sodium-restricted diets.
Iron (Fe)	Dissolved from almost all rocks and soils. May also be derived from iron pipes, pumps, and other equipment.	On exposure to air, iron in groundwater oxidizes to reddish-brown sediment. More than about 0.3 mg/L stains laundry and fixtures. Objectionable for food processing, beverages, dying, bleaching, ice manufacture, brewing, and other processes.

Copyright © 2008, 2001 by The McGraw-Hill Companies, Inc. Click here for terms of use.

Constituent or physical property	Source or cause	Significance
		Iron and manganese should not together exceed 0.3 mg/L. Larger quantities cause unpleasant taste and favor growth of iron bacteria, but do not endanger health. Excessive iron may also interfere with the efficient operation of exchange-silicate water softeners. Iron may be removed from water by aeration of the water followed by settling or filtration.
Manganese (Mn)	Dissolved from some rocks and soils. Not as common as iron. Large quantities often associated with high iron content and acid waters.	Same objectionable features as iron. Causes dark-brown or black stain. Iron and manganese should not exceed 0.3 mg/L for taste and aesthetic reasons.
Silica (SiO_2)	Dissolved from almost all rocks and soils, usually in small amounts (5 to 30 mg/L), but often more from acidic volcanic rocks.	Forms hard scale in pipes and boilers. Carried over in steam of high-pressure boilers to form deposits on blades of steam turbines. Inhibits deterioration of zeolite water softeners.
Bicarbonate (HCO_3^-) and Carbonate (CO_3^{-2})	Action of carbon dioxide in water on carbonate rocks such as limestone and dolomite, and oxidation of organic carbon.	Bicarbonate and carbonate produce alkalinity. Bicarbonates of calcium and magnesium in steam boilers and hot-water facilities form scale and release carbon dioxide gas.
Chloride (Cl^-)	Dissolved from rocks and soils. Present in sewage and found in large amounts in ancient brines, sea water, and industrial brines.	Chloride salts in excess of 100 mg/L give a salty taste to water. When combined with calcium and magnesium may increase the corrosive activity of water. It is recommended that chloride content should not exceed 250 mg/L.
Sulfate (SO_4^{-2})	Dissolved from rocks and soils containing gypsum, iron sulfides, and other sulfur compounds. Usually present in some industrial wastes.	Sulfate in water containing calcium forms hard scale in steam boilers. In large amounts, sulfate in combination with other ions gives a bitter taste to water. Concentrations above 250 mg/L may have a laxative effect, but 500 mg/L is considered safe. Some calcium sulfate is beneficial in the brewing process. Domestic waters in Montana containing as much as 1,000 mg/L sulfate are for drinking in the absence of a less mineralized water supply.

Constituent or physical property	Source or cause	Significance
Nitrate (NO_3^-)	Decaying organic matter, sewage, nitrates in soil, and fertilizers.	Concentrations greater than the local average may suggest pollution. High concentrations are generally characteristic of individual wells and not whole aquifers. Nitrate has been shown to be helpful in reducing intercrystalline cracking of boiler steel. Nitrate encourages the growth of algae and other organisms, which produce undesirable tastes and odors. There is evidence that more than about 10 mg/L (as N) may cause a type of methemoglobinemia ("blue babies") in infants, which may be fatal.
Fluoride (F^-)	Dissolved in small to minute quantities from most rocks and soils. Most hot and warm springs contain more than the recommended concentration of fluoride.	Fluoride in drinking water reduces the incidence of tooth decay in children when the water is consumed during the period of enamel calcification, but it may cause mottling of teeth, depending upon the concentration of fluoride, the age of the child, the amount of drinking water consumed, and the susceptibility of the individual. 0.8 to 1.7 mg/L is optimal, depending upon air temperature.
Hydrogen-ion activity (pH)	Acids, acid-generating salts, and free carbon dioxide lower pH. Carbonates, bicarbonates, hydroxides, silicates, and borates raise the pH.	The pH is a measure of the activity of the hydrogen ions (H^+). A pH of 7.0 indicates neutrality of a solution. Values higher than 7.0 denote increasing alkalinity; values lower than 7.0 indicate increasing acidity. Corrosiveness of water generally increases with decreasing pH, but excessively alkaline waters may also attack metals. Accurate pH can be made only at the well. Laboratory values willvary somewhat from the real value. A pH range between 6.0 and 8.5 is acceptable and is normal for most waters in Montana.
Dissolved Solids	Chiefly mineral constituents dissolved from rocks and soils. Includes all material that is in solution in the water.	Dissolved solids should not exceed 1,000 mg/L, but 1,000 mg/L is acceptable for drinking water if no other supply is available. Amounts exceeding 1,000 mg/L are unacceptable for most uses.

Constituent or physical property	Source or cause	Significance
Specific Conductance	Dissolved mineral in the water.	Specific conductance is a measurement of the water's capacity to conduct an electric current. This varies with the temperature and the degree of ionization of the dissolved constituents. When measured in micromhos/cm or microsiemens/cm, it is generally 1.0 to 1.5 times the total dissolved-solids content.
Hardness as $CaCO_3$	In most water nearly all hardness is due to calcium and magnesium. All of the metallic cations besides the alkaline earths also cause hardness.	Hard water consumes soap before a lather will form, deposits soap curd on bathtubs, and forms scale in boilers, water heaters, and pipes. Hardness equivalent to the bicarbonate and carbonate content is called carbonate hardness. Any hardness in excess of this is called non-carbonate hardness. Waters of hardness as much as 60 mg/L are termed soft; 61 to 120 mg/L moderately hard; 121 to 180 mg/L hard; and more that 180 mg/L very hard.
Alkalinity	Formed in the presence of certain anions in solution. Some organic materials may also produce alkalinity.	Alkalinity is an indicator of the relative amounts of carbonate, bicarbonate, and hydroxide ions and some anions (acid ligands).
Sodium Adsorption Ratio	SAR is defined by the equation $SAR = Na/([Ca + Mg]/2)^{0.5}$ Where the concentrations are expressed in milli-equivalents per liter (meq/L).	High sodium concentration combined with low alkaline-earth element concentration usually reduces soil tilth and affects plant growth.
Hydrogen Sulfide (H_2S)	Natural decomposition of organic material and from the reduction of sulfates.	Causes objectionable odor when in concentration above 1 mg/L and taste when in excess of 0.05 mg/L Presence may limit water usefulness in the food and beverage industry.
Trace metals	Dissolved from rocks and soils. Some metals may be released from plumbing piping, etc. Check the limits for your area.	Limits are usually recommended for health reasons. Limits for drinking water normally are conservative, and higher concentrations may be permitted if the water is the best available supply (e.g., copper).

Glossary

acquisition First of the three divisions of geophysical exploration (data acquisition). The process of designing geophysical surveys recording and recording geophysical measurements.

aggrading A stream reach building up sediments in its channel or floodplain by being supplied more sediment than it can carry. It is a stream reach characterized by active sedimentation.

amplitude Maximum departure of a wave from the average value (Sheriff 1991).

anisotropic *See* isotropy

aplite A dike rock of granitic composition that has very fine-grained crystals. The appearance is usually very felsic or light colored.

approach velocity (V_a) As groundwater moves towards the well screen the velocity increases. If the velocity exceeds a critical limit, finer particles from the aquifer will become entrained and move into the gravel packing. This critical limit is known as the approach velocity (V_a). It is not the same as an entrance velocity because it is specific discharge at the damage zone of the borehole wall.

aquicludes Units of extreme low permeability that form barriers to fluid flow. They are usually six orders of magnitude or less than surrounding units.

aquifer A formation, part of a formation, or group of formations that contain sufficient saturated permeable material to yield significant quantities of water to wells or springs.

aquifer hydraulics Evaluation of aquifer properties by stressing the aquifer and measuring and analyzing the response. Stressing the aquifer may be conducted through pumping tests or slug tests in the field. The drawdown response is plotted and analyzed to estimate the hydraulic properties.

aquitard A saturated unit of low hydraulic conductivity that can store and slowly transmit groundwater either upward or downward depending on the vertical hydraulic gradient.

aquitards Units of low hydraulic conductivity that can store and release groundwater at a slow rate.

Copyright © 2008, 2001 by The McGraw-Hill Companies, Inc. Click here for terms of use.

arrays Geometrical arrangement of sources or receivers used in a geophysical survey. Certain arrangements can be used to enhance particular qualities of the recording.

artesian *See* confined aquifer

average linear velocity (V_{ave}) *See* seepage velocity

backwashing A process of well development. In the development process water in the well casing is lifted by air for several minutes followed by shutting off the air for several minutes. As this is repeated, groundwater comes from the formation through the screen into the well casing and then from the well casing back out into the formation once again.

barrier boundaries Boundaries that inhibit groundwater flow. Examples are faults, bedrock, or thinning of an aquifer unit.

batholiths Igneous rock masses that are greater than 40 square miles (100 km^2).

bed A subunit of a member with distinguishable enough characteristics to be mappable in the field. An example would be a coal bed, within the member of a formation.

bolt method A method of protecting a mini-piezometer from crimping while pounding it to its completion depth. A bolt is taped to the bottom of the mini-piezometer, hence the name.

borehole dilution A type of tracer test where the volume of tracer introduced to a well is diluted by the volume of groundwater within the well bore.

Bouwer and Rice A method used to estimate the hydraulic conductivity in a partially penetrating or fully penetrating well in a unconfined aquifer from slug-test data.

breccia pipe A zone of fractured or angular rock materials that became fragmented during the migration of pressurized gasses towards the land surface along a plane or zone of weakness. The origin of the volatile gasses are associated with a magma source.

bulk density Density of a geologic medium that may be different than the densities of its constituents.

caldera A ring-shaped depression structure formed from the collapse of a magma chamber. The diameter of the crater rim usually exceeds 1 mile (1.6 km).

chargeability One of several units of induced polarization in the time domain. The ratio of initial decay voltage (or secondary voltage) to primary voltage (Sheriff 1991).

circulation A term indicating whether drill cutting and fluids are returning to the land surface. Fluids are injected at the bit, which in turn lift the cutting and fluid to the surface.

columnar jointing A phenomenon that occurs as lava contracts to form a solid. During the cooling process, polygonal prismatic shapes from to accommodate the escaping heat. The polygonal prismatic shapes extend down through the thickness of the lava flow to form columns.

compressional Seismic wave motion described by particle motion in the same direction as the wavefront propagation direction. Compressional waves are also called *P*-waves.

conceptual model A simplified representation of the groundwater system that indicates flow directions and boundary conditions affecting fluid flow.

conductance The product of conductivity and thickness. Indication of ease of current flow in a medium.

conductivity The ability of a material to conduct electrical current. In isotropic material, the reciprocal of resistivity (Sheriff 1991). Units are siemens per meter.

cone of depression A depression in the water table or potentiometric surface surrounding a pumping well. The shape of this depression is similar to an inverted cone.

confined aquifer An aquifer that is isolated has confining layers to maintain the pressure in the system at a pressure greater than atmospheric pressure. This causes the water levels in cased wells to rise above the top of the aquifer. The pressure results from the weight of the water elevation near the recharge area to be propagated throughout the system.

confining layers Layers that have a hydraulic conductivity two to three orders of magnitude less than a layer above or below it.

contact metamorphism A recrystallization of country rock into new compositions as a result of a nearby magma source. In this zone, high temperatures and low pressures are characteristics.

converging test A tracer test where the tracer is introduced under a nonstressed condition, but the sampling well is pumped.

crest-stage gauge A gauging apparatus useful in estimating peak flood events. A tube with grounded up cork or another floating material adheres to the sides of a tube at the place of maximum stream stage.

critical refraction The angle of incidence for which the refracted wave grazes the surface of contact between two media of different velocities.

cross-line Characterizes the direction perpendicular to a measurement direction (see in-line).

current density Current per unit cross-sectional area, determined by the velocity and density of charge carriers (Sheriff 1991).

Darcian velocity *See* specific discharge

Darcy's Law An equation that relates the volume of water per time moving through a given cross-sectional area of aquifer.

dart valve A valve on the bottom of a bailer that opens, when compressed, to allow cuttings and fluids into the bailer. The valve closes when the weight of the bailer is relaxed when lifted off of the bottom of the hole.

degrading The process of lowering a surface by removing sediments via air or water. Degrading streams are actively eroding sediments. This occurs from a stream with too flat a gradient for the volume of discharge.

delayed yield The second or delayed Theisian response after a recharge response indicated on the field plot of time-drawdown data during a pumping test. During the initial part of the time-drawdown plot the early-time data follow the Theis curve. This is followed by a flattening of the drawdown curve below the characteristic Theis curve indicating a recharge response. At late time, the data climb back on a secondary Theis curve once again.

diagenesis The process whereby unconsolidated sediments turn into solid rock. This occurs through burial, compaction, replacement, metamorphism, and cementation.

dikes Tabular igneous features that are discordant or cut across existing rocks.

dip The degree of inclination of a tilted bed from a horizontal plane.

discharge The loss of water from an aquifer system through an upward gradient in hydraulic head.

dispersion Variation of velocity with frequency. Surface waves exhibit dispersion, the analysis of which allows the calculation of shear wave velocity with depth.

distance-drawdown plots Plots of drawdown (on arithmetic scale) versus distance (in log scale) indicating the drawdown at a pumping well, observation wells, and the distance of the range of influence. These plots can also be used to estimate the hydraulic properties of aquifers.

diverging test A tracer test where initial injection of a point-source occurs, but pumping of the sampling well is not performed.

drawdown The amount of water level change from the static water level position during a pumping test.

drawworks A heavy cable with the top section laterally connected to a heavy chain along the drill rig mast that is designed to lift the drill string. The driller can raise and lower the drill string by the drawworks while the kelly bar slides past the kelly bushings in the rotary table.

dual-wall reverse circulation A drilling method where drill fluids are injected down the outer passageway of the drill pipe and the cuttings and fluids are drawn up through the center passageway. The inner sleeve is sealed by an O ring. During this method, the only place the drilling fluids contact the formation is near the bit. This allows a continuous sampling of the formation with minimal disturbance and reduces the chances of cross contamination.

dynamic viscosity (μ) It is a value equal to the shear stress divided by the velocity gradient, indicating a fluids resistance to flow.

effective radius (r_e) The distance from the center of a drillhole to the borehole wall where the formation was disturbed by drilling.

effective porosity (η_e) That proportion of porosity available to fluid flow. The effective porosity if often estimated by the value of specific yield.

effective grain size (d_{10}) The diameter of a sieved soil at 10% finer by weight.

Eh or E_H A measure of the oxidation status of the aqueous system, represented as: $E_H = E_H{}^o + (2.303RT/nF) \log_{10} [P_i\{ox\}^{n_i}/P_j\{red\}^{n_j}]$, where n is the number of electrons involved in the reaction, F is the Faraday's constant, R is the gas constant, T is the temperature in degrees Kelvin, $P_i\{ox\}^{n_i}$ is the product of the activities of the products of the reaction (as written, by convention the oxidized form of the element is on the product side of the reaction and the reduced form is on the reactant side; note that all components *except* the electrons are present in these terms) and $P_j\{red\}^{n_j}$ is the product of the activities of the reactants in the reaction as written. $E_H{}^o$ is the potential measured (in volts) when all of the species in the reaction are present at unit activities (the reference state for the reaction) and the rest of the terms are the correction for constituents not being present at unit activities. If all products and reactants are present at unit activities ($a_I = 1$), the right-hand term becomes the log of 1, which is zero, and the terms other than $E_H{}^o$ disappear.

elastic The ability to return to original shape after removal of a distorting stress (Sheriff 1991). Characterizes the ability of most rocks in response to a small disturbance.

electromagnetic surveying A method in which the magnetic and/or electric fields associated with artificially generated subsurface currents are measured. In general, electromagnetic methods are those in which the electric and magnetic fields in the earth satisfy the diffusion equation but not Laplace's equation or the wave equation (Sheriff 1991).

electromagnetic Referring to measurement methods which make use of electric and magnetic properties.

entropy Classically defined by physical chemists for reversible reactions at a uniform temperature as: $dS = dQ/T$, where Q is heat, T is absolute temperature, and S is entropy. In the real world all reactions are irreversible and a second term is added: $dS = dQ/T + dQ'/T$, where $dQ' < 0$ because of the nonideal (irreversibility) nature of real systems. In explaining entropy to geologists, it is often better to start off with stating that it is a measure of the disorder or randomness of the system studied. The use of entropy by Back and Hanshaw (1971) is that it is an indication of the degradation of the system or an index of the exhaustion of the system. They convert head change to potential energy available as heat, and derive the entropy from the head change (always positive values), and convert the water chemistry data into degree of saturation with respect to calcite, dolomite, and gypsum getting entropy values that are always negative.

eolian Pertaining to deposits formed under the influence of the wind.

equipotential lines Lines of equal hydraulic head.

evapotranspiration The amount of moisture loss from the transpiration of plants *and* the evaporation from soils.

exfoliation The process by which concentric layers of the rock fracture and peel off in sheets parallel the rock mass similar to onion layers. This is very characteristic in granites.

extrusive The process of eruption and the rocks that form on the surface.

facies The nature of sedimentary or metamorphic rocks reflective of the condition of their environment when they formed. It represents an areally restricted part of a formation with a particular characteristic. In sedimentary rocks, a coarse-grained facies may grade into a medium-grained facies as the energy in the environment decreases. In metamorphic rocks a greenschist facies may grade into an amphibolite facies as the temperature and pressure conditions increase.

falling-head test A slug test where the slug is instantaneously placed below the static water level in the well bore, displacing the water upward. Measurements of the falling water levels over time are recorded. In this case groundwater is entering the formation from the well.

first break The first recognizable part of a seismic trace attributable to seismic wave travel from a known source.

first arrival *See* first break.

float method A crude method of estimating stream velocity by tossing a float into a stream and measuring the time it takes to move a measured distance. This is repeated several times to obtain an average. A factor is multiplied by the result to account for drag and vegetative effects.

flow net A two-dimensional representation of steady-state groundwater flow. The flow net consists of intersecting lines of equal hydraulic head and associated flow lines.

fluvial Pertaining to a river or deposits formed by a river.

fluvial plain A relatively planar feature containing the active stream channel, floodplain and associated fluvially derived sediments.

foliation A planar textural term related to any rock, but is especially characteristic in metamorphic rocks. In this case there is a well defined orientation structure of minerals that formed during recrystallization. The minerals form perpendicular to the applied stresses.

footwall The rock mass below a fault plane.

formation A body of rock that is mappable in the field. Usually a formation consists of a similar lithology or group of lithologies formed in the same depositional environment.

forward modeling The process of calculating predicted data by inputting selected parameters into a desired model (see inverse modeling). For example, calculating seismic traveltimes by performing calculations from earth parameters.

frequency The inverse of period. The units of frequency are inverse seconds, inverse minutes, etc. Inverse seconds are given the unit hertz (Hz). One Hz represents one cycle per second.

gaining stream A stream that receives discharging water from a groundwater system. Discharge occurs because the head in the groundwater system is higher than the stage elevation of the stream.

geophones Instruments consisting of a magnet and coil arrangement used to record earth movement for recording by a seismograph. Transforms seismic energy into electrical energy (Sheriff 1991).

graben An extensional valley bounded on both sides by normal faults.

grading An engineering term pertaining to the division of sediments into grain sizes. Well grade indicates a wide range of grains sizes present, where poorly graded sediments indicate a narrow range of grain sizes.

group of formations A body of rocks composed of two or more formations.

hanging wall The rock mass above a fault plane.

head waves The wave created in medium 1 by a critically refracted wave in medium 2.

heaving sands Unconsolidated sands that forge into the borehole under pressure. The pressure deferential often results from the difference in fluid level in the casing compared to sands underlying clay zones.

heterogeneous *See* homogeneity.

hidden layer An earth layer which cannot be detected by seismic refraction methods. A layer of lower velocity lying beneath a layer of higher-velocity high-frequency approximation (Sheriff 1991).

homogeneity Relating to the physical properties of an aquifer from point A to point B, including packing, thickness, cementation. Homogenous units have similar properties from point A to point B and heterogeneous units differ in physical properties from point A to point B.

homogeneous *See* homogeneity.

horsts An elongate uplifted crustal unit left from the down-dropping of rock masses on either side from extension.

Hvorslev method A slug test analytical method used to estimate the hydraulic conductivity of an aquifer in the screened portion of a well. In can be used for confined or unconfined aquifers.

hydraulic conductivity (*K*) A value representing the relative ability of water to move through a geologic material of a given permeability. The specific weight and kinematic viscosity are also considered in determining the hydraulic conductivity.

hydraulic gradient The slope of the potentiometric surface. It is the rate of change of head per length of flow in a given direction.

hydraulic head The sum of the elevation head, pressure head, and velocity head at a given point in an aquifer.

hydrostratigraphy The division of stratigraphic units into aquifers and confining layers.

hyporheic zone That portion of the saturated zone in which surface water and groundwater mix. Physical, geochemical, and biological evidence of intermixing are used to define the hyporheic zone. Mixing can occur at many scales, through the stream bed, along the banks, and across meander bends. If seismic waves are characterized as having very high frequencies, the wavefronts will have very high curvature and can be described as arcs of circles with small radii. For high enough frequencies producing small enough radii, the wavefronts approximate the seismic ray.

induced polarization An exploration method involving measurement of the slow decay of voltage in the ground following the cessation of an excitation current pulse (time-domain method) or low-frequency (below 100 Hz) variations of earth impedance (Sheriff 1991).

in-line Characterizes the direction along a measurement direction such as along a line of geophones.

image well theory A theory used to simulate the effects of boundaries encountered during a pumping test. To simulate the boundary effect an imaginary well is placed on the other side of the boundary at an equal distance away from the pumping well to the boundary. The sign of the imaginary well (pumping or discharging) depends on the boundary type and whether the well is pumping or injecting. If the boundary is a barrier condition the imaginary well has the same sign as the real well. If the boundary condition is a recharge condition the imaginary well has the opposite sign of the real well.

infiltration The process of precipitation waters migrating into the soil horizon.

intercept time Time obtained by extrapolating the refraction alignment on a refraction t-x plot back to zero offset (Sheriff 1991).

interpretation Third of the three divisions of geophysical exploration (data interpretation). Estimating geological and lithological parameters from processed geophysical measurements.

intrinsic permeability (k_i) The ability of a fluid to move through a porous medium under a given gradient independent of the properties of the fluid. It is generally a function of grain size.

intrusive A process of injection into existing rock and igneous rocks that form from magma under the earth's surface.

inverse modeling The process of estimating model or desired parameters from measured data (see forward modeling). For example, estimating earth parameters from seismic traveltimes.

isotropy The ability of a fluid to move in a given direction at a given point within an aquifer. Fluids that can move equally in all directions are said to be isotropic and those that differ in one direction over another are said to be anisotropic.

joints Undisplaced fractures in rocks that have been subjected to tectonic forces.

kelly A steel bar on the drill rig that connects to the drill string. The power from the rig turns the rotary table which is transmitted to the kelly bar that rotates the drill pipe and bit.

kilobars A unit of pressure denoting 1,000 bars of pressure; one bar is a centimeter-gram-second unit of pressure, equal to 1,000,000 dynes per square centimeter.

knock-out plate or plug A plate placed near the bit of a hollow-stem auger to keep cutting from entering the center cavity of the hollow stem. The plate is knocked out during monitoring well completion.

lag time The time delay it takes for drill cuttings near the bit to appear at the surface.

landstreamer An array of geophones connected by cabling such that it can be towed efficiently on the ground surface. Similar in concept to a marine streamer which is towed behind a seismic survey vessel on the water.

lava Naturally occurring molten rock materials that flow above the land surface.

law of reflection The angle of incidence equals the angle of reflection. Geometric description of wave reflection from an interface.

leakance The rate of discharge of groundwater through an aquitard.

lineaments Linear features visible on the topographic surface that extend for more than 1 mile (1.6 km). These features are often believed to reflect crustal structure.

longitudinal dispersivity A coefficient representing the mixing that takes place along the direction of the flow path.

losing stream A stream that recharges a groundwater system through the loss of surface water. Surface water is lost because the stage is at a higher elevation than the local groundwater system.

lystric A normal fault that begins at a steep angle near the surface whose angle flattens with depth.

mafic Dark or related to rocks containing ferromagnesium minerals.

magma Naturally occurring molten rock materials occurring under the land surface.

magnetotellurics A method in which orthogonal components of the horizontal electric and magnetic fields induced by natural primary sources are measured simultaneously as a function of frequency (Sheriff 1991).

MASW Multichannel Analysis of Surface Waves. An analysis technique that uses surface wave information recorded from multiple geophones to produce a shear wave velocity profile with depth.

match point A selected point where values on the Theis curve and the overlaid time-drawdown data coincide. The match point defines where the well function, value of $1/u$, the time, and drawdown are to be used in the Theis equation. The most convenient place to select a match point is where the well function and the value for $1/u$ equals 1.0.

member A part of a formation with distinguishable enough characteristics to be mappable in the field. For example, a member may have unique fossil assemblages.

metasomatism A process where the compositions of rocks change from chemically active pore fluids without changes in the features or structures of the rock. The fluids are active in removing and replacing minerals.

mini-piezometers Small-diameter wells with short slot lengths (less than 6 in, 15 cm) used to measure hydraulic head. A series of these driven to different depths are useful in evaluating vertical gradients.

noise Any unwanted signal. For example, in geophysical exploration, 60 Hz electrical noise, wind noise, traffic noise, pump noise.

normal type curve A type curve where values of the well function and values for u are plotted forming a characteristic curve in log-log scale.

normal fault A fault forming under extensional conditions where the hanging wall moves down relative to the footwall.

optimum offset The optimum source/receiver separation or offset that results in seismic reflections that have minimal interference with other types of seismic waves.

peak Maximum excursion (positive) of a seismic wavelet or pulse (Sheriff 1991).

perched aquifer An aquifer that occurs above the regional water table with a vadose zone beneath it.

period The time for one cycle of a periodic signal. The time corresponding to one wavelength. Period can be measured in s, ms, micros, etc.

permeability The ability of a porous medium to transmit fluid under a given gradient.

phenocrysts Visible crystals in an igneous rock that are conspicuously larger than the surrounding matrix material.

pitless adapters A fitting from the riser pipe discharge line into a welded port in the casing allowing water to be discharged in a water line to a house. These are placed in areas below the frost line. Wells without pitless adapters have discharge lines that make a 90° turn with an elbow toward the house in a pit dug below the frost line.

porosity (η) The volume of void space within earth materials. Primary porosity occurs with the formation of a rock mass. Secondary porosity represents void spaces that occur after the rock mass formed.

potentiometric surface A surface estimated by the level to which cased wells will rise. This surface represents total head, which includes elevation head and pressure head.

price meter A meter used to perform stream guaging in larger deeper streams. A price meter is used to determine stream velocities per fraction of cross-sectional area. It has a horizontal wheel approximately 5 in (12.7 cm) in diameter, with small cups attached. The wheel rotates in the current on a cam attached to the spindle. An electrical contact creates a "click" sound with each rotation. The clicks are transmitted to a headset worn by the field person to obtain a clear signal. The clicks are counted for 30 or 60 s or sent to a direct readout meter. The number of clicks are compared with a calibration curve to obtain the velocity.

processing The second of the three divisions of geophysical exploration (data processing). Enhancing geophysical measurements and eliminating unwanted signals to aid geophysical interpretation.

profiling A geophysical survey in which the measuring system is moved about an area with the objective of characterizing lateral variations in the subsurface (Sheriff 1991).

pseudosection A plot of electrical measurements or calculations, often of apparent resistivity or induced polarization as a function of position and electrode spacing. A pseudosection indicates how the parameter varies with location and depth, but it can only be converted into a 2D model by inversion. For the dipole-dipole electrode configuration, the

data are plotted beneath the midpoint between the dipoles at a depth of half the distance between the dipole centers (Sheriff, 1991).

pumice A volcanic froth that has hardened into rock. Pumice forms where volatile gasses are expelled into lava. It is often sufficiently buoyant to float on water.

pygmy meter A small version of the price meter, used in shallower streams. *See* price meter.

range of influence The distance away from the pumping well to where the drawdown is zero.

ray A geometric construction everywhere perpendicular to wavefronts (in isotropic media). Used to characterize seismic wave travel paths.

recharge The addition of water to a groundwater system results in a downward gradient in hydraulic head.

recharge boundaries Boundaries that supply groundwater. Examples include hydraulically connected streams, coarser-grained units, or a thickening of the aquifer.

recirculation test A tracer test where both wells are stressed. The injection well receives "clean" or pumped water from another source.

recovery data The recovery response of drawdown after a pumping has stopped.

reflection Energy or wave from a seismic source which has been reflected (returned) from an acoustic-impedance contrast or series of contrasts within the earth (Sheriff 1991).

refraction The change in direction of a seismic ray upon passing into a medium with a different velocity (Sheriff 1991). Arises from Snell's law.

regional metamorphism A term referring to the metamorphism of an extensive region from tectonic activity. There may be a sequence metamorphic rock types that occur as a result of changes in temperature, pressure, and fluids associated with colliding tectonic plates.

residual drawdown plot A residual drawdown plot is constructed by plotting the ratio of the time since pumping started (t) to time since pumping stopped (t') (t/t') versus residual drawdown (s') to estimate aquifer transmissivity.

residual drawdown (s') The amount of drawdown recovery since pumping stopped.

resistance Opposition to the flow of electric current. Resistance takes into account resistivity and the geometry of the material.

resistivity The property of a material that resists the flow of electrical current. Units are ohm meters.

resolution The ability to separate two features which are close together. The minimum separation of two bodies before their individual identities are lost on the resultant map or cross section (Sheriff 1991).

reverse A fault forming under compressional conditions where the hanging wall moves up relative to the footwall.

reverse type curve The more commonly used form of the Theis curve. In this case values of the well function and values for $1/u$ are plotted forming a characteristic curve in log-log scale.

rifting A condition where tectonic forces extend or pull apart. This results in cracking, volcanism, and graben valleys.

riparian zone The riparian zone is commonly referred to as the interface between the terrestrial and aquatic interface. It is characterized by trees and other large vegetation and generally does not contain surface water except during episodic floods. In smaller stream systems, the riparian zone may be characterized by willows or other shrubs.

rising-head test A slug test where the slug is extracted from the well bore, displacing the static water level downward. Measurements of the rising recovering water levels over time are recorded. In this test recovering groundwater comes from the formation.

runoff The amount of precipitation that moves down a topographic slope that can not enter the soil horizon.

sand line An auxiliary cable on a drill rig other than the main cable used to retrieve pipe, pick up casing, other lifts and heavy tools.

saturated thickness (*b*) The thickness of saturated permeable material in an unconfined aquifer from the water table to lowermost confining layer. In a confined aquifer it is the thickness of saturated permeable material between two confining layers. In a pumping test it represents the contributing saturated thickness to the well screen, which is a function of pumping time and geologic conditions.

scoria A highly vesicular cindery zone at the tops and bottoms of lava flows from escaping gasses and burning vegetation.

seepage velocity The average rate of movement of a fluid over a given distance. It is calculated by dividing the specific discharge by the effective porosity.

seepage meter A seepage meter is an open-bottomed container that is inserted into the stream sediments to measure seepage rates. The time

it takes a volume of water to flow into or out of a bag connected to the container is measured to estimate the seepage.

seismic source A device that releases energy, such as an explosion or an air gun release (Sheriff 1991). Any of a variety of devices used to create seismic, electrical or other pulses for propagation through the earth.

seismic velocity Speed of propagation of a seismic disturbance through a medium. *P*-wave velocities are approximately twice as large as *S*-wave velocities.

seismic section A plot of seismic data along a line. The vertical scale is usually arrival time but sometimes depth (Sheriff 1991).

seismic tomography A method for estimating earth parameters from a multitude of observations using combinations of source and receiver locations. For example, CAT scans in medical imaging (see inverse modeling).

seismograph An instrument or system used to record seismic wave disturbances. Used in conjunction with geophones.

shear Seismic wave motion described by particle motion in a plane perpendicular to the wavefront propagation direction. Shear waves are also called *S*-waves.

sills Tabular igneous features that are concordant or are injected parallel to existing rocks.

sinks Extractions of groundwater from a system, such as pumping wells, and surface water discharge.

Snell's Law Describes the change in propagation direction of a seismic wave when it crosses a medium. The direction change depends on the seismic velocities of the media.

sorting The process of dividing sediments according to size during transport. This is done through a variety of processes, such water, wind, or ice. Well sorted indicates the sizes are similar and poorly sorted indicates a wide range of grain sizes represented.

sounding A geophysical survey in which the measuring system is moved about an area with the objective of characterizing vertical variations in the subsurface.

sources Contributions of water to a groundwater system, such as precipitation, injection wells, or imported water.

specific weight (γ) The weight of a given substance per unit volume.

specific yield (S_y) The ratio of volume of water from a saturated rock mass to the total volume that was yielded by gravity drainage.

specific retention (S_r) The ratio of the volume of water retained against the force of gravity to the total volume of rock.

specific storage (S_s) The volume of water that will yield due to compression of the mineral skeleton and decompression of water in a confined aquifer. It is also known as elastic storage.

specific discharge The apparent velocity of a fluid in an aquifer under laminar conditions that would flow if no geologic materials were present.

specific gravity The ratio of the density of a volume material to the density of an equal volume of water at a specified temperature.

specific capacity (S_c) The pumping rate in gallons per minute divided by the drawdown in feet. It is an expression of the productivity of a well and varies with time.

speed of propagation Speed at which a pulse or disturbance is transmitted through earth materials. Typically used to describe seismic or electromagnetic wave propagation.

spontaneous potential Observation of the static natural voltage existing between sets of points on the ground, sometimes caused by the electrochemical effects of ore bodies (Sheriff 1991).

stacking The process of making a composite trace by combining traces from different records. The constituent traces meet the condition of being reflected from the same earth point.

static water level The ambient water level elevation in a cased well where the aquifer has not been stressed.

storage coefficient (S) The volume of an aquifer takes into or releases from storage per unit surface area of an aquifer per unit change in head. In an unconfined aquifer it is estimated to be the specific yield and in a confined aquifer it represents the specific storage multiplied by the saturated thickness.

storativity (S) *See* storage coefficient.

strain Rock deformation as a result of stresses applied. Examples are folding or faulting of rocks.

strike The directional orientation of a structure resulting with intersection of a horizontal plane with an inclined plane.

support-rod method A method of protecting a mini-piezometer from crimping while pounding it to its completion depth by inserting a metal

support rod inside the mini-piezometer. The support rod is retracted after the desired depth is achieved.

synoptic survey A detailed stream guaging survey along a reach of stream, accounting for every gain or loss from diversion ditches or incoming ditches along the path. It is performed as a flux balance approach to stream flow. One can also identify losing or gaining stretches if the values exceed the error limitations of the equipment.

***t-x* plot** A plot of times for a selected seismic event (e.g., first arrival) versus distance (e.g., geophone offset from the shot).

transversal dispersivity A coefficient representing the mixing that takes place normal or transverse to the direction of the flow path.

tectonics The forces within the earth's crust which create structures or crustal movement.

tellurics Of the earth. A natural electrical earth current of low frequency which extends over a large region (Sheriff 1991).

three-point problem A geometric method of determining the strike and dip from three accurately determined positions of a structural surface.

tortuosity The actual sinuous flow path length divided by the straight-line distance.

trace A record of the data from one seismic channel, one electromagnetic channel, etc. (Sheriff 1991).

tracer test A field test where a traceable substance is introduced into the groundwater system at an injection point and tracked and measured to estimate hydraulic or hydrochemical properties.

transmissivity (T) The product of the hydraulic conductivity and the saturated thickness. It represents the ability of a given thickness of aquifer under a given gradient to transmit fluids.

tremie pipe A small-diameter pipe used as an access tube to place gravel packing materials around a well screen.

tripping in A drilling term referring to connecting the drill pipe and running it back into a drill hole after changing the drill bit or some other task requiring the drill pipe to be extracted.

tripping out A drilling term referring to the process of extracting the drill pipe from a drill hole.

trough Minimum excursion (maximum negative) of a seismic wavelet or pulse.

unconfined aquifer An aquifer whose upper surface is at atmospheric pressure.

uniformity coefficient (C_u) The ratio of the diameter of a given sieved soil at 60% finer by weight to the diameter at 10% finer by weight (effective grain size). Values less than 4 indicate well-sorted soils and values greater than 6 indicate poorly sorted soils.

vesicular An igneous rock texture associated with trapped gas bubbles.

viscosity The physical property of a fluid to resist flow. It is a measure of the shear stress to shear strain.

water table The top of the saturated zone of an unconfined aquifer where the pressure is at atmospheric pressure.

water-table aquifer *See* unconfined aquifer.

wave A disturbance that is propagated through the body or on the surface of a medium without involving net movement of material. Waves are usually characterized by periodicity (Sheriff 1991). For example, seismic waves, electromagnetic waves.

wavefronts The surface over which the phase of a traveling wave disturbance is the same. The wavefront follows the path defined by the seismic ray (see ray).

wavelength The distance between successive similar points on two adjacent cycles of a single frequency wave (Sheriff 1991). Used to quantify resolution in geophysical exploration.

well function ($W_{(u)}$) It is the infinite series term of the Theis equation. The well function includes relationships between the radial distance of an observation well and the hydraulic properties of the aquifer.

zero flux plane Basically, this is a "split the difference" approach to estimating the fraction of the soil moisture that actually recharges the groundwater system. It requires a bell-shaped curve of total hydraulic head (data from the tensiometers) versus depth. This approach presumes that the drainable soil moisture below the peak in the bell curve will continue moving downward to the water table, and that soil moisture above the peak will be drawn upward and be evapotranspired.

zero-offset The situation in which the source is at the same location as the receiver.

Reference

Sheriff, R.E., 1991. *Encyclopedic Dictionary of Exploration Geophysics*. Society of Exploration Geophysicists, Tulsa, OK.

Index

Acid rock drainage, 316, 370
Activated carbon, 676, 680, 684, 685, 687, 689–698
Analysis
  water budget, 4, 7
  traditional pumping test, 443
Alkalinity, 289–292, 304–310, 314–317
Andesite, 41–43, 45
Anisotropy, 119, 120, 438, 456, 471, 490
Apparent resistivity, 153–164
Approach velocity, 375, 379–382, 387
Aquifer, 91, 437
  artesian, 114
  boundary, 91, 114, 117–119
  combining, 116, 223, 228, 229
  concepts, 111, 120
  confined, 111, 114, 115, 118, 121, 122, 169, 438, 439, 441–443, 447, 455, 456, 458–463, 466, 473, 477, 483, 498
  confining layers, 91, 94, 114, 116, 122
  karst, 604, 615, 620, 627, 629, 633–638, 666, 697
  leaky-confined, 102, 441, 458–460, 462, 498
  perched, 94
  properties, 91, 119
  semiconfined, 102, 103
  unconfined, 94, 102, 111, 113, 115, 118, 122, 439, 441, 442, 455, 456, 458–463, 468, 470, 473, 477–479, 485–487
Aquifer hydraulics, 437, 438
Aquitards, 111, 459, 460
ASR, 1
Atomic absorption spectrophotometry, 307
Auger drilling 346, 347
  hollow-stem, 347, 363–368
  solid-stem, 346, 347, 364
Auger flights, 347, 364, 367
Axial plane, 73, 74

Back pressure, 411, 425, 426
Backwashing, 389
Bailer, 333, 361
Barometric pressure, 420, 433, 466
Barrier boundaries, 482, 484
Basalt, 41, 42, 45–50, 58, 62
  hydrologic properties, 49
Batholith, 50, 52
Batteries, 195, 207, 214, 215, 247, 292, 298, 428
Beaded cable, 205–207
Beaverhead Valley, 504, 505, 529, 542
Bentonite, 368, 369, 373, 593
Berkeley Pit, 7, 8
Bernoulli equation, 176, 177, 179, 229
Bighorn Basin, 75, 83
Bighorn Mountains, 83
Blacktail Creek, 224, 225
Blacktail Deer Creek, 541
Blanks, 290, 312, 313
Body waves, 134, 148
Bolt method, 255, 259
Bouwer and Rice test, 501, 512–520, 523–525
Bowen reaction series, 61
Breccia pipe, 38, 40
Bridge-slot, 382
Brunton compass, 69–71
Bubbling pressure, 581
Butte, Montana, 440, 441

Caldera, 48
Calibration, 19, 27, 28, 288, 292, 299, 304, 312, 313
Casing 188, 199–201, 203, 206–208, 212, 215, 219, 221, 344–349, 351, 356, 357, 363, 365–370, 373, 375, 378, 383, 385–387, 504, 506, 510, 513–517, 519, 523, 539–541, 565, 592–594
  advancement, 344

Copyright © 2008, 2001 by The McGraw-Hill Companies, Inc. Click here for terms of use.

Casing (*Cont.*):
driver, 344
hammer, 344
Cavitation, 395, 404
Cave(s), 627–633, 636, 637
controlling factors, 629, 630
passageways, 630, 631
Cenotes, 618, 619
Centralizers, 212, 215
Chain of command, 28, 29
Chain of custody, 292, 297, 308
Channel
active, 231, 237, 237, 277
geomorphology, 237
orientation, 234
Charge balance, 314–316
Chart recorders, 201, 205–209, 221
Chemical mass balance, 243, 280
Chemograph, 639, 640
Chip samples, 355
Circulation, 34, 336–339, 341–345, 358, 359, 387
Collecting samples, 310
Columnar joining, 46, 47
Conceptual model, 5, 16, 33, 35, 37, 116, 177, 123
Conductance
electrical, 129, 151, 641
Conductivity, 151, 168, 169
hy1draulic, 5, 34, 94, 101, 104–111, 114–116, 118–122, 173–182, 184, 186, 187, 191, 192, 203, 227, 229, 233, 263, 266–268, 278, 440, 441, 444, 456, 459, 463–466, 473, 485–490, 492, 493, 498, 501, 502, 504, 505, 512, 513, 515, 517, 519, 523–526, 529, 543, 554–562, 566, 567, 571, 572, 574, 575, 577–579, 581, 583, 586, 597, 661, 663–665, 669, 673
Cone of depression, 176, 397, 399, 401, 403, 404, 416, 425, 431, 435, 437–442, 460, 462, 463, 470, 472, 479, 481, 483
Cone of impression, 479
Confined aquifer, 111, 114, 115, 118, 121, 122, 169, 438, 439, 441–443, 447, 455, 456, 458–463, 466, 473, 477, 483, 498
Confining layers, 91, 94, 114, 116, 122, 397, 443, 460
Conservation of mass, 4, 183
Continuous-slot, 382, 383
Cooper-Jacob plot, 437, 448, 450–452, 454–456, 463, 470, 474, 482, 483
Core samples, 22, 355
Crest-stage gauge, 243, 251–253
Critical angle 137,
calculation, 139–140
Critical
refraction, 137, 138
time, 457
Current density, 153, 154, 164
Cuttings, 21, 22, 25, 321, 323, 327, 329, 333, 334, 336–338, 340–345, 347, 354, 356–359, 363, 364, 368, 375

Damping parameter, 526, 537–539, 541, 543
Darcy, 105
Darcy's law, 173, 174, 176, 179–182, 186, 187, 189, 229, 440, 512, 554, 557, 559, 561, 566, 567, 572
Dart valve, 333
Data
statistical analysis, 317
Data logger, 26, 193, 207–210, 219, 222, 265, 411, 418–420, 422–424, 430–432, 502–504, 506, 507, 511, 512, 537, 538
Decontaminating equipment, 218
Delayed yield, 398, 400, 430, 461–467, 495, 496, 498
Density
dry bulk, 99, 101
Depositional environment, 59, 64, 66, 67, 108, 109, 117, 120, 186, 187, 192, 397, 611
Diagenesis, 64
Dikes, 50, 53, 55, 57, 87
Dillon, Montana, 504, 505, 541, 542
Dip, 55, 69–72
Direct measuring
psychrometer, 584–586
tensiometer, 558, 583, 584
Direct sampling
lysimeter, 562, 594
Direct-push method, 347, 349–351
Discharge, 8, 10, 30, 81, 122, 165, 189–191, 231, 236, 240, 249, 250, 262, 265, 274, 278, 414, 425, 426
area, 10, 15, 118, 173, 183, 187–189–191, 193, 223, 225, 227, 228, 234, 236, 397
chamber, 333, 334
line, 27, 411, 416, 425–427, 429, 435
rate, 174, 396, 411

Discharge (*Cont.*):
spring, 8, 122
system, 411, 425, 435
tube, 344, 345
Dissolved oxygen, 290, 291, 298, 303, 318
Distance-drawdown plots, 397, 438, 462, 470–474, 476, 477, 479–481
Diurnal, 5, 265, 318, 319
Diverging test, 653, 653
Dolomite problem, 614
Domestic wells, 13, 28, 53, 112, 175, 198, 201, 215, 260, 383, 385, 457, 478, 485
Double straight-line effect, 519
Drag bit, 338, 339
Drainable porosity, 553
Drainage
ephemeral, 236, 251, 252
Sand Creek, 5, 6
Silver Bow Creek, 7, 58
Drawdown, 208, 383, 397, 399–411, 419, 420, 423–425, 430, 431, 433–435, 528
residual, 474, 475
Drawworks, 335, 337, 356
Drill hole
logging, 344, 354, 356
Drillers, 356, 358, 360, 361, 364, 365, 367, 370, 376, 385–387, 390
Drilling and well completion, 321
Drilling fluids, 330, 336, 337, 339, 341, 343, 347, 351
Drive shoe, 342
Dry bulk density, 99, 101
Dual porosity model, 438, 495–497
Duct tape, 208, 222, 254, 273, 274, 292, 372, 411, 420, 427, 429
Dunham classification, 613
Dynamic viscosity, 104

Eagle Sandstone, 264
Edwards aquifer, 8, 9
Effective column length, 527, 529, 538
Effective grain size, 107, 108, 110, 375
Effective porosity, 96, 122, 175, 177, 379
Effective radius, 473, 474, 513, 515, 517, 543
Effective stress, 529, 530, 532
Effective water column, 526, 527, 534
Efficiency (well), 379, 405–407, 484
Eh, 290–292, 303, 304
El Nino, 36
Elastic behavior, 474
Electrical neutrality, 314
Electrode configurations
arrays, 155
Electrode spacing, 148, 154–159, 163
Electromagnetic
surveying, 152
techniques, 165, 589, 641, 643
Entrance velocity, 375, 379, 382, 384
Environmental Protection Agency, 11, 289, 290, 308, 309, 312, 313, 316
Eosine, 680, 681, 683–686, 691, 693–695, 697
Ephemeral drainage, 236, 251, 252
Epikarst, 623–625, 634, 635, 696, 697
Equipment
batteries, 195, 207, 214, 215, 247, 292, 298, 428
calibration, 19, 27, 28, 288, 299, 304, 312, 313
decontamination, 215, 219, 222
detangling, 217, 218
retrieving, 215
Equipotential lines, 183, 189
E-tapes, 27, 201–205, 209, 211–213, 215–218, 221, 222, 504, 512, 672
Evaporation, 1, 5, 7, 8, 12, 559, 561, 562, 578, 584
Evapotranspiration, 5, 8, 11, 554, 562, 563, 564, 566, 567
Exfoliation, 51, 62, 63
Exported water, 5
Extrusive rocks, 38

Facies, 58
Falling-head test, 506–508, 512
Fault, 18, 37, 49, 51, 52, 63, 68, 69, 71, 75, 78, 86
lystric, 75
normal, 75–77, 79
reverse, 75–77
thrust, 75, 76, 82
Field book, 18, 19, 21, 24–27, 355, 411, 412, 430, 431, 435
Field equipment 203, 290, 297, 317, 412
Field hydrogeology, 1, 35
Field notes, 18, 19, 24, 28
field sketches, 19
lithologic logs, 19, 21, 359
Field parameters, 287, 290, 293, 298
Fillable porosity, 575
Filter pack, 366, 367, 377–380
First arrival, 132, 133
First break, 132, 139, 140

Fluorescein, 677, 678, 680–686, 693–695, 697
Flow meter, 411, 426, 427, 429, 430
Flow nets, 183, 184, 186–191, 229
Flowing well
  pumping test, 495, 497
Fluid
  movement, 104
  potential, 154
Fluvial plain, 231–242
Fold geometry, 73, 74
Foliated rock, 56
Foliation, 56, 58, 69
Folk classification, 612, 613
Footwall, 75
Formation, 37, 55, 67–69, 71, 73, 76–79, 84, 87, 189
Forward modeling, 128, 162
Fracture flow analysis, 462, 472, 492, 497
Fractured media, 492, 493, 495

Gaining stream, 189, 190, 247, 259, 274, 280
Gauging
  stream, 243–245, 247–249, 251, 253, 260, 278–282, 429
Generator, 411–414, 428, 430, 432
Geographic information system, 15, 31
Geologic model, 37
Geologic terms, 37, 66, 88
  history, 87
  map, 71, 340, 341, 355
  time, 84, 85
Geomorphology, 237
Geophone, 131, 132, 134, 135, 138–140, 142, 145, 146, 148, 149
Geophysical investigation, 126, 128, 141
Geophysical survey, 127, 130, 151, 156
Geophysical techniques 125–127
  active, 127
  overview, 127
  passive, 127, 148
Geophysics, 125, 126, 130, 131
GEOREF, 14, 15
Global positioning system, 23, 195
Goldich weathering sequence, 61
Goldich weathering series, 61
Gradient
  hydraulic, 104, 115, 118, 119, 173–176, 183–187, 192, 261, 263, 440, 493, 494, 550, 554, 555, 558, 561, 566, 577, 578, 586, 593
Grading, 65
Grain size
  sorting, 64–66
Gravel packing, 375, 377–379
Ground-penetrating radar, 129, 145, 169
Groundwater, 1–3, 30, 165, 169, 207, 530
  characterization, 30
  chemistry, 287
  discharge, 10–11, 189, 190
  monitoring wells, 184, 186, 192
  planning, 30
  use, 29
  vertical flow, 261
Groundwater contamination, 34
Groundwater flow
  boundary concepts, 117
  conceptual model, 5, 9, 16, 33, 35, 37, 116, 177, 123
  refraction, 191
Groundwater monitoring, 184, 186, 192, 193, 207, 211, 218, 321, 361, 362
Groundwater/surface water
  flow-through, 232, 234, 235
  gaining, 232, 234, 240, 278, 280
  losing, 232, 234, 237, 238, 280
  parallel, 232, 234, 236, 238, 280
Grouting material, 25, 368
Gypsum blocks, 586–588

Hanging wall, 75
Hazen equation, 107–110
Hazen method, 108
  ranges, 108
Head losses, 404, 405, 425, 485
Head waves, 137, 139
Heaving sands, 334, 339, 384
Homestake Pass, 52–54
Homogeneity, 119
Horizontal drilling, 353, 354
Hualapai Plateau, 116, 117
Hvorslev method, 512–514, 516, 519, 524, 525, 541, 543
Hydraulic conductivity, 5, 34, 94, 101, 104–111, 114–116, 118–122, 173–182, 184, 186, 187, 191, 192, 203, 227, 229, 233, 263, 266–268, 278, 440, 441, 444, 456, 459, 463–466, 473, 485–490, 492, 493, 498, 501, 502, 504, 505, 512, 513, 515, 517, 519, 523–526, 529, 543, 554–562, 566, 567, 571, 572, 574, 575, 577–579, 581, 583, 586, 597, 661, 663–665, 669, 673

Hydraulic gradient, 104, 115, 118, 119, 173–176, 183–187, 192, 261, 263, 440, 493, 494, 550, 554, 555, 558, 561, 566, 577, 578, 586, 593
Hydrogeologic investigation, 184–186
  site location, 16
Hydrogeology
  field, 1, 35
Hydrograph, 2, 32, 206, 221, 226, 227, 236, 435,
Hydrologic cycle, 1–4, 35
Hydrostratigraphic unit, 37, 64, 68
Hydrostratigraphy, 116, 117, 122
Hyporheic zone, 231, 236, 238, 240–242, 272, 275, 278, 280

iButton, 272–274
Igneous rocks
  classification, 39
  extrusive, 38, 41, 46, 49, 50
  geologic properties, 38
  intrusive, 38, 41, 49–51, 53, 59
Image well theory, 438, 482–484
Imported water, 5, 7, 8
In situ, 291, 298–300
Indirect measuring
  neutron probe, 565, 577–579, 591, 592
  resistance method, 574, 586, 587
Induced polarization, 129, 152, 162
Inductively coupled argon plasma spectrometry, 291, 307
Inertial effects, 526, 527, 530, 531, 533, 535
Inertial parameter, 537, 539
Infiltration, 27, 87, 547, 559–562, 566–568, 574–579
  galleries, 32
  rates, 560–562, 575–579
Infinite transmissivity, 470
Inflow, 4, 5
Injection wells, 475, 479–481, 651, 653, 658, 660, 662, 671, 678
Inorganic constituents, 287, 315
Intermittent streams, 31
Interpretation of geophysical, 125, 127, 128, 130, 140, 142, 145, 151, 152, 154, 156, 157, 159, 161, 163, 165, 166, 169
Intrinsic permeability, 91, 101, 104, 105
Inverse modeling, 128
Ion chromatography, 291, 308
Ionic balance (*see* charge balance)
Isotropy, 119–121

Kalispell, Montana, 531, 532
Karren, 622, 623
Karst, 66, 79, 82–84, 603–606, 675, 680, 697
  aquifer, 82, 604, 615, 619, 627, 633–638, 697
  cockpit, 605, 608
  cone, 607, 608
  covered, 606, 608
  epikarst, 623–625, 634, 635, 696, 697
  fluvio, 608, 609
  landscape, 604, 606, 608, 609, 615, 620, 623, 636, 643
  pavement, 608, 609
  paleo, 67, 606
  sinkhole, 66, 79, 82, 603, 605, 608–610, 615–618, 620, 626, 629, 630, 637, 639, 642, 680, 696
  springs, 615, 625–627, 633–635, 640, 643, 680
  tower, 603, 607, 616
  valleys, 620, 622
Kelly bar, 335, 347
Kipp method, 526, 528, 533, 535, 537–539, 541–543
Knock-out plate, 363–365

Laboratory blank, 313
Laboratory protocol, 29, 33, 297, 307, 313, 314
Laboratory QA, 313
Lacustrine, 66, 401
Lag time, 358, 359
Laminar flow, 250, 404, 406–408
Lava, 38, 41–43, 45, 46, 48, 86
Law of Reflection, 135
Leakance, 459, 482
Level measurement 192, 220
  defining, 194, 211
  errors, 213, 215, 223, 227
  in flowing wells, 219
  taking, 197, 201
Level measurement methods
  automated, 207, 208, 211, 222
  manual, 221
Level measurement devices 201, 211
  electronic cable, 196
  probe design, 194
  well probes, 195
Light nonaqueous phase liquid, 227
Lithologic logs, 19–21
Little Bitterroot Valley, 401
Long Island, NY, 435

Longitudinal dispersivity, 661, 669
Losing stream, 190, 191, 231, 236, 248
Lysimeter, 562–565, 593, 594

Macroinvertebrates, 236, 240
Mafic, 38
Magma, 38, 41, 46, 49, 50, 52, 53, 56–58, 62
Magnetic surveying, 126, 152
Magnetotellurics, 152, 164, 165
Manning equation, 252, 253
Manometer tube, 427, 429, 430
Match point, 445–447, 454, 460–462, 466, 467, 495
Matric potential, 548–550, 566
Maximum concentration, 660, 662, 668, 669
Mean sea level, 178, 180, 194
Measurement
  water-quality, 27
Metamorphic rock, 55
  contact, 56, 57
  geologic properties, 58
  plate tectonic settings, 57
  regional, 56, 58
Metasomatism, 55
Meters
  pH, 288, 298, 300, 301, 303, 305
  specific conductance, 290, 298, 300, 302
Miles Crossing, 463, 466
Minipiezometer, 240, 243, 253–255, 259–261, 263, 264, 280
MINTEQ, 315, 316
Monitoring well, 331, 347, 360, 363
  groundwater, 184, 186, 192, 360, 363
  level measurements, 180, 190, 220

Net positive suction head, 416, 418
Neutron probe, 565, 577–579, 591, 592
Noise, 125
Nonwell injections, 665
Nutrient exchange, 236–238
  retention, 238
  samples, 291, 319

Observation well, 27, 208, 360, 396, 398–401, 403, 404, 412, 428, 431, 434, 438, 439, 442, 447, 451, 452, 455, 462–470, 475, 486, 495–497, 528, 532, 656–658, 662, 668, 671
Optimum offset method, 146
Organic carbon, 291, 294, 298, 308, 314, 319, 684
Osmotic potential, 585
Outflow, 4, 5, 8
Outwash deposits, 92
Overpumping, 372, 378, 387

P-waves, 134, 148, 149, 151
Packing, 94, 97, 98, 119, 120
Paleokarst, 67, 606
Paradox basin, 78, 79
Parasitic fold, 78, 79
Parshall flume, 243, 249–251
Partial penetration, 398, 455, 456, 484, 485
Pathogenic organisms, 31
Peoples Republic of China, 328, 346
Percent open area, 382–384
Perched aquifer, 94, 228, 229, 362, 547, 550, 565, 593
Percolation, 567
  deep, 559, 565–568
Period, 131
Permeability, 94, 104, 120, 122
  intrinsic,91, 101, 104, 105
Personal protective equipment, 329, 330, 355
Petroleum County, 497
pH, 27–29, 211, 219, 227, 238, 239, 274, 288–292, 298–301, 303, 305–307, 310, 314–316, 318, 319
pH meters, 288, 298, 300, 301, 303, 305
Phenocrysts, 49
PHREEQC, 316
Pipestone, Montana, 53
Pitless adapter, 215
Plate-jack method, 256, 278
Point-source infrastructure, 656, 662
Polarization, 129, 152, 162, 514, 517, 553
Porosity, 7, 39, 94, 95, 98, 113, 653
  aquifer storage, 94
  drainable, 494
  dual, 95, 438, 495–497
  effective, 34, 96, 175, 263, 660, 661, 665, 673
  fillable, 574
  primary, 51, 59, 95
  ranges, 49, 97
  secondary, 51, 59, 80, 84, 95, 119
  total, 94, 96, 97, 99, 494
  triple, 80, 81, 94, 635
Potentiometric surface, 5, 114, 115, 118, 174, 178–180, 183–186, 195, 248, 403, 438, 439, 479, 536

Precipitation, 1, 2, 5–8, 11, 15, 91, 173, 189, 223, 225–227, 249, 252, 341, 547, 559–562, 566–568, 603, 615, 620, 622, 640, 687
Pressure head, 114, 177–180, 219, 227, 401, 439, 466, 550, 553–559, 567, 569, 577, 578, 583, 584
Pressure transducer, 207–209, 211, 219, 222, 264, 353, 420, 423, 497, 502, 504, 511, 526, 574, 584, 672
Price meter, 243, 246
Primary porosity, 51, 59, 95
Production-well completion, 374
Profiling, 146, 155–157, 159
Propagation, 131–135, 138
Pseudosection, 157–160, 166
Psychrometer, 584–586
Pumice, 39, 43
Pump liner, 383, 385
Pumping rate, 9, 26, 27, 96, 379, 387, 388, 404–409, 425, 430, 438, 439, 442, 444, 447–452, 454–456, 459, 462, 467, 472, 473, 475, 476, 478, 497, 484, 490, 491, 665
Pumping test, 5, 19, 25, 26, 96, 101, 110, 111, 202–204, 208, 211, 215, 219, 381, 395–401, 404, 405, 409, 411–414, 419, 421, 423–427, 431, 433–435, 437, 441–443, 445, 447–449, 452, 453, 455–458, 463, 467–470, 472–476, 484–488, 492, 495–497, 501, 519, 529–532, 543, 635, 665
  barometric pressure, 209, 419
  data, 381, 419,
  designing, 397
  equipment, 411, 412, 420
  example, 395
  geologic conditions, 396–398
  manual readings, 395, 421, 428, 430, 431
  safety, 413, 432
  setup procedure, 427
  time intervals, 431
Pumps sampling, 404, 412–414, 425
  submersible, 404, 414
  turbine, 397, 414, 415, 427
Purge, 25, 28, 289, 292, 293, 298
Pygmy meter, 246
Pyranine, 682–686, 694–697

Ramsay, Montana, 441, 442
Range of influence, 463, 470–473
Receptor, 658–662, 668–670, 673, 674
Recharge, 8, 10, 11, 13, 93, 178, 223, 226, 235, 264, 266, 398, 559, 565–569
  area, 15, 31, 114, 118, 122, 173, 187, 188, 190, 191, 219, 223, 227, 228, 397, 434
  boundary, 434, 439, 460, 462, 463
  well, 479, 482–484, 495
Recirculating tracer test, 652, 653, 663
Recovery plots, 474–477
Redox, 294, 296, 316
  state, 298, 303
Reflection, 129, 131, 133, 135, 136, 138, 140, 143–147, 643
Refraction, 127–133, 135, 137–140, 142–146, 149, 160, 162, 642, 643
Residual drawdown, 47, 475
Resistance blocks, 586, 587
Resistivity, 129, 151, 154–160, 162, 164, 168
  electrical, 130, 140, 152
Resolution, 128, 144, 151, 154
Retention curve, 551, 556, 569, 571, 581
Reverse type curve, 446–448, 483
Rhodamine B, 683
Rhodamine WT, 274–276, 278, 279, 652, 654–656, 677, 680, 683–686, 693–695, 697
Rhyolite, 38, 41, 42
Rifting, 39, 41, 49
Rio Grande River, 182
Riparian doctrine, 30
Riparian zone, 236–238, 240, 241, 243
Riser pipe, 27, 203, 205, 208, 209, 215–217, 411, 416, 422, 425, 457,
Rising-head test, 506–508, 512, 538
Riverine valley, 232

Safety, 324, 325, 328–330, 351, 354
Sampler
  carbon, 676, 680, 684, 689, 695–697
  water, 680, 684, 292–294, 297
Samples 22, 99, 109
  blank, 313
  chip, 22, 355, 356
  collecting, 99, 292–298, 310, 311, 344, 347, 355, 356, 375–377, 583, 589, 592–595, 670, 686, 689–694
  core, 22, 349, 635
  duplicate, 308
  environmental, 308–310
  soil, 569
  spike, 312

Samples (*Cont.*):
water, 28, 29, 86, 287–299, 301–307, 311–314, 317, 689–694
Sand Creek, 5, 6, 248
Sand line, 323, 333, 346, 365
Sand lock, 367
Sand size, 60, 366
Saturated thickness, 102, 111, 174, 398, 406, 438, 460, 462, 467, 468, 485–487, 492
Screen entrance velocity, 375, 379, 382, 384
Sea level, 178, 180, 194
Secondary porosity, 51, 59, 80, 84, 95, 119
Sediment, 61, 64–66, 79, 82, 206, 232–237, 242, 252–256, 258–268, 270, 276, 277, 282
grading, 65
sorting, 64–66
transport, 63, 64
Sediment classification
grain size, 60
Wentworth, 60
Sedimentary rock, 53, 59, 61, 62, 69, 84, 87
Seepage
meter, 260–265
velocity (average linear), 106, 107, 175–177, 187, 263, 275, 276
Seismic, 142–144, 642
layer, 128
reflection, 129, 131, 133, 135, 136, 138, 140, 143–147, 643
refraction, 127–133, 135, 137–140, 142–146, 149, 160, 162, 642, 643
section, 144–147, 159
source, 131, 139, 141, 142, 146, 148
velocity, 127, 135, 139
Seismograph, 131, 140
Shenandoah National Park, 275, 277
Shepard method, 108–110
Sieve, 356, 358, 366
analysis, 375–377, 381, 384
Silica sand, 366
Sills, 51, 53, 57
Silver Bow Creek, 7, 233, 248, 249
Silver Gate, Montana, 260–262, 281, 282
Sinkhole, 66, 79, 82, 603, 605, 608–610, 615–618, 620, 626, 629, 630, 637, 639, 642, 680, 696
Skin effect, 365, 404, 405, 510, 515, 526, 533, 543
Skin factor, 539
Slack time, 18, 19, 24, 324
Slide hammer, 569
Slot size, 366, 375–380, 383
Slug test,
Bouwer and Rice, 518, 519, 521, 523–525
Butler, 501, 526, 533, 543
Hvorslev, 513–515, 519, 524, 525
Kipp, 526, 528, 535–539, 541
van der Kamp, 526–528, 533, 534, 541
Snell's Law, 137, 138, 191
Soil moisture, 569
Soil moisture determination, 569
Soil-water potential, 550, 551, 554, 565, 583–586, 595
Sounding, 155–157, 159
Source-water protection, 1, 30–34
Speciation, 292, 310, 315, 316
Specific capacity, 457, 472, 477, 478
Specific conductance, 290, 298, 300, 302
Specific discharge, 175
Specific gravity, 99, 101
Specific retention, 96–98
Specific storage, 102, 455
Specific water capacity, 566
Specific weight, 104
Specific yield, 96–98, 100, 102, 441, 455, 463, 466–468, 470
Spectroscopy, 307–309
Spectrophotometer, 288, 292, 308, 311
Speleothems, 631, 632
Spike recovery, 312, 313
Spikes, 289, 308, 312, 313
Spontaneous potential, 129, 152, 163
Springs, 8, 9, 32, 42, 43, 82, 84, 111, 113, 119–121, 615, 625–627, 633–635, 640, 643, 680
Spudding beam, 331, 332
Stacking, 142, 144
Standard operating procedure (SOP), 289, 290, 292, 294, 296, 309, 317
Static water level, 16, 24, 25, 27, 34, 192, 199, 202, 205, 211, 219, 220, 342, 343, 359, 404, 438, 463, 477, 502, 506, 508, 510–513, 517, 527, 538, 543
Steel tapes, 201–203, 205, 213, 221
Step-drawdown test, 404, 407–410, 430
Storage coefficient or storage, 94, 101, 441, 445, 461, 480, 490, 491
casing, 456–457
fracture, 494
specific, 102, 455
water, 559, 561, 563, 565, 567

Storativity, 101, 102, 441, 459–461
  confined aquifers, 102, 441, 461
Straight-line plot,
  Cooper-Jacob, 448, 450–454, 466, 482, 483
  distance drawdown, 470–472
  recovery, 475
Stratigraphy, 64, 67, 68
Stream
  aggrading, 237, 238
  braided, 231, 233, 234, 236
  channel orientation, 234
  connectivity, 237, 258
  degrading, 237, 238
  ecology, 275
  ephemeral, 236, 251, 252
  gaining, 189, 190, 247, 259, 274, 280
  health, 240–243, 249
  hyporheic zone, 231, 236, 238, 240–242, 272, 275, 278, 280
  intermittent, 31, 66, 236, 238
  losing, 190, 191, 231, 236, 248
  meandering, 231, 233, 235–237
Stream gauging, 243, 244, 248, 260, 280–282
  float method, 244
  gauging station, 245, 253, 281
  pygmy meter, 246
  synoptic survey, 246, 248–250
  tag line, 247
Streambed topography, 240, 241
Strike, 69–73, 78–81
Structure-contour maps, 15, 72
Subsurface
  cavities, 129
  geophysics, 129
  investigations, 126, 141, 142
  materials, 125, 152, 157
  properties, 127, 144, 152, 154
  shallow, 125, 159
Sulforhodamine B, 680, 683–686, 693–695, 697
Superfund, 440
Support-rod method, 255, 256
Survey
  reconnaissance, 131, 165
  seismic refraction, 127, 128, 132, 133, 135, 140, 142–146
  synoptic, 246, 248–250
Surveying
  electromagnetic, 152
  magnetic, 126
Surveying (*Cont.*):
  reflection, 135, 140, 143–146
  refraction, 127, 128, 132, 133, 135, 140, 142–146
S-waves, 134, 135, 148–151
Synoptic survey, 246, 248–250

Tag line, 247
Tailing effect, 516, 519, 523, 524
Takings, 33
Talus slope, 62
Tectonics, 69
Telluric currents, 152, 164
Tellurics, 152
  magneto, 152, 164, 165
Tensiometer, 556, 558, 574, 577–579, 583, 584
Theis
  equations, 444, 448, 454
  method, 437, 438, 443, 452, 474
  normal plot, 446
  reverse plot, 446–448, 452, 459, 463, 482
  type A curve, 459, 461–463, 466, 467
  type B curve, 461–463, 466, 467
Three-point problem, 71, 72
Time-of-travel studies, 273–275
Top of casing, 200
Topographic maps, 5, 15, 17, 23
Tortuosity, 492, 493
Total depth drilled, 24, 201, 448
Total dissolved solids, 292, 301, 309, 310
Total head, 118, 176–180, 438, 557, 558
Total porosity, 94, 96, 97, 99, 100
Tracer
  agents, 274, 567, 568, 638, 652, 670, 681–686
  concentration, 278, 656, 660, 668,
  initial mass, 657, 658, 662, 670, 696, 697
  peak concentration, 275, 660, 661, 669
  studies, 273–275, 278, 279, 651, 663–665, 669, 670, 677, 678, 694
Tracer test, 106, 273–279, 651, 663–665, 669, 670, 675
  design and completion, 653–658, 686–689, 692, 696
  detection limits, 689–692, 695, 696
  dye, 274, 638, 639, 675–679
  heat, 265, 272, 655, 658
  misconceptions, 673, 674, 679–681
  objectives, 652, 656, 657
  point-source, 276, 662

Tracer test (*Cont.*):
procedure, 278, 663–669
recirculating, 668, 671
single well, 652, 662–665
tracer material, 653–655, 681–686
Transducer, 201, 207–209, 211, 212, 219, 222, 411, 418–422
Transmissivity, 110, 111, 184, 184, 186, 227, 440, 441, 444–447, 450–453, 456–458, 462, 467, 471–473, 477, 486, 492, 495
Transpiration, 5
Transversal dispersivity, 660, 661, 663, 668, 669
Tri-cone bit, 338, 339
Tripping in, 323, 346
Tripping out, 323, 346
Trough, 132

Unconfined aquifer, 94, 102, 111, 113, 115, 118, 122, 439, 441, 442, 455, 456, 458–463, 468, 470, 473, 477–479, 485–487
Uniformity coefficient, 108, 110, 375, 378

Vadose zone, 1, 93, 94, 176, 177, 185, 238, 547, 548, 550, 551, 554–556, 559, 562, 565–569, 575, 583, 588, 592, 593, 627, 629, 630, 634, 663, 690
van der Kamp method, 526–528, 533, 534, 541
Vertical gradient, 261, 263
Velocity
seepage or average linear, 51, 59, 80, 84, 95, 119
stream, 243–250, 252
vertical, 12, 13, 259, 268
Vesicular lava, 38, 41, 49
Viscosity, 104, 105

Water
imported, 5, 7, 8
storage, 5
water-balance, 502
Water chemistry, 287, 294, 318
results, 287, 291, 298, 306, 312–314, 317–319
sampling, 287–291, 293–295, 297, 298, 307–309
Water content, 551–558, 563, 565–569, 577–579, 591, 592
gravimetric, 551, 589
profiles, 561, 562
Water content (*Cont.*):
residual, 553
volumetric, 551, 588, 589
Water flux, 567, 568
Water table, 5, 11–13, 91, 93, 96, 99, 113–115, 126, 140, 152, 163, 177, 178, 181, 184–186, 205, 223, 228, 232, 327, 340, 364, 403, 404, 439, 442, 456, 487, 491, 514, 515, 517, 547, 565, 567, 568, 574, 575, 627–631, 635, 663, 664
aquifer, 113,
perched, 94
regional, 93, 94, 547
Water witching, 390
dowsing, 390
witcher, 341, 390
Water-budget analysis, 4, 7
Water-budget myth, 10
Water-laid soils
grain-size distribution, 109
physical properties, 109
Water-level data
misinterpretation, 222, 229
Water-level devices, 201
Water-level measurement
carpenter's chalk, 202, 221
chart recorder, 201, 205–209, 221
E-tapes, 27, 201–205, 209, 211–213, 215–217, 221, 222, 258, 411, 419, 424, 425, 429, 430, 504, 512
steel tapes, 27, 201–203, 205, 213, 221
Water-quality 5, 287, 297
down-hole, 292
measurements, 19, 27, 32, 33, 298, 299
Water-quality sample
sources of error, 289, 290, 314, 317
Watershed, 3, 4–6, 11, 30
Wave, 131–133, 146, 148
form, 132, 134
fronts, 131–135
head, 137, 139, 144
length, 131–133, 136
P-, 134, 148, 149, 151
radio, 169
S-, 134, 135, 148–151
Weather conditions, 25, 27, 28
Weathering, 50–52, 61, 68
chemical, 62–64
mechanical, 62–64
sequence, 61
spheroidal, 63, 64

Well construction
materials comparison, 371
monitoring, 360
Well drilling, 19
auger, 346–348, 356, 363, 364, 367
cable-tool method, 331–334, 441, 375, 383
circulation, 336–339, 345, 358, 359
completion, 20, 22, 24, 25, 32, 33, 346, 367, 368, 372, 373, 374, 375, 383, 385
forward rotary method, 329, 334–336, 338, 339, 344, 356, 389
horizontal, 353, 354
methods, 321, 330–332, 344, 351, 354
reverse circulation, 341–344, 387
rotosonic (mini), 351, 352
safety, 324, 325, 328–330, 351, 354
safety points summary, 328, 329
total depth, 24, 201, 448
wire-line, 344–346
Well efficiency, 379, 405–407, 484
Well function, 444–446, 449, 451, 454, 461, 494
Well screen criteria, 378, 382
Well-bore storage, 356, 357
Wells, 5, 8, 24, 25, 34, 43, 60, 93, 96, 114, 128, 184, 243, 253, 264, 281, 316, 326, 333, 338, 339, 342, 355, 360–362, 371, 375, 383, 438–441, 455, 463, 471–473, 478, 479, 484, 495, 509, 525, 529, 555, 592, 628, 637, 652, 653, 675, 678, 690
cluster, 373, 374
completion, 20, 22, 24, 25, 32, 33, 346, 367, 368, 372, 373, 374, 375, 383, 385, 397
deep, 205, 383
development, 385
drilling, 330
function, 444–446, 449, 451, 454, 461, 494
imaginary, 475, 476, 483, 484
Wells (*Cont.*):
monitoring, 21, 64, 186, 188, 189, 197, 199–201, 212, 215, 218, 226, 227, 272–274, 288, 292–294, 307, 331, 347, 350, 360, 363, 371, 373, 398–400, 504, 510, 543, 657, 668, 671, 676, 690–692
multi-level, 373
nested, 373
observation, 27, 208, 360, 396, 398–401, 403, 404, 412, 428, 431, 434, 438, 439, 442, 447, 451, 452, 455, 462–470, 475, 484, 485, 494, 495–497, 656
production, 41, 42, 48, 49, 94, 321, 346, 371, 374, 375, 378, 385, 397
partial penetration, 398, 455, 456, 484, 485
Well sentinel, 207, 209–211, 222, 272, 411, 418–421, 423, 429, 430, 504, 508, 509, 512
Wenner array, 155, 159
Wentworth classification, 60
Wetlands, 31, 293
Wetted perimeter, 252
Wetting front, 555, 560, 561, 574, 575

Yellow, 21, 62, 326, 611, 681, 682
Yellowstone National Park, 41–43, 62, 260, 457, 458
geothermal area, 43
Yield, specific, 96–98, 100, 102, 441, 455, 463, 466–468, 470

Zero, 132, 185, 208, 222, 236, 314, 356, 511, 538, 549, 550, 555, 660
drawdown, 450–452, 463, 470, 471, 473, 475, 494
pressure, 93, 177
reading, 422, 423
time, 507, 511, 513, 515, 517–519, 521, 533, 535, 540, 541
Zero flux plane, 513
Zero-offset, 144